Justus-Liebig-Universität Gießen

Fachbereich Medizin

Zentrum für Zahn-, Mund- und Kieferheilkunde

Klinik- und Poliklinik für Mund-, Kiefer- und Gesichtschirurgie

Das freie mikrovaskuläre Fibulatransplantat zur Kieferrekonstruktion

-

Virtuelle präoperative Planung und Untersuchungen zu Einflussfaktoren auf den Transplantaterfolg

Kumulative Habilitationsschrift

zur Erlangung der Venia legendi

für das Fach Mund-Kiefer-Gesichtschirurgie

des Fachbereichs Medizin

der Justus-Liebig-Universität Gießen

vorgelegt von

Dr. med. Dr. med. dent.

Heinz Michael Knitschke

aus Krefeld

Gießen 2022

Die Naturwissenschaft braucht der Mensch zum Erkennen,
den Glauben zum Handeln.

Auch eine Enttäuschung, wenn sie nur gründlich und endgültig ist,
bedeutet einen Schritt vorwärts.

(Max Planck, 1858 – 1947)

Für meine Familie

Abkürzungsverzeichnis

ABI	Ankle-brachial-index (Knöchel-Arm-Index)
ASA	American society of anesthesiologists
ATA	*A. tibialis anterior*
ATP	*A. tibialis posterior*
BMI	Body mass index
CAD	Computer aided design
CAM	Computer aided manufacturing
CAS	Computer assisted surgery
COU	Vollständige Verknöcherung (Complete osseus union)
CS	Vollständiger Lappenerfolg (Complete success)
CTA	Computertomographie-Angiographie
DM	Distante Metastasen (Fernmetastasen)
FA	*Arteria fibularis*
HO	Heterotope Ossifikation
IOU	Inkomplette Verknöcherung (Incomplete osseus union)
LNM	Lymphknotenmetastase
LTR	Lokales Tumorrezidiv
MRONJ	Medikamente assoziierte Kiefernekrose
ORN	Osteoradionekrose
pAVK	periphere arterielle Verschlusskrankheit
PB	Periosteal branch der *A. fibularis*
PFF	Teilweiser Lappenerfolg (Partial flap failure)
PSI	Patienten-spezifisches Implantat
SCP	Septo-cutaneous branch der *A. fibularis*
SLM	Selective laser melting
TFF	Vollständiger Lappenverlust (Total flap failure)
TTI	Time to therapy initiation
VSP	Virtual surgical planning
WHD	Wundheilungsstörung (Wound healing disorder)

1. Einleitung

1.1. Rückblick

Der Ursprung der plastisch-rekonstruktiven Mund-, Kiefer- und Gesichtschirurgie (MKG-Chirurgie) geht auf den ersten Weltkrieg zurück. Kriegerische Auseinandersetzungen gingen mit Hochgeschwindigkeitsverletzungen und kombinierten, schweren Hart- und Weichgewebsverlusten der Gesichtsregion einher. Zu Beginn des 20. Jahrhunderts standen lokale Lappenplastiken und kleine freie Knochentransplante zur Verfügung. Der Versorgung kiefer- und gesichtsversehrter Soldaten nahm sich der Düsseldorfer Zahnarzt *Christian Bruhn* an und gründete im Jahr 1917 die Westdeutsche Kieferklinik in Düsseldorf. Die Klinik wuchs schnell und bereits 1920 verfügte sie über 100 Betten, die von zwölf Ärzten und Zahnärzten betreut wurden. Diese älteste Fachklinik kann als Keimzelle der heutigen MKG-Chirurgie Deutschlands aufgefasst werden [1]. Im Vergleich dazu verfügte das Vereinigte Königreich mit Ausbruch des zweiten Weltkrieges über die vier plastischen Chirurgen *Harold Gillies*, *Thomas Pomfred Kilner*, *Archibald McIndoe* und *Rainsford Mowlem*. Von britischen und amerikanischen plastischen Chirurgen werden sie als „The big four" bezeichnet [2].

Das erste freie Knochentransplantat am Menschen wird *van Meekeren* im Jahr 1662 zur Deckung eines Kalottendefekts zugeschrieben. Bemerkenswerterweise handelte es sich bei dem Transplantat um xenogenes Spenderknochengewebe eines Hundes [3-5]. Das erste autologe Knochentransplantat wurde von *von Walther* 1821 beschrieben [4, 6]. In der Mitte des 19. Jahrhunderts erarbeitete der französische Chirurg *Leopold Ollier* Verfahren zur Knochenheilung und Rekonstruktion mit Transplantaten. Auf seine Arbeiten gehen die heute noch verwendeten Begriffe *autogen*, *allogen* und *xenogen* zurück [7]. *Erich Lexer* und *Georg Axhausen* sorgten für die Weiterentwicklung und Verbreitung freier Knochentransplantate. Sie vertraten dabei die Meinung, dass die Osteoneogenese durch das Knochengewebe und die darin enthaltenen Zellen getriggert wird [8, 9]. Dieser sogenannten Osteoblastenlehre stand die Induktionslehre gegenüber, bei der das Transplantatbett für die Osteoneogenese als maßgeblich erachtet wurde [10]. Es ist *Wolfgang Axhausen*s Verdienst, beide Theorien zusammengeführt zu haben. Er beobachtete, dass die Knochenregeneration vom Transplantat selbst als auch durch das Transplantatbett

ausgelöst wird [11]. Schnell wurde deutlich, dass die freien Knochentransplantate aufgrund ihrer Versorgung per Diffusion anfällig für Komplikationen wie Infektionen waren. Weiterhin fiel auf, dass die Transplantate teils gravierenden Resorptionsvorgängen unterworfen waren [12]. *Bardenheuer* berichtete 1892 über die Verwendung kortikaler Knochentransplantate [13]. *Walther* beschrieb 1911 das freie Fibulatransplantat zur Rekonstruktion des Radius [14, 15]. In der rekonstruktiven Chirurgie des Ersten Weltkrieges erlangten Rippe und Schienbein als typische Spenderregion große Popularität [16]. Zumeist handelte es sich um freie Blocktransplantate. Bei diesen ergaben sich jedoch ähnliche entzündliche und resorptive Komplikationen, deren Frequenz erst mit Etablierung gefäßgestielter Transplantate reduziert werden konnte. Der gefäßgestielte Transplantattyp war sehr vielseitig einsetzbar, da das Transplantat – analog zum klassischen Rundstiel-Wanderlappen – bis zur Einheilung für die Blutversorgung mit der Entnahmestelle verbunden blieb. Es konnte an beinahe jeder Stelle eingesetzt werden. So wurden beispielsweise Transplantate der Fibula zur Rekonstruktion von Tibia und Femur verwendet [17]. In den 1960er Jahren wurde partikulierte Beckenkammspongiosa in Metallschalen zur Defektüberbrückung eingesetzt. Das Verfahren war ebenfalls mit hohen Infektions- und Verlustraten verbunden. Gefäßgestielte Rippenknochen- und Clavicula-Transplantate wurden bereits im 20. Jahrhundert zur Rekonstruktion der Mandibula angewandt [18]. Der zunächst notwendige, ernährende Gefäßstiel brachte Schwierigkeit bei der Inkorporation und der Ernährung mit sich. Gegen Ende der 1970er Jahre wurden – zum Teil neu entwickelt und zum Teil wiedereingeführt – die gestielten myo-kutanen und kombinierten Transplantate wie das *Serratus anterior* Transplantat mit Rippenknochen, der *Pectoralis major* Lappen mit Rippenknochen, *Clavicula*, *Sternum* oder gestielte Skapulaknochen zur Rekonstruktion herangezogen. Diese Techniken galten als relativ einfach, aber die Gefäßversorgung und die Qualität des Knochens war schlecht, und die Flexibilität bei der Lappenpositionierung war außerdem begrenzt [19]. Mitte der 1970er Jahre wurden Überbrückungsplatten aus Stahl zur Wiederherstellung der Unterkieferkontinuität nach Segmentresektionen eingesetzt [20].

Mit der Entwicklung mikrochirurgischer Techniken und vaskularisierter Transplantate ließen sich die Probleme Infektion und Resorption freier, avaskulärer Transplantate lösen [21]. Die erste Beschreibung eines freien Transplantates stammt von

McCullough und *Fredrickson* aus dem Jahre 1972. Ihnen gelang die freie Transplantation einer Rippe in einen Defekt des Unterkiefers [22]. Fünf Jahre später konnten *Buncke et al.* das erste mikrovaskuläre, freie osteokutane Rippentransplantat zur Rekonstruktion der Tibia verpflanzen [23].

1.2. Meilenstein Mikrochirurgie

Die erste „Seit-zu-Seit“ Anastomose führte *Eck* 1877 zwischen der *V. portae* und der *V. cava inferior* durch [24]. *Jassinowski* berichtete im Jahr 1889 über die Technik der Gefäßnaht und konstatierte, dass das Nahtmaterial die endoluminale Intima nicht durchgreifen solle [25]. *Alexis Carrel* publizierte 1902 die erste End-zu-End Anastomose in Triangulations- (oder Aufspann-) Technik [26]. Im Folgejahr wurde die erste erfolgreiche Extremitätenreplantation bei einem Hund durchgeführt [27]. Bereits zehn Jahre nach Einführung seiner auch heute noch angewandten Nahttechnik wurde *Carrel* für seine weitreichende Innovation im Jahr 1912 für den Nobel-Preis nominiert [28]. Heute zählt er gemeinsam mit *Guthrie* zu den Pionieren und Wegbereitern der Mikrochirurgie. Ein weiterer bedeutender Schritt war die Entdeckung des Heparins durch den Medizinstudenten *Jay McLean* sowie *Howell* und *Holt* im Jahr 1916 [29, 30]. Schon kurze Zeit später erfolgte der praktische Einsatz, und es folgten erste klinische Studien durch *Charles* und *Scott* Anfang der 1930er Jahre [31].

Die Entstehung der Mikrochirurgie ist eng mit der technologischen Entwicklung von Vergrößerungshilfen und konkret mit Mikroskopen verknüpft. Dem schwedischen HNO-Arzt *Nylén* wird die erste Verwendung eines für operative Zwecke benutzbaren Stativmikroskops im Jahr 1921 zugeschrieben [32]. *Nyléns* akademischer Vater *Gunnar Holmgren* an der *Karolinska Medical School* in Stockholm (Schweden) entwickelte 1923 ein binokulares Mikroskop, was räumliches Sehen ermöglichte [33].

Erst 1960 wurde die erste erfolgreiche Gefäßanastomose unter einem OP-Mikroskop durch *Jacobson* und *Suarez* durchgeführt [34-36]. Beide entwickelten für die spezifischen Belange der Mikrochirurgie ein filigranes Instrumentarium. Auf das Jahr 1965 wird der erste mikrovaskuläre Lappen am Hund durch *Krizek et al.* datiert. Dabei handelte es sich um einen abdominofaszialen Hautlappen basierend auf den

Vasa epigastricae superficiales [37]. Der erste mikrovaskuläre Rippentransfer durch *Strauch et al.* erfolgte 1971 in den Unterkiefer eines Hundes [38].

Nur ein Jahr später – 1972 – wurde der weltweit erste freie Hautlappen am Menschen durch *Harii et al.* im Bereich der Kopfhaut durchgeführt [39]. In der Literatur werden jedoch zumeist *Daniel* und *Taylor* (1973) als Erstbeschreiber eines erfolgreichen mikrovaskulären Leistenlappens (groin flap) genannt [40]. In den Folgejahren wuchs das Verständnis der Gefäßanatomie und territorialen Ausbreitung [41] und Erfahrung in mikrovaskulären Techniken. In schneller zeitlicher Folge wurden verschiedene Lappen entwickelt. So erschienen bereits 1975 Berichte über das freie, mikrovaskuläre Beckenkammtransplantat [42]. 1976 wurde von *Baudet et al.* der Begriff "muskulokutaner Lappen" geprägt und der freie myo-kutane Latissimus-dorsi-Lappen beschrieben [43]. In China wurde 1978 der an der *Arteria radialis* gestielte freie faszio-kutane Unterarm-Lappen entwickelt. Sowohl *Yang et al*. 1981 [44] als auch *Song et al*. 1982 [45] veröffentlichten ihre Ergebnisse erst nach über 100 erfolgreichen Transplantation des „Chinese flaps“ – dem Radialislappen.

1.3. Das mikrovaskuläre Fibulatransplantat

Taylor beschrieb im Jahr 1975 als Erster das freie mikrovaskuläre Fibulatransplantat (FFF) zur Versorgung eines Tibiadefektes [42]. Ergänzend muss erwähnt werden, dass *Ueba* und *Fujikawa* im Jahr 1982 von einem neunjährigen Follow-up eines mikrovaskulären Fibulatransplantats berichteten, das sie 1973 verpflanzt hatten. Sie sind somit als weitere Entdecker dieses Transplantats zu nennen [46]. *Gilbert* entwickelte und beschrieb 1979 die heute noch angewandte Entnahmetechnik über den postero-lateralen Zugang ventral des *Septum intermusculare posterius* [47].
Das Fibulatransplantat ist das heutige „Workhorse“ der rekonstruktiven MKG-Chirurgie [42, 48, 49]. Es wird aufgrund zahlreicher günstiger Eigenschaften bevorzugt zur Rekonstruktion der Mandibula und Maxilla eingesetzt [50]. Die zur Verfügung stehende Knochenlänge ist zumeist ausreichend für eine Rekonstruktion des Unterkiefers bis zu einer Defekt-Klasse Typ IVc nach *Brown et al.* [51]. Es bietet die Möglichkeit auf implantologische Rehabilitation [52-58], einen ausreichend langen Gefäßstiel zum Einsatz in der gesamten Kopf-Hals-Region zwischen Stirn und Schlüsselbein [59] und

eine insgesamt geringe Entnahmemorbidität [60]. Die Wiederherstellung der knöchernen Kontinuität des Unterkiefers führt zu einer erheblichen Verbesserung der Lebensqualität. Studien ergaben, dass dies besonders ausgeprägt bei Patienten mit infizierter Osteoradionekrosen des Kiefers zutrifft [61, 62].

Wurde initial noch eine stabile und suffiziente Gefäßversorgung der septo-kutanen Hautinsel angezweifelt [63], wuchs mit zunehmender Verbreitung des Transplantats das Wissen über die vaskuläre Versorgung über septo-kutane Perforatorgefäße der *A. fibularis* (FA), die im *Septum intermuscualare posterius* gelegen sind. Untersuchungen zeigten weiterhin, dass auch im *Musculus soleus* relevante Perforatoren gelegen sein können [64-66]. *Yadav et al.* erarbeiteten an 386 Fibulatransplantaten vier Versorgungstypen der Hautinsel [67]. Dabei bezieht der häufigste Typ A (95,8 %) die Blutversorgung ausschließlich aus Ästen der *A. fibularis*, Typ B (3,6 %) aus den *Aa. fibularis* und *tibialis posterior* [68], Typ C (0,5 %) über myo-cutane Äste aus der *A. tibialis posterior* [66, 69, 70] und Typ D aus Ästen der *A. poplitea* [65].

Das Fibulatransplantat wurde von nun an stetig weiterentwickelt. So wurde 1983 erstmals ein vaskularisiertes, osteo-faszio-myo-cutanes Fibulatransplantat beschrieben, bei welchem zusätzlich zur Gefäßachse und Knochen auch Haut und umgebendes Muskelgewebe entnommen wurde [71]. *Jones et al.* berichteten 1988 über die „Double-Barrel“-Technik, bei welcher durch zwei parallel eingebrachte Fibula-Segmente eine größere Knochenbreite zur Rekonstruktion eines Femurs erreicht werden konnte [72]. Schließlich ist es *Hidalgo*s Verdienst, 14 Jahre nach *Taylor*s Erstbeschreibung, das Fibulatransplantat zur Rekonstruktion der Mandibula eingesetzt zu haben. Er berichtete über die erfolgreiche Versorgung von zwölf Patienten [73]. Fünf Jahre später folgte die erste Rekonstruktion eines Oberkiefers von *Nakayama* mittels mikovaskulärem Fibulatransplantat [74]. *Bähr et al.* übertrugen die Aufdopplungstechnik – „Double-Barrel“ – in die Kieferregion zum Erreichen einer ausreichenden Knochenhöhe der nicht-atrophen Mandibula [75]. *Chang et al.* entwickelten das osteo-fasziale Fibulatransplantat als Alternative, wenn intraoperativ keine septo-kutanen Perforatoren zur Versorgung der Hautinsel exploriert werden können. Dabei verwendeten sie das Fasziengewebe des *M. soleus* und der *Mm. peronei* zur Rekonstruktion des Mundbodens und überließen es der freien Epithelisierung. Die Donorseite konnte primär verschlossen werden und heilte stets

ohne Komplikationen ab. Sie beobachteten bei Anwendung dieser Technik keine lappenbedingten Komplikationen [76, 77]. Ein weiterer Meilenstein markiert im Jahr 2005 die Einführung computergestützter Verfahren [78], durch das die Passgenauigkeit mittels CAD/CAM-Techniken erhöht und die Operationszeit verringert werden konnte [79].

1.4. Die Entwicklung Computer assistierter und virtuell geplanter Chirurgie (VSP)

Der Weg von analog geplanten, ein- zu mehrgliederigen und weiter zu virtuell entworfenen ein- und mehrgliederigen knöchernen Rekonstruktionen war von mehreren technologischen Entwicklungssprüngen begleitet. So orientierte sich die freihändige Modellierung des Fibulatransplantats zunächst am Defekt und dem anatomischen Spiegelbild der Kiefergegenseite. Es determinierte mitunter die Lage der Osteotomielinien und die Positionierung der Osteosyntheseplatten [73, 80]. Mit Aufkommen und weiten Verbreitung der Digitalisierung, leistungsstarken Computern und Speichermedien konnten auf der Basis hochauflösender Computertomographien die ersten 3D-Modelle des Gesichtsschädels erstellt werden.
Diese erleichterten die Operationsplanung komplexer Rekonstruktionen [81, 82]. Einen wegweisenden Impuls gab der amerikanische Physiker *Hull*. Er entwickelte das Stereolithographieverfahren und ließ sich dieses 1983 patentieren. Dabei handelt es sich um ein additives Fertigungsverfahren, bei dem iterativ (zeilen- bzw. schrittweise) ein digital modellierter Körper gefertigt wird. Damit gelang erstmals die Überführung eines digital geformten Körpers in ein haptisches Modell. Solche wurden und werden bei der Operationsplanung verschiedener operativer Disziplinen eingesetzt [83-85]. Während beispielsweise 3-D-Oberflächenrekonstruktionen in den 1990er Jahren noch als aufwendige technische und rechenintensive Raffinesse anmuteten, hat sich die Realtime 3-D-Oberflächenrekonstruktion etabliert und bietet zahlreiche Anwendungsgebiete, insbesondere im Bereich der knochenbasierten Chirurgie. Die **Abbildung *1*** illustriert den Entwicklungsprozess der Volumenoberflächen-rekonstruktion über die letzten 20 Jahre bis zur heute möglichen photorealistischen Darstellung mit der Cinematic Volume Rendering Technik [86-88].

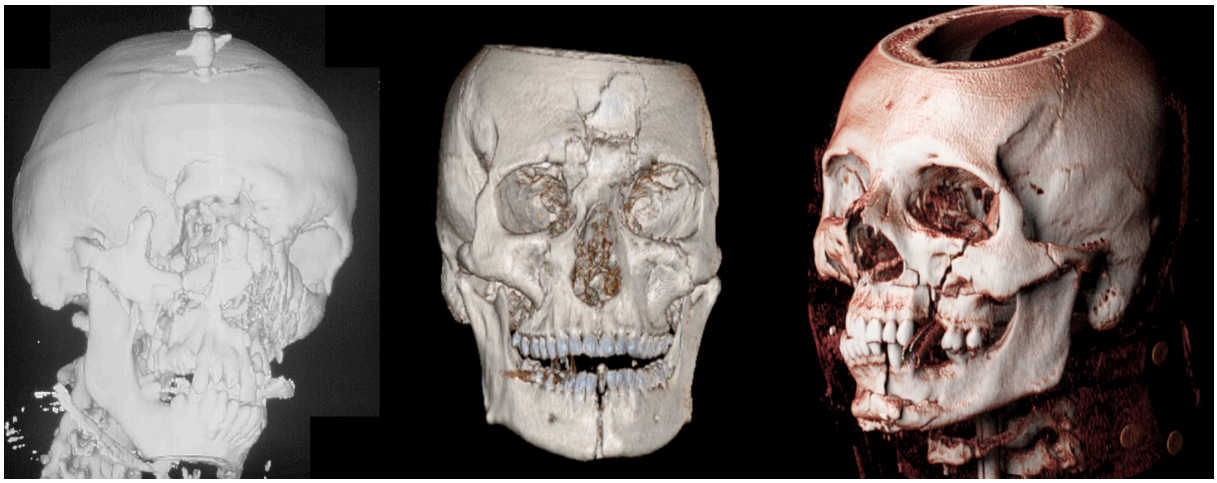

Abbildung 1. Oberflächenrekonstruktionen panfazialer Frakturen. Links: Aufnahmedatum 1998, Software: Unbekannt, Mitte: 2014, Software: syngo.via (Siemens Heathineers, Forchheim, Deutschland), Rechts: 2021, Software: MeVisLab (MeVis Medical Solutions AG, Bremen, Deutschland)

Die Computer assistierte Chirurgie hat in der MKG-Chirurgie inzwischen an zahlreichen Stellen mit CAD/CAM-Technologien einen festen Stellenwert. Das Einsatzgebiet reicht von Schablonen für die geführte dentale Implantologie [89, 90] über Osteotomieschablonen, patienten-spezifische Osteosyntheseplatten und Okklusionssplinten (sog. Wafer) für die orthognathe Chirurgie [91, 92], über patienten-spezifische Implantate für die Traumatologie des Gesichtsschädels inklusive Orbitarekonstruktion [93-95] sowie bei mikrovaskulären osteo-faszialen Transplantanten in Form von patienten-spezifischen Osteosyntheseplatten, wie sie beim Fibulatransplantat zur Anwendung kommen [96].

Die erste volldigitale, virtuelle Planung einer Unterkieferrekonstruktion (virtual surgical planning, VSP) wurde im Jahr 2005 von *Eckardt* und *Swennen* beschrieben [78]. Die Technik wurde seitdem weiterentwickelt [97-101]. Einzeitige onkologische Resektionen der Mandibula und Rekonstruktion mit einem freien Fibulatransplantat wurden zunächst virtuell geplant und rekonstruiert. Als Planungsergebnis wurden Modelle im 3-D-Druck wie z.B. im sterolithographischen Verfahren hergestellt. Notwendige Positionierungs- und Resektionsschablonen wurden dann auf dem Modell angepasst und z.B. eine Rekonstruktionsplatte am Modell ideal angebogen [102]. Durch die digitale Kombination von Spender- und Empfängerregion können virtuell – nach chirurgischen Regeln und Erfahrungen – ideale Rekonstruktionen erreicht werden. Mit virtuell konstruierten (CAD) und gefertigten (CAM) Resektionsschablonen

kann ein hohes Maß an Genauigkeit erreicht werden [103, 104]. Die Rückführung digitaler Daten in Form eines gedruckten Modells reduziert jedoch die ursprüngliche Genauigkeit der virtuell geplanten Rekonstruktionen, wenn dazu eine manuell vorgebogene Rekonstruktionsplatte aufgrund des Systemwechsels zur klinischen Umsetzung erforderlich ist [103]. Derartige Ungenauigkeiten könnten sich insbesondere auf der Ebene der Okklusion auswirken.

Heute stehen verschiedene 3-D-Druckverfahren zur Verfügung, wobei folgende Methoden im Prinzip unterschieden werden können: Lichtgehärtetes Polymer, verklebter und gesinterter Pulverdruck sowie thermoplastischer Druck. Im Prinzip wird mithilfe eines zweiachsig geführten Lasers ein lichtaktivierbares Polymer schichtweise durch einen Laser ausgehärtet [105]. Weiterhin kann anstelle eines lichtaktivierbaren Polymers ein Metallpulver erwärmt und gezielt mittels Laser aufgeschmolzen und so schichtweise geformt werden [106]. Dieses Verfahren wird als selektives Laserschmelzverfahren bezeichnet („selective laser melting“, SLM; z. B. KLS Martin, Tuttlingen). Im Gegensatz hierzu verarbeiten Filamentdrucker thermoplastische Kunststoffe von der Rolle (fused deposition modelling), was den Vorteil bietet, dass unterschiedliche Farben für einen Werkkörper benutzt werden können [105]. Die CAD/CAM-Technologie ermöglicht die Herstellung von – teils sogar in-house/chairside – individuell gefertigten Resektions- und Sägeschablonen sowie die industrielle Fertigung patienten-spezifischer Implantate (PSI) bzw. Osteosyntheseplatten [107-113]. Die Entwicklung und Produktion eben dieser (syn. Rekonstruktionsplatten) sind das zentrale Bindeglied zwischen virtueller Planung und der realen operativen Rekonstruktionsumsetzung der Neo-Mandibula [109]. Bei PSI handelt es sich um individuell geformte und 3-D-gefertigte Osteosyntheseplatten und diese sind der Schlüssel für die dreidimensionale Konfiguration der ursprünglichen und der transplantierten Knochensegmente [109, 114]. Die Genauigkeit dieser Technik wurde bereits umfassend untersucht [108, 109, 113, 115, 116]. Die Ausführungen sind variabel in der Plattendicke, Anzahl, Positionierung und Angulation von Schraubenlöchern. Eine Nachbearbeitung mit fräsenden Verfahren (z.B. Gewinde für Locking-Schrauben) ist zudem möglich. Ein wesentlicher Innovationstreiber dieser technologischen Evolution waren die Entwicklung von industriellen 3-D-Druckern und die Entwicklung des SLM zur wirtschaftlichen Herstellung – rapid prototyping – der PSI. Daneben stehen subtraktive, fräsende (CNC) oder erodierende Verfahren zur

Fertigung zur Verfügung [96]. Der digitale und klinische Workflow einer Unterkieferrekonstruktion ist anhand eins Beispiels in **Abbildung *2*** dargestellt.

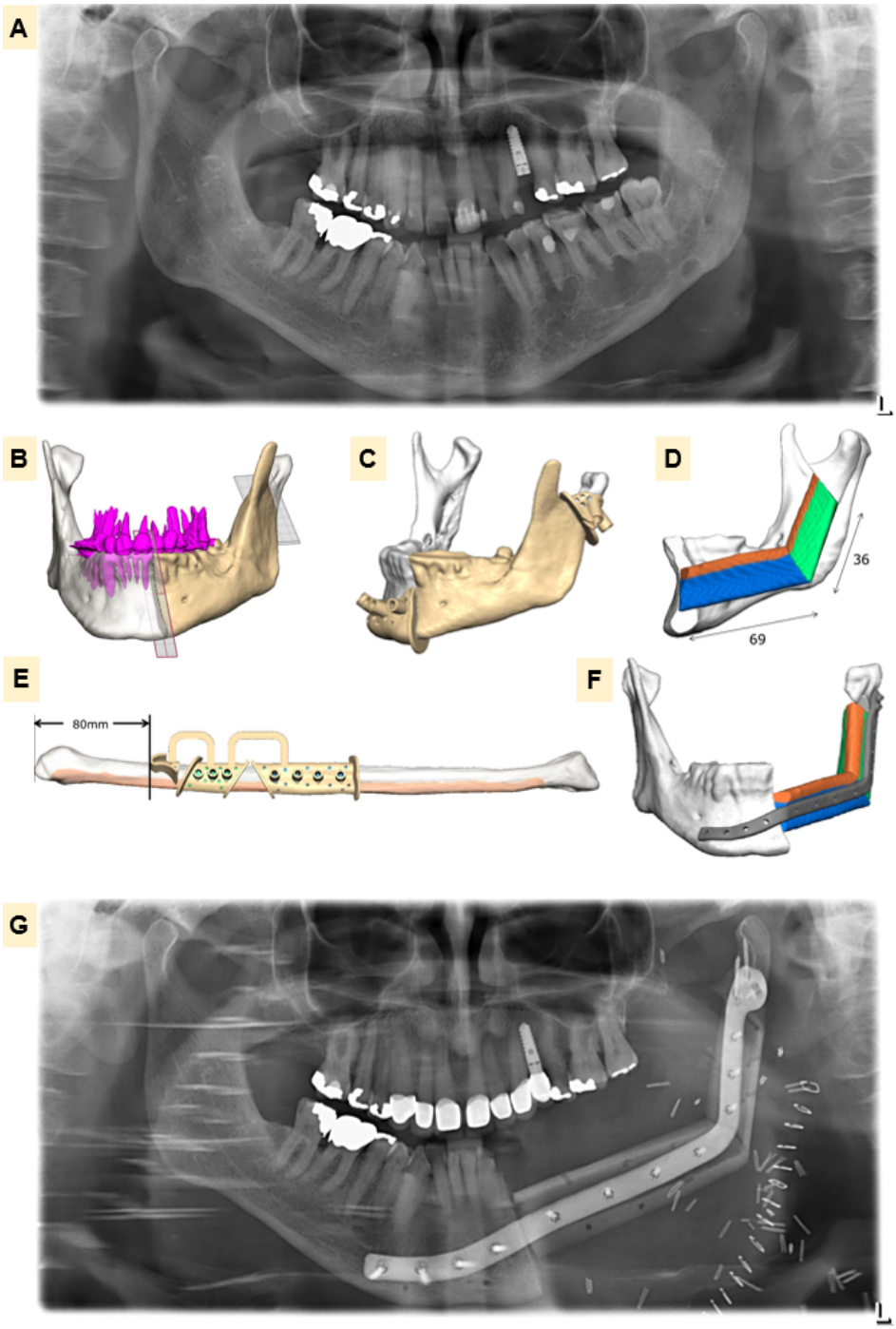

Abbildung 2. Klinischer Workflow einer virtuell geplanten Resektion und Rekonstruktion. **A**: Ausgangsbefund bei drittem Rezidiv einer odontogen Keratozyste (früher: Keratozystisch odontogener Tumor, KZOT) in regio 36-37. **B**: Festlegen von Resektionsebenen am virtuellen 3-D-Oberflächenmodell und **C**: Planung von Resektionsschablonen. **D**: Rekonstruktion der Mandibula mit bi-segmentalem Fibula-transplantat. **E**: Fibula mit modellierten Schablonen und Bedarfsschablone für Kondylusersatz. **F**: Finales Modell der Neo-Mandibula mit PSI (Verwendung mit freundlicher Genehmigung von KLS Martin). **G**: Postoperative OPG-Kontrolle.

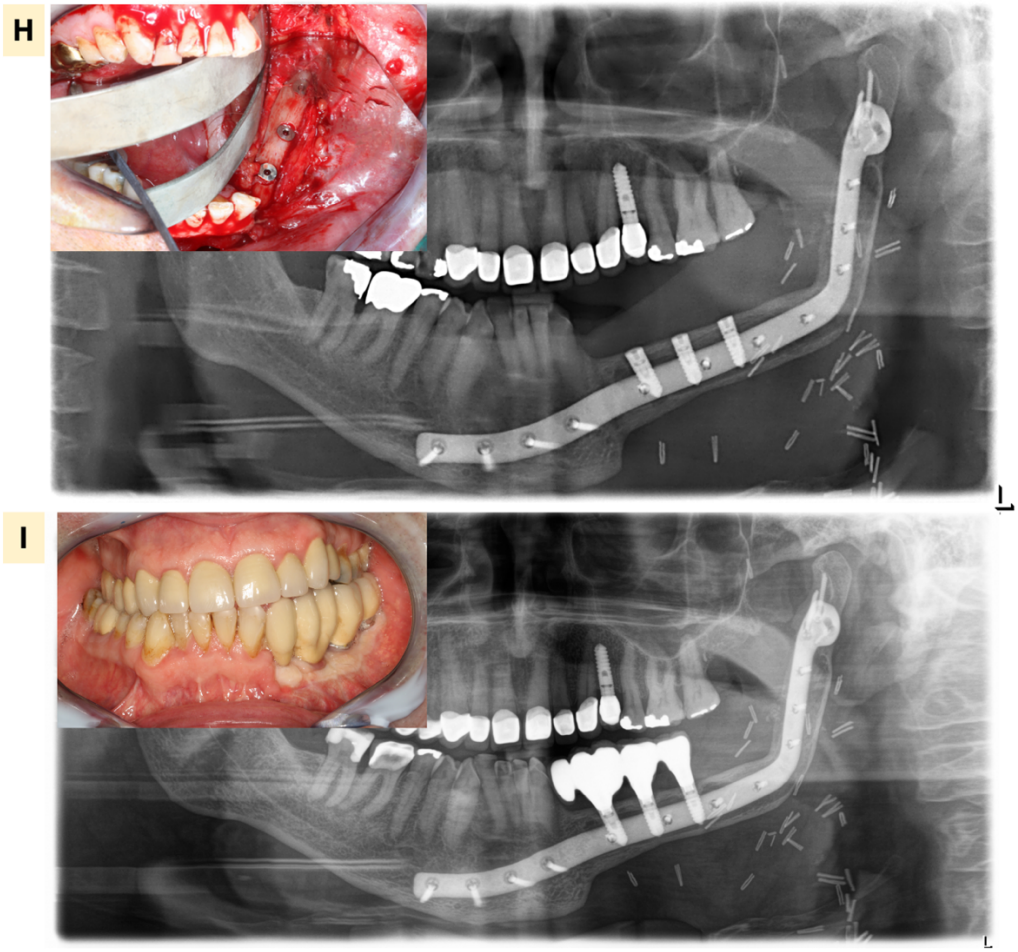

Abbildung 2 (Fortsetzung): G: Postoperative OPG-Kontrolle. **H**: Z.n. Insertion dentaler Implantate und Trimmung der Hautinsel **I**: Abschlussdokumentation nach prothetischer Versorgung.

1.5. Verbliebene Herausforderungen des mikrovaskulären Gewebetransfers

Mikrovaskuläre Rekonstruktionen haben sich in den letzten Jahren fest im Spektrum der rekonstruktiven, plastischen Chirurgie etabliert. Weiterentwicklungen mikrochirurgischer Techniken ermöglichen die erfolgreiche Anastomisierung feinster Blut- [117-122] und Lymphgefäße [123-125]. Des Weiteren konnten durch die Einführung von Gefäß-Coupler-Systemen [126-129], virtuell geplanten Rekonstruktionen und der Anwendung von PSI Verkürzungen der Operationszeit erreicht werden. Das Monitoring der postoperativen Lappendurchblutung ist eine weitere klinische Herausforderung. Apparative peri- und postoperative Lappen-Monitorverfahren [130, 131] sowie das interdisziplinäre anästhesiologische und intensivmedizinische Patientenmanagement haben dazu beigetragen, Erfolgsraten von 90 – 95% für das osteo-faszio-kutane Fibulatransplantat zu erreichen [49, 132-134].

Trotz der ausgewiesenen Erfolgsrate kommt es in der klinischen Routine immer wieder zu un- bzw. vollständigen Lappenverlusten mit weitreichenden Folgen für die betroffenen Patienten. Neben der krankheitsassoziierten spezifischen Morbidität durch den – zumeist onkologischen – Primäreingriff, können (sub-)totale Transplantatverluste zu einer Verzögerung beispielsweise adjuvanter strahlentherapeutischer Maßnahmen und zur Notwendigkeit operativer Folgeeingriffe wie Revisionen und Sekundärlappen führen.

Tabelle 1. Beispiele für Einflussfaktoren auf den Erfolg des mikrovaskulären Fibulatransplantats

Parameter		
Patient	Geschlecht	
	Alter	
	BMI	
	ASA	
	Präoperative Anämie	
	Vorerkrankungen	- Diabetes mellitus
		- Vaskulärer Status
	Risikofaktoren	- Alkohol
		- Rauchen
		- Antikoagulation
Operation	Voroperation Hals	-
	Vorbestrahlt	-
	Rekonstruktionszeitpunkt	- Ein- vs. zweizeitig
	Rekonstruktionsverfahren	- Analog (Konventionell), Non-VSP
		- Digital (VSP)
		- Digital (VSP) mit PSI
	Chirurgische OP-Dauer	- Schnitt-Naht-Zeit
		- Ischämiezeit
	Anästhesiologische Parameter	- Ausgangshämoglobinkonzentration
		- Arterieller Mitteldruck
		- Körpertemperatur
		- Blutverlust, intraoperativ
		- Blutprodukte (EK, TZ, FFP)
		- Katecholamine
		- Dauer: OP
		- Dauer: OPINT
		- Tracheotomie
		- Postoperatives Delir
Makroperfusions-störung	Lappenmonitoring	- Arteriell
		- Venös
		- Beides (Oberflächenverfahren)
	Gefäßstiel	- Hämodynamische Ursachen
		- Mechanische Ursache
Mikroperfusions-störung	Mechanisches Trauma:	- Osteosynthese:
		- Schrauben
		- Platte
		- Periost
		- Periostale Gefäße
	Segmentosteotomien	
	Aufpassung von Schablonen	
	Präparation Gefäßstiel	
	Anzahl Segmente	
	Segmentlänge	
Langzeiterfolg	Heterotope Ossifikation	

Defektmorphologie:	- Maxilla - Lateral: Brown I(c) – II(c) - Anterior: Brown III – IV(c)
Verknöcherung	- M - F (distal)
Transitionszone:	- F - F (intersegmental) - F - M (proximal)
Osteoradionekrose	
Okklusion	

1.5.1. Aspekt 1: Die Patientenselektion

Nichtsdestotrotz bleibt die besondere Herausforderung bei mikrovaskulären Rekonstruktionen die sorgfältige Patientenselektion um Lappenverluste – also Misserfolge – zu vermeiden. International haben verschiedene Studien u.a. den Einfluss des Patientenalters, des BMI, der ASA-Klasse und des Voroperationsstatus des Halses bei mikrovaskulären Lappenoperationen sowie eine stattgehabte präoperative wie auch postoperative Strahlentherapie auf den Lappenerfolg untersucht. Weiterhin wurde der Einfluss von hämodynamischen Parametern (u.a. Volumentherapie, arterieller Mitteldruck, intraoperative Hämoglobinkonzentration und Transfusionsbedarf, Notwendigkeit intravenöser Katecholamin-Verabreichung) hinsichtlich des Transplantationserfolges beforscht – teils mit widersprüchlichen Ergebnissen (**Tabelle *1***). Weitgehend ungeklärt ist bislang, wie sich die patientenseitigen Faktoren bei Anwendung der Methode der virtuellen chirurgischen Planung (VSP) in Kombination mit PSI auf den Transplantaterfolg auswirken.

1.5.2. Aspekt 2: Die Übertragung der virtuellen Planung auf den Patientensitus

Technische Innovationen wie endoskopisch bzw. laparoskopisch durchgeführte Operationen, OP-Roboter (z.B. Davinci®) unterstützte Eingriffe, aber auch die Computer unterstützte Chirurgie (CAS, computer assisted surgery) sind von Vorteil die Operationszeit als wesentlichen Kostenfaktor zu reduzieren und gleichzeitig eine Verbesserung der Qualität zu erreichen [135]. Digital geplante Kieferrekonstruktionen tragen zu einer Verkürzung der Operationszeit und der stationären Verweildauer bei [136, 137]. Jedoch benötigt die Überführung der virtuellen Planung die Herstellung

individueller Resektions- und Rekonstruktionsschablonen sowie patienten-spezifischer Osteosyntheseplatten (bzw. Implantate) und damit eine entsprechende Vorlaufzeit von Planung und Fertigung über Logistik und Sterilisation [138]. Der Einfluss auf einzeitige Rekonstruktionen nach ablativer onkologischer Chirurgie ist bislang lückenhaft untersucht. Es muss die Frage erörtert werden, inwiefern sich die verfahrensbedingte Vorlaufzeit bis zur operativen onkologischen Therapie auf den Resektionsstatus auswirkt und ob das onkologische Outcome hierdurch beeinflusst wird.

1.5.3. Aspekt 3: Bildgebung und Berücksichtigung kleiner Gefäße

Für das osteo-faszio-kutane Fibulatransplantat kann konstatiert werden, dass kein nicht-invasives Routine-Verfahren zur Bewertung der Qualität der Gefäßversorgung des Unterschenkels - analog zum Allen-Test am Unterarm - zur Verfügung steht. Als klinisches Screening-Verfahren auf das Vorliegen der peripheren arteriellen Verschlusskrankheit (pAVK) wird der Ankle-Brachial-Index (ABI) als kostengünstiges und nicht-invasives Untersuchungsverfahren genannt [139].
Für die chirurgische Planung wird die präoperative Angiographie des Unterschenkels kombiniert mit einer für die virtuelle Rekonstruktionsplanung notwendigen CT-Untersuchung und zu einer CT-Angiographie (CTA) der unteren Extremität zusammengefasst. Es stellt sich daher die Frage, ob die CT-Angiographie Hinweise auf einen potenziellen (sub-)totalen Lappenverlust liefern kann. Zusätzlich ist die Einbeziehung der kleinen Gefäße in die virtuelle Planung mono- und polysegmentaler Rekonstruktion nicht im Hauptfokus der klinischen Forschung.
Die Auswertung der CTA-Bilddaten mit besonderem Augenmerk auf den Verlauf, Dichte und Verteilung der großen und kleinen Gefäße scheint vielversprechende Aspekte für die chirurgische Planung insbesondere im Rahmen der virtuellen Planung liefern zu können.

1.5.4. Aspekt 4: PSI assoziierte Komplikationen

Wie eingangs erwähnt, können Kieferrekonstruktionen mit PSI zu einer Verkürzung der Operationsdauer und Erhöhung der Rekonstruktionsgenauigkeit führen [136, 137]. Andererseits zeigt die klinische Erfahrung eine Häufung von lokalen Komplikationen im Zusammenhang mit PSI im Vergleich zu herkömmlichen Mini-Platten. Die werkstofflichen und fertigungstechnischen Eigenschaften bedingen eine höhere Rigidität des PSI [140]. Die Rigidität reduziert funktionelle, osteoinduktive Reize auf den Knochen bzw. auf den „Osteotomiespalt“ [141-144]. Zudem haben Untersuchungen anderer Arbeitsgruppen aufgezeigt, dass das distale Transplantatsegment – insbesondere bei mehrgliedrigen Rekonstruktionen – eine verminderte Perfusion aufweist [145, 146]. Hier erscheint es klinisch relevant, eine Auswertung der Kieferrekonstruktionen durchzuführen und die Verknöcherung der Osteotomiespalten am Übergang Mandibula zu Fibula sowie intersegmental bei polysegmentalen Rekonstruktionen zu beurteilen.

1.6. Einordnung der Arbeit

Die kumulative Habilitationsschrift zur klinischen Versorgungsforschung fokussiert sich auf Komplikationen, deren Tragweite im klinischen Alltag und Einflussfaktoren für den langfristigen Erfolg der Kieferrekonstruktion mit dem Fibulatransplantat. In der Literatur sind zahlreiche Einflussfaktoren und Komplikationen mit zum Teil erheblicher Spanne in der beobachteten Prävalenz und mit gegensätzlichem Informationsgehalt aufgeführt. In der auf retrospektiven Auswertungen basierenden kumulativen Forschungsschrift werden Fibulatransplantate über einen Zeitraum von bis zu 19 Jahren untersucht. Es wird eine systematische Bewertung des angewandten Rekonstruktionsverfahrens (konventionell vs. VSP/PSI) mit Blick auf bekannte Einflussfaktoren auf den Transplantaterfolg und die onkologische Sicherheit durchgeführt. Dabei werden nicht nur Aspekte für den kurz-, sondern auch für den mittel- und langfristigen Lappenerfolg untersucht. So wird unter anderem das Auftreten von heterotopen Ossifikationen entlang des Transplantats analysiert und klassifiziert. Die Bedeutung der periostalen Äste der *A. fibularis* sowie der septo-kutanen Perforatoren für den Erfolg des Fibulatransplantats ist unstrittig. Der Stellenwert dieser scheint in der präoperativen Planung bislang eine untergeordnete Rolle zu spielen. Im

Zusammenhang mit der heute vielerorts durchgeführten virtuellen, digitalen Rekonstruktionsplanung auf der Basis von CT-Untersuchungen wird untersucht, ob die CT-Angiographien zum einen ein ausreichendes Auflösungsvermögen zur Darstellung der kleinen Gefäße haben und andererseits die Dichte und Verteilung mit dem Transplantationsergebnis korrelieren. Zudem wurde als „neue“ Visualisierungsmethode das *Cinematic Volume Rendering* (CVR) auf der Basis von kontrastierten CT bzw. CT-Angiographien angewandt, um u.a. die infra-popliteale Gefäßarchitektur intuitiv erfassbar zu machen.

2. Fragestellung und Zielsetzungen der Arbeit

Mit der Untersuchung sollen Ergebnisse mikrovaskulärer Kieferrekonstruktionen mit dem Fibulatransplantat (FFF) kritisch analysiert werden. Einflussfaktoren auf den Lappenerfolg stehen somit im Mittelpunkt dieser Forschungsarbeit. Die durchgeführte Aufarbeitung postoperativer Komplikationen konzentriert sich darauf, eine Standortbestimmung durchzuführen und Verbesserungspotenzial in der bisherigen präoperativen Planung und der operativen Prozedur zu diskutieren. Diese Ergebnisse zielen darauf ab, die Ergebnisqualität weiter zu optimieren und damit die Lebensqualität der Patienten positiv beeinflussen zu können.

Zur Untersuchung dieser Zusammenhänge erfolgte die Analyse von Patienten, die sich in der Klinik für MKG-Chirurgie der Justus-Liebig-Universität Gießen zwischen 2002 und 2020 einer Kieferrekonstruktion mit einem Fibulatransplantat unterzogen hatten.

Mit drei Kernfragen soll die besondere Herausforderung der mikrovaskulären Kieferrekonstruktion bearbeitet werden:

I. Wie hoch ist die Rate der Lappenverluste bei Kieferrekonstruktionen mit dem Fibulatransplantat und in welcher Form treten sie auf?

   Neben der Erhebung der Transplantatverlustrate soll die Frequenz partiellen oder vollständigen Verlusts der septo-kutanen Hautinsel und/oder von

knöchernen Transplantatsegmenten ermittelt werden. Dabei sollen Ursachen und gewählte chirurgische „Rettungsverfahren“ untersucht werden.

II. Wie unterscheiden sich die Erfolgs- und Komplikationsraten zwischen analog/konventionell und digital/virtuell geplanten Rekonstruktionen?

Es ist von besonderem Interesse, ob ein Einfluss des verwendeten Planungs- und Rekonstruktionsverfahrens auf den Resektionsstatus (R0-Situation) besteht. Dies spielt im klinischen Alltag eine große Rolle, da sich Zeitspanne von Diagnosestellung bis zur chirurgischen Therapie zwischen beiden Methoden Planungs- und Fertigungsbedingt maßgeblich unterscheiden.
Insgesamt hat sich zwar die Anwendung von CAD/CAM gefertigten patienten-spezifischen Implantaten (PSI) im Rahmen von Kieferrekonstruktionen in der Literatur bewährt, jedoch sind noch Fragen zur Verknöcherung der segmentalen Übergänge unvollständig bearbeitet.

III. Wie kann der klinisch tätige Chirurg den funktionellen Lappenerfolg in der Planungsphase positiv beeinflussen?

Ein Aspekt in diesem Zusammenhang ist die Analyse der präoperativ durchgeführten CT-Angiographien. Es ergibt sich die Frage, ob die in den CT-Angiographien sichtbare vaskuläre Versorgung des bzw. der geplanten knöchernen Fibulasegmente und der optional anhängenden septo-kutanen Hautinsel Rückschlüsse auf den Lappenerfolg erlaubt. Im Rahmen dessen wurde zudem die Methode *Cinematic Volume Rendering* eingeführt. Auf der Basis von kontrastierten CT-Untersuchungen bzw. CT-Angiographien erlaubt dieses postprozedurale Bildverarbeitungsverfahren einen intuitiven plastischen Eindruck der anatomischen Strukturen.

3. Eigene Arbeiten

3.1. <u>Originalarbeit 1:</u> Partial and Total Flap Failure after Fibula Free Flap in Head and Neck Reconstructive Surgery: Retrospective Analysis of 180 Flaps over 19 Years.

Knitschke, M.; Sonnabend, S.; Bäcker, C.; Schmermund, D.; Böttger, S.; Howaldt, H.-P.; Attia, S. Partial and Total Flap Failure after Fibula Free Flap in Head and Neck Reconstructive Surgery: Retrospective Analysis of 180 Flaps over 19 Years. Cancers **2021**, 13, 865.
https://doi.org/10.3390/cancers1304086 **IF: 6,639**

<u>Zusammenfassung:</u>

Das freie, mikrovaskuläre Fibulatransplantat ist in der rekonstruktiven Kopf- und Halschirurgie weit verbreitet und wird bevorzugt zur Kieferrekonstruktion eingesetzt. Die meisten Daten über das Fibulatransplantat in der MKG-Chirurgie sind auf kleine Stichprobengrößen und kurze Nachbeobachtungszeiträume beschränkt. Die monozentrische, retrospektive Studie untersuchte insgesamt 180 Fälle über einen Zeitraum von 19 Jahren (Januar 2002 bis Juni 2020). Es erfolgte die Zuordnung in die beiden Hauptgruppen partielle (*PFF*) und vollständige Lappenverluste (*TFF*: 11,1 %). PFF trat in *n* = 16 (8,9 %) und *TFF* in *n* = 20 (11,1 %) Fällen auf. Die Gruppe der PFF setzte sich aus Teilverlusten der Hautinsel (*n* = 11), dem Verlust einzelner Transplantatsegmente (*n* = 4) sowie einer Kombination beider Komponenten (*n* = 1) zusammen.
Statistisch signifikante Unterschiede konnten in Bezug auf Patientenalter, Geschlecht, BMI, ASA-Klasse, Planungs- und Rekonstruktionsverfahren (Non-VSP vs. VSP) und Zeitpunkt der Rekonstruktion (ein- vs. zweizeitig) nicht ermittelt werden. Die verlängerte Dauer des Krankenhausaufenthalts der Gruppe *TFF* unterschied sich auf signifikantem Niveau von der *PFF*-Gruppe ($p = 0{,}038$). Es bestanden jedoch keine wegweisenden Unterschiede hinsichtlich der Operationszeit und der Dauer des Aufenthalts auf der Intensivstation.

Partielles Lappenversagen (*PFF*) scheint in der Literatur unterrepräsentiert zu sein. Ein teilweises oder vollständiges Versagen der Hautinsel führt zu klinischen

Beschwerden wie freiliegenden Knochensegmenten und Plattenexposition. Teilweise oder vollständige Transplantatverluste erhöhen die Morbidität durch die Notwendigkeit weiterer chirurgischer Eingriffe z.B. zur Entfernung des transplantierten Knochens und ggf. auch Einbringung neuer, zumeist Weichgewebstransplantate und können den Beginn adjuvanter Maßnahmen verzögern. *PFF* von Fibulasegmenten kann durch Strahlentherapie induziert werden. Abschließend kann festgestellt werden, dass *PFF* der Hautinsel in der Non-VSP und Fibulasegmentverluste in der VSP Gruppe dominierten.

Ausblick:

Die Ergebnisse der langjährigen monozentrischen, retrospektiven Untersuchung sind eine Stellungnahme zum Lappenerfolg und zu Teil- und Totalverlustraten, die durch eine sorgfältige Patientenselektion und einen Zwei-Team-Ansatz zur Verkürzung der Operationszeit erreicht wurden. Die Beobachtung, dass (sub-)totale Verluste der septo-kutanen Hautinsel in der überwiegenden Zahl der Fälle in der Non-VSP Gruppe auftraten, wirft die Frage auf, inwiefern durch eine Schablone das Trauma für das anhängende Weichgewebe kontrolliert und minimiert werden kann. Andererseits traten Knochensegmentverluste zum überwiegenden Teil in der VSP-Gruppe auf, was Fragen bzgl. Segmentgröße, Präparationstrauma und Folgen einer adjuvanten Strahlentherapie aufwirft.

cancers

MDPI

Article

Partial and Total Flap Failure after Fibula Free Flap in Head and Neck Reconstructive Surgery: Retrospective Analysis of 180 Flaps over 19 Years

Michael Knitschke *, Sophia Sonnabend, Christina Bäcker, Daniel Schmermund, Sebastian Böttger, Hans-Peter Howaldt and Sameh Attia

Department of Oral and Maxillofacial Surgery, Justus-Liebig-University, Klinikstrasse 33, 35392 Giessen, Germany; Sophia.M.Sonnabend@dentist.med.uni-giessen.de (S.S.); Christina.Baecker-2@dentist.med.uni-giessen.de (C.B.); Daniel.Schmermund@uniklinikum-giessen.de (D.S.); Sebastian.Boettger@uniklinikum-giessen.de (S.B.); HP.Howaldt@uniklinikum-giessen.de (H.-P.H.); Sameh.Attia@dentist.med.uni-giessen.de (S.A.)

* Correspondence: Michael.Knitschke@uniklinikum-giessen.de

Simple Summary: Most data concerning fibula free flaps after cancer resection in the head and neck region are limited to small sample sizes and a short period of follow-up. This retrospective study aims to evaluate the flap success, failure, and complications at the recipient site in 180 cases over 19 years. The flap failure is classified as partial and total flap necrosis. A correlation between flap failure and patients' medical status, age, sex, BMI, ASA-Score, planning type, and reconstruction time point was performed. Our findings help head and neck surgeons understand the factors that influence flap failure and assess risk factors. Our observations could optimize the treatment of cancer patients receiving a fibula free flap in the future.

Abstract: Fibula free flap (FFF) is widely used in head and neck reconstructive surgery and is considered as a standard and therapy of choice after ablative cancer surgery. The aim of this retrospective monocenter study was to determine the success rates of fibula free flaps for jaw reconstruction after ablative tumor surgery. The disease course of patients who underwent jaw reconstructive surgery with FFF from January 2002 to June 2020 was evaluated regarding the flap success rate. Flap failure was analyzed in detail and categorized into two groups: partial flap failure (PFF) and total flap failure (TFF). A total of 180 free fibular flaps were performed over the last 19 years and a total of 36 flap failures were recorded. TFF occurred in n = 20 (56.6%) and PFF in n = 16 cases (44.4%) cases. No statistically significant differences were found concerning patients' age at flap transfer, sex, BMI, ASA-Score, preoperative non-virtual or virtual surgical planning (non-VSP vs. VSP), and time of reconstruction (immediately vs. delayed). Duration of hospitalization shows statistically significant differences between both groups (p = 0.038), but no differences concerning operating time and duration on Intensive Care Unit (ICU). Partial flap failure appears to be underreported in literature. Sub- and complete failure of the skin paddle leads to clinical complaints like uncovered bone segments and plate exposure. Partial or complete FFF failure lead to infections on the recipient site and prolonged wound healing and therefore may cause a delay of the beginning of adjuvant radiation therapy (RT). PFF of hard tissue can be induced by RT.

Keywords: fibula free flap; head and neck cancer; reconstructive surgery; FFF success rate; FFF failure rate

Citation: Knitschke, M.; Sonnabend, S.; Bäcker, C.; Schmermund, D.; Böttger, S.; Howaldt, H.-P.; Attia, S. Partial and Total Flap Failure after Fibula Free Flap in Head and Neck Reconstructive Surgery: Retrospective Analysis of 180 Flaps over 19 Years. *Cancers* **2021**, *13*, 865. https://doi.org/10.3390/cancers13040865

Academic Editor: Sven Otto

Received: 19 January 2021
Accepted: 16 February 2021
Published: 18 February 2021

1. Introduction

Since the first mandibular reconstruction with a fibula free flap (FFF) by Hidalgo in 1989, it has been shown that FFF is a reliable and versatile graft [1,2]. Currently, FFF is considered as standard therapy in head and neck reconstructive surgery, providing

the optimal precondition for dental implant success and therefore for oral and dental rehabilitation [3,4]. Long-term complications on the donor-site are relatively low. Most patients have been satisfied with the functional and aesthetic results [5,6]. The number of free tissue transfers of soft and/or bone tissue defects have increased significantly in recent years [7]. The flap provides the opportunity to include a septo-cutaneous skin paddle of up to 200 cm^2. Cadaver studies investigating skin perfusion through selective injection have shown that a skin area of 12 × 7 cm can be perfused by a single perforating vessel [8]. A recent milestone in operative techniques is the possibility of computer-assisted surgery (CAS) and virtual surgical planning (VSP) in reconstructions of jaws [9–11]. VSP initially focused on bone grafts. The innovative potential lies in the design of a cutting guide that takes into account the course of the cutaneous perforating vessels based on preoperative CT and sonographic measurements [12,13]. For skin paddle harvesting, the support of perforator vessels is crucial. Fibular flaps have been reported to allow a success rate of up to 95% [7,14–16]. The causes of flap failure are anastomosis insufficiency, more frequent venous congestion (e.g., edema, hematoma), rare arterial occlusion (e.g., embolism, thrombus, kinking), vasospasms, postoperative bleeding, and coagulopathies [17–20].

However, detailed data about partial FFF loss are rare and seem to be underreported in literature. An analysis of risk factors for flap failure and complications in a low-level center of 129 FFFs over a time span of 20 years reported a PFF rate of 7.8%. By definition, (sub-)total flap loss describes the failure of the skin paddle and/or the loss of one or more bone graft segments in poly-segmental reconstructions [21]. The data published to date lack a differentiation concerning soft and/or hard tissue loss. A comparative investigation on computer-assisted versus conventional FFF technique for craniofacial reconstruction found six skin paddle and two segmental graft failures, which corresponded to a PFF rate of 11.76% (n = 8 out of 68) and a TFF rate of 4.41% (n = 3) [22]. Comparative results of partial loss were reported with a range of 3–14% [16,23]. This should be considered when the often-described advantage of the skin paddle as a vital monitor is advocated [24,25]. Gennaro et al. mentioned that a thin muscle cuff around bone, e.g., the fibula or vascularized iliac crest bone flap, is needed for flap harvesting. In these cases, a direct clinical assessment even without the use of a Doppler probe is advisable [26]. However, if PFF or TFF occurs, therapeutic options and decisions must be made to reduce local infection, functional impairment, and increase the patient's quality of life. In this study, we have assessed and discussed the therapeutic options in the setting of TFF.

The aims of this study are:

1. to estimate the rate of partial flap loss ((sub-)total loss of skin paddle and/or failure of graft segments) and total flap failure over a long time period of 19 years, and to suggest further therapy procedures according to localization and defect type;
2. to examine a correlation between age at flap transfer, BMI, ASA-Score, and risk factors in terms of partial and total flap failure; and
3. to investigate whether there is a correlation between non-VSP vs. VSP and time of reconstruction (immediate vs. delayed).

2. Materials and Methods

2.1. Study Design and Patient Population

The study was conducted as a monocentric, retrospective study. Medical records of all patients who underwent FFF in the head and neck region from January 2002 to June 2020 were analyzed in respect of success of the flap transfer procedure. Flap failure was stratified into two groups: partial flap failure (PFF) and total flap failure (TFF) (Figure 1). PFF was defined as any loss of parts of the skin paddle (Skin) (Figure 2), parts or segments (poly-segmental reconstruction) of bone grafts (Bone) (Figure 3), or a combination of both (Both). The major characteristic of PFF is the remaining blood supply by the vascular pedicle. In contrast to PFF, TFF is characterized by discontinued perfusion of the graft (i.e., thrombosis). Intra- or extraoral wound dehiscences around the skin paddle alone did not match the criteria for PFF and were not included.

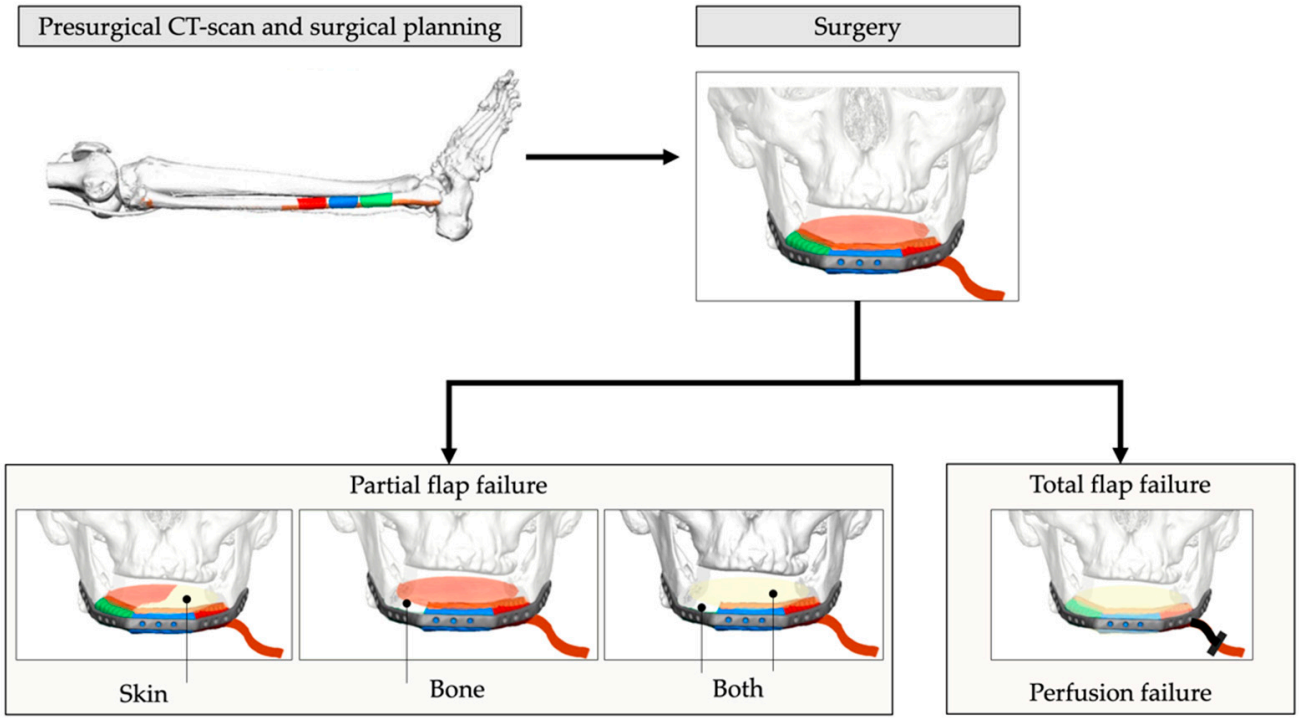

Figure 1. Schematic illustration of reconstructive workflow and stratification in partial and total flap failure groups. The major characteristic of PFF is the remaining blood supply by the vascular pedicle. In contrast to this, TFF is characterized by interrupted graft perfusion.

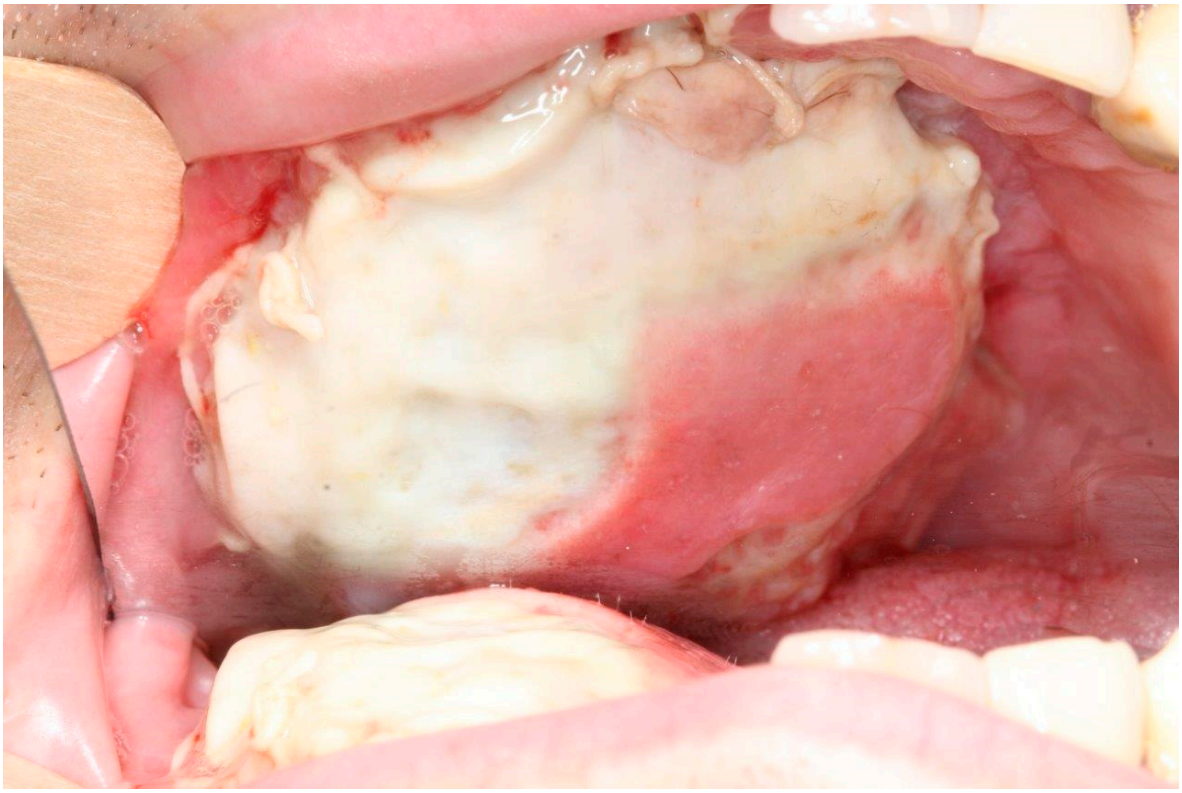

Figure 2. Example of 'PFF skin' after maxilla reconstruction.

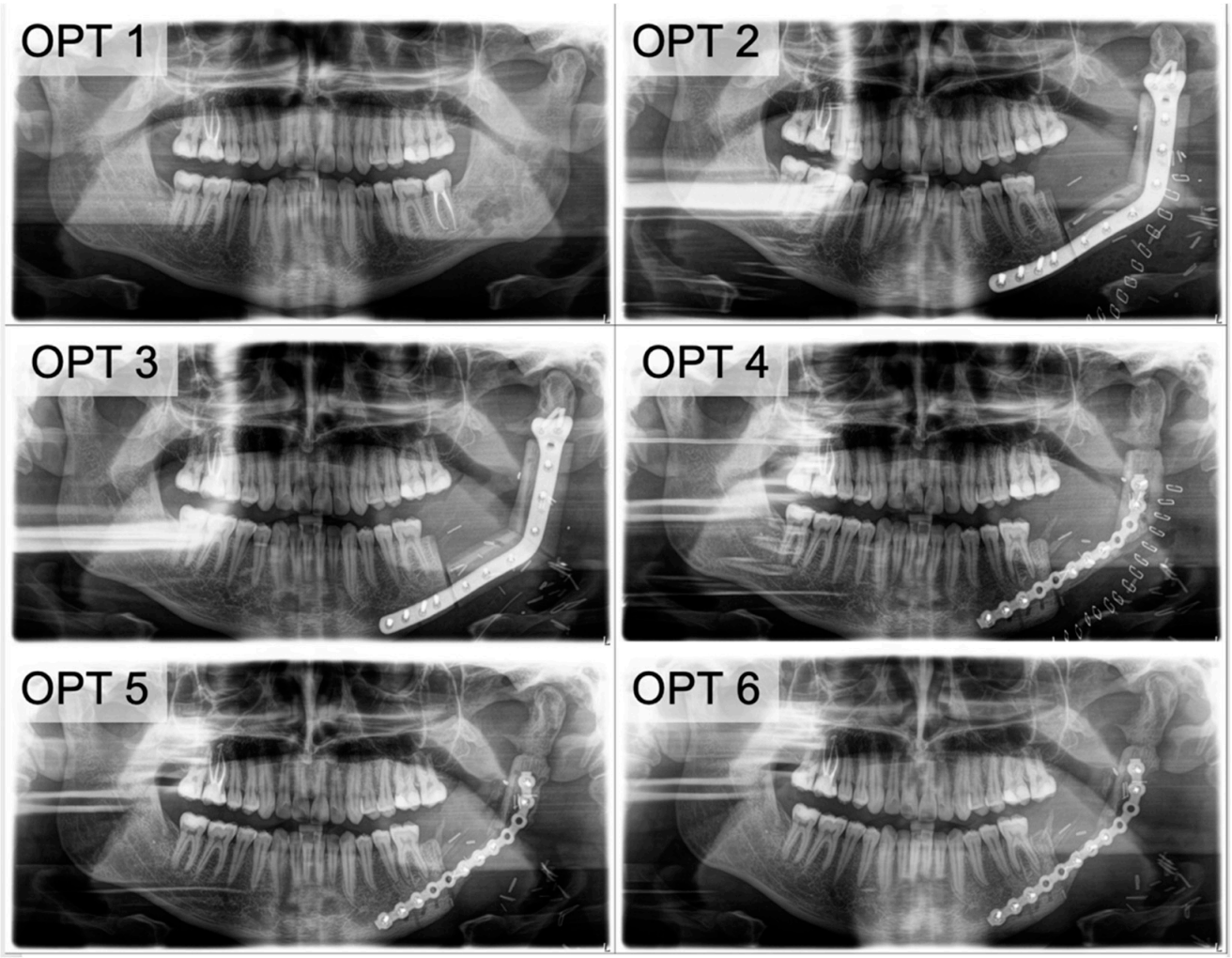

Figure 3. The clinical course of PFF. (**OPT 1**) Due to the recurrence of an ossifying fibroma (odontogenic tumor) in the ramus ascendens mandibulae in a 22-year-old patient, (**OPT 2**) a continuity resection and simultaneous reconstruction with a bi-segmental fibula and CAD/CAM plate was planned. (**OPT 3**) The clinical submandibular fistula had a connection to the plate (Figure 4A). (**OPT 4**) An OPT image was obtained after removal of the avital fibular segments and re-stabilization of the remaining graft. There is initial evidence of incipient bone healing on the proximal resection-site. (**OPT 5**) Follow-up visit at 9 weeks after re-stabilization. In the condylar segment, bone healing is pictured, and at the distal segment, progressive resorption is visible. (**OPT 6**) Progressive bone healing and callus formation originating from the resection site is visible 19 weeks after re-stabilization.

All patients underwent a preoperative CT or MRI angiography to ensure the presence of a three fibular vessel anatomy and the absence of significant arteriosclerotic changes in the lower leg. Free fibula flap dissection was performed by Gilbert's lateral approach [27]. To preserve knee and ankle stability, respectively, a bone length of 8 cm proximal to the harvest site and a distal bone length of 6–8 cm of distal to the harvest site were left in situ. When an osseo-cutaneous free flap was harvested, a muscle cuff with parts of soleus and flexor hallucis longus muscle was included to protect the perforators. Before donor-site wounds were closed, a vacuum drainage (Redon) was installed. Wound closure at the lower limb was performed using a split skin graft over the harvested skin flap or primarily in all cases of sole bone flaps without skin paddles.

Examples for the clinical course of a subtotal bone graft loss (PFF) were illustrated in Figures 3–5 and an example of TFF is demonstrated in Figure 6.

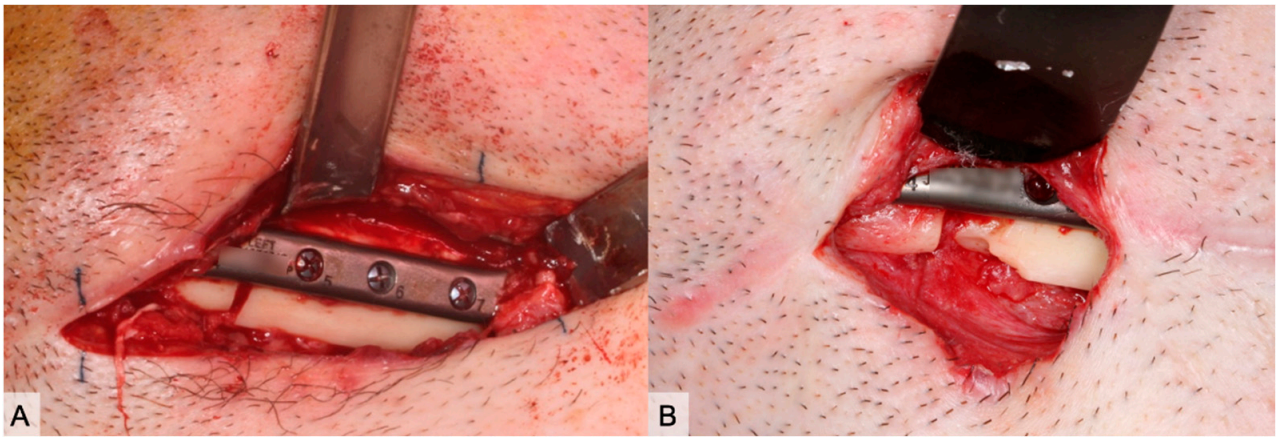

Figure 4. (**A**) Clinical aspect 4 weeks after reconstruction. After reopening the submandibular approach and excision of the skin fistula, there was no evidence of screw loosening. Temporary unscrewing of the screw (No. 5) leads to bleeding. (**B**) With a new fistula, the site was reentered 8 weeks after surgery and the screw was removed again. There was no clear bleeding from the screw hole. In addition, the anterior-caudal edge of the bone was removed.

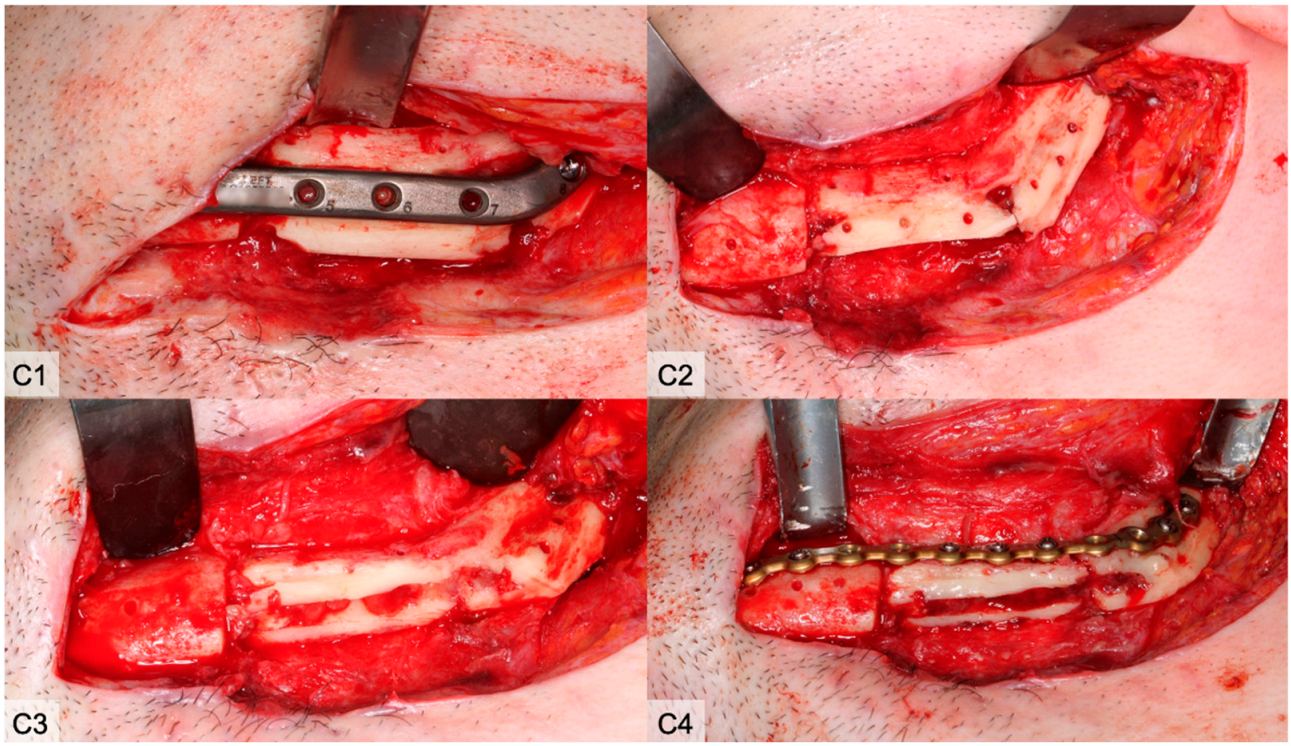

Figure 5. (**C1**) The CAD/CAM plate was removed 14 weeks after surgery when the fistula was productive again. (**C1**–**C3**) A sharp demarcation line caudal to the crestal edge of the plate became visible and was conspicuous. (**C2**) Between the fibula segments, an incipient ossification of the gap was observed. The underlying bone was pale. (**C3**) The bone was removed caudally. The bone marrow was replaced by granulation tissue and was removed. (**C4**) The intersegmental ossification was not yet sufficient so that stabilization again was necessary.

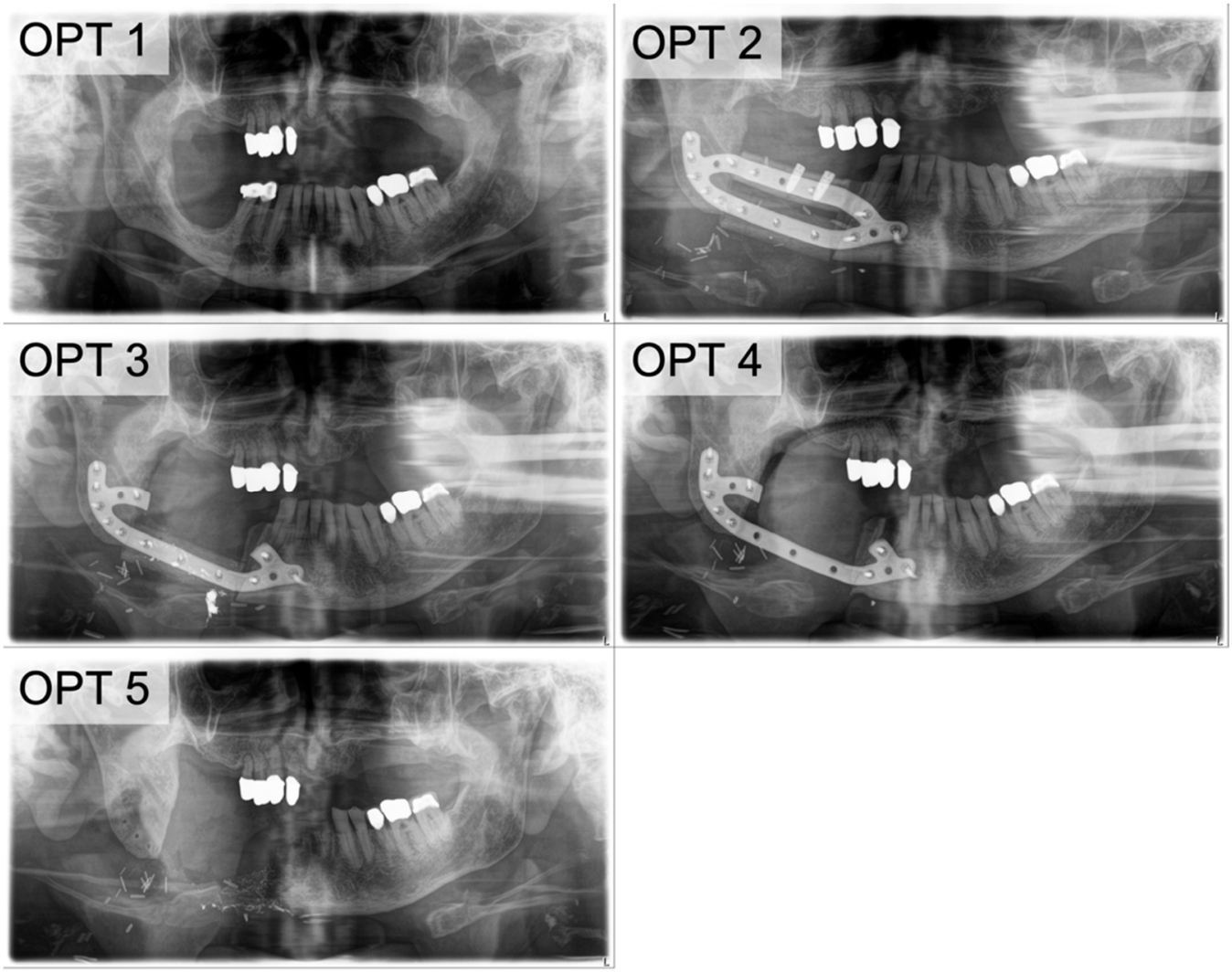

Figure 6. The following OPTs outline the clinical course of TFF in a 76-year-old patient in good general condition who suffered from osseous metastasis of prostate cancer and underwent FFF. (**OPT 1**) A pathologic fracture occurred after the removal of necrotic bone in the right lower jaw in the setting of bisphosphonate induced MRONJ stage III (treatment with Zoledronacid/Denosumab in prostate cancer) [28]. (**OPT 2**) Virtual planning of double-barrel fibula was performed. CAD/CAM plate was used for stabilization and the simultaneous insertion of two dental implants was performed. (**OPT 3**) At 3 weeks post-surgery, the skin paddle was lost. A surgical exploration ended with the removal of an avital distal graft segment and modification of the plate in situ. The vascular pedicle of the remaining FFF still rendered a clear signal in the Doppler ultrasonic probe. (**OPT 4**) At 16 weeks after surgery, the remaining graft segment also had to be removed in the setting of continued inflammation and the absence of a Doppler signal. (**OPT 5**) At 22 weeks after surgery: The screws loosened in the anterior mandible segment so that the remaining plate with teeth 32–42 and a bone sequester had to be taken out.

2.2. Study Parameters and Evaluator Calibration

The following parameters were collected: Patient age at the time of flap transfer, sex, primary diagnosis, planning procedure, location, type of defect classified according to Brown et al. [29,30], number of fibula segments, reconstruction time (immediately vs. delayed), flap condition, part of flap loss, and reason for flap loss. Patients' medical records were analyzed independently for flap outcomes.

2.3. Inclusion and Exclusion Criteria for Study Subjects

In this study, we enrolled all patients who underwent a reconstruction of the maxilla or mandible (immediately or delayed) with a FFF. Only cases with incomplete data sets and/or medical records were excluded (n = 2).

2.4. Statistical Analyses

Fischer test and Freeman–Halton extension [31] were used to compare flap outcome with sex, ASA-Score, alcohol and tobacco abuse, time and method of reconstruction, and the number of fibular bone segments. Students t-test was performed to compare the mean age at FFF-transfer, operating time, duration in the ICU, and time of hospitalization between the three flap outcome groups after verification of normality. $p < 0.05$ was defined as statistically significant. The statistical analysis was carried out with SPSS 25 (SPSS Inc., Chicago, IL, USA).

2.5. Ethics Statement/Confirmation of Patients' Permission

The study was approved by the local Ethics Committee of the Justus-Liebig University Giessen (AZ35/20) and patients' consent was not necessary for this retrospective study. The patients consented that their intraoral pictures and X-ray images may be used anonymously in the publication. All data in the Microsoft Excel spreadsheet were pseudonymized.

3. Results

A total of 180 fibula free flaps (FFF) were performed over a period from January 2002 to June 2020. Complete flap success was recorded in 144 cases (80.0%). The remaining 36 flap failures were categorized into the two major groups partial (PFF) and total flap failure (TFF). PFF occurred in n = 16 (44.4%) and TFF in n = 20 (56.6%) cases (Table 1). No statistically significant difference concerning the age at flap transfer, sex, time, and method of reconstruction was apparent. Furthermore, no significant differences were detected in relation to surgical parameters (neck dissection, tracheostomy, radiation therapy) and general risk factors (alcohol and tobacco abuse). There is a significant difference concerning the duration of hospitalization between the groups PFF (mean 22.6 $\pm$ 9.7 days) and TFF (mean 33.8 $\pm$ 18.8 days) (p = 0.038). No statistically significant differences concerning operating time and duration in the ICU between PFF and TFF were detected.

While TFF occurred in a median 8.5 days, PFF was clinically incident later. All TFF were an early complication. Out of 20 TFF (100%), four arterial and four venous thrombosis were found during anastomosis revision. The aetiology of the flap failure of the remaining 12 cases (60%) are unknown. PFF of the skin paddle (n = 11) was observed in a median time of 22.5 days and therefore considered as a late complication. The onset of PFF of bone segments without skin paddles (n = 4) was detected much later at a median time of 101.5 days.

PFF was analyzed in detail. After maxillary reconstruction, two partial and three total flap failures were found in the investigation. This corresponds to 13.5% (n = 5) of the study collective. Two cases of PFF of the skin paddle was found after maxilla reconstructions (Brown Class II and III) with uni-segmental fibular, and three TFF were observed in uni- (n = 2) and bi-segmental reconstruction (n = 1).

In mandible reconstruction, PFF was observed in 87.5% of cases. A total number of 14 partial flap failures—nine losses of the skin paddle, four isolated bone graft losses, and one combination of both—were found in mandible reconstructions after tumor recurrence (Table 2). Out of 11 skin paddle losses (PFF), 81.81% (n = 9) occurred in the conventional non-VSP group.

Table 1. Clinical details of partial (PFF; n = 16) and total flap failures (TFF; n = 20) after jaw reconstruction with fibular free flaps.

N = 36	**PFF N = 16 (44.4%)**	**TFF N = 20 (56.6%)**	***p*-Value**
Age (years), SD	59.9 ± 14.4	62.5 ± 9.5	$p = 0.520$
Follow-up (months), SD	48 ± 42.9	31.5 ± 31.6	$p = 0.193$
Type of flap loss			
PFF, Skin paddle	11		
PFF, Bone segment	4		
PFF, Both	1		
Total flap loss (TFF)		20	
Sex			
Female	5	6	$p = 0.609$
Male	11	14	
Diagnosis			
Benign tumor	1		
Malignant tumor	15	15	
MRONJ		2	
ORN		3	
Reconstruction			
Immediate	14	17	$p = 0.610$
Delayed	2	3	
Reconstruction			
Non-VSP	10	10	$p = 0.341$
VSP	6	10	
Neck dissection			
Unilateral	11	13	n.s.
Bilateral	3	3	
None	2	4	
Tracheostomy			
None	6	8	n.s.
Primary	9	11	
Secondary	1	1	
Irradiation			
Preoperative	1	3	n.s.
Postoperative	8	4	
None	7	13	
Risk factors			
Alcohol abuse	5	9	$p = 0.348$
Tobacco abuse	9	13	$p = 0.546$
Operating time (min)	546.2 ± 94.9	524.4 ± 97.2	$p = 0.504$
Duration ICU (days)	2 ± 1.3	2.1 ± 1.7	$p = 0.847$
Hospitalization (days)	22.6 ± 9.7	33.8 ± 18.8	$p = 0.038$
BMI			
≤18		1	
18 ≤ 25	9	9	
25 ≤ 30	3	7	
30 ≤ 35	4	2	
>35		1	
ASA-Score			
ASA 2	10	7	
ASA 3	6	12	
ASA 4		1	

n.s. = not significant; ORN, Osteoradionecrosis; MRONJ, Medication-related osteonecrosis of the jaw; VSP, virtual surgical planning; BMI, Body mass index; SD, standard deviation.

Table 2. Table depicting the locations according to the classification by Brown et al. where PFF (n=16) and TFF (n=20) occurred [29,30].

Type of Defect	PFF Skin (*n* = 11)	PFF Bone (*n* = 4)	PFF Both (*n* = 1)	TFF (*n* = 20)
Maxilla				
II	1	-	-	2
III	1	-	-	1
Mandible				
I	4	-	1	7
Ic	-	-	-	1
II	2	2	-	6
IIc	-	1	-	-
III	3	1	-	2
IV	-	-	-	1

TFF was observed mostly in Brown class I (*n* = 7) and II (*n* = 6) defects. Subtotal loss of the skin paddle was incident in 68.7% of cases (*n* = 11 out of 16). Isolated loss of fibular bone segments was found in 25.0% (*n* = 4) and a combination of both was reported in only one case (6.3%). PFF was found in 50.0% (8 out of 16 cases) of uni-segmental, 25.0% (*n* = 4) of bi-segmental, and 25.0% (*n* = 4) of tri-segmental jaw reconstructions. A total flap loss occurred in 55.0% of cases after bi-segmental and in 40.0% of cases after uni-segmental reconstructions (Figure 7). There was a non-significant trend towards TFF in poly-segmental reconstructions ($p = 0.114$).

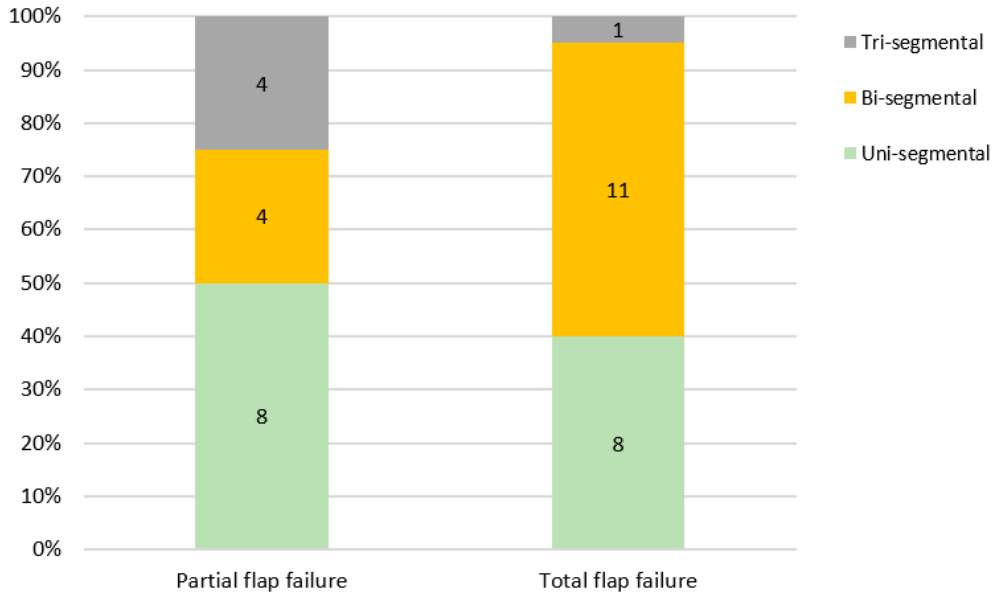

Figure 7. Partial or total flap failure in relation to the number of fibula segments ($p = 0.114$).

A total loss of the skin paddle (*n* = 11) was observed at a mean of 27 days (median 22 days, range 2–67 days) and an isolated loss of bone graft segments at 181 days (*n* = 4; median: 101.5 days, range 37–499 days) post surgery. Kaplan–Meier survival function was calculated and visualizes the different periods of partial soft and hard tissue failure (Figure 8).

In comparison to the beginning of radiation therapy in the complete success group (*n* = 40, mean 52.9 days, median 49 days, range 21–98 days), PFF of the skin paddle generates a delay (Figure 9). Radiation therapy started at a mean of 63.5 days (*n* = 4, median 50.5 days, range 39–114 days). The difference remains without any statistical significance ($p = 0.358$).

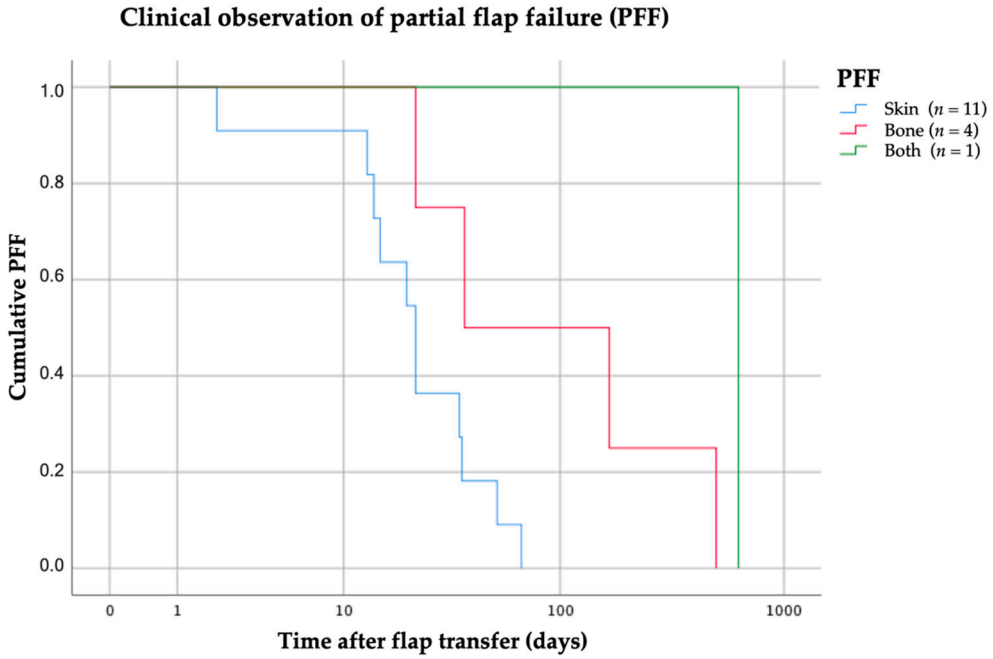

Figure 8. Kaplan–Meier function was drawn for the three sub-groups of PFF. The abscissa axis "time" (days) is drawn on a logarithmic scale.

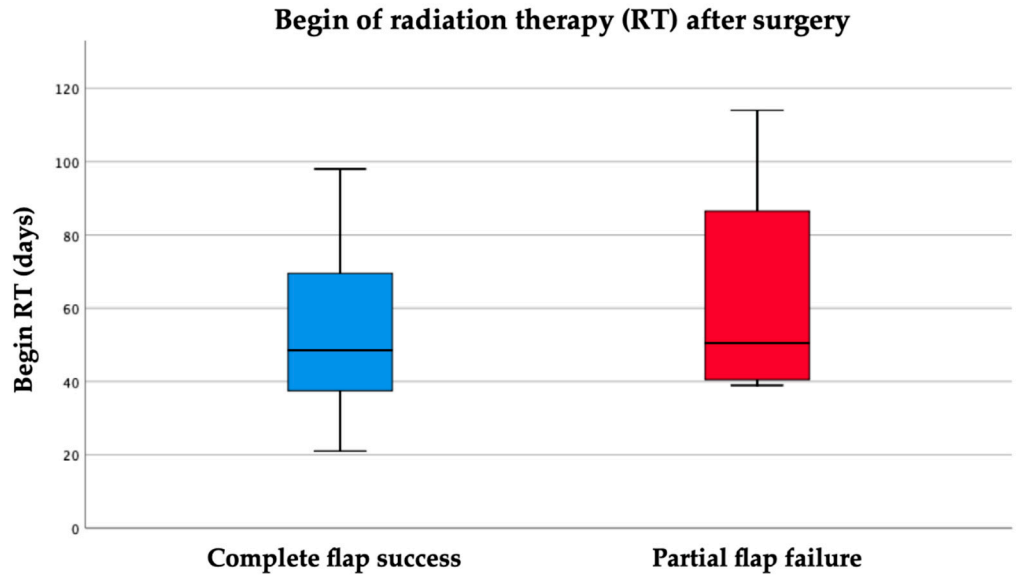

Figure 9. Comparison of the onset of adjuvant radiation therapy between the groups of complete flap success (n = 40) and PFF skin (n = 4).

Clinical flap necrosis and time of bone graft removal were compared with the number of bone segments used. Statistical analysis showed no significant differences between the uni- and bi-segmental graft losses. Overall, clinical flap loss was observed at a mean of 12 days after surgery (Median 8.5 days, range 0–40 days) and surgical removal of the avital grafts at a mean of 86.4 postoperative days (Median 22.5 days, range 2–503 days) (Figure 10).

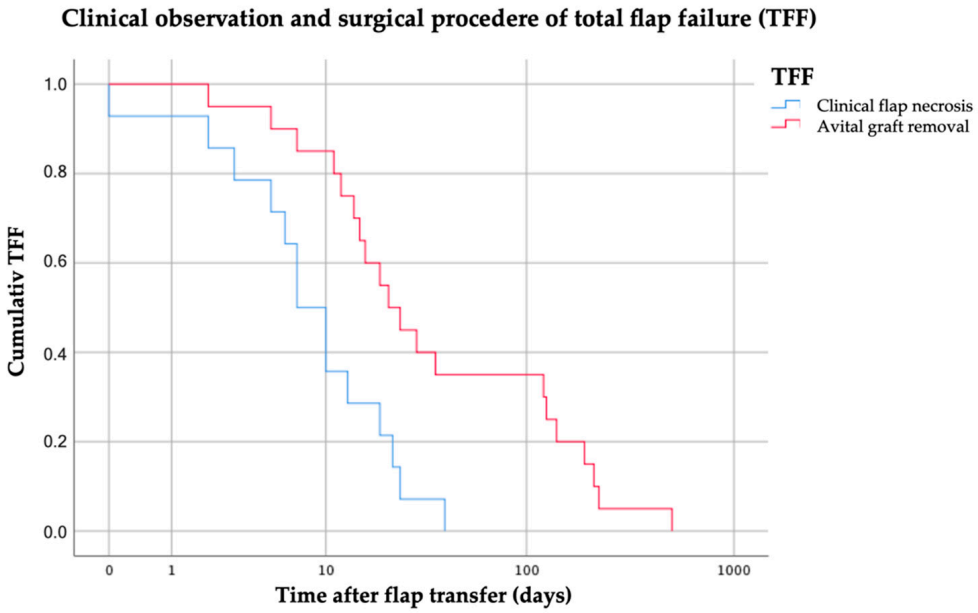

Figure 10. TFF concerning the first clinical signs of flap necrosis and time of removal of the avital graft was visualized by Kaplan–Meier function. The abscissa axis "time" (days) is drawn on a logarithmic scale.

Comparing TFF after maxillary and mandibular reconstruction, it is noticeable that maxillary TFF cases were a mean of 73.3 years old, and thus older than mandibular TFF cases (62.5 years). Therefore, with unequal variance, there is a statistically highly significant difference, which can be explained by the composition of the collective ($p < 0.001$). Regarding the first clinical sign of impending TFF, signs of TFF were documented after 3.3 days in the upper jaw and after 14.4 days in the lower jaw (Table 3). This observation is statistically significant ($p = 0.007$). Concerning further surgical procedure and removal of the necrotic graft, no statistically significant difference between maxilla and mandible was observed (Figure 11).

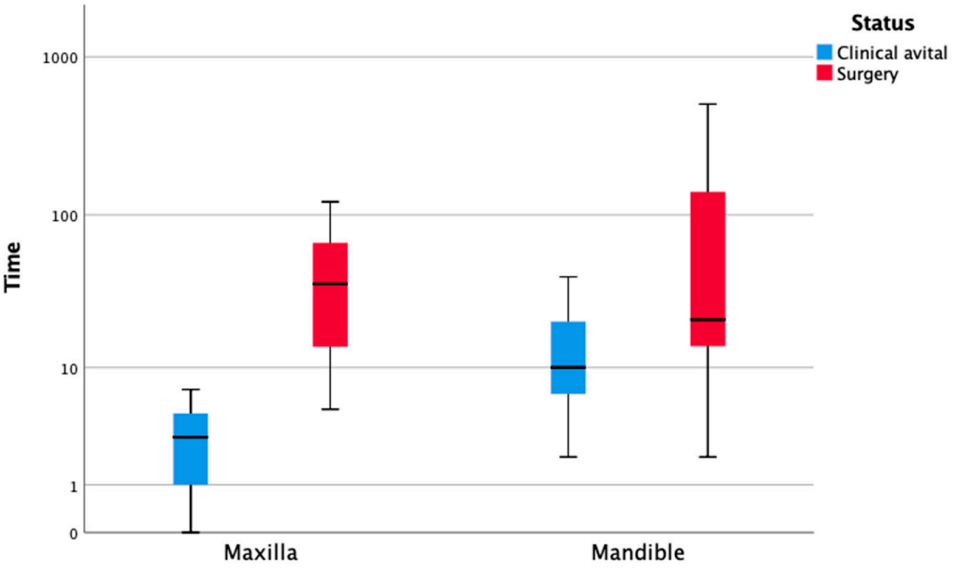

Figure 11. TFF analysis. Clinically diagnosed flap necrosis and further surgical interventions (removal of graft) are shown according to jaw location (maxilla or mandible) in the postoperative time course. The ordinate axis "time" (days) is drawn on a logarithmic scale.

Table 3. Clinical details of total flap failures (n = 20).

N = 20	Maxilla (n = 3)	Mandible (n = 17)	Overall (n = 20)	p
Age (years), SD	73.3 ± 1.8	60.6 ± 8.9	62.5 ± 9.5	$p = 0.001$ ^
Follow-up (months), SD	10.3 ± 9.7	35.2 ± 32.8	31 ± 31.6	
The earliest sign of flap dysfunction (days)	3. 3 ± 3.5 (Median 3)	14.4 ± 11.1 (Median 10)	12 ± 10.9 (Median 8.5)	$p = 0.007$ ^
Surgical validation and avital flap treatment procedure (days)	54 ± 60.1 (Median 36)	92.1 ± 132.0 (Median 21)	86.5 ± 123.6 (Median 22.5)	$p = 0.449$ ^
Anastomosis revisions	2	6	8	
Arterial thrombosis ‡	2	2	4	
Venous thrombosis ‡	-	4	4	n.s
Unknown	1	11	12	
Explantation of bone graft	2	16	18	
Osteosynthesis (PSI) removal	1	11	12	
Re-osteosynthesis	-	3	3	
Second flap	1	8	9	
Temporalis muscle flap	1	1	2	
Deltopectoral flap	-	1	1	
Pectoralis major flap	-	2	2	
RFF	-	1	1	
FFF	-	2	2	
Hip graft (non-DCIA)	-	1	1	

‡ Kind of thrombosis was evaluated during microsurgical revision. (n.s. = not significant; ^ Equal variances not assumed; DCIA, deep circumflexia iliac artery; PSI, patient-specific implant; SD, standard deviation; RFF, radial forearm flap).

4. Discussion

4.1. Rate of PFF and TFF

Thrombosis, kinking, and spasm of the vessels have been reported as common causes of total free-flap failure in the early phase after microvascular anastomosis [32]. Venous thrombosis is more common than arterial thrombosis due to the low-flow and low-pressure venous system. Unrecognized venous thrombosis can lead to backward perfusion failure up to total stasis in the arterial system. This is followed by flap ischemia, no-reflow, and subsequent flap loss [33,34]. Fibular flaps are reported with success rates of up to 95.0% [7,14–16]. Study findings have shown a cumulative success rate of 88.9% (80.0% complete success and 8.9% partial flap failure). The total failure rate in the presented study is 11.1% over the last 19 years and over all types of indications for reconstruction, time of reconstruction, and method of planning (Non-VSP vs. VSP). In comparison to the here reported investigations, other reconstructive centers report total fibular flap failure rates of up to 12.4% (Table 4). Comparability of the results must be ensured concerning the chosen definition of flap success and PFF/TFF. In the presented study, strict criteria for PFF and TFF was defined. Only clear definitions will engage the collection of comparable data. Retrospective study design without standardization is often of poor data quality due to incomplete follow up data and different investigators. However, data collection over 19 years by a single investigator appears to be impractical. Loss and removal of the whole graft are clear parameters for TFF. From the clinical course and as a result of perfusion disorder through its vascular pedicle, TFF is an early flap failure. Therefore, minor, insufficient perfusion of flap elements leads to malnutrition, and thus to consecutive (sub-)total loss of skin paddle and/or bone segments. This was defined as PFF. PFF therefore does include the functional use of the flap and appears as a late flap failure. Most published data lack a differentiation between soft and hard tissue loss. Partial flap failure was reported with an incidence of 3–14% but has not been further differentiated in most cases (Table 4).

Table 4. Overview of FFF total and partial flap failure rates in the literature.

Authors	Investigation Period	*n*	Total Flap Failure	Partial Flap Failure
This study	2002–2020	180	11.1%	8.9%
Colletti et al. [16]	2002–2010	99	7%	3%
Gallegos-Hernandez et al. [35]	1996–2006	87	16.1%	-
Götze et al. [12]	2013–2015	24	12.5%	8.3%
Lopez-Arcas et al. [36]	1992–2006	117	-	8.5%
Momoh et al. [23]	2005–2009	157	1%	14%
Mücke et al. [37]	2009–2013	76	9.2%	-
Seruya et al. [22]	2003–2012	68	4.41%	11.76%
Shroff et al. [14]	2009–2013	30	6.66%	-
Verhelst et al. [21]	1996–2016	129	12.4%	7.8%

A retrospective single-center study on 129 FFF transfers over the last 20 years found TFF in 12.4% and PFF in 7.8% of cases [21]. An investigation on 20 virtual planned FFF showed that preoperative planning based on preoperative CT-scan allows to include the preoperatively planned skin paddle area [13]. Another clinical trial included preoperatively marked perforator vessels for skin paddle in digital planning and noted a survival rate of 92% (n = 24) in FFF transfer with three total and two partial skin paddle losses [12]. Other investigators observed seven total flap losses and three losses of skin paddle in a total of 99 FFFs [16].

In the present study, there were four losses of fibular bone segments and only two of them occurred after radiation therapy (RT). Loss of the skin paddle occurred in two cases of maxillary reconstruction and in nine cases of uni- and poly-segmental reconstruction of the mandible. After an average time of 27 days (median: 22 days, range 2–67 days), partial loss of the skin paddle was observed whereas partial bone loss occurred after mean 181 days (Median: 101.5 days, range 37–499 days). Swelling and edema are results of ongoing inflammatory processes and wound healing immediately after surgery. A critically reduced perfusion of the septo-cutaneous perforators could be the consequence. Its maximum dimension can be expected 2–3 days after surgery. The unusually late appearance of visible (sub-)total dysfunction of the skin paddle perfusion after more than the median time of 3 weeks should be interpreted with caution and as result of documentation bias. Any influence of RT in this respect can be excluded, since RT always started after PFF was already observed. The onset of adjuvant RT in the group PFF skin was at median 50.5 days (range 39–114 days) after surgery in comparison to the control group comprising complete flap success (n = 40), in which RT began in median 49 days (range 21–98 days) after surgery. A statistically significant difference could not be observed. However, an adjuvant RT for oncologic reasons was not to be delayed by a PFF. The results must be interpreted with caution due to the small number of cases. In the literature, the effect of prior irradiation on partial or complete loss of FFF compared with unirradiated grafts has often been reported to be statistically insignificant [38–42]. The effect of postoperative irradiation on partial flap failure in microvascular head and neck reconstruction has not been well described in literature and indicates that further studies are needed in this area. Verhelst et al. focused on perioperative irradiation but it was not identified as a statistically insignificant risk factor for flap failure [21]. In a study by He et al., 9 of 17 patients were irradiated postoperatively and all grafts sustained [43]. In this study, no cases of PFF were detected during or after RF. Under RT conditions, PFF could be similar to radiogenic oral mucositis, which is associated with an early inflammatory response [44,45]. These factors provide a target for biology-based mucositis-prevention strategies [46,47], and thus for PFF prevention. Further, the option of an additional skin paddle for defect

closure after oncologic resection is without doubt one of the major advantages of the FFF in addition to its clinical and technical function of flap monitoring. On the other site, wound healing disorder of the donor site after skin paddle harvesting appears at a rate of 1.07–31.2% [23,48,49]. In literature, different techniques for closure of the donor site have been described [50]. Focused only on monitor function, the price for an unreliable monitor skin paddle seems to be high and should be critically reflected. Nevertheless, some authors believe that the reliability of the skin paddle for the closure of recipient site defects is insufficient in non-irradiated [51] and especially in irradiated patients [52]. In a retrospective investigation, Thome et al. observed 20% of skin paddle failures (n = 27) and came to a similar conclusion [53]. Other authors found a stable and sufficient vascular supply of the septo-cutaneous skin paddle by the septum intermusculare posterius and perforator vessels around the musculus soleus [54–56]. They emphasize the necessity of a muscle cuff around the posterior septum, which contains vessels that are crucial for skin paddle survival [24].

Partial bone loss may occur more frequently than previously observed and described in the literature as a result of malnutrition. Sufficient neovascularization to allow free-flap survival independent of the vascular pedicle has been reported to occur within 7 to 10 days in myo-cutaneous flaps [57–59]. In contrast, a comparative prospective clinical study measured hemoglobin oxygenation and capillary flow in 50 flaps (25 forearm flaps, 15 osseo-cutaneous fibular flaps, and 10 anterolateral thigh flaps) at 4 and 12 postoperative weeks. The authors found that flap autonomization rates were significantly higher in the lower jaw and non-irradiated defect sites. In addition, fascio-cutaneous flaps were found to be autonomized faster than osseo-myo-cutaneous free flaps. Myo-cutaneous flaps were never found to be autonomized after 4 weeks [60]. Kumar et al. studied blood supply of fascio-septo-cutaneous free flaps several months after surgery and found no significant blood flow through vessels across the flap inset [59]. Mücke et al. found that osseo-myo-cutaneous free flaps are significantly dependent on vascularity of the original anastomoses even 1 year after surgery [60]. According to their data, our findings should be interpreted as an adverse effect of radiation therapy (n = 2) and two "real" partial bone segment failures. The risk to develop osteoradionecrosis is decreased in patients with high body mass indices and on steroid therapy [61] through adequate soft-tissue bulk paired with the high-quality vascularized fibula bone [62]. Data published in the literature show that osteoradionecrosis of the original mandible occurred after a median time of 10.9 months (range 1.8–89.7 months) after RT and 90% occurred within 37.4 months [63]. In contrast, our data show bone loss after a median time of 3.38 months (range 1.23–16.63 months) and more than 6 months earlier. This observation should be interpreted with caution due to the low number of cases and should be further studied in larger study groups.

Early TFF was incident in n = 3 maxillary and n = 17 mandible reconstructions. TFF was found after mandible reconstruction in anterior defects (Classes III-IV, 3 out of 17 cases, 17.6%) and more frequently in lateral defects (Classes I–II, n = 14, 82.4%). Uni- and bi-segmental were commonly used for these Classes I–II reconstructions. Reasons for increased TFF in class I and II were critical pedicle course (inner surface of mandible and mouth floor), kinking of the vascular bundle [64] and length [21,65,66]. In addition to known general risk and complicating factors, further risk factors for flap failure include postoperative swelling and edema, hematoma, movement of the neck, circular tracheal tube fixation loop, and course of the vessel through the neck [33].

The therapeutic procedure for partial skin or isolated bone loss depends on the jaw affected. If PFF of the skin paddle occurs in the maxilla, it is usually an uncritical situation and wound healing from peri-osseous tissue can be expected. When bone loss in the maxilla occurs, a "simple" prosthetic rehabilitation by obturator prosthetic is a therapeutic alternative [67,68] if another microvascular bone graft is not desired. Large defects can be downsized with local tissue advancement. Functional impairment (eg. scars) might be

addressed in a two-staged procedure. Safe flaps routinely used in our department are the temporal myo-fascial [69], pectoralis major [70,71], and deltopectoral flaps [72].

In the mandible, skin paddle loss is often noncritical when the primary bone graft is vital. After wound healing local flaps and staged scars, loosing procedures can be necessary to improve dysfunction such as trismus [73]. Flaps of choice in this situation are often radial forearm [74], pectoralis major [70,71], and deltopectoral flaps [72]. When PFF of bone segments or TFF after mandible reconstructions appear, there are different strategies available that need to be evaluated in light of the patient's condition. If patient's condition is poor and the avital graft showed no signs of inflammation, it was left in the oral cavity (Figure 6). If inflammation and/or loosening of osteosynthesis material occurred around the avital segment, removal is necessary. Sometimes further use of osteosynthesis is possible, especially if patient-specific osteosynthesis was used. However, in the majority of cases, removal of the osteosynthesis will become necessary (Table 3). Re-osteosyntheses could be useful in combination with distant flaps like pectoralis major flaps, deltopectoral flaps, and bone hip grafts. The staged procedure of second attempts microvascular bone graft is possible after critical evaluation. The removal of the avital graft and the anticipation of stable scars building and "functional" pseudarthrosis is a further option (Figure 6).

4.2. Influence of Age at Flap Transfer, BMI, ASA-Score and Risk Factors in Terms of Flap Success in Relation to PFF and TFF

In this study, no significant differences between patients' age at flap transfer and flap outcome were observed. This confirms other investigations that patients' age at flap transfer is not crucial for flap success [75,76]. It is a surrogate parameter for the general condition of the patient [77,78]. A prospective study on 215 patients found that age $\geq$ 70 years had a significantly higher ASA-Score and shorter duration of surgery. Age was a risk factor for longer ICU stay and complication rate. They found no influence of age on the length of hospital stay and overall success of microvascular reconstructions [79]. In this study, more than 92% were rated ASA 2 or 3. All partial flap failures and all but one total flap occurred in both groups. ASA score and duration of the operation were found to be independent risk factors for operative revisions [76]. In literature, ASA-Rating is correlated with a higher number of postoperative complications after microvascular reconstructions [80,81] and the overall survival [82]. We calculated the relation between 'Age at flap transfer' and BMI and found an evenly distributed pattern.

Concerning alcohol and tobacco abuse in the investigated group, no statistically significant differences were found. In published literature, alcohol abuse was identified as a risk factor for postoperative adverse events [82]. Tobacco abuse was shown to reduce overall survival time compared with non- and never-smokers [83,84]. A review by Van Imhoff et al. stated that survival rates are lower and recurrence rates are higher in patients who continued to smoke after having being diagnosed with Head and Neck SCC in comparison to patients who stopped smoking [85].

BMI had no statistically significant influence on flap success in this study. Low BMI or underweight at diagnosis was an independent, unfavorable prognostic factor [86,87]. Obesity was associated with better outcome and was not an independent risk factor for postoperative complications of free tissue transfer [88,89]. Other investigators found that higher BMI/obesity is a risk factor for peri- and postoperative medical complications [90].

The duration of hospitalization was calculated with a mean of 22.6 days in the PFF group and a mean of 33.8 days in the TFF group. Statistically significant differences (p = 0.038) were found in the occurrence of partial or total flap failures (Table 1). While the majority (68.75%, n= 11 out of 16) of all partial flap failures are a dysfunction of the skin paddle failures (mean duration of hospitalization partial flap loss group 20.71 days), we conclude that loss of that skin loss does not result in significantly longer hospital stay than in total flap losses. Stepwise removing of avital flap parts, deperiostizing of the bone graft, and covering with oral mucosa is an attempt for flap salvage. However, the initial stay at the ICU seems to have no statistical influence concerning upcoming PFF or TFF. It was calculated in both groups with a mean of approximately 2.0 days.

No statistically significant difference concerning mean operating time (PFF: meantime 546 min, TFF: meantime 524 min) and flap outcome was found. Surgery time is described as a risk factor for postoperative complications [91–93]. Increased operating time may also be the result of a younger surgeon learning and being taught by an older instructing surgeon. However, operating time should be reduced whenever possible [92]. The study could not include ischemia time in the risk analysis because this parameter was not recorded or was incomplete.

4.3. PFF and TFF in Non-VSP vs. VSP and Reconstruction Methods (Immediate vs. Delayed)

The majority of isolated skin paddle losses occurred in the non-VSP group. Reasons can be seen in mechanical trauma and manipulation during free-hand transplant forming i.e., preparation of bone segments and revised application of osteosynthesis. Individually custom-made cutting guides stabilize and preserve intersegmental connectors for stabilization of several bone segments, which provide a valuable support on the vascular pedicle during transplant preparation and shaping.

No statistically significant differences were found concerning patients' preoperative planning procedure (non-VSP vs. VSP) and time of reconstruction (immediately vs. delayed). The results confirmed the findings of other clinical investigations [94]. A retrospective study of 128 osseous free flaps with a minimum follow-up of 12 months evaluated plate-related complications in patient-specific versus conventional fixation systems. They found more complications with patient-specific plates (e.g., wound healing disorders, plate exposure, fixation failure, and subtotal osseous union) in comparison to conventional reconstruction plates, but the differences were statistically insignificant.

One possible reason for (sub-)total bone loss despite maintained perfusion of the vascular pedicle might be trauma during preparation, segmentation, and shaping of the fibula graft. Preoperatively planned and fabricated saw guides and patient-specific implants ease and accelerate the surgical procedure itself, which should be helpful in avoiding mistakes and facilitating the handling of the fibula graft. More complex shaping and osteotomization of bone segments leads to manipulation of the vascular pedicle during dissection and puts it at risk [22]. Furthermore, the impact of VSP and patient-specific plates in terms of wound healing abnormalities, plate exposure, and subtotal osseous union shows a trend towards increased complication rates compared with non-VSP with hand-bended plates. Plate-related complications were increased with radiotherapy and multi-segment flaps [95].

Further investigations on partial flap loss of osseomyocutaneous FFF are needed.

5. Conclusions

The fibula free flap constitutes a standard therapy for jaw reconstructive surgery. The present results of 180 fibula free flap over a period of 19 years shows a cumulative success rate of 88.9%, which is well comparable with other studies. The findings of our long term monocenter retrospective investigation are a position statement about flap success and partial and total loss rates, which was achieved by careful patient selection and a two team approach to reduce operating time. In partial or total flap failure, no statistically significant correlation was observed between patient age, sex, ASA, BMI, alcohol and tobacco abuse, time, and method of reconstruction (virtual versus non-virtual surgical planning). Total flap failure caused significantly prolonged hospitalization time. Partial flap failure affected mainly the skin paddle. Two-thirds of these cases were found in the non-VSP group and only two cases were observed in the virtual surgical planning group. This could be attributed to protective effects of the cutting-guide template, which possibly decrease the mechanical trauma during surgery.

Author Contributions: Conceptualization, M.K.; methodology, S.S., M.K., C.B.; formal analysis, M.K.; investigation, M.K., and S.S; data curation, M.K. and S.S.; writing—original draft preparation, M.K., S.S., S.A. and S.B.; writing—review and editing, M.K., S.S., S.A., C.B., D.S., H.-P.H. and S.B.; visualization, M.K., D.S., H.-P.H. and S.A.; supervision, M.K., H.-P.H., S.B. and S.A.; project administration, M.K. All authors have read and agreed to the published version of the manuscript.

Funding: This research received no external funding.

Institutional Review Board Statement: The study was conducted according to the guidelines of the Declaration of Helsinki, and approved by the Ethics Committee of Justus-Liebig University Giessen (AZ35/20, approval 25.5.2020).

Informed Consent Statement: Patient consent was waived as the study is a retrospective data analysis.

Data Availability Statement: The data presented in this study are available upon request from the corresponding author.

Acknowledgments: The authors are grateful for the consent of the patient for presented X-rays and clinical images. This publication is part of the second author's dental doctoral thesis (SS).

Conflicts of Interest: The authors declare no conflict of interest.

References

1. Hidalgo, D.A. Fibula free flap: A new method of mandible reconstruction. *Plast. Reconstr. Surg.* **1989**, *84*, 71–79.
2. Zlotolow, I.M.; Huryn, J.M.; Piro, J.D.; Lenchewski, E.; Hidalgo, D.A. Osseointegrated implants and functional prosthetic rehabilitation in microvascular fibula free flap reconstructed mandibles. *Am. J. Surg.* **1992**, *164*, 677–681. [CrossRef]
3. Attia, S.; Wiltfang, J.; Streckbein, P.; Wilbrand, J.-F.; El Khassawna, T.; Mausbach, K.; Howaldt, H.-P.; Schaaf, H. Functional and aesthetic treatment Outcomes after immediate jaw reconstruction using a fibula flap and dental implants. *J. Cranio-Maxillofacial Surg.* **2019**, *47*, 786–791. [CrossRef]
4. Attia, S.; Wiltfang, J.; Pons-Kühnemann, J.; Wilbrand, J.-F.; Streckbein, P.; Kähling, C.; Howaldt, H.-P.; Schaaf, H. Survival of dental implants placed in vascularised fibula free flaps after jaw reconstruction. *J. Cranio Maxillofac. Surg.* **2018**, *46*, 1205–1210. [CrossRef]
5. Attia, S.; Diefenbach, J.; Schmermund, D.; Böttger, S.; Pons-Kühnemann, J.; Scheibelhut, C.; Heiss, C.; Howaldt, H.-P. Donor-Site Morbidity after Fibula Transplantation in Head and Neck Tumor Patients: A Split-Leg Retrospective Study with Focus on Leg Stability and Quality of Life. *Cancers* **2020**, *12*, 2217. [CrossRef]
6. Knitschke, M.; Siu, K.; Bäcker, C.; Attia, S.; Howaldt, H.-P.; Böttger, S. Heterotopic Ossification of the Vascular Pedicle after Maxillofacial Reconstructive Surgery Using Fibular Free Flap: Introducing New Classification and Retrospective Analysis. *J. Clin. Med.* **2020**, *10*, 109. [CrossRef]
7. Kansy, K.; Mueller, A.A.; Mücke, T.; Kopp, J.-B.; Koersgen, F.; Wolff, K.D.; Zeilhofer, H.-F.; Hölzle, F.; Pradel, W.; Schneider, M.; et al. Microsurgical reconstruction of the head and neck—Current concepts of maxillofacial surgery in Europe. *J. Cranio-Maxillofac. Surg.* **2014**, *42*, 1610–1613. [CrossRef]
8. Wolff, K.-D. The supramalleolar flap based on septocutaneous perforators from the peroneal vessels for intraoral soft tissue replacement. *Br. J. Plast. Surg.* **1993**, *46*, 151–155. [CrossRef]
9. Ciocca, L.; Mazzoni, S.; Fantini, M.; Persiani, F.; Marchetti, C.; Scotti, R. CAD/CAM guided secondary mandibular reconstruction of a discontinuity defect after ablative cancer surgery. *J. Cranio Maxillofac. Surg.* **2012**, *40*, 511–515. [CrossRef]
10. Weitz, J.; Bauer, F.; Hapfelmeier, A.; Rohleder, N.; Wolff, K.-D.; Kesting, M. Accuracy of mandibular reconstruction by three-dimensional guided vascularised fibular free flap after segmental mandibulectomy. *Br. J. Oral Maxillofac. Surg.* **2016**, *54*, 506–510. [CrossRef]
11. Cornelius, C.-P.; Smolka, W.; Giessler, G.A.; Wilde, F.; Probst, F.A. Patient-specific reconstruction plates are the missing link in computer-assisted mandibular reconstruction: A showcase for technical description. *J. Cranio Maxillofac. Surg.* **2015**, *43*, 624–629. [CrossRef]
12. Goetze, E.; Kämmerer, P.W.; Al-Nawas, B.; Moergel, M. Integration of Perforator Vessels in CAD/CAM Free Fibula Graft Planning: A Clinical Feasibility Study. *J. Maxillofac. Oral Surg.* **2019**, *19*, 61–66. [CrossRef]
13. Battaglia, S.; Maiolo, V.; Savastio, G.; Zompatori, M.; Contedini, F.; Antoniazzi, E.; Cipriani, R.; Marchetti, C.; Tarsitano, A. Osteomyocutaneous fibular flap harvesting: Computer-assisted planning of perforator vessels using Computed Tomographic Angiography scan and cutting guide. *J. Cranio Maxillofac. Surg.* **2017**, *45*, 1681–1686. [CrossRef]
14. Shroff, S.S.; Nair, S.C.; Shah, A.; Kumar, B. Versatility of Fibula Free Flap in Reconstruction of Facial Defects: A Center Study. *J. Maxillofac. Oral Surg.* **2016**, *16*, 101–107. [CrossRef]
15. Hölzle, F.; Kesting, M.; Hölzle, G.; Watola, A.; Loeffelbein, D.; Ervens, J.; Wolff, K.-D. Clinical outcome and patient satisfaction after mandibular reconstruction with free fibula flaps. *Int. J. Oral Maxillofac. Surg.* **2007**, *36*, 802–806. [CrossRef]

16. Colletti, G.; Autelitano, L.; Rabbiosi, D.; Biglioli, F.; Chiapasco, M.; Mandalà, M.; Allevi, F. Technical refinements in mandibular reconstruction with free fibula flaps: Outcome-oriented retrospective review of 99 cases. *Acta Otorhinolaryngol. Ital.* **2014**, *34*, 342–348.
17. Chang, E.I.; Carlsen, B.T.; Festekjian, J.H.; Da Lio, A.L.; Crisera, C.A. Salvage Rates of Compromised Free Flap Breast Reconstruction After Recurrent Thrombosis. *Ann. Plast. Surg.* **2013**, *71*, 68–71. [CrossRef]
18. Koshima, I.; Fukuda, H.; Yamamoto, H.; Moriguchi, T.; Soeda, S.; Ohta, S. Free anterolateral thigh flaps for reconstruction of head and neck defects. *Plast. Reconstr. Surg.* **1993**, *92*, 421–428; discussion 429–430.
19. Siemionow, M.; Arslan, E. Ischemia/reperfusion injury: A review in relation to free tissue transfers. *Microsurgery* **2004**, *24*, 468–475. [CrossRef]
20. Yang, Q.; Ren, Z.; Chickooree, D.; Wu, H.; Tan, H.; Wang, K.; He, Z.; Gong, C.; Ram, V.; Zhang, S. The effect of early detection of anterolateral thigh free flap crisis on the salvage success rate, based on 10 years of experience and 1072 flaps. *Int. J. Oral Maxillofac. Surg.* **2014**, *43*, 1059–1063. [CrossRef]
21. Verhelst, P.-J.; Dons, F.; Van Bever, P.-J.; Schoenaers, J.; Nanhekhan, L.; Politis, C. Fibula Free Flap in Head and Neck Reconstruction: Identifying Risk Factors for Flap Failure and Analysis of Postoperative Complications in a Low Volume Setting. *Craniomaxillofacial Trauma Reconstr.* **2019**, *12*, 183–192. [CrossRef]
22. Seruya, M.; Fisher, M.; Rodriguez, E.D. Computer-Assisted versus Conventional Free Fibula Flap Technique for Craniofacial Reconstruction. *Plast. Reconstr. Surg.* **2013**, *132*, 1219–1228. [CrossRef]
23. Momoh, A.O.; Yu, P.; Skoracki, R.J.; Liu, S.; Feng, L.; Hanasono, M.M. A Prospective Cohort Study of Fibula Free Flap Donor-Site Morbidity in 157 Consecutive Patients. *Plast. Reconstr. Surg.* **2011**, *128*, 714–720. [CrossRef]
24. Yadav, P.S.; Ahmad, Q.G.; Shankhdhar, V.K.; Nambi, G. Skin paddle vascularity of free fibula flap—A study of 386 cases and a classification based on contribution from axial vessels of the leg. *Indian J. Plast. Surg.* **2012**, *45*, 058–061. [CrossRef]
25. Yu, P.; Chang, E.I.; Hanasono, M.M. Design of a Reliable Skin Paddle for the Fibula Osteocutaneous Flap: Perforator Anatomy Revisited. *Plast. Reconstr. Surg.* **2011**, *128*, 440–446. [CrossRef]
26. Gennaro, P.; Della Monaca, M.; Aboh, I.V.; Priore, P.; Facchini, A.; Valentini, V. "Naked Microvascular Bone Flap" in Oral Reconstruction. *Ann. Plast. Surg.* **2014**, *73*, 164–169. [CrossRef]
27. Gilbert, A. Vascularised transfer of the fibula shaft. *Int. J. Microsurg.* **1979**, *1*, 100.
28. Ruggiero, S.L.; Dodson, T.B.; Fantasia, J.; Goodday, R.; Aghaloo, T.; Mehrotra, B.; O'Ryan, F. American Association of Oral and Maxillofacial Surgeons Position Paper on Medication-Related Osteonecrosis of the Jaw—2014 Update. *J. Oral Maxillofac. Surg.* **2014**, *72*, 1938–1956. [CrossRef]
29. Brown, J.S.; Shaw, R.J. Reconstruction of the maxilla and midface: Introducing a new classification. *Lancet Oncol.* **2010**, *11*, 1001–1008. [CrossRef]
30. Brown, J.S.; Barry, C.; Ho, M.; Shaw, R. A new classification for mandibular defects after oncological resection. *Lancet Oncol.* **2016**, *17*, 23–30. [CrossRef]
31. Freeman, G.H.; Halton, J.H. Note on an exact treatment of contingency, goodness of fit and other problems of significance. *Biometrika* **1951**, *38*, 141–149.
32. Gluckman, J.L.; McDonough, J.; Donegan, J.O. The role of the free jejunal graft in reconstruction of the pharynx and cervical esophagus. *Head Neck Surg.* **1982**, *4*, 360–369. [CrossRef]
33. Bui, D.T.; Cordeiro, P.G.; Hu, Q.-Y.; Disa, J.J.; Pusic, A.; Mehrara, B.J. Free Flap Reexploration: Indications, Treatment, and Outcomes in 1193 Free Flaps. *Plast. Reconstr. Surg.* **2007**, *119*, 2092–2100. [CrossRef]
34. Chaine, A.; Pitak-Arnnop, P.; Dhanuthai, K.; Ruhin-Poncet, B.; Bertrand, J.-C.; Bertolus, C. A treatment algorithm for managing giant mandibular ameloblastoma: 5-year experiences in a Paris university hospital. *Eur. J. Surg. Oncol. (EJSO)* **2009**, *35*, 999–1005. [CrossRef]
35. Gallegos-Hernández, J.F.; Martínez-Miramón, A.; Reyes-Vivanco, A. Seguimiento a largo plazo del colgajo libre de peroné en la reconstrucción mandibular. *Cirugía y Cirujanos* **2019**, *87*, 267–271. [CrossRef]
36. López-Arcas, J.M.; Arias, J.; del Castillo, J.L.; Burgueño, M.; Navarro, I.; Moran, M.J.; Chamorro, M.; Martorell, V. The Fibula Osteomyocutaneous Flap for Mandible Reconstruction: A 15-Year Experience. *J. Oral Maxillofac. Surg.* **2010**, *68*, 2377–2384. [CrossRef]
37. Mücke, T.; Ritschl, L.M.; Roth, M.; Güll, F.D.; Rau, A.; Grill, S.; Kesting, M.R.; Wolff, K.-D.; Loeffelbein, D.J. Predictors of free flap loss in the head and neck region: A four-year retrospective study with 451 microvascular transplants at a single centre. *J. Cranio Maxillofac. Surg.* **2016**, *44*, 1292–1298. [CrossRef]
38. Las, D.E.; de Jong, T.; Zuidam, J.M.; Verweij, N.M.; Hovius, S.E.; Mureau, M.A. Identification of independent risk factors for flap failure: A retrospective analysis of 1530 free flaps for breast, head and neck and extremity reconstruction. *J. Plast. Reconstr. Aesthetic Surg.* **2016**, *69*, 894–906. [CrossRef]
39. Suh, J.D.; Sercarz, J.A.; Abemayor, E.; Calcaterra, T.C.; Rawnsley, J.D.; Alam, D.; Blackwell, K.E. Analysis of Outcome and Complications in 400 Cases of Microvascular Head and Neck Reconstruction. *Arch. Otolaryngol. Head Neck Surg.* **2004**, *130*, 962–966. [CrossRef]
40. Tan, N.C.; Lin, P.-Y.; Chiang, Y.-C.; Chew, K.-Y.; Chen, C.-C.; Fujiwara, T.; Kuo, Y.-R. Influence of neck dissection and preoperative irradiation on microvascular head and neck reconstruction-Analysis of 853 cases. *Microsurgery* **2014**, *34*, 602–607. [CrossRef]

41. Bourget, A.; Chang, J.T.C.; Wu, D.B.-S.; Chang, C.J.; Wei, F.C. Free Flap Reconstruction in the Head and Neck Region following Radiotherapy: A Cohort Study Identifying Negative Outcome Predictors. *Plast. Reconstr. Surg.* **2011**, *127*, 1901–1908. [CrossRef]
42. Deek, N.F.A.L.; Wei, F.-C. Computer-Assisted Surgery for Segmental Mandibular Reconstruction with the Osteoseptocutaneous Fibula Flap. *Plast. Reconstr. Surg.* **2016**, *137*, 963–970. [CrossRef]
43. He, Y.; Zhang, Z.Y.; Zhu, H.G.; Sader, R.; He, J.; Kovacs, A.F. Free Fibula Osteocutaneous Flap for Primary Reconstruction of T3-T4 Gingival Carcinoma. *J. Craniofacial Surg.* **2010**, *21*, 301–305. [CrossRef]
44. Cvek, J.; Kubes, J.; Skacelikova, E.; Otahal, B.; Kominek, P.; Halamka, M.; Feltl, D. Hyperfractionated accelerated radiotherapy with concomitant integrated boost of 70–75 Gy in 5 weeks for advanced head and neck cancer. *Strahlenther. Onkol.* **2012**, *188*, 666–670. [CrossRef]
45. Wygoda, A.; Rutkowski, T.; Hutnik, M.; Składowski, K.; Goleń, M.; Pilecki, B. Acute mucosal reactions in patients with head and neck cancer. *Strahlenther. Onkol.* **2013**, *189*, 547–551. [CrossRef]
46. Moura, J.F.B.; Mota, J.M.S.C.; Leite, C.A.V.; Wong, D.V.T.; Bezerra, N.P.; Brito, G.A.D.C.; Lima, V.; Cunha, F.Q.; Ribeiro, R.A. A novel model of megavoltage radiation-induced oral mucositis in hamsters: Role of inflammatory cytokines and nitric oxide. *Int. J. Radiat. Biol.* **2015**, *91*, 500–509. [CrossRef]
47. Logan, R.M.; Gibson, R.J.; Sonis, S.T.; Keefe, D.M. Nuclear factor-κB (NF-κB) and cyclooxygenase-2 (COX-2) expression in the oral mucosa following cancer chemotherapy. *Oral Oncol.* **2007**, *43*, 395–401. [CrossRef]
48. Fang, H.; Liu, F.; Sun, C.; Pang, P. Impact of wound closure on fibular donor-site morbidity: A meta-analysis. *BMC Surg.* **2019**, *19*, 1–6. [CrossRef]
49. Ling, X.F.; Peng, X. What Is the Price to Pay for a Free Fibula Flap? A Systematic Review of Donor-Site Morbidity following Free Fibula Flap Surgery. *Plast. Reconstr. Surg.* **2012**, *129*, 657–674. [CrossRef]
50. Bach, C.A.; Guilleré, L.; Yildiz, S.; Wagner, I.; Darmon, S.; Chabolle, F. Comparison of negative pressure wound therapy and conventional dressing methods for fibula free flap donor site management in patients with head and neck cancer. *Head Neck* **2015**, *38*, 696–699. [CrossRef]
51. Schusterman, M.A.; Reece, G.P.; Miller, M.J.; Harris, S. The osteocutaneous free fibula flap: Is the skin paddle reliable? *Plast. Reconstr. Surg.* **1992**, *90*, 787–794; discussion 794–798.
52. Torroni, A.; Gennaro, P.; Aboh, I.V.; Longo, G.; Valentini, V.; Iannetti, G. Microvascular Reconstruction of the Mandible in Irradiated Patients. *J. Craniofacial Surg.* **2007**, *18*, 1359–1369. [CrossRef]
53. Thome, J. Das mikrovaskuläre Fibulatransplantat in der Mund-, Kiefer—Und Gesichtschirurgie—Eine Literaturübersicht—Dissertation. University Cologne, Cologne, Germany, 2008.
54. Jones, N.F.; Monstrey, S.; Gambier, B.A. Reliability of the Fibular Osteocutaneous Flap for Mandibular Reconstruction: Anatomical and Surgical Confirmation. *Plast. Reconstr. Surg.* **1996**, *97*, 707–716. [CrossRef]
55. Wong, C.-H.; Tan, B.-K.; Wei, F.-C.; Song, C. Use of the Soleus Musculocutaneous Perforator for Skin Paddle Salvage of the Fibula Osteoseptocutaneous Flap: Anatomical Study and Clinical Confirmation. *Plast. Reconstr. Surg.* **2007**, *120*, 1576–1584. [CrossRef]
56. Winters, H.A.H.; de Jongh, G.J. Reliability of the Proximal Skin Paddle of the Osteocutaneous Free Fibula Flap: A Prospective Clinical Study. *Plast. Reconstr. Surg.* **1999**, *103*, 846–849. [CrossRef]
57. Millican, P.; Poole, M. Peripheral neovascularisation of muscle and musculocutaneous flaps. *Br. J. Plast. Surg.* **1985**, *38*, 369–374. [CrossRef]
58. Khoo, C.; Bailey, B. The behaviour of free muscle and musculocutaneous flaps after early loss of axial blood supply. *Br. J. Plast. Surg.* **1982**, *35*, 43–46. [CrossRef]
59. Kumar, K.; Jaffe, W.; London, N.J.M.; Varma, S.K. Free Flap Neovascularization: Myth or Reality? *J. Reconstr. Microsurg.* **2004**, *21*, 31–34. [CrossRef]
60. Mücke, T.; Wolff, K.-D.; Rau, A.; Kehl, V.; Mitchell, D.A.; Steiner, T. Autonomization of free flaps in the oral cavity: A prospective clinical study. *Microsurgery* **2012**, *32*, 201–206. [CrossRef]
61. Goldwaser, B.R.; Chuang, S.-K.; Kaban, L.B.; August, M. Risk Factor Assessment for the Development of Osteoradionecrosis. *J. Oral Maxillofac. Surg.* **2007**, *65*, 2311–2316. [CrossRef]
62. Celik, N.; Wei, F.-C.; Chen, H.-C.; Cheng, M.-H.; Huang, W.-C.; Tsai, F.-C.; Chen, Y.-C. Osteoradionecrosis of the Mandible after Oromandibular Cancer Surgery. *Plast. Reconstr. Surg.* **2002**, *109*, 1875–1881. [CrossRef]
63. Aarup-Kristensen, S.; Hansen, C.R.; Forner, L.; Brink, C.; Eriksen, J.G.; Johansen, J. Osteoradionecrosis of the mandible after radiotherapy for head and neck cancer: Risk factors and dose-volume correlations. *Acta Oncol.* **2019**, *58*, 1373–1377. [CrossRef]
64. Cummins, D.M.; Kim, B.; Kaleem, A.; Zaid, W. Pedicle Orientation in Free-Flap Microvascular Maxillofacial Reconstruction. *J. Oral Maxillofac. Surg.* **2017**, *75*, 875.e1–875.e4. [CrossRef]
65. Zhang, C.; Sun, J.; Zhu, H.; Xu, L.; Ji, T.; He, Y.; Yang, W.; Hu, Y.; Yang, X.; Zhang, Z. Microsurgical free flap reconstructions of the head and neck region: Shanghai experience of 34 years and 4640 flaps. *Int. J. Oral Maxillofac. Surg.* **2015**, *44*, 675–684. [CrossRef]
66. Chiu, Y.-H.; Chang, D.-H.; Perng, C.-K. Vascular Complications and Free Flap Salvage in Head and Neck Reconstructive Surgery. *Ann. Plast. Surg.* **2017**, *78*, S83–S88. [CrossRef]
67. Costa, H.; Zenha, H.; Sequeira, H.; Coelho, G.; Gomes, N.; Pinto, C.; Martins, J.; Santos, D.; Andresen, C. Microsurgical reconstruction of the maxilla: Algorithm and concepts. *J. Plast. Reconstr. Aesthetic Surg.* **2015**, *68*, e89–e104. [CrossRef]
68. Cao, Y.; Yu, C.; Liu, W.; Miao, C.; Han, B.; Yang, J.; Li, L.; Li, C. Obturators versus flaps after maxillary oncological ablation: A systematic review and best evidence synthesis. *Oral Oncol.* **2018**, *82*, 152–161. [CrossRef]

69. Colmenero, C.; Martorell, V.; Colmenero, B.; Sierra, I. Temporalis myofascial flap for maxillofacial reconstruction. *J. Oral Maxillofac. Surg.* **1991**, *49*, 1067–1073. [CrossRef]
70. Ariyan, S. The Pectoralis Major Myocutaneous Flap A Versatile Flap for Reconstruction in the Head and Neck. *Plast. Reconstr. Surg.* **1979**, *63*, 73–81. [CrossRef]
71. Ariyan, S. Pectoralis Major, Sternomastoid, and Other Musculocutaneous Flaps for Head and Neck Reconstruction. *Clin. Plast. Surg.* **1980**, *7*, 89–109. [CrossRef]
72. Bakamjian, V.; Poole, M. Maxillo-facial and palatal reconstructions with the deltopectoral flap. *Br. J. Plast. Surg.* **1977**, *30*, 17–37. [CrossRef]
73. de Pablo, A.; Chen, Y.-T.; Chen, J.-K.; Tsao, C.-K. Trismus surgical release and free flap reconstruction after radiation therapy in oral and oropharyngeal squamous cell carcinoma. *J. Surg. Oncol.* **2018**, *117*, 142–149. [CrossRef]
74. Chang, T.S.; Wang, W.; Hsu, C.Y. The free forearm flap–a report of 25 cases. *Ann. Acad. Med. Singap.* **1982**, *11*, 236–240.
75. Ludolph, I.; Lehnhardt, M.; Arkudas, A.; Kneser, U.; Pierer, G.; Harder, Y.; Horch, R.E. Plastisch rekonstruktive Mikrochirurgie beim alten Patienten. *Handchir. · Mikrochir. · Plast. Chir.* **2017**, *50*, 118–125. [CrossRef]
76. Wolfer, S.; Wohlrath, R.; Kunzler, A.; Foos, T.; Ernst, C.; Schultze-Mosgau, S. Scapular free flap as a good choice for mandibular reconstruction: 119 out of 280 cases after resection of oral squamous cell carcinoma in a single institution. *Br. J. Oral Maxillofac. Surg.* **2020**, *58*, 451–457. [CrossRef]
77. Hwang, K.; Lee, J.P.; Yoo, S.Y.; Kim, H. Relationships of comorbidities and old age with postoperative complications of head and neck free flaps: A review. *J. Plast. Reconstr. Aesthetic Surg.* **2016**, *69*, 1627–1635. [CrossRef]
78. Sierakowski, A.; Nawar, A.; Parker, M.; Mathur, B. Free flap surgery in the elderly: Experience with 110 cases aged ≥70 years. *J. Plast. Reconstr. Aesthetic Surg.* **2017**, *70*, 189–195. [CrossRef]
79. Kesting, M.R.; Hölzle, F.; Wolff, K.-D.; Wagenpfeil, S.; Hasler, R.J.; Wales, C.J.; Steinstraesser, L.; Rohleder, N.H. Use of microvascular flap technique in older adults with head and neck cancer: A persisting dilemma in reconstructive surgery? *J. Am. Geriatr. Soc.* **2011**, *59*, 398–405. [CrossRef]
80. Grill, F.D.; Wasmaier, M.; Mücke, T.; Ritschl, L.M.; Wolff, K.-D.; Schneider, G.; Loeffelbein, D.J.; Kadera, V. Identifying perioperative volume-related risk factors in head and neck surgeries with free flap reconstructions—An investigation with focus on the influence of red blood cell concentrates and noradrenaline use. *J. Cranio Maxillofac. Surg.* **2020**, *48*, 67–74. [CrossRef]
81. Clark, J.R.; McCluskey, S.A.; Hall, F.; Lipa, J.; Neligan, P.; Brown, D.; Irish, J.; Gullane, P.; Gilbert, R. Predictors of morbidity following free flap reconstruction for cancer of the head and neck. *Head Neck* **2007**, *29*, 1090–1101. [CrossRef]
82. Loeffelbein, D.; Ritschl, L.; Güll, F.; Roth, M.; Wolff, K.-D.; Mücke, T. Influence of possible predictor variables on the outcome of primary oral squamous cell carcinoma: A retrospective study of 392 consecutive cases at a single centre. *Int. J. Oral Maxillofac. Surg.* **2017**, *46*, 413–421. [CrossRef]
83. Chen, A.M.; Chen, L.M.; Vaughan, A.; Farwell, D.G.; Luu, Q.; Purdy, J.A.; Vijayakumar, S. Head and Neck Cancer Among Lifelong Never-Smokers and Ever-Smokers. *Am. J. Clin. Oncol.* **2011**, *34*, 270–275. [CrossRef]
84. Fortin, A.; Wang, C.S.; Vigneault, É. Influence of Smoking and Alcohol Drinking Behaviors on Treatment Outcomes of Patients With Squamous Cell Carcinomas of the Head and Neck. *Int. J. Radiat. Oncol.* **2009**, *74*, 1062–1069. [CrossRef]
85. Van Imhoff, L.C.; Kranenburg, G.G.; Macco, S.; Nijman, N.L.; van Overbeeke, E.J.; Wegner, I.; Grolman, W.; Pothen, A.J. Prognostic value of continued smoking on survival and recurrence rates in patients with head and neck cancer: A systematic review. *Head Neck* **2015**, *38*, E2214–E2220. [CrossRef]
86. Crippen, M.M.; Brady, J.S.; Mozeika, A.M.; Eloy, J.A.; Baredes, S.; Park, R.C.W. Impact of Body Mass Index on Operative Outcomes in Head and Neck Free Flap Surgery. *Otolaryngol. Neck Surg.* **2018**, *159*, 817–823. [CrossRef]
87. Gama, R.R.; Song, Y.; Zhang, Q.; Brown, M.C.; Wang, J.; Habbous, S.; Tong, L.; Huang, S.H.; O'Sullivan, B.; Waldron, J.; et al. Body mass index and prognosis in patients with head and neck cancer. *Head Neck* **2017**, *39*, 1226–1233. [CrossRef]
88. de La Garza, G.; Militsakh, O.N.; Panwar, A.; Galloway, T.L.; Jorgensen, J.B.; Ledgerwood, L.G.; Kaiser, K.; Bs, C.K.; Shnayder, Y.; Neumann, C.A.; et al. Obesity and perioperative complications in head and neck free tissue reconstruction. *Head Neck* **2016**, *38*, E1188–E1191. [CrossRef]
89. Khan, M.N.; Russo, J.; Spivack, J.; Pool, C.; Likhterov, I.; Teng, M.; Genden, E.M.; Miles, B.A. Association of Body Mass Index With Infectious Complications in Free Tissue Transfer for Head and Neck Reconstructive Surgery. *JAMA Otolaryngol. Neck Surg.* **2017**, *143*, 574–579. [CrossRef]
90. Thai, L.; McCarn, K.; Stott, W.; Watts, T.; Wax, M.K.; Andersen, P.E.; Gross, N.D. Venous thromboembolism in patients with head and neck cancer after surgery. *Head Neck* **2012**, *35*, 4–9. [CrossRef]
91. Eskander, A.; Kang, S.; Tweel, B.; Sitapara, J.; Old, M.; Ozer, E.; Agrawal, A.; Carrau, R.; Rocco, J.W.; Teknos, T.N. Predictors of Complications in Patients Receiving Head and Neck Free Flap Reconstructive Procedures. *Otolaryngol. Neck Surg.* **2018**, *158*, 839–847. [CrossRef]
92. Cannady, S.B.; Hatten, K.M.; Bur, A.M.; Brant, J.; Fischer, J.P.; Newman, J.G.; Chalian, A.A. Use of free tissue transfer in head and neck cancer surgery and risk of overall and serious complication(s): An American College of Surgeons-National Surgical Quality Improvement Project analysis of free tissue transfer to the head and neck. *Head Neck* **2017**, *39*, 702–707. [CrossRef]
93. Offodile, A.C.; Aherrera, A.; Wenger, J.; Rajab, T.K.; Guo, L. Impact of increasing operative time on the incidence of early failure and complications following free tissue transfer? A risk factor analysis of 2,008 patients from the ACS-NSQIP database. *Microsurgery* **2015**, *37*, 12–20. [CrossRef]

94. Tang, N.S.; Ahmadi, I.; Ramakrishnan, A. Virtual surgical planning in fibula free flap head and neck reconstruction: A systematic review and meta-analysis. *J. Plast. Reconstr. Aesthetic Surg.* **2019**, *72*, 1465–1477. [CrossRef]
95. Rendenbach, C.; Steffen, C.; Hanken, H.; Schluermann, K.; Henningsen, A.; Beck-Broichsitter, B.; Kreutzer, K.; Heiland, M.; Precht, C. Complication rates and clinical outcomes of osseous free flaps: A retrospective comparison of CAD/CAM versus conventional fixation in 128 patients. *Int. J. Oral Maxillofac. Surg.* **2019**, *48*, 1156–1162. [CrossRef]

cancers

an Open Access Journal by MDPI

Indexed in: PubMed | CITESCORE 4.4 SCOPUS | IMPACT FACTOR 6.639

CERTIFICATE OF PUBLICATION

Certificate of publication for the article titled:

Partial and Total Flap Failure after Fibula Free Flap in Head and Neck Reconstructive Surgery: Retrospective Analysis of 180 Flaps over 19 Years

Authored by:

Michael Knitschke; Sophia Sonnabend; Christina Bäcker; Daniel Schmermund; Sebastian Böttger; Hans-Peter Howaldt;
Sameh Attia

Published in:

Cancers **2021**, Volume 13, Issue 4, 865

MDPI Academic Open Access Publishing since 1996

Basel, October 2021

3.2. Originalarbeit 2: Heterotopic Ossification of the Vascular Pedicle after Maxillofacial Reconstructive Surgery Using Fibular Free Flap: Introducing New Classification and Retrospective Analysis.

Knitschke, M.; Siu, K.; Bäcker, C.; Attia, S.; Howaldt, H.-P.; Böttger, S. Heterotopic Ossification of the Vascular Pedicle after Maxillofacial Reconstructive Surgery Using Fibular Free Flap: Introducing New Classification and Retrospective Analysis. J. Clin. Med. **2021**, 10, 109.
https://doi.org/10.3390/jcm10010109 **IF: 4,241**

Zusammenfassung:
Heterotope Ossifikation (HO) des Gefäßstiels sind in der Literatur ein beschriebenes Phänomen nach Kieferrekonstruktionen mit dem freien Fibulatransplantat.
Ziel der retrospektiven Studie war die Erhebung der Häufigkeit von radiologischen und klinischen Zeichen der HO, sowie die Erfassung von klinisch symptomatischen Verläufen, bei denen eine chirurgische Therapie zur Symptomkontrolle notwendig wurde. Von 102 Patienten wurden CT-Untersuchungen nach Kieferrekonstruktion mit dem Fibulatransplantat auf das Vorliegen von HO hin untersucht. Anschließend wurden die Patientenakten ausgewertet, um die Fälle mit klinischen Symptomen und Komplikationen im Zusammenhang mit dem Vorhandensein von HO zu identifizieren. Von 102 Patienten wiesen *n* = 29 (28,43 %) den radiologischen Befund einer HO auf. Klinische Symptome wurden in *n* = 10 Fällen (9,8 %) in Form von Dysphagie (*n* = 5), Trismus (*n* = 3) und knöchernen Massen (*n* = 2) erhoben. Von diesen musste in fünf Fällen (4,9 %) eine operative Entfernung der HO erfolgen.
HO trat im untersuchten Kollektiv häufiger bei jüngeren und männlichen Patienten auf (Durchschnittsalter 52,3 ± 14,4 Jahre). Es wurde keine Korrelation zwischen dem Auftreten von HO und der Planungsmethode (analog, Non-VSP vs. digital, VSP) und dem Zeitpunkt der Rekonstruktion (ein- vs. zweizeitig) festgestellt. Nach Rekonstruktionen des Oberkiefers wurde HO radiologisch sechs Monate früher als nach der Wiederherstellung des Unterkiefers in der CT registriert. Nach jeder dritten Oberkiefer- und jeder vierten Unterkieferrekonstruktion konnte in der hier untersuchten Patientengruppe eine HO beobachtet werden.

In dieser Studie wurde zum ersten Mal eine Klassifizierung von vier verschiedenen HO-Mustern entwickelt. Die HO-Typen 1 und 2 wurden überwiegend nach Unterkieferrekonstruktion und Typ 4 zumeist nach Oberkieferrekonstruktionen beobachtet.

Trismus, Kauschmerzen und/oder palpable, derbe submandibuläre Massen können ein Indikator für HO sein, wenn postoperative Narben und Tumorrezidive ausgeschlossen werden können. Eine modifizierte Entnahmetechnik ohne verbliebenes Periost entlang des Gefäßstiels scheint eine Methode zur Vermeidung heterotoper Ossifikationen zu sein, was den Stellenwert des periostalen Gewebes in der Genese unterstreicht. Im Falle ausgedehnter HO-Verläufe können modellierende Osteotomien und die Anwendung schraubenfixierter Verbandsplatten als therapeutische Strategie in Betracht gezogen werden. In keinem Fall wurde ein Transplantatverlust aufgrund einer HO registriert.

Ausblick:

Extraossäre, heterotope Ossifikation (HO) sind ein häufiges radiologisches, aber klinisch nur selten symptomatisches Phänomen nach freiem Fibulatransplantat zur Kieferrekonstruktion.

Zur Vermeidung klinisch symptomatischer Verläufe ist eine Modifikation bei der Fibulaentnahmetechnik und der Präparation des Gefäßstiels im Bereich des zu verwerfenden proximalen Fibulaabschnitts zu diskutieren. Unseres Wissens ist dies die erste Studie, die eine Klassifizierung von vier verschiedenen radiologischen HO-Mustern beschreibt. Weitere Studien zur Validierung der Klassifizierung sind erforderlich.

Journal of
Clinical Medicine

MDPI

Article

Heterotopic Ossification of the Vascular Pedicle after Maxillofacial Reconstructive Surgery Using Fibular Free Flap: Introducing New Classification and Retrospective Analysis

Michael Knitschke *, Kelly Siu, Christina Bäcker, Sameh Attia, Hans-Peter Howaldt and Sebastian Böttger

Department of Oral and Maxillofacial Surgery, Justus-Liebig-University, Klinikstrasse 33, 35392 Giessen, Germany; kelly.siu@dentist.med.uni-giessen.de (K.S.); christina.baecker-2@dentist.med.uni-giessen.de (C.B.); Sameh.Attia@dentist.med.uni-giessen.de (S.A.); HP.Howaldt@uniklinikum-giessen.de (H.-P.H.); Sebastian.Boettger@uniklinikum-giessen.de (S.B.)
* Correspondence: Michael.Knitschke@uniklinikum-giessen.de

Abstract: Heterotopic ossification (HO) is one of the described phenomena after maxillofacial reconstructive surgery using fibular free flap (FFF) at the reception-site. The aim of this study was to determine the radiological incidence and form of HO along the fibular vascular pedicle as well as the rate of clinical symptoms if present. CT-scans of 102 patients who underwent jaw reconstructive surgery by using FFF from January 2005 to December 2019 were evaluated concerning the presence of HO. Subsequently, the patient files were evaluated to identify the cases with clinical signs and complications related to the presence of HO. A radiological classification of four different HO types was developed. Out of 102 patients, 29 (28.43%) presented radiological findings of HO. Clinical symptoms were recorded in 10 cases (9.8%) (dysphagia (n = 5), trismus (n = 3), bony masses (n = 2)) and from these only five (4.9%) needed surgical removal of calcified structures. HO occurs significantly in younger patients (mean 52.3 year). In maxillary reconstructions, HO was radiologically visible six months earlier than after mandibular reconstruction. Furthermore, HO is observed after every third maxilla and every fourth mandible reconstruction. This study developed for the first time a classification of four distinct HO patterns. HO types 1 and 2 were mostly observed after mandible reconstruction and type 4 predominantly after maxilla reconstruction.

Keywords: reconstructive surgery; microsurgery; fibular free flap; FFF; heterotopic ossification

Citation: Knitschke, M.; Siu, K.; Bäcker, C.; Attia, S.; Howaldt, H.-P.; Böttger, S. Heterotopic Ossification of the Vascular Pedicle after Maxillofacial Reconstructive Surgery Using Fibular Free Flap: Introducing New Classification and Retrospective Analysis. *J. Clin. Med.* **2021**, *10*, 109. https://doi.org/10.3390/jcm10010109

Received: 21 October 2020
Accepted: 27 December 2020
Published: 30 December 2020

1. Introduction

The fibular free flap (FFF) is the workhorse of defect-oriented reconstruction after combined hard and soft tissue resections within the maxillofacial region [1]. The graft was firstly introduced by Hidalgo et al. [2] and quickly considered as a safe and reliable osteo-fascio-cutaneous graft which is widely used worldwide. The available bone length is usually sufficient for reconstruction of the lower jaw up to class IV [3], offering the possibility of satisfactory oral rehabilitation using endosseous dental implants [4–6]. FFF provides a vascular pedicle of sufficient length for use in the entire head and neck region between forehead and clavicula [7] and shows an overall low donor site morbidity [8]. Furthermore, there is the option of forming one or more septo-cutaneous skin paddles, which are suitable for flap monitoring as well as for closing soft tissue defects of the head and neck region. Initially, a stable and sufficient vascular supply of the septo-cutaneous skin paddle was doubted [9], but as this graft became more widespread, knowledge of vascular supply via the perforator vessels of the septum intermusculare posterius and perforator vessels around the musculus soleus was improved [10–12].

There is still debate about the reconstruction time point, and whether it is best to perform reconstruction immediately or at a delayed time after the ablative oncological procedure. The necessity of cervical lymphadenectomy offers an ideal approach to suitable vessels for

micro-anastomosis. Therefore the time of oncologic resection is the best time for reconstruction [13]. Another advantage is a decrease in surgical procedures and the opportunity for oral rehabilitation in less time [14]. Improved morphological assessment techniques such as frozen-section analysis and flat-panel volume computed tomography of the removed tissues allows an assessment regarding the complete resection of the tumor [15]. Such extended defects are often complex. Combined soft and hard tissue defects after surgery require free vascularized tissue transplant [16]. Wound healing at soft and hard tissue starts immediately after transfer of a combined osteo-fascio-cutaneous FFF. Fracture healing between the original jaw and fibular bone is a highly complex process. Several molecular interactions and gene regulatory processes are necessary for physiological bone growth. Bone healing and regeneration, as with wound healing of any other tissue, follow a sequential process with hematoma formation, tissue inflammation, and recruitment of stem cells. Finally, angiogenesis and bone remodeling will be initiated and continued [17]. Often described complications after reconstruction of maxillofacial structures are delayed wound healing and infection at both donor and receptor-site, (sub-)total flap loss [8,18], plate-related complications (infection, loosing of screw), plate exposure, and osseous non-union [19,20]. Additionally, function problems such as dysphagia, speech complaints, bulky skin paddle, reduced mouth opening, and scars were recorded [18]. Another reason for complaints and functional impairment at the reconstructed area is so-called heterotopic ossification (HO) [21,22].

HO is defined as mature lamellar bone tissue in extra-skeletal soft tissues [23]. Regardless of its genesis, HO has an endochondral structure, which lays on a cartilaginous matrix [24]. Concerning free flaps, HO of the vascular pedicle is described in the literature as a known complication of FFF [25–28]. Remarkably, evaluation of CT-scans shows frequencies up to 65% [22,29,30]. In detail, there is a broad discrepancy between radiological presence and clinical symptoms of HO. Until now, no literature has been published on the role of virtual planning, necessary patient specific cutting guides for transplant shaping, or the onset of HO. Different theories of origin are discussed, considering the periosteal tissue of the vascular pedicle [26] as well as local mechanic factors and cytokine interactions as the keys role [31]. There is some evidence that FFF harvesting technique and remaining periosteum at the vascular pedicle play a relevant role in HO formation [21,32]. Interestingly HO is also reported in non-osseus transplants like fascio-cutaneous radial forearm free flaps and septomyo-cutaneous lateral upper arm flap, all without any contact to, or included, periosteum [33,34].

The aims of this study are:

1. to estimate the radiological and clinical form and frequency of HO,
2. to define and compare different radio-morphological HO types introducing a new classification,
3. to report the surgical intervention rate for removing calcified structures,
4. and to investigate whether there is a correlation between: analog vs. digital planning, reconstruction methods (immediate vs. delayed), fibular segments and the occurrence of HO.

2. Material and Methods

2.1. Study Design and Patient Population

The study was conducted as a monocentric, retrospective study. CT scans and cone beam CTs (CBCT) of patients who underwent successful FFF in the head and neck region from January 2005 to December 2019 were analyzed concerning the presence of heterotopic ossification (HO). The evaluated CT-scans were initiated either within the course of radiation planning or routine follow-up examination. CBCT were mostly performed to plan the insertion of dental implants for oral rehabilitation.

2.2. Study Parameters and Evaluator Calibration

The following parameters were collected: age at flap transfer, sex, primary diagnosis, planning procedure, location and type of defect, number of used fibula segments, extension of

neck dissection, irradiation, clinical symptoms of HO and need for surgical intervention if HO was clinically symptomatic. All CT and CBCT-scans were analyzed independently for presence of HO by two authors (KS and MK). If they disagreed, it was planned to take a third author's opinion (SB) in consideration, which was not necessary. MK and SB are experienced maxillofacial surgeons. KS is a fifth year dental medicine student.

2.3. Inclusion and Exclusion Criteria for Study Subjects

All patients who underwent a successful reconstruction of the maxilla or mandible (simultaneous or two-staged) with a FFF were enrolled in this study. Inclusion criteria were the presence of at least two CT-scans of the region of interest. Only CT-scans with a slice thickness $\leq$5 mm were included to ensure optimal HO detection. The minimum follow-up interval was four months. Cases with incomplete data sets, patient records, and those with less than two postoperative CT- or CBCT-scans of the head and neck region or a CT layer thickness >5 mm were excluded.

2.4. A New Classification of HO of the Vascular Pedicle and Periosseous Tissue Based on Radiological and Clinical Follow-Up

Systematic evaluation of the patient records was performed to identify the cases in which the clinical presence of HO in the vascular pedicle region (palpable submandibular "bone-hard" swelling, ongoing difficulty swallowing and/or the periosteal tissue) led to clinical complications. For the radiological description, five types of HO patterns were defined (Figures 1 and 2): no recognizable ossification of the vascular pedicle or perosseous tissue corresponds to type 0. Type 1 shows an ossification at the transition zone from fibula graft to vascular pedicle. Type 2 shows isolated ossification of the vascular pedicle without contact to the fibula. Type 3 is defined as an isolated HO of periosseous tissue without pedicle-associated ossification. Type 4 is a combination of HO of the vascular bundle and periosseous tissue.

2.5. Statistical Analyses

Chi-square-test was used to compare the frequency of HO in males and females. Students *t*-test was performed to compare the mean age at FFF-transfer between groups with and without radiological sign of HO, after verification of normality. $p < 0.05$ was defined as statistically significant. The statistical analysis (analogous to Kaplan-Meier survival function) was carried out with SPSS 25 (SPSS Inc., Chicago, IL, USA, http://www.spss.com).

2.6. Ethics Statement/Confirmation of Patients' Permission

The study was approved by the local Ethics Committee of Justus-Liebig University Giessen (AZ34/20) and patients' permission/consent was not necessary in this retrospective study. The patients consented that their intraoral pictures and X-ray images could be used anonymously in the publication. In addition, all data in the Microsoft Excel spreadsheet were pseudonymized.

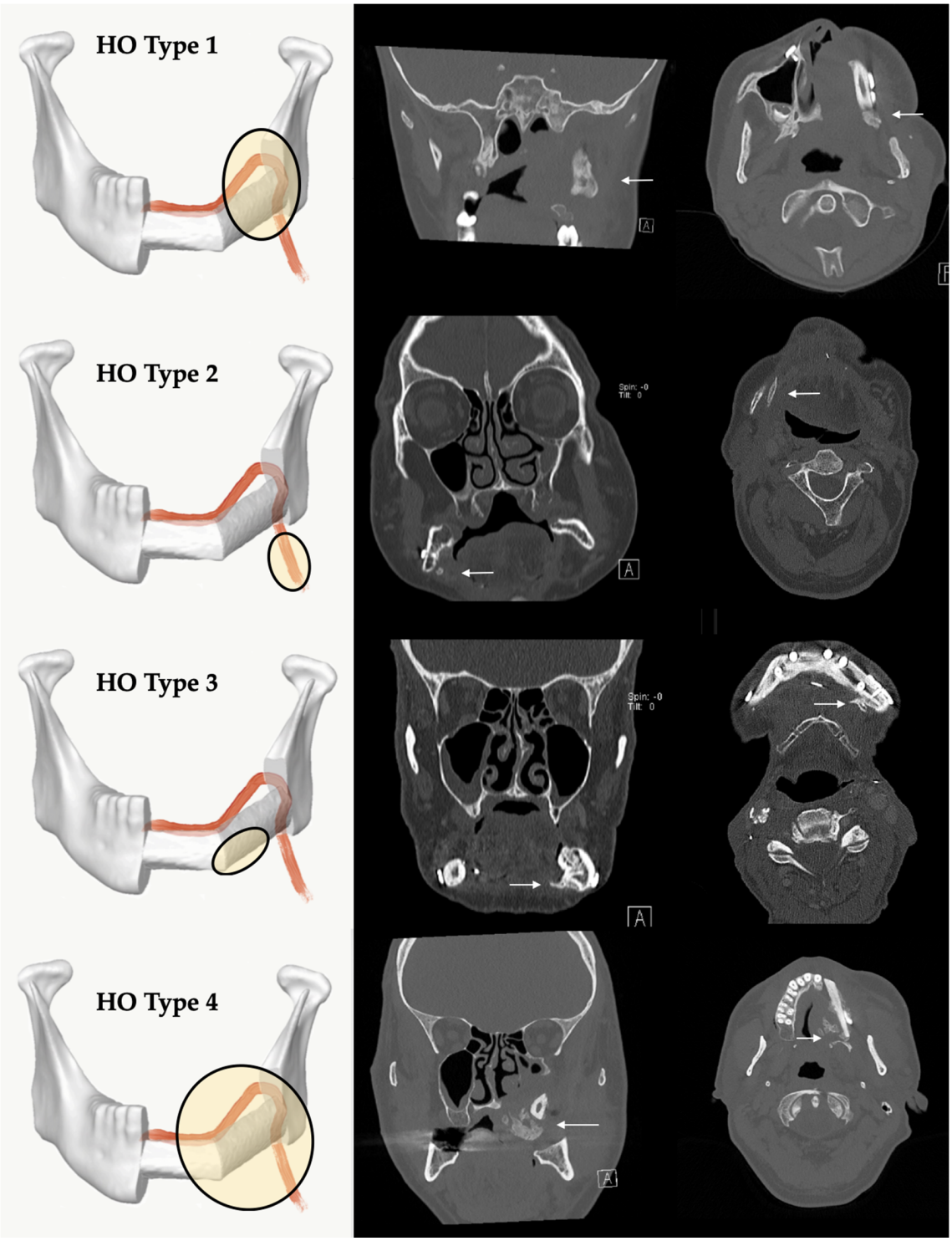

Figure 1. Classification of different radiological types of heterotopic ossification (HO): Type 1 = HO at the transition zone from fibula graft to vascular pedicle, Type 2 = HO isolated at the pedicle without contact to the fibula, Type 3 = HO appears isolated at the periosseous tissue without involvement of the vascular pedicle, Type 4 = a combination with ossification of the pedicle and periosseous tissue. The white arrows mark region of interest. A = Anterior.

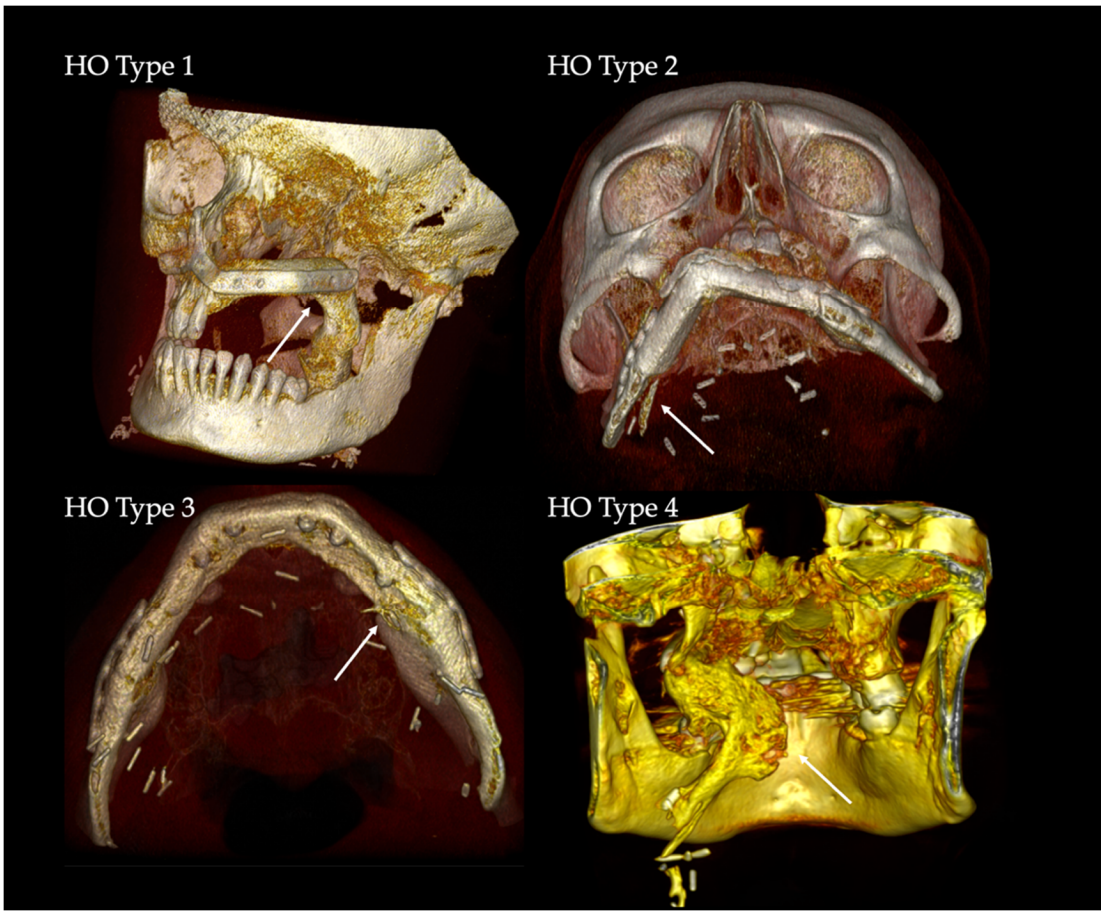

Figure 2. 3D-volume rendering of clinical examples of HO Types 1–4. The white arrows mark the regions of interest.

3. Results

A total of 149 cases fulfilled the defined inclusion and 47 cases matched the exclusion criteria. A total of 102 FFF cases (M: n = 66 (64.7%), F: n = 36 (35.3%)) with complete data records during the period January 2005 to December 2019 were analyzed in the study (Table 1). The average age at surgery time in the HO- group was 58.69 ± 11.92 year (median 59.91 years, range 32.58–82.75 years) (follow-up 45.16 ± 44.49 months) and in the HO+ group 52.30 ± 14.39 years (median 53.92 years, range 14.75–76.83 years) (follow-up 66.59 ± 45.04 months). Both groups were tested for normal distribution. There was a significant age difference between the HO+ and HO- group (p = 0.0236). FFF was used for maxillary reconstruction in 26 cases and for mandibular reconstruction in 76 cases.

Table 1. Clinical details of 102 patients after reconstruction of continuity defects of maxilla and mandible with fibular free flaps.

n = 102	**HO−** **n = 73 (71.57%)**	**HO+** **n = 29 (28.43%)**	
Age (year), SD	58.69 ± 11.92	52.30 ± 14.39	p = 0.0236
Follow-up (months), SD	45.16 ± 44.49	66.59 ± 45.04	
HO duration until observation (months)		mean 13.48, median 9 ± 16.54	
Surgical intervention		5	
Sex			
Male	41 (40.20%)	25 (24.51%)	
Female	32 (31.37%)	4 (3.92%)	p = 0.5096

Table 1. *Cont.*

n = 102	HO− *n* = 73 (71.57%)	HO+ *n* = 29 (28.43%)	
Preoperative planning/osteosynthesis			
Analog/hand-bent	45 (44.12%)	15 (14.71%)	
Virtual/custom-made	28 (27.45%)	14 (13.73%)	$p = 0.3806$
Reconstruction			
Immediately	60 (58.82%)	19 (18.63%)	
Delayed	13 (12.75%)	10 (9.80%)	$p = 0.1128$
Diagnosis			
Malignant	69 (67.65%)	22 (21.57%)	
Benign	4 (3.92%)	4 (3.92%)	
Other (ORN, BPONJ, OM)		3 (2.94%)	
Location			
Maxilla	17 (16.67%)	9 (8.82%)	
Mandibula	56 (54.90%)	20 (19.61%)	$p = 0.4553$
Maxilla defect type (Brown et Shaw 2010) [35]			
II	15 (57.69%)	8 (30.77%)	
III	2 (7.69%)	1 (3.85%)	
Mandible defect type (Brown et al. 2016) [3]			
I	15 (19.74%)	7 (9.21%)	
Ic	4 (5.26%)		
II	13 (17.11%)	3 (3.95%)	
IIc	1 (1.32%)	1 (1.32%)	
III	22 (28.95%)	7 (9.21%)	
IV	1 (1.32%)	2 (2.63%)	
Reconstruction			
Maxilla 1 FS	14 (53.85%)	7 (26.92%)	
Maxilla 2 FS	3 (11.54%)	2 (7.69%)	
Mandibula 1 FS	24 (31.58%)	8 (10.53%)	
Mandibula 2 FS	19 (25.00%)	6 (7.89%)	
Mandibula 3 FS	13 (17.11%)	6 (7.89%)	
Neck dissection (ND)			
None	14 (13.73%)	12 (11.76%)	
Selective ND	23 (22.55%)	4 (3.92%)	
MR ND	36 (35.29%)	13 (12.75%)	n.s.
Neck surgery			
One side	54 (52.94%)	23 (22.55%)	
Both sides	19 (18.63%)	6 (5.66%)	$p = 0.6213$
Postoperative irradiation			
None	31 (30.39%)	16 (15.69%)	
< 60 Gy	20 (19.61%)	10 (9.80%)	
≥ 60 Gy	20 (19.61%)	2 (1.96%)	
Dosage unknown	2 (1.96%)	1 (0.98%)	n.s.

n.s. = not significant; ORN, Osteoradionecrosis; BPONJ, Bisphosphonate related osteonecrosis of the jaw; FS, number of used fibula segments; OM, Osteomyelitis; selective ND summarizes submandibular or supraomohyoidal neck dissection; MRND, modified radical ND.

Table S1 in the supplementary material depicts the collected data of our 29 patients with radiological HO (M: $n = 25$ (86.2%), F: $n = 4$ (13.8%)). Extraosseous ossification occurred in 34.6% ($n = 9$ out of 26) after maxillary and in 26.3% ($n = 20$ out of 76) after mandibular reconstruction. The difference was not statistically significant ($p = 0.4553$).

The onset of HO in the CT-scan was drawn as incidence function (Kaplan Meier function), cumulative for reconstruction of maxilla and mandible with FFF (Figure 3). After an average time of 13.48 months (median 9.0 months), HO was observed in CT scans. Comparing time of detection of HO after maxillary (median = 5 months, 95% CI = 4.0–20.0 months) and mandibular reconstruction, it is noticeable that maxillary HO occurred six months earlier than mandibular HO (median = 9.5 months, 95% CI = 5.0–13.0 months) (Figure 4).

Incidence functions for reconstruction of continuity of mandible and maxilla were calculated separately (Figure 4).

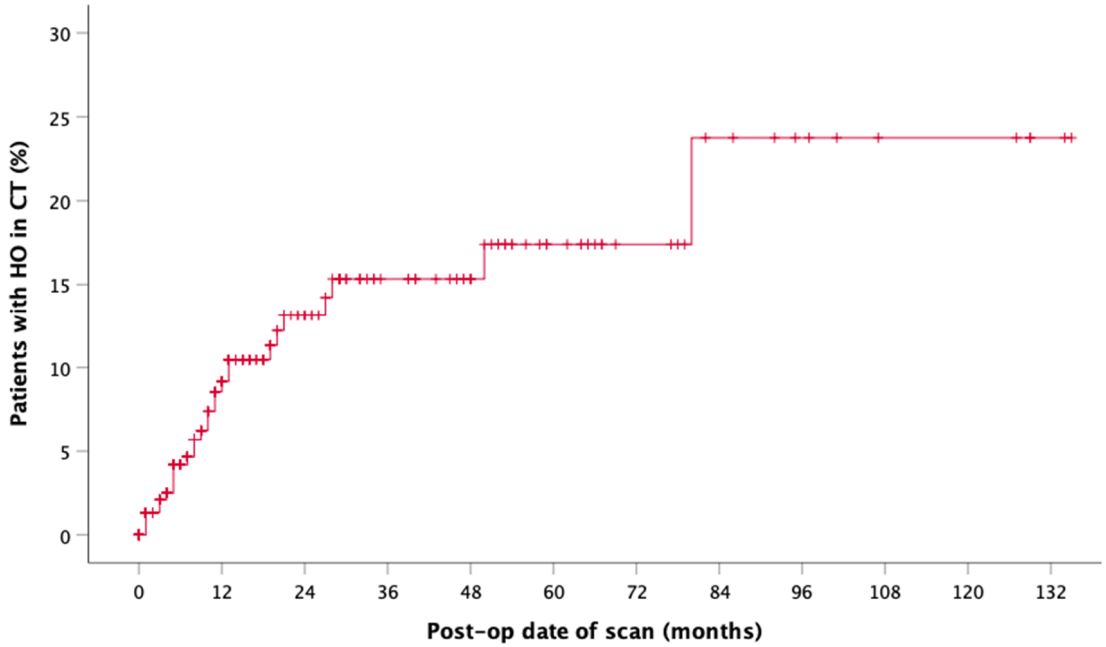

Figure 3. Incidence function shows the overall radiographic presence of HO aligned to the postoperative date of CT (n = 29).

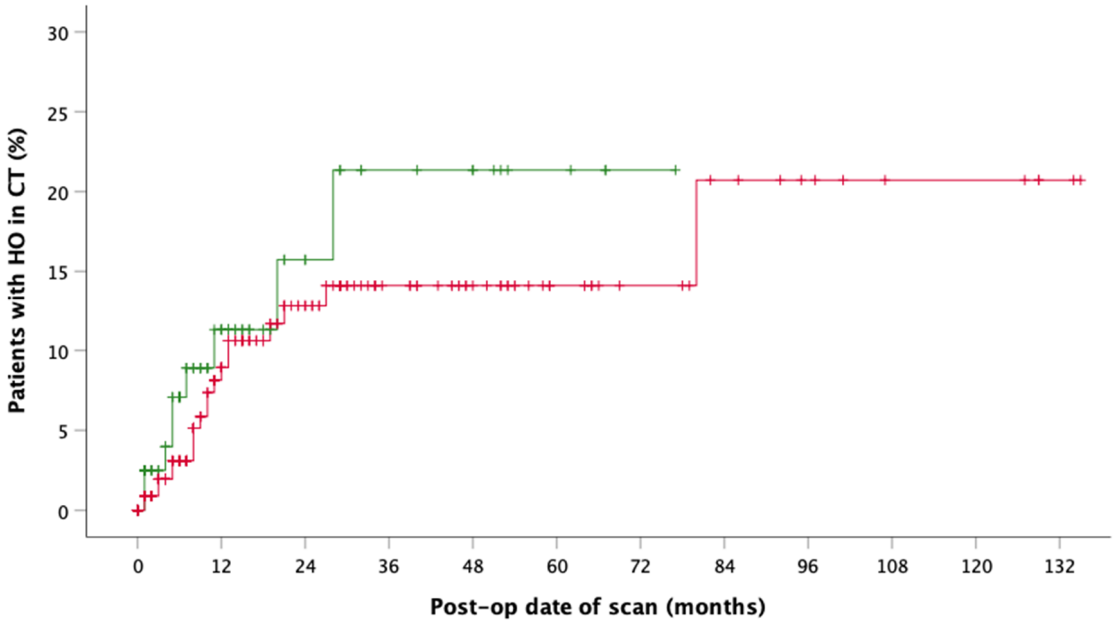

Figure 4. Incidence function shows the radiographic presence of HO by postoperative date of CT in maxillary (green, n = 9) and mandible (red, n = 20) reconstruction.

There were no statistically significant differences in the presence of radiological HO with regards to time of reconstruction (p = 0.1128) and the planning procedure, which was either analog (hand-bent, freehand osteotomized) or virtual (CAD/CAM plate, CAD/CAM cutting guides) (p = 0.3806). Jaw reconstruction was necessary in case of malignant disease in 89.22% of cases (n = 91) and 22 out of 91 developed HO. Reconstructions of continuity of the maxilla and mandible were classified by site and extent of the defect (Table 1).

The extent of cervical lymphonodectomy (selective vs. modified radical neck dissection) and no lymphonodectomy showed no influence on the presence of HO.

After adjuvant radiotherapy (RT) with <60 Gy, however, a near to similar incidence (n = 10 out of 30 (33.3%)) was observed compared to no RT (n = 16 of 47 (34.0%)). Within the subgroup of total irradiation dose of ≥60 Gy, two cases of HO (n = 2 of 22 (9.1%)) were documented. These observations were not statistically significant.

The analysis of the CT-scans showed four different patterns (types) of HO. Distribution and results are shown in Table 2. HO Type 1 was most frequently observed in four cases after maxilla (13.79%) and in 10 cases after mandible (34.48%) reconstruction with FFF. Isolated ossification of the pedicle (Type 2) accounted for seven cases in the mandible (24.14%) and 6.9% (n = 2) in the maxilla. In three cases, combined ossification (Type 4) after maxilla reconstruction (10.34%) and only one case after mandibular reconstruction were recorded. HO Type 3 was only recorded in two cases after mandibular reconstruction (6.9%). Figure 5 illustrates the distribution of HO types according to the number of fibula segments used. A homogeneous distribution of HO Type 1 is shown across all reconstruction localizations and shapes, while Type 2 and Type 4 are found in both types of jaw reconstruction. Type 3 could only be observed after mandibular reconstruction. Figure 6 outlines the appearance of HO in CT scans considering the number of used fibula segments in maxillary or mandible reconstruction. HO occurred more frequently after bi-segmental (33.3%) maxillary reconstruction compared to mono-segmental (29.1%) maxillary reconstruction. In the mandible, HO was most frequently observed after tri-segmental (26%) reconstruction compared to mono-segmental (20%) and bi-segmental (15%) reconstruction.

Table 2. HO was classified into four distinct radiological identifiable patterns. The distribution of HO types according to site of appearance (maxilla or mandible) and mean age (Minimum/Maximum), clinical impairments, and necessary surgical interventions are shown (Max., Maxilla; Mand., Mandible).

HO Type	Maxilla		Mandible		Cumulative		Complaints		Surgery	
	n	Age (Year) (Min/Max)	*n*	Age (Year) (Min/Max)	*n*	Age (Year) ± SD	Max.	Mand.	Max.	Mand.
0	17	58.65 (32.58/79.08)	56	58.70 (32.83/82.75)	73	58.69 ± 11.92				
1	4 (13.79%)	47.63 (14.75/68.25)	10 (34.48%)	54.59 (37.75/76.83)	14	52.60 ± 15.85	2	1	1	-
2	2 (6.90%)	63.5 (53.92/73.08)	7 (24.14%)	53.81 (30.0/65.66)	9	55.96 ± 13.61	1	2	1	-
3			2 (6.90%)	51.21 (46.08/56.33)	2	51.20 ± 7.25		1		-
4	3 (10.34%)	40.25 (24.41/54.0)	1 (3.45%)	53.58	4	43.58 ± 13.87	3		3	-
	9 (31.03%)	48.69 (14.75/73.08)	20 (68.97%)	53.92 (30.0/76.83)	29	52.30 ± 14.39				

T-test showed a significant difference for the parameter 'age' and presence of HO (p = 0.0236) disregarding reconstructed upper or lower jaw. A statistical sub-analysis of the parameter 'age' concerning occurrence of HO in maxillary (p = 0.158) or mandible (p = 0.232) reconstruction revealed no statistically significant difference.

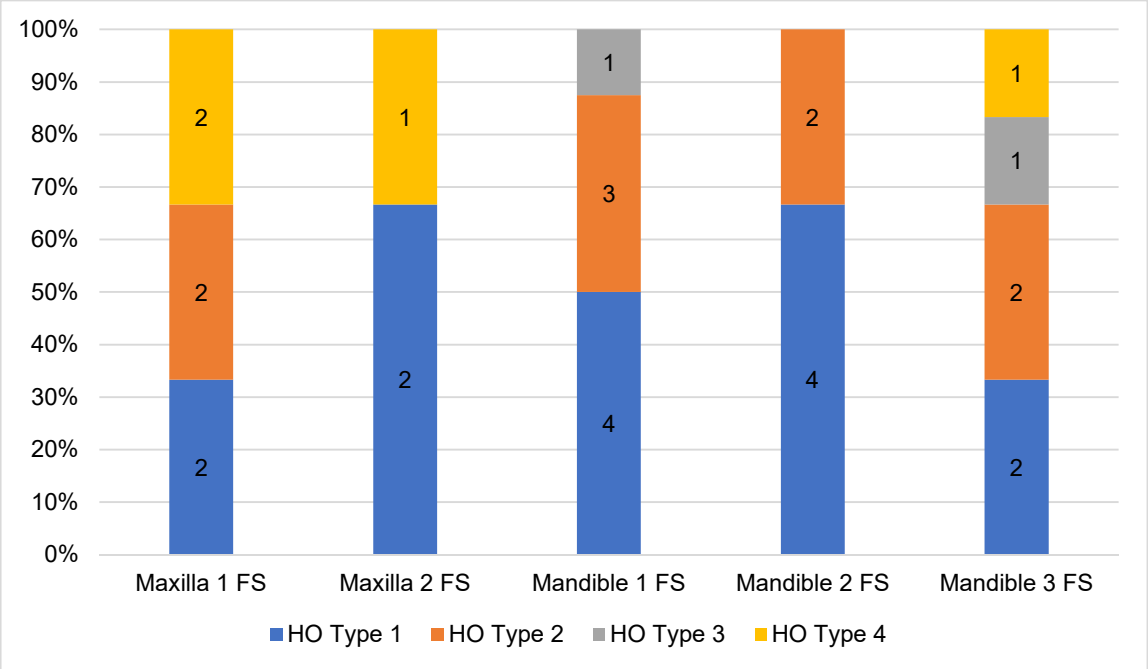

Figure 5. Distribution of HO types according to the number of used fibula segments for jaw reconstruction.

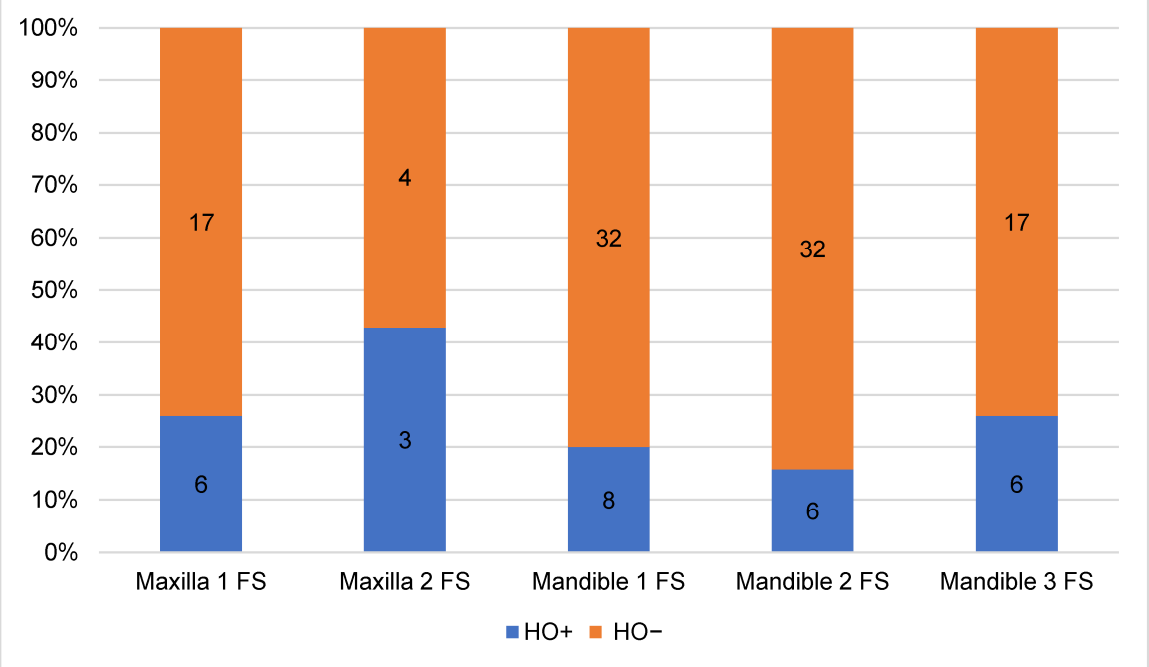

Figure 6. Relative proportion of HO in relation to localization and number of fibula segments (FS) used for jaw reconstruction.

The evaluated medical records of the HO+ group showed clinical symptoms in 10 cases with swallowing difficulties ($n = 5$), trismus ($n = 3$), and palpable bony masses in level I ($n = 2$). Clinical complaints occurred after an average time of 6.3 months. Surgical intervention with a removal of calcification was only necessary in five cases. One of the patients (Figure 7) had a two-staged, virtually planned mono-segmental maxillary reconstruction after previous resection of a recurrence of a odontogenic kerato-cyst (OKC). Early after flap transfer there was an extensive overgrowth of granulation tissue with subsequent periosteal ossification in the area of the palate and parts of the vascular pedicle (HO type 4). He suffered from

severe dyspnea and dysphagia, prompting the surgical removal of the granulation tissue and parts of the heterotopic ossification. As a temporary wound closure, the defect was covered with a split skin graft and a screw-fixed dressing plate for five days. With further progress, a modelling osteotomy was performed simultaneously with the insertion of dental implants. Histopathologic evaluation of the tissue specimen confirmed the presence of mature bone tissue (Figure 7).

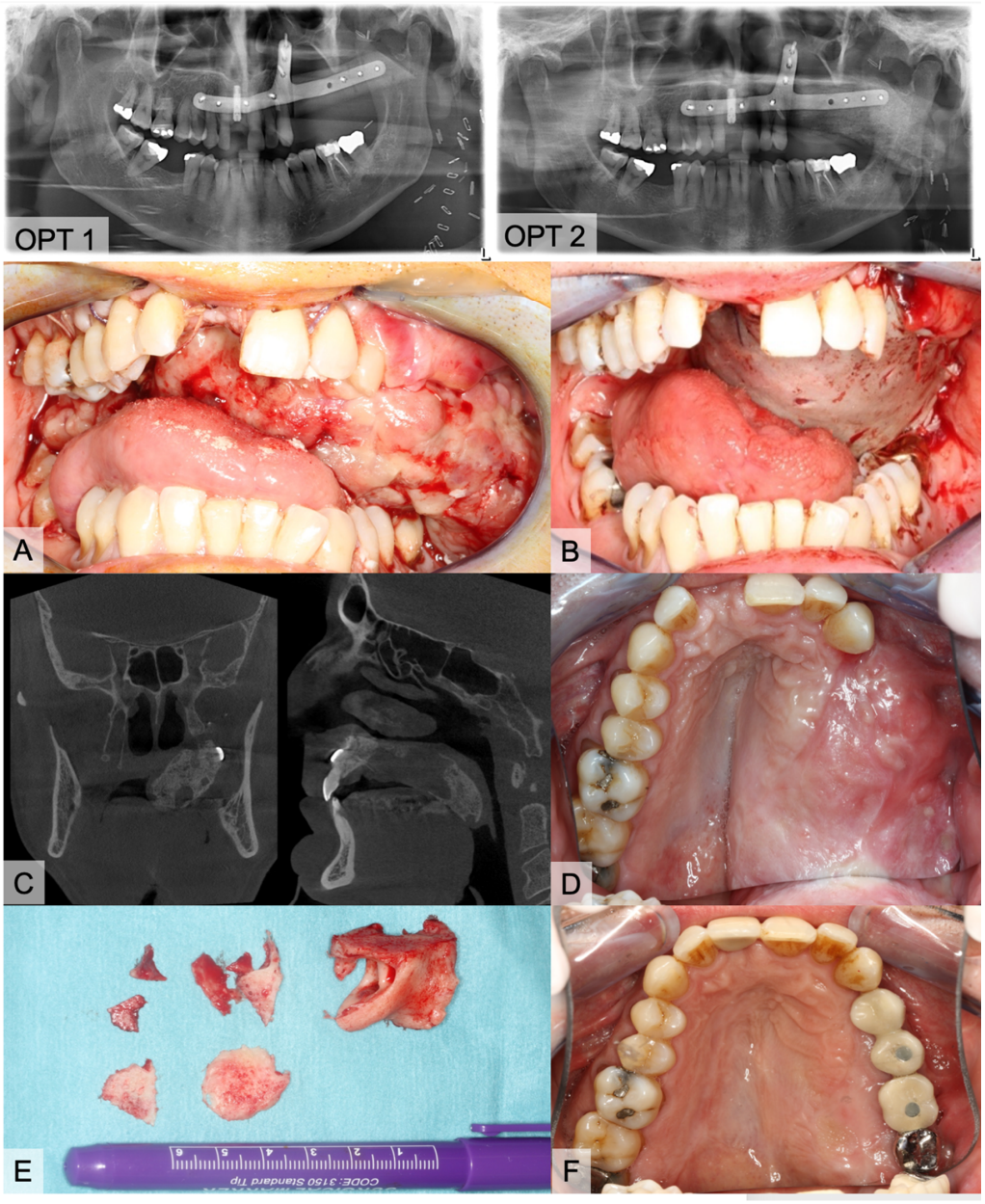

Figure 7. Images of an 54-year-old, healthy male who underwent subtotal hemi-maxillectomy due to a second recurrence of an odontogenic kerato-cyst (OKC). After more than one year later, we performed a virtually planned mono-segmental FFF transfer without a skin paddle for maxillary reconstruction (OPT 1). Three days after discharge, he consulted the emergency unit with progressive dyspnea and fear of asphyxiation in dorsal position. Clinical inspection showed large masses of soft and vulnerable granulation tissue (**A**). After carefully removing the tissue, we covered the bone with a split skin graft from the thigh (**B**). Six months later, we planned implantological rehabilitation. OPT and CBCT were accomplished and presented large bone masses at the palate (**C**, OPT 2). Clinical impression is shown on image (**D**). Prior to the insertion of four dental implants, we molded the FFF and removed bone masses (**E**). Implants were exposed four months later. Figure (**F**) shows the final prosthetic rehabilitation.

4. Discussion

4.1. HO after FFF in Literature

Radiologically detected ossifications of the vascular pedicle of osteo-fascio-cutaneous FFF are described in the literature with a high incidence of up to 65% [22,29,30]. Table 3 lists publications that reported the radiological and clinical incidences of HO after FFF. Individual case reports on the occurrence of HO after radialis flap [34], lateral upper arm flap [33], and scapula flap [36] have been published. HO rarely seems to lead to clinical symptoms and surgical correction is required even less frequently.

Table 3. Heterotopic ossification (HO): overview published cases.

Authors	Flap (*n*)	Incidence on Radiographs	Imaging	Clinical Symptoms/Surgical Removal
Deschler et al., 1997 [37]	FFF (*n* = 38)	No data available	OPT	8% (*n* = 3)
Smith et al., 2003 [27]	FFF, CR		CT	(*n* = 1)
Autelitano et al., 2008 [26]	FFF (*n*~100)	No data available		~4% (*n* = 4)
Gonzales-Garcia et al., 2011 [25]	FFF, CR		CT	(*n* = 1)
Colletti et al., 2014 [38]	FFF (*n* = 92)	No data available		4.3% (*n* = 4)
Acarturk et al., 2011 [39]	FFF, CR		CT	(*n* = 1)
DeConde et al., 2011 [22]	FFF (*n* = 520) *	65% (*n* = 43 out of 66)	CT	2.6% (*n* = 14 out of 520)
Myon et al., 2012 [36]	FFF (*n* = 149) SF (*n* = 13)	9.2% (*n* = 15) (*n* = 14) (*n* = 1)	OPT, CT	3.7% (*n* = 6)
Karagozoglu et al., 2013 [30]	FFF (*n* = 74)	27% (*n* = 20)	OPT	No data
Tarsitano et al., 2013 [21]	FFF sp (*n*= 41) mp (*n* = 20)	17% (*n* = 7) 0%	OPT, CT	4.9% (*n* = 2)
Glastonbury et al., 2014 [29]	FFF (*n* = 32)	50% (*n* = 16)	CT	3.13% (*n* = 1)
Baserga et al., 2016 [28]	FFF (*n* = 68)	No data		4.4% (*n* = 3)
This study	FFF (*n*=102)	28.4% (*n* = 29)	CT, CBCT	9.8% (*n* = 10)/ 4.9% (*n* = 5)

CR Case Report, FFF = fibular free flap, SF = scapula flap, sp = standard procedure, mp = modified supra-periosteal procedure, * from 520 cases only 66 CT-scans were available for multiplanar reconstruction and analysis.

Different theories on the origin of HO are discussed. In osteo-fascio-cutaneous flaps, periosteal tissue near to the vascular pedicle seems to play a central role [26] as well as local mechanical factors and cytokine interactions [31]. The FFF harvesting technique with remaining periosteum on the vascular pedicle has significant influence on the development of HO [21,32]. All FFF in the investigation were harvested by the lateral approach [40] on the angled, perfused lower leg. In case of multi-segmental reconstructions, the corresponding preparation of the fibula was completed with the application of miter cuts (freestyle or prefabricated cutting guides) and osteosynthesis (hand-bent or custom-made). The proximal, free fibula segment was de-periosted, osteotomized and either discarded or used as a free graft (e.g., particulate). The exposed periosteum partially remains on the vascular pedicle, which is surrounded by a muscle layer. Preferred microvascular recipient vessels were the A. thyroidea superior or A. facialis. Direct end-to-end anastomosis of the external carotid artery was rarely used. While a long vascular pedicle facilitates microsurgical-vascular handling, it increases the risk of kinking pedicle. The longer vascular pedicle is prepared to a larger extent than the area with remaining adherent periosteum will be, from which HO can commence. Especially in young patients, careful periosteum-free

vascular pedicle preparation should therefore be emphasized [39]. Tarsitano et al. could not observe any case of HO [36] by this modified harvesting technique (n = 20) with removal of the periosteum adhering to the vascular pedicle, which emphasizes a possible key role of osseo-inductive cells of the periosteum in the etiology of HO [21]. The periosteum is suspected to be a privileged target of recombinant human bone morphogenetic protein 2 [36]. Colletti et al. conclude that careful separation of the vascular pedicle from the periosteum seems to prevent HO [38]. An additional modification of this FFF harvesting procedure described by Kim et al. [32] suggests that, due to virtual planning, the extent of required fibula is exactly known and thus supra-periosteal proximal preparation can be performed after branching out of the fibular artery to the planned proximal osteotomy. They state that it is possible to omit one surgical step and thus shorten flap harvesting time [32]. Despite supra-periosteal dissection, there are cases in which pedicle ossification occurs [41]. The supra-periosteal dissection was not performed in the investigated group.

In addition to the outlined role of periosteal osteoprogenitor cells, other theories are discussed. The theory of fracture repair focuses on the presence of all cellular and molecular players such as bone morphogenetic protein (BMP), which are important for bone healing [42]. The ligands of the BMP signaling pathway, BMP-2 and BMP-4, have been known to induce bone formation for several decades [43,44]. Multiple studies have used this fact to recreate HO in vivo [45–47] or analyze the mechanistic basis of HO in vitro [48,49].

Blood flow and perfusion theory aims at changed pressure conditions in the arterial and venous system of the FFF after transfer of the arterial moderate and relative venous high pressure situation (valves, muscle pump) on the lower leg compared to the high arterial and low venous pressure situation of the head and neck region [36]. In addition, after microsurgical anastomosis of the vessels, there were changes in the flap perfusion. After flap dissection small arterial and venous collaterals were interrupted. Both factors, a higher arterial perfusion pressure at the cervical acceptor site and less opportunity of flap drainage to the surrounded tissue, can inflate the flap tissue. The mechanical theory describes the influence of physiological forces due to micro-stress on the callus and the bone healing of the attachment surfaces in the upper and lower jaw [21,25,31,36].

4.2. Classification of Four Different HO Patterns and Biological Etiology

The HO classification suggested in this study distinguishes four types of HO. Type 1 is the most frequently observed variant across all reconstruction sites and forms. Concerning the referred theories of HO etiology, the bone healing/fracture repair theory describes the origin of HO from the resection site. Functional stress to the stabilized bone graft induces micromotion and enhances bone healing and callus growth [36]. We hypothesize that, as a result, the calcified tissue is a type of excessive bone healing that originates from the resection site and courses along the remaining periosteum at the pedicle by molecular stimulation from osteoprogenitor recruitment [31,42,50].

Type 2 may be the result of isolated periosteal cells in contact with osteocytes along the pedicle from osteo-cutaneous FFF [26,51–53]. A long vascular pedicle with remaining periosteal cells therefore offers more potential for the development of HO [25]. We expected that HO Type 2 will be more common, especially in maxillary reconstructions but we found only two cases after maxilla, but seven cases after mandible reconstruction. However, molecular interactions and the influence of BMPs on the induction of wound healing could promote HO formation [31]. Local factors could have additional influence after bone resections.

HO Type 3 was only observed after mandible reconstruction. Its clinical appearance is similar to torus mandibularis. The occurrence of ectopic oral bone formation is probably the result of functional aspects of mastication [54,55]. Thus, this HO type could be triggered by manipulation of the periosteum and its dissection during preparation and maintained by functional factors induced by mastication. In addition, mechanical stress (tension) supports BMP signaling [31]. Keeping this in mind, we expected to find HO Type 3 occurring more frequently in poly-segmental reconstructions close to the resection sites

and more particularly at intersegmental graft sites. There are discrepancies between cross sections of resection sites and FFF. Remnant free periosteum after poly-segmental shaping procedure around vascular bundle needs to be considered as an origin of HO. There were no clear reasons why HO Type 3 was not found after maxillary reconstruction. One thinkable hypothesis is that HO Type 3 origin might be an hyperperfused and inflated bone feeder vessel via the above-mentioned mechanisms of blood flow and perfusion theory. For maxillary reconstruction the strong and rigid tissue of the gum might be a sufficient resistance to prevent its development in compare to the more loose and wide tissue of the floor of the mouth.

Changes in blood flow and pressure could also induce HO Type 4 [36]. Three cases after maxilla and one after mandible reconstruction can be assigned to HO Type 4. This pattern was observed in younger patients (mean age 43.58 y). Focused on the morphological architecture of the surrounding soft tissue, the micro-vessels seem to be inflated. There is also an increase in bone and blood vessels during callus healing normally reported in stabilized fractures [56]. In the clinical case presented in Figure 7, we hypothesize that the overwhelming granulation of the soft tissue might be an early clinical expression of upcoming HO. Only in this case was no skin paddle used to cover the soft tissue of the graft which obviously led to granulation tissue. The low pressure from the surrounding functional soft tissue (tongue, floor of mouth, cheek) appears to be one possible cofactor in the development of HO. In maxilla reconstruction, a tunnel for the vascular pedicle has to be dissected bluntly. Following McCarthy's remarks, a superficial tunnel in the face-lift plane facilitates the course of vessels and, if the maxillary tubercle is resected, access can be gained by a parapharyngeal approach medial to the mandible [57]. Here, we also recognized HO (Figures 1, 2 and 7). In mandible reconstruction, HO Type 4 was not as distinctive as in maxilla reconstruction. It is conceivable that the neck tissue surrounding the vascular pedicle sufficiently counteracts the changed perfusion pressures after flap transfer. This could be a reason why pronounced changes such as in the tunnel area of the oral cavity after maxilla reconstruction could not be observed.

4.3. Impact of Analogous and Virtual Planning

In the literature, HO appears to occur more frequently in maxillary reconstructions [27,36]. HO was found in 34% (n = 9 of 26) of all cases of maxillary reconstructions with FFF. This corresponds to a ratio of approximately 1:3. However, overall, more than two thirds of radiological observed HO cases (69%, n = 20) were recorded after mandibular reconstruction. At a total number of 76 successfully performed mandibular reconstructions, we identified 20 cases of HO. This corresponds to a ratio of about 1:4. Since 2015, we have been planning jaw reconstructions digitally. The results show a radiological incidence after analogous (11.45%) and digitally (10.69%) planning procedures. However, in the early years of jaw reconstruction, cases were planned analogously and were realized "manually" [58]. In recent years computer-assisted planning is clinical routine and, in addition to custom-made resection and cutting guides, patient-specific manufactured osteosynthesis plates are available [59–64]. The selection of the donor region and reconstruction morphology is the subject of current research into the use of algorithm-based automated procedures [65]. There was no significant difference in the presence of HO between virtually planned and CAD/CAM stabilized fibula (10.69%) grafts than in those of analog and hand-bent osteosynthesis (11.45%).

4.4. Frequency of Clinical Symptoms and Surgical Removal of HO

Although the ossification of the vascular pedicle according to radiological criteria seems to be common [29], clinical complications seems to be rare. Despite a radiological incidence of over 28.43%, we identified 10 cases of clinically symptomatic HO (9.8%) in the investigated collective with swallowing difficulties (n = 5), trismus (n = 3), and bony masses in level I (n = 2). Only five patients (4.9%) needed a surgical intervention to remove calcification. On average, clinical complaints occurred after 4.4 months and surgical removal of calcified structures was performed after 12.6 months. HO and the planned

removal of HO-related structures is a definite indication for surgery. In our opinion, changing the surgical harvesting procedure (supra-periosteal preparation of the proximal pedicle) does not seem to be advisable regarding the background of the low incidence of clinical symptomatic HO and the multifactorial genesis, where the periosteum plays an essential role.

However, excessive new bone formation in the entire graft area (HO Type 4) can result in massive clinical impairment [27]. Depending on graft location, the course of the vascular bundle and the region of anastomosis, the incidence of HO may be underestimated. According to the literature, HO is rarely symptomatic in a way that surgical intervention is indicated. However, removal of ectopic bone mass may be necessary in cases of impaired movement of mandibula, pain during mastication or disturbing submandibular masses in neck level I or II after exclusion of a recurrence of the proper oncological disease [21,36]. It is remarkable that all five surgically treated cases in the present investigation occurred after maxillary reconstruction, because of functional impairment (Table 2). In case of extensive periosseous HO, modelling osteotomy for recontouring and application of a screw-fixed dressing plate may be considered as a therapeutic strategy. Ossification of the vascular pedicle at the transition from FFF to pedicle (Type 1) and isolated HO of the pedicle (Type 2) can be treated surgically if clinical symptoms are clear. Careful, subtle preparation of vascular stalk is only necessary during the early phase after transplantation until the graft is adequately perfused with blood. Myon et al. report that, in one case, the removal of a pedicle-associated HO did not lead to any reduction of the flap vitality [36]. Sufficient neovascularization to allow FFF survival independent of the vascular pedicle has been reported to occur within 4 to 12 weeks [66].

4.5. Effect of Irradiation on HO Occurrence

It is interesting to note that adjuvant irradiation (group <60 Gy and ≥60 Gy) leads to a decrease of the number of HO cases (not statistically significant). In orthopedic surgery, the hip is the most common site of HO development and treatment. Radiotherapy (RT) has been shown to be particularly effective in the hip, knee, and elbow area. In studies, uni-fractionated radiation application of 7 Gy was performed after elbow surgery and was associated with favorable functional and radiological result [67]. Another study of nine patients with clinically significant HO at the elbow reported a majority of clinical improvement after irradiation. In this study, 5 Gy in two fractions and 6–7 Gy in one fraction were applied. The mean follow-up was 7.7 months [68]. For prevention of HO after hip endo-prosthetics, prophylactic radiotherapy with 1 × 7 Gy immediately before or up to 24 h after surgery is recommended [69]. This leads to the question of the influence of fractionation at overall low doses of 7 to 16–17 Gy. In adjuvant radiotherapy in the head and neck region single applications between 1.8–2.2 Gy are normally used. In summary, there are four main differences in oncological adjuvant RT in head and neck: low single application dosage between 1.8–2.2 Gy per fraction, onset of RT up to four weeks after operation, overall cumulative irradiation dose (56–72 Gy), and amount of 33–34 fractions.

4.6. Limitations of This Study

The evaluation shows statistically significant differences concerning 'Age' and the occurrence of HO. However, subgroup analysis concerning maxillary or mandible reconstruction mean age was without any significant results. However, where there is a difference in mean of 10 years between the HO+ and HO− groups in maxilla reconstructions, the number of cases is too small and the age distribution too broad to reach statistical significance.

Limitations of the presented study are the retrospective design and the lack of defined imaging time points, so that the mean or median first observation time of HO at 3.48 and 9.0 months appears late. Glastonbury et al. described typical imaging findings of HO in three cases only one month after FFF [29]. However, the incidence functions show that about half of the observed cases become visible in CT scan within the first 12 postoperative

months. The second half only develop in the following six years. The reasons for this remain unclear. Bone or fracture healing is complete so that continuous remodeling processes could play a role. Our mixed patient collective was mostly formed of oncologic patients (87.78%). Two third were male and one third female. About 86% of the radiologically detected HO cases were male patients which could be a selection bias. Therefore, the bias continued in the clinical (M = 8, F = 2) and in the surgically treated group (M = 4, F = 1).

Finally, further investigation and more data is necessary to validate this newly introduced classification. Any new classification in medicine should be verified by an independent cohort.

5. Conclusions

Extraosseous heterotopic ossification (HO) is a known phenomenon of osteo-cutaneous fibular free flap (FFF) after ablative tumor surgery and jaw reconstruction and can lead to clinical complications. Trismus, mastication pain and/or rough submandibular masses could be an indicator of HO if postoperative scars and tumor recurrence are excluded.

Radiologically, HO appears to occur more frequently in younger and male patients. No correlation between HO and the method of planning (analog vs. digital), the type of osteosynthesis (hand-bent vs. custom-made), or time of reconstruction (immediately vs. delayed) were found. A modified harvesting technique with a vascular pedicle without periosteal tissue seems to be an effective method to avoid heterotopic ossifications. This method could prevent the development of HO in maxillary reconstruction. In case of extensive HO, the modelling osteotomy for jaw recontouring and the application of a screw-fixed dressing plate could be considered as a therapeutic strategy.

To our knowledge, this is the first study to describe a classification of four different radiological HO patterns. Further studies for the classification's validation are required.

Supplementary Materials: The following are available online at https://www.mdpi.com/2077-0383/10/1/109/s1, Table S1: Characteristics of HO+ cases (n= 29) after FFF.

Author Contributions: Conceptualization, M.K., S.A. and H.-P.H.; Data curation, M.K. and K.S.; Formal analysis, M.K., K.S., C.B. and S.A.; Investigation, M.K. and K.S.; Methodology, M.K.; Project administration, S.B.; Supervision, H.-P.H. and S.B.; Validation, M.K.; Visualization, M.K. and S.B.; Writing—original draft, M.K. and K.S.; Writing—review & editing, C.B., S.A., H.-P.H. and S.B. All authors have read and agreed to the published version of the manuscript.

Funding: This research received no external funding.

Institutional Review Board Statement: The study was conducted according to the guidelines of the Declaration of Helsinki and approved by the Ethics Committee of Justus-Liebig University Giessen (AZ34/20).

Informed Consent Statement: Patients' permission/consent was not necessary in this retrospective study.

Data Availability Statement: The data presented in this study are available on request from the corresponding author.

Acknowledgments: The authors are grateful for the consent of the patient for presented X-rays and clinical images. This publication forms part of the dental doctoral thesis of the second author (KS).

Conflicts of Interest: The authors declare no conflict of interest.

References

1. Hayden, R.E.; Mullin, D.P.; Patel, A.K. Reconstruction of the segmental mandibular defect: Current state of the art. *Curr. Opin. Otolaryngol. Head Neck Surg.* **2012**, *20*, 231–236. [CrossRef]
2. Hidalgo, D.A. Fibula free flap: A new method of mandible reconstruction. *Plast. Reconstr. Surg.* **1989**, *84*, 71–79. [CrossRef]
3. Brown, J.S.; Barry, C.; Ho, M.; Shaw, R. A new classification for mandibular defects after oncological resection. *Lancet Oncol.* **2016**, *17*, e23–e30. [CrossRef]
4. Hakim, S.G.; Kimmerle, H.; Trenkle, T.; Sieg, P.; Jacobsen, H.C. Masticatory rehabilitation following upper and lower jaw reconstruction using vascularised free fibula flap and enossal implants-19 years of experience with a comprehensive concept. *Clin. Oral Investig.* **2015**, *19*, 525–534. [CrossRef]

5. Attia, S.; Wiltfang, J.; Streckbein, P.; Wilbrand, J.F.; El Khassawna, T.; Mausbach, K.; Howaldt, H.P.; Schaaf, H. Functional and aesthetic treatment outcomes after immediate jaw reconstruction using a fibula flap and dental implants. *J. Craniomaxillofac. Surg.* **2019**, *47*, 786–791. [CrossRef]
6. Attia, S.; Wiltfang, J.; Pons-Kuhnemann, J.; Wilbrand, J.F.; Streckbein, P.; Kahling, C.; Howaldt, H.P.; Schaaf, H. Survival of dental implants placed in vascularised fibula free flaps after jaw reconstruction. *J. Craniomaxillofac. Surg.* **2018**, *46*, 1205–1210. [CrossRef]
7. Bluebond-Langner, R.; Rodriguez, E.D. Application of skeletal buttress analogy in composite facial reconstruction. *Craniomaxillofac. Trauma Reconstr.* **2009**, *2*, 19–25. [CrossRef]
8. Attia, S.; Diefenbach, J.; Schmermund, D.; Böttger, S.; Pons-Kühnemann, J.; Scheibelhut, C.; Heiss, C.; Howaldt, H.-P. Donor-Site Morbidity after Fibula Transplantation in Head and Neck Tumor Patients: A Split-Leg Retrospective Study with Focus on Leg Stability and Quality of Life. *Cancers* **2020**, *12*, 2217. [CrossRef]
9. Schusterman, M.A.; Reece, G.P.; Miller, M.J.; Harris, S. The osteocutaneous free fibula flap: Is the skin paddle reliable? *Plast. Reconstr. Surg.* **1992**, *90*, 787–793. [CrossRef]
10. Jones, N.F.; Monstrey, S.; Gambier, B.A. Reliability of the fibular osteocutaneous flap for mandibular reconstruction: Anatomical and surgical confirmation. *Plast. Reconstr. Surg.* **1996**, *97*, 707–716. [CrossRef]
11. Wong, C.H.; Tan, B.K.; Wei, F.C.; Song, C. Use of the soleus musculocutaneous perforator for skin paddle salvage of the fibula osteoseptocutaneous flap: Anatomical study and clinical confirmation. *Plast. Reconstr. Surg.* **2007**, *120*, 1576–1584. [CrossRef]
12. Winters, H.A.; de Jongh, G.J. Reliability of the proximal skin paddle of the osteocutaneous free fibula flap: A prospective clinical study. *Plast. Reconstr. Surg.* **1999**, *103*, 846–849. [CrossRef]
13. Schusterman, M.A.; Harris, S.W.; Raymond, A.K.; Goepfert, H. Immediate free flap mandibular reconstruction: Significance of adequate surgical margins. *Head Neck* **1993**, *15*, 204–207. [CrossRef] [PubMed]
14. Chana, J.S.; Chang, Y.M.; Wei, F.C.; Shen, Y.F.; Chan, C.P.; Lin, H.N.; Tsai, C.Y.; Jeng, S.F. Segmental mandibulectomy and immediate free fibula osteoseptocutaneous flap reconstruction with endosteal implants: An ideal treatment method for mandibular ameloblastoma. *Plast. Reconstr. Surg.* **2004**, *113*, 80–87. [CrossRef]
15. Schaaf, H.; Wahab-Gothe, T.; Kerkmann, H.; Streckbein, P.; Obert, M.; Pons-Kuehnemann, J.; Ahrens, M.; Howaldt, H.P.; Attia, S. Comparison between flat-panel volume computed tomography and histologic assessments of bone invasion of maxillofacial tumors: Utility of an instantaneous radiologic diagnostic tool. *Oral Surg. Oral Med. Oral Pathol. Oral Radiol.* **2017**, *124*, 191–198. [CrossRef]
16. Iizuka, T.; Hafliger, J.; Seto, I.; Rahal, A.; Mericske-Stern, R.; Smolka, K. Oral rehabilitation after mandibular reconstruction using an osteocutaneous fibula free flap with endosseous implants. Factors affecting the functional outcome in patients with oral cancer. *Clin. Oral Implants Res.* **2005**, *16*, 69–79. [CrossRef]
17. Marsell, R.; Einhorn, T.A. The biology of fracture healing. *Injury* **2011**, *42*, 551–555. [CrossRef]
18. Verhelst, P.J.; Dons, F.; Van Bever, P.J.; Schoenaers, J.; Nanhekhan, L.; Politis, C. Fibula Free Flap in Head and Neck Reconstruction: Identifying Risk Factors for Flap Failure and Analysis of Postoperative Complications in a Low Volume Setting. *Craniomaxillofac. Trauma Reconstr.* **2019**, *12*, 183–192. [CrossRef]
19. Zavattero, E.; Fasolis, M.; Garzino-Demo, P.; Berrone, S.; Ramieri, G.A. Evaluation of plate-related complications and efficacy in fibula free flap mandibular reconstruction. *J. Craniofac. Surg.* **2014**, *25*, 397–399. [CrossRef]
20. Rendenbach, C.; Steffen, C.; Hanken, H.; Schluermann, K.; Henningsen, A.; Beck-Broichsitter, B.; Kreutzer, K.; Heiland, M.; Precht, C. Complication rates and clinical outcomes of osseous free flaps: A retrospective comparison of CAD/CAM versus conventional fixation in 128 patients. *Int. J. Oral Maxillofac. Surg.* **2019**, *48*, 1156–1162. [CrossRef]
21. Tarsitano, A.; Sgarzani, R.; Betti, E.; Oranges, C.M.; Contedini, F.; Cipriani, R.; Marchetti, C. Vascular pedicle ossification of free fibular flap: Is it a rare phenomenon? Is it possible to avoid this risk? *Acta Otorhinolaryngol. Ital.* **2013**, *33*, 307–310. [PubMed]
22. DeConde, A.S.; Vira, D.; Blackwell, K.E.; Moriarty, J.M.; Sercarz, J.A.; Nabili, V. Neck mass due to pedicle ossification after oromandibular reconstruction. *Laryngoscope* **2011**, *121*, 2095–2099. [CrossRef] [PubMed]
23. Edwards, D.S.; Clasper, J.C. Heterotopic ossification: A systematic review. *J. R. Army Med. Corps* **2015**, *161*, 315–321. [CrossRef] [PubMed]
24. Dey, D.; Wheatley, B.M.; Cholok, D.; Agarwal, S.; Yu, P.B.; Levi, B.; Davis, T.A. The traumatic bone: Trauma-induced heterotopic ossification. *Transl. Res.* **2017**, *186*, 95–111. [CrossRef] [PubMed]
25. Gonzalez-Garcia, R.; Manzano, D.; Ruiz-Laza, L.; Moreno-Garcia, C.; Monje, F. The rare phenomenon of vascular pedicle ossification of free fibular flap in mandibular reconstruction. *J. Craniomaxillofac. Surg.* **2011**, *39*, 114–118. [CrossRef]
26. Autelitano, L.; Colletti, G.; Bazzacchi, R.; Biglioli, F. Ossification of vascular pedicle in fibular free flaps: A report of four cases. *Int. J. Oral Maxillofac. Surg.* **2008**, *37*, 669–671. [CrossRef]
27. Smith, R.B.; Funk, G.F. Severe trismus secondary to periosteal osteogenesis after fibula free flap maxillary reconstruction. *Head Neck* **2003**, *25*, 406–411. [CrossRef]
28. Baserga, C.; Massarelli, O.; Bolzoni, A.R.; Rossi, D.S.; Beltramini, G.A.; Baj, A.; Gianni, A.B. Fibula free flap pedicle ossification: Experience of two centres and a review of the literature. *J. Craniomaxillofac. Surg.* **2018**, *46*, 1674–1678. [CrossRef]
29. Glastonbury, C.M.; van Zante, A.; Knott, P.D. Ossification of the vascular pedicle in microsurgical fibular free flap reconstruction of the head and neck. *AJNR Am. J. Neuroradiol.* **2014**, *35*, 1965–1969. [CrossRef]

30. Karagozoglu, K.H.; Winters, H.A.; Forouzanfar, T.; Schulten, E.A. Periosteal ossification of the vascular pedicle after reconstruction of continuity defects of the mandible and the maxilla with fibular free flaps: A retrospective study. *Br. J. Oral Maxillofac. Surg.* **2013**, *51*, 965–967. [CrossRef]
31. Yu, Y.Y.; Lieu, S.; Lu, C.; Colnot, C. Bone morphogenetic protein 2 stimulates endochondral ossification by regulating periosteal cell fate during bone repair. *Bone* **2010**, *47*, 65–73. [CrossRef] [PubMed]
32. Kim, B.B.; Kaleem, A.; Alzahrani, S.; Yeoh, M.; Zaid, W. Modified fibula free flap harvesting technique for prevention of heterotopic pedicle ossification. *Head Neck* **2019**, *41*, E104–E112. [CrossRef] [PubMed]
33. Jehn, P.; Zimmerer, R.; Dittmann, J.; Fedchenko, M.; Gellrich, N.C.; Spalthoff, S. Ossification of the Vascular Pedicle After Microsurgical Soft Tissue Transfer of the Lateral Upper Arm Free Flap. *Ann. Plast. Surg.* **2019**, *83*, e39–e42. [CrossRef] [PubMed]
34. Gangidi, S.R.; Courtney, D. "You reap what you sow"—A case of heterotopic ossification within a fasciocutaneous radial forearm free flap reconstruction. *Int. J. Oral Maxillofac. Surg.* **2013**, *42*, 458–459. [CrossRef] [PubMed]
35. Brown, J.S.; Shaw, R.J. Reconstruction of the maxilla and midface: Introducing a new classification. *Lancet Oncol.* **2010**, *11*, 1001–1008. [CrossRef]
36. Myon, L.; Ferri, J.; Genty, M.; Raoul, G. Consequences of bony free flap's pedicle calcification after jaw reconstruction. *J. Craniofac. Surg.* **2012**, *23*, 872–877. [CrossRef]
37. Deschler, D.G.; Hayden, R.E. Bone spur presenting as a submandibular mass following free fibula reconstruction of the mandible. *Am. J. Otolaryngol.* **1997**, *18*, 425–427. [CrossRef]
38. Colletti, G.; Autelitano, L.; Rabbiosi, D.; Biglioli, F.; Chiapasco, M.; Mandala, M.; Allevi, F. Technical refinements in mandibular reconstruction with free fibula flaps: Outcome-oriented retrospective review of 99 cases. *Acta Otorhinolaryngol. Ital.* **2014**, *34*, 342–348.
39. Acarturk, T.O.; Aslaner, E.E. Periosteal ossification from the vascular pedicle of a free fibular flap. *J. Craniofac. Surg.* **2011**, *22*, e29–e32. [CrossRef]
40. Gilbert, A. Vascularised transfer of the fibula shaft. *Int. J. Microsurg.* **1979**, *1*, 100.
41. Mays, A.C.; Gillenwater, A.M.; Garvey, P.B. Rare presentation of heterotopic ossification along a fibula free flap pedicle in a high-volume microvascular reconstruction practice. *Head Neck* **2018**, *40*, E21–E24. [CrossRef] [PubMed]
42. Kwong, F.N.; Harris, M.B. Recent developments in the biology of fracture repair. *J. Am. Acad. Orthop. Surg.* **2008**, *16*, 619–625. [CrossRef] [PubMed]
43. Urist, M.R.; Mikulski, A.; Lietze, A. Solubilized and insolubilized bone morphogenetic protein. *Proc. Natl. Acad. Sci. USA* **1979**, *76*, 1828–1832. [CrossRef] [PubMed]
44. Takagi, K.; Urist, M.R. The reaction of the dura to bone morphogenetic protein (BMP) in repair of skull defects. *Ann. Surg.* **1982**, *196*, 100–109. [CrossRef]
45. Lounev, V.Y.; Ramachandran, R.; Wosczyna, M.N.; Yamamoto, M.; Maidment, A.D.; Shore, E.M.; Glaser, D.L.; Goldhamer, D.J.; Kaplan, F.S. Identification of progenitor cells that contribute to heterotopic skeletogenesis. *J. Bone Joint Surg. Am.* **2009**, *91*, 652–663. [CrossRef]
46. Liu, X.; Kang, H.; Shahnazari, M.; Kim, H.; Wang, L.; Larm, O.; Adolfsson, L.; Nissenson, R.; Halloran, B. A novel mouse model of trauma induced heterotopic ossification. *J. Orthop. Res.* **2014**, *32*, 183–188. [CrossRef]
47. Uchibe, K.; Son, J.; Larmour, C.; Pacifici, M.; Enomoto-Iwamoto, M.; Iwamoto, M. Genetic and pharmacological inhibition of retinoic acid receptor gamma function promotes endochondral bone formation. *J. Orthop. Res.* **2017**, *35*, 1096–1105. [CrossRef]
48. Tian, X.B.; Sun, L.; Yang, S.H.; Fu, R.Y.; Wang, L.; Lu, T.S.; Zhang, Y.K.; Fu, D.H. Ectopic osteogenesis of mouse bone marrow stromal cells transfected with BMP 2/VEGF(165) genes in vivo. *Orthop. Surg.* **2009**, *1*, 322–325. [CrossRef]
49. Peterson, J.R.; De La Rosa, S.; Sun, H.; Eboda, O.; Cilwa, K.E.; Donneys, A.; Morris, M.; Buchman, S.R.; Cederna, P.S.; Krebsbach, P.H.; et al. Burn injury enhances bone formation in heterotopic ossification model. *Ann. Surg.* **2014**, *259*, 993–998. [CrossRef]
50. Shirley, D.; Marsh, D.; Jordan, G.; McQuaid, S.; Li, G. Systemic recruitment of osteoblastic cells in fracture healing. *J. Orthop. Res.* **2005**, *23*, 1013–1021. [CrossRef]
51. Burstein, F.D.; Canalis, R.F. Studies on the osteogenic potential of vascularized periosteum: Behavior of periosteal flaps transferred onto soft tissues. *Otolaryngol. Head Neck Surg.* **1985**, *93*, 731–735. [CrossRef] [PubMed]
52. Ortak, T.; Ozdemir, R.; Uysal, A.; Ulusoy, M.G.; Sungur, N.; Sahin, B.; Kocer, U.; Sensoz, O. Osteogenic capacities of periost grafts, periost flaps and prefabricated periosteal flaps: Experimental study. *J. Craniofac. Surg.* **2005**, *16*, 594–600. [CrossRef] [PubMed]
53. Takato, T.; Harii, K.; Nakatsuka, T.; Ueda, K.; Ootake, T. Vascularized periosteal grafts: An experimental study using two different forms of tibial periosteum in rabbits. *Plast. Reconstr. Surg.* **1986**, *78*, 489–497. [CrossRef] [PubMed]
54. Cortes, A.R.; Jin, Z.; Morrison, M.D.; Arita, E.S.; Song, J.; Tamimi, F. Mandibular tori are associated with mechanical stress and mandibular shape. *J. Oral Maxillofac. Surg.* **2014**, *72*, 2115–2125. [CrossRef] [PubMed]
55. Morrison, M.D.; Tamimi, F. Oral tori are associated with local mechanical and systemic factors: A case-control study. *J. Oral Maxillofac. Surg.* **2013**, *71*, 14–22. [CrossRef] [PubMed]
56. Claes, L.; Eckert-Hubner, K.; Augat, P. The effect of mechanical stability on local vascularization and tissue differentiation in callus healing. *J. Orthop. Res.* **2002**, *20*, 1099–1105. [CrossRef]
57. McCarthy, C.M.; Cordeiro, P.G. Microvascular reconstruction of oncologic defects of the midface. *Plast. Reconstr. Surg.* **2010**, *126*, 1947–1959. [CrossRef]
58. Pellini, R.; Mercante, G.; Spriano, G. Step-by-step mandibular reconstruction with free fibula flap modelling. *Acta Otorhinolaryngol. Ital.* **2012**, *32*, 405–409.

59. Wilde, F.; Cornelius, C.P.; Schramm, A. Computer-Assisted Mandibular Reconstruction using a Patient-Specific Reconstruction Plate Fabricated with Computer-Aided Design and Manufacturing Techniques. *Craniomaxillofac. Trauma Reconstr.* **2014**, *7*, 158–166. [CrossRef]
60. Cornelius, C.P.; Smolka, W.; Giessler, G.A.; Wilde, F.; Probst, F.A. Patient-specific reconstruction plates are the missing link in computer-assisted mandibular reconstruction: A showcase for technical description. *J. Craniomaxillofac. Surg.* **2015**, *43*, 624–629. [CrossRef]
61. Wilde, F.; Hanken, H.; Probst, F.; Schramm, A.; Heiland, M.; Cornelius, C.P. Multicenter study on the use of patient-specific CAD/CAM reconstruction plates for mandibular reconstruction. *Int. J. Comput. Assist. Radiol. Surg.* **2015**, *10*, 2035–2051. [CrossRef] [PubMed]
62. Liu, X.J.; Gui, L.; Mao, C.; Peng, X.; Yu, G.Y. Applying computer techniques in maxillofacial reconstruction using a fibula flap: A messenger and an evaluation method. *J. Craniofac. Surg.* **2009**, *20*, 372–377. [CrossRef] [PubMed]
63. Modabber, A.; Ayoub, N.; Mohlhenrich, S.C.; Goloborodko, E.; Sonmez, T.T.; Ghassemi, M.; Loberg, C.; Lethaus, B.; Ghassemi, A.; Holzle, F. The accuracy of computer-assisted primary mandibular reconstruction with vascularized bone flaps: Iliac crest bone flap versus osteomyocutaneous fibula flap. *Med. Devices* **2014**, *7*, 211–217. [CrossRef] [PubMed]
64. Wilde, F.; Winter, K.; Kletsch, K.; Lorenz, K.; Schramm, A. Mandible reconstruction using patient-specific pre-bent reconstruction plates: Comparison of standard and transfer key methods. *Int. J. Comput. Assist. Radiol. Surg.* **2015**, *10*, 129–140. [CrossRef]
65. Raith, S.; Rauen, A.; Mohlhenrich, S.C.; Ayoub, N.; Peters, F.; Steiner, T.; Holzle, F.; Modabber, A. Introduction of an algorithm for planning of autologous fibular transfer in mandibular reconstruction based on individual bone curvatures. *Int. J. Med. Robot.* **2018**, *14*. [CrossRef]
66. Mucke, T.; Wolff, K.D.; Rau, A.; Kehl, V.; Mitchell, D.A.; Steiner, T. Autonomization of free flaps in the oral cavity: A prospective clinical study. *Microsurgery* **2012**, *32*, 201–206. [CrossRef]
67. Robinson, C.G.; Polster, J.M.; Reddy, C.A.; Lyons, J.A.; Evans, P.J.; Lawton, J.N.; Graham, T.J.; Suh, J.H. Postoperative single-fraction radiation for prevention of heterotopic ossification of the elbow. *Int. J. Radiat. Oncol. Biol. Phys.* **2010**, *77*, 1493–1499. [CrossRef]
68. Heyd, R.; Strassmann, G.; Schopohl, B.; Zamboglou, N. Radiation therapy for the prevention of heterotopic ossification at the elbow. *J. Bone Joint Surg. Br.* **2001**, *83*, 332–334. [CrossRef]
69. Seegenschmiedt, M.H.; Makoski, H.B.; Micke, O.; the German Cooperative Group on Radiotherapy for Benign Diseases. Radiation prophylaxis for heterotopic ossification about the hip joint—A multicenter study. *Int. J. Radiat. Oncol. Biol. Phys.* **2001**, *51*, 756–765. [CrossRef]

Journal of
Clinical Medicine

Indexed in: PubMed
Indexed in: Scopus
IMPACT FACTOR 4.241

an Open Access Journal by MDPI

CERTIFICATE OF PUBLICATION

Certificate of publication for the article titled:

Heterotopic Ossification of the Vascular Pedicle after Maxillofacial Reconstructive Surgery Using Fibular Free Flap: Introducing New Classification and Retrospective Analysis

Authored by:

Michael Knitschke; Kelly Siu; Christina Bäcker; Sameh Attia; Hans-Peter Howaldt; Sebastian Böttger

Published in:

J. Clin. Med. **2021**, Volume 10, Issue 1, 109

MDPI Academic Open Access Publishing since 1996

Basel, October 2021

3.3. <u>Originalarbeit 3:</u> Impact of Planning Method (Conventional versus Virtual) on Time to Therapy Initiation and Resection Margins: A Retrospective Analysis of 104 Immediate Jaw Reconstructions.

Knitschke, M.; Bäcker, C.; Schmermund, D.; Böttger, S.; Streckbein, P.; Howaldt, H.-P.; Attia, S. Impact of Planning Method (Conventional versus Virtual) on Time to Therapy Initiation and Resection Margins: A Retrospective Analysis of 104 Immediate Jaw Reconstructions. Cancers **2021**, 13, 3013.
https://doi.org/10.3390/cancers13123013 **IF: 6,639**

Zusammenfassung:
Das Verfahren der virtuellen chirurgischen Planung (VSP) und Rekonstruktion mit patienten-spezifischen Implantaten (PSI) findet zunehmend Verbreitung bei der einzeitigen Kieferrekonstruktionen in Folge Malignom bedingter Knocheninfiltration. Die retrospektive, monozentrische Studie analysiert den Einfluss der verfahrensbedingten Vorlaufzeit für VSP mit PSI Herstellung vs. Non-VSP für die Rekonstruktionsplanung und Osteosynthese hinsichtlich des Status der pathohistologischen Weich- und Hartgeweberesektionsränder. In der Studie konnten 104 Patienten (Non-VSP: *n* = 63 und VSP: *n* = 41) mit einzeitiger Kieferrekonstruktion mit Fibulatransplantat (01/2002 – 12/2020) eingeschlossen und ausgewertet werden. Die Ergebnisse zeigten einen statistisch signifikanten Unterschied ($p = 0{,}008$) im Sinne einer Verzögerung bis zum chirurgischen Therapiebeginn bei Anwendung der Methode VSP mit PSI von 11 Tagen (VSP = 42,0 Tage vs. Non-VSP = 31,0 Tage).
Die beobachtete Zeitverzögerung ergab keinen signifikanten Unterschied hinsichtlich der Resektionsstatus der Weich- und Hartgewebeschnittränder.
Eine statistisch signifikant verlängerte Zeitdauer bis zum Therapiebeginn von im Median 46,5 Tage ergab sich zudem, wenn eine in-domo Gewebebiopsie mit der VSP/PSI-Methode im Vergleich zur Non-VSP-Methode (33,0 Tage) praktiziert wurde. Erfolgte die Biopsie extern, so beschleunigte das die Zeit vom ersten Klinikbesuch bis zur Operation (VSP 35,0 vs. Non-VSP 31,0 Tage), verlängerte aber die Prozesszeit von der Biopsie bis zur Operation in beiden Gruppen auf im Median 46,0 Tage. Die erweiterte Radikalität führte in unserer Studiengruppe zudem zu einer geringeren Rate an lokalen Tumorrezidiven bei fast gleicher Rate an Lymphknoten- und Fernmetastasen. Unterschiede konnten nicht auf einem signifikanten Niveau

beobachtet werden. VSP mit PSI ermöglicht eine präzise sofortige Rekonstruktion nach ablativer onkologischer Chirurgie und verkürzt die Schnitt-Naht-Zeit im Vergleich zur konventionellen Methode. Diese Methode wird somit aus unserer Sicht als onkologisch sicher beurteilt.

Ausblick:

Es sind weitere Studien notwendig, um Aspekte bezüglich der kaufunktionellen implantat-prothetischen Rehabilitation nach VSP mit PSI zu untersuchen. Es liegen Hinweise vor, dass aufgrund der mechanischen Rigidität der Patienten-spezifischen Implantate eine höhere Rate unvollständiger (verzögerter) Verknöcherungen der Übergangszone Mandibula-Fibula und bei polysegmentalen Rekonstruktionen zwischen den einzelnen Fibulasegmenten auftritt. Zudem ist unklar, ob sich die Rate plattenassoziierter Komplikationen (Lockerung, Infektion, Exposition) zwischen PSI vs. konventionellen Osteosyntheseverfahren unterscheidet. Diese Fragen werden in der Originalarbeit 6 untersucht.

cancers

MDPI

Article

Impact of Planning Method (Conventional versus Virtual) on Time to Therapy Initiation and Resection Margins: A Retrospective Analysis of 104 Immediate Jaw Reconstructions

Michael Knitschke *, Christina Bäcker, Daniel Schmermund, Sebastian Böttger, Philipp Streckbein, Hans-Peter Howaldt and Sameh Attia

Department of Oral and Maxillofacial Surgery, Justus-Liebig-University, Klinikstrasse 33, 35392 Giessen, Germany; Christina.Baecker-2@dentist.med.uni-giessen.de (C.B.); Daniel.Schmermund@uniklinikum-giessen.de (D.S.); Sebastian.Boettger@uniklinikum-giessen.de (S.B.); Philipp.Streckbein@uniklinikum-giessen.de (P.S.); HP.Howaldt@uniklinikum-giessen.de (H.-P.H.); Sameh.Attia@dentist.med.uni-giessen.de (S.A.)

* Correspondence: Michael.Knitschke@uniklinikum-giessen.de

Simple Summary: Computer-aided design and manufacturing of osseous reconstructions are currently widely used in jaw reconstructive surgery, providing an improved surgical outcome and decreased procedural stumbling block. However, data on the influence of planning time on the time-to-surgery initiation and resection margin are missing in the literature. This retrospective, monocentric study compares process times from the first patient contact in hospital, time of in-house or out-of-house biopsy for tumor diagnosis and surgical therapy of tumor resection, and immediate reconstruction of the jaw with free fibula flaps (FFF). Two techniques for reconstruction are used: Virtual surgical planning (VSP) and non-VSP. A total of 104 patients who underwent FFF surgery for immediate jaw reconstruction from 2002 to 2020 are included. The study findings fill the gaps in the literature and obtain clear insights based on the investigated study subjects.

Abstract: Virtual surgical planning (VSP) and patient-specific implants are currently increasing for immediate jaw reconstruction after ablative oncologic surgery. This technique contributes to more accurate and efficient preoperative planning and shorter operation time. The present retrospective, single-center study analyzes the influence of time delay caused by VSP vs. conventional (non-VSP) reconstruction planning on the soft and hard tissue resection margins for necessary oncologic safety. A total number of 104 cases of immediate jaw reconstruction with free fibula flap are included in the present study. The selected method of reconstruction (conventionally, non-VSP: $n = 63$; digitally, VSP: $n = 41$) are analyzed in detail. The study reveals a statistically significant ($p = 0.008$) prolonged time to therapy initiation with a median of 42 days when the VSP method compared with non-VSP (31.0 days) is used. VSP did not significantly affect bony or soft tissue resection margin status. Apart from this observation, no significant differences concerning local tumor recurrence, lymph node, and distant metastases rates are found according to the reconstruction method, and affect soft or bone tissue resection margins. Thus, we conclude that VSP for immediate jaw reconstruction is safe for oncological purposes.

Keywords: oral cancer; head and neck tumor; fibula free flap; virtual surgical planning

Citation: Knitschke, M.; Bäcker, C.; Schmermund, D.; Böttger, S.; Streckbein, P.; Howaldt, H.-P.; Attia, S. Impact of Planning Method (Conventional versus Virtual) on Time to Therapy Initiation and Resection Margins: A Retrospective Analysis of 104 Immediate Jaw Reconstructions. *Cancers* **2021**, *13*, 3013. https://doi.org/10.3390/cancers13123013

Academic Editor: Jan Egger

Received: 27 May 2021
Accepted: 13 June 2021
Published: 16 June 2021

1. Introduction

Oral squamous cell cancer (OSCC) is the most common malignancy of the upper aerodigestive tract, with about 90–95% prevalence [1,2]. Five-year survival rates of the progressed staged disease were estimated at 50–60% [3], and its pathohistological residual status (R-category) has been described in the literature as a prognostic factor for tumor recurrence [4–8]. Surgical therapy is aimed to excise the neoplasia with a surrounding

safety margin of ≥5 mm (R0-resection) [9], corresponding to an intraoral distance of 10 mm to the palpable tumor border [10]. Further fixation and processing for pathohistological assessment distort measurements, due to tissue shrinkage and, therefore, changes concerning margin evaluation [11].

The margin of excision was defined as close when the distance to the tumor border was between 1–5 mm [12,13]. The involved margin (R1-resection) was described when the distance from the tumor border to the margin of excision was less than 1 mm. This corresponds to an invasive tumor. Close and involved margins were reasons for adjuvant therapy. Published literature concerning resection margins after tumor resection of the oral cavity showed that about 3% were categorized as R1 and 16.3% as close margins [14]. Other investigators found clear margins in half of their collective 896 patients [15]. To increase the safety margin, segmental resection or resection of continuity of the mandible must be performed depending on the location of the tumor site [16,17]. The best time for reconstruction has been debated for some time. Today, immediate reconstruction with osteo-fascio-cutaneous transplants, such as the free fibula flap (FFF) [18], has become the gold standard in maxillofacial reconstruction, due to its advantages and versatility [18,19]. Currently, FFF is the standard therapy for head and neck reconstructive surgery, providing the optimal precondition for later placement of dental implants and, therefore, for oral and dental rehabilitation [20,21]. The immediate insertion of dental implants is sometimes performed simultaneously to jaw reconstruction [22–26]. Nowadays, virtual planned surgery combined with custom-made osteosynthesis—or so-called patient-specific implants, manufactured in a titan laser melting process—has become routine in daily practice. Often pronounced advantages of maxillofacial reconstruction are increased accuracy, decreased operation and ischemia time, reduced length of hospitalization time, improved patient outcomes, highly effective results, and minimized intersegmental gap size [27–34]. Reported disadvantages of VSP are planning time [35], preparation time, and cost aspects, which must be considered [36] as patient-specific (laser-melted titanium) implants are expensive and will decrease the gain on total proceeds.

While high-volume reconstructive centers often use rapid in-house prototyping to manufacture cutting guides and prebending fixation devices. In contrast, low-volume institutions use purpose-made, web-based interfaces for virtual surgical planning of resections and the design of custom-made implants. The time interval of out-of-house service until delivery causes a delay of several days, while tumor growing continues [37–39]. Time to therapy initiation (TTI) was a significant influencing factor of upstaging in patients with head and neck SCC (HNSCC) [40].

Published data concerning TTI and quality of excision margins were weak and showed contrary results [27,41,42]. This study aims to estimate the TTI and rate of clean (R0), and close/involved (R1) margins in soft and hard tissue tumor excision when using VSP and PSI for immediate jaw reconstruction with FFF. The study also examines the following oncologic aspects:

Are there differences in the TTI when using a VSP vs. non-VSP (conventional) technique?

What is the influence of resection margins concerning local tumor recurrence, lymph node metastasis, and distant metastasis with respect to the used reconstruction technique?

2. Material and Methods

2.1. Study Design and Patient Population

The study was conducted as a monocentric, retrospective study. Medical records of patients suffering from SCC who underwent FFF in the head and neck region from January 2002 to December 2020 were analyzed.

Patients were treated with tumor ablation and neck dissection. Immediate reconstruction of the mandibular defect was performed with microsurgical FFF. From 2002 to 2015, reconstructions were conventionally planned (non-VSP) by free-hand during surgery with hand-bent osteosynthesis. Since early 2015, virtual surgical planning (VSP) combined with

patient-specific, custom-made implants (PSI) has been performed based on the patient's preoperative CT scans of the fibula, donor, and tumor recipient site.

Patients were treated according to German guidelines published by Wolf et al. [10].

2.2. Study Parameters and Evaluator Calibration

The following parameters were collected: Age at flap transfer, gender, tumor location, time lapse between diagnosis and surgery, initial clinic visit, time in-house vs. out-of-house biopsy, time to therapy initiation, disease-free survival, pathohistological tumor parameters (T-, N-, and R-Category), planning mode, type of defect [43,44], number of used fibular bone segments, overall length of the fibular flap, and flap outcome (Figure 1). Pathohistological records were assessed and categorized into clear, and close, or involved margins concerning soft tissue and bone. Tumor excision was defined as R0-resection (clear margin) when a surrounding safety margin of $\geq$5 mm was achieved. Margins were described as close when the distance to the tumor border was between 1–5 mm and involved when it was less than 1 mm (R1-resection).

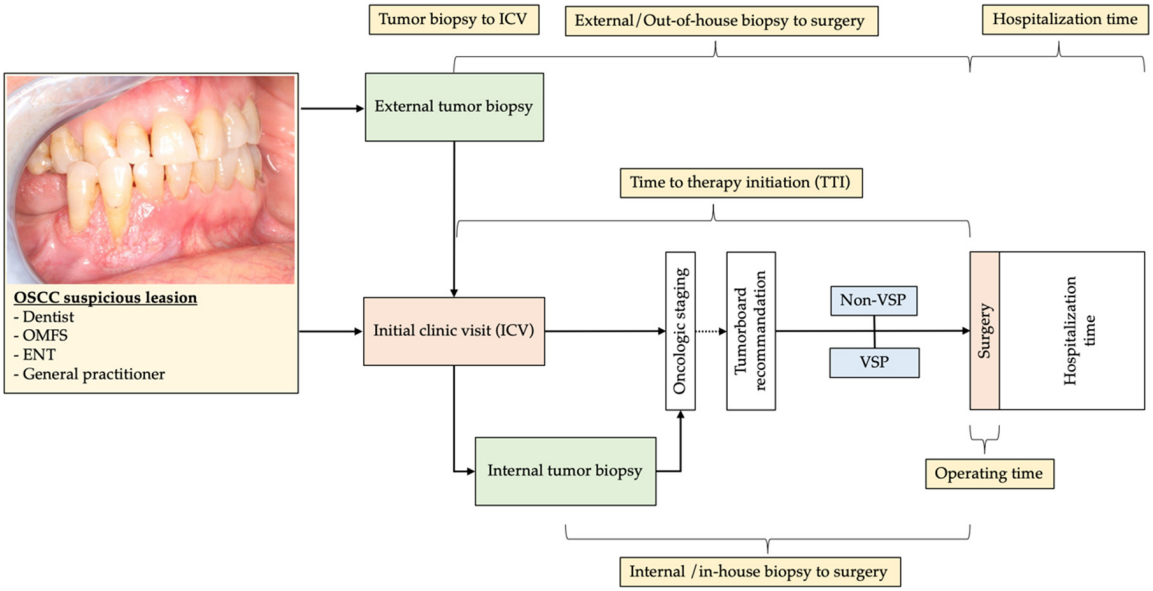

Figure 1. The typical workflow of the first diagnosis of OSCC and referral to oncologic reconstructive OMFS-department and initial clinic visit (ICV). Time intervals of study interest are marked in yellow boxes and correlated to the method of immediate jaw reconstruction.

2.3. Inclusion and Exclusion Criteria for Study Subjects

We enrolled patients diagnosed with SCC of the oral cavity for an initial surgical treatment with immediate reconstruction of the jaws with FFF. Only cases with complete data sets and/or medical records were included. Patients with previous chemotherapy, other malignant oncologic diseases, or earlier neoadjuvant irradiation therapy of the head and neck were excluded.

2.4. Statistical Analyses

Pearson's χ^2 test, Fischer's exact test, and the Freeman–Halton extension [45] were conducted on the categorical variables used to compare both methods of reconstruction concerning gender, external vs. internal biopsy, lymph node involvement, bone invasion and erosion, hard and soft tissue margin, oncologic therapy, number of fibular bone segments, microanastomosis revision rate, and flap success. Student's *t*-test was performed to compare the mean age at FFF-transfer, tumor diameter, overall length of transplanted FFF, UICC tumor stage, time intervals—tumor biopsy to initial clinic visit and surgery, operating time, and hospitalization time between the study groups after verification of

normality. $p < 0.05$ was defined as statistically significant. The statistical analysis was carried out using SPSS 25 (SPSS Inc., Chicago, IL, USA).

2.5. Ethics Statement/Confirmation of Patients' Permission

The local Ethics Committee of Justus-Liebig University Giessen approved the study (AZ27/21), and patients' permission/consent was not necessary for this retrospective study. The patients consented to their intraoral pictures being used anonymously in the publication. All data in the Microsoft Excel spreadsheet were pseudonymized.

3. Results

The tumor database contains 612 records from January 2002 to December 2020. A total number of 104 cases (34 females (32.7%), 70 males (67.3%), mean age of 60.3 ± 9.6 years, age range of 37.0–82.8 years) fulfilled the chosen inclusion criteria for analyses. Secondary reconstruction after tumor recurrence or delayed jaw reconstruction with FFF, as well as cases in which flaps other than FFF had been used, were excluded from this investigation. Over the study period of 18 years, a core team of four, senior, experienced oral and maxillofacial oncologic and reconstructive surgeons performed immediate jaw reconstructions. One surgeon overlooked the whole observation time, the second 16 years, and the other two observed eight years. Collected data were categorized concerning FFF planning procedure: Non-VSP, conventional ($n = 63$) vs. VSP, and digital workflow ($n = 41$). The groups were tested for normal distribution. The detailed demographic parameters and results are summarized in Table 1.

Table 1. Demographic parameters of study groups (VSP, virtual surgical planning; FFF, free fibula flap; SD, standard deviation; S; surgery; RT, radiation therapy; RCT, radiation, and chemotherapy).

***N* = 104**	**VSP FFF (%) 41 (39.4%)**	**Non-VSP FFF (%) 63 (60.6%)**	***p***
Age (years), mean ± SD	62.0 ± 10.0	59.2 ± 9.2	0.146
Follow-up (months), mean ± SD	20.5 ± 16.4	64.9 ± 52.1	0.502
Sex, *n* (%)			
Male	26 (63.4%)	44 (68.5%)	
Female	15 (36.6%)	19 (31.5%)	0.318
Tumor site, *n* (%)			
Gingiva of alveolar crest	6 (14.6%)	24 (34.8%)	
Mouth floor	12 (29.3%)	23 (33.3%)	
Retromolar region	18 (43.9%)	10 (14.5%)	
Maxilla	5 (12.2%)	5 (7.2%)	
Planum buccale	-	1 (1.4%)	
UICC tumor stage, *n* (%)			
Stage I	5 (12.2%)	5 (7.2%)	
Stage II	1 (2.4%)	10 (14.5%)	
Stage III	6 (14.6%)	6 (8.7%)	
Stage IV	29 (70.7%)	42 (60.9%)	
Tumor diameter (mm), mean ± SD	37.0 ± 16.4	33.5 ± 16.0	0.283
Node-positive, *n* (%)	20 (48.8%)	31 (49.2%)	0.562
Extracapsular spread, *n* (%)	6 (14.6%)	-	
Bone invasion, *n* (%)	23 (56.1%)	32 (50.8%)	0.372
Bone erosion, *n* (%)	6 (14.6%)	12 (19.0%)	0.559

Table 1. *Cont.*

***N* = 104**	**VSP FFF (%) 41 (39.4%)**	**Non-VSP FFF (%) 63 (60.6%)**	***p***
Bone margin, *n* (%)			
Clear	39 (95.1%)	61 (96.8%)	
Close	-	-	
Involved	2 (4.9%)	2 (3.2%)	0.516
Soft tissue margin, *n* (%)			
Clear	26 (63.4%)	46 (73.0%)	
Close	10 (24.4%)	13 (20.6%)	
Involved	5 (12.2%)	4 (6.3%)	0.470
Oncologic therapy, *n* (%)			
S	13 (31.7%)	33 (52.4%)	
S + RT	13 (31.7%)	12 (19.0%)	
S + RCT	15 (36.6%)	18 (28.6%)	0.102

Two-thirds of the whole study group were male. OSCC was mainly localized in the conventional group at the gingiva of an alveolar crest (34.8%) and mouth floor (33.3%). In contrast, in the virtual planned group, the tumor mainly affected the retromolar region (43.9%) and the mouth floor (29.3%). In both groups, about 80% were stratified as UICC tumor stage III or IV. Tumor diameter was measured, resulting in a mean of 37.0 ± 16.4 mm, and all near 4 mm larger than the maximal extension in the non-VSP group. The finding was without statistical significance. Lymph node metastasis was found in both groups in half of the cases. Extracapsular spreading was recorded since 2015 and, therefore, only observed in 14.6% of the VSP-group.

The bone invasion was more frequent in the VSP group (56.1% vs. 50.8%), while bone erosion was slightly more often recorded in the non-VSP group (19.0% vs. 14.6%). Clear bone resection margins (R0-resection) were found slightly more often in the non-VSP group (96.8% vs. 95.1%). The assessment of soft tissue margins revealed clear margins of excision (R0-resection) in 63.4% of patients after virtual and 73.0% after conventional planning. Differences concerning resection margins of the bone ($p = 0.516$) and soft tissue ($p = 0.470$) were not statistically significant.

Surgery only was 52.4%, and surgery in combination with RCT was 28.6% as the treatment of choice in the non-VSP group. In comparison, in the VSP group, surgery only and in combination with adjuvant RT and RCT was performed in a third of the cases.

Defect and FFF-associated parameter data are summarized in Table 2. Maxillary reconstructions have been performed in both groups with a frequency of about 10.0% [44]. The majority of immediate reconstructions were mandible defects. Findings showed a trend in reconstructions of Brown class I and II defects (59.0% vs. 46.4%) with the conventional non-VSP method to class III and IV digitally planned, larger reconstructions (41.4% vs. 33.4%) [43]. The overall length of transplanted FFF was significantly longer in the VSP-group ($p = 0.002$) with a mean of 9.02 ± 2.8 cm. Further, in the VSP-group, polysegmental reconstructions (75.6%) were used significantly more frequently ($p = 0.014$) than in the non-VSP group (52.4%).

Table 2. Defect and associated FFF parameters of the study groups (VSP, virtual surgical planning; FFF, free fibula flap; SD, standard deviation) [43,44].

***N* = 104**	**VSP FFF (%) 41 (39.4%)**	**Non-VSP FFF (%) 63 (60.6%)**	***p***
Maxilla (Brown class), *n* (%)			
II	3 (7.3%)	5 (7.9%)	-
III	1 (2.4%)	-	-
IV	1 (2.4%)	-	-
Mandible (Brown class), *n* (%)			
I	9 (22.0%)	19 (30.2%)	-
II	10 (24.4%)	18 (28.6%)	-
III	14 (34.1%)	20 (31.7%)	-
IV	3 (7.3%)	1 (1.6%)	-
Reconstruction length (cm), mean ± SD	9.02 ± 2.80	7.23 ± 1.83	0.002
Number of segments, *n* (%)			
1	10 (24.4%)	30 (47.6%)	
2	20 (48.8%)	20 (31.7%)	
3	11 (26.8%)	13 (20.6%)	0.014

Diagnosis, surgery-associated parameters, and comparisons of intraoperative factor parameter data are shown in Table 3. The time interval from the initial clinic visit (ICV) to surgery was significantly ($p = 0.008$) longer in the VSP group (47.2 ± 24.5 days) compared with the conventional group (35.7 ± 18.6 days).

Table 3. Diagnosis, surgery-associated parameters, and comparison of intraoperative factors.

***N* =104**	**VSP FFF *n* = 41 (39.4%)**	**Non-VSP FFF *n* = 63 (60.6%)**	***p***
Tumor biopsy, *n* (%)			
Internal/In-house	27 (65.9%)	40 (63.5%)	-
External/Out-of-house	14 (34.1%)	23 (36.5%)	0.806
ICV to surgery (days), mean ± SD (median)			
Internal/In-house	53.5 ± 26.8 (46.5)	36.8 ± 21.1 (33.0)	0.006
External/Out-of-house	35.8 ± 15.5 (35.0)	33.9 ± 13.4 (31.0)	0.696
Biopsy to surgery (days), mean ± SD (median)			
Internal/In-house	47.7 ± 25.2 (43.0)	34.5 ± 20.6 (34.5)	0.022
External/Out-of-house	44.7 ± 15.4 (46.0)	44.7 ± 14.1 (46.0)	0.995
ICV to (days), mean ± SD (median)			
Internal/In-house	5.6 ± 9.0 (1.0)	2.3 ± 4.0 (1.0)	0.045
External/Out-of-house *	−9.6 ± 6.2 (−7.0)	−8.0 ± 5.6 (−7.0)	0.424
CT recipient site	10.1 ± 9.5 (8.0)	13.4 ± 12.8 (10.0)	0.160
CTA/MRA donor site	14.6 ± 11.6 (14.0)	15.7 ± 11.8 (13.0)	0.641
Kickoff VSP	21.3 ± 15.6 (8.0)	-	-
Approval VSP	34.4 ± 17.8 (34.5)	-	-
Shipping VSP/PSI	38.6 ± 18.5 (35.5)	-	-
Surgery	47.2 ± 24.5 (42.0)	35.7 ± 18.6 (31.0)	0.008
Oncologic board **	14.9 ± 8.9 (14.0)	-	-

Table 3. *Cont.*

***N* =104**	**VSP FFF *n* = 41 (39.4%)**	**Non-VSP FFF *n* = 63 (60.6%)**	***p***
Entire VSP turnaround time	16.9 ± 8.5 (15.0)	-	-
CT recipient site–surgery (days), mean ± SD (median)	34.8 ± 17.6 (32.0)	25.09 ± 17.2 (22.0)	0.008
Operating time (minutes), mean ± SD	508.2 ± 88.8	562.6 ± 98.5	0.005
Hospitalization time (days), mean ± SD	22.5 ± 12.0	20.33 ± 9.0	0.285
Microanastomosis revision, *n* (%)	4 (9.8%)	5 (7.9%)	0.504
Flap success, *n* (%)	35 (85.4%)	57 (90.6%)	0.310

* Annotation: Negative values mean that the biopsy occurred before the initial consultation in the outpatient clinic. ** Interdisciplinary pretherapeutic oncologic board was established in 2015 simultaneously to VSP. (VSP, virtual surgical planning; FFF, free fibula flap; SD, standard deviation; ICV, initial clinic visit; CTA, computed tomography angiography; MRA, magnetic resonance angiography; PSI, patient-specific implant).

In both groups, near to two-thirds of the tumor biopsies and initial pathohistological assessments were performed in-house. The time of ICV to surgery showed significant differences when tumor biopsy was performed in-house (p = 0.006). VSP was associated with a longer (53.5 ± 26.8 days) lead time compared with conventional planning (36.8 ± 21.1 days). It was insignificant when the tumor was confirmed by external biopsy (p = 0.696). The results of ICV to tumor confirmed biopsy showed insignificant differences when the biopsy was conducted externally, with a median of −7.0 days before the patient's first consultation in the outpatient clinic. In-house tumor diagnosis was confirmed by pathohistological assessment after 5.6 ± 9.0 days in the VSP and after 2.3 ± 4.0 days in the conventional (non-VSP) group; the difference was significant (p = 0.045). Time from in-house biopsy to surgical therapy initiation was significantly (p = 0.022) longer in the VSP group (47.7 ± 25.2 days) compared with the conventional group (34.5 ± 20.6 days). No statistically significant differences (44.7 ± 15.4 days vs. 44.7 ± 14.1 days) were observed concerning time from out-of-house biopsy to surgical therapy initiation (p = 0.995) when both methods of reconstruction were compared.

Operating time resulted in a mean of 508.2 ± 88.8 minutes in the VSP group and was significantly shorter (p = 0.005) than in the non-VSP group at 562.5 ± 98.5 minutes. Furthermore, the time from ICV to CT scans of the donor and recipient site were performed slightly earlier in the VSP (recipient site, 10.1 ± 9.5 days; donor site, 14.6 ± 11.6 days) compared with the conventional group (recipient site, 13.4 ± 12.8 days; donor site, 15.7 ± 11.8 days). These observed differences were insignificant. For VSP, the entire turnaround time from kickoff (ICV-kickoff: mean, 21.3 ± 15.6 days; median, 8.0 days) until the delivery of the patient-specific implant (ICV-shipping VSP/PSI: mean, 38.6 ± 18.5 days; median, 35.5 days) was a median of 15.0 days (mean, 16.9 ± 8.5 days).

Hospitalization was found in the VSP group with a mean of 22.5 ± 12.0 days, two days longer than in the non-VSP group. In both groups, the microanastomosis revision rate was lower than 10%. Microanastomosis revision became necessary for flap salvage slightly more frequently in the VSP-group (9.8% vs. 7.9%). Total flap success rate was estimated with 85.4% in the VSP and 90.6% in the conventional group. Differences concerning hospitalization time, microanastomosis revision rate, and flap success were without statistical significance between the groups.

In summary, the shortest time interval between tumor biopsy and surgery at a median of 32.0 days was found when in-house biopsy and non-VSP for immediate jaw reconstruction were performed. If VSP was used, the gap was 45.5 days. Out-of-house biopsy to surgery was estimated with a median time of 42 days in the VSP and 38.0 days in the non-VSP group (Figure 2).

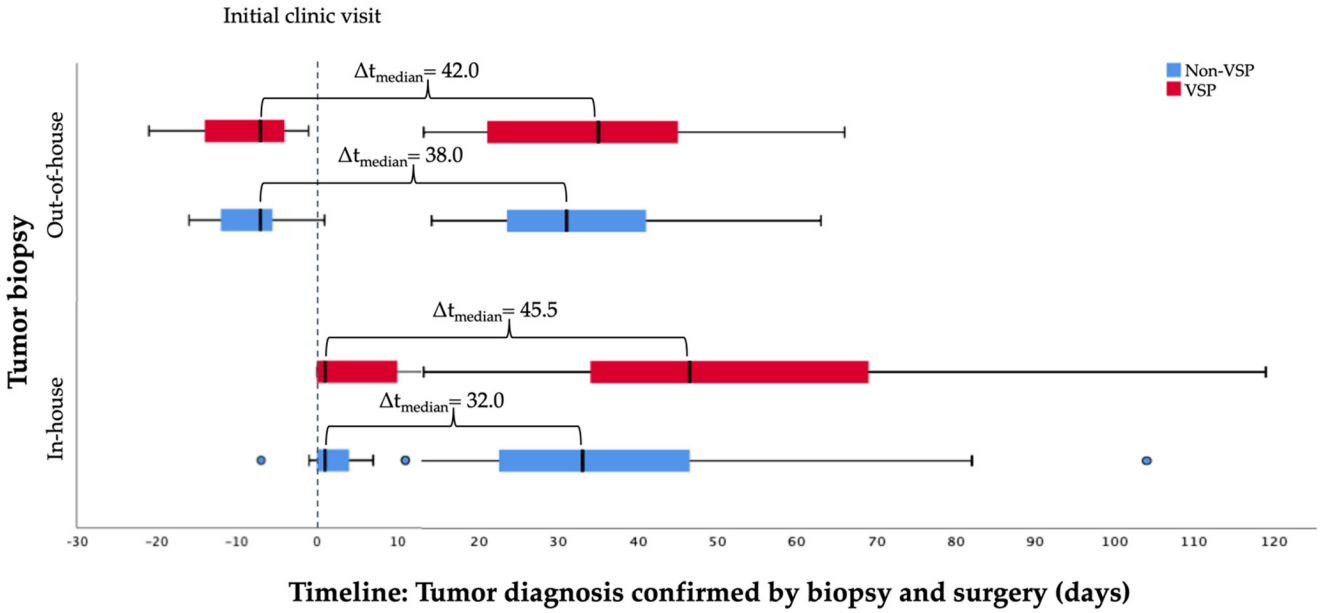

Figure 2. Timeline: In-house vs. out-of-house tumor biopsy to surgery categorized by method of reconstruction planning.

Further, stages of diagnostic and planning procedures from the first contact in the outpatient clinic to surgery were drawn in Figure 3. Overall, the initial oncologic staging procedure was completed after CT scan of the lower limb for transplant planning in both groups near a mean of 15 days after ICV (Table 3). Finally, surgery was performed later in the non-VSP than in the VSP group (non-VSP, 35.7 ± 18.6 days; VSP, 47.2 ± 24.5 days). When VSP was performed, data shows a wide range from VSP-kickoff after ICV was initiated (mean, 21.3 ± 15.6 days; median, 8.0 days). The whole VSP-procedure turnaround time from kickoff to patient-specific implant shipping to our department took an average of 16.9 ± 8.5 days (median, 15.0 days).

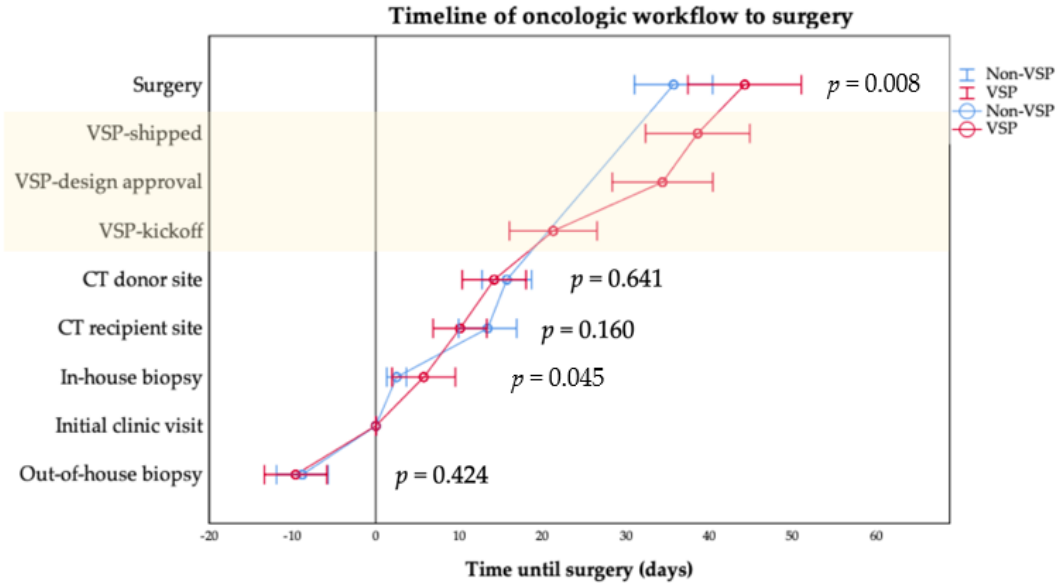

Figure 3. Mean time of diagnostic and planning procedure from the initial clinic visit to surgery categorized by method of reconstruction planning. The 95% confidence intervals are given by whisker bars. Statistically significant differences were found for intervals of the initial clinic visit to in-house biopsy ($p = 0.045$) and surgery ($p = 0.008$) (Table 3). Annotation: The light yellow background marks VSP parameters.

Although differences between the planning groups and resection margins of soft and bony tissue were insignificant (Table 1), 36.6% close and involved margins in the VSP group compared with 26.9% in the conventional, non-VSP group were found. Therefore, the rate of local tumor recurrence (LTR), lymph node metastasis (LNM), and distant metastasis (DM) were evaluated concerning resection margins of soft (Figure 4) and bony tissue (Figure 5) concerning the used planning mode of reconstruction.

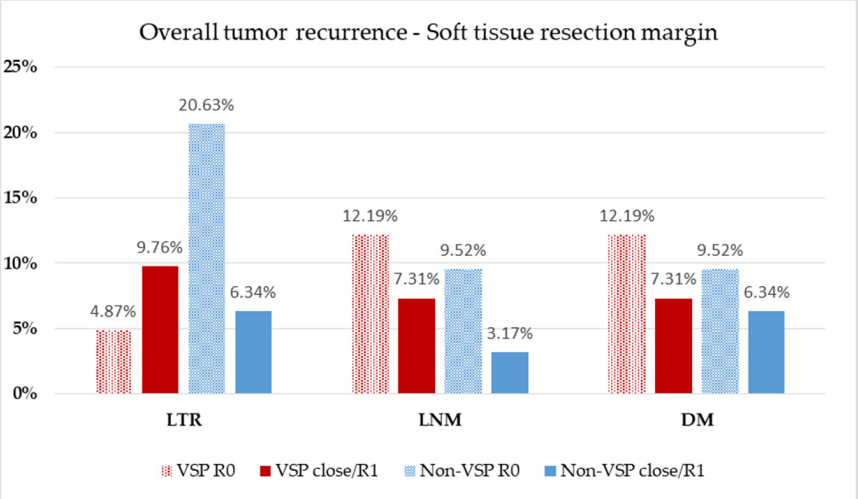

Figure 4. Evaluation of soft tissue resection margin. Relative distribution of local tumor recurrence (LTR), lymph node metastasis (LNM), and distant metastasis (DM) according to the method of reconstruction planning. Patients at risk: VSP group, $n = 41$ (follow-up, 20.6 ± 16.4 months); non-VSP group: $n = 63$ (follow-up, 64.9 ± 52.1 months).

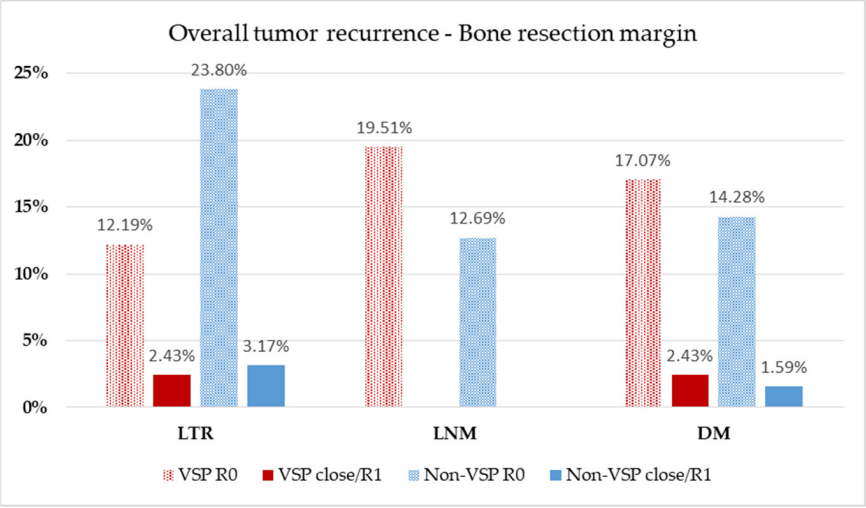

Figure 5. Evaluation of bony resection margin. Relative distribution of local tumor recurrence (LTR), lymph node metastasis (LNM), and distant metastasis (DM) according to the method of reconstruction planning. Patients at risk: VSP group, $n = 41$ (follow-up, 20.5 ± 16.4 months); non-VSP group, $n = 63$ (follow-up, 64.9 ± 52.1 months).

For comparison of LTR, LNM, and DM, patients at risk were classified according to the method of reconstruction and assessed on soft tissue margin status (Figure 4) in the recorded follow-up interval (Table 1). A total 14.63% of VSP reconstructions suffered LTR, which occurred about two-times more often when close or involved margins (VSP: R0 = 4.87%, $n = 2$, close/R1 = 9.76%, $n = 4$) were assessed. In the conventional, non-VSP

group, LTR was detected in 26.97% of patients and occurred three times more often in the non-VSP group with a clear resection margin than in the close/R1 group (non-VSP: R0 = 20.63%, n = 13, close/R1 = 6.34%, n = 4). LNM showed 19.51% occurrence in the VSP group and 12.69% in the non-VSP group. In both groups, LNM was slightly more frequently observed in the clean margin group (VSP: R0 = 12.19%, n = 5, close/R1 = 7.31%, n = 3; non-VSP: R0 = 9.52%, n = 6, close/R1 = 3.17%, n = 2). DM were found in 19.51% of the VSP group and 15.86% of the non-VSP group. In both groups, DM was slightly more frequently observed in the clean margin group (VSP: R0 = 12.19%, n = 5, close/R1 = 7.31%, n = 3; non-VSP: R0 = 9.52%, n = 6, close/R1 = 6.34%, n = 4).

Analogous to soft tissue resection margin, rates of LTR, LNM, and DM, were evaluated for bony resection margin status and also according to the method of reconstruction (Figure 5) about the recorded follow-up interval (Table 1). Together, 14.63% of VSP reconstructions suffered LTR, which occurred about five times more often when clean margins (VSP: R0 = 12.19%, n = 5, close/R1 = 2.43%, n = 1) were assessed. In the conventional, non-VSP group, LTR was detected in 26.97% of patients and occurred three times more often in the non-VSP group with a clear resection margin than in the close/R1 group (non-VSP: R0 = 23.80%, n = 15, close/R1 = 3.17%, n = 2). LNM occurred in 19.51% of the VSP group and 15.86% of the non-VSP group. In both groups, LNM was observed despite clean bony resection margins (VSP: R0 = 19.51%, n = 8; non-VSP: R0 = 12.69%, n = 8). DM were found in 19.51% of the VSP group and 15.86% of the non-VSP group. In both groups, DM was observed more frequently in the clean margin group (VSP: R0 = 17.07%, n = 7, close/R1 = 2.43%, n = 1; non-VSP: R0 = 14.28%, n = 9, close/R1 = 1.59%, n = 1).

4. Discussion

The free fibula flap (FFF) has become the gold standard in maxillofacial reconstruction, due to its advantages and versatility [18,19]. Vascular pathologies of the lower limb vessels, such as peripheral arterial occlusive disease, stenoses, and vascular anomalies were considered as contraindications for FFF [46]. Preoperatively computed tomography angiography (CTA) [47–50] or magnetic resonance angiography (MRA) was performed in all cases to ensure three-vessel status to prevent postoperatively critical ischemia of the donor site leg [51,52]. In those cases, patients were excluded for FFF, and alternative reconstructive procedures, such as vascularized deep circumflex iliac artery flap (DCIA) [53], and a hand-bent or customized, patient-specific reconstruction plate [54] was used.

The present study found a significantly longer time to therapy initiation (TTI) when virtual surgical planning (VSP) was used for immediate jaw reconstruction. Concerning TTI, some authors emphasized the necessity for tumor resection during a few days within three weeks after diagnosis and doubted whether this can be achieved with a digital workflow [27]. Compared with the non-VSP group, a significant time delay to TTI was about 12 days in the VSP-group, with a mean therapy initiation at 47.2 days. The observed delay mainly arises from the VSP turnaround time of a median of 15.0 days (mean, 16.9 $\pm$ 8.5 days) and time from PSI delivery to surgery of 6.7 $\pm$ 4.5 days (median, 5.0 days). However, another study found in their individual setting an insignificant shorter TTI of 59 $\pm$ 16 days when VSP was used compared with conventional immediate reconstruction [41]. Published data from the national cancer database of the United States showed that prolonged TTI is currently affecting survival and a TTI of greater than 46 to 52 days introduced an increased risk of death. The risk of death was adverse beyond 60 days [55]. Furthermore, in advanced HNSCC, multidisciplinary treatment is necessary. It was also found that increasing delays in postoperative and radiation intervals were associated independently with an escalating risk of mortality. When the entire treatment period is considered, delays in initiating therapy fade into the background [56]. However, published literature has shown that increased TTI did not impact overall survival [57].

Surgical treatment of oral SCC is based on tumor resection with a circular safety margin, including the continuity of the mandible or extended parts of the maxilla, if tumor invasion was assumed [58]. Immediate microvascular reconstructions have become

popular, safe, and reliable [59]. They admit the quality of life, which is comparable to segmental resections of the jaw [60]. While conventional immediate reconstructions have been performed in the past, VSP has become popular in many reconstructive centers. Some high-volume reconstructive centers often maintain their own "in-house" planning and rapid prototype printing devices for bending models or use an "out-of-house" service with the option of a patient-specific implant [37–39]. Custom-made (CAD/CAM) osteosynthesis plates are the transfer key that enable three-dimensional configuration of the original and transplanted bone segments [61,62]. The accuracy of the technique has been widely investigated [35,63–65]. Our data concur with the results of other studies that the duration of surgery is significantly shortened [35,36,66], due to more accurate and efficient intraoperative fibular osteotomies and faster shaping of the neomandible, and elimination of free-hand contouring and stepwise plate bending [67–69]. Statistically significant differences concerning the duration of hospitalization, microanastomosis revision rate, and total flap failures were not found between the observed groups.

However, the crux of VSP is that it is addressed to the snapshot of the CT scan of the recipient site, which is timely localized at the beginning of the staging procedure. The time interval between the CT scan of the tumor (recipient) site and defining the virtual resection planes should be as short as possible to surgery [70]. Prolonged time to therapy initiation (TTI) is a disadvantage of VSP and leads to further tumor growth [37,39,66,71]. Thus, tumor progress should be kept minimal, and involvement of the resection border should be prevented to exclude unexpected modifications of the virtual surgical plan. Possible changes in the resection margins have the consequence that in a two-team approach setting, the shaping of the neomandible must be stopped until the affected bone section has been evaluated. For intraoperative assessment of bony resection margins, flat-panel volume computed tomography could be used to increase tumor-free bony margins [72]. An ever-present risk is that a prepared PSI must be discarded if the bony resection margins change or unforeseen limitations occur on the soft tissue site.

Study findings revealed that CT scans of the recipient (tumor) site were about 10 days older in the VSP group than in the non-VSP group at the time of surgery (VSP, 34.8 $\pm$ 17.6 days vs. non-VSP, 25.09 $\pm$ 17.2 days). This result is the consequence of the VSP preparation time. In virtual planning, soft and hard tissue tumor involvement is estimated, and a necessary safety distance is mentally drawn. However, the time difference between the CT scan and later virtual planned resection did not have a relevant impact on the frequency of LTR, due to close or involved resection margins during the ongoing follow-up period.

Involved or close resection margins after ablative oncologic treatment increase the risk for local tumor recurrence and development of distant metastasis [73]. Infiltration of the bone correlates with a worse prognosis [74]. An oncologic safety margin of about 5 mm should be the aim for pathohistological classification of free margins status (R0) [9]. Therefore, excision was recommended at about a 10 mm distance around the palpable tumor [10] and 10 mm length to the visible tumor border in the bone. There are some reports in the literature that pathohistological safety distance can be achieved when using the VSP procedure [27,41,42,68,71,75]. Literature shows that rates of local recurrence following margin-free surgical resections can range from 16% to 20% [76]. The failure to obtain clear (R0) surgical margins increases the probability of local tumor recurrence [77]. R1 or R2 are found to occur 1.7 times more frequently in OSCC than in other head and neck subsites [78–80]. The study results show that LTR rates concerning clean, soft tissue margins are 20.63% in the conventional non-VSP group, which are well comparable with literature, and are 4.87% in the VSP group. The authors believe that the low rate of LTR in the VSP group was a result of the necessary intensive preoperative oncologic case study for ideal addressing of the tumor location and consequent ablative concept. In our eyes, this is a decisive advantage of the virtual method, aside from the accessible precision of the reconstructions.

To the best of our knowledge, only one study has been published investigating the influence of the time delay on VSP of custom-made implants (PSI) for oncologic reasons

and impacts on bony and soft tissue margins [41]. They evaluated n = 28 conventional and n = 25 VSP primary, immediate mandible reconstructions and found that VSP did not significantly affect bony or soft tissue margin status. Our findings confirm their results concerning the impact of VSP on excision margins. The aforementioned workgroup found, in their individual setting in Ireland, a shorter time interval from clinic visit to surgery in the VSP than in the conventional group (59 ± 16 days vs. 65 ± 30 days) [41], which might be a benefit for the patient. The results of the present study found that the conventional planning method led to surgery faster (35.7 ± 18.6 days) than the virtual method (47.2 ± 24.5 days). The environment of our evaluated university setting revealed a faster time to surgery of around 12 days compared with their TTI. However, the time delay is the critical aspect of the VSP method because tumor progression is time-sensitive [40]. In addition, no differences concerning local tumor recurrence, lymph node, and distant metastases rates were found according to the method of reconstruction that affected soft or bone tissue resection margins.

Furthermore, the time of biopsy must be considered. In both study groups, about a third of the tumor biopsies were performed out-of-house. Process time from biopsy to surgery was almost equal in both groups and independent from the planning method, with a median of 46 days. In contrast to this, TTI was faster when an in-house biopsy for diagnosis was performed. This time advantage supports the recommendation for in-house biopsy at the oncologic and reconstructive center of choice. A median TTI of 43 days was found in the VSP group and 34.5 days in the non-VSP group. However, several influencing variables may bias the extended TTI in VSP. First, the institutional tumor board conference has taken place once a week since 2015. In the specific setting of the department, a schedulable intensive care bed capacity was more or less limited to one day a week. The whole process and production time is a median of 15 days after VSP kickoff and an initial web-meeting. In summary, the longer TTI in the VSP group was mainly influenced by VSP workflow, weekly oncologic board schedule, and limited ICU capacities.

Limitations of the Study

The retrospective analysis is at risk of various biases. Historical and documentation bias must be considered. Data was extracted out of medical records and the anesthetists' database. Therefore, transmission error could not be excluded. Pathologists' reports and assessments were not standardized and had not been prepared for the present investigation. The main focus was on the bone resection margins, but an essential limitation of the current study is the small number of cases involving bony resection margins. However, the findings showed no increase of involved or close resection margins of the bone in our out-of-house setting when virtual surgical planning combined with a patient-specific implant (custom-made osteosynthesis plate) was used. Regarding soft tissue resection margins, a statistically insignificant low increase in close and involved margins was found.

5. Conclusions

The present retrospective study is a single-center analysis of 104 cases of immediate jaw reconstruction with free fibula flap, which were conventionally (non-VSP, n = 63) or digitally (VSP, n = 41) planned. The study revealed a statistically significant prolonged time to therapy initiation in the median of 46.5 days when the VSP method and in-house tumor biopsy were used compared with non-VSP (33.0 days). External biopsies accelerated time from initial clinic visit to surgery (VSP 35.0 vs. non-VSP 31.0 days), but prolonged overall process time from biopsy to surgery. The observed time delay did not significantly affect the soft and bony resection margins. Thus, oncologically-necessary extended resections can be adequately reconstructed using the VSP method. With increasing tumor category, the complexity also increases, leading to a decrease in R0 resections. Nevertheless, we found a lower rate of local tumor recurrence (LTR) under VSP with almost the same rate of lymph node metastasis (LNM) and distant metastases (DM). VSP allows precise immediate reconstruction after ablative oncologic surgery and reduces the entire operation

time compared with traditional methods. Further randomized clinical trials are necessary to validate the study findings.

Author Contributions: Conceptualization, M.K.; methodology, P.S., M.K., and C.B.; formal analysis, M.K.; investigation, M.K., and P.S.; data curation, M.K. and P.S.; writing—original draft preparation, M.K., P.S., S.A., and S.B.; writing—review and editing, M.K., P.S., S.A., C.B., D.S., H.-P.H., and S.B.; visualization, M.K., D.S., H.-P.H., and S.A.; supervision, M.K., H.-P.H., and S.A.; project administration, M.K. All authors have read and agreed to the published version of the manuscript.

Funding: This research received no external funding.

Institutional Review Board Statement: The study was conducted according to the guidelines of the Declaration of Helsinki and approved by the Ethics Committee of Justus-Liebig University Giessen (AZ27/21).

Informed Consent Statement: Patient consent was waived, as the study is a retrospective data analysis.

Data Availability Statement: The data presented in this study are available upon request from the corresponding author.

Acknowledgments: The authors are grateful for the consent of the patient to use presented X-rays and clinical images.

Conflicts of Interest: The authors declare no conflict of interest.

References

1. Markopoulos, A.K. Current aspects on oral squamous cell carcinoma. *Open Dent. J.* **2012**, *6*, 126–130. [CrossRef]
2. Ferlay, J.; Soerjomataram, I.; Dikshit, R.; Eser, S.; Mathers, C.; Rebelo, M.; Parkin, D.M.; Forman, D.; Bray, F. Cancer incidence and mortality worldwide: Sources, methods and major patterns in GLOBOCAN 2012. *Int. J. Cancer* **2015**, *136*, E359–E386. [CrossRef]
3. Bray, F.; Ferlay, J.; Soerjomataram, I.; Siegel, R.L.; Torre, L.A.; Jemal, A. Global cancer statistics 2018: GLOBOCAN estimates of incidence and mortality worldwide for 36 cancers in 185 countries. *CA Cancer J. Clin.* **2018**, *68*, 394–424. [CrossRef]
4. Chang, A.M.; Kim, S.W.; Duvvuri, U.; Johnson, J.T.; Myers, E.N.; Ferris, R.L.; Gooding, W.E.; Seethala, R.R.; Chiosea, S.I. Early squamous cell carcinoma of the oral tongue: Comparing margins obtained from the glossectomy specimen to margins from the tumor bed. *Oral Oncol.* **2013**, *49*, 1077–1082. [CrossRef]
5. Hinni, M.L.; Ferlito, A.; Brandwein-Gensler, M.S.; Takes, R.P.; Silver, C.E.; Westra, W.H.; Seethala, R.R.; Rodrigo, J.P.; Corry, J.; Bradford, C.R.; et al. Surgical margins in head and neck cancer: A contemporary review. *Head Neck* **2013**, *35*, 1362–1370. [CrossRef] [PubMed]
6. Maxwell, J.H.; Thompson, L.D.; Brandwein-Gensler, M.S.; Weiss, B.G.; Canis, M.; Purgina, B.; Prabhu, A.V.; Lai, C.; Shuai, Y.; Carroll, W.R.; et al. Early oral tongue squamous cell carcinoma: Sampling of margins from tumor bed and worse local control. *JAMA Otolaryngol. Head Neck Surg.* **2015**, *141*, 1104–1110. [CrossRef] [PubMed]
7. Meier, J.D.; Oliver, D.A.; Varvares, M.A. Surgical margin determination in head and neck oncology: Current clinical practice. The results of an International American Head and Neck Society Member Survey. *Head Neck* **2005**, *27*, 952–958. [CrossRef] [PubMed]
8. Thomas Robbins, K.; Triantafyllou, A.; Suarez, C.; Lopez, F.; Hunt, J.L.; Strojan, P.; Williams, M.D.; Braakhuis, B.J.M.; de Bree, R.; Hinni, M.L.; et al. Surgical margins in head and neck cancer: Intra- and postoperative considerations. *Auris Nasus Larynx* **2019**, *46*, 10–17. [CrossRef]
9. Muller, S.; Boy, S.C.; Day, T.A.; Magliocca, K.R.; Richardson, M.S.; Sloan, P.; Tilakaratne, W.M.; Zain, R.B.; Thompson, L.D.R. Data set for the reporting of oral cavity carcinomas: Explanations and recommendations of the guidelines from the International Collaboration of Cancer Reporting. *Arch. Pathol. Lab. Med.* **2019**, *143*, 439–446. [CrossRef] [PubMed]
10. Leitlinienprogramm Onkologie (Deutsche Krebsgesellschaft, Deutsche Krebshilfe, AWMF): S3-Leitlinie Diagnostik und Therapie des Mundhöhlenkarzinoms, Langversion 3.01 (Konsultationsfassung), 2019, AWMF Registernummer: 007/100OL. 2019. Available online: https://www.leitlinienprogramm-onkologie.de/leitlinien/mundhoehlenkarzinom/ (accessed on 7 February 2021).
11. Chen, C.H.; Hsu, M.Y.; Jiang, R.S.; Wu, S.H.; Chen, F.J.; Liu, S.A. Shrinkage of head and neck cancer specimens after formalin fixation. *J. Chin. Med. Assoc.* **2012**, *75*, 109–113. [CrossRef]
12. Looser, K.G.; Shah, J.P.; Strong, E.W. The significance of "positive" margins in surgically resected epidermoid carcinomas. *Head Neck Surg.* **1978**, *1*, 107–111. [CrossRef] [PubMed]
13. Ribeiro, N.F.; Godden, D.R.; Wilson, G.E.; Butterworth, D.M.; Woodwards, R.T. Do frozen sections help achieve adequate surgical margins in the resection of oral carcinoma? *Int. J. Oral Maxillofac. Surg.* **2003**, *32*, 152–158. [CrossRef]
14. Fridman, E.; Na'ara, S.; Agarwal, J.; Amit, M.; Bachar, G.; Villaret, A.B.; Brandao, J.; Cernea, C.R.; Chaturvedi, P.; Clark, J.; et al. The role of adjuvant treatment in early-stage oral cavity squamous cell carcinoma: An international collaborative study. *Cancer* **2018**, *124*, 2948–2955. [CrossRef]
15. Jayasooriya, P.R.; Pitakotuwage, T.N.; Mendis, B.R.; Lombardi, T. Descriptive study of 896 Oral squamous cell carcinomas from the only University based Oral Pathology Diagnostic Service in Sri Lanka. *BMC Oral Health* **2016**, *16*, 1. [CrossRef]

16. Friedland, P.L.; Bozic, B.; Dewar, J.; Kuan, R.; Meyer, C.; Phillips, M. Impact of multidisciplinary team management in head and neck cancer patients. *Br. J. Cancer* **2011**, *104*, 1246–1248. [CrossRef] [PubMed]
17. Gou, L.; Yang, W.; Qiao, X.; Ye, L.; Yan, K.; Li, L.; Li, C. Marginal or segmental mandibulectomy: Treatment modality selection for oral cancer: A systematic review and meta-analysis. *Int. J. Oral Maxillofac. Surg.* **2018**, *47*, 1–10. [CrossRef] [PubMed]
18. Hidalgo, D.A. Fibula free flap: A new method of mandible reconstruction. *Plast. Reconstr. Surg.* **1989**, *84*, 71–79. [CrossRef] [PubMed]
19. Zlotolow, I.M.; Huryn, J.M.; Piro, J.D.; Lenchewski, E.; Hidalgo, D.A. Osseointegrated implants and functional prosthetic rehabilitation in microvascular fibula free flap reconstructed mandibles. *Am. J. Surg.* **1992**, *164*, 677–681. [CrossRef]
20. Attia, S.; Wiltfang, J.; Streckbein, P.; Wilbrand, J.F.; El Khassawna, T.; Mausbach, K.; Howaldt, H.P.; Schaaf, H. Functional and aesthetic treatment outcomes after immediate jaw reconstruction using a fibula flap and dental implants. *J. Craniomaxillofac. Surg.* **2019**, *47*, 786–791. [CrossRef]
21. Attia, S.; Wiltfang, J.; Pons-Kuhnemann, J.; Wilbrand, J.F.; Streckbein, P.; Kahling, C.; Howaldt, H.P.; Schaaf, H. Survival of dental implants placed in vascularised fibula free flaps after jaw reconstruction. *J. Craniomaxillofac. Surg.* **2018**, *46*, 1205–1210. [CrossRef]
22. Chang, Y.M.; Wei, F.C. Fibula jaw-in-a-day with minimal computer-aided design and manufacturing: Maximizing efficiency, cost-effectiveness, intraoperative flexibility, and quality. *Plast. Reconstr. Surg.* **2021**, *147*, 476–479. [CrossRef]
23. Garrido-Martinez, P.; Pena-Cardelles, J.F.; Pozo-Kreilinger, J.J.; Esparza-Gomez, G.; Montesdeoca-Garcia, N.; Cebrian-Carretero, J.L. Jaw in a day: Osseointegration of the implants in the patient's leg before reconstructive surgery of a maxilla with ameloblastoma. A 4-year follow-up case report. *J. Clin. Exp Dent.* **2021**, *13*, e81–e87. [CrossRef] [PubMed]
24. Khatib, B.; Cheng, A.; Sim, F.; Bray, B.; Patel, A. Challenges with the jaw in a day technique. *J. Oral Maxillofac. Surg.* **2020**, *78*, 1869.e1–1869.e10. [CrossRef] [PubMed]
25. Patel, A.; Harrison, P.; Cheng, A.; Bray, B.; Bell, R.B. Fibular reconstruction of the maxilla and mandible with immediate implant-supported prosthetic rehabilitation: Jaw in a day. *Oral Maxillofac. Surg. Clin. N. Am.* **2019**, *31*, 369–386. [CrossRef]
26. Sukato, D.C.; Hammer, D.; Wang, W.; Shokri, T.; Williams, F.; Ducic, Y. Experience with "Jaw in a Day" technique. *J. Craniofac. Surg.* **2020**, *31*, 1212–1217. [CrossRef]
27. Han, H.H.; Kim, H.Y.; Lee, J.Y. The pros and cons of computer-aided surgery for segmental mandibular reconstruction after oncological surgery. *Arch. Craniofac. Surg.* **2017**, *18*, 149–154. [CrossRef] [PubMed]
28. Alassaf, M.H.; Li, W.; Joshi, A.S.; Hahn, J.K. Computer-based planning system for mandibular reconstruction. *Stud. Health Technol. Inf.* **2014**, *196*, 6–10.
29. Ciocca, L.; De Crescenzio, F.; Fantini, M.; Scotti, R. CAD/CAM and rapid prototyped scaffold construction for bone regenerative medicine and surgical transfer of virtual planning: A pilot study. *Comput. Med. Imaging Graph.* **2009**, *33*, 58–62. [CrossRef]
30. Ciocca, L.; Mazzoni, S.; Fantini, M.; Persiani, F.; Marchetti, C.; Scotti, R. CAD/CAM guided secondary mandibular reconstruction of a discontinuity defect after ablative cancer surgery. *J. Craniomaxillofac. Surg.* **2012**, *40*, e511–e515. [CrossRef]
31. Ciocca, L.; Marchetti, C.; Mazzoni, S.; Baldissara, P.; Gatto, M.R.; Cipriani, R.; Scotti, R.; Tarsitano, A. Accuracy of fibular sectioning and insertion into a rapid-prototyped bone plate, for mandibular reconstruction using CAD-CAM technology. *J. Craniomaxillofac. Surg.* **2015**, *43*, 28–33. [CrossRef]
32. Toto, J.M.; Chang, E.I.; Agag, R.; Devarajan, K.; Patel, S.A.; Topham, N.S. Improved operative efficiency of free fibula flap mandible reconstruction with patient-specific, computer-guided preoperative planning. *Head Neck* **2015**, *37*, 1660–1664. [CrossRef] [PubMed]
33. Culie, D.; Dassonville, O.; Poissonnet, G.; Riss, J.C.; Fernandez, J.; Bozec, A. Virtual planning and guided surgery in fibular free-flap mandibular reconstruction: A 29-case series. *Eur. Ann. Otorhinolaryngol. Head Neck Dis.* **2016**, *133*, 175–178. [CrossRef]
34. Hanken, H.; Schablowsky, C.; Smeets, R.; Heiland, M.; Sehner, S.; Riecke, B.; Nourwali, I.; Vorwig, O.; Grobe, A.; Al-Dam, A. Virtual planning of complex head and neck reconstruction results in satisfactory match between real outcomes and virtual models. *Clin. Oral Investig.* **2015**, *19*, 647–656. [CrossRef] [PubMed]
35. Wilde, F.; Hanken, H.; Probst, F.; Schramm, A.; Heiland, M.; Cornelius, C.P. Multicenter study on the use of patient-specific CAD/CAM reconstruction plates for mandibular reconstruction. *Int. J. Comput. Assist. Radiol. Surg.* **2015**, *10*, 2035–2051. [CrossRef]
36. Mazzola, F.; Smithers, F.; Cheng, K.; Mukherjee, P.; Hubert Low, T.H.; Ch'ng, S.; Palme, C.E.; Clark, J.R. Time and cost-analysis of virtual surgical planning for head and neck reconstruction: A matched pair analysis. *Oral Oncol.* **2020**, *100*, 104491. [CrossRef] [PubMed]
37. Bosc, R.; Hersant, B.; Carloni, R.; Niddam, J.; Bouhassira, J.; De Kermadec, H.; Bequignon, E.; Wojcik, T.; Julieron, M.; Meningaud, J.P. Mandibular reconstruction after cancer: An in-house approach to manufacturing cutting guides. *Int. J. Oral Maxillofac. Surg.* **2017**, *46*, 24–31. [CrossRef] [PubMed]
38. Mottini, M.; Seyed Jafari, S.M.; Shafighi, M.; Schaller, B. New approach for virtual surgical planning and mandibular reconstruction using a fibula free flap. *Oral Oncol.* **2016**, *59*, e6–e9. [CrossRef]
39. Smithers, F.A.E.; Cheng, K.; Jayaram, R.; Mukherjee, P.; Clark, J.R. Maxillofacial reconstruction using in-house virtual surgical planning. *ANZ J. Surg.* **2018**, *88*, 907–912. [CrossRef]
40. Xiao, R.; Ward, M.C.; Yang, K.; Adelstein, D.J.; Koyfman, S.A.; Prendes, B.L.; Burkey, B.B. Increased pathologic upstaging with rising time to treatment initiation for head and neck cancer: A mechanism for increased mortality. *Cancer* **2018**, *124*, 1400–1414. [CrossRef]

41. Barry, C.P.; MacDhabheid, C.; Tobin, K.; Stassen, L.F.; Lennon, P.; Toner, M.; O'Regan, E.; Clark, J.R. 'Out of house' virtual surgical planning for mandible reconstruction after cancer resection: Is it oncologically safe? *Int. J. Oral Maxillofac. Surg.* **2020**. [CrossRef]
42. Liu, X.J.; Gui, L.; Mao, C.; Peng, X.; Yu, G.Y. Applying computer techniques in maxillofacial reconstruction using a fibula flap: A messenger and an evaluation method. *J. Craniofac. Surg.* **2009**, *20*, 372–377. [CrossRef]
43. Brown, J.S.; Barry, C.; Ho, M.; Shaw, R. A new classification for mandibular defects after oncological resection. *Lancet Oncol.* **2016**, *17*, e23–e30. [CrossRef]
44. Brown, J.S.; Shaw, R.J. Reconstruction of the maxilla and midface: Introducing a new classification. *Lancet Oncol.* **2010**, *11*, 1001–1008. [CrossRef]
45. Freeman, G.H.; Halton, J.H. Note on an exact treatment of contingency, goodness of fit and other problems of significance. *Biometrika* **1951**, *38*, 141–149. [CrossRef] [PubMed]
46. Holzle, F.; Ristow, O.; Rau, A.; Mucke, T.; Loeffelbein, D.J.; Mitchell, D.A.; Wolff, K.D.; Kesting, M.R. Evaluation of the vessels of the lower leg before microsurgical fibular transfer. Part I: Anatomical variations in the arteries of the lower leg. *Br. J. Oral Maxillofac. Surg.* **2011**, *49*, 270–274. [CrossRef]
47. Battaglia, S.; Maiolo, V.; Savastio, G.; Zompatori, M.; Contedini, F.; Antoniazzi, E.; Cipriani, R.; Marchetti, C.; Tarsitano, A. Osteomyocutaneous fibular flap harvesting: Computer-assisted planning of perforator vessels using Computed Tomographic Angiography scan and cutting guide. *J. Craniomaxillofac. Surg.* **2017**, *45*, 1681–1686. [CrossRef]
48. Ribuffo, D.; Atzeni, M.; Saba, L.; Guerra, M.; Mallarini, G.; Proto, E.B.; Grinsell, D.; Ashton, M.W.; Rozen, W.M. Clinical study of peroneal artery perforators with computed tomographic angiography: Implications for fibular flap harvest. *Surg. Radiol. Anat.* **2010**, *32*, 329–334. [CrossRef]
49. Abou-Foul, A.K.; Borumandi, F. Anatomical variants of lower limb vasculature and implications for free fibula flap: Systematic review and critical analysis. *Microsurgery* **2016**, *36*, 165–172. [CrossRef]
50. Ettinger, K.S.; Alexander, A.E.; Arce, K. Computed Tomographic Angiography Perforator Localization for Virtual Surgical Planning of Osteocutaneous Fibular Free Flaps in Head and Neck Reconstruction. *J. Oral Maxillofac. Surg.* **2018**, *76*, 2220–2230. [CrossRef]
51. Kelly, A.M.; Cronin, P.; Hussain, H.K.; Londy, F.J.; Chepeha, D.B.; Carlos, R.C. Preoperative MR angiography in free fibula flap transfer for head and neck cancer: Clinical application and influence on surgical decision making. *AJR Am. J. Roentgenol.* **2007**, *188*, 268–274. [CrossRef] [PubMed]
52. Rosson, G.D.; Singh, N.K. Devascularizing complications of free fibula harvest: Peronea arteria magna. *J. Reconstr Microsurg.* **2005**, *21*, 533–538. [CrossRef]
53. Cariati, P.; Farhat, M.C.; Dyalram, D.; Ferrari, S.; Lubek, J.E. The deep circumflex iliac artery free flap in maxillofacial reconstruction: A comparative institutional analysis. *Oral Maxillofac. Surg.* **2021**, 1–6. [CrossRef]
54. Jehn, P.; Spalthoff, S.; Korn, P.; Zeller, A.N.; Dittmann, J.; Zimmerer, R.; Tavassol, F.; Gellrich, N.C. Patient-specific implant modification for alloplastic bridging of mandibular segmental defects in head and neck surgery. *J. Craniomaxillofac. Surg.* **2020**, *48*, 315–322. [CrossRef] [PubMed]
55. Murphy, C.T.; Galloway, T.J.; Handorf, E.A.; Egleston, B.L.; Wang, L.S.; Mehra, R.; Flieder, D.B.; Ridge, J.A. Survival impact of increasing time to treatment initiation for patients with head and neck cancer in the United States. *J. Clin. Oncol.* **2016**, *34*, 169–178. [CrossRef] [PubMed]
56. Ho, A.S.; Kim, S.; Tighiouart, M.; Mita, A.; Scher, K.S.; Epstein, J.B.; Laury, A.; Prasad, R.; Ali, N.; Patio, C.; et al. Quantitative survival impact of composite treatment delays in head and neck cancer. *Cancer* **2018**, *124*, 3154–3162. [CrossRef] [PubMed]
57. DeGraaff, L.H.; Platek, A.J.; Iovoli, A.J.; Wooten, K.E.; Arshad, H.; Gupta, V.; McSpadden, R.P.; Kuriakose, M.A.; Hicks, W.L., Jr.; Platek, M.E.; et al. The effect of time between diagnosis and initiation of treatment on outcomes in patients with head and neck squamous cell carcinoma. *Oral Oncol.* **2019**, *96*, 148–152. [CrossRef]
58. Abler, A.; Roser, M.; Weingart, D. On the indications for and morbidity of segmental resection of the mandible for squamous cell carcinoma in the lower oral cavity. *Mund Kiefer Gesichtschir.* **2005**, *9*, 137–142. [CrossRef]
59. Kansy, K.; Mueller, A.A.; Mucke, T.; Kopp, J.B.; Koersgen, F.; Wolff, K.D.; Zeilhofer, H.F.; Holzle, F.; Pradel, W.; Schneider, M.; et al. Microsurgical reconstruction of the head and neck-current concepts of maxillofacial surgery in Europe. *J. Craniomaxillofac. Surg.* **2014**, *42*, 1610–1613. [CrossRef]
60. Rogers, S.N.; Devine, J.; Lowe, D.; Shokar, P.; Brown, J.S.; Vaugman, E.D. Longitudinal health-related quality of life after mandibular resection for oral cancer: A comparison between rim and segment. *Head Neck* **2004**, *26*, 54–62. [CrossRef]
61. Cornelius, C.P.; Smolka, W.; Giessler, G.A.; Wilde, F.; Probst, F.A. Patient-specific reconstruction plates are the missing link in computer-assisted mandibular reconstruction: A showcase for technical description. *J. Craniomaxillofac. Surg.* **2015**, *43*, 624–629. [CrossRef]
62. Weitz, J.; Bauer, F.J.; Hapfelmeier, A.; Rohleder, N.H.; Wolff, K.D.; Kesting, M.R. Accuracy of mandibular reconstruction by three-dimensional guided vascularised fibular free flap after segmental mandibulectomy. *Br. J. Oral Maxillofac. Surg.* **2016**, *54*, 506–510. [CrossRef] [PubMed]
63. Wilde, F.; Cornelius, C.P.; Schramm, A. Computer-assisted mandibular reconstruction using a patient-specific reconstruction plate fabricated with computer-aided design and manufacturing techniques. *Craniomaxillofac. Trauma Reconstr.* **2014**, *7*, 158–166. [CrossRef] [PubMed]

64. Rustemeyer, J.; Busch, A.; Sari-Rieger, A. Application of computer-aided designed/computer-aided manufactured techniques in reconstructing maxillofacial bony structures. *Oral Maxillofac. Surg.* **2014**, *18*, 471–476. [CrossRef]
65. Deek, N.F.; Wei, F.C. Computer-assisted surgery for segmental mandibular reconstruction with the osteoseptocutaneous fibula flap: Can we instigate ideological and technological reforms? *Plast. Reconstr. Surg.* **2016**, *137*, 963–970. [CrossRef]
66. Wang, Y.Y.; Zhang, H.Q.; Fan, S.; Zhang, D.M.; Huang, Z.Q.; Chen, W.L.; Ye, J.T.; Li, J.S. Mandibular reconstruction with the vascularized fibula flap: Comparison of virtual planning surgery and conventional surgery. *Int. J. Oral Maxillofac. Surg.* **2016**, *45*, 1400–1405. [CrossRef]
67. Bell, R.B. Computer planning and intraoperative navigation in cranio-maxillofacial surgery. *Oral Maxillofac. Surg. Clin. N. Am.* **2010**, *22*, 135–156. [CrossRef]
68. Antony, A.K.; Chen, W.F.; Kolokythas, A.; Weimer, K.A.; Cohen, M.N. Use of virtual surgery and stereolithography-guided osteotomy for mandibular reconstruction with the free fibula. *Plast. Reconstr. Surg.* **2011**, *128*, 1080–1084. [CrossRef]
69. Modabber, A.; Legros, C.; Rana, M.; Gerressen, M.; Riediger, D.; Ghassemi, A. Evaluation of computer-assisted jaw reconstruction with free vascularized fibular flap compared to conventional surgery: A clinical pilot study. *Int. J. Med. Robot.* **2012**, *8*, 215–220. [CrossRef]
70. Roser, S.M.; Ramachandra, S.; Blair, H.; Grist, W.; Carlson, G.W.; Christensen, A.M.; Weimer, K.A.; Steed, M.B. The accuracy of virtual surgical planning in free fibula mandibular reconstruction: Comparison of planned and final results. *J. Oral Maxillofac. Surg.* **2010**, *68*, 2824–2832. [CrossRef] [PubMed]
71. Ciocca, L.; Mazzoni, S.; Fantini, M.; Persiani, F.; Baldissara, P.; Marchetti, C.; Scotti, R. A CAD/CAM-prototyped anatomical condylar prosthesis connected to a custom-made bone plate to support a fibula free flap. *Med. Biol. Eng. Comput.* **2012**, *50*, 743–749. [CrossRef] [PubMed]
72. Schaaf, H.; Wahab-Gothe, T.; Kerkmann, H.; Streckbein, P.; Obert, M.; Pons-Kuehnemann, J.; Ahrens, M.; Howaldt, H.P.; Attia, S. Comparison between flat-panel volume computed tomography and histologic assessments of bone invasion of maxillofacial tumors: Utility of an instantaneous radiologic diagnostic tool. *Oral Surg. Oral Med. Oral Pathol. Oral Radiol.* **2017**, *124*, 191–198. [CrossRef]
73. Slootweg, P.J.; Hordijk, G.J.; Schade, Y.; van Es, R.J.; Koole, R. Treatment failure and margin status in head and neck cancer. A critical view on the potential value of molecular pathology. *Oral Oncol.* **2002**, *38*, 500–503. [CrossRef]
74. Ebrahimi, A.; Murali, R.; Gao, K.; Elliott, M.S.; Clark, J.R. The prognostic and staging implications of bone invasion in oral squamous cell carcinoma. *Cancer* **2011**, *117*, 4460–4467. [CrossRef]
75. Rodby, K.A.; Turin, S.; Jacobs, R.J.; Cruz, J.F.; Hassid, V.J.; Kolokythas, A.; Antony, A.K. Advances in oncologic head and neck reconstruction: Systematic review and future considerations of virtual surgical planning and computer aided design/computer aided modeling. *J. Plast. Reconstr. Aesthet. Surg.* **2014**, *67*, 1171–1185. [CrossRef] [PubMed]
76. Yanamoto, S.; Yamada, S.; Takahashi, H.; Yoshitomi, I.; Kawasaki, G.; Ikeda, H.; Minamizato, T.; Shiraishi, T.; Fujita, S.; Ikeda, T.; et al. Clinicopathological risk factors for local recurrence in oral squamous cell carcinoma. *Int. J. Oral Maxillofac. Surg.* **2012**, *41*, 1195–1200. [CrossRef] [PubMed]
77. Zanoni, D.K.; Migliacci, J.C.; Xu, B.; Katabi, N.; Montero, P.H.; Ganly, I.; Shah, J.P.; Wong, R.J.; Ghossein, R.A.; Patel, S.G. A Proposal to redefine close surgical margins in squamous cell carcinoma of the oral tongue. *JAMA Otolaryngol. Head Neck Surg.* **2017**, *143*, 555–560. [CrossRef] [PubMed]
78. Chen, W.C.; Lai, C.H.; Fang, C.C.; Yang, Y.H.; Chen, P.C.; Lee, C.P.; Chen, M.F. Identification of high-risk subgroups of patients with oral cavity cancer in need of postoperative adjuvant radiotherapy or chemo-radiotherapy. *Medicine* **2016**, *95*, e3770. [CrossRef]
79. Magliocca, K.R. Surgical margins: The perspective of pathology. *Oral Maxillofac. Surg. Clin. N. Am.* **2017**, *29*, 367–375. [CrossRef] [PubMed]
80. Smits, R.W.; Koljenovic, S.; Hardillo, J.A.; Ten Hove, I.; Meeuwis, C.A.; Sewnaik, A.; Dronkers, E.A.; Bakker Schut, T.C.; Langeveld, T.P.; Molenaar, J.; et al. Resection margins in oral cancer surgery: Room for improvement. *Head Neck* **2016**, *38*, E2197–E2203. [CrossRef] [PubMed]

cancers

an Open Access Journal by MDPI

Indexed in: PubMed | CITESCORE 4.4 SCOPUS | IMPACT FACTOR 6.639

CERTIFICATE OF PUBLICATION

Certificate of publication for the article titled:

Impact of Planning Method (Conventional versus Virtual) on Time to Therapy Initiation and Resection Margins: A Retrospective Analysis of 104 Immediate Jaw Reconstructions

Authored by:

Michael Knitschke; Christina Bäcker; Daniel Schmermund; Sebastian Böttger; Philipp Streckbein; Hans-Peter Howaldt; Sameh Attia

Published in:

Cancers **2021**, Volume 13, Issue 12, 3013

MDPI Academic Open Access Publishing since 1996

Basel, October 2021

3.4. <u>Originalarbeit 4:</u> Computed Tomography Angiography (CTA) before Reconstructive Jaw Surgery Using Fibula Free Flap: Retrospective Analysis of Vascular Architecture.

Knitschke, M.; Baumgart, A.K.; Bäcker, C.; Adelung, C.; Roller, F.; Schmermund, D.; Böttger, S.; Howaldt, H.-P.; Attia, S. Computed Tomography Angiography (CTA) before Reconstructive Jaw Surgery Using Fibula Free Flap: Retrospective Analysis of Vascular Architecture. Diagnostics **2021**, 11, 1865.
https://doi.org/10.3390/diagnostics11101865 **IF: 3,706**

Zusammenfassung:

Die Computertomographie-Angiographie (CTA) wird zur präoperativen Beurteilung des Gefäßsystems der unteren Extremitäten zur Planung der Kieferrekonstruktion mit freiem Fibulatransplantat eingesetzt. In der retrospektiven klinischen Studie wurden angefertigte CTA (*n* = 72) der Beine für die virtuelle chirurgische Planung ausgewertet. Ziel war es, die Struktur der Gefäßversorgung der Fibula in der „Routine"-CTA-Bildgebung zu erforschen. Besonderer Fokus lag auf der „Architektur" des infra-poplitealen Gefäßsystems und der Dichte und Verteilung der kleinen Gefäße der *A. fibularis* insbesondere der periostalen Äste (PB) und der septo-kutanen Perforatoren (SCPs).

Insgesamt wurden 144 untere Gliedmaßen ausgewertet (Durchschnittsalter: 58,5 ± 15,3 Jahre; Frauen: *n* = 28, 38,9 %; Männer: *n* = 44, 61,1 %). Das Gefäßsystem wurde in 140 Fällen (97,2 %) gemäß der Klassifizierung von *Kim et al.* als regelrecht (Typ I-A bis II-C) eingestuft. Es wurden hypoplastische *A. tibialis anterior* (Typ III-A, *n* = 2) und hypo- und aplastische *A. tibialis posterior* (Typ III-B, *n* = 2) festgestellt. Stenosen wurden meist in der *A. fibularis* (*n* = 11), einmal in der *A. tibialis anterior* und zweimal in der *A. tibialis posterior* beobachtet. Insgesamt wurden *n* = 361 periostale Äste und *n* = 231 septo-kutane Perforatoren registriert. Während sich für die periostalen Äste entlang der Fibula ein Verteilungsmuster mit zwei Häufigkeitsgipfeln ergab, wurde für die septo-kutane Äste ein eher dreigeteiltes Verteilungsmuster aufgezeichnet. Eine geringere Dichte wurde für periostale Äste der *A. fibularis* im Vergleich zu einer experimentellen Studie an humanen Fibulapräparaten gefunden. Je weiter proximal ein Fibulaabschnitt untersucht wurde, desto häufiger wurde ein periostaler Ast in der CTA beobachtet, was wichtige Informationen zur Auswahl der

geeigneten Entnahmestelle liefert. Wir folgerten, dass die konventionelle CTA für die virtuelle chirurgische Planung des Fibulatransplantates in der Lage ist, septo-kutane (SCP) und periostale Äste (PB) darzustellen.

Ausblick:

Während die Studie die vaskuläre „Architektur“ der unteren Extremität unabhängig von der Kenntnis der gewählten Entnahmeseite und des Transplantationsergebnisses des Fibulatransplantates untersuchte, können weitere Untersuchungen an eben dieser Studiengruppe geeignet sein, um u.a. diese klinisch relevanten Fragen zu beantworten:

1. Wie wirken sich Stenosen der *A. fibularis* auf das Transplantationsergebnis des Fibulatransplantates aus?
2. Wie beeinflusst die Verteilung der mittels CTA nachgewiesenen periostalen Äste (PB) und der septo-kutanen Perforatoren (SCPs) das chirurgische Ergebnis von mono- und polysegmentalen Kieferrekonstruktionen sowie (sub-) totalen Lappenverlust?
3. Beeinflusst die beobachtete Verteilung der periostalen Äste und der septo-kutanen Perforatoren die Wundheilung der Spenderstelle?

Die Kenntnis über die Lage der Perforatoren kann bei der Planung der Segmentlängen und des Umrisses der Hautinsel helfen, um drohende Komplikationen im Sinne von (sub-)totalen Transplantatverlusten zu vermeiden. Die auf den Ergebnissen aufbauende Originalarbeit 5 vergleicht die Studienergebnisse mit den virtuellen chirurgischen Planungen und den Transplantationsergebnissen.

diagnostics

MDPI

Article

Computed Tomography Angiography (CTA) before Reconstructive Jaw Surgery Using Fibula Free Flap: Retrospective Analysis of Vascular Architecture

Michael Knitschke [1,*], Anna Katrin Baumgart [1], Christina Bäcker [1], Christian Adelung [2], Fritz Roller [2], Daniel Schmermund [1], Sebastian Böttger [1], Hans-Peter Howaldt [1] and Sameh Attia [1]

1 Department of Oral and Maxillofacial Surgery, Justus-Liebig-University, Klinikstrasse 33, 35392 Giessen, Germany; Anna.Baumgart@ymail.com (A.K.B.); Christina.Baecker-2@dentist.med.uni-giessen.de (C.B.); Daniel.Schmermund@uniklinikum-giessen.de (D.S.); Sebastian.Boettger@uniklinikum-giessen.de (S.B.); HP.Howaldt@uniklinikum-giessen.de (H.-P.H.); Sameh.Attia@dentist.med.uni-giessen.de (S.A.)

2 Department of Radiology, Justus-Liebig-University, Klinikstrasse 33, 35392 Giessen, Germany; Christian.Adelung@radiol.med.uni-giessen.de (C.A.); fritz.c.roller@radiol.med.uni-giessen.de (F.R.)

* Correspondence: Michael.Knitschke@uniklinikum-giessen.de

Abstract: Computed tomography angiography (CTA) is widely used in preoperative evaluation of the lower limbs' vascular system for virtual surgical planning (VSP) of fibula free flap (FFF) for jaw reconstruction. The present retrospective clinical study analysed $n = 72$ computed tomography angiographies (CTA) of lower limbs for virtual surgical planning (VSP) for jaw reconstruction. The purpose of the investigation was to evaluate the morphology of the fibular bone and its vascular supply in CTA imaging, and further, the amount and distribution of periosteal branches (PB) and septo-cutaneous perforators (SCPs) of the fibular artery. A total of 144 lower limbs was assessed (mean age: 58.5 ± 15.3 years; 28 females, 38.9%; 44 males, 61.1%). The vascular system was categorized as regular (type I-A to II-C) in 140 cases (97.2%) regarding the classification by Kim. Absent anterior tibial artery (type III-A, $n = 2$) and posterior tibial artery (type III-B, $n = 2$) were detected in the left leg. Stenoses were observed mostly in the fibular artery ($n = 11$), once in the anterior tibial artery, and twice in the posterior tibial artery. In total, $n = 361$ periosteal branches (PBs) and $n = 231$ septo-cutaneous perforators (SCPs) were recorded. While a distribution pattern for PBs was separated into two clusters, a more tripartite distribution pattern for SCPs was found. We conclude that conventional CTA for VSP of free fibula flap (FFF) is capable of imaging and distinguishing SCPs and PBs.

Keywords: oral cancer; head and neck tumor; fibula free flap; virtual surgical planning

Citation: Knitschke, M.; Baumgart, A.K.; Bäcker, C.; Adelung, C.; Roller, F.; Schmermund, D.; Böttger, S.; Howaldt, H.-P.; Attia, S. Computed Tomography Angiography (CTA) before Reconstructive Jaw Surgery Using Fibula Free Flap: Retrospective Analysis of Vascular Architecture. *Diagnostics* **2021**, *11*, 1865. https://doi.org/10.3390/diagnostics11101865

Academic Editors: Maciej Misiolek and Joanna Katarzyna Strzelczyk

Received: 15 September 2021
Accepted: 8 October 2021
Published: 11 October 2021

1. Introduction

Fourteen years after the first description of the free fibula flap (FFF) by Taylor in 1975 [1], the FFF was used for mandibular reconstruction by Hidalgo [2]. This flap is reliable and widely applicable in reconstructive surgery [3]. It offers the possibility of reconstructing both bony and soft tissue defects with a free flap from only one donor site. The FFF can be shaped to almost an ideal form of the missing parts of the jaw and represents the gold standard in mandibular reconstruction [4]. Additionally, it increases the patient's quality of life after ablative cancer surgery [5,6]. The osseous FFF facilitates prosthetic rehabilitation with dental implants with stable long-term results [7,8].

The vascular supply of the fibula flap is based on the fibular artery (FA), which arises from the truncus tibiofibularis (TTF) after branching the posterior tibial artery (PTA). The truncus continues as the popliteal artery (PA) after debranching the anterior tibial artery (ATA). Preoperative imaging of the vascular status of the lower limb is mandatory for the diagnosis of any anatomical variants. Hypo- or aplasia of the typical three-vessel architecture of the lower leg is crucial to prevent critical limb ischemia [9–11]. Peripheral

arterial occlusive disease (PAOD) and stenoses have been mentioned as contraindications for flap raising, as they may lead to critical ischemia of the donor-site leg [12–14].

Computed tomography angiography (CTA) [15–18], digital subtraction angiography (DSA) [9,19], or magnetic resonance angiography (MRA) [9,12,17,20,21] are often used as objective techniques for visualization of the lower limbs vascular status. Today CTA and MRA often replace invasive catheter arteriography [14]. Present nephrocytotoxic effects of iodinated contrast media and exposure to radiation are disadvantages of CTA and DSA. Acute renal failure is assigned to endothelial cell damage resulting in endothelial dysfunction [22]. There is a correlation between dosage and an increased risk of renal dysfunction in predisposed patients with impaired renal function (e.g., diabetic patients) [23–25]. Reduction of the contrast agent volume would minimize damage to renal function and systemic toxicity [26]. CTA offers numerous advantages as a non-invasive imaging system in comparison to DSA with treating complications of intraarterial application (pseudoaneurysm, arteriovenous fistula) [27]. CTA arises from the standard imaging of the infra-popliteal system in PAOD diagnosis [28]. Further, CTA has been reported to be superior to MRA for visualization of the perforator system [29], and is frequently available, sufficiently precise, and cost-effective [16,30,31]. Other authors prefer MRA as a radiation-free, non-invasive diagnostic, and operator-independent tool [32,33]. In addition, a systematic review, which compared both methods for PAOD diagnosis, found no significant differences [34].

Currently, virtual surgical planning (VSP) and facilitating custom-made, titan-laser-melted patient-specific osteosynthesis plates, CT scans, and DICOM data sets of the donor and recipient site are obligatory [35–37]. Performing pre-operative MRA and CTA as standard evaluation before jaw reconstruction will be cost and time expensive. The three-dimensional design and the configured plate allow the translation from virtual planning to surgery site [38]. Due to this planning method, precisely predictable uni- and poly-segmental bony reconstructions are possible [35,39,40]. In literature, 90–95% of FFF success rates were reported in high-volume reconstructive centers [41–44].

Despite those significant advantages, surgery remains challenging in modifying the planned flap design or a prepared patient specific implant (PSI); if perforator vessels are insufficient, unforeseen difficulties on the vascular bundle occur, or the prepared oncologic resection margins are inadequate [45,46]. The necessity for exploring the contralateral leg and/or dissection of an additional microvascular flap can arise. To minimize this risk, extensive preoperative analysis of the vascular system is necessary, and CTA should be run before every fibula harvest to increase flap safety [47]. CTA facilitates simultaneous evaluation of the bone and vascular system. The preoperative planning for an ideal defect-related skin paddle based on cutaneous perforator vessels is of current research interest. Based on preoperative CTA, assessment of position and run-off of the small vessels has to be performed to design a fibular cutting guide that includes those perforators to increase flap safety [15]. Clinical trials have been carried out on the feasibility of integrating Doppler sonography to detect and locate perforator vessels of the lower leg and facilitate manual transfer to VSP software for presurgical planning [48].

The present retrospective clinical study aimed to determine whether the prospective CTA provides additive aspects for FFF segment molding for VSP. Thus, the purpose of the investigation was to evaluate the morphology of the fibular bone and its vascular supply (lower limb vascular architecture, FA run-off, and distance to the fibula) in CTA imaging, and further, the amount and distribution of PBs and SCPs of the FA. Furthermore, this study aimed to give a clear answer to the following questions:

1. What is the prevalence of vascular anomalies in the present sample?
2. Is it possible to record and distinguish periosteal branches (PBs) and septo-cutaneous perforators (SCPs) of the FA, and up to which diameter can these vessels be detected in routinely run preoperative CTA for VSP?
3. What is the frequency and distribution of PBs and SCPs of the FA?

2. Materials and Methods

2.1. Study Design and Patient Population

The investigation was conducted as a monocentric, retrospective clinical study on patients who received virtual planned for immediate or delayed jaw reconstruction with FFF from January 2015 to December 2020. The prospective (pre-operative) CTA of the lower limbs was analyzed retrospectively (Figure 1). Out of a total sample size of $n = 80$ VSP cases, 77 CTA datasets of the lower limb were evaluable (MRA instead of CTA, $n = 3$). Of those, five instances of repeated reconstruction after primary flap graft loss ($n = 4$) and tumor recurrence ($n = 1$) were excluded because of one vessel CTA. Finally, a number of ($n = 72$) cases was available for the analysis. The blinded observer was not given any information concerning the elected donor site for FFF transplant.

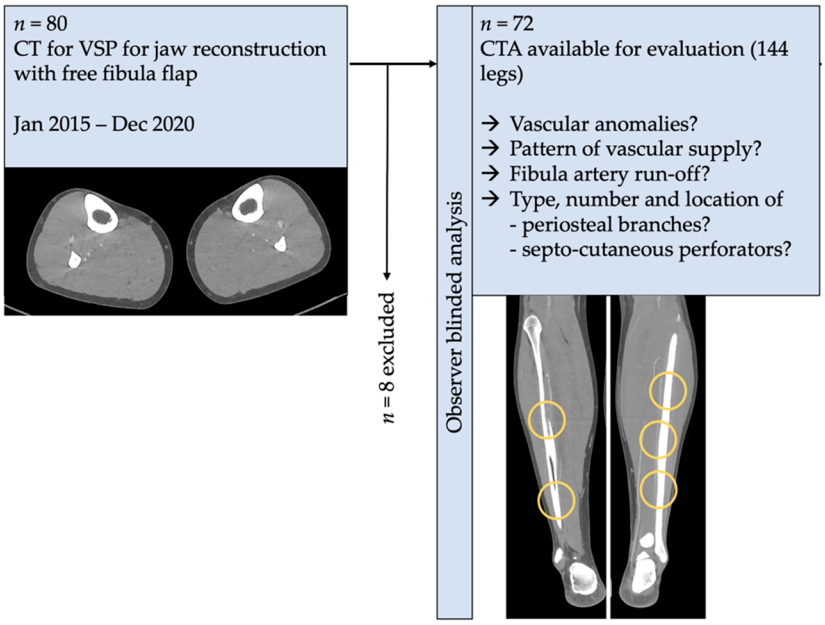

Figure 1. Schematic workflow of the present study. Only computed tomography angiography (CTA) DICOM-datasets of virtual planned jaw reconstructions were included in the investigation. The architecture of lower leg vascular perfusion was analyzed. Number, type of perforator (periosteal branch, septo-cutaneous), and distance to the distal tip of the fibula and between the branches were assessed.

2.2. Inclusion and Exclusion Criteria for Study Subjects

Patients with virtual surgical planning of immediate or delayed jaw reconstruction with FFF and pre-operative CTA and a layer thickness of $\leq$1.5 mm were enrolled. When previous (VSP) FFF failed and total flap loss occurred, only the datasets of the initial reconstruction attempt with FFF (two fibulae CTA) were included.

2.3. Methods, Study Parameters, and Evaluator Calibration

CTA analyses of pseudo-anonymized DICOM data sets (including gender and patient's age at CTA scan) were performed by a blinded investigator (A.K.B.).

All CTA studies were performed in the Department of Diagnostic and Interventional Radiology of the University Hospital Giessen. The CTA scans were performed on a first- and third-generation dual-energy CT (SOMATOM Definition AS & Force, Siemens Healthineers, Forchheim, Germany). The CTAs used the following standard operating procedure: The first acquisition determined the level for bolus tracking and the scan length. The examination of both legs was done with a slice thickness $\leq$ 1.5 mm above the aortic bifurcation (chest vertebral body 12) to the feet (70 kV, 300 mA max, pitch 0.5, collimation 0.6 mm, matrix size 512 $\times$ 512).

The scans were started when the enhancement peak was observed, and the Bolus tracking approach was utilized to determine the contrast media filling of the relevant vessels. The zone of interest for monitoring vessel filling was positioned in the abdominal aorta at a set level, centered within the artery, and sized to contain only the lumen. Non-ionic contrast medium containing 350 mg of iodine per milliliter (Ultravist 370, Bayer, Leverkusen, Germany) was injected intravenously into an antecubital vein using an 18-gauge needle and a power injector at maximum flow rates of 4.5 or 5.0 mL/s. For a typical scan period of 40 s, the volume of contrast material ranged from 100 to 120 mL (adjusted to patient's weight).

CTA DICOM data sets were analyzed in HOROS-Software for Macintosh (Version 4.0.0 RC5, Horosproject). Horos is a free and open-source code software (FOSS) program distributed free of charge under the LGPL license at Horosproject.org and sponsored by Nimble Co LLC d/b/a Purview in Annapolis, MD, USA.

The CTA quality was assessed by side-by-side comparison with a region of interest (ROI) in the center of the popliteal artery and dorsal vessels of the dorsum of the foot. For every CTA, the measurements were performed on both patient's legs.

Based on axial acquired data, the multiplanar three-dimensional reconstructions were performed. Maximum intensity projection (MIP) [49,50] and volume-rendered technique (VRT) reconstructions were used. When MIP and VRT reconstructions are coupled [51], precise identification of tiny vessels in the axial plane, as well as determination of pedicle length and diameters, is achievable. The maximal length of the fibular bone was assessed (Figure 2). The images were studied in the coronal and axial plane for the presence of relevant pathologies (stenoses, PAOD) or anatomic anomalies of the infrapopliteal vascular system. The findings were recorded regarding their localization. The vascular anatomy of the lower limb was categorized concerning the infrapopliteal branching pattern classification described by Kim et al. [52]. The length of the TTF, distance after branching of ATA to the bifurcation of PTA, and FA were measured.

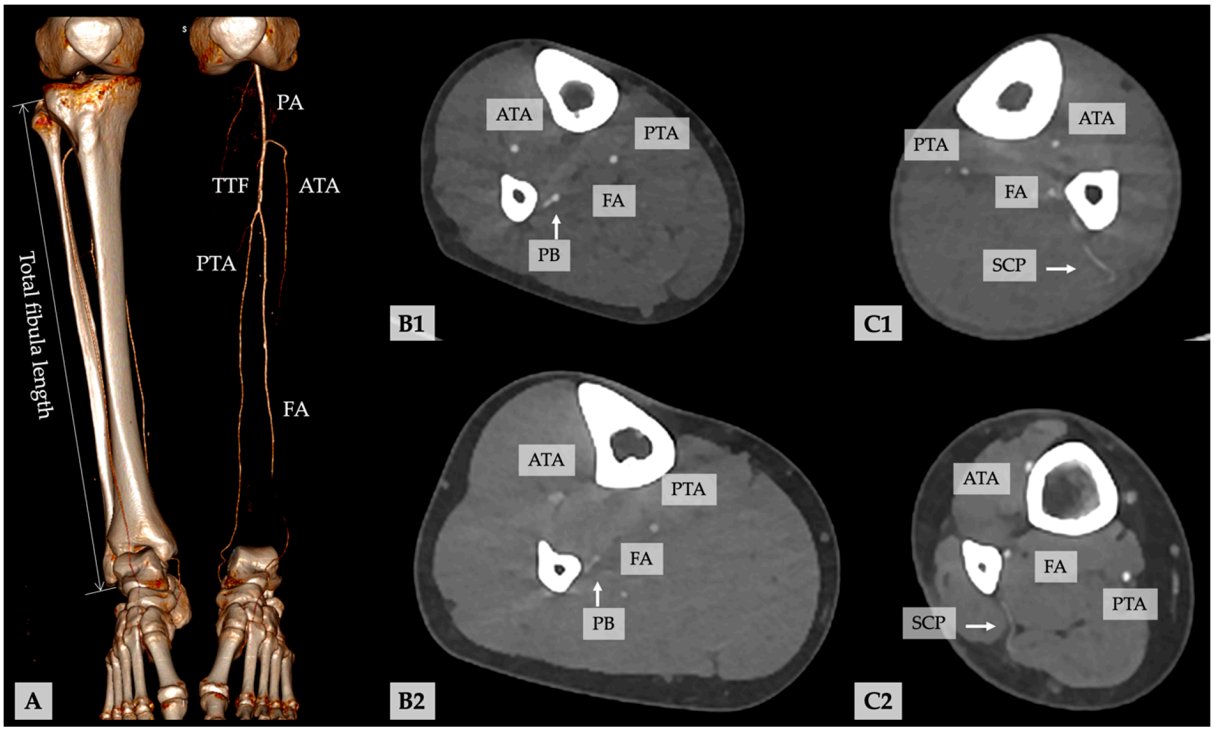

Figure 2. (**A**) Volume rendering and virtual excision of the left tibia and fibula illustrate the vessel run-off along the lower leg. (**B1**,**B2**) Representative examples of periosteal branches (PB) and (**C1**,**C2**) septo-cutaneous perforators (SCP) of the FA in the axial CTA planes (ATA, anterior tibial artery; FA, fibular artery; PA, popliteal artery; PTA, posterior tibial artery; TTF, truncus tibiofibularis).

The localization of the main visible (musculo-)septo-cutaneous perforators and periosteal branches (PB) of the FA were identified in the axial plane on CTA (Figure 2), and the distance of the exit of the perforators of the FA to the distal tip of the fibula was recorded. The shortest distance between the surface of the fibular bone and the center of the FA and the diameter of the FA were recorded in 0.5 mm intervals and 50 mm above the distal tip of the fibula bone. The internal diameter of perforators was also recorded. In cases of doubt, impartial, experienced radiologists (C.A. and F.R.) were consulted.

The following parameters were assessed:

Fibula length, bone and vascular anomalies, vascular anatomy and branching pattern of the calf [52], length of the TTF, the shortest distance between the surface of fibular bone and center of the fibular artery (FA) in the axial plane, the internal diameter of the FA, and the number and length of skin perforators and bone feeders from the distal tip of the fibular bone to branching and between the branches (Figure 2). All measurements were recorded in millimeters. Body weight and height were collected from the medical records.

2.4. Statistical Analyses

Pearson's χ^2 test, Fisher's exact test, and the Freeman-Halton extension [53] were conducted on the categorical variables. The continuous parameters (age, total length of the fibula, length of the FA from origin to the distal tip of the fibula bone, diameter of the FA, length and diameter of the TTF, number and distance of SCPs, and PBs) were verified for normality. The distribution was presented as a mean (standard deviation), and Student's *t*-test was performed. $p < 0.05$ was defined as statistically significant. The statistical analysis was carried out with SPSS 25 (SPSS Inc., Chicago, IL, USA).

2.5. Ethics Statement/Confirmation of Patients' Permission

The local Ethics Committee of Justus-Liebig-University Giessen approved the study (AZ33/20), and patients' permission/consent was not necessary for this retrospective study. All collected data in the Microsoft Excel spreadsheet were pseudonymized.

3. Results

A total of 72 patients (28 females, 38.9%; 44 males, 61.1%) fulfilled the inclusion criteria. The mean age was 58.5 ± 15.3 years (range: 14.8–82.6 years). A series of eight virtual planned reconstructions were excluded due to missing data (MRA instead of CTA, $n = 3$, one leg CTA: reconstruction with contralateral fibula after flap loss, $n = 4$ and after tumor recurrence, $n = 1$).

A total of 144 lower limbs were assessed. The groups were tested for normal distribution. More than half (61.1 %, $n = 44$), of the included study participants were male. Their mean age was 56.8 ± 14.6 years, and they were 4.3 years younger than the female patients; the difference was non-significant ($p = 0.257$). The length of the fibula revealed a gender-specific, significant difference within the mean near to 45 mm more prominent bone in males ($p \leq 0.001$). The detailed demographic parameters and results are summarized in Table 1.

The run-off of the fibular artery (FA) concerning the surface of the fibular bone and the total length is depicted gender-separated in Figure 3A,B. A significant difference in total length of the fibular bone was found (male: $n = 88$, mean ± SD: 39.08 ± 2.35 cm vs. female: $n = 56$, mean ± SD: 34.60 ± 1.70 cm; $p \leq 0.001$). Despite the observed difference of the gender- and body-height-dependent run-off of the FA, the LOESS curves with the inclusion of 50% of the assessed points run almost congruent in the interval between 5.0 cm and 15.0 cm. While between 5.0 cm and 11.0 cm, the FA was found nearer to the surface of the fibula in females than males, by over 11.0 cm to 15.0 cm, the FA was detected, on average, 1.0 mm in the median and the proximal third and more than 2.0 mm farther distant to the fibula in females than in males (Figure 3B).

Table 1. CTA assessment for bone and vascular system parameters of the study group categorized for gender (cm, centimeter; FA, fibular artery; PB, periosteal branch; SCP, septo-cutaneous perforator; SD, standard deviation; TTF, truncus tibiofibularis). Annotation: ‡ Length and diameter of TTF were only assessed for type I-A branching pattern.

***n* = 72 Patients**	***n* (%)**	***n* = 144 Lower Limbs**	***p*-Value**
Age at CT-scan (years), mean ± SD			
Male	44 (61.1)	56.8 ± 14.6	
Female	28 (38.9)	61.1 ± 16.1	0.257
Body weight (kilogram), mean ± SD			
Male (range)	44 (61.1)	77.7 ± 15.7 (37.5–113.0)	
Female (range)	28 (38.9)	66.5 ± 14.1 (43.2–104.0)	0.003
Body height (cm), mean ± SD			
Male (range)	44 (61.1)	177.5 ± 7.2 (159.8–198.0)	
Female (range)	28 (38.9)	161.4 ± 5.6 (150.0–176.0)	≤0.001
BMI (kg/m^2), mean ± SD			
Male (range)	44 (61.1)	24.6 ± 4.9 (14.7–40.0)	
Female (range)	28 (38.9)	25.4 ± 5.4 (17.3–40.0)	0.518
Length of fibula, mean (mm) ± SD			
Male (range)	44 (61.1)	390.8 ± 23.5 (340.2–460.1)	
Female (range)	28 (38.9)	346.0 ± 17.0 (310.0–390.2)	≤0.001
Length of TTF, mean (mm) ± SD ‡			
Male (range)	80 (62.5)	35.15 ± 14.07 (6.0–67.2)	
Female (range)	48 (37.5)	28.20 ± 11.51 (10.0–64.5)	0.0045
Diameter of TTF, mean (mm) ± SD ‡			
Male (range)	80 (62.5)	4.44 ± 1.00 (2.67–6.78)	
Female (range)	48 (37.5)	3.64 ± 0.65 (2.30–5.12)	≤0.001
Length of FA, mean (mm) ± SD			
Male (range)	44 (61.1)	25.66 ± 3.72 (7.0–35.85)	
Female (range)	28 (38.9)	22.42 ± 3.65 (4.65–26.6)	≤0.001
Diameter of FA, mean (mm) ± SD			
Male (range)	44 (61.1)	3.41 ± 0.78 (1.88–5.40)	
Female (range)	28 (38.9)	2.78 ± 0.64 (1.46–4.27)	≤0.001
Diameter of SCP, mean (mm) ± SD			
Male (range)	127 (59.6)	0.91 ± 0.26 (0.53–1.82)	
Female (range)	86 (40.4)	0.96 ± 0.35 (0.52–2.43)	0.233
Diameter of PB, mean (mm) ± SD			
Male (range)	230 (63.7)	0.88 ± 0.25 (0.40–1.89)	
Female (range)	131 (36.3)	0.86 ± 0.26 (0.35–2.26)	0.472

The gender characteristic difference was also found for the length of FA ($p \leq 0.001$), and diameter of the FA (male: n = 88, mean ± SD: 3.41 ± 0.78 mm vs. female: n = 56, mean ± SD: 2.78 ± 0.64 mm; $p \leq 0.001$). Analogous gender-associated results were found for the length (male: n = 80, mean ± SD: 35.15 ± 14.07 mm vs. female: n = 48, mean ± SD: 28.20 ± 11.51 mm; p = 0.045) and diameter (male: n = 80, mean ± SD: 4.44 ± 1.00 mm vs. female: n = 48, mean ± SD: 3.64 ± 0.65 mm; $p \leq 0.001$) of TTF in the type I-A branching pattern of the infra-popliteal vessels (Table 1).

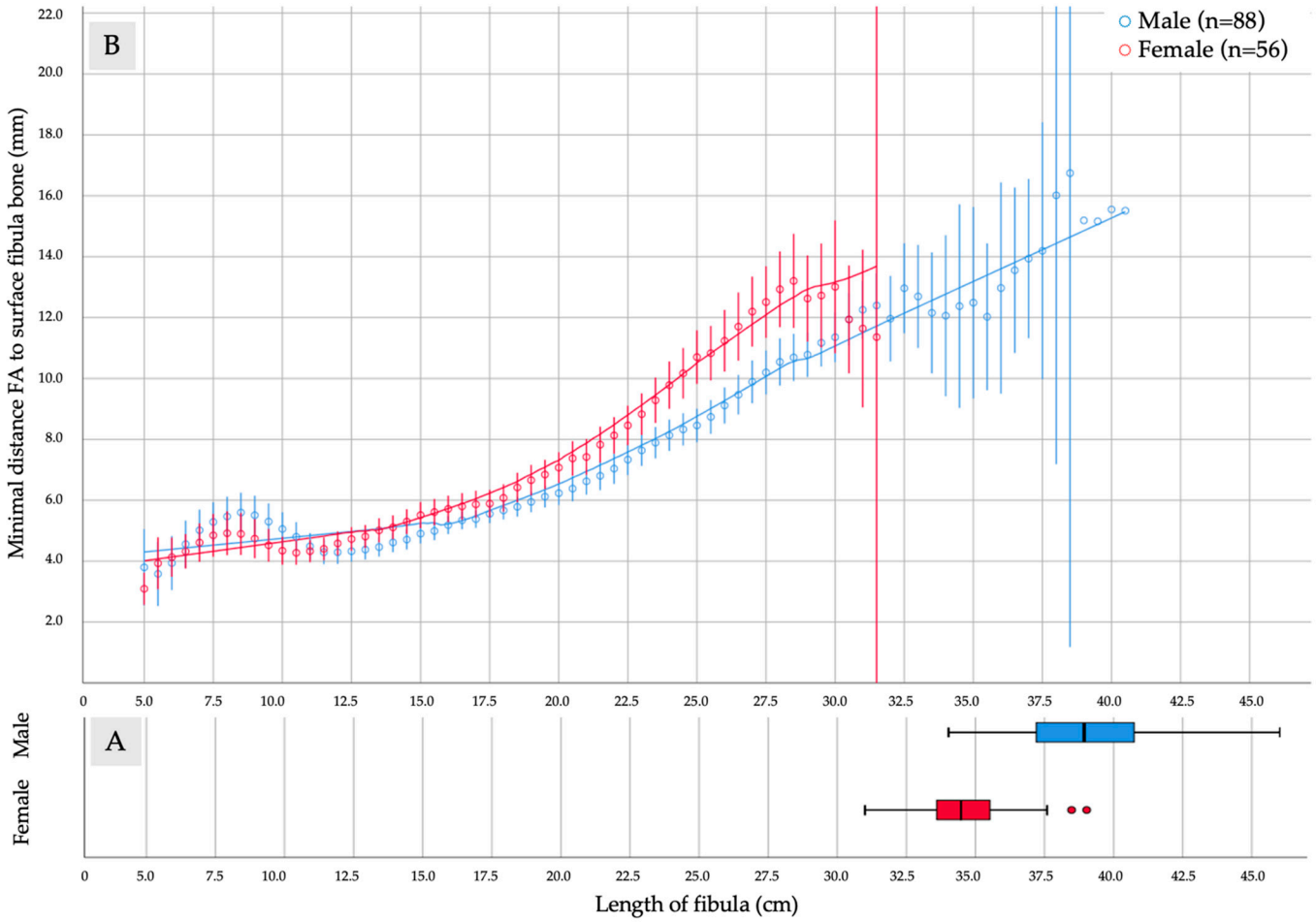

Figure 3. The diagram summarizes assessed parameters of (**A**) length of fibula and (**B**) distance and length of the fibular artery (FA) in relation to fibular bone surface in CTA of 144 lower limbs in 72 patients. (**A**) A significant difference for total length of the fibular bone was measured (male: $n = 88$, mean ± SD: 39.08 ± 2.35 cm vs. female: $n = 56$, mean ± SD: 34.60 ± 1.70 cm; $p = 0.0001$). (**B**) Comparison of the minimal distance of FA run-off (mm) in males ($n = 88$) and females ($n = 56$) measured in axial planes from the distal tip of the fibula (cm). LOESS curves with the inclusion of 50% of the assessed points were drawn.

A total number ($n = 361$) of periosteal branches (PB) and ($n = 231$) septo-cutaneous perforators (SCP) was recorded. The distribution of CTA-based detected PB and SCP is shown in Figure 4. The histogram of scaled vessel origins demonstrates a bi- for PB and trimodal distribution for SCP. The distal PB cluster was narrow, with its maximum placed around 0.30 RD (relative distance), and the proximal one is broader with a frequency peak between 0.55 RD and 0.70 RD. A tripartite distribution pattern was found in SCPs. The distal clustering was narrow and located around 0.30 RD. The mean clustering was broad and located between 0.45 RD and 0.60 RD. Proximally, a third cluster appeared at 0.70 RD. Insignificant differences were recorded concerning gender and diameter of PB ($p = 0.472$) and SCP ($p = 0.233$) of the FA. The diameter of PB ranged from 0.35 mm to 2.26 mm (male: $n = 230$, mean ± SD: 0.88 ± 0.25 mm vs. female: $n = 131$, mean ± SD: 0.86 ± 0.26 mm; $p = 0.472$). SCP ranged from 0.52 mm to 2.43 mm (male: $n = 127$, mean ± SD: 0.91 ± 0.26 mm vs. female: $n = 86$, mean ± SD: 0.96 ± 0.35 mm; $p = 0.233$). The diameter of both vessel types was measured at the origin of the FA (Table 1).

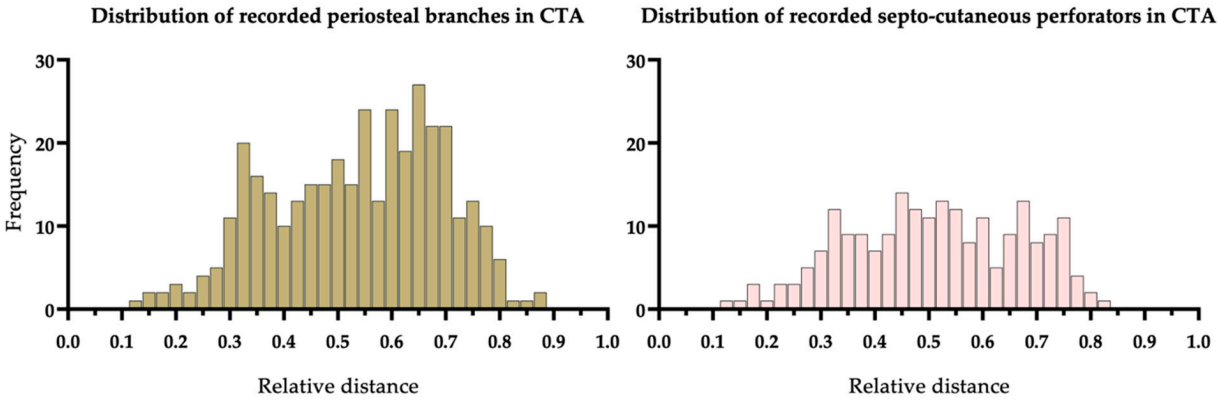

Figure 4. (**Left**) Distribution of periosteal branches (n = 361) and (**Right**) septo-cutaneous perforators (n = 213) of the FA demonstrated by the CTA. The origin of the vessels is scaled concerning the total length of the fibula and given as relative distance.

The evaluated parameters of the lower leg and the vascular system are summarized in Table 2. In a side-by-side comparison, non-significant differences for the total length of the fibular bone were assessed (p = 0.953). One case of a healed isolated fibula fracture was found. In the investigated sample of n = 144 lower legs, the vascular system was categorized as regular (type I-A to II-C) in 140 cases (97.2%) [52]. Absent ATA (type III-A, n = 2) and PTA (type III-B, n = 2) were detected in the left leg (Table 3). Stenoses were mostly observed in FA (n = 11), once in the ATA, and twice in the PTA. While the number of detected SCP of the FA were nearly similar (left: n = 103; right: n = 108), a remarkable difference of 12.5% was observed concerning the number of PB on the right leg (left: n = 168; right: n = 193). The average diameter of PB differed significantly in side-to-side comparisons (p = 0.033) and was larger in the right lower leg.

Table 2. CTA assessment for the study sample's fibula bone and vascular system parameters (SD, standard deviation; ATA, anterior tibial artery; FA, fibular artery; PB, periosteal branch; PTA, posterior tibial artery; SCP, septo-cutaneous perforator; TTF, truncus tibiofibularis). Annotation: ‡ Length and diameter of TTF were only assessed for type I-A branching pattern.

***n* = 144**	**Left Fibula *n* = 72**	**Right Fibula *n* = 72**	***p*-Value**	**Total**
Fibula length, mean (mm) ± SD	373.5 ± 30.8	373.2 ± 30.4	0.953	144
Fibula bone anomalies, *n*			-	
Fracture	1	0		1
Infrapopliteal branching pattern [52]			-	
Regular (I-A to II-C)	68	72		140
Absent ATA (III-A)	2	-		2
Absent PTA (III-B)	2	-		2
Stenoses, *n*			-	
ATA	1	-		1
PTA	2	-		2
FA	5	6		11
Length of TTF, mean (mm) ± SD ‡	30.37 ± 12.78	35.03 ± 14.26	0.053	128
Diameter of TTF, mean (mm) ± SD ‡	4.06 ± 0.92	4.14 ± 0.97	0.663	128
Length of FA, mean (mm) ± SD	244.5 ± 41.3	243.4 ± 39.2	0.809	144
Diameter of FA, mean (mm) ± SD	3.17 ± 0.80	3.16 ± 0.78	1.0	144
Distance to the fibular bone, mean (mm) ± SD	8.58 ± 3.74	8.55 ± 3.81	0.974	144
Overall found SCP, *n*	104	109		213
Mean SCP per fibula (mm) ± SD	1.44 ± 1.10	1.51 ± 1.13	0.647	1.48 ± 1.12
Overall found PB, *n*	168	193		361
Mean PB per fibula (mm) ± SD	2.33 ± 1.46	2.68 ± 1.62	0.033	2.51 ± 1.55

Table 3. Infra-popliteal arterial branching variations of the study sample (n = 144) were categorized according the classification by Kim et al. [52].

Type n (%)	Left Leg, n = 72	Right Leg, n = 72	All, n = 144
I-A	63 (87.5)	65 (90.3)	128 (88.9)
I-B	2 (2.8)	1 (1.4)	3 (2.1)
I-C	1 (1.4)	-	1 (0.7)
II-A	1 (1.4)	2 (2.8)	3 (2.1)
II-B	1 (1.4)	4 (5.6)	5 (3.6)
II-C	-	-	-
III-A	2 (2.8)	-	2 (1.4)
III-B	2 (2.8)	-	2 (1.4)
III-C	-	-	-

The study found an average amount (±SD) of 2.51 ± 1.55 (median: 3.0; range: 0–7) PB and 1.48 ± 1.12 (median: 1.0; range: 0–4) SCP with a mean (±SD) distance between them of 5.17 ± 3.07 cm (median: 4.6 cm; range: 0.1–15.5 cm) of the FA in each fibula in the region of interest between the origin of FA from TTF and 5.0 cm above the distal tip of the fibular bone. One PB was found in 10.77% of the 1 cm segments, 21.07% of the 2.0 cm segments, and 29.17% of the 3 cm segments. One SCP was found in 6.46% of the 1 cm segments, 12.25% of the 2.0 cm segments, and 17.84% of the 3 cm segments (Table 4).

Table 4. Number (%) of fibular segments that were supplied by periosteal branches (PB, n = 361) and corresponding septo-cutaneous perforators (SCP, n = 213) of FA of all lower legs (n = 144).

Size of Segment (cm)/Vessel Type	None	One	Two or More
1.0 PB	89.05%	10.77%	0.18%
2.0 PB	78.33%	21.07%	0.68%
3.0 PB	68.28%	29.17%	2.55%
1.0 SCP	93.54%	6.46%	0
2.0 SCP	87.22%	12.25%	0.54%
3.0 SCP	81.28%	17.84%	0.88%

4. Discussion

Over the past three decades, there has been debate about the best technique for vascular evaluation of fibular grafts [54], which was abandoned in favor of the CT for VSP, which can easily be modified as CTA. Numerous investigations have shown the impact of CTA as a sensitive and specific method for microsurgical free flap [15–18] and perforator flap harvesting in reconstructive surgery [55–63].

4.1. What Is the Prevalence of Vascular Anomalies in the Present Sample?

In the evaluated sample of n = 144 lower limbs, a majority of 88.9% (n = 128) were assigned as type I-A concerning the classification by Kim [52], and four limbs (2.8%) with dominant FA variants (type III-A: n = 2 and III-B: n = 2) were found. The results are comparable to the literature [64]. The sample revealed no cases of a peronea arteria magna (type III-C), in which FA is the main blood-supplying vessel for the lower limb and foot.

Before FFF harvesting, it is crucial to detect this specific, singular vasculature to prevent significant and critical limb and foot ischemia [13,65,66]. In comparison to the vascular supply of the forearm by the superficial and deep palmar arterial arch, for which sufficient perfusion is evaluable by Allen's test, anatomical anomalies like type III-A-C elude simple clinical examination [12,67–69]. In type III-A and -B, blood supply of the foot is shared between the FA and non-hypoplastic ATAs or PTAs, and the diameter of the FA is then often enlarged [14,68,70]. The prevalence of such a dominant FA was published

with 5.2% of any leg, and furthermore, critical vascular anomalies of the lower limb were recorded in 10% of the population [17]. The findings of the present study show dominant FA variants in 2.8% of the investigated sample. Vascular anomalies (stenoses n = 14) had been recorded in 9.7% in the present investigation and were well comparable to the study [17]. Stenoses were mainly found in n = 11 FAs.

Other studies found that the FA is less severely affected by the PAOD than the tibial arteries [11,12,54]. For its diagnosis, the ankle-brachial index (ABI) is reported as a cheap and non-invasive test [71]. Suspicious scores of 0.9 or less implicate further diagnosis of PAOD [72–74] by MRA or CTA [75,76]. According to the literature, findings of preoperative clinical examination of the vascular system with ABI were not predictive of a problem when color flow Doppler sonography and angiography results were not physiological [77–79]. A combined ABI and handheld Doppler sonography examination were not accurate enough and are not sufficient for developing the surgical plan for a FFF [78].

Further investigations found that pathologic ABI was related to difficulty with the microvascular anastomosis [80]. Furthermore, the wide variability concerning sensitivity and specificity of the ABI test must be considered [81]. Because of insufficient evidence, US Institutions do not recommend the ABI test for PAOD screening in asymptomatic individuals [82]. However, in the present study the ABI test was not performed in our preoperative routine.

4.2. Is It Possible to Record and to Distinguish Periosteal Branches and Septo-Cutaneous Perforators of the FA, and up to Which Diameter Can These Vessels Be Detected in Routinely Run Preoperative CTA for VSP?

The evaluated prospective—in daily routine—CTA studies in the present investigation were sufficient to evaluate the lower limb's vascular system and perforator system. PBs and SCPs were distinguishable by their course and direction to the skin. Numerous investigations have shown the impact of CTA as a sensitive and specific method for microsurgical free flap [15–18,83] and perforator flap harvesting in plastic and reconstructive surgery [55–63]. Previous studies on lower limbs found that CTA demonstrated all the size, course, and penetration patterns of perforators over 0.3 mm in diameter [16]; these patterns were demonstrated more clearly in perforators with a diameter larger than 1 mm [56,62]. In the present study, the mean diameter of SCPs was 0.93 $\pm$ 0.30 mm (range: 0.52–2.43 mm) and of PBs, 0.87 $\pm$ 0.25 mm (range: 0.35–2.26 mm). Other studies found that CTA is accurate for estimating fibular length, run-off, and course of the infra-popliteal vasculature and the perforator subsystem but less precise in predicting perforator vessel diameter [31]. The disadvantage is, in our experience without clinical contribution because of the dissection of the posterior intermuscular septum on-sight and inclusion of a small cuff of soleus muscle for a safe and reliable supply of the skin paddle (musculo-septo-cutaneous perforators).

Therefore, it is crucial, that the CTA method in our setting can mark/visualize small vessels down to a diameter 0.35 mm in routine CTA for VSP. The rate of undetected PBs and SCPs remains unclear. Preoperative information about the location and course of those vessels could be helpful for planning and achieving reliable single or bi-partitioned skin paddles [32,84] and poly-segmental jaw reconstructions [83].

4.3. What Is the Frequency and Distribution of PBs and SCPs of the FA?

The results of the study show different distribution patterns for PBs and SCPs. A more extended bone section increases the probability of finding a perforator. PBs were encountered with about twice the frequency of SCP. Of particular note is the observation that for a fibula segment of 3.0 cm in length, a PB was found on average 29.17% and a SCP in 17.84% in CTA assessment. However, the observed distribution patterns reflect PB and SCP clustering and confirm the high variability of the localization and course. We found a bimodal distribution pattern for PBs and three peaks for SCPs in performed CTA for VSP. These patterns are comparable to the results of other studies [21,31,85].

Published literature shows that CT scans after barium latex mixture in fresh frozen cadaver lower limbs showed in mean 12.8 periosteal branches of the fibula artery with

a mean distance of 1.36 cm between them [86]. It was observed that one branch was found in 65.1% in 1.0 cm segments, in 83.4% of 1.5 cm segments, and 94% of the 2.0 cm segments. Another CTA in vivo study demonstrated all perforator size, course, and penetration patterns were over 0.3 mm in diameter [16]. Present study findings show different results. Only in 10.77%, was one PB found in a 1.0 cm fibula segment in our defined region of interest between the origin of the FA and a plane 5 cm above the distal tip of the fibula. The likelihood increased in 2.0 cm segments to 21.07% and in 3.0 cm segment lengths to 29.17%, having included at least one PB (Table 4). However, a comparison of the results of the cadaver study is only limited, possibly because of the differences in method, radiation dosage, and type and application of the contrast agent [86]. Nevertheless, the findings support the possibility of including even small segments in jaw reconstruction. For VSP our team avoids segment length less than 30 mm to achieve sufficient bone segment perfusion to prevent partial and total flap loss.

Previous studies found that the skin paddle of the FFF can be categorized into four subtypes concerning its vascular supply. Detailed information about the vascular pattern of the skin paddle is required, especially to salvage larger paddles [87]. The course of the perforator system is crucial in difficult situations (e.g., loss or discharge of previous graft) for precise planning. CTA imaging allows individual mapping of the vasculature.

4.4. Limitations of the Study

Our study sample was formed by benign and malign pathologies and included immediate and delayed jaw reconstructions with VSP FFF. The performed CTAs had not been run under experimental conditions but in clinical routine. Intraoperative matching would be of great value to validate the number and distribution of PBs and SCPs observed using CTA, but the study cannot give an answer about the number of undetected PBs and SCPs in our sample. It has to be expected that several PBs and SCPs were not observed in the CTA evaluation. Further clinical investigations are necessary for this purpose.

4.5. Implications

While the present study evaluated the vascular architecture of the lower limb independent of flap outcome, further investigations on the study sample are necessary to assess the following questions:

1. How do fibular artery stenoses effects the outcome of flap surgery?
2. How does the distribution of CTA- detected PBs and SCPs influence the surgical result of mono- and poly-segmental jaw reconstructions, as well as partial and total flap loss?
3. Does the observed distribution of PBs and SCPs impact wound healing of the donor site?

It is planned to match the study results with the virtual surgical planning, and further to analyze them regarding flap success and failure.

5. Conclusions

Routinely run CTA for virtual surgical planning of free fibula flap (FFF) is capable of imaging and distinguishing septo-cutaneous perforators (SCPs) and periosteal branches (PBs) of the fibula artery. The density and distribution obtained differ from those of anatomical cadaver studies. The more proximal the FFF segment, the more frequently a potential PB was observed in the CTA. Knowledge of perforator location may help to plan segment lengths and outline of skin paddles to avoid impending complications.

Author Contributions: Conceptualization, M.K. and S.A.; data curation, D.S. and S.B.; formal analysis, M.K.; funding acquisition, H.-P.H.; investigation, M.K. and A.K.B.; methodology, M.K., A.K.B., C.A. and F.R.; supervision, H.-P.H. and S.A.; validation, S.A.; visualization, C.B.; writing—original draft, M.K.; writing—review and editing, A.K.B., C.B., C.A., F.R., D.S., S.B., H.-P.H. and S.A. All authors have read and agreed to the published version of the manuscript.

Funding: None of the authors has a financial interest to declare in relation to the content of this article. No funding was received for this work.

Institutional Review Board Statement: The study was approved by the local Ethics Committee of Justus-Liebig University Giessen (AZ33/20, approval 25 May 2020).

Informed Consent Statement: Patient consent was waived as the study is a retrospective data analysis.

Data Availability Statement: The datasets generated and/or analyzed during the current study are available from the corresponding author upon reasonable request.

Acknowledgments: This publication is part of the dental doctoral thesis of the second author (A.K.B.).

Conflicts of Interest: The authors declare no conflict of interest.

References

1. Taylor, G.I.; Miller, G.D.H.; Ham, F.J. The free vascularized bone graft: A clinical extension of microvascular techniques. *Plast. Reconstr. Surg.* **1975**, *55*, 533–544. [CrossRef]
2. Hidalgo, A.D. Fibula free flap: A new method of mandible reconstruction. *Plast. Reconstr. Surg.* **1989**, *84*, 71–79. [CrossRef] [PubMed]
3. Cordeiro, P.G.; Disa, J.J.; Hidalgo, D.A.; Hu, Q.Y. Reconstruction of the mandible with osseous free flaps: A 10-year experience with 150 consecutive patients. *Plast. Reconstr. Surg.* **1999**, *104*, 1314–1320. [CrossRef] [PubMed]
4. Kumar, B.P.; Venkatesh, V.; Kumar, K.A.J.; Yadav, B.Y.; Mohan, S.R. Mandibular reconstruction: Overview. *J. Maxillofac. Oral Surg.* **2015**, *15*, 425–441. [CrossRef] [PubMed]
5. Nyberg, M.; Karlsson, T.; Thórarinsson, A.; Kjeller, G.; Lidén, M.; Fröjd, V.; Löfstrand, J. Quality of life after free fibula flap reconstruction of segmental mandibular defects. *J. Reconstr. Microsurg.* **2017**, *34*, 108–120. [CrossRef] [PubMed]
6. Tarsitano, A.; Ciocca, L.; Cipriani, R.; Scotti, R.; Marchetti, C. Mandibular reconstruction using fibula free flap harvested using a customised cutting guide: How we do it. *Acta Otorhinolaryngol. Ital.* **2015**, *35*, 198–201.
7. Attia, S.; Wiltfang, J.; Streckbein, P.; Wilbrand, J.-F.; El Khassawna, T.; Mausbach, K.; Howaldt, H.-P.; Schaaf, H. Functional and aesthetic treatment outcomes after immediate jaw reconstruction using a fibula flap and dental implants. *J. Cranio Maxillofac. Surg.* **2019**, *47*, 786–791. [CrossRef] [PubMed]
8. Petrovic, I.; Baser, R.; Blackwell, T.; McCarthy, C.; Ganly, I.; Patel, S.; Cordeiro, P.; Shah, J. Long-term functional and esthetic outcomes after fibula free flap reconstruction of the mandible. *Head Neck* **2019**, *41*, 2123–2132. [CrossRef]
9. Hölzle, F.; Franz, E.P.; von Diepenbroick, V.H.; Wolff, K.D. Evaluation of the lower leg vessels before microsurgical fibula transfer—Magnetic resonance angiography versus digital subtraction angiography. *Mund Kiefer Gesichtschir.* **2003**, *7*, 246–253. [CrossRef]
10. Hölzle, F.; Ristow, O.; Rau, A.; Mücke, T.; Loeffelbein, D.J.; Mitchell, D.A.; Wolff, K.D.; Kesting, M.R. Evaluation of the vessels of the lower leg before microsurgical fibular transfer. Part I: Anatomical variations in the arteries of the lower leg. *Br. J. Oral Maxillofac. Surg.* **2011**, *49*, 270–274. [CrossRef]
11. Young, D.; Trabulsy, P.; Anthony, J. The Need for preoperative leg angiography in fibula free flaps. *J. Reconstr. Microsurg.* **1994**, *10*, 283–287. [CrossRef]
12. Kelly, A.M.; Cronin, P.; Hussain, H.K.; Londy, F.J.; Chepeha, D.B.; Carlos, R.C. Preoperative MR angiography in free fibula flap transfer for head and neck cancer: Clinical application and influence on surgical decision making. *Am. J. Roentgenol.* **2007**, *188*, 268–274. [CrossRef] [PubMed]
13. Rosson, G.D.; Singh, N.K. Devascularizing complications of free fibula harvest: Peronea arteria magna. *J. Reconstr. Microsurg.* **2005**, *21*, 533–538. [CrossRef] [PubMed]
14. Abou-Foul, A.; Fasanmade, A.; Prabhu, S.; Borumandi, F. Anatomy of the vasculature of the lower leg and harvest of a fibular flap: A systematic review. *Br. J. Oral Maxillofac. Surg.* **2017**, *55*, 904–910. [CrossRef] [PubMed]
15. Battaglia, S.; Maiolo, V.; Savastio, G.; Zompatori, M.; Contedini, F.; Antoniazzi, E.; Cipriani, R.; Marchetti, C.; Tarsitano, A. Osteomyocutaneous fibular flap harvesting: Computer-assisted planning of perforator vessels using Computed Tomographic Angiography scan and cutting guide. *J. Cranio Maxillofac. Surg.* **2017**, *45*, 1681–1686. [CrossRef]
16. Ribuffo, D.; Atzeni, M.; Saba, L.; Guerra, M.; Mallarini, G.; Proto, E.B.; Grinsell, D.; Ashton, M.W.; Rozen, W.M. Clinical study of peroneal artery perforators with computed tomographic angiography: Implications for fibular flap harvest. *Surg. Radiol. Anat.* **2010**, *32*, 329–334. [CrossRef]
17. Abou-Foul, A.K.; Borumandi, F. Anatomical variants of lower limb vasculature and implications for free fibula flap: Systematic review and critical analysis. *Microsurgery* **2016**, *36*, 165–172. [CrossRef]
18. Ettinger, K.S.; Alexander, A.E.; Arce, K. Computed Tomographic angiography perforator localization for virtual surgical planning of osteocutaneous fibular free flaps in head and neck reconstruction. *J. Oral Maxillofac. Surg.* **2018**, *76*, 2220–2230. [CrossRef]
19. Wales, C.J.; Morrison, J.; Drummond, R.; Devine, J.C.; McMahon, J. Pre-operative evaluation of vascularised fibula donor sites: A UK maxillofacial e-survey. *Br. J. Oral Maxillofac. Surg.* **2010**, *48*, 192–194. [CrossRef]
20. Akashi, M.; Nomura, T.; Sakakibara, S.; Sakakibara, A.; Hashikawa, K. Preoperative MR angiography for free fibula osteocutaneous flap transfer. *Microsurgery* **2013**, *33*, 454–459. [CrossRef]
21. Schuderer, J.; Meier, J.; Klingelhöffer, C.; Gottsauner, M.; Reichert, T.; Wendl, C.; Ettl, T. Magnetic resonance angiography for free fibula harvest: Anatomy and perforator mapping. *Int. J. Oral Maxillofac. Surg.* **2020**, *49*, 176–182. [CrossRef]

22. Sendeski, M.M.; Persson, A.B.; Liu, Z.Z.; Busch, J.F.; Weikert, S.; Persson, P.; Hippenstiel, S.; Patzak, A. Iodinated contrast media cause endothelial damage leading to vasoconstriction of human and rat vasa recta. *Am. J. Physiol. Physiol.* **2012**, *303*, F1592–F1598. [CrossRef]
23. Levy, E.M.; Viscoli, C.M.; Horwitz, I.R. The effect of acute renal failure on mortality—A cohort analysis. *JAMA* **1996**, *275*, 1489–1494. [CrossRef]
24. McCullough, A.P.; Wolyn, R.; Rocher, L.L.; Levin, R.N.; O'Neill, W.W. Acute renal failure after coronary intervention: Incidence, risk factors, and relationship to mortality. *Am. J. Med.* **1997**, *103*, 368–375. [CrossRef]
25. Mitchell, A.M.; Kline, J.A.; Jones, A.E.; Tumlin, J.A. Major Adverse events one year after acute kidney injury after contrast-enhanced computed tomography. *Ann. Emerg. Med.* **2015**, *66*, 267–274. [CrossRef] [PubMed]
26. Ten Dam, M.A.; Wetzels, J.F. Toxicity of contrast media: An update. *Neth. J. Med.* **2008**, *66*, 416–422. [PubMed]
27. Napoli, A.; Anzidei, M.; Zaccagna, F.; Marincola, B.C.; Zini, C.; Brachetti, G.; Cartocci, G.; Fanelli, F.; Catalano, C.; Passariello, R. Peripheral arterial occlusive disease: Diagnostic performance and effect on therapeutic management of 64-Section CT angiography. *Radiology* **2011**, *261*, 976–986. [CrossRef] [PubMed]
28. Shwaiki, O.; Rashwan, B.; Fink, M.A.; Kirksey, L.; Gadani, S.; Karuppasamy, K.; Melzig, C.; Thompson, D.; D'Amico, G.; Rengier, F.; et al. Lower extremity CT angiography in peripheral arterial disease: From the established approach to evolving technical developments. *Int. J. Cardiovasc. Imaging* **2021**, 1–14. [CrossRef]
29. Rozen, W.M.; Phillips, T.; Ashton, M.W.; Stella, D.; Gibson, R.N.; Taylor, G.I. Preoperative imaging for diea perforator flaps: A comparative study of computed tomographic angiography and doppler ultrasound. *Plast. Reconstr. Surg.* **2008**, *121*, 1–8. [CrossRef]
30. Razek, A.A.; Denewer, A.; Hegazy, M.; Hafez, M. Role of computed tomography angiography in the diagnosis of vascular stenosis in head and neck microvascular free flap reconstruction. *Int. J. Oral Maxillofac. Surg.* **2014**, *43*, 811–815. [CrossRef]
31. Garvey, P.B.; Chang, E.I.; Selber, J.C.; Skoracki, R.J.; Madewell, J.E.; Liu, J.; Yu, P.; Hanasono, M.M. A prospective study of preoperative computed tomographic angiographic mapping of free fibula osteocutaneous flaps for head and neck reconstruction. *Plast. Reconstr. Surg.* **2012**, *130*, 541e–549e. [CrossRef] [PubMed]
32. Fukaya, E.; Saloner, D.; León, P.; Wintermark, M.; Grossman, R.F.; Nozaki, M. Magnetic resonance angiography to evaluate septocutaneous perforators in free fibula flap transfer. *J. Plast. Reconstr. Aesthetic Surg.* **2010**, *63*, 1099–1104. [CrossRef] [PubMed]
33. Varga-Szemes, A.; Wichmann, J.L.; Schoepf, U.J.; Suranyi, P.; De Cecco, C.N.; Muscogiuri, G.; Caruso, D.; Yamada, R.T.; Litwin, S.E.; Tesche, C.; et al. Accuracy of noncontrast quiescent-interval single-shot lower extremity MR angiography versus CT angiography for diagnosis of peripheral artery disease: Comparison with digital subtraction angiography. *JACC Cardiovasc. Imaging* **2017**, *10*, 1116–1124. [CrossRef] [PubMed]
34. Jens, S.; Koelemay, M.J.W.; Reekers, J.A.; Bipat, S. Diagnostic performance of computed tomography angiography and contrast-enhanced magnetic resonance angiography in patients with critical limb ischaemia and intermittent claudication: Systematic review and meta-analysis. *Eur. Radiol.* **2013**, *23*, 3104–3114. [CrossRef] [PubMed]
35. Wilde, F.; Hanken, H.; Probst, F.; Schramm, A.; Heiland, M.; Cornelius, C.-P. Multicenter study on the use of patient-specific CAD/CAM reconstruction plates for mandibular reconstruction. *Int. J. Comput. Assist. Radiol. Surg.* **2015**, *10*, 2035–2051. [CrossRef]
36. Wilde, F.; Winter, K.; Kletsch, K.; Lorenz, K.; Schramm, A. Mandible reconstruction using patient-specific pre-bent reconstruction plates: Comparison of standard and transfer key methods. *Int. J. Comput. Assist. Radiol. Surg.* **2015**, *10*, 129–140. [CrossRef]
37. Wilde, F.; Schramm, A. Computer-aided reconstruction of the facial skeleton: Planning and implementation in clinical routine. *HNO* **2016**, *64*, 641–649. [CrossRef]
38. Cornelius, C.-P.; Smolka, W.; Giessler, G.A.; Wilde, F.; Probst, F.A. Patient-specific reconstruction plates are the missing link in computer-assisted mandibular reconstruction: A showcase for technical description. *J. Cranio Maxillofac. Surg.* **2015**, *43*, 624–629. [CrossRef]
39. Wilde, F.; Cornelius, C.-P.; Schramm, A. Computer-assisted mandibular reconstruction using a patient-specific reconstruction plate fabricated with computer-aided design and manufacturing techniques. *Craniomaxillofac. Trauma Reconstr.* **2014**, *7*, 158–166. [CrossRef]
40. Geusens, J.; Sun, Y.; Luebbers, H.-T.; Bila, M.; Darche, V.; Politis, C. Accuracy of computer-aided design/computer-aided manufacturing-assisted mandibular reconstruction with a fibula free flap. *J. Craniofacial Surg.* **2019**, *30*, 2319–2323. [CrossRef]
41. Kansy, K.; Mueller, A.A.; Mücke, T.; Kopp, J.-B.; Koersgen, F.; Wolff, K.D.; Zeilhofer, H.-F.; Hölzle, F.; Pradel, W.; Schneider, M.; et al. Microsurgical reconstruction of the head and neck—Current concepts of maxillofacial surgery in Europe. *J. Cranio Maxillofac. Surg.* **2014**, *42*, 1610–1613. [CrossRef]
42. Shroff, S.S.; Nair, S.C.; Shah, A.; Kumar, B. Versatility of fibula free flap in reconstruction of facial defects: A center study. *J. Maxillofac. Oral Surg.* **2017**, *16*, 101–107. [CrossRef]
43. Hölzle, F.; Kesting, M.; Hölzle, G.; Watola, A.; Loeffelbein, D.; Ervens, J.; Wolff, K.-D. Clinical outcome and patient satisfaction after mandibular reconstruction with free fibula flaps. *Int. J. Oral Maxillofac. Surg.* **2007**, *36*, 802–806. [CrossRef]
44. Colletti, G.; Autelitano, L.; Rabbiosi, D.; Biglioli, F.; Chiapasco, M.; Mandalà, M.; Allevi, F. Technical refinements in mandibular reconstruction with free fibula flaps: Outcome-oriented retrospective review of 99 cases. *Acta Otorhinolaryngol. Ital.* **2014**, *34*, 342–348.

45. Barry, C.; MacDhabheid, C.; Tobin, K.; Stassen, L.; Lennon, P.; Toner, M.; O'Regan, E.; Clark, J. 'Out of house' virtual surgical planning for mandible reconstruction after cancer resection: Is it oncologically safe? *Int. J. Oral Maxillofac. Surg.* **2021**, *50*, 999–1002. [CrossRef] [PubMed]
46. Knitschke, M.; Bäcker, C.; Schmermund, D.; Böttger, S.; Streckbein, P.; Howaldt, H.-P.; Attia, S. Impact of planning method (conventional versus virtual) on time to therapy initiation and resection margins: A retrospective analysis of 104 immediate jaw reconstructions. *Cancers* **2021**, *13*, 3013. [CrossRef] [PubMed]
47. Ma, C.; Wang, L.; Tian, Z.; Qin, X.; Zhu, D.; Qin, J.; Shen, Y. Standardize routine angiography assessment of leg vasculatures before fibular flap harvest: Lessons of congenital and acquired vascular anomalies undetected by color Doppler and physical examinations. *Acta Radiol.* **2021**. [CrossRef] [PubMed]
48. Goetze, E.; Kämmerer, P.W.; Al-Nawas, B.; Moergel, M. Integration of perforator vessels in CAD/CAM free fibula graft planning: A clinical feasibility study. *J. Maxillofac. Oral Surg.* **2020**, *19*, 61–66. [CrossRef] [PubMed]
49. Napel, S.; Rubin, G.D.; Jeffrey, R.B., Jr. STS-MIP: A new reconstruction technique for CT of the chest. *J. Comput. Assist. Tomogr.* **1993**, *17*, 832–838. [CrossRef] [PubMed]
50. Prokop, M.; Shin, H.O.; Schanz, A.; Schaefer-Prokop, C.M. Use of maximum intensity projections in CT angiography: A basic review. *Radiographics* **1997**, *17*, 433–451. [CrossRef]
51. Johnson, P.T.; Heath, D.G.; Kuszyk, B.S.; Fishman, E.K. CT angiography with volume rendering: Advantages and applications in splanchnic vascular imaging. *Radiology* **1996**, *200*, 564–568. [CrossRef] [PubMed]
52. Kim, D.; Orron, D.E.; Skillman, J.J. Surgical significance of popliteal arterial variants: A unified angiographic classification. *Ann. Surg.* **1989**, *210*, 776–781. [CrossRef] [PubMed]
53. Freeman, G.H.; Halton, J.H. Note on an exact treatment of contingency, goodness of fit and other problems of significance. *Biometrika* **1951**, *38*, 141–149. [CrossRef]
54. Oxford, L.; Ducic, Y. Use of fibula-free tissue transfer with preoperative 2-vessel runoff to the lower extremity. *Arch. Facial Plast. Surg.* **2005**, *7*, 261–264. [CrossRef] [PubMed]
55. Alonso-Burgos, A.; García-Tutor, E.; Bastarrika, G.; Cano, D.; Martínez-Cuesta, A.; Pina, L. Preoperative planning of deep inferior epigastric artery perforator flap reconstruction with multislice-CT angiography: Imaging findings and initial experience. *J. Plast. Reconstr. Aesthetic Surg.* **2006**, *59*, 585–593. [CrossRef]
56. Chiu, W.-K.; Lin, W.-C.; Chen, S.-Y.; Tzeng, W.-D.; Liu, S.-C.; Lee, T.-P.; Chen, S.-G. Computed tomography angiography imaging for the chimeric anterolateral thigh flap in reconstruction of full thickness buccal defect. *ANZ J. Surg.* **2011**, *81*, 142–147. [CrossRef]
57. Duymaz, A.; Karabekmez, F.E.; Vrtiska, T.J.; Mardini, S.; Moran, S.L. Free Tissue transfer for lower extremity reconstruction: A study of the role of computed angiography in the planning of free tissue transfer in the posttraumatic setting. *Plast. Reconstr. Surg.* **2009**, *124*, 523–529. [CrossRef]
58. Gelati, C.; Miralles, M.E.L.; Morselli, P.G.; Fabbri, E.; Cipriani, R. Deep inferior epigastric perforator breast reconstruction with computer-aided design/computer-aided manufacturing sizers. *Ann. Plast. Surg.* **2020**, *84*, 24–29. [CrossRef]
59. Higueras Sune, M.C.; Lopez Ojeda, A.; Narvaez Garcia, J.A.; De Albert De Las Vigo, M.; Roca Mas, O.; Perez Sidelnikova, D.; Carrasco Lopez, C.; Palacin Porte, J.A.; Serra Payro, J.M.; Vinals, J.M. Use of angioscanning in the surgical planning of perforator flaps in the lower extremities. *J. Plast. Reconstr. Aesthetic Surg.* **2011**, *64*, 1207–1213. [CrossRef]
60. Masia, J.; Clavero, J.; Larrañaga, J.; Alomar, X.; Pons, G.; Serret, P. Multidetector-row computed tomography in the planning of abdominal perforator flaps. *J. Plast. Reconstr. Aesthetic Surg.* **2006**, *59*, 594–599. [CrossRef]
61. Ngaage, L.M.; Hamed, R.; Oni, G.; Di Pace, B.; Ghorra, D.T.; Koo, B.B.C.; Malata, C.M. The Role of CT angiography in assessing deep inferior epigastric perforator flap patency in patients with pre-existing abdominal scars. *J. Surg. Res.* **2019**, *235*, 58–65. [CrossRef] [PubMed]
62. Prokop, M. Multislice CT angiography. *Eur. J. Radiol.* **2000**, *36*, 86–96. [CrossRef]
63. Zhang, Y.; Pan, X.; Yang, H.; Yang, Y.; Huang, H.; Rui, Y. Computed tomography angiography for the chimeric anterolateral thigh flap in the reconstruction of the upper extremity. *J. Reconstr. Microsurg.* **2016**, *33*, 211–217. [CrossRef] [PubMed]
64. Yanik, B.; Bulbul, E.; Demirpolat, G. Variations of the popliteal artery branching with multidetector CT angiography. *Surg. Radiol. Anat.* **2015**, *37*, 223–230. [CrossRef]
65. Futran, N.D.; Stack, B.C., Jr.; Zachariah, A.P. Ankle-arm index as a screening examination for fibula free tissue transfer. *Ann. Otol. Rhinol. Laryngol.* **1999**, *108*, 777–780. [CrossRef]
66. Astarci, P.; Siciliano, S.; Verhelst, R.; Lacroix, V.; Noirhomme, P.; Rubay, J.; Poncelet, A.; Funken, J.; Glineur, D.; El Kourhy, G. Intra-operative acute leg ischaemia after free fibula flap harvest for mandible reconstruction. *Acta Chir. Belg.* **2006**, *106*, 423–426. [CrossRef]
67. Sandhu, G.S.; Rezaee, R.P.; Wright, K.; Jesberger, J.A.; Griswold, M.A.; Gulani, V. Time-Resolved and bolus-chase MR angiography of the leg: Branching pattern analysis and identification of septocutaneous perforators. *Am. J. Roentgenol.* **2010**, *195*, 858–864. [CrossRef]
68. Carroll, W.R.; Esclamado, R. Preoperative vascular imaging for the fibular osteocutaneous flap. *Arch. Otolaryngol. Head Neck Surg.* **1996**, *122*, 708–712. [CrossRef]
69. Blackwell, K.E. Donor site evaluation for fibula free flap transfer. *Am. J. Otolaryngol.* **1998**, *19*, 89–95. [CrossRef]
70. Seres, L.; Császár, J.; Borbély, L.; Vörös, E. Donor site digital subtraction angiography before mandible reconstruction with free fibula transplantation. *Fogorvosi Szle.* **2001**, *94*, 15–20.

71. Doobay, A.V.; Anand, S.S. Sensitivity and specificity of the ankle–brachial index to predict future cardiovascular outcomes: A systematic review. *Arter. Thromb. Vasc. Biol.* **2005**, *25*, 1463–1469. [CrossRef]
72. Yao, S.T.; Hobbs, J.T.; Irvine, W.T. Ankle pressure measurement in arterial disease of the lower extremities. *Br. J. Surg.* **1968**, *55*, 859–860. [PubMed]
73. Fowkes, F.G.R. The measurement of atherosclerotic peripheral arterial disease in epidemiological surveys. *Int. J. Epidemiol.* **1988**, *17*, 248–254. [CrossRef]
74. Fowkes, F.G.; Housley, E.; Macintyre, C.C.; Prescott, R.J.; Ruckley, C.V. Variability of ankle and brachial systolic pressures in the measurement of atherosclerotic peripheral arterial disease. *J. Epidemiol. Community Health* **1988**, *42*, 128–133. [CrossRef] [PubMed]
75. Anzidei, M.; Lucatelli, P.; Napoli, A.; Jens, S.; Saba, L.; Cartocci, G.; Sedati, P.; D'Adamo, A.; Catalano, C. CT angiography and magnetic resonance angiography findings after surgical and interventional radiology treatment of peripheral arterial obstructive disease. *J. Cardiovasc. Comput. Tomogr.* **2015**, *9*, 165–182. [CrossRef] [PubMed]
76. Mishra, A.; Jain, N.; Bhagwat, A. CT Angiography of peripheral arterial disease by 256-slice scanner: Accuracy, advantages and disadvantages compared to digital subtraction angiography. *Vasc. Endovasc. Surg.* **2017**, *51*, 247–254. [CrossRef]
77. Futran, N.D.; Stack, B.C., Jr.; Zaccardi, M.J. Preoperative color flow doppler imaging for fibula free tissue transfers. *Ann. Vasc. Surg.* **1998**, *12*, 445–450. [CrossRef] [PubMed]
78. Klein, S.; Hage, J.J.; van der Horst, C.M.; Lagerweij, M. Ankle-arm index versus angiography for the preassessment of the fibula free flap. *Plast. Reconstr. Surg.* **2003**, *111*, 735–743. [CrossRef]
79. Smith, R.B.; Thomas, R.D.; Funk, G.F. Fibula free flaps: The role of angiography in patients with abnormal results on preoperative color flow Doppler studies. *Arch. Otolaryngol. Head Neck Surg.* **2003**, *129*, 712–715. [CrossRef]
80. Bartella, A.K.; Luderich, C.; Kamal, M.; Braunschweig, T.; Steegmann, J.; Modabber, A.; Kloss-Brandstätter, A.; Hölzle, F.; Lethaus, B. Ankle brachial index predicts for difficulties in performing microvascular anastomosis. *J. Oral Maxillofac. Surg.* **2020**, *78*, 1020–1026. [CrossRef]
81. Aboyans, V.; Criqui, M.H.; Abraham, P.; Allison, M.A.; Creager, M.A.; Diehm, C.; Fowkes, F.G.R.; Hiatt, W.R.; Jönsson, B.; Lacroix, P.; et al. Measurement and interpretation of the ankle-brachial index: A scientific statement from the American Heart Association. *Circulation* **2012**, *126*, 2890–2909. [CrossRef]
82. Moyer, V.A.; Force, U.P.S.T. Screening for peripheral artery disease and cardiovascular disease risk assessment with the ankle-brachial index in adults: U.S. preventive services task force recommendation statement. *Ann. Intern. Med.* **2013**, *159*, 342–348. [CrossRef]
83. Yu, P.; Chang, E.I.; Hanasono, M.M. Design of a reliable skin paddle for the fibula osteocutaneous flap: Perforator anatomy revisited. *Plast. Reconstr. Surg.* **2011**, *128*, 440–446. [CrossRef]
84. Fukaya, E.; Grossman, R.F.; Saloner, D.; Leon, P.; Nozaki, M.; Mathes, S.J. Magnetic resonance angiography for free fibula flap transfer. *J. Reconstr. Microsurg.* **2007**, *23*, 205–211. [CrossRef] [PubMed]
85. Jones, N.F.; Monstrey, S.; Gambier, B.A. Reliability of the fibular osteocutaneous flap for mandibular reconstruction: Anatomical and surgical confirmation. *Plast. Reconstr. Surg.* **1996**, *97*, 707–716. [CrossRef] [PubMed]
86. Fry, A.; Laugharne, D.; Jones, K. Osteotomising the fibular free flap: An anatomical perspective. *Br. J. Oral Maxillofac. Surg.* **2016**, *54*, 692–693. [CrossRef] [PubMed]
87. Yadav, P.S.; Ahmad, Q.G.; Shankhdhar, V.K.; Nambi, G. Skin paddle vascularity of free fibula flap—A study of 386 cases and a classification based on contribution from axial vessels of the leg. *Indian J. Plast. Surg.* **2012**, *45*, 58–61. [CrossRef]

diagnostics

an Open Access Journal by MDPI

Indexed in: PubMed | CITESCORE 1.4 SCOPUS | IMPACT FACTOR 3.706

CERTIFICATE OF PUBLICATION

Certificate of publication for the article titled:

Computed Tomography Angiography (CTA) before Reconstructive Jaw Surgery Using Fibula Free Flap: Retrospective Analysis of Vascular Architecture

Authored by:

Michael Knitschke; Anna Katrin Baumgart; Christina Bäcker; Christian Adelung; Fritz Roller; Daniel Schmermund;
Sebastian Böttger; Hans-Peter Howaldt; Sameh Attia

Published in:

Diagnostics **2021**, Volume 11, Issue 10, 1865

MDPI Academic Open Access Publishing since 1996

Basel, October 2021

3.5. Originalarbeit 5: Impact of Periosteal Branches and Septo-Cutaneous Perforators on Free Fibula Flap Outcome: A Retrospective Analysis of Computed Tomography Angiography Scans in Virtual Surgical Planning.

Knitschke, M.; Baumgart, A.K.; Bäcker, C.; Adelung, C.; Roller, F.; Schmermund, D.; Böttger, S.; Howaldt, H.-P.; Attia, S. Impact of Periosteal Branches and Septo-Cutaneous Perforators on Free Fibula Flap Outcome: A Retrospective Analysis of Computed Tomography Angiography Scans in Virtual Surgical Planning.
Front Oncol. **2021**;11:821851
https://doi.org/10.3389/fonc.2021.821851 **IF: 6,244**

Zusammenfassung:
Die virtuelle chirurgische Planung (VSP) für die Kieferrekonstruktion mit freiem Fibulalappen ist zu einem Routineverfahren geworden. Die präoperative Computertomographie-Angiographie (CTA) ermöglicht die Beurteilung des Gefäßsystems der unteren Extremität und des Knochens mit einem bildgebenden Verfahren.
Ziel der retrospektiven klinischen Studie war es, den Einfluss der Verteilung und Dichte der in der CT-Angiographie sichtbaren kleinen Gefäße der *A. fibularis*, der periostalen Äste (PB) und der septo-kutanen Perforatoren (SCP) auf den Lappenerfolg zu analysieren. Dazu wurde die präoperative CT-Angiographie des infra-poplitealen Gefäßsystems von 72 Patienten ausgewertet, die sich einer virtuell geplanten Rekonstruktion mit einem freien Fibulatransplantat zur Kieferrekonstruktion zwischen 2015 und 2020 unterzogen hatten. Das Ergebnis des Lappentransfers, einschließlich der Wundheilung der Donorregion und (sub-)totalem Lappenverlust, wurde mit der segmentalen Gefäßversorgung abgeglichen.
Insgesamt *72* Patienten (Frauen: *n* = 28, 38,9 %; Männer: *n* = 44, 61,1 %) erfüllten die Einschlusskriterien. Das Durchschnittsalter betrug 58,5 ± 15,3 Jahre. Ein vollständiger Lappenerfolg wurde bei *n* = 59 (82,0 %), ein partieller bei *n* = 4 (5,5 %) und totaler Lappenverlust bei *n* = 9 (12,5 %) registriert. Bezogen auf die Gesamtzahl der präparierten Segmente (*n* = 121) waren 46,7 % (*n* = 7) der mono-, 40,4 % (*n* = 21) der bi- und 31,5 % (*n* = 17) der tri-segmentalen freien Fibulatransplantate in der Erfolgsgruppe mindestens von einem PB versorgt. Das entspricht einer kumulativen

Rate von 37,2 % (*n* = 45 von 121) aller erfolgreichen Fibulatransplantate im Vergleich zu einer relativen Rate von 42,9 % (*n* = 6 von 14) diskret versorgter Segmente in der Gruppe der totalen Lappenverluste. Weiterhin ergab sich, dass proximal gelegene Fibulatransplantatsegmente bei mehrgliedrigen Kieferrekonstruktion eine höhere Rate von periostalen Ästen pro Lappensegment zeigten als weiter distal gelegene Segmente. Es wurde kein statistisch signifikanter Zusammenhang zwischen Wundheilungsstörungen der Donorregion und der Dichte und Verteilung der septo-kutanen Perforatoren gefunden.

Zusammenfassend konnte keine Korrelation zwischen höheren Raten von periostalen Ästen (PB) und den septo-kutanen Abgängen (SCP) der *A. fibularis* und dem Lappenerfolg in der untersuchten Studienstichprobe statistisch nachgewiesen werden. Wir kommen zu dem Schluss, dass die präoperative Mapping der kleinen Gefäße auf der Grundlage der routinemäßigen CTA-Bildgebung nicht zur Vorhersage des Lappenergebnisses geeignet ist.

<u>Ausblick:</u>

Die Ergebnisse der Studie zeigten weder eine positive noch eine negative Korrelation für die kleinen Gefäßen der unteren Gliedmaßen und dem Transplantationsergebnis.

1. Weitere Studien unter Verwendung einer weiterentwickelten Volumenvisualisierungssoftware sind notwendig, um die Darstellung dieser kleinen Gefäße im Rahmen eines zukünftigen Forschungsschritts zu diesem Thema zu verbessern.
2. Zudem muss der Frage nachgegangen werden, inwiefern sich die nach distal abnehmende Dichte und Anzahl von periostalen Ästen (PB) und den septo-kutanen Abgängen (SCP) entlang der Fibula bei der Verknöcherung des distalen Fibulaendes bzw. der distalen Übergangszone bemerkbar macht.

Frage 2 wird in der Originalarbeit 6 bearbeitet.

frontiers in Oncology

ORIGINAL RESEARCH
published: 19 January 2022
doi: 10.3389/fonc.2021.821851

Impact of Periosteal Branches and Septo-Cutaneous Perforators on Free Fibula Flap Outcome: A Retrospective Analysis of Computed Tomography Angiography Scans in Virtual Surgical Planning

Michael Knitschke[1], Anna Katrin Baumgart[1], Christina Bäcker[1], Christian Adelung[2], Fritz Roller[2], Daniel Schmermund[1], Sebastian Böttger[1], Philipp Streckbein[1], Hans-Peter Howaldt[1] and Sameh Attia[1]*

[1] Department of Oral and Maxillofacial Surgery, Justus-Liebig-University, Giessen, Germany, [2] Department of Diagnostic and Interventional Radiology and Pediatric Radiology, Justus-Liebig-University, Giessen, Germany

OPEN ACCESS

Edited by:
Florian M. Thieringer,
University Hospital Basel, Switzerland

Reviewed by:
Salvatore Battaglia,
Maxillofacial Surgery Unit, Italy
Xiaofeng Shan,
Peking University Hospital of Stomatology, China

***Correspondence:**
Michael Knitschke
Michael.Knitschke@uniklinikum-giessen.de

Specialty section:
This article was submitted to Head and Neck Cancer, a section of the journal Frontiers in Oncology

Received: 24 November 2021
Accepted: 24 December 2021
Published: 19 January 2022

Citation:
Knitschke M, Baumgart AK, Bäcker C, Adelung C, Roller F, Schmermund D, Böttger S, Streckbein P, Howaldt H-P and Attia S (2022) Impact of Periosteal Branches and Septo-Cutaneous Perforators on Free Fibula Flap Outcome: A Retrospective Analysis of Computed Tomography Angiography Scans in Virtual Surgical Planning. Front. Oncol. 11:821851. doi: 10.3389/fonc.2021.821851

Background: Virtual surgical planning (VSP) for jaw reconstruction with free fibula flap (FFF) became a routine procedure and requires computed tomography angiography (CTA) for preoperative evaluation of the lower limbs vascular system and the bone. The aim of the study was to assess whether the distribution and density of periosteal branches (PB) and septo-cutaneous perforators (SCP) of the fibular artery have an impact on flap success.

Method: This retrospective clinical study assessed preoperative CTA of the infra-popliteal vasculature and the small vessel system of 72 patients who underwent FFF surgery. Surgical outcome of flap transfer includes wound healing, subtotal, and total flap loss were matched with the segmental vascular supply.

Result: A total of 72 patients (28 females, 38.9 %; 44 males, 61.1 %) fulfilled the study inclusion criteria. The mean age was 58.5 (± 15.3 years). Stenoses of the lower limbs' vessel (n = 14) were mostly detected in the fibular artery (n = 11). Flap success was recorded in n = 59 (82.0%), partial flap failure in n = 4 (5.5%) and total flap loss in n = 9 (12.5%). The study found a mean number (± SD) of 2.53 ± 1.60 PBs and 1.39 ± 1.03 SCPs of the FA at the donor-site. The proximal FFF segment of poly-segmental jaw reconstruction showed a higher rate of PB per flap segment than in the distal segments. Based on the total number of prepared segments (n = 121), 46.7% (n = 7) of mono-, 40.4% (n = 21) of bi-, and 31.5 % (n = 17) of tri-segmental fibula flaps were at least supplied by one PB in the success group. Overall, this corresponds to 37.2% (45 out of 121) of all successful FFF. For total flap loss (n = 14), a relative number of 42.9% (n = 6) of distinct supplied segments was recorded. Wound healing disorder of the donor site was not statistically significant influenced by the detected rate of SCP.

Conclusion: In general, a correlation between higher rates of PB and SCP and the flap success could not be statistically proved by the study sample. We conclude, that preoperative PB and SCP mapping based on routine CTA imaging is not suitable for prediction of flap outcome.

Keywords: virtual surgical planning, jaw reconstruction, CTA, flap failure, head and neck tumor, fibula free flap

INTRODUCTION

Taylor presented the free fibula flap (FFF) for the first time in 1975 (1), and Hidalgo employed it for mandible reconstruction 14 years later (2). This flap has a high success rate and is commonly used in reconstructive surgery (3). It allows the treatment of both bone and soft tissue defects with a single free flap from a single donor site (4). The FFF is the gold standard in mandibular reconstruction as it may be molded to a nearly ideal form of the missing jaw sections (5). Sufficient jaw reconstruction improves the quality of life (QoL) after ablative cancer surgery. After successful treatment, the overall QoL is comparable to that of the general population (6, 7). The osseous FFF permits for stable long-term prosthetic rehabilitation with dental implants with manageable donor-site complications (8–11). Computed tomography (CT) scans and DICOM data sets of the donor and recipient sites are required for virtual surgical planning (VSP) and the facilitation of custom-made, laser-melted, patient-specific titanium osteosynthesis plates (12, 13), which becomes widespread routine in many reconstructive centers (14). MRA was found as a reliable and non-invasive technique to identify anatomical variants and arterial stenoses (15, 16) without radiation in preoperative FFF planning (17). But CTA has been shown to be better than MRA for perforator mapping (18), as well as being more widely available, adequately accurate, and economic (19–21). The method of VSP was described by Eckardt and Swennen in 2005 for mandible reconstruction (22) and becomes more popular since than (23–27). The transfer from virtual planning to operating fields became accurate due to the possible because of the three-dimensionally designed and configured plate (28). Thank this planning method an exact and predictable uni- and poly-segmental bone restorations are possible (14, 29, 30). Success rates of the FFF ranging between 90% to 95% have been reported in the literature (31–34). Despite these significant benefits, surgery remains challenging in terms of insufficient perforator vessels, vascular bundle complications, or inadequate resections margins (35, 36). A thorough preoperative examination of the vascular system using a computed tomography angiography scan (CTA) to reduce those risks is required, as CTA scans allow for simultaneous evaluation of bony and vascularly structures (37).

The descriptive term periosteal branch (PB) is very general and has to be precise. Studies showed that bone perfusion of the skeleton is maintained by a system of three types of vessels (38, 39): endosteal nutrient vessels, penetrating periosteal vessels, and non-penetrating periosteal vessels. There are crosslinks between periosteal and endosteal vessels but without clear borders of perfusion. Experimental studies show that the inner two-thirds of the cortical bone is supplied by the endosteal system and the outer third by the periosteal system (40). Age seems to play a vital role, as the endosteal supply dominates the perfusion of cortical bone in youth, while in advanced age, a greater cortical thickness can be supplied by periosteum (41). While the nutrient vessels contribute to periosteal and endosteal blood supply (41), the non-penetrating branches do not appear to have a contribution to the endosteal perfusion (39, 42). The FFF is supplied by the non-penetrating perforator vessel subtypes direct periosteal and musculo-periosteal and nutrient vessels (1, 43). Several studies supported the thesis that non-penetrating branches only perfuse the outer section of the cortical bone (42, 44).

An anatomical examination of 30 formalin-fixed legs revealed that 27 legs (90%) had a singular nutrient vessel, and two (6.6 %) had a double nutrient vessel. In one leg, no nutrient vessel was observed. These vessels enter the fibula predominantly in the middle third, at its medial crest. In contrast, only one entered from the posterior surface and showed, on average, a diameter of 0.9 mm – 1.5 mm (45). Based on 54 cadaveric legs, it was found that the fibular nutrient artery, which arose from the fibular artery as a short descending branch, penetrated the M. flexor hallucis longus to enter the fibular nutrient foramen (46). Between the distal half of the first-quarter and second-quarter segments of the fibula, the fibular nutrient artery, and up to three arcuate arteries were located constantly (47). The term periosteal branch summarizes, therefore, nutrient and non-penetrating vessels.

Previous radiological analyzes of our research group on the same study sample revealed different distribution patterns and frequencies for PB and SCP based on CTA scans of both legs. A bimodal distribution pattern for PB and three peaks for SCP in performed CTA for VSP were recorded (48). Further, significant differences concerning the number of periosteal branches in the bone segment of different sizes were found compared to cadaver studies (49). The more proximal the FFF segment, the more frequently a potential PB was observed in the CTA scans. So that a comparison of the previous published radiological findings to the clinical data of the same patient's collection is of great interest, which is the topic of this paper.

This investigation aimed to evaluate the impact of detected small vessels (PB and SCP) on the surgical outcome after VSP of uni- and poly-segmental mandible reconstruction with FFF. Additionally, the following questions were evaluated in the study.

1. How do infra-popliteal branching pattern and fibular artery vascular anomalies (stenoses) affect the outcome of flap surgery?
2. How does the distribution of CTA-based detected PB and SCP influence the surgical result of mono- and poly-segmental jaw reconstructions with partial or total flap loss?

3. Does the observed distribution of PB and SCP impact wound healing of the donor site?

MATERIAL AND METHODS

Patient Collection, Ethical Consideration and Inclusion Criteria

The ethics committee of the Justus-Liebig-University Giessen approved the study (approval number: AZ33/20, approval date: 25.5.2020). No written obtained consent was required from the considered patients. Individuals meeting the following criteria were included: Immediate or delayed mandible reconstruction using FFF planned virtually, availability of preoperative CTA scans with a maximum slice thickness of 1.5 mm, treatment performed between January 2015 and December 2020.

A total number of 77 patients fulfilled the inclusion criteria. Five could not be included because of one fibula CTA after reconstruction with contralateral fibula after flap loss (n = 4) and after tumor recurrence (n = 1). Finally, 72 patients with CTA scans of 144 legs were available for the analyzis (**Figure 1**).

Dissection of the fibula flap was conducted using Gilbert's lateral approach (50). A segment of 8cm at the proximal end and the distal end, a 6-8cm length, was left in place to preserve knee and ankle stability. When a composite flap was harvested, the perforators were protected with a muscle cuff of M. soleus and M. flexor hallucis longus. A summarized clinical example is given in **Figures 2–4**. Wound closure of the donor site was done primarily in cases of non-composite FFF. When composite FFF were harvested, all donor site defects were covered with meshed split thickness skin graft.

All CTA scans were done at the University Hospital Giessen's Departments of Diagnostic and Interventional Radiology and Pediatric Radiology. The CT scans were done using a first-generation dual-energy CT scanner and a third-generation dual-energy CT scanner (SOMATOM Definition AS & Force, Siemens Healthineers, Forchheim, Germany). Above the aortic bifurcation to the feet, scans of both legs were performed with a slice thickness of 1.5 mm (70 kV, 300 mA max, pitch 0.5, collimation 0.6 mm, matrix size 512 x 512). Intravenously, non-ionic contrast fluids containing 350 mg of iodine per milliliter (Ultravist 370, Bayer, Leverkusen, Germany) were given. The amount of contrast media used is determined on the patient's weight.

CTA DICOM data sets were analyzed in HOROS-Software for Mac (Version 4.0.0 RC5, Horosproject). Horos is a free and open-source code software (FOSS) program distributed free of charge under the LGPL license at Horosproject.org and sponsored by Nimble Co LLC d/b/a Purview in Annapolis, MD, USA. The CTA quality was assessed by side-by-side comparison with an ROI in the center of the popliteal artery and dorsal vessels of the dorsum of the foot. For every CTA, the measurements were performed on both patients' legs.

Study Parameters

The following parameters were collected in a previous investigation on the study sample: Length of the fibula, bone and

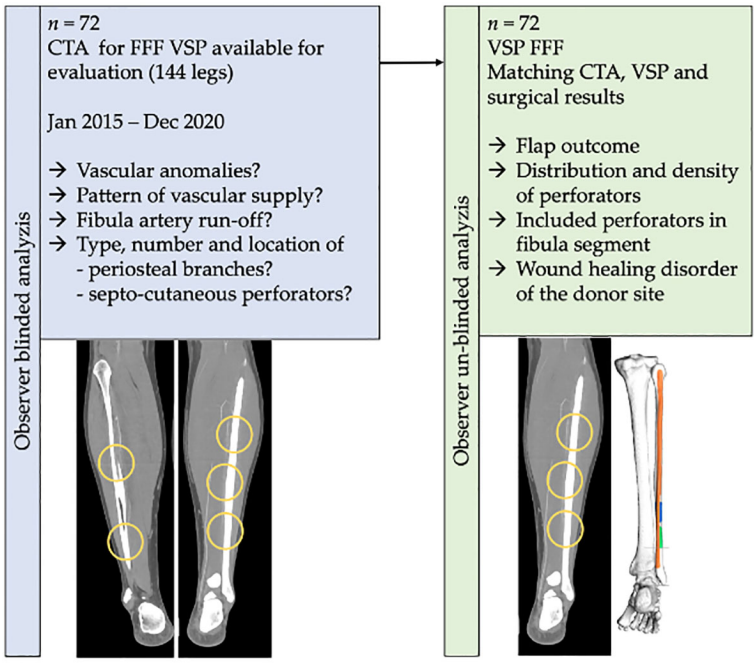

FIGURE 1 | Workflow of the present study. A total number of n = 72 computed tomography angiography (CTA) DICOM-datasets of virtual planned jaw reconstructions with a free fibula flap were included in the investigation. Findings on the vascular infra-popliteal branching pattern, stenoses, and distribution and density of periosteal branches and septo-cutaneous perforators of the fibular artery were matched with flap surgery outcome.

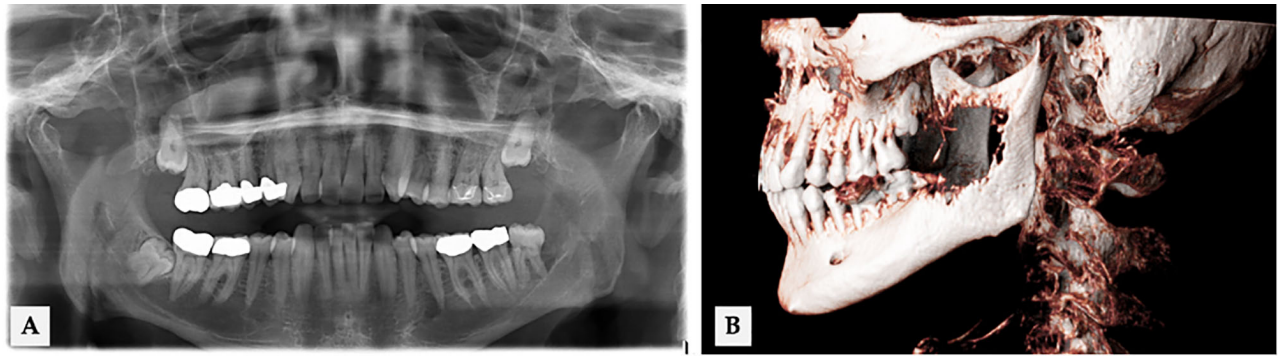

FIGURE 2 | 56 years old male with an infiltrative growth of oral squamous cell carcinoma (T4) in regio 38 (ID 18 in **Figure 5**). **(A)** Extension of osseous destruction in OPT and **(B)** cinematic volume rendering CT reconstruction.

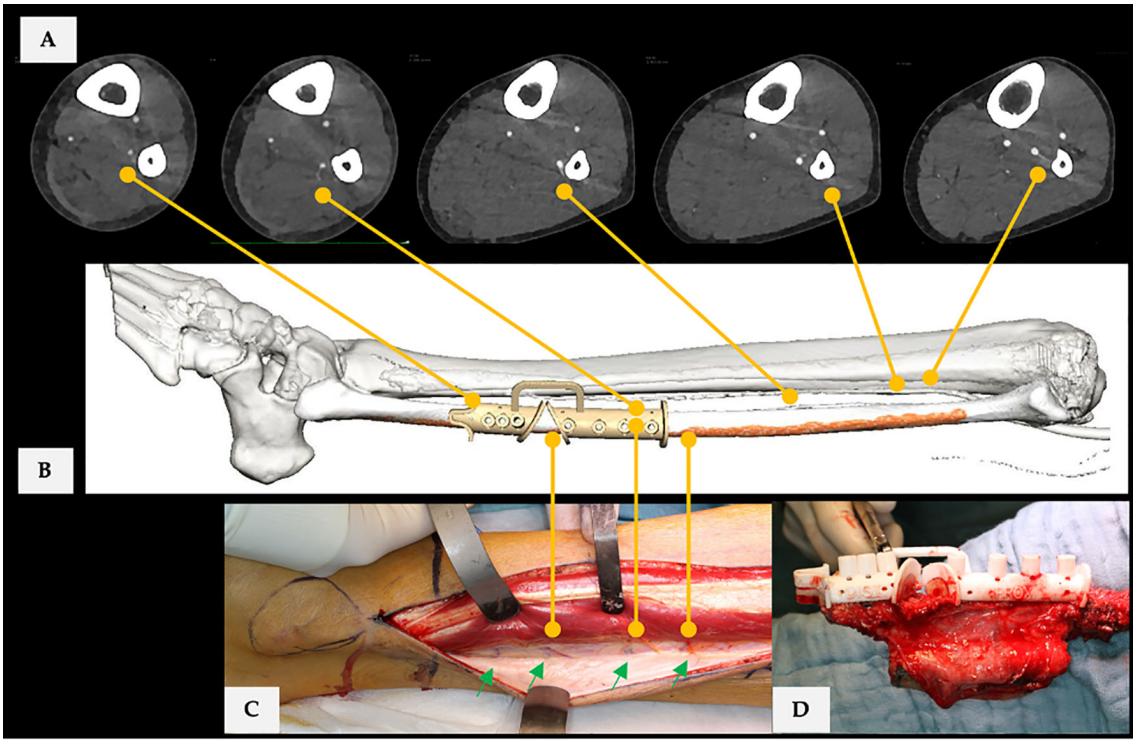

FIGURE 3 | **(A)** CTA scan (axial plane) of the donor site. Yellow lines connect found PB and SCP with virtual surgical planning. **(B)** Final virtual surgical planning for bi-segmental mandible reconstruction with free fibula flap. **(C)** Yellow lines connect corresponding vessels with the operating field. **(D)** Applied cutting guide, performed osteotomies, and shaped neo-condyle. Case is ID 18 in **Figure 5**. In CTA assessment were 5 PB and one SCP of the FA at donor site recorded. Each fibula flap segment was supplied by one PB, while three were located proximal to the designed flap. The CTA-based SCP position was in the middle of the skin paddle in the proximal fibula flap segment. The radiological examination of the FA was without pathological findings (type I-B: infra-popliteal branching pattern, which means trifurcation of the popliteal artery in ATA, PTA, and FA). Overall, there were no radiological reservations or restrictions to surgery. **Figure 3A, C** shows that there was a discrepancy between the radiological and the operative findings. The number of SCP was at least 4 (green arrows).

vascular anomalies, vascular anatomy and branching pattern of the infra-popliteal vessels will the classified concerning Kim et al. (51), length of TTF, number and localization of SCPs and PBs from the distal tip of the fibula bone to branching and between the branches.

These findings were matched with the surgical outcome including: Patient's age (at CT scan), gender, body height, and weight, BMI, flap-type (composite or non-composite flap), site of flap harvesting, distance to the distal tip of the fibula (ankle), as well

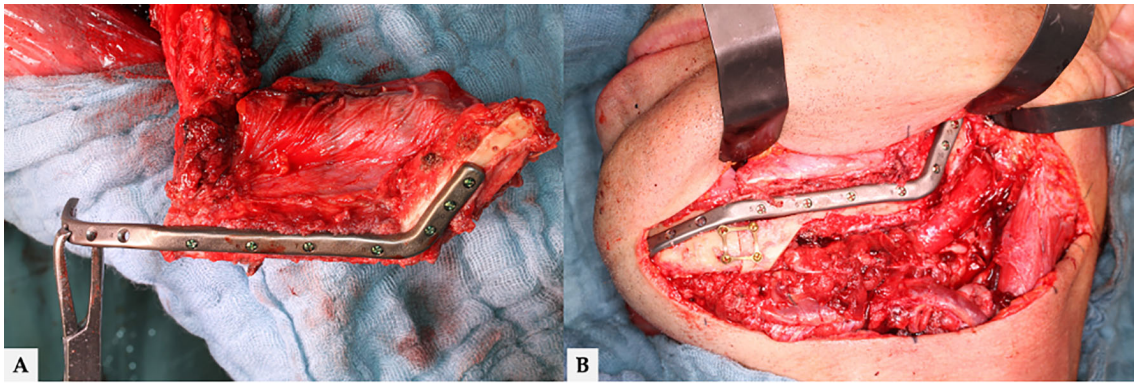

FIGURE 4 | **(A)** Final molded bi-segmental composite fibula flap and **(B)** neo-mandible. Additional triangular free bone transplant to smooth the contour of neo-mandible's jawline. Finally, total flap loss occurred in this case. The surgical revision revealed a combined arterial and venous thrombosis.

as the number, length, and position of fibula segments. Additionally, total transplant length, which were taken out of the virtual planning report was recorded. Information about flap status (complete flap success, partial (bone or skin paddle), or total flap loss) was extracted from the medical records. PFF was defined as any loss of parts of the skin paddle (skin), parts or segments (poly-segmental reconstruction) of bone grafts (bone), or a combination of both (52). The donor site's wound healing disorder (WHD) was classified as minor WHD when only a conservative wound had been performed. Major WHD implicates large wounds with exposed tendons and surgical treatment by applying split-thickness skin graft after wound debridement.

Statistical Analysis

Pearson's $\chi 2$ test, Fisher's exact test, and the Freeman–Halton extension (53) were conducted on the categorical variables used to analyze flap outcome concerning: gender, flap-type (composite or non-composite flap), donor site, number of bone segments, and number and type of included perforators and ASA-score. Kruskal-Wallis test was performed to analyze defined flap outcome groups concerning metric parameters. The continuous parameters: age, body height, and weight, body-mass-index (BMI), the total length of the fibula, the length of the fibular artery (FA) from origin to the distal tip of the fibula bone, the diameter of the fibular artery, the length and the diameter of the truncus tibiofibularis (TTF), the number and the distance of septo-cutaneous perforators (SCP), the periosteal branches (PB), overall reconstruction length, and the segment length were verified for normality. The distribution was presented as a mean (standard deviation), and Student's t-test was performed. $p < 0.05$ was defined as statistically significant. The statistical analyzes were carried out with SPSS (IBM SPSS Statistics, v28.0, Armonk, NY, USA).

RESULTS

A total of 72 patients (28 women, 38.9 %; 44 men, 61.1 %) fulfilled the inclusion criteria. The mean age was 58.5 ± 15.3 years (range: 14.8 – 82.6 years). Firstly, the vascular system of the study sample was assessed and the sample was categorized into donor and non-donor site for further analyzis.

In the gender-mixed sample, no significant difference in fibular bone length was found. Concerning the infra-popliteal branching pattern type as classified by Kim et al., all donor fibulae had a regular vascular supply equivalent to types I-A through II-C. In contrast, at the non-donor site, two cases of type III-A and two cases of type III-B were found (51). Out of 144 legs, 88.9 % (n = 128) were assigned as type I-A. Detailed evaluation of the donor site vascular architecture revealed that type I-A was found in 93.1 % (non-donor site: 84.7 %). Two donor site vascular systems were classified as type I-B, and one case was assigned to categories I-C to II-B. Four legs of the non-donor site showed dominant fibular artery (FA) variants (III-A: n = 2; III-B: n = 2). No type III-C branching pattern was observed, defined as a dominant fibular artery, that can lead to critical perfusion (**Tables 1** and **2**).

At all, 14 stenoses of the lower limbs' vessels were recognized. Five stenoses of the FA were detected at the donor site, while in the non-donor site, stenoses in all three vessels had been found (FA: n = 6; ATA: n = 1; PTA: n = 2). In donor vs. non-donor site comparison, no significant differences for the total length of the TTF and FA and the diameters were found. PB and SCP were located in equal parts at donor- vs. non-donor sites. The study detected a mean number (± SD) of 2.53 ± 1.60 PB and 1.39 ± 1.03 SCP of the FA at the donor-site in the region of interest between the exit of FA from the TTF and 5.0 cm above the distal tip of the fibula bone. Compared to the non-donor site, a non-significant difference in the mean number of recorded PB and SCP was found.

The findings were matched with virtual surgical planning (VSP) and surgery results, and flap outcome was categorized concerning complete flap success (FS), partial (PFF), and total flap failure (TFF). Partial flap failure was defined as (sub-)total loss of the skin paddle and/or parts or segments of poly-segmental reconstructions. The detailed results are summarized in **Table 3** and **Figure 5**. Total flap loss was recorded in n = 9 cases (12.5%). The highest average age with 64.9 ± 8.0 years was found in the TFF-group, while the lowest

TABLE 1 | CTA assessment for fibular bone and vascular system parameters of the study sample.

n = 144	Donor site (*n* = 72)	Non-donor site (*n* = 72)	Total	*p*-value
Fibula length, mean (mm) ± SD	373.9 ± 30.2	372.8 ± 30.9	142	0.829
Fibula bone anomalies				
Fracture	0	1	1	–
Branching pattern of the calf (51)				
Regular (I-A to II-C)	72	68	140	
Absent ATA (III-A)	0	2	2	
Absent PTA (III-B)	0	2	2	0.119
Stenoses				
ATA	0	1	1	
PTA	0	2	2	
FA	5	6	11	0.670
Length of TTF, mean (mm) ± SD	32.6 ± 12.9 (*n* = 67)	32.5 ± 14.6 (*n* = 61)	128	0.965
Diameter of TTF, mean (mm) ± SD	4.13 ± 0.95 (*n* = 67)	4.16 ± 1.0 (*n* = 61)	128	0.862
Length of FA, mean (mm) ± SD	244.9 ± 36.9	243.0 ± 43.3	142	0.777
Diameter of FA, mean (mm) ± SD	3.12 ± 0.79	3.21 ± 0.78	142	0.493
Overall found SCP, *n* (%)	101 (47.4%)	112 (52.6%)	213	
Diameter SCP, mean (mm) ± SD	0.93 ± 0.28	0.93 ± 0.32	0.93 ± 0.30	1.0
Mean SCP per fibula (mm) ± SD	1.39 ± 1.03	1.52 ± 1.23	1.40 ± 1.01	0.407
Overall found PB, *n* (%)	185 (51.2%)	176 (48.8%)	361	
Diameter PB, mean (mm) ± SD	0.87 ± 0.24	0.87 ± 0.26	0.87 ± 0.56	1.0
Mean PB per fibula (mm) ± SD	2.53 ± 1.60	2.42 ± 1.60	2.47 ± 1.54	0.514

SD, standard deviation; ATA, anterior tibial artery; FA, fibular artery; PB, periosteal branch; PTA, posterior tibial artery; SCP, septo-cutaneous perforator; TTF, truncus tibiofibularis.

mean age with 49.8 ± 20.6 years was estimated in the PFF group. The finding was without statistical significance. Differences concerning body weight were found significant for PFF in comparison to FS (PFF: 92.3 ± 10.6 kg vs. TFF: 64.9 ± 8.0 kg; p = 0.012) and a trend towards significance concerning the TFF (PFF: 92.3 ± 10.6 kg vs. FS: 58.4 ± 15.6 kg; p = 0.061). About 43.1 % of the study sample were classified at least ASA-score 3. PFF and TFF were found only for ASA-score 2 and 3 and within each class in equal proportions. All registered PFFs and TFFs (except for one type, I-B) occurred in a I-A branching pattern.

The donor site was in nearly two-thirds of the cases (63.9 %) the right leg, and a minimal distance to the distal tip of the fibular of more than 70 mm was planned in 91.7 % of our cases to preserve ankle stability. TFF has not been observed when tri-segmental jaw reconstruction has been performed.

No significant difference (p = 0.431) was found for the length of TTF concerning flap outcome (FS: 31.3 ± 12.2 mm vs. TFF: 40.1 ± 14.9 mm).

Only when composite flaps were used, wound healing disorders of the donor site were registered. Harvesting defects were standardized covered with a meshed split-thickness skin graft (0.4 mm). The proportion of significant wound healing disorders (WHD) was almost twice as high as that of minor WHD in the FS-group (33.9 % vs. 18.6 %). In the TFF-group, this proportion quadrupled and must be viewed critically due to the small number of cases. No WHD was observed summarized in half of the patients in all groups (**Table 4**).

The total number of in FFF included SCP and PB of the FA were analyzed in relation to the found vessels beyond the flap and classified concerning flap outcome (**Figure 6**). No significant differences were observed for different flap outcomes and the number of included SCP (CS 46.3 % vs. PFF 50.0 %, TFF 45.4 %) and PB (CS 37.7 % vs. PFF 38.5 %, TFF 28.6 %).

Further, the number of every single segment of a mono- and poly-segmental reconstruction which was supplied by at least one PB (**Table 5**), and analog for SCP (only for composite flaps, n = 61) (**Table 6**) was assessed. Based on the number of prepared segments, at least one PB supplied 46.7% in the mono-, 40.4% in the bi-, and 31.5 % in the tri-segmental group. Overall, this corresponds to 37.2% (45 out of 121) of all successful FFF. For TFF, a relative number of 42.9% of single addressed segments was calculated. The findings were non-significant. In summary, the number of SCP per segment were lower in poly-segmental composite FFF than in mono-segmental composite reconstruction (**Table 6**). These results are without significance.

Minimal and maximal segment length of each virtually shaped FFF segment was assessed and categorized concerning flap outcome. With an increasing number of used FFF segments for reconstruction, the mean segment length decreases (**Table 3**). With the same number of used segments, no statistically significant differences could be found. In detail, the shortest segment length was found in mean with ≥ 34.5 ± 14.2 mm for successful tri-segmental reconstructions, with ≥ 27.1 ± 6.4 mm for partial flap failure in tri-segmental reconstructions, and with ≥ 40.3 ± 16.8 mm

TABLE 2 | Infrapopliteal arterial branching variations were classified by Kim (51) of the investigated sample (n = 144).

Type	Donor site (*n* = 72) *n* (%)	Non-donor site (*n* = 72) *n* (%)	Total (*n* = 144) *n* (%)
I-A	67 (93.1)	61 (84.7)	128 (88.9)
I-B	2 (2.8)	1 (1.4)	3 (2.1)
I-C	1 (1.4)	–	1 (0.7)
II-A	1 (1.4)	2 (2.8)	3 (2.1)
II-B	1 (1.4)	4 (5.6)	5 (3.6)
II-C	–	–	–
III-A	–	2 (2.8)	2 (1.4)
III-B	–	2 (2.8)	2 (1.4)
III-C	–	–	–

TABLE 3 | Demographic and surgery-associated parameters.

***n* = 72**	**Flap success 59 (82.0%)**	**Partial flap failure 4 (5.5%)**	**Total flap failure 9 (12.5%)**	***p*-value**
Age (years), mean ± SD	58.4 ± 15.6	49.8 ± 20.6	64.9 ± 8.0	0.338
Gender, n (%)				
Male	33 (44.1)	4 (100.0)	7 (77.8)	
Female	26 (55.9)	0	2 (22.2)	0.150
Body weight (kg), mean ± SD	71.7 ± 15.7	92.3 ± 10.6	74.6 ± 15.2	*0.012
Body height (cm), mean ± SD	169.9 ± 10.0	179.3 ± 3.9	176.8 ± 11.3	0.067
BMI (kg/m^2), mean ± SD	24.7 ± 5.2	28.8 ± 3.6	23.6 ± 4.8	0.189
ASA-score, n (%)				
1	3 (5.1)	0	0	
2	31 (52.5)	2 (50.0)	5 (55.6)	
3	23 (39.0)	2 (50.0)	4 (44.4)	
4	2 (3.4)	0	0	0.973
Reconstruction site				
Maxilla	15 (25.4)	1 (25.0)	2 (22.2)	
Mandibula	44 (74.6)	3 (75.0)	7 (77.8)	1.0
FFF type, n (%)				
Composite flap	51 (86.5)	3 (75.0)	7 (77.8)	
Non-composite flap	8 (13.5)	1 (25.0)	2 (22.2)	0.573
Donor site, n (%)				
Left	22 (37.3)	0	4 (44.4)	
Right	37 (62.7)	4 (100.0)	5 (55.6)	0.384
Distance to the tip of the fibula (ankle), mean ± SD				
60 mm	6 (10.2)	0	0	
70 mm	31 (52.5)	4 (100.0)	5 (55.6)	
80 mm	17 (28.8)	0	2 (22.2)	
90 mm	5 (8.5)	0	1 (11.1)	
118.9 mm	0	0	1 (11.1)	0.175
Number of segments, n (%)				
1	15 (25.4)	1 (25.0)	4 (44.4)	
2	26 (44.1)	2 (50.0)	5 (55.6)	
3	18 (30.5)	1 (25.0)	0	0.351
Total transplant length (mm), mean ± SD (range)				
1	56.1 ± 15.3 (35.0 – 94.9)	55.0	68.1 ± 17.8 (47.3 – 90.2)	0.458
2	106.6 ± 21.5 (71.0 – 143.6)	99.8 ± 18.2 (86.9 – 112.6)	109.9 ± 18.7 (90.5 – 133.1)	0.804
3	142.3 ± 21.2 (103.7 – 176.3)	126.7	–	0.361
Minimal segment length (mm), mean ± SD (range)				
1	45.3 ± 16.8 (17.0 – 84.7)	32.0	52.6 ± 12.5 (34.0 – 60.2)	0.261
2	36.7 ± 14.3 (16.0 – 64.8)	37.0 ± 14.7 (28.4 – 59.0)	40.3 ± 16.8 (22.7 ± 73.0)	0.926
3	34.5 ± 14.2 (16.7 – 71.3)	27.1 ± 6.4 (25.8 – 29.5)	–	0.650
Maximal segment length (mm), mean ± SD (range)				
1	53.7 ± 16.4 (29.0 – 91.5)	52	62.2 ± 12.1 (45.0 – 71.5)	0.464
2	49.4 ± 16.1 (20.0 – 80.2)	45.1 ± 14.7 (32.9 – 64.5)	47.2 ± 16.1 (32.3 ± 79.3)	0.809
3	43.1 ± 13.5 (27.4 – 89.5)	36.8 ± 2.1 (29.9 – 42.4)	–	0.508
Length of TTF, mean ± SD (n‡)	31.3 ± 12.2 (55)	32.3 ± 11.7 (4)	40.1 ± 14.9 (8)	‡0.034

*BMI, body mass index; FFF, free fibula flap; PB, periosteal branch; SCP, septo-cutaneous perforator; SD, standard deviation; TTF, truncus tibiofibularis; WHD, wound healing disorder. *Significant difference was only found between flap success and partial flap failure group. ‡TTF was only assessed in type I-A branching pattern.*

for total flap failure in bi-segmental reconstructions. The length of each fibula flap segment was non-significant different in mono- ($p = 0.194$) and bi-segmental ($p = 0.752$) reconstructions concerning flap success. In poly-segmental jaw reconstructions, the proximal FFF segments (proximal in bi- and proximal > medial in tri-segmental reconstruction), a higher rate of PB per flap segment was assessed than in the distal segments (**Figure 7**).

DISCUSSION

Despite advances in the planning of free flaps, improvements of microsurgical techniques (54), and flap monitoring (55–57), the result of surgical reconstruction is still threatened by perfusion disorders of macro- and microcirculation. Flap loss severely disturbs patients' quality of life and increases the risk of further surgical procedures. Intensive preoperative assessment and imaging evaluation are necessary to decrease peri- and postoperative complications and increase flap success (58–63). CTA has been shown as a sensitive and specific method for microsurgical free flap (21, 64–66) and perforator flap harvesting in reconstructive surgery (67–75).

Over 43 % (n = 31) of the included study subjects were classified at least ASA-score 3. PFF occurred in 2 cases (6.5 %) and TFF in 4 cases (12.9 %). On the other hand, in the ASA-score 1 and 2 groups (n = 41), we documented n = 2 PFF (4.9 %) and n

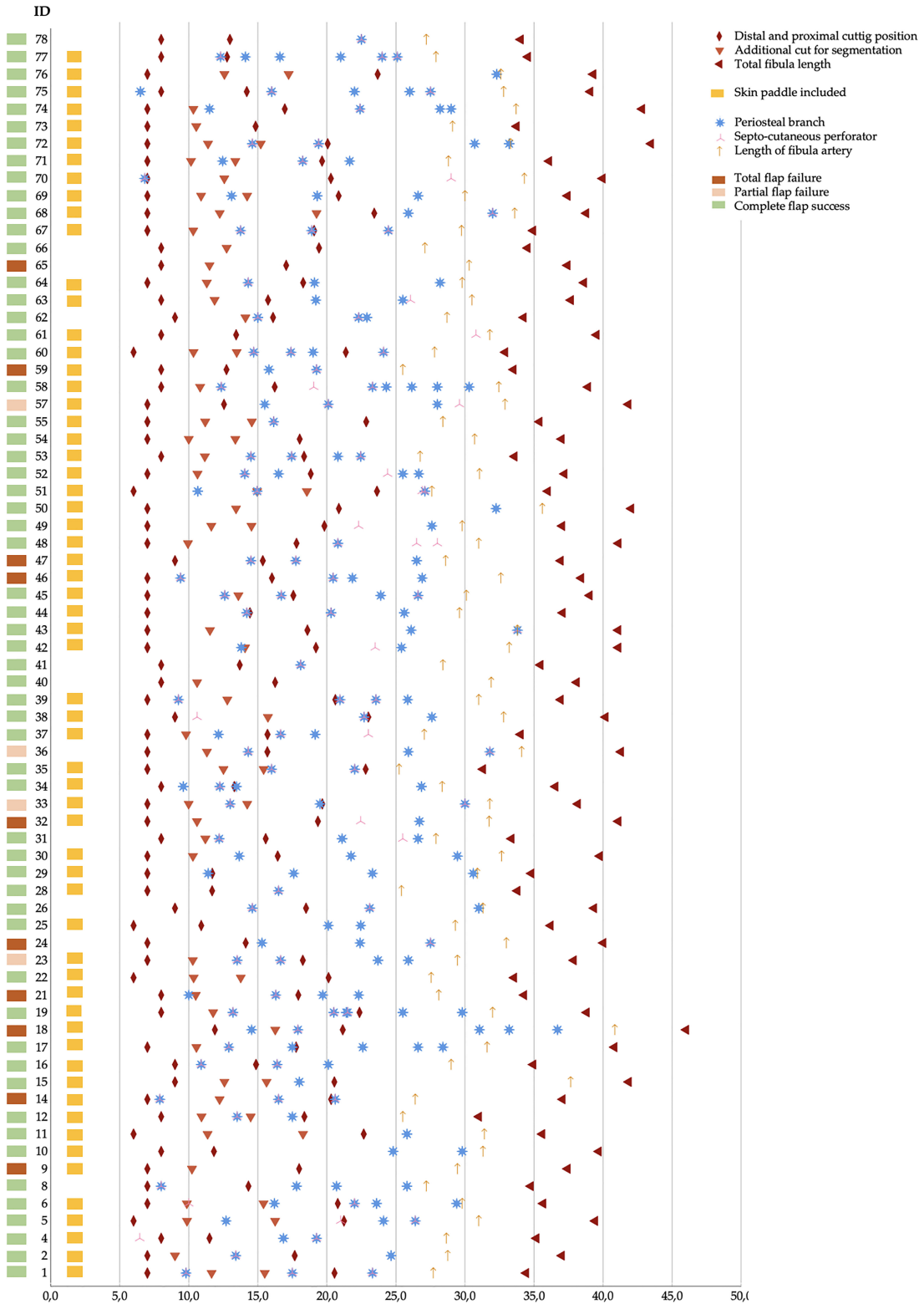

FIGURE 5 | Sample of n = 72 virtual planned jaw reconstructions. Matching virtually planned parameters, CTA detected vessels (PB and SCP), and surgical outcome. All position marks (x-axis) are given in centimeters.

TABLE 4 | Wound healing disorders of the donor site.

n = 72	Flap success 59 (82.0%)	Partial flap failure 4 (5.5%)	Total flap failure 9 (12.5%)	*p*-value
Composite flap, n (%)				
None	20 (33.9)	1 (25.0)	2 (22.2)	
Minor WHD	11 (18.6)	0	1 (11.1)	
Major WHD	20 (33.9)	2 (50.0)	4 (44.4)	
Non-composite flap				
None	8 (13.6)	1 (25.0)	2 (22.2)	0.523

= 5 (12.2 %) TFF. Despite the presence of comorbidities, we did not observe an increase in complications and flap loss. These results are comparable to the literature reported by other study groups (76–78).

How do Infra-Popliteal Branching Pattern and Fibular Artery Vascular Anomalies (Stenoses) Affect the Outcome of Flap Surgery?

Evaluation of the donor site vascular architecture revealed that type I-A was found in 93.1 % (non-donor site: 84.7 %) according to the classification by Kim et al. (51). Two donor site vascular systems were classified as type I-B, and one case was assigned to categories I-C to II-B. Four legs of the non-donor site showed dominant FA variants (III-A: n = 2; III-B: n = 2). The foot's blood supply is then shared between FA and non-hypoplastic ATA or PTA in type III-A and B, and FA is enlarged as a result (79–81). It was previously estimated that 5.2 % of limbs have dominant FAs (66). The study sample presented either on the donor or non-donor site none peroneal artery magna (type III-C), in which FA supplies blood to the lower leg and foot.

Overall, the distribution of the recorded branching variants of the popliteal artery is comparable to previous published data (82). However, it is imperative to identify this particular singular vasculature before FFF harvesting to prevent critical limb and foot ischemia (63, 83, 84). The investigation revealed that all but one of the PFF and TFF cases could be assigned to type I-A and I-B branching patterns. In accordance with the literature, type I-A is the most common branching pattern. Successful flap transfers occurred in types I-B, I-C, II-A, and II-B (each n = 1).

9.7 % of cases with vascular stenoses (n = 14) were identified in the sample, and from these, 11 were localized in the FA. There were five stenoses in the distal course of the FA run-off at the donor site, and two of these were associated with TFF. On the other hand, three cases of FA stenoses did not impact flap success. Remarkably, the majority of the recorded stenoses were located in FA. Other studies suggest the FA is not as severely affected by the peripheral arterial occlusive disease (PAOD) as the tibial arteries (60, 85, 86). Despite vascular calcifications impacting the flap vascular pedicle, successful microvascular FFF has been described, with a 0 % complete flap failure rate and a 7 % partial flap failure rate (87). Preoperative optimizing of leg perfusion by endovascular interventions has also been reported as a therapeutic option in possible critical limb perfusion (88).

Further study findings revealed significant differences concerning the length of TTF in the flap failure group compared to flap success and were assessed with an extended length of 40.1 ± 14.9 mm (p = 0.034). A more prolonged TTF implicates a decreasing length of the FA and, therefore, the entire vascular pedicle of the FFF. While short pedicle length can aggravate microsurgical anastomosis (89), a long pedicle is

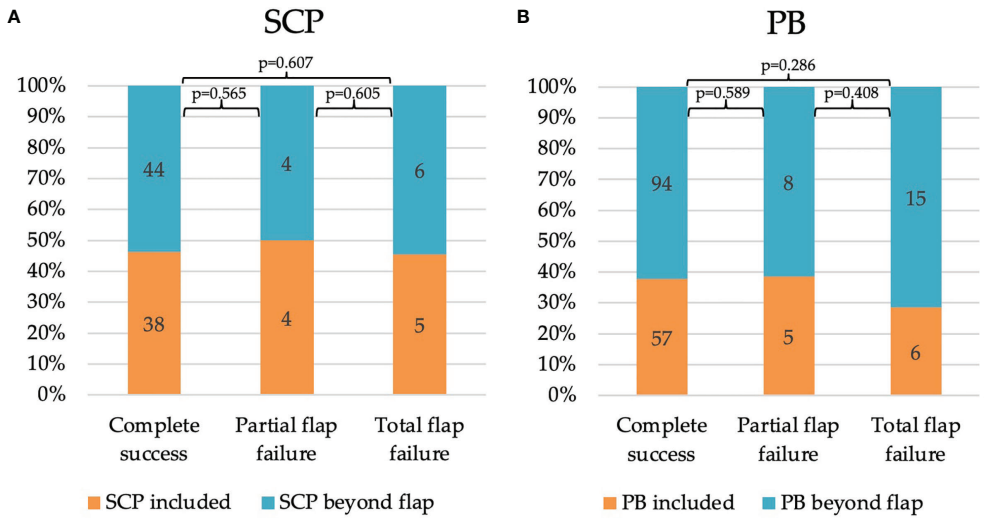

FIGURE 6 | Impact of relative distribution of **(A)** SCP and **(B)** PB concerning FFF outcome: Complete success, *n* = 59; Partial flap failure, *n* = 4; Total flap failure, *n* = 9. An absolute number of recorded vessel types are noted in the bars. Annotation: All possible SCP were recorded without consideration of including a skin paddle (composite FFF type). FFF, free fibula flap; PB, periosteal branch; SCP, septo-cutaneous perforator.

TABLE 5 | Absolute (n) and relative (%) number of fibular segments were addressed by at least one periosteal branch (PB) based on preoperative CTA for VSP.

PB ≥1 per segment (total segments *n* = 143)	Flap success 121 (= 59 FFF)	Partial flap failure 8 (= 4 FFF)	Total flap failure 14 (= 9 FFF)
1 SFFF, n (%)	7 (46.7)	0	2 (50.0)
2 SFFF, n (%)	21 (40.4)	2 (50.0)	4 (40.0)
3 SFFF, n (%)	17 (31.5)	2 (66.7)	–
All, n (%)	45 (37.2)	4 (50.0)	6 (42.9)

TABLE 6 | Absolute (n) and relative (%) number of fibula segments of composite FFF, which were addressed by at least one septo-cutaneous perforator (SCP) based on preoperative CTA for VSP.

SCP ≥1 per segment (total segments *n* = 126)	Flap success 109 (= 51 FFF)	Partial flap failure 6 (= 3 FFF)	Total flap failure 11 (= 7 FFF)
1 SFFF, n (%)	4 (36.4)	0	2 (66.7)
2 SFFF, n (%)	13 (29.5)	1 (50.0)	3 (37.5)
3 SFFF, n (%)	12 (22.2)	1 (33.3)	–
All, n (%)	29 (26.6)	2 (33.3)	5 (45.4)

endangered for kinking and twisting with critical blood flow of the vascular axis (90). Published literature hypothesizes a relation between length and course of TTF and high body mass. This condition may contribute to enlarged and curved/twisted TTF, promoting local atherosclerosis and impeding microsurgery (91).

Summarized, the infra-popliteal branching pattern types I-A to II-B did not affect the flap surgery outcome in the present study. Furthermore, despite recorded vascular stenoses of the FA, flap success was observed in more than the half of those cases.

How Does the Distribution of CTA-Based Detected PB and SCP Influence the Surgical Result of Mono- and Poly-Segmental Jaw Reconstructions With Partial or Total Flap Loss?

The results of this study show that a PB and SCP (musculo-fascio-periosteal perforators) could not be visualized in every virtually planned and transplanted segment in the preoperatively performed lower limb CTA scan. Nevertheless, mono- and poly-segmental reconstructions were successful when no PB was found in CTA evaluation and failed, although PB (and SCP) were verifiable.

When matching harvested segments with detected PB, 38.5 % of all virtual planned segments (n = 143 in 72 patients) were congruent to one or more PB localization. If the segments which at least one PB distinctively supplied are assigned to the defined flap outcome groups, it was found that the FS group has the lowest rate with 37.2 %, the PFF group has the highest rate with 50.0 %, and the TFF group is between both with 42.9 % (**Table 5**). Therefore, the rate of in CTA detected PB found per segment did not provide information concerning expected flap success. The explored distribution patterns reflect PB and SCP clustering and confirm the high variability of the localization and course. It is noticeable that in poly-segmental reconstructions, the probability of observing a PB in the CTA increases in the more proximal segment. Previous investigations on the study sample revealed a bimodal distribution pattern for PB and three peaks for SCP in performed CTA for VSP (48). These patterns of distribution are similar to the results of other studies (17, 20, 92).

Investigations of CT-scans in fresh frozen cadaver lower limbs showed in mean 12.8 periosteal branches of the fibular artery with a mean intersegmental distance of 1.36 cm between them, and at least one branch in 65.1% in 1.0 cm segments, and up to 94% of the 2.0 cm segments (49). Their radiological findings of the detected periosteal branches (49) support the measurements of fibular segments perfusion in cadavers (93), but differ from our conclusions presented. The previous analysis of the study sample has shown that in 10.8 %, one PB was found in a 1.0 cm fibula section in our defined region of interest between the origin of the FA and a plane 5 cm above the distal tip of the fibula section. The likelihood increases in 2.0 cm segment up to 21.1 % and in 3.0 cm segment length to 29.2 %, having included at least one PB (48). Further, there is no difference regarding the density of periosteal and musculo-periosteal vessels in the long and short fibula segments. Existing collaterals between the superficial, periosteal, and the internal endoperiosteal system, were not able to compensate for the work of the non-functional vessels if the segment length was too short. However, this is more likely to occur if the segments are longer (93). Larger segments and fewer osteotomies were associated with higher perfusion (94). Battaglia et al. reported a series of 20 patients in matching in CTA images identified perforators with the intraoperative perforator location while FFF harvesting (65). An average distance between CTA perforator positions and intraoperative perforator positions of 1 mm (range 0 to 2 mm) was assessed. They concluded that preoperative CTA evaluation to investigate lower-extremity vascular patterns for patients undergoing composite FFF is a valuable approach for reducing VSP complications due to variable vascular anatomy. Still, more follow-up studies are needed to assess this modern technique's long-term outcomes and benefits (65). Ettinger et al. report that further development of CTA imaging protocols and existing VSP workflows is necessary to be optimized to allow faster and more accurate preoperative modeling of cutaneous perforator anatomy for consideration in VSP of reconstructions (64). These authors point out also, that CTA for VSP allows taking the position of perforators into account when planning poly-segmental reconstruction and skin paddle (64). A previous study found that CTA could detect the size, course, and penetration pattern of all perforators with a diameter more than 0.3 mm (21). Recent investigation on the study population confirmed these statements (48). However, it can be assumed that the discrepancy in anatomical findings is based on the quality of the CTA scans. Several other factors influence CTA scan accuracy, including the timing, dosage, and coordination of the contrast bolus with the sequence of images (95).

Overall, the rate of CTA detected PB per segment did not indicate flap success. Mono- and poly-segmental reconstructions were successful when no PB (and SCP) were found in the CTA evaluation and even were unsuccessful when PB (and SCP) were recorded.

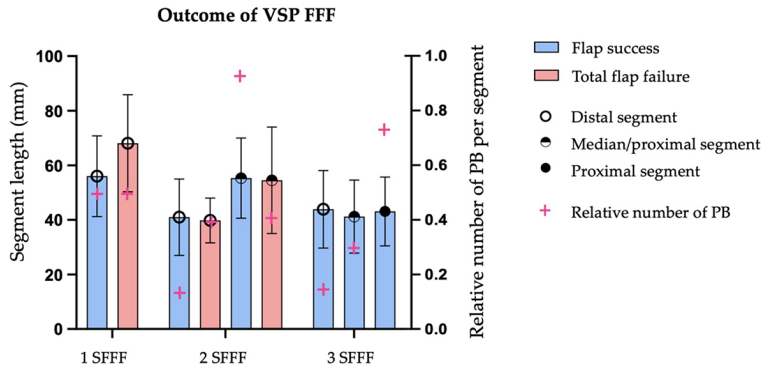

FIGURE 7 | Impact of FFF outcome concerning length of fibular bone segments of mono- (1 SFFF), bi- (2 SFFF) or tri-segmental (3 SFFF) flap for achieving jaw reconstruction (left y-axis). The relative number of periosteal branches (PB) per segment (right y-axis) was calculated and superimposed (magenta cross). 1 SFFF flap success: *n* = 16 vs. total flap failure: *n* = 4; 2 SFFF flap success: *n* = 28 vs. *n* = 5; 3 SFFF flap success: *n* = 19 vs. *n* = 0; Amount of observed PB in region of transplanted fibular bone segments *n* = 66 based on the preoperative CTA.

Does the Observed Distribution of PB and SCP Impact Wound Healing of the Donor Site?

WHD of the donor site were recorded only in the composite flap group, and the proportion of WHD was less high in the TFF-group (55.5 %) than in the FS-group (52.5 %). The differences should be viewed critically according to the small number of cases. A separation between minor WHD (small wound area and local therapy) and major WHD (large wound, exposed tendon, and need of surgical therapy with debridement, new skin grafting) had been done and showed, that major WHD (33.9%) had been recorded near to twice than minor WHD (18.6%) in the FS-group. In summary, more than 52.8 % of the entire study sample WHD were found. Published literature shows complication rates from 0% to 33% (62, 96, 97). In the present study, donor site defect of composite FFF were covered in all cases with a meshed split-thickness skin graft, and every (sub-)total graft loss was counted and defined as WHD. Primarily wound closure was only performed after non-composite FFF harvesting, and wound healing disorder was not found in this group.

According to SCP per segment matching rate, only composite flaps were evaluated. A total number of n = 126 segments in 64 patients has shown that overall, 28.6 % of all virtual planned segments were congruent to one or more SCP localization. However, this finding does not allow providing information concerning wound healing disorder. On the one hand, the authors believe that the size of the skin paddle and the donor site defect, and the patient's general condition with comorbidities play a decisive role in wound healing. Heavy tobacco use was found to have as a risk factor for wound impairment (97).

The problem of WHD as a donor site morbidity has been known in the literature for a long time. Up to now, closure of the donor site is controversial and ranges from primarily closure, open wound healing, split-thickness skin graft, full skin graft, free flap (96, 98). Open healing of the fibular donor site and meshing of the surrounded tissue has been reported as a modification to decrease the wound area and avoid the morbidity associated with graft and resulted in a good cosmetic outcome (99). The use of vacuum-assisted closure allows patients to be mobilized sooner, assures greater graft acceptance, and reduces healing time up to 50% (100).

Up to now, information about the number and course of PB and SCP has not been of interest in our entire virtual planning process. Designing the composite flap and especially the skin paddle's dimension depends on the defect size and visible SCP in the posterior intermuscular septum. From our clinical experience, we agree with others that handheld Doppler sonography examination is often unsuitable in general anesthesia to identify SCP reliably. Identifying tiny perforators and distinguishing between superficial muscular perforators and cutaneous perforators is difficult (101). Islam et al. discovered that real-time, color-flow Doppler ultrasonography was beneficial in the planning and harvesting free perforator flaps and suggested that it be used more widely than traditional hand-held Doppler equipment (102). We prefer the direct assessment and visualization of the SCP during dissection (**Figure 3**).

The distribution of in preoperative CTA detected PB and SCP per segment was not associated with the rate of wound healing disorders of the donor site after composite flap harvesting.

Limitations of the Study

There are some limitations in this retrospective study. Only patients who underwent the following FFF procedure were included in the investigation. Patients who were not suitable for FFF after CTA scan were not included, and the number of cases remains unclear. The investigated study population consisted a mixture of malignant and benign diseases which give an inhomogeneity to the study subjects. Another limitation is that multiple surgeons were involved in the treatment of the study population. Three different surgeons were involved in FFF harvesting over the entire study period. Evaluated CTA scans were not performed under experimental, controlled conditions. Instead, they were run as routine clinical imaging which reported by different radiologists.

Furthermore, as concluded in a previous study, the in CTA observed number of PBs and SCPs is substantially less than accurate as the anatomical findings (48). Therefore, the number of small vessels could be underestimated. Further studies using better developed volume visualization software to improve the illustration of small vessels are necessary as a future research step in this topic.

CONCLUSION

Preoperatively CTA for VSP of free fibula flap (FFF) is suitable for vascular mapping of the infra-popliteal vascular system and smaller vessels. Despite recorded stenoses of fibular artery in five cases, FFF was in 60% successful.

Correlation between higher rates of PB, SCP and the flap success could not be statistically proved in study sample. We conclude, that preoperative PB and SCP mapping based on routine CTA imaging is not suitable for prediction of flap outcome.

DATA AVAILABILITY STATEMENT

The raw data supporting the conclusions of this article will be made available by the authors, without undue reservation.

ETHICS STATEMENT

The study was approved by the local Ethics Committee of Justus-Liebig University Giessen (AZ33/20, approval 25.5.2020). Written informed consent for participation was not required for this study in accordance with the national legislation and the institutional requirements.

AUTHOR CONTRIBUTIONS

Conceptualization, MK and SA. Data curation, DS and SB. Formal analysis, MK and PS. Funding acquisition, H-PH. Investigation, MK and AB. Methodology, MK, AB, CA, and FR. Supervision, H-PH and SA. Validation, SA. Visualization, CB. Writing – original draft, MK. Writing – review & editing, AB, CB, CA, FR, DS, SB, PS, H-PH, and SA. All authors have read and agreed to the published version of the manuscript.

ACKNOWLEDGMENTS

This publication is part of the dental doctoral thesis of AB.

REFERENCES

1. Taylor GI, Miller GD, Ham FJ. The Free Vascularized Bone Graft. A Clinical Extension of Microvascular Techniques. *Plast Reconstr Surg* (1975) 55 (5):533–44. doi: 10.1097/00006534-197505000-00002
2. Hidalgo DA. Fibula Free Flap: A New Method of Mandible Reconstruction. *Plast Reconstr Surg* (1989) 84(1):71–9. doi: 10.1097/00006534-198907000-00014
3. Cordeiro PG, Disa JJ, Hidalgo DA, Hu QY. Reconstruction of the Mandible With Osseous Free Flaps: A 10-Year Experience With 150 Consecutive Patients. *Plast Reconstr Surg* (1999) 104(5):1314–20. doi: 10.1097/00006534-199910000-00011
4. Wei FC, Chen HC, Chuang CC, Noordhoff MS. Fibular Osteoseptocutaneous Flap: Anatomic Study and Clinical Application. *Plast Reconstr Surg* (1986) 78 (2):191–200. doi: 10.1097/00006534-198608000-00008
5. Kumar BP, Venkatesh V, Kumar KA, Yadav BY, Mohan SR. Mandibular Reconstruction: Overview. *J Maxillofac Oral Surg* (2016) 15(4):425–41. doi: 10.1007/s12663-015-0766-5
6. Löfstrand J, Nyberg M, Karlsson T, Thórarinsson A, Kjeller G, Lidén M, et al. Quality of Life After Free Fibula Flap Reconstruction of Segmental Mandibular Defects. *J Reconstr Microsurg* (2018) 34(2):108–20.
7. Tarsitano A, Ciocca L, Cipriani R, Scotti R, Marchetti C. Mandibular Reconstruction Using Fibula Free Flap Harvested Using a Customised Cutting Guide: How We do it. *Acta Otorhinolaryngol Ital* (2015) 35 (3):198–201.
8. Attia S, Wiltfang J, Streckbein P, Wilbrand JF, El Khassawna T, Mausbach K, et al. Functional and Aesthetic Treatment Outcomes After Immediate Jaw Reconstruction Using a Fibula Flap and Dental Implants. *J Craniomaxillofac Surg* (2019) 47(5):786–91. doi: 10.1016/j.jcms.2018.12.017
9. Attia S, Diefenbach J, Schmermund D, Bottger S, Pons-Kuhnemann J, Scheibelhut C, et al. Donor-Site Morbidity After Fibula Transplantation in Head and Neck Tumor Patients: A Split-Leg Retrospective Study With Focus on Leg Stability and Quality of Life. *Cancers (Basel)* (2020) 12(8). doi: 10.3390/cancers12082217
10. Attia S, Wiltfang J, Pons-Kühnemann J, Wilbrand JF, Streckbein P, Kähling C, et al. Survival of Dental Implants Placed in Vascularised Fibula Free Flaps After Jaw Reconstruction. *J Craniomaxillofac Surg* (2018) 46(8):1205–10. doi: 10.1016/j.jcms.2018.05.008
11. Petrovic I, Baser R, Blackwell T, McCarthy C, Ganly I, Patel S, et al. Long-Term Functional and Esthetic Outcomes After Fibula Free Flap Reconstruction of the Mandible. *Head Neck* (2019) 41(7):2123–32. doi: 10.1002/hed.25666
12. Wilde F, Winter K, Kletsch K, Lorenz K, Schramm A. Mandible Reconstruction Using Patient-Specific Pre-Bent Reconstruction Plates: Comparison of Standard and Transfer Key Methods. *Int J Comput Assist Radiol Surg* (2015) 10(2):129–40. doi: 10.1007/s11548-014-1065-1
13. Wilde F, Schramm A. [Computer-Aided Reconstruction of the Facial Skeleton : Planning and Implementation in Clinical Routine]. *HNO* (2016) 64(9):641–9. doi: 10.1007/s00106-016-0220-0
14. Wilde F, Hanken H, Probst F, Schramm A, Heiland M, Cornelius CP. Multicenter Study on the Use of Patient-Specific CAD/CAM Reconstruction Plates for Mandibular Reconstruction. *Int J Comput Assist Radiol Surg* (2015) 10(12):2035–51. doi: 10.1007/s11548-015-1193-2
15. Ersoy H, Rybicki FJ. MR Angiography of the Lower Extremities. *AJR Am J Roentgenol* (2008) 190(6):1675–84. doi: 10.2214/AJR.07.2223
16. Lorbeer R, Grotz A, Dörr M, Völzke H, Lieb W, Kühn JP, et al. Reference Values of Vessel Diameters, Stenosis Prevalence, and Arterial Variations of the Lower Limb Arteries in a Male Population Sample Using Contrast-Enhanced MR Angiography. *PLoS One* (2018) 13(6):e0197559. doi: 10.1371/journal.pone.0197559
17. Schuderer JG, Meier JK, Klingelhöffer C, Gottsauner M, Reichert TE, Wendl CM, et al. Magnetic Resonance Angiography for Free Fibula Harvest: Anatomy and Perforator Mapping. *Int J Oral Maxillofac Surg* (2020) 49 (2):176–82. doi: 10.1016/j.ijom.2019.09.005
18. Rozen WM, Phillips TJ, Ashton MW, Stella DL, Gibson RN, Taylor GI. Preoperative Imaging for DIEA Perforator Flaps: A Comparative Study of Computed Tomographic Angiography and Doppler Ultrasound. *Plast Reconstr Surg* (2008) 121(1 Suppl):1–8. doi: 10.1097/01.prs.0000293874.71269.c9
19. Abdel Razek AA, Denewer AT, Hegazy MA, Hafez MT. Role of Computed Tomography Angiography in the Diagnosis of Vascular Stenosis in Head and Neck Microvascular Free Flap Reconstruction. *Int J Oral Maxillofac Surg* (2014) 43(7):811–5. doi: 10.1016/j.ijom.2014.03.014
20. Garvey PB, Chang EI, Selber JC, Skoracki RJ, Madewell JE, Liu J, et al. A Prospective Study of Preoperative Computed Tomographic Angiographic Mapping of Free Fibula Osteocutaneous Flaps for Head and Neck

Reconstruction. *Plast Reconstr Surg* (2012) 130(4):541e–9e. doi: 10.1097/PRS.0b013e318262f115
21. Ribuffo D, Atzeni M, Saba L, Guerra M, Mallarini G, Proto EB, et al. Clinical Study of Peroneal Artery Perforators With Computed Tomographic Angiography: Implications for Fibular Flap Harvest. *Surg Radiol Anat* (2010) 32(4):329–34. doi: 10.1007/s00276-009-0559-y
22. Eckardt A, Swennen GR. Virtual Planning of Composite Mandibular Reconstruction With Free Fibula Bone Graft. *J Craniofac Surg* (2005) 16 (6):1137–40. doi: 10.1097/01.scs.0000186306.32042.96
23. Seruya M, Fisher M, Rodriguez ED. Computer-Assisted Versus Conventional Free Fibula Flap Technique for Craniofacial Reconstruction: An Outcomes Comparison. *Plast Reconstr Surg* (2013) 132(5):1219–28. doi: 10.1097/PRS.0b013e3182a3c0b1
24. Han HH, Kim HY, Lee JY. The Pros and Cons of Computer-Aided Surgery for Segmental Mandibular Reconstruction After Oncological Surgery. *Arch Craniofac Surg* (2017) 18(3):149–54. doi: 10.7181/acfs.2017.18.3.149
25. Saini V, Gaba S, Sharma S, Kalra P, Sharma RK. Assessing the Role of Virtual Surgical Planning in Mandibular Reconstruction With Free Fibula Osteocutaneous Graft. *J Craniofac Surg* (2019) 30(6):e563–6. doi: 10.1097/SCS.0000000000005538
26. Tang NSJ, Ahmadi I, Ramakrishnan A. Virtual Surgical Planning in Fibula Free Flap Head and Neck Reconstruction: A Systematic Review and Meta-Analysis. *J Plast Reconstr Aesthet Surg* (2019) 72(9):1465–77. doi: 10.1016/j.bjps.2019.06.013
27. Barr ML, Barr ML, Haveles CS, Rezzadeh KS, Nolan IT, Castro R, Lee JC, et al. Virtual Surgical Planning for Mandibular Reconstruction With the Fibula Free Flap: A Systematic Review and Meta-Analysis. *Ann Plast Surg* (2020) 84(1):117–22. doi: 10.1097/SAP.0000000000002006
28. Cornelius CP, Smolka W, Giessler GA, Wilde F, Probst FA. Patient-Specific Reconstruction Plates are the Missing Link in Computer-Assisted Mandibular Reconstruction: A Showcase for Technical Description. *J Craniomaxillofac Surg* (2015) 43(5):624–9. doi: 10.1016/j.jcms.2015.02.016
29. Wilde F, Cornelius CP, Schramm A. Computer-Assisted Mandibular Reconstruction Using a Patient-Specific Reconstruction Plate Fabricated With Computer-Aided Design and Manufacturing Techniques. *Craniomaxillofac Trauma Reconstr* (2014) 7(2):158–66. doi: 10.1055/s-0034-1371356
30. Geusens J, Sun Y, Luebbers HT, Bila M, Darche V, Politis C. Accuracy of Computer-Aided Design/Computer-Aided Manufacturing-Assisted Mandibular Reconstruction With a Fibula Free Flap. *J Craniofac Surg* (2019) 30(8):2319–23. doi: 10.1097/SCS.0000000000005704
31. Kansy K, Mueller AA, Mücke T, Kopp JB, Koersgen F, Wolff KD, et al. Microsurgical Reconstruction of the Head and Neck–Current Concepts of Maxillofacial Surgery in Europe. *J Craniomaxillofac Surg* (2014) 42(8):1610–3. doi: 10.1016/j.jcms.2014.04.030
32. Shroff SS, Nair SC, Shah A, Kumar B. Versatility of Fibula Free Flap in Reconstruction of Facial Defects: A Center Study. *J Maxillofac Oral Surg* (2017) 16(1):101–7. doi: 10.1007/s12663-016-0930-6
33. Hölzle F, Kesting MR, Hölzle G, Watola A, Loeffelbein DJ, Ervens J, et al. Clinical Outcome and Patient Satisfaction After Mandibular Reconstruction With Free Fibula Flaps. *Int J Oral Maxillofac Surg* (2007) 36(9):802–6. doi: 10.1016/j.ijom.2007.04.013
34. Colletti G, Autelitano L, Rabbiosi D, Biglioli F, Chiapasco M, Mandala M, et al. Technical Refinements in Mandibular Reconstruction With Free Fibula Flaps: Outcome-Oriented Retrospective Review of 99 Cases. *Acta Otorhinolaryngol Ital* (2014) 34(5):342–8.
35. Barry CP, MacDhabheid C, Tobin K, Stassen LF, Lennon P, Toner M, et al. 'Out of House' Virtual Surgical Planning for Mandible Reconstruction After Cancer Resection: Is it Oncologically Safe? *Int J Oral Maxillofac Surg* (2020). doi: 10.1016/j.ijom.2020.11.008
36. Knitschke M, Bäcker C, Schmermund D, Böttger S, Streckbein P, Howaldt HP, et al. Impact of Planning Method (Conventional Versus Virtual) on Time to Therapy Initiation and Resection Margins: A Retrospective Analysis of 104 Immediate Jaw Reconstructions. *Cancers (Basel)* (2021) 13(12). doi: 10.3390/cancers13123013
37. Ma C, Wang L, Tian Z, Qin X, Zhu D, Qin J, et al. Standardize Routine Angiography Assessment of Leg Vasculatures Before Fibular Flap Harvest: Lessons of Congenital and Acquired Vascular Anomalies Undetected by Color Doppler and Physical Examinations. *Acta Radiol* (2021) p:284185120980001. doi: 10.1177/0284185120980001
38. Panje W, Cutting C. Trapezius Osteomyocutaneous Island Flap for Reconstruction of the Anterior Floor of the Mouth and the Mandible. *Head Neck Surg* (1980) 3(1):66–71. doi: 10.1002/hed.2890030112
39. Sparks DS, Saleh DB, Rozen WM, Hutmacher DW, Schuetz MA, Wagels M. Vascularised Bone Transfer: History, Blood Supply and Contemporary Problems. *J Plast Reconstr Aesthet Surg* (2017) 70(1):1–11. doi: 10.1016/j.bjps.2016.07.012
40. Menck J, Sander A. [Periosteal and Endosteal Blood Supply of the Human Fibula and its Clinical Importance]. *Acta Anat (Basel)* (1992) 145(4):400–5. doi: 10.1159/000147397
41. Simpson AH. The Blood Supply of the Periosteum. *J Anat* (1985) 140(Pt 4):697–704.
42. Rhinelander FW. Tibial Blood Supply in Relation to Fracture Healing. *Clin Orthop Relat Res* (1974) 105):34–81. doi: 10.1097/00003086-197411000-00005
43. Schmidt AB, Giessler GA. The Muscular and the New Osteomuscular Composite Peroneus Brevis Flap: Experiences From 109 Cases. *Plast Reconstr Surg* (2010) 126(3):924–32. doi: 10.1097/PRS.0b013e3181e3b74d
44. Kofoed H, Sjontoft E, Siemssen SO, Olesen HP. Bone Marrow Circulation After Osteotomy. Blood Flow, Po2, Pco2, and Pressure Studied in Dogs. *Acta Orthop Scand* (1985) 56(5):400–3. doi: 10.3109/17453678508994357
45. Kocabiyik N, Yalcin B, Ozan H. Variations of the Nutrient Artery of the Fibula. *Clin Anat* (2007) 20(4):440–3. doi: 10.1002/ca.20442
46. Anetai H, Kinose S, Sakamoto R, Onodera R, Kato K, Kawasaki Y, et al. Anatomic Characterization of the Tibial and Fibular Nutrient Arteries in Humans. *Anat Sci Int* (2021) 96(3):378–85. doi: 10.1007/s12565-020-00600-9
47. Zhu YL, Xu YQ, Yang J, Li J, Lan XF. An Anatomic Study of Vascularized Fibular Grafts. *Chin J Traumatol* (2008) 11(5):279–82. doi: 10.1016/S1008-1275(08)60056-5
48. Knitschke M, Baumgart AK, Bäcker C, Adelung C, Roller F, Schmermund D, et al. Computed Tomography Angiography (CTA) Before Reconstructive Jaw Surgery Using Fibula Free Flap: Retrospective Analysis of Vascular Architecture. *Diagnostics (Basel)* (2021) 11(10). doi: 10.3390/diagnostics11101865
49. Fry AM, Laugharne D, Jones K. Osteotomising the Fibular Free Flap: An Anatomical Perspective. *Br J Oral Maxillofac Surg* (2016) 54(6):692–3. doi: 10.1016/j.bjoms.2015.11.009
50. Gilbert A. Vascularised Transfer of the Fibula Shaft. *Int J Microsurg* (1979) 1:100.
51. Kim D, Orron DE, Skillman JJ. Surgical Significance of Popliteal Arterial Variants. A Unified Angiographic Classification. *Ann Surg* (1989) 210 (6):776–81. doi: 10.1097/00000658-198912000-00014
52. Knitschke M, Sonnabend S, Bäcker C, Schmermund D, Böttger S, Howaldt HP, et al. Partial and Total Flap Failure After Fibula Free Flap in Head and Neck Reconstructive Surgery: Retrospective Analysis of 180 Flaps Over 19 Years. *Cancers (Basel)* (2021) 13(4). doi: 10.3390/cancers13040865
53. Freeman GH, Halton JH. Note on an Exact Treatment of Contingency, Goodness of Fit and Other Problems of Significance. *Biometrika* (1951) 38 (1-2):141–9. doi: 10.1093/biomet/38.1-2.141
54. Wieker H, Fritz Schomaker MC, Florke C, Karayurek F, Naujokat H, Acil Y, et al. A Retrospective Analysis of the Surgical Outcomes of Different Free Vascularized Flaps Used for the Reconstruction of the Maxillofacial Region: Hand-Sewn Microvascular Anastomosis vs Anastomotic Coupler Device. *J Craniomaxillofac Surg* (2021) 49(3):191–5. doi: 10.1016/j.jcms.2020.12.015
55. Thiem DGE, Frick RW, Goetze E, Gielisch M, Al-Nawas B, Kämmerer PW. Hyperspectral Analysis for Perioperative Perfusion Monitoring-a Clinical Feasibility Study on Free and Pedicled Flaps. *Clin Oral Investig* (2021) 25 (3):933–45. doi: 10.1007/s00784-020-03382-6
56. Salgado CJ, Moran SL, Mardini S. Flap Monitoring and Patient Management. *Plast Reconstr Surg* (2009) 124(6 Suppl):e295–302. doi: 10.1097/PRS.0b013e3181bcf07b
57. Ludolph I, Lehnhardt M, Arkudas A, Kneser U, Pierer G, Harder Y, et al. [Plastic Reconstructive Microsurgery in the Elderly Patient - Consensus Statement of the German Speaking Working Group for Microsurgery of the Peripheral Nerves and Vessels]. *Handchir Mikrochir Plast Chir* (2018) 50 (2):118–25. doi: 10.1055/s-0043-115730

58. Akashi M, Nomura T, Sakakibara S, Sakakibara A, Hashikawa K. Preoperative MR Angiography for Free Fibula Osteocutaneous Flap Transfer. *Microsurgery* (2013) 33(6):454–9. doi: 10.1002/micr.22128
59. Bretzman PA, Manaster BJ, Davis WL, Coleman DA. MR Angiography for Preoperative Evaluation of Vascularized Fibular Grafts. *J Vasc Interv Radiol* (1994) 5(4):603–10. doi: 10.1016/S1051-0443(94)71561-X
60. Kelly AM, Cronin P, Hussain HK, Londy FJ, Chepeha DB, Carlos RC. Preoperative MR Angiography in Free Fibula Flap Transfer for Head and Neck Cancer: Clinical Application and Influence on Surgical Decision Making. *AJR Am J Roentgenol* (2007) 188(1):268–74. doi: 10.2214/AJR.04.1950
61. Kessler P, Wiltfang J, Schultze-Mosgau S, Lethaus B, Greess H, Neukam FW. The Role of Angiography in the Lower Extremity Using Free Vascularized Fibular Transplants for Mandibular Reconstruction. *J Craniomaxillofac Surg* (2001) 29(6):332–6. doi: 10.1054/jcms.2001.0251
62. Ling XF, Peng X. What is the Price to Pay for a Free Fibula Flap? A Systematic Review of Donor-Site Morbidity Following Free Fibula Flap Surgery. *Plast Reconstr Surg* (2012) 129(3):657–74. doi: 10.1097/PRS.0b013e3182402d9a
63. Rosson GD, Singh NK. Devascularizing Complications of Free Fibula Harvest: Peronea Arteria Magna. *J Reconstr Microsurg* (2005) 21(8):533–8. doi: 10.1055/s-2005-922432
64. Ettinger KS, Alexander AE, Arce K. Computed Tomographic Angiography Perforator Localization for Virtual Surgical Planning of Osteocutaneous Fibular Free Flaps in Head and Neck Reconstruction. *J Oral Maxillofac Surg* (2018) 76(10):2220–30. doi: 10.1016/j.joms.2018.04.002
65. Battaglia S, Maiolo V, Savastio G, Zompatori M, Contedini F, Antoniazzi E, et al. Osteomyocutaneous Fibular Flap Harvesting: Computer-Assisted Planning of Perforator Vessels Using Computed Tomographic Angiography Scan and Cutting Guide. *J Craniomaxillofac Surg* (2017) 45 (10):1681–6. doi: 10.1016/j.jcms.2017.07.017
66. Abou-Foul AK, Borumandi F. Anatomical Variants of Lower Limb Vasculature and Implications for Free Fibula Flap: Systematic Review and Critical Analysis. *Microsurgery* (2016) 36(2):165–72. doi: 10.1002/micr.30016
67. Alonso-Burgos A, Garcia-Tutor E, Bastarrika G, Cano D, Martinez-Cuesta A, Pina LJ. Preoperative Planning of Deep Inferior Epigastric Artery Perforator Flap Reconstruction With Multislice-CT Angiography: Imaging Findings and Initial Experience. *J Plast Reconstr Aesthet Surg* (2006) 59 (6):585–93. doi: 10.1016/j.bjps.2005.12.011
68. Chiu WK, Lin WC, Chen SY, Tzeng WD, Liu SC, Lee TP, et al. Computed Tomography Angiography Imaging for the Chimeric Anterolateral Thigh Flap in Reconstruction of Full Thickness Buccal Defect. *ANZ J Surg* (2011) 81(3):142–7. doi: 10.1111/j.1445-2197.2010.05483.x
69. Duymaz A, Karabekmez FE, Vrtiska TJ, Mardini S, Moran SL. Free Tissue Transfer for Lower Extremity Reconstruction: A Study of the Role of Computed Angiography in the Planning of Free Tissue Transfer in the Posttraumatic Setting. *Plast Reconstr Surg* (2009) 124(2):523–9. doi: 10.1097/PRS.0b013e3181addafa
70. Gelati C, Lozano Miralles ME, Morselli PG, Fabbri E, Cipriani R. Deep Inferior Epigastric Perforator Breast Reconstruction With Computer-Aided Design/Computer-Aided Manufacturing Sizers. *Ann Plast Surg* (2020) 84 (1):24–9. doi: 10.1097/SAP.0000000000002020
71. Higueras Sune MC, Lopez Ojeda A, Narvaez Garcia JA, De Albert De Las Vigo M, Roca Mas O, Perez Sidelnikova D, et al. Use of Angioscanning in the Surgical Planning of Perforator Flaps in the Lower Extremities. *J Plast Reconstr Aesthet Surg* (2011) 64(9):1207–13. doi: 10.1016/j.bjps.2011.03.015
72. Masia J, Clavero JA, Larranaga JR, Alomar X, Pons G, Serret P. Multidetector-Row Computed Tomography in the Planning of Abdominal Perforator Flaps. *J Plast Reconstr Aesthet Surg* (2006) 59(6):594–9. doi: 10.1016/j.bjps.2005.10.024
73. Ngaage LM, Hamed R, Oni G, Di Pace B, Ghorra DT, Koo BBC, et al. The Role of CT Angiography in Assessing Deep Inferior Epigastric Perforator Flap Patency in Patients With Pre-Existing Abdominal Scars. *J Surg Res* (2019) 235:58–65. doi: 10.1016/j.jss.2018.09.059
74. Prokop M. Multislice CT Angiography. *Eur J Radiol* (2000) 36(2):86–96. doi: 10.1016/S0720-048X(00)00271-0
75. Zhang Y, Pan X, Yang H, Yang Y, Huang H, Rui Y. Computed Tomography Angiography for the Chimeric Anterolateral Thigh Flap in the Reconstruction of the Upper Extremity. *J Reconstr Microsurg* (2017) 33 (3):211–7. doi: 10.1055/s-0036-1597587
76. Piazza C, Grammatica A, Paderno A, Taglietti V, Del Bon F, Marengoni A, et al. Microvascular Head and Neck Reconstruction in the Elderly: The University of Brescia Experience. *Head Neck* (2016) 38 Suppl 1:E1488–92. doi: 10.1002/hed.24264
77. van Gemert JTM, Abbink JH, van Es RJJ, Rosenberg A, Koole R, Van Cann EM. Early and Late Complications in the Reconstructed Mandible With Free Fibula Flaps. *J Surg Oncol* (2018) 117(4):773–80. doi: 10.1002/jso.24976
78. Lodders JN, Schulten EA, de Visscher JG, Forouzanfar T, Karagozoglu KH. Complications and Risk After Mandibular Reconstruction With Fibular Free Flaps in Patients With Oral Squamous Cell Carcinoma: A Retrospective Cohort Study. *J Reconstr Microsurg* (2016) 32(6):455–63. doi: 10.1055/s-0036-1571794
79. Abou-Foul AK, Fasanmade A, Prabhu S, Borumandi F. Anatomy of the Vasculature of the Lower Leg and Harvest of a Fibular Flap: A Systematic Review. *Br J Oral Maxillofac Surg* (2017) 55(9):904–10. doi: 10.1016/j.bjoms.2017.08.363
80. Carroll WR, Esclamado R. Preoperative Vascular Imaging for the Fibular Osteocutaneous Flap. *Arch Otolaryngol Head Neck Surg* (1996) 122(7):708–12. doi: 10.1001/archotol.1996.01890190006003
81. Seres L, Csaszar J, Borbely L, Voros E. [Donor Site Digital Subtraction Angiography Before Mandible Reconstruction With Free Fibula Transplantation]. *Fogorv Sz* (2001) 94(1):15–20.
82. Yanik B, Bulbul E, Demirpolat G. Variations of the Popliteal Artery Branching With Multidetector CT Angiography. *Surg Radiol Anat* (2015) 37(3):223–30. doi: 10.1007/s00276-014-1346-y
83. Futran ND, Stack BC Jr, Zachariah AP. Ankle-Arm Index as a Screening Examination for Fibula Free Tissue Transfer. *Ann Otol Rhinol Laryngol* (1999) 108(8):777–80. doi: 10.1177/000348949910800811
84. Astarci P, Siciliano S, Verhelst R, Lacroix V, Noirhomme P, Rubay J, et al. Intra-Operative Acute Leg Ischaemia After Free Fibula Flap Harvest for Mandible Reconstruction. *Acta Chir Belg* (2006) 106(4):423–6. doi: 10.1080/00015458.2006.11679921
85. Young DM, Trabulsy PP, Anthony JP. The Need for Preoperative Leg Angiography in Fibula Free Flaps. *J Reconstr Microsurg* (1994) 10(5):283–7; discussion 287-9. doi: 10.1055/s-2007-1006596
86. Oxford L, Ducic Y. Use of Fibula-Free Tissue Transfer With Preoperative 2-Vessel Runoff to the Lower Extremity. *Arch Facial Plast Surg* (2005) 7 (4):261–4; discussion 265. doi: 10.1001/archfaci.7.4.261
87. Lee MK, Blackwell KE, Kim B, Nabili V. Feasibility of Microvascular Head and Neck Reconstruction in the Setting of Calcified Arteriosclerosis of the Vascular Pedicle. *JAMA Facial Plast Surg* (2013) 15(2):135–40. doi: 10.1001/2013.jamafacial.208
88. Kim RY, Burkes JN, Broker HS, Williams FC. Preoperative Vascular Interventions to Improve Donor Leg Perfusion: A Report of Two Fibula Free Flaps Used in Head and Neck Reconstruction. *J Oral Maxillofac Surg* (2019) 77(3):658–63. doi: 10.1016/j.joms.2018.10.017
89. Lorenz RR, Esclamado R. Preoperative Magnetic Resonance Angiography in Fibular-Free Flap Reconstruction of Head and Neck Defects. *Head Neck* (2001) 23(10):844–50. doi: 10.1002/hed.1123
90. Bui DT, Cordeiro PG, Hu QY, Disa JJ, Pusic A, Mehrara BJ. Free Flap Reexploration: Indications, Treatment, and Outcomes in 1193 Free Flaps. *Plast Reconstr Surg* (2007) 119(7):2092–100. doi: 10.1097/01.prs.0000260598.24376.e1
91. Wood NB, Zhao SZ, Zambanini A, Jackson M, Gedroyc W, Thom SA, et al. Curvature and Tortuosity of the Superficial Femoral Artery: A Possible Risk Factor for Peripheral Arterial Disease2006. *J Appl Physiol (1985)* (2006) 101 (5):1412–8. doi: 10.1152/japplphysiol.00051.2006
92. Jones NF, Monstrey S, Gambier BA. Reliability of the Fibular Osteocutaneous Flap for Mandibular Reconstruction: Anatomical and Surgical Confirmation. *Plast Reconstr Surg* (1996) 97(4):707–16; discussion 717-8. doi: 10.1097/00006534-199604000-00003
93. Bähr W. Blood Supply of Small Fibula Segments: An Experimental Study on Human Cadavers. *J Craniomaxillofac Surg* (1998) 26(3):148–52. doi: 10.1016/S1010-5182(98)80004-8
94. Fichter AM, Ritschl LM, Georg R, Kolk A, Kesting MR, Wolff KD, et al. Effect of Segment Length and Number of Osteotomy Sites on Cancellous Bone Perfusion in Free Fibula Flaps. *J Reconstr Microsurg* (2018).
95. Chang EI, Chu CK, Chang EI. Advancements in Imaging Technology for Microvascular Free Tissue Transfer. *J Surg Oncol* (2018) 118(5):729–35. doi: 10.1002/jso.25194

96. Momoh AO, Yu P, Skoracki RJ, Liu S, Feng L, Hanasono MM. A Prospective Cohort Study of Fibula Free Flap Donor-Site Morbidity in 157 Consecutive Patients. *Plast Reconstr Surg* (2011) 128(3):714–20. doi: 10.1097/PRS.0b013e318221dc2a
97. Shindo M, Fong BP, Funk GF, Karnell LH. The Fibula Osteocutaneous Flap in Head and Neck Reconstruction: A Critical Evaluation of Donor Site Morbidity. *Arch Otolaryngol Head Neck Surg* (2000) 126(12):1467–72. doi: 10.1001/archotol.126.12.1467
98. Fang H, Liu F, Sun C, Pang P. Impact of Wound Closure on Fibular Donor-Site Morbidity: A Meta-Analysis. *BMC Surg* (2019) 19(1):81. doi: 10.1186/s12893-019-0545-1
99. Fry AM, Patterson A, Orr RL, Colver GB. Open Wound Healing of the Osseocutaneous Fibula Flap Donor Site. *Br J Oral Maxillofac Surg* (2014) 52 (9):861–3. doi: 10.1016/j.bjoms.2014.05.003
100. Bach CA, Guillere L, Yildiz S, Wagner I, Darmon S, Chabolle F. Comparison of Negative Pressure Wound Therapy and Conventional Dressing Methods for Fibula Free Flap Donor Site Management in Patients With Head and Neck Cancer. *Head Neck* (2016) 38(5):696–9. doi: 10.1002/hed.23952
101. Yu P, Youssef A. Efficacy of the Handheld Doppler in Preoperative Identification of the Cutaneous Perforators in the Anterolateral Thigh Flap. *Plast Reconstr Surg* (2006) 118(4):928–33. doi: 10.1097/01.prs.0000232216.34854.63
102. Islam S, Ansari U, Walton GM. Role of Real-Time Colour-Flow Doppler in Perforator Free Flap Head and Neck Reconstruction. *Br J Oral Maxillofac Surg* (2021) 59(1):111–3. doi: 10.1016/j.bjoms.2020.08.008

Conflict of Interest: The authors declare that the research was conducted in the absence of any commercial or financial relationships that could be construed as a potential conflict of interest.

3.6. Originalarbeit 6: Osseous Union after Mandible Reconstruction with Fibula Free Flap using manually bent Plates vs. Patient-Specific Implants: A Retrospective Analysis of 89 Patients.

Knitschke, M.; Sonnabend, S.; Roller, F; Pons-Kühnemann, J; Schmermund, D.; Streckbein, P; Attia, S.; Howaldt, H.-P.; Böttger, S.;
Osseous Union after Mandible Reconstruction with Fibula Free Flap using manually bent Plates vs. Patient-Specific Implants: A Retrospective Analysis of 89 Patients.
Curr. Oncol. **2022**, *29*(5), 3375-3392;
https://doi.org/10.3390/curroncol29050274 **IF: 3.677**

Zusammenfassung:
Die monozentrische retrospektive Studie untersuchte Unterkieferrekonstruktionen mit mikrovaskulärem Fibulatransplantat. Das konventionelle Osteosyntheseverfahren mit handgebogener Platte (Unilock-2,0 mm) wurde mit dem des patientenspezifischen Implantats (PSI) hinsichtlich der Komplikationsraten verglichen. Dazu wurden Panoramaröntgenaufnahmen (OPG), Computertomographien (CT) oder DVT von Patienten aus dem Zeitraum 01/2005 – 12/2020 ausgewertet, bei denen eine Unterrekonstruktion mit einem Fibulatransplantat durchgeführt worden war. Die Übergangszonen zwischen originärem Unterkiefer und Fibula sowie bei polysegmentalen Rekonstruktionen zwischen den einzelnen Fibulasegmenten wurden auf das Vorliegen einer voll- bzw. unvollständigen Verknöcherung hin untersucht. Es konnten 89 Fälle (Frauen: *n* = 28, 31,5 %; Männer: *n* = 61, 68,5 %), Durchschnittsalter: 58,2 ± 11,3 Jahre, Spanne: 22,8 – 82,7 Jahre) in die Studie eingeschlossen werden (konventionell: *n* = 44 vs. PSI: *n* = 45).
Es wurde eine Rate von 24,7 % unvollständiger Verknöcherungen auf der Basis von 89 Patienten (PSI: 35,6 % vs. konventionell: 13,6 %; *p* = 0,017) bzw. bezogen auf 249 Osteotomiespalten zwischen Mandibula und Fibula sowie intersegmental von 12,4 % (PSI: 19,4 % (*n* = 25) vs. konventionell: 6 (*n* = 5,0 %); *p* < 0,001) ermittelt. Für die Übergänge zwischen einzelnen Fibulasegmenten wurde eine Rate unvollständiger Verknöcherungen von 16,0 % in der PSI-Gruppe bestimmt, während in der konventionellen Gruppe kein Fall einer unvollständigen Verknöcherung für diese Kategorie beobachtet werden konnte. Mit Blick auf die Segmentorientierung ergaben sich kumulative Raten unvollständiger Verknöcherung von 10,6 % proximal und

16,3 % im Bereich des distalen Fibulaendes. Unvollständige Verknöcherungen traten signifikant häufiger in polysegmentalen ($p = 0.041$) und lateralen ($p = 0.016$) - nicht Mittellinien überschreitenden - mit PSI stabilisierten Rekonstruktionen auf. Der verwendete Plattentyp und eine Plattenexposition konnten als unabhängige Risikofaktoren für unvollständige Verknöcherung identifiziert werden. Eine vorangegangene oder begleitende Strahlentherapie hatte keinen Einfluss auf den Status der Verknöcherung. Die Rigidität des PSI ist in Kombination mit der Topografie des Defekts und des daraus resultierenden mechanischen Stimulus als mögliche Hauptursache für die verminderte oder verzögerte Verknöcherung zu bezeichnen. Um den funktionellen Stimulus für die Ossifikation zu erhöhen, sollte ein durchgehendes patientenspezifisches Implantat durch unterbrochene, separate Platten ersetzt werden, damit das physiologische Knochenremodelling gefördert wird.

Ausblick:

Der in einer Voruntersuchung vermutete Einfluss zwischen geringerer Verteilungsdichte der kleinen Gefäße (periostaler Äste) und dem berichteten Auftreten einer gehäuften gestörten Verknöcherungen am distalen Transplantatende konnte in der Untersuchung nicht bestätigt werden. Die mechanische Rigidität des PSI ist in Kombination mit der Topographie des Defekts und des daraus resultierenden mechanischen Stimulus wahrscheinlich der Hauptfaktor für die verminderte Verknöcherung. Weitere klinische Follow-up-Untersuchungen sind notwendig, um den natürlichen „zeitlichen“ Verlauf einer unvollständigen Verknöcherung am Patienten erfassen und das Verknöcherungsmuster beurteilen zu können.

Current Oncology

MDPI

Article

Osseous Union after Mandible Reconstruction with Fibula Free Flap Using Manually Bent Plates vs. Patient-Specific Implants: A Retrospective Analysis of 89 Patients

Michael Knitschke [1,*], Sophia Sonnabend [1], Fritz Christian Roller [2], Jörn Pons-Kühnemann [3], Daniel Schmermund [1], Sameh Attia [1], Philipp Streckbein [1], Hans-Peter Howaldt [1] and Sebastian Böttger [1]

[1] Department of Oral and Maxillofacial Surgery, Justus-Liebig-University, Klinikstrasse 33, 35392 Giessen, Germany; sophia.m.sonnabend@dentist.med.uni-giessen.de (S.S.); daniel.schmermund@uniklinikum-giessen.de (D.S.); sameh.attia@dentist.med.uni-giessen.de (S.A.); philipp.streckbein@uniklinikum-giessen.de (P.S.); hp.howaldt@uniklinikum-giessen.de (H.-P.H.); sebastian.boettger@uniklinikum-giessen.de (S.B.)

[2] Department of Diagnostic and Interventional Radiology and Pediatric Radiology, Justus-Liebig-University, Klinikstrasse 33, 35392 Giessen, Germany; fritz.c.roller@radiol.med.uni-giessen.de

[3] Institute of Medical Informatics, Justus-Liebig-University Giessen, 35392 Giessen, Germany; joern.pons@informatik.med.uni-giessen.de

* Correspondence: michael.knitschke@uniklinikum-giessen.de

Abstract: The aim of this monocentric, retrospective clinical study was to evaluate the status of osseous union in uni- and poly-segmental mandible reconstructions regarding conventional angle-stable manually bent osteosynthesis plates (Unilock 2.0 mm) versus titan laser-melted PSI patient-specific implant's (PSI). The clinical impact of PSI's high stiffness fixation methods on bone healing and regeneration is still not well addressed. The special interest was in evaluating the ossification of junctions between mandible and fibula and between osteotomized fibula free flap (FFF) segments. Panoramic radiograph (OPT), computed tomography (CT) scans, or cone-beam CTs (CBCT) of patients who underwent successful FFF for mandible reconstruction from January 2005 to December 2020 were analyzed. A total number of 89 cases (28 females (31.5%), 61 males (68.5%), mean age 58.2 ± 11.3 years, range: 22.8–82.7 years) fulfilled the chosen inclusion criteria for analysis (conventional: $n = 44$ vs. PSI: $n = 45$). The present study found an overall incomplete ossification (IOU) rate of 24.7% (conventional: 13.6% vs. PSI: 35.6%; $p = 0.017$) for mandible to fibula and intersegmental junctions. Between osteotomized FFF segments, an IOU rate of 16% was found in the PSI-group, while no IOU was recorded in the conventional group ($p = 0.015$). Significant differences were registered for IOU rates in poly-segmental ($p = 0.041$), and lateral ($p = 0.016$) mandibular reconstructions when PSI was used. Multivariate logistic regression analysis identified plate exposure and type of plate used as independent risk factors for IOU. Previous or adjuvant radiotherapy did not impact incomplete osseous union in the evaluated study sample. PSI is more rigid than bent mini-plates and shields functional mechanical stimuli, and is the main reason for increasing the rate of incomplete ossification. To enhance the functional stimulus for ossification it has to be discussed if patient-specific implants can be designed to be thinner, and should be divided into segmental plates. This directs chewing forces through the bone and improves physiological bone remodeling.

Keywords: osseous free flaps; patient-specific implants; plate-related complications; free fibula flap; bone healing; osseous union; ossification

Citation: Knitschke, M.; Sonnabend, S.; Roller, F.; Pons-Kühnemann, J.; Schmermund, D.; Attia, S.; Streckbein, P.; Howaldt, H.-P.; Böttger, S. Osseous Union after Mandible Reconstruction with Fibula Free Flap Using Manually Bent Plates vs. Patient-Specific Implants: A Retrospective Analysis of 89 Patients. *Curr. Oncol.* **2022**, *29*, 3375–3392. https://doi.org/10.3390/curroncol29050274

Received: 11 April 2022
Accepted: 5 May 2022
Published: 6 May 2022

1. Introduction

Jaw reconstruction with a free fibula flap (FFF) has been raised to today's gold standard [1–3]. The FFF offers numerous advantages such as flap harvesting in a two-team approach to decrease operating time and a single or bi-partitioned septo-cutaneous skin

paddle for jaw reconstruction [4]. Jaw reconstruction is in the current focus of research for increasing and reliable results, minimizing complications, and accelerating dental rehabilitation [5–8]. Virtual surgical planning (VSP) is an essential tool for craniomaxillofacial surgery, from demolition to reconstruction, including orthognathic surgery and oral rehabilitation [9]. Studies showed that VSP facilitates the precise positioning of the bone graft, decreases ischemia time and the entire operating time if the neo-mandible was stabilized with a patient-specific implant (PSI) [10–14]. As an alternative for the stabilization of neo-mandible with PSI, conventional manual-bendable mini-plates and reconstruction plates are still available with each specific advantages and disadvantages [15]. Further improvements can be made by varying the plate design, plate thickness and fixation methods (locking or non-locking screws).

Data about osseous union after jaw reconstruction with FFF concerning the stabilization methods, especially the comparison PSI vs. conventional plates, are rare in the literature. Virtual surgical planning in combination with CAD/CAM plates is a widespread and promising technology. However, the clinical impact of PSI high stiffness fixation methods on bone healing and regeneration is still not well addressed. Therefore, the current study is designed to fill the gap.

This investigation aimed to evaluate the status of osseous union in uni- and polysegmental mandible reconstructions regarding conventional angle-stable manually bent osteosynthesis plates (2.0 mm) versus PSIs. Furthermore, plate-related complications should be evaluated. The authors hypothesized that the chosen plate system could not influence the osseous union of the inter-segment gaps and related complications. The study focusses on giving detailed answers to the following questions:

Are there differences in incomplete osseous union rates (IOU) according to the used plate type (conventional vs. PSI)?

How is the distribution and frequency of complete and incomplete osseous union regarding FFF's proximal or distal end?

What is the frequency of plate-related complications (loosening of osteosynthesis, plate exposure)?

2. Material and Methods

2.1. Study Design and Patient Population

The study was conducted as a monocentric, retrospective study. We enrolled the investigation for immediate and delayed mandible reconstructions. Panoramic radiograph (OPT), computed tomography (CT) scans, and cone-beam CTs (CBCT) of patients who underwent successful FFF for jaw reconstruction from January 2005 to December 2020 were reviewed concerning the osseous union of the intersegmental gaps between mandible and fibula and between fibula segments themselves. The stabilization of the neo-mandible was performed either with conventional plates or individual CAD/CAM-planned patient specific plates after virtual surgical planning. Conventional manually bent plates of 2.0 mm thickness (Unilock 2.0 system, DePuy Synthes CMF, Oberdorf, Switzerland) were compared with laser-melted patient-specific CAD/CAM titanium plates (PSI) with layer thicknesses of 2.0 to 2.5 mm (KLS Martin, Tuttlingen, Germany) in terms of reconstructive features, and complication rates (Figure 1). Conventional plates were placed segmentally, while PSI were applied as continuous plates. Only in the PSI group were cutting guides used for flap harvesting at the donor site and for defining resection planes at the recipient site. In the conventional group, free hand osteotomies were performed for the resection and shaping of the fibula segments. Both conventional and patient-specific plates were almost secured with bi-cortical locking screws in the mandibula. The decision to use locking or non-locking screws for plate anchoring to the FFF was done by a surgeon intraoperatively.

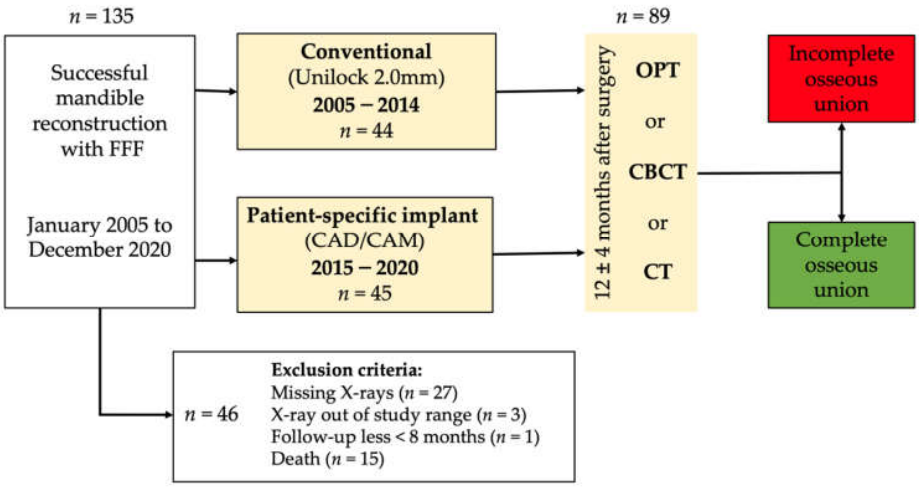

Figure 1. Schematic study design. OPT: Panoramic radiograph; CT: computed tomography; CBCT: cone-beam CT; CAD: computer-aided design; CAM: computer-aided manufacturing; FFF: fibula free flap.

2.2. Inclusion and Exclusion Criteria for Study Subjects

All patients who underwent mandible reconstruction (immediately or delayed) with FFF were enrolled in this study. Inclusion criteria were the presence of OPT, CBCT or CT-scan of the jaw 12 ± 4 months after surgery. The minimum follow-up interval was eight months after surgery. A total of n = 135 successful FFF were performed over the entire study period, and n = 89 patients fulfilled the chosen inclusion criteria. A total number of n = 46 cases were excluded from the analysis because of missing X-rays (n = 27), death (n = 15) and one patient lost to follow-up. Three cases were excluded, because X-ray of the jaws was admitted at least 22 months after surgery and did not match our inclusion criteria.

2.3. Study Parameters and Evaluator Calibration

The patients' medical records were evaluated for the type of used plate system and complications such as exposed osteosynthesis plates (intraoral and/or extraoral) or material loosening (screw loosening). The reconstruction was categorized according to the classification of Brown et al. [16]. For further evaluation, this was simplified and summarized. Classes I(c) to II(c) correspond to unilateral defects and classes III to IV(c) to anterior, bilateral defects.

The following parameters were collected: age at flap transfer, gender, diagnosis, number of used fibula segments, and ossification status of each gap concerning the orientation of the fibular bone (distal/proximal end). Complete (COU) and incomplete osseous union (IOU) rates were calculated in relation to the related reference group (patients, all gaps at risk, or intersegmental only) of all assessable junctions. The available radiographs (OPT, CT, and CBCT-scans) were analyzed independently for the ossification of each gap by two authors (SS and MK). Ossification in OPT was defined as incomplete (IOU) if the interosseous transition zone appeared less than 50% ossified or as complete (COU) if it appeared more than 50% ossified (Figure 2). In CBCT and CT, axial imaging was considered for assessment. IOU was rated if initial callus formation or a persistent gap between segments or subtotal osseous bridging between corresponding bone cortices or marrow were found. COU was rated if the corresponding cortices were joined without significant gaps. Every gap was assessed by two investigators individually. Any disagreements between the two authors were discussed and judged by a third author (FR) who is a radiologist. If a CT or CBCT was available in addition to an OPT, a higher-quality image source

was evaluated for assessment. The evaluated CT scans were initiated within the course of routine follow-up examination. CBCT was mainly performed to plan the insertion of dental implants for oral rehabilitation. Radiological control was performed between the ninth and 14th postoperative months.

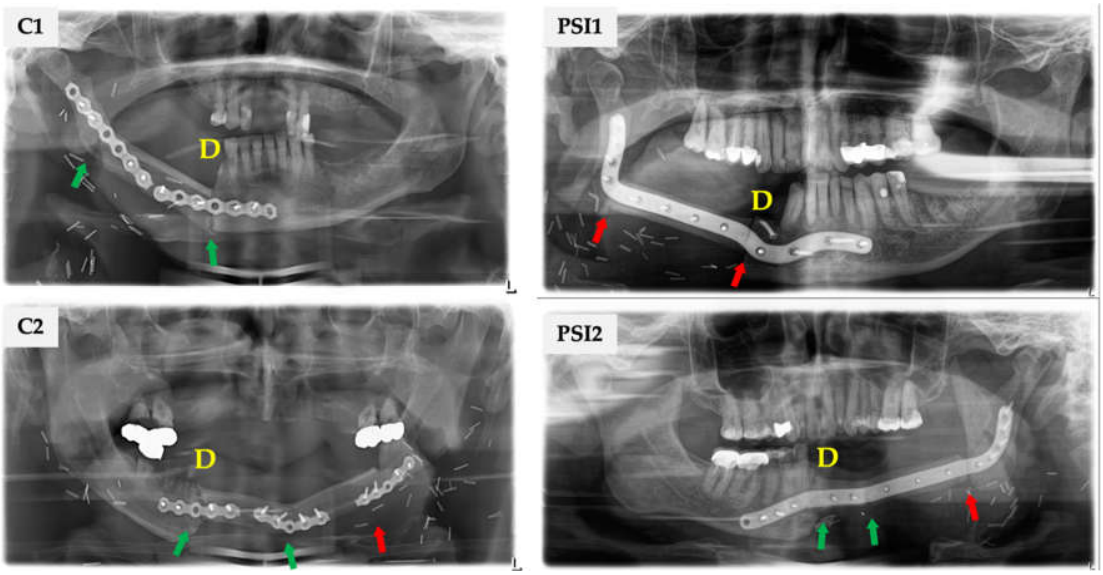

Figure 2. Note: D, distal end of fibula; green arrow: complete osseous union (COU); red arrow: incomplete osseous union (IOU). **C1:** Uni-segmental, lateral reconstruction of mandible. Two distinct mini-plates Unilock 2.0 system (DePuy Synthes CMF®, Raynham, MA, USA) were used for internal fixation. Each junction was addressed with a single plate and locking screws. COU was assessed for the proximal (angle) and distal (anterior corpus) junction. **C2:** Bi-segmental, bilateral mandible reconstruction, and conventional stabilization. IOU of the proximal transition zone at the posterior corpus region, while the distal (canine) and inter-segment junctions showed COU. **PSI1:** Uni-segmental, lateral mandible reconstruction and stabilization with PSI (KLS Martin, Tuttlingen, Germany). IOU of the proximal (angle) and distal (anterior corpus) transition zone. **PSI2:** Bi-segmental, bilateral mandible reconstruction and stabilization with PSI. IOU of the proximal junctions at the posterior corpus region, while the distal (canine) and intersegmental junctions show COU.

2.4. Statistical Analyses

Continuous variables were reported using mean, standard deviation, median and interquartile interval (Q1, Q3). Categorical data were recorded as frequencies and percentages. Binary logistic regression statistics was performed. The bivariate analysis included Student's t-test to compare continuous quantitative variables between both groups (Conventional vs. PSI) after verifying normality (Shapiro–Wilk-test). Chi-square and Fisher tests were performed for categorical variables. Cohen's Kappa (κ) statistics was calculated to assess the interobserver reliability between SS and MK. $P < 0.05$ was defined as statistically significant. The statistical analysis was performed in collaboration with the Institute of Medical Informatics of Justus Liebig University Giessen using SPSS software version 28 (SPSS Inc., Chicago, IL, USA).

2.5. Ethics Statement/Confirmation of Patients' Permission

The local Ethics Committee of Justus-Liebig University Giessen, Faculty of Medicine, approved the study (AZ35/20 on 25 May 2020). Patients' permission/consent was not necessary for this retrospective study. The patients consented that their X-ray images could be used anonymously in the publication.

3. Results

A total number of $n = 89$ cases (28 females (31.5%), 61 males (68.5%), mean age 58.2 ± 11.3 years, range: 22.8–82.7 years) fulfilled the inclusion criteria for analysis. They were classified in non-VSP, conventional ($n = 44$) and digitally planned PSI ($n = 45$) groups. The parameters age and time of image acquisition ('Image osseous union') were verified for normal distribution for both osteosynthesis groups. No statistically significant differences were found. The study sample structure was almost similar in both groups (age, gender, ASA-Score, BMI). The detailed demographic parameters and results are summarized in Table 1.

Table 1. Details of the study sample. Conventional osteosynthesis with Unilock 2.0 system (DePuy Synthes CMF, Oberdorf, Switzerland), CAD/CAM-osteosynthesis with PSI (KLS Martin, Tuttlingen, Germany). IQI: Interquartile interval; MRONJ: Medication-related osteonecrosis of the jaw; PSI: patient-specific implant; Q: quartile; SD: standard deviation.

	Conventional (Unilock 2.0) ($n = 44$)	**CAD/CAM (PSI) ($n = 45$)**	***p*-Value**
Age (years), mean ± SD	58.54 ± 10.46	59.23 ± 12.23	0.777
Image osseous union (months), mean ± SD	11.25 ± 2.52	11.0 ± 2.90	0.665
Follow-up (months), median; IQI (Q1, Q3)	88.0 (35.75, 125.5)	19.0 (12.5, 34.5)	0.001
Gender, *n* (%)			
Male	31 (70.4)	30 (66.7)	
Female	13 (29.6)	15 (33.3)	0.699
Image type			
OPT	29 (65.9)	23 (51.1)	
CBCT	2 (4.5)	2 (4.4)	
CT	13 (29.5)	20 (44.4)	0.321
Pathology, *n* (%)			
Benign tumor	1 (2.3)	5 (11.1)	
Malignant tumor	41 (93.1)	36 (80.0)	
MRONJ	-	1 (2.2)	
Osteoradionecrosis	1 (2.3)	1 (2.2)	
Osteomyelitis	1 (2.3)	2 (4.4)	0.366
ASA, *n* (%)			
1	4 (9.1)	1 (2.2)	
2	22 (50.0)	22 (48.9)	
3	18 (40.9)	21 (46.7)	
4	-	1 (2.2)	0.389
BMI (kg/m^2), *n* (%)			
<18	3 (6.8)	3 (6.7)	
18 ≥ 25	24 (54.5)	22 (48.9)	
25 ≥ 30	12 (27.3)	14 (31.1)	
30 ≥ 35	3 (6.8)	5 (11.1)	
>35	2 (4.5)	1 (2.2)	0.901
Tobacco abuses, *n* (%)	32 (72.7)	29 (64.4)	0.495
Alcohol abuses, *n* (%)	16 (36.4)	21 (46.7)	0.392
Time of reconstruction, *n* (%)			
Immediate	42 (95.5)	39 (86.7)	
Delayed	2 (4.5)	6 (13.3)	0.266
Brown Classification, *n* (%)			
I(c)	16 (36.4)	10 (22.2)	
II(c)	12 (27.3)	16 (35.6)	

III	16 (36.4)	16 (35.6)	
IV(c)	-	3 (6.7)	0.175
Number of segments			
1	19 (43.2)	8 (17.8)	
2	19 (43.2)	21 (46.7)	
3	6 (13.6)	16 (35.6)	0.010

The main reasons for mandible reconstruction were benign and malign tumors infiltrating the bone (conventional: 95.4% vs. PSI: 91.1%). Medication-related osteonecrosis of the jaw (MRONJ), osteoradionecrosis, and osteomyelitis contributed 4.6% vs. 8.8% to the analyzed groups. The main reconstruction method was immediate (95.5% vs. 86.7%). In the PSI group, 77.8% of defects with classified at least as class II(c) or higher according to the classification of Brown et al. [16], whereas in the conventional group only 63.6% showed a classification of at least II(c). Therefore, a trend for larger and more complex reconstructions can be assumed in the PSI group. Nineteen patients (43.2%) in the conventional group and eight (17.8%) in the PSI group underwent mono-segmental reconstruction. Poly-segmental mandibular reconstruction accounted for 82.2% of the PSI group and 56.8% in the conventional group. Regarding general conditions of the patients there were 61 cases of chronic tobacco abuse (conventional: 72.7% vs. PSI: 64.4%; $p = 0.495$) and 35 of pathologic alcohol usage (conventional: 36.4% vs. PSI: 46.7%; $p = 0.392$).

Complications of the donor and recipient sites are presented in Table 2. In total, there were $n = 21$ cases of plate exposure (conventional: 22.7% vs. PSI: 24.4%; $p = 1.000$) and eleven plate related fixation failures (conventional: 9.1% vs. PSI: 15.6%; $p = 0.522$). Preoperative radiotherapy (RT) occurred only in exceptional cases (conventional: 11.4% vs. PSI: 13.3%) while postoperative RT was frequently used (conventional: 34.1% vs. PSI: 53.3%). The rate of non-irradiated patients has decreased (conventional: 54.5% vs. PSI: 33.3%).

Table 2. Complication rates of the conventional vs. PSI groups. (FFF: free fibula flap; F: fibula; M: mandibula; PSI: patient-specific implant); IOU: incomplete osseous union; COU: complete osseous union; OU: osseous union. Note: In CAD/CAM-PSI group only $n = 79$ junctions in $n = 45$ patients were assessed, because eleven gaps were not interpretable by artifacts of the plate ($n = 1$) and free ending without any contact to the origin mandible ($n = 10$).

	Conventional (Unilock 2.0) (*n* = 44)	**CAD/CAM (PSI) (*n* = 45)**	***p*-Value**
Plate related fixation failures, *n* (%)	4 (9.1)	7 (15.6)	0.522
Plate exposure, *n* (%)	10 (22.7)	11 (24.4)	1.000
Radiotherapy, *n* (%)			
Preoperative	5 (11.4)	6 (13.3)	
Postoperative	15 (34.1)	24 (53.3)	
None	24 (54.5)	15 (33.3)	0.121
OU: M ↔ F and F ↔ F, *n* (%)	44	45	
COU	38 (86.4)	29 (64.6)	
IOU	6 (13.6)	16 (35.6)	0.017
OU: M ↔ F and F ↔ F, *n* = all junctions (%)	120	129	
COU	114 (95.0)	104 (80.6)	
IOU	6 (5.0)	25 (19.4)	<0.001
OU: M ↔ F, *n* = only proximal and distal junctions, (%)	88	79	

COU	82 (93.2)	62 (78.5)	
IOU	6 (6.8)	17 (21.5)	0.006
OU: F ↔ F, *n* = only intersegmental junctions, (%)	32	50	
COU	32 (100.0)	42 (84.0)	
IOU	0	8 (16.0)	0.015
OU uni-segmental reconstruction, *n* (%)	19	8	
COU	16 (84.2)	5 (62.5)	
IOU	3 (15.8)	3 (37.5)	0.215
OU poly-segmental reconstruction, *n* (%)	25	37	
COU	22 (88.0)	24 (64.9)	
IOU	3 (12.0)	13 (35.1)	0.041
OU lateral reconstruction, *n* (%)	28	25	
COU	24 (85.7)	14 (56.0)	
IOU	4 (14.3)	11 (44.0)	0.016
OU anterior reconstruction, *n* (%)	16	20	
COU	14 (87.5)	15 (75.0)	
IOU	2 (12.5)	5 (25.0)	0.346

Inter-observer reliability was obtained for the graduation of osseous union. The κ value of 0.934 indicates a good match between the observers. In total, IOU of at least one osteotomy junction between mandibula to fibula or intersegmental in the study sample was found in 35.6% (n = 16 out of 45) in the PSI group and in 13.6% (n = 6 out of 44) in the conventional group (Table 2). The difference was statistically significant (p = 0.017). The difference becomes more apparent when OU was referred to all junctions at risk (conventional: n = 6; 5.0% vs. PSI: n = 25; 19.4%; $p < 0.001$). In detail, there were n = 23 IOU out of assessable n = 167 appositions between the native mandibula and the free flap bone, indicating an overall IOU rate of 13.1% (conventional: n = 6; 6.8% vs. PSI: n = 17; 21.5%; p = 0.006). IOU was recorded at the distal junction in n = 13 (conventional: n = 5 vs. PSI: n = 8), at the proximal junction in n = 10 patients (conventional: n = 1 vs. PSI: n = 9). Regarding the intersegmental junctions eight IOU were found in the PSI group while no IOU could be found in the conventional group (conventional: 0/32 vs. PSI: 8/50; p = 0.015). Thus, an overall rate of 16.0% IOU was found. Only six patients had IOU of more than one junction in the PSI group.

Ossification status was assessed for the distal and proximal inter-segment junctions and assigned to regions of the mandible (Table 3). The evaluation revealed cumulative rates of IOU at the proximal end of 10.6% (PSI: 19.5% vs. conventional: 2.2%; p = 0.009) and the distal end of 16.3% (22.2% vs. 11.4%; p = 0.190). In the conventional group only one proximal and five distal cases (11.4%) were recorded. IOU was found to be more frequent at fibula's distal end. Finally, no preferred region was found in which IOU was observed more frequently. Uni- and poly-segmental mandibular reconstructions were analyzed for the status of osseous union (Table 3). Statistically significant differences for the presence of IOU were found in poly-segmental reconstructions with PSI (p = 0.041). The comparison of lateral and anterior reconstructions showed that IOU was found more often after lateral reconstructions with PSI (p = 0.016). The relation between the risk factor variables and binary outcomes was assessed by a generalized linear model for binary logistic regression (Table 4). When PSI was used as plate system (OR = 3.494; 95%-CI: 1.216–10.040; p = 0.017), plate exposure (OR = 3.173; 95%-CI: 1.105–9.110; p = 0.027) and screw loosening (OR = 4.650; 95%-CI: 1.257–17.197; p = 0.014) were identified as significant risk factors. Multivariate analysis revealed that only the variables plate system (OR = 3.682; 95%-CI: 1.236–10.966; p = 0.019) and plate exposure (OR = 3.389; 95%-CI: 1.118–10.275; p = 0.031)

are independent risk parameters for incomplete osseous union (Table *5*). The model is significant in the Omnibus-Test ($p = 0.05$; Nagelkerkes $R^2 = 0.166$). The data were not able to distinguish the reasons for screw loosing (fixation problems vs. osteoradionecrosis). The parameter screw loosing was excluded from multivariate analysis.

Table 3. Overall incomplete (IOU) versus complete osseous union (COU) was categorized concerning the used plate system and according to the distal or proximal end of the FFF. Co: Condyle; Sco: subcondyle; A: angle; Pc: posterior corpus mandibulae; Ac: anterior corpus mandibulae; C: canine; COU: complete osseous union; IOU: incomplete osseous union; PSI: patient-specific implant.

	Co	Sco	A	Pc	Ac	C	All	IOU-Rate	*p*-Value
Distal junction							(89) 80 *	16.3% *	
COU, conventional	-	5	4	12	10	8	39	-	
IOU, conventional	-	1	1	-	1	2	5	11.4%	
COU, PSI	(9) 0 *	10	3	9	2	4	(37) 28 *	-	
IOU, PSI	-	2	1	1	2	1	8	22.2% *	0.190
Proximal junction							(87) 85 ‡	10.6% ‡	
COU, conventional	-	5	9	15	6	8	43	-	
IOU, conventional	-	1	-	-	-	-	1	2.2%	
COU, PSI	-	(2) 1 ‡	5	9	7	11	(34) 33 ‡	-	
IOU, PSI	-	1	2	(2) 1 ‡	2	2	(9) 8 ‡	19.5%	0.009

Note: * When resection of the mandible including the condyle was done, the fibula's distal end was shaped into a neo-condyle. Therefore, no osseous union can be expected for this region and $n = 9$ were excluded from the statistical analysis. ‡ Proximal region in PSI-group was in two cases not interpretable, because of artifacts by the plate ($n = 1$) and free ending without any contact to the origin mandible ($n = 1$).

Table 4. Univariate analysis of patient, surgery, and complication-related parameters on the incomplete osseous union. 95%-CI: 95%-confidence interval; OR: Odds ratio; PSI: patient-specific implant; SD: standard deviation; WHD: wound healing disorder.

		Incomplete Osseous Union			
		Yes, *n* (%)	**No, *n* (%)**	***p*-Value**	**OR [95%-CI]**
Patient-related parameter					
Age, years (Mean ± SD)		58.91 ± 12.70	58.79 ± 10.92	0.967	1.001 [0.959; 1.045]
Gender	Male	14 (63.6)	47 (70.1)	0.568	0.745 [0.270; 2.053]
	Female	8 (36.4)	20 (29.9)		
Tobacco	Yes	16 (72.7	45 (67.2)	0.626	1.304 [0.448; 3.793]
	No	6 (27.3)	22 (32.8)		
Alcohol	Yes	9 (40.9)	28 (41.8)	0.942	0.964 [0.362; 2.566]
	No	13 (59.1)	39 (58.2)		
ASA-Score ≥ 3	Yes	8 (36.4)	31 (46.3)	0.417	1.958 [0.428; 8.959]
	No	14 (63.6)	36 (53.7)		
BMI (Mean ± SD)		24.81 ± 3.71	24.54 ± 4.90	0.811	1.013 [0.913; 1.124]
Surgery related parameter					
Operation duration, minutes (Mean ± SD)		533 ± 132	512 ± 91	0.395	1.002 [0.997; 1.007]
Reconstruction	Immediate	19 (86.4)	62 (92.5)	0.380	1.958 [0.428; 8.959]
	Delayed	3 (13.6)	5 (7.5)		
Plate system	Conventional	6 (27.3)	38 (56.7)	0.017	3.494 [1.216; 10.040]
	PSI	16 (72.7)	29 (43.3)		
Fibular segments	1	6 (27.3)	21 (31.3)	0.800	0.919 [0.479; 1.765]
	2	15 (54.5)	28 (41.8)		

Reconstruction site	3	4 (18.2)	18 (26.9)	0.406	0.650 [0234; 1.803]
	Unilateral	15 (68.2)	39 (58.2)		
	Bilateral	7 (31.8)	28 (41.8)		
Radiotherapy	None	8 (36.4)	31 (46.3)	0.432	1.231 [0.733; 2.068]
	Preoperative	3 (13.6)	8 (11.9)		
	Postoperative	11 (50.0)	28 (41.8)		
Complication					
Plate exposure	Yes	9 (40.9)	12 (17.9)	0.027	3.173 [1.105; 9.110]
	No	13 (59.1)	55 (82.1)		
Plate related complication (screw loosening)	Yes	6 (27.3)	5 (7.5)	0.014	4.650 [1.257; 17.197]
	No	16 (72.7)	62 (92.5)		

Table 5. Multivariate analysis of significant risk factors on the incomplete osseous union in univariate binary logistic regression.

Parameter	*p*-Value	OR	95% CI	
Plate system	0.019	3.682	1.236	10.966
Plate exposure	0.031	3.389	1.118	10.275

4. Discussion

Virtual surgical planning (VSP) in combination with custom-made osteosynthesis (patient-specific implants, PSI) has become popular in jaw reconstruction. VSP allows for more extensive, complex and precise reconstructions than the conventional freehand method [17–19]. VSP was described for ideal placement of miniplates on a virtual 3D model and adapting these plates in further step on a printed model. The specific advantage of this approach requires a minimum of money and time [20]. However, CAD/CAM implants allow highly precise mono- and poly-segmental shaping and molding of a free fibula flap for ideal jaw reconstruction [21–23]. Increased precision of mandibula and maxilla reconstruction, shortened surgery and ischemia time, reduced length of hospital stay, and improved patient outcomes were all common advantages in maxillofacial reconstruction [24–29]. However, there are disadvantages concerning the VSP method with PSI such as the prolonged time to surgery [30] and abnormalities in the ossification of the transition zone between the fibula and mandibular stumps. Yang et al. compared $n = 33$ patients (conventional: $n = 16$, PSI: $n = 17$) and found improved accuracy of reconstruction in terms of bilateral mandibular angles and bone grafts, but the accuracy of the osteotomy was similar in both groups. There was no change in intraoperative blood loss, total operation time, or hospital stay [31]. More plate exposure and a higher rate of incomplete osseous union was found for patient-specific plates [32]. Incomplete osseous union (IOU) was described to be more prevalent at the junction zone of the distal fibula segment and in poly-segmental reconstructions [33,34].

4.1. Are There Differences in Incomplete Osseous Union (IOU) Rates According to the Used Plate Type (Conventional vs. PSI)?

IOU was found between fibula and mandible stumps and between fibula segments in both osteosynthesis groups (Table 2). The present study revealed an overall IOU rate of 24.7%, which is well comparable to the literature with reported rates between 5% and 45.9% [32,35–40]. The study results show in detail a higher IOU rate related to all junctions at risk and referred to the number of patients in the PSI group of 35.6% in comparison to the conventional group with 13.6% ($p = 0.017$). Rendenbach et al. found subtotal osseous union rates in their study sample ($n = 128$) after mandible reconstruction with a rate of 45.9% for PSI in comparison to conventional plating with 33.0% [32].

Significant differences were registered in the present study for IOU rates in polysegmental ($p = 0.041$), and in lateral ($p = 0.016$) mandibular reconstructions when PSI instead of conventional plate was used. A shielding of mechanical forces due to robust plate systems reduces inter-osteotomy micromotions below a critical functional minimum for bone healing stimulation [41–44]. In patients with reduced dentition or without postoperative occlusion, and therefore minimal functional loading on the bone, a higher rate of IOU has been reported [32,41]. This underlines the importance of mechanical factors such as strain, pressure, stability, stimulation for bone healing [45]. Thus, one reason for the higher IOU rate in the PSI group is attributed to the increased plate rigidity of CAD/CAM plates [46]. Another difference is the functional force transmission into the bone in the systems used. Conventional plates were placed segmentally, so that each junction (mandible-fibula and fibula-fibula) was addressed with a separate osteosynthesis. The applied masticatory force is thus directed through each link of the "bone chain" and contributes to functional stimulation. In PSI stabilization, the bone segments are adapted to a single plate and introduced forces are absorbed by the continuous load-bearing patient-specific plate. Therefore, the functional stimulus on each bone segment must be lower than in segmentally joined jaw reconstruction. Kreutzer et al. have proposed to replace the PSIs with patient-specific mini-plates [47], and presented recently a feasibility study with $n = 8$ patients [48]. According to their findings and limitations of the small sample size due the feasibility study they concluded, that mandible reconstruction with FFF using patient-specific 3D-printed miniplates is possible and related to good precision, bone healing, and distant soft tissue problems [48]. Alternatively, the planning of predefined separation points in the PSI, which can be divided after the neojaw's shaping, should be considered. This will increase the force transmission through the "bone chain", enhances functional stimuli for bone healing, and simplifies later intraoral plate removal if necessary.

Compared to conventional plating methods, the bone-to-plate contact area is increased in PSIs [46]. Due to the ideal bone surface congruent shape of the PSI, the blood circulation of the periosteum can be impaired by compression [49–51]. As a result, bone resorption and screw loosening can occur if non-locking screws are used [52]. In addition to PSI's technical and biomechanical aspects, additional guides for jaw resection and transplant molding should also be mentioned as a reason for IOU as a result of periosteal trauma and decreased perfusion [53,54]. After VSP for jaw reconstruction, a patient-specific plate had to be applied, either 3-dimensional printed CAD/CAM [17,18] or universal, reusable saw guides [55,56] for resection and donor-site were required. The soft-tissue at the resection site and, in particular, the periosteum of the donor-site disturbs the correct fit of the individual cutting and drill guides. This implicates inaccuracy concerning resection planes and miter cuts. For FFF harvesting it is recommended to leave a preserving muscle cuff of 1 to 2 mm thickness during flap dissection around fibular bone [57], because of the split osseous blood supply of the fibula bone in endosteal and periosteal portions [2,58]. The endosteal blood supply is responsible for over two-thirds of cortical bone blood flow and is the leading player for blood supply in tubular bones [59]. The interruption of the periosteum or endosteum's integrity appears to impair bone healing in both experimental and clinical studies, but disturbance of either one of these structures does not affect total fracture healing [54,60,61]. Numerous animal studies have shown that the healing potential of cortical bone is dependent on endosteal and periosteal blood flow, which can be impaired due to osteosynthesis [53,54].

4.2. How Is the Distribution and Frequency of Complete and Incomplete Osseous Union Regarding FFF's Proximal or Distal End?

IOU was found to be slightly more frequent at fibula's distal end with a rate of 16.3% (PSI: 22.2% vs. conventional: 11.4%; $p = 0.190$) than proximal 10.6% (19.5% vs. 2.2%; $p = 0.009$). A comparison of the IOU presence concerning the defined transition zones shows no preferred region in which IOU has been found more frequently.

A retrospective study on $n = 104$ mandibular or maxillary resections and subsequent reconstructions with osseous(-cutaneous) free flaps revealed a partial union or non-union rate of 47%. The authors observed significantly higher COU rates between intersegmental junctions (fibula to fibula) than the native mandible [38]. They reported that it was unlikely to detect COU if the intersegmental gap width was broader than 1 mm, and recommended precise shaping to reduce intersegmental gap width to a minimum [38]. The current study observed an IOU rate of 16.0% ($n = 8$) for intersegmental junctions in the PSI group ($n = 8$ out of 50), and no case has been detected in the conventional plating group ($n = 0$ out of 32). This statistically significant ($p = 0.015$) observation must be critically evaluated because of the PSI group's higher number of poly-segmental reconstructions compared to conventional plates (Table 1).

Bone healing and intersegmental osseous union can be recorded two months after surgery, and structural changes in X-ray become visible, and is dependent on functional stimuli, stress, and shearing [62]. While primary bone healing is dependent on gap width up to 1 mm, broader gaps can heal by secondary bone healing due to callous formation, completing the connection of the two bone segments [63]. Regardless of the accuracy of VSP and individual cutting guides, it is presumable that in the majority of junctions secondary bone healing will occur. Greksa et al. highlighted the impact of periosteal and endosteal microcirculation in bone healing in a case of non-union of the tibia bone after osteosynthesis [64]. When micro-motions occur between the fractured sections of bones covered by the periosteum, endochondral bone repair is the predominant way of bone healing in long bones [51,65]. The importance of the endosteum in bone healing is commonly underestimated due to the periosteum's essential function [66,67]. The authors hypothesized that the combination of impaired endosteal and periosteal circulation after (multiple) segmentation and decreased mechanical stimulation through the PSI contributes to the higher IOU rates in poly-segmental reconstructions. Visual control for bleeding from the bone marrow is routinely performed after osteotomy of each fibula segment. Clinical experience shows that a significant bleeding does not occur in all cases. What impact this observation has on the osseous union of the junctions remains still unclear.

Following fractures and osteotomies, the size of the interfragmentary gap changes the mechanical environment. Therefore, increasing gap size results in significantly reduced strength and stiffness in mechanical and histological outcomes [62,68,69]. Successful segmental mandible reconstruction with FFF was also reported when mini-plates were used [46,70], but it is recommended not to use them if a radiation therapy is planned [13,71]. *Robey* et al. reviewed $n = 117$ patients after mandible reconstruction with FFF, and compared complication rates when using mini-plates ($n = 86$) and reconstruction plates ($n = 31$). They found a decreased incidence of osteoradionecrosis in the mini-plate group (5% vs. 38%; $p = 0.02$) [43]. This finding must be interpreted cautiously because of the small sample size. However, for PSI there is a leak of data regarding its influence on the incidence of osteoradionecrosis. Shimamoto et al. assessed scatter doses for various dental metals and titanium of the buccal mucosa and different types of radiation therapy in an experimental setting. Except for gold, there were no variations in the scatter doses caused by specific dental metals in the direction of the buccal mucosa in 3D conformal radiation therapy and in intensity-modulated radiation therapy [72].

FFF dissection, multiple osteotomies, and mechanical trauma decrease the endosteal blood flow in the distal segment [73]. Both segmental osteotomies and fixation osteosynthesis plates or screws reduce blood supply to the most distal fibula segment, according to animal investigations on a vascularized pig fibula [73,74]. Segment length and the frequency of proximal osteotomies were associated to distal segment bone perfusion. Longer segments and fewer osteotomies were associated with higher perfusion [33]. These results are in accordance with the observation of a higher complication and non-union rate in the distal segment in poly-segmental mandible reconstructions [34]. Therefore, it is recommended to reduce the number of osteotomies to a minimum, to ensure segmental periosteal circulation and to decrease operating time [75,76]. A human cadaver experiment was

conducted to assess the critical segment length. They determined that fibula segments can be revascularized in the recipient bed if they are at least 2 cm long. It can work even in shorter segments, but only partially. Segments smaller than 0.5 cm in length are likely to fail to revascularize and become non-vascularized grafts. Thus, they are recommended not to be used in infected areas or have been subjected to radiation treatment or trauma [77]. During VSP, awareness is necessary to prevent small bone segments to ensure sufficient bone segment perfusion to avoid partial or total flap failure [78]. According to our experience, segments length should not be less than 3.0 cm.

Our results confirmed the findings of other studies [32–34], and found only a slightly higher rate of the incomplete osseous union of the distal compared to the proximal gap regarding the entire study population.

4.3. What Is the Frequency of Plate-Related Complications (Loosening of Osteosynthesis, Plate Exposure)?

Plate exposure has been recorded in our sample with 23.6% (PSI: 24.4%. vs. conventional: 22.7%), which is almost similar to the literature (PSI vs. conventional: 29.7% vs. 18.7%) [32]. In our study, despite using a composite FFF, conventional and CAD/CAM plates, exposure occurred in all cases intraorally at the canine region around the junction zone of two fibula segments or at the junction fibula to mandible. Dehiscence occurred between the skin paddle and the oral mucosa of the vestibulum or planum buccale. One PSI was exposed through the skin near to the mandible's angle (Table 2).

Infection, non-union, fistulae, and plate exposure are among the complications linked with mandibulotomies [79]. Some authors argue that bone incision and fixation procedures are likely encouraging factors, while others believe that radiation is involved. Others found no evidence for a single factor, radiation, or fixation type, contributing to a non-union, and recommended careful surgical technique [80]. Plate exposure rates are reported in literature after segmental mandible reconstruction ranging from 4% to 46% [81]. Infection at the surgical site is an independent risk factor for plate exposure [81]. Yao et al. found that postoperative surgical site infection, kind of mandibulectomy defects, and plate profile/thickness were associated with plate exposure in their univariable analysis [81]. In current research concerning removal of PSI following segmental mandible reconstruction, Kreutzer et al. observed that using a FFF septo-cutaneous intraoral skin paddle did not reduce the complication rate resulting in plate removal. They emphasized reviewing critically the indication of a skin paddle to improve donor-side morbidity and subsequent peri-implant soft tissue situation. [47]. Furthermore, the application of resection guides after VSP on the recipient-site requires more extensive hard and soft tissue exposure, and therefore an increasing wound area. It is presumed that a more extended bone exposure is correlated with a higher rate of local infections and plate exposure in the early postoperative course [81].

Plate-related fixation failures were assessed in the present study with 12.3% (PSI: 15.6%. vs. conventional: 9.1%), which is slightly higher than comparable results in the literature (PSI vs. conventional: 8.1% vs. 6.6%) [32]. The PSI group's higher rate of adjuvant radiation (53.3% vs. 34.1%) has certainly an influence on fixation failure rates but without significance. Based on our clinical experience radiation therapy increases the complications rate postoperatively. This can be confirmed and displayed on irradiated FFF in our study subjects with a screw loosening rate of 42.8% in the PSI group (n = 3 out of 7) and 25% in the conventional osteosynthesis group (n = 1 out of 4). In two PSI cases, osteoradionecrosis of the FFF occurred, which was reasonable for screw loosening. However, no statistically significant relation could be found regarding screw loosening and radiotherapy, presumably because of the limited number of affected patients. Plate-related problems, however, are nonetheless prevalent when utilizing patient-specific reconstruction plates and may not occur only in patients with significant risk factors such as radiation or poly-segmental reconstructions [48].

Without doubt, technical innovations in smaller plate profiles of reconstructions plates increases biocompatibility and decreases the risk for plate exposure [82,83]. Avoiding bone edges and ridges can help prevent plate exposure. Scarring soft tissue retraction can only be controlled to a limited extent. Therefore, special attention must be paid to the canine region in anterior, poly-segmental reconstructions to design smooth intersegmental transition sections during VSP to decrease the risk of plate exposure. Reducing neomandible's chin prominence in combination with a skin paddle can contribute to a sufficient soft tissue coverage and decreases in our experience the risk of plate exposure. For the beneficial use of a skin paddle different opinions can be found in the literature [47].

Likhterov et al. report their routine fixation procedure with 2.0 or 2.4 locking plates and up to four bi-cortical screws for attaching the plate to the native mandible and one to two mono-cortical screws securing the flap segments to the plate [71]. For PSI fixation, mono-cortical locking [47] or non-locking screws [32] for the fibula flap segment and bi-cortical locking screws to the mandible were described. The advantage of using locking screws for PSI and graft fixation was emphasized in a finite element analysis of a three-segment anterior mandibular reconstruction [49].

In summary, the status of ossification in terms of radiological findings was significantly more frequently assessed as incomplete at the junction between mandible and FFF and between fibula segments in the PSI group compared to the conventional group. These significant differences also remained when comparing the localization (anterior vs. lateral) and the number of segments (uni- vs. poly-segmental) used. Therefore, together with the discussed literature, it can be assumed that the properties of PSI contribute to incomplete ossification.

5. Implications

Further studies are necessary to improve PSI's design and hardware parameters (plate extension, thickness, stiffness, locking vs. non-locking fixation to jaw and graft segments). While bone healing after fracture is well described in the literature, there is a knowledge gap about bone healing of microvascular osseous flaps regarding time interval for the complete osseous union. Additional follow-up trails can be useful to close the data gap regarding the clinical impact of incomplete osseous and its influence on dental rehabilitation with implants.

6. Limitations

Limitations of the present study need to be addressed. First, despite the well-known problems of retrospective studies, they allow the covering of a long period of time. Over the study period of 15 years, a core team of four, senior, experienced oral and maxillofacial oncologic and reconstructive surgeons performed immediate jaw reconstructions. Two surgeons overlooked the whole observation time, and the other two observed eight years.

Second, the study focuses on a single image taken around the first year after surgery, and therefore the progression of subtotal ossifications of the free flap segment remains unclear. Although the assessment and classification of ossification were performed independently by two investigators, it was not blinded and was predominantly based on OPTs. Standardized CBCT or CT scans for comparison were not available in all cases. Third, the individual progress of IOU and its clinical impact is left unclear in every single patient's case. Follow-up evaluation is required to conclude IOU's impact on necessary surgical treatment and dental rehabilitation.

7. Conclusions

Patient-specific implants allow highly accurate poly-segmental, and therefore more complex shaping and molding of a fibula free flap. Incomplete ossification was observed more frequently in the PSI group than in the conventional group. Plate exposure and used plate type were identified as independent risk factors for incomplete osseous union in

logistic regression analysis. Previous or adjuvant radiotherapy did not impact incomplete osseous union in the evaluated study sample. This finding should be interpreted carefully as the evidence coming from a limited number of affected patients. Further optimization of the PSI system is required to improve the fibula-jaw bone healing and lowering post-operative complications. To enhance the functional stimulus for ossification it has to be discussed if patient-specific implants can be designed to be thinner, and should be divided into segmental plates. This directs chewing forces through the bone and improves physiological bone remodeling.

Author Contributions: Conceptualization, M.K. and F.R.; Data curation, M.K. and S.S.; Formal analysis, J.P.-K.; Investigation, M.K., S.S. and S.A.; Methodology, M.K. and S.A.; Project administration, D.S., P.S.; Resources, H.-P.H.; Supervision, H.-P.H. and S.B.; Validation, S.A.; Writing—original draft, M.K.; Writing—review & editing, D.S., F.R., J.P.-K., S.S., S.A., P.S., H.-P.H. and S.B. All authors have read and agreed to the published version of the manuscript.

Funding: None of the authors has a financial interest to declare in relation to the content of this article. No funding was received for this work.

Institutional Review Board Statement: The study was approved by the local Ethics Committee (AZ35/20, approval 25 May 2020). Patients' permission/consent was not necessary for this retrospective study.

Informed Consent Statement: Patient consent was waived due to this retrospective study.

Data Availability Statement: The data presented in this study are available on request from the corresponding author.

Acknowledgments: The authors are grateful for the patients' consent for presented X-rays. This publication forms part of the dental doctoral thesis of the second author (S.S.).

Conflicts of Interest: We have no conflicts of interest.

Abbreviations

A: angle; Ac, anterior corpus mandibulae; BMI, body mass index; C, canine; Co, condyle; COU, complete osseous union; F, fibula; FFF, fibula free flap; IOU, incomplete osseous union; IQI, Interquartile interval; M, mandibula; MRONJ, medication-related osteonecrosis of the jaw; OU, osseous union; Pc, posterior corpus mandibulae; PSI, patient-specific implant; Q, quartile; Sco, subcondyle; SD, standard deviation; VSP, virtual surgical planning.

References

1. Taylor, G.I.; Miller, G.D.; Ham, F.J. The free vascularized bone graft. A clinical extension of microvascular techniques. *Plast. Reconstr. Surg.* **1975**, *55*, 533–544. https://doi.org/10.1097/00006534-197505000-00002.
2. Wei, F.C.; Chen, H.C.; Chuang, C.C.; Noordhoff, M.S. Fibular osteoseptocutaneous flap: Anatomic study and clinical application. *Plast. Reconstr. Surg.* **1986**, *78*, 191–200. https://doi.org/10.1097/00006534-198608000-00008.
3. Kansy, K.; Mueller, A.A.; Mücke, T.; Kopp, J.B.; Koersgen, F.; Wolff, K.D.; Zeilhofer, H.F.; Hölzle, F.; Pradel, W.; Schneider, M.; et al. Microsurgical reconstruction of the head and neck—Current concepts of maxillofacial surgery in Europe. *J. Cranio-Maxillofac. Surg.* **2014**, *42*, 1610–1613. https://doi.org/10.1016/j.jcms.2014.04.030.
4. Cordeiro, P.G.; Disa, J.J.; Hidalgo, D.A.; Hu, Q.Y. Reconstruction of the mandible with osseous free flaps: A 10-year experience with 150 consecutive patients. *Plast. Reconstr. Surg.* **1999**, *104*, 1314–1320. https://doi.org/10.1097/00006534-199910000-00011.
5. Chana, J.S.; Chang, Y.M.; Wei, F.C.; Shen, Y.F.; Chan, C.P.; Lin, H.N.; Tsai, C.Y.; Jeng, S.F. Segmental mandibulectomy and immediate free fibula osteoseptocutaneous flap reconstruction with endosteal implants: An ideal treatment method for mandibular ameloblastoma. *Plast. Reconstr. Surg.* **2004**, *113*, 80–87. https://doi.org/10.1097/01.PRS.0000097719.69616.29.
6. Attia, S.; Wiltfang, J.; Streckbein, P.; Wilbrand, J.F.; El Khassawna, T.; Mausbach, K.; Howaldt, H.P.; Schaaf, H. Functional and aesthetic treatment outcomes after immediate jaw reconstruction using a fibula flap and dental implants. *J. Cranio-Maxillofac. Surg.* **2019**, *47*, 786–791. https://doi.org/10.1016/j.jcms.2018.12.017.
7. Chen, X.F.; Chen, Y.M.; Gokavarapu, S.; Shen, Q.C.; Ji, T. Free flap reconstruction for patients aged 85 years and over with head and neck cancer: Clinical considerations for comprehensive care. *Br. J. Oral Maxillofac. Surg.* **2017**, *55*, 793–797. https://doi.org/10.1016/j.bjoms.2017.07.003.
8. Shroff, S.S.; Nair, S.C.; Shah, A.; Kumar, B. Versatility of fibula free flap in reconstruction of facial defects: A center study. *J. Maxillofac. Oral Surg.* **2017**, *16*, 101–107. https://doi.org/10.1007/s12663-016-0930-6.

9. Barone, S.; Cosentini, G.; Bennardo, F.; Antonelli, A.; Giudice, A. Incidence and management of condylar resorption after orthognathic surgery: An overview. *Korean J. Orthod.* **2022**, *52*, 29–41. https://doi.org/10.4041/kjod.2022.52.1.29.
10. Rustemeyer, J.; Busch, A.; Sari-Rieger, A. Application of computer-aided designed/computer-aided manufactured techniques in reconstructing maxillofacial bony structures. *Oral Maxillofac. Surg.* **2014**, *18*, 471–476. https://doi.org/10.1007/s10006-014-0462-5.
11. Mascha, F.; Winter, K.; Pietzka, S.; Heufelder, M.; Schramm, A.; Wilde, F. Accuracy of computer-assisted mandibular reconstructions using patient-specific implants in combination with CAD/CAM fabricated transfer keys. *J. Cranio-Maxillofac. Surg.* **2017**, *45*, 1884–1897. https://doi.org/10.1016/j.jcms.2017.08.028.
12. Knitschke, M.; Sonnabend, S.; Bäcker, C.; Schmermund, D.; Böttger, S.; Howaldt, H.P.; Attia, S. Partial and total flap failure after fibula free flap in head and neck reconstructive surgery: Retrospective analysis of 180 flaps over 19 years. *Cancers* **2021**, *13*, 865. https://doi.org/10.3390/cancers13040865.
13. Zavattero, E.; Fasolis, M.; Garzino-Demo, P.; Berrone, S.; Ramieri, G.A. Evaluation of plate-related complications and efficacy in fibula free flap mandibular reconstruction. *J. Craniofac. Surg.* **2014**, *25*, 397–399. https://doi.org/10.1097/SCS.0000000000000656.
14. Chan, A.; Sambrook, P.; Munn, Z.; Boase, S. Effectiveness of computer-assisted virtual planning, cutting guides and pre-engineered plates on outcomes in mandible fibular free flap reconstructions over traditional freehand techniques: A systematic review protocol. *JBI Database Syst. Rev. Implement. Rep.* **2019**, *17*, 2136–2151. https://doi.org/10.11124/JBISRIR-2017-003875.
15. Möllmann, H.L.; Apeltrath, L.; Karnatz, N.; Wilkat, M.; Riedel, E.; Singh, D.D.; Rana, M. Comparison of the accuracy and clinical parameters of patient-specific and conventionally bended plates for mandibular reconstruction. *Front. Oncol.* **2021**, *11*, 719028. https://doi.org/10.3389/fonc.2021.719028.
16. Brown, J.S.; Barry, C.; Ho, M.; Shaw, R. A new classification for mandibular defects after oncological resection. *Lancet Oncol.* **2016**, *17*, e23–e30. https://doi.org/10.1016/S1470-2045(15)00310-1.
17. Bartier, S.; Mazzaschi, O.; Benichou, L.; Sauvaget, E. Computer-assisted versus traditional technique in fibular free-flap mandibular reconstruction: A CT symmetry study. *Eur. Ann. Otorhinolaryngol. Head Neck Dis.* **2021**, *138*, 23–27. https://doi.org/10.1016/j.anorl.2020.06.011.
18. De Maesschalck, T.; Courvoisier, D.S.; Scolozzi, P. Computer-assisted versus traditional freehand technique in fibular free flap mandibular reconstruction: A morphological comparative study. *Eur. Arch. Otorhinolaryngol.* **2017**, *274*, 517–526. https://doi.org/10.1007/s00405-016-4246-4.
19. Ren, W.; Gao, L.; Li, S.; Chen, C.; Li, F.; Wang, Q.; Zhi, Y.; Song, J.; Dou, Z.; Xue, L.; et al. Virtual planning and 3D printing modeling for mandibular reconstruction with fibula free flap. *Med. Oral Patol. Oral Cir. Bucal* **2018**, *23*, e359–e366. https://doi.org/10.4317/medoral.22295.
20. Egger, J.; Wallner, J.; Gall, M.; Chen, X.; Schwenzer-Zimmerer, K.; Reinbacher, K.; Schmalstieg, D. Computer-aided position planning of miniplates to treat facial bone defects. *PLoS ONE* **2017**, *12*, e0182839. https://doi.org/10.1371/journal.pone.0182839.
21. Wilde, F.; Cornelius, C.P.; Schramm, A. Computer-assisted mandibular reconstruction using a patient-specific reconstruction plate fabricated with computer-aided design and manufacturing techniques. *Craniomaxillofac. Trauma Reconstr.* **2014**, *7*, 158–166. https://doi.org/10.1055/s-0034-1371356.
22. Wilde, F.; Hanken, H.; Probst, F.; Schramm, A.; Heiland, M.; Cornelius, C.P. Multicenter study on the use of patient-specific CAD/CAM reconstruction plates for mandibular reconstruction. *Int. J. Comput. Assist. Radiol. Surg.* **2015**, *10*, 2035–2051. https://doi.org/10.1007/s11548-015-1193-2.
23. Geusens, J.; Sun, Y.; Luebbers, H.T.; Bila, M.; Darche, V.; Politis, C. Accuracy of computer-aided design/computer-aided manufacturing-assisted mandibular reconstruction with a fibula free flap. *J. Craniofac. Surg.* **2019**, *30*, 2319–2323. https://doi.org/10.1097/SCS.0000000000005704.
24. Han, H.H.; Kim, H.Y.; Lee, J.Y. The pros and cons of computer-aided surgery for segmental mandibular reconstruction after oncological surgery. *Arch. Craniofac. Surg.* **2017**, *18*, 149–154. https://doi.org/10.7181/acfs.2017.18.3.149.
25. Alassaf, M.H.; Li, W.; Joshi, A.S.; Hahn, J.K. Computer-based planning system for mandibular reconstruction. *Stud. Health Technol. Inform.* **2014**, *196*, 6–10.
26. Ciocca, L.; Marchetti, C.; Mazzoni, S.; Baldissara, P.; Gatto, M.R.; Cipriani, R.; Scotti, R.; Tarsitano, A. Accuracy of fibular sectioning and insertion into a rapid-prototyped bone plate, for mandibular reconstruction using CAD-CAM technology. *J. Cranio-Maxillofac. Surg.* **2015**, *43*, 28–33. https://doi.org/10.1016/j.jcms.2014.10.005.
27. Toto, J.M.; Chang, E.I.; Agag, R.; Devarajan, K.; Patel, S.A.; Topham, N.S. Improved operative efficiency of free fibula flap mandible reconstruction with patient-specific, computer-guided preoperative planning. *Head Neck* **2015**, *37*, 1660–1664. https://doi.org/10.1002/hed.23815.
28. Culie, D.; Dassonville, O.; Poissonnet, G.; Riss, J.C.; Fernandez, J.; Bozec, A. Virtual planning and guided surgery in fibular free-flap mandibular reconstruction: A 29-case series. *Eur. Ann. Otorhinolaryngol. Head Neck Dis.* **2016**, *133*, 175–178. https://doi.org/10.1016/j.anorl.2016.01.009.
29. Hanken, H.; Schablowsky, C.; Smeets, R.; Heiland, M.; Sehner, S.; Riecke, B.; Nourwali, I.; Vorwig, O.; Grobe, A.; Al-Dam, A. Virtual planning of complex head and neck reconstruction results in satisfactory match between real outcomes and virtual models. *Clin. Oral Investig.* **2015**, *19*, 647–656. https://doi.org/10.1007/s00784-014-1291-5.
30. Knitschke, M.; Bäcker, C.; Schmermund, D.; Böttger, S.; Streckbein, P.; Howaldt, H.P.; Attia, S. Impact of planning method (conventional versus virtual) on time to therapy initiation and resection margins: A retrospective analysis of 104 immediate jaw reconstructions. *Cancers* **2021**, *13*, 3013. https://doi.org/10.3390/cancers13123013.

31. Yang, W.F.; Choi, W.S.; Wong, M.C.; Powcharoen, W.; Zhu, W.Y.; Tsoi, J.K.; Chow, M.; Kwok, K.W.; Su, Y.X. Three-dimensionally printed patient-specific surgical plates increase accuracy of oncologic head and neck reconstruction versus conventional surgical plates: A comparative study. *Ann. Surg. Oncol.* **2021**, *28*, 363–375. https://doi.org/10.1245/s10434-020-08732-y.
32. Rendenbach, C.; Steffen, C.; Hanken, H.; Schluermann, K.; Henningsen, A.; Beck-Broichsitter, B.; Kreutzer, K.; Heiland, M.; Precht, C. Complication rates and clinical outcomes of osseous free flaps: A retrospective comparison of CAD/CAM versus conventional fixation in 128 patients. *Int. J. Oral Maxillofac. Surg.* **2019**, *48*, 1156–1162. https://doi.org/10.1016/j.ijom.2019.01.029.
33. Fichter, A.M.; Ritschl, L.M.; Georg, R.; Kolk, A.; Kesting, M.R.; Wolff, K.D.; Mücke, T. Effect of segment length and number of osteotomy sites on cancellous bone perfusion in free fibula flaps. *J. Reconstr. Microsurg.* **2019**, *35*, 108–116. https://doi.org/10.1055/s-0038-1667364.
34. Mücke, T.; Ritschl, L.M.; Roth, M.; Güll, F.D.; Rau, A.; Grill, S.; Kesting, M.R.; Wolff, K.D.; Loeffelbein, D.J. Predictors of free flap loss in the head and neck region: A four-year retrospective study with 451 microvascular transplants at a single centre. *J. Cranio-Maxillofac. Surg.* **2016**, *44*, 1292–1298. https://doi.org/10.1016/j.jcms.2016.04.029.
35. Chang, E.I.; Jenkins, M.P.; Patel, S.A.; Topham, N.S. Long-term operative outcomes of preoperative computed tomography-guided virtual surgical planning for osteocutaneous free flap mandible reconstruction. *Plast. Reconstr. Surg.* **2016**, *137*, 619–623. https://doi.org/10.1097/01.prs.0000475796.61855.a7.
36. Foster, R.D.; Anthony, J.P.; Sharma, A.; Pogrel, M.A. Vascularized bone flaps versus nonvascularized bone grafts for mandibular reconstruction: An outcome analysis of primary bony union and endosseous implant success. *Head Neck* **1999**, *21*, 66–71. https://doi.org/10.1002/(sici)1097-0347(199901)21:1<66::aid-hed9>3.0.co;2-z.
37. Mehra, P.; Murad, H. Internal fixation of mandibular angle fractures: A comparison of 2 techniques. *J. Oral Maxillofac. Surg.* **2008**, *66*, 2254–2260. https://doi.org/10.1016/j.joms.2008.06.024.
38. Swendseid, B.; Kumar, A.; Sweeny, L.; Zhan, T.; Goldman, R.A.; Krein, H.; Heffelfinger, R.N.; Luginbuhl, A.J.; Curry, J.M. Natural history and consequences of nonunion in mandibular and maxillary free flaps. *Otolaryngol. Head Neck Surg.* **2020**, *163*, 956–962. https://doi.org/10.1177/0194599820931069.
39. Yeh, D.H.; Lee, D.J.; Sahovaler, A.; Fung, K.; MacNeil, D.; Nichols, A.C.; Yoo, J. Shouldering the load of mandible reconstruction: 81 cases of oromandibular reconstruction with the scapular tip free flap. *Head Neck* **2019**, *41*, 30–36. https://doi.org/10.1002/hed.25342.
40. Yla-Kotola, T.M.; Bartlett, E.; Goldstein, D.P.; Armstrong, K.; Gilbert, R.W.; Hofer, S.O. Union and bone resorption of free fibular flaps in mandibular reconstruction. *J. Reconstr. Microsurg.* **2013**, *29*, 427–432. https://doi.org/10.1055/s-0033-1343953.
41. Claes, L.E.; Heigele, C.A.; Neidlinger-Wilke, C.; Kaspar, D.; Seidl, W.; Margevicius, K.J.; Augat, P. Effects of mechanical factors on the fracture healing process. *Clin. Orthop. Relat. Res.* **1998**, *355*, S132–S147. https://doi.org/10.1097/00003086-199810001-00015.
42. Kennady, M.C.; Tucker, M.R.; Lester, G.E.; Buckley, M.J. Stress shielding effect of rigid internal fixation plates on mandibular bone grafts. A photon absorption densitometry and quantitative computerized tomographic evaluation. *Int. J. Oral Maxillofac. Surg.* **1989**, *18*, 307–310. https://doi.org/10.1016/s0901-5027(89)80101-8.
43. Robey, A.B.; Spann, M.L.; McAuliff, T.M.; Meza, J.L.; Hollins, R.R.; Johnson, P.J. Comparison of miniplates and reconstruction plates in fibular flap reconstruction of the mandible. *Plast. Reconstr. Surg.* **2008**, *122*, 1733–1738. https://doi.org/10.1097/PRS.0b013e31818a9ac5.
44. Zoumalan, R.A.; Hirsch, D.L.; Levine, J.P.; Saadeh, P.B. Plating in microvascular reconstruction of the mandible: Can fixation be too rigid? *J. Craniofac. Surg.* **2009**, *20*, 1451–1454. https://doi.org/10.1097/SCS.0b013e3181af156a.
45. Ghiasi, M.S.; Chen, J.; Vaziri, A.; Rodriguez, E.K.; Nazarian, A. Bone fracture healing in mechanobiological modeling: A review of principles and methods. *Bone Rep.* **2017**, *6*, 87–100. https://doi.org/10.1016/j.bonr.2017.03.002.
46. Rendenbach, C.; Sellenschloh, K.; Gerbig, L.; Morlock, M.M.; Beck-Broichsitter, B.; Smeets, R.; Heiland, M.; Huber, G.; Hanken, H. CAD-CAM plates versus conventional fixation plates for primary mandibular reconstruction: A biomechanical in vitro analysis. *J. Cranio-Maxillofac. Surg.* **2017**, *45*, 1878–1883. https://doi.org/10.1016/j.jcms.2017.08.024.
47. Kreutzer, K.; Steffen, C.; Nahles, S.; Koerdt, S.; Heiland, M.; Rendenbach, C.; Beck-Broichsitter, B. Removal of patient-specific reconstruction plates after mandible reconstruction with a fibula free flap: Is the plate the problem? *Int. J. Oral Maxillofac. Surg.* **2021**, *51*, 182–190. https://doi.org/10.1016/j.ijom.2021.04.003.
48. Kreutzer, K.; Steffen, C.; Koerdt, S.; Doll, C.; Ebker, T.; Nahles, S.; Flügge, T.; Heiland, M.; Beck-Broichsitter, B.; Rendenbach, C. Patient-specific 3D-printed miniplates for free flap fixation at the mandible: A feasibility study. *Front. Surg.* **2022**, *9*, https://doi.org/10.3389/fsurg.2022.778371.
49. Zhong, S.; Shi, Q.; Sun, Y.; Yang, S.; van Dessel, J.; Gu, Y.; Chen, X.; Lubbers, H.T.; Politis, C. Biomechanical comparison of locking and non-locking patient-specific mandibular reconstruction plate using finite element analysis. *J. Mech. Behav. Biomed. Mater.* **2021**, *124*, 104849. https://doi.org/10.1016/j.jmbbm.2021.104849.
50. Kristina, H. Finite Element Analysis of Orthopaedic Plates and Screws to Reduce the Effects of Stress Shielding. Ph.D. Thesis, University of Ottawa, Ottawa, ON, Canada, 2009.
51. Koo, H.; Hupel, T.; Zdero, R.; Tov, A.; Schemitsch, E.H. The effect of muscle contusion on cortical bone and muscle perfusion following reamed, intramedullary nailing: A novel canine tibia fracture model. *J. Orthop. Surg. Res.* **2010**, *5*, 89. https://doi.org/10.1186/1749-799X-5-89.
52. Coletti, D.P.; Ord, R.; Liu, X. Mandibular reconstruction and second generation locking reconstruction plates: Outcome of 110 patients. *Int. J. Oral Maxillofac. Surg.* **2009**, *38*, 960–963. https://doi.org/10.1016/j.ijom.2009.03.721.

53. Lippuner, K.; Vogel, R.; Tepic, S.; Rahn, B.A.; Cordey, J.; Perren, S.M. Effect of animal species and age on plate-induced vascular damage in cortical bone. *Arch. Orthop. Trauma Surg.* **1992**, *111*, 78–84. https://doi.org/10.1007/BF00443472.
54. Whiteside, L.A.; Ogata, K.; Lesker, P.; Reynolds, F.C. The acute effects of periosteal stripping and medullary reaming on regional bone blood flow. *Clin. Orthop. Relat. Res.* **1978**, *131*, 266–272.
55. Leiggener, C.; Messo, E.; Thor, A.; Zeilhofer, H.F.; Hirsch, J.M. A selective laser sintering guide for transferring a virtual plan to real time surgery in composite mandibular reconstruction with free fibula osseous flaps. *Int. J. Oral Maxillofac. Surg.* **2009**, *38*, 187–192. https://doi.org/10.1016/j.ijom.2008.11.026.
56. Weitz, J.; Wolff, K.D.; Kesting, M.R.; Nobis, C.P. Development of a novel resection and cutting guide for mandibular reconstruction using free fibula flap. *J. Cranio-Maxillofac. Surg.* **2018**, *46*, 1975–1978. https://doi.org/10.1016/j.jcms.2018.09.007.
57. Pitak-Arnnop, P.; Hemprich, A.; Dhanuthai, K.; Pausch, N.C. Fibular flap for mandibular reconstruction: Are there old tricks for an old dog? *Rev. Stomatol. Chir. Maxillo-Fac. Chir. Orale* **2013**, *114*, 15–18. https://doi.org/10.1016/j.stomax.2012.05.001.
58. Menck, J.; Sander, A. Periosteal and endosteal blood supply of the human fibula and its clinical importance. *Acta Anat.* **1992**, *145*, 400–405.
59. Strachan, R.K.; Mccarthy, I.; Fleming, R.; Hughes, S.P.F. The role of the tibial nutrient artery—Microsphere estimation of blood-flow in the osteotomised canine tibia. *J. Bone Jt. Surg.-Br. Vol.* **1990**, *72*, 391–394.
60. Kregor, P.J.; Senft, D.; Parvin, D.; Campbell, C.; Toomey, S.; Parker, C.; Gillespy, T.; Swiontkowski, M.F. Cortical bone perfusion in plated fractured sheep tibiae. *J. Orthop. Res.* **1995**, *13*, 715–724. https://doi.org/10.1002/jor.1100130511.
61. Seibold, R.; Schlegel, U.; Kessler, S.B.; Cordey, J.; Perren, S.M.; Schweiberer, L. Healing of spiral fractures in the sheep tibia comparing different methods—Osteosynthesis with internal fixation, interlocking nailing and dynamic compression plate. *Unfallchirurg* **1995**, *98*, 620–626.
62. Bartnikowski, N.; Claes, L.E.; Koval, L.; Glatt, V.; Bindl, R.; Steck, R.; Ignatius, A.; Schuetz, M.A.; Epari, D.R. Modulation of fixation stiffness from flexible to stiff in a rat model of bone healing. *Acta Orthop.* **2017**, *88*, 217–222. https://doi.org/10.1080/17453674.2016.1256940.
63. Yoda, N.; Zheng, K.; Chen, J.; Liao, Z.; Koyama, S.; Peck, C.; Swain, M.; Sasaki, K.; Li, Q. Biomechanical analysis of bone remodeling following mandibular reconstruction using fibula free flap. *Med. Eng. Phys.* **2018**, *56*, 1–8. https://doi.org/10.1016/j.medengphy.2018.03.008.
64. Greksa, F.; Butt, E.; Csonka, E.; Javor, P.; Tuboly, E.; Torok, L.; Szabo, A.; Varga, E.; Hartmann, P. Periosteal and endosteal microcirculatory injury following excessive osteosynthesis. *Injury* **2021**, *52* (Suppl. 1), S3–S6. https://doi.org/10.1016/j.injury.2020.11.053.
65. Kowalski, M.J.; Schemitsch, E.H.; Kregor, P.J.; Senft, D.; Swiontkowski, M.F. Effect of periosteal stripping on cortical bone perfusion: A laser doppler study in sheep. *Calcif. Tissue Int.* **1996**, *59*, 24–26. https://doi.org/10.1007/s002239900080.
66. Schemitsch, E.H.; Kowalski, M.J.; Swiontkowski, M.F.; Harrington, R.M. Comparison of the effect of reamed and unreamed locked intramedullary nailing on blood flow in the callus and strength of union following fracture of the sheep tibia. *J. Orthop. Res.* **1995**, *13*, 382–389. https://doi.org/10.1002/jor.1100130312.
67. Shapiro, F. Bone development and its relation to fracture repair. The role of mesenchymal osteoblasts and surface osteoblasts. *Eur. Cells Mater.* **2008**, *15*, 53–76. https://doi.org/10.22203/ecm.v015a05.
68. Augat, P.; Margevicius, K.; Simon, J.; Wolf, S.; Suger, G.; Claes, L. Local tissue properties in bone healing: Influence of size and stability of the osteotomy gap. *J. Orthop. Res.* **1998**, *16*, 475–481. https://doi.org/10.1002/jor.1100160413.
69. Claes, L.; Augat, P.; Suger, G.; Wilke, H.J. Influence of size and stability of the osteotomy gap on the success of fracture healing. *J. Orthop. Res.* **1997**, *15*, 577–584. https://doi.org/10.1002/jor.1100150414.
70. Hidalgo, D.A. Titanium miniplate fixation in free flap mandible reconstruction. *Ann. Plast. Surg.* **1989**, *23*, 498–507. https://doi.org/10.1097/00000637-198912000-00005.
71. Likhterov, I.; Roche, A.M.; Urken, M.L. Contemporary osseous reconstruction of the mandible and the maxilla. *Oral Maxillofac. Surg. Clin. North Am.* **2019**, *31*, 101–116. https://doi.org/10.1016/j.coms.2018.08.005.
72. Shimamoto, H.; Sumida, I.; Kakimoto, N.; Marutani, K.; Okahata, R.; Usami, A.; Tsujimoto, T.; Murakami, S.; Furukawa, S.; Tetradis, S. Evaluation of the scatter doses in the direction of the buccal mucosa from dental metals. *J. Appl. Clin. Med. Phys.* **2015**, *16*, 5374. https://doi.org/10.1120/jacmp.v16i3.5374.
73. Chiodo, A.A.; Gur, E.; Pang, C.Y.; Neligan, P.C.; Boyd, J.B.; Binhammer, P.M.; Forrest, C.R. The vascularized pig fibula bone flap model: Effect of segmental osteotomies and internal fixation on blood flow. *Plast. Reconstr. Surg.* **2000**, *105*, 1004–1012. https://doi.org/10.1097/00006534-200003000-00025.
74. Gur, E.; Chiodo, A.; Pang, C.Y.; Mendes, M.; Pritzker, K.P.; Neligan, P.C.; Shpitzer, T.; Forrest, C.R. The vascularized pig fibula bone flap model: Effects of multiple segmental osteotomies on growth and viability. *Plast. Reconstr. Surg.* **1999**, *103*, 1436–1442. https://doi.org/10.1097/00006534-199904050-00012.
75. Strackee, S.D.; Kroon, F.H.; Jaspers, J.E.; Bos, K.E. Modeling a fibula transplant in mandibular reconstructions: Evaluation of the effects of a minimal number of osteotomies on the contour of the jaw. *Plast. Reconstr. Surg.* **2001**, *108*, 1915–1921. https://doi.org/10.1097/00006534-200112000-00010.
76. Wei, F.C.; Santamaria, E.; Chang, Y.M.; Chen, H.C. Mandibular reconstruction with fibular osteoseptocutaneous free flap and simultaneous placement of osseointegrated dental implants. *J. Craniofac. Surg.* **1997**, *8*, 512–521. https://doi.org/10.1097/00001665-199711000-00018.

77. Bähr, W. Blood supply of small fibula segments: An experimental study on human cadavers. *J. Cranio-Maxillofac. Surg.* **1998**, *26*, 148–152. https://doi.org/10.1016/s1010-5182(98)80004-8.
78. Knitschke, M.; Baumgart, A.K.; Bäcker, C.; Adelung, C.; Roller, F.; Schmermund, D.; Böttger, S.; Streckbein, P.; Howaldt, H.P.; Attia, S. Impact of periosteal branches and septo-cutaneous perforators on free fibula flap outcome: A retrospective analysis of computed tomography angiography scans in virtual surgical planning. *Front. Oncol.* **2021**, *11*, 821851. https://doi.org/10.3389/fonc.2021.821851.
79. Trignano, E.; Fallico, N.; Faenza, M.; Rubino, C.; Chen, H.C. Free fibular flap with periosteal excess for mandibular reconstruction. *Microsurgery* **2013**, *33*, 527–533. https://doi.org/10.1002/micr.22159.
80. Smeele, L.E.; Slotman, B.J.; Mens, J.W.; Tiwari, R. Local radiation dose, fixation, and non-union of mandibulotomies. *Head Neck* **1999**, *21*, 315–318. https://doi.org/10.1002/(sici)1097-0347(199907)21:4<315::aid-hed4>3.0.co;2-w.
81. Yao, C.M.; Ziai, H.; Tsang, G.; Copeland, A.; Brown, D.; Irish, J.C.; Gilbert, R.W.; Goldstein, D.P.; Gullane, P.J.; de Almeida, J.R. Surgical site infections following oral cavity cancer resection and reconstruction is a risk factor for plate exposure. *J. Otolaryngol. Head Neck Surg.* **2017**, *46*, 30. https://doi.org/10.1186/s40463-017-0206-2.
82. Zhang, Z.L.; Wang, S.; Sun, C.F.; Xu, Z.F. Miniplates versus reconstruction plates in vascularized osteocutaneous flap reconstruction of the mandible. *J. Craniofac. Surg.* **2019**, *30*, e119–e125. https://doi.org/10.1097/SCS.0000000000005020.
83. Militsakh, O.N.; Wallace, D.I.; Kriet, J.D.; Girod, D.A.; Olvera, M.S.; Tsue, T.T. Use of the 2.0-mm locking reconstruction plate in primary oromandibular reconstruction after composite resection. *Otolaryngol. Head Neck Surg.* **2004**, *131*, 660–665. https://doi.org/10.1016/j.otohns.2004.04.033.

Current Oncology

an Open Access Journal by MDPI

CERTIFICATE OF ACCEPTANCE

Certificate of acceptance for the manuscript (**curroncol-1700737**) titled:

Osseous Union and Complication Rates after Mandible Reconstruction with Fibula Free Flap using manually bent Plates vs. Patient-Specific Implants: A Retrospective Analysis of 89 Patients

Authored by:

Michael Knitschke; Sophia Sonnabend; Fritz Christian Roller; Jörn Pons-Kühnemann; Daniel Schmermund; Sameh Attia; Philipp Streckbein; Hans-Peter Howaldt; Sebastian Böttger

has been accepted in *Curr. Oncol.* (ISSN 1718-7729) on 05 May 2022

MDPI Academic Open Access Publishing since 1996

Basel, May 2022

3.7. Unveröffentlichte Arbeiten

3.7.1. Cinematic Volume Rendering

Mithilfe der freierhältlichen (Freeware) Software MeVisLab (MeVis Medical Solutions AG, Bremen, Deutschland) wurde eigenständig ein Modul entwickelt, mit dem *Cinematic Volume Rendering* (CVR)-Rekonstruktionen aus DICOM-Datensätzen generiert werden können (**Abbildung *4*** bis **Abbildung *8***). Die Hauptvorteile von CVR liegen in der intuitiven Auswertung verschiedener anatomischer Strukturen. Außerdem ermöglicht CVR die farbige Darstellung von in Graustufen abgespeicherten CT-Bilddaten [147, 148]. Um also zu vermeiden, dass kritische Informationen verloren gehen, sollten CVR-Bilder immer mit den konventionellen multiplanaren Rekonstruktions-Bildern verglichen werden. Schließlich sollte bedacht werden, dass die Visualisierung von Bilddaten mit CVR - wie bei anderen Nachbearbeitungstechniken wie beispielsweise der Maximalen-Intensitäts-Projektion (MIP) - dem Betrachter nie mehr Informationen über das hinausgeben können, was in den Originalbildern vorhanden ist. Klinische Entscheidungen erfordern eine schnelle Beurteilung der in schichtbildgebenden Verfahren gewonnenen Informationen. Obwohl die Betrachtung medizinischer Bilder auf der Grundlage der multiplanaren Rekonstruktion in der diagnostischen Bildgebung nach wie vor vorherrschend ist, nimmt die Bedeutung der dreidimensionalen Visualisierung von Bilddaten zu. Dies ist darauf zurückzuführen, dass diese Methoden ein viel schnelleres Verständnis räumlicher anatomischer Strukturen ermöglichen und das Potenzial haben, die Sensitivität und Spezifität medizinischer Bilder zu erhöhen. Vor allem Nichtradiologen, medizinisches Assistenz- und Fachpersonal, das nicht in der planaren Bildbetrachtung geschult ist, sowie Patienten profitieren von solchen Visualisierungen.

Fortschritte in der Computergrafik haben interaktive, physikalisch basierte Volumenvisualisierungstechniken möglich gemacht. Solche Techniken reproduzieren komplexe Beleuchtungseffekte in computergenerierten Bildern, indem sie die reale Interaktion von Licht mit Materie nachahmen. Das Ergebnis sind physikalisch plausible Bilder, die für das menschliche Gehirn oft leichter zu interpretieren sind, da das Gehirn darauf trainiert ist, kleinste Schattierungshinweise zu interpretieren, um Form- und Tiefeninformationen zu rekonstruieren. Solche Schattierungshinweise fehlen oft bei computergenerierten Bildern. Es bleibt immer eine Option für eine andere Darstellung

der Bilddaten, die bei anatomisch komplexen Strukturen und Krankheiten und für eine einfachere und verständliche Illustration von Bildgebungsbefunden hilfreich sein kann [87]. In der Literatur sind bereits CVR-Anwendungen für Fragestellungen der Traumatologie [149, 150], HNO [151], Neurochirurgie [152], Onkologie und der Herzkranzgefäße [153] beschrieben.
Eigenständig durchgeführte Rekonstruktionen für Aspekte der Traumatologie, der Darstellung heterotoper Ossifikationen sowie der Visualisation der infra-poplitealen Gefäßarchitektur zur Planung de Kieferrekonstruktion sind in dieser Schrift in den **Abbildungen 1c, 3c, 7, 8, 13, 19, 21** und **22** und exemplarisch abgedruckt.

Die Darstellung von periostalen und septo-kutanen Ästen ist bislang nicht in der virtuellen Routineplanung von Kieferrekonstruktionen berücksichtigt. Daher schlagen wir vor, weitere Studien unter Verwendung der entwickelten Volumenvisualisierungssoftware durchzuführen, um die Darstellung kleiner Gefäße als einen zukünftigen Forschungsschritt zu diesem Thema zu verbessern. In einer bereits projektierten und durch die lokale Ethikkommission der Justus-Liebig-Universität positiv beschiedenen Studie (AZ 256/21, 21.01.2022) soll der Einsatz von *Cinematic Volume Rendering* (CVR)-Rekonstruktionen aus CT-Angiographie-Datensätzen zur Darstellung der kleinen Gefäße mit dem intraoperativen Situs verglichen werden (**Abbildung 3**).
Einen guten Eindruck über das Ortauflösungsvermögen gibt **Abbildung 21** im Abschnitt 4.3. In diesem Fallbespiel sind die septo-kutanen Abgänge der *A. fibularis* und der *A. tibialis posterior* deutlich zu erkennen.

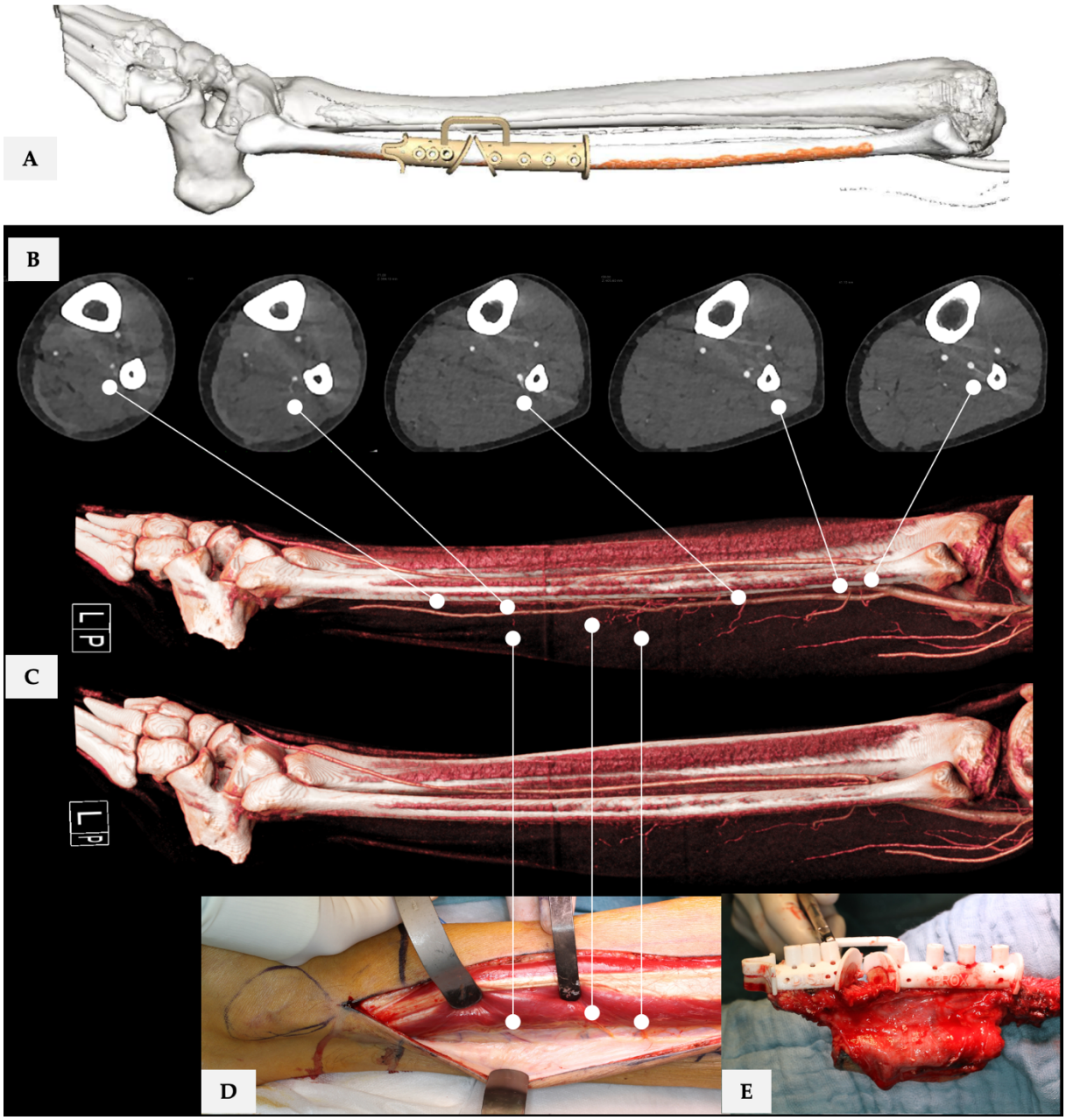

Abbildung 3. (A) Virtuelle chirurgische Planung für eine bi-segmentale Unterkieferrekonstruktion mit freiem Fibulatransplantat aus unserer Klinik bei einem 56-jährigen Patienten mit cT4 Plattenepithelkarzinom (Verwendung mit freundlicher Genehmigung von KLS Martin). (**B**) CTA-Scan (axiale Ebene) der Entnahmeseite. Weiße Linien verbinden die gefundenen periostalen (PB) und septo-kutanen Äste (SCP) mit dem CVR-Bild (**C**) Die Cinematic Volume Rendering-CT-Rekonstruktion zeigt septo-kutane Perforatoren und periostale Äste der *Arteria fibularis*. Software: MeVisLab (MeVis Medical Solutions AG, Bremen, Deutschland). (**D**) Weiße Linien verbinden die entsprechenden Gefäße mit dem Operationsfeld. (**E**) Durchgeführte Osteotomien und Formung des Neokondylus. In dem präsentierten Beispiel fanden sich in der CTA-Beurteilung fünf periostale Äste und ein septo-kutaner Abgang. Die Abbildungen (**C**) und (**D**) zeigen, dass es eine Diskrepanz zwischen dem radiologischen und dem operativen Befund gab. Die Anzahl septo-kutaner Perforatoren ist mindestens vier.

Das Programm MeVisLab (MeVis Medical Solutions AG, Bremen, Deutschland) hat eine graphische Programmieroberfläche und eine umfangreiche Bibliothek freier Module. Diese können entsprechend verknüpft und spezifisch konfiguriert werden (***Abbildung 4***). Die DICOM-Daten werden über ein Interface importiert (***Abbildung 5***) und dann an den 2D LUT Editor SoLUTEditor2D übergeben (***Abbildung 6***). Im Modul SoPathTracerVolume wird der Schicht- in einen Oberflächendatensatz umgewandelt.

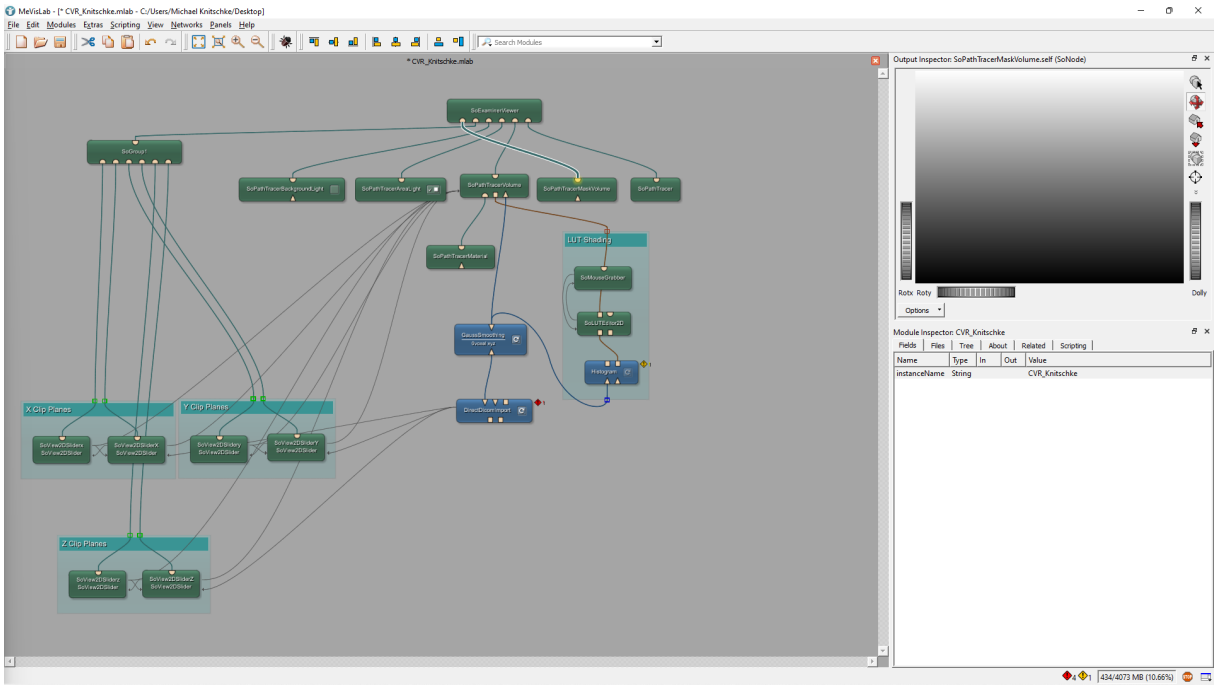

Abbildung 4. Die Benutzeroberfläche von MeVisLab (MeVis Medical Solutions AG, Bremen, Deutschland).

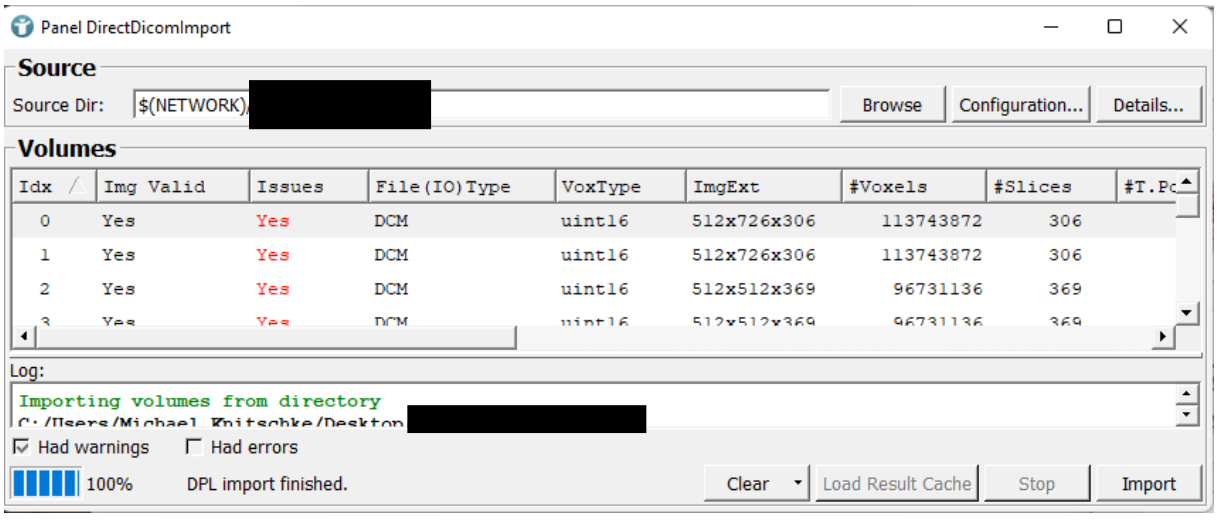

Abbildung 5. Das Panel DirectDICOMImport von MeVisLab (MeVis Medical Solutions AG, Bremen, Deutschland).

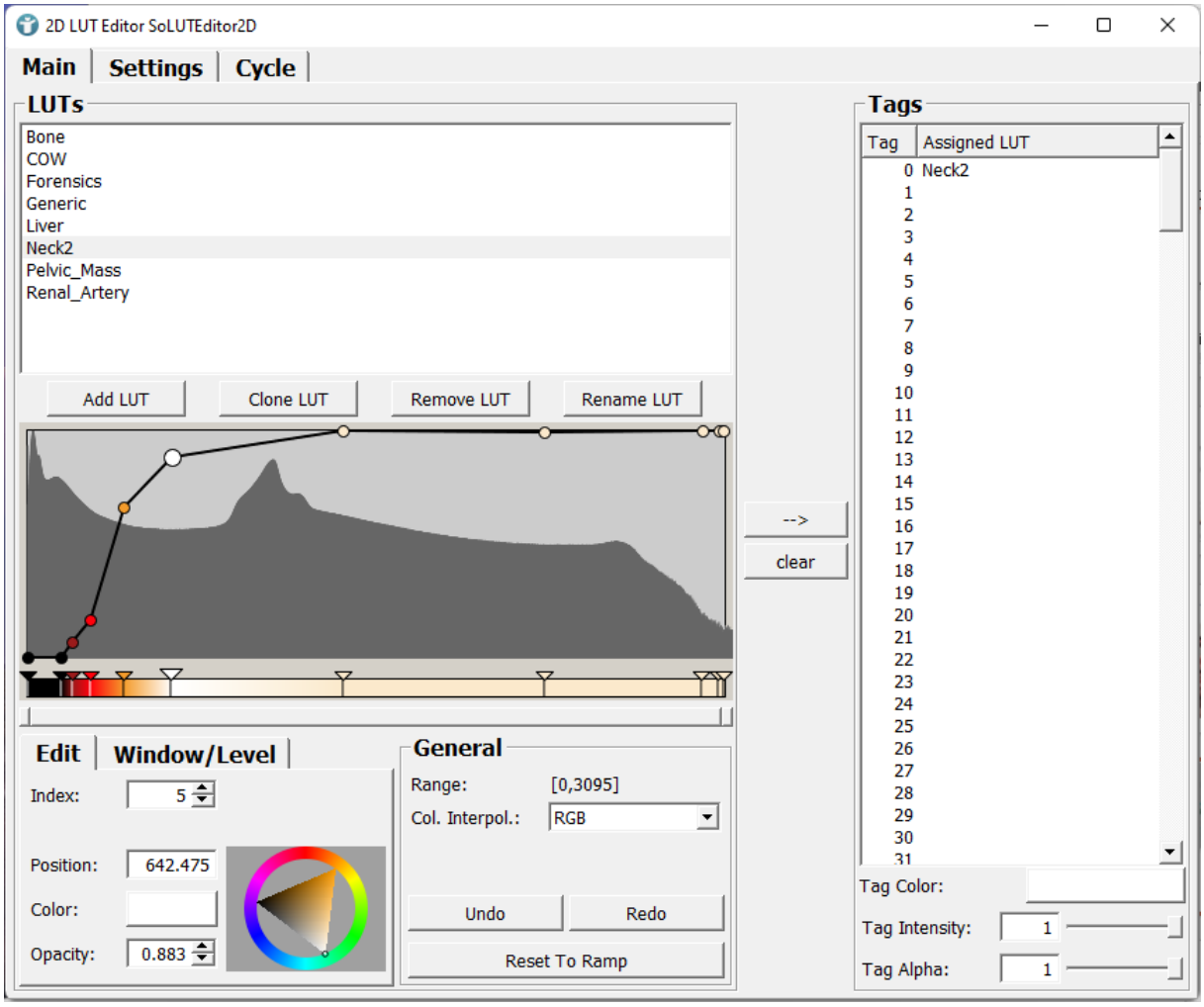

Abbildung 6. Der 2D LUT Editor SoLUTEditior2D von MeVisLab (MeVis Medical Solutions AG, Bremen, Deutschland).

Im Prinzip können im 2D LUT Editor SoLUTEditior2D beliebige Profile hinterlegt werden, um unterschiedliche Strukturen in Abhängigkeit ihres Hounsfield-Werts abzubilden. Das Ergebnis wird dann im Viewer SoExaminerViewer in Echtzeit gezeigt (**Abbildung 7**).

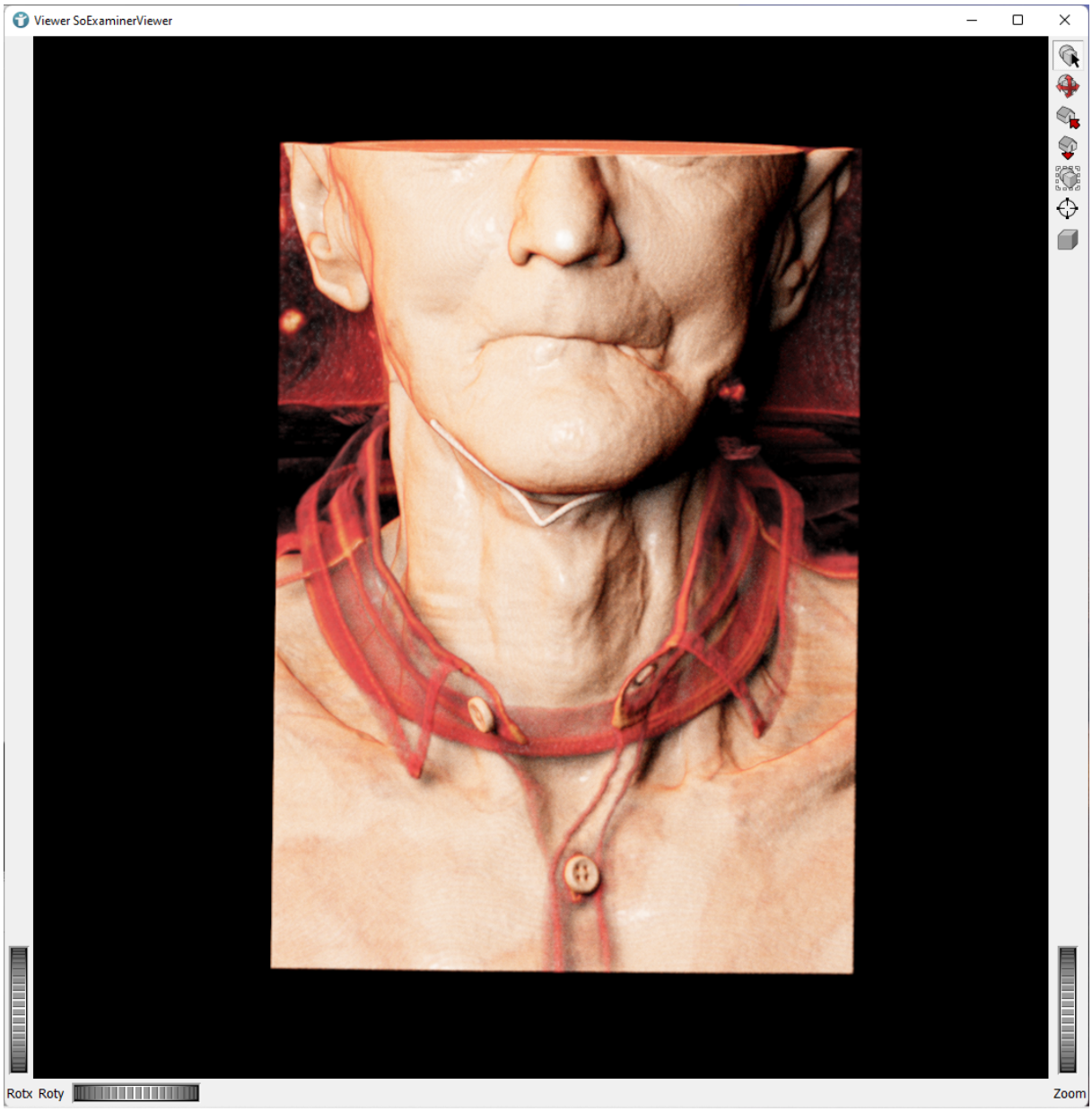

Abbildung 7. Der Viewer SoExaminerViewer von MeVisLab (MeVis Medical Solutions AG, Bremen, Deutschland).

Durch Anpassung der „Gradientenfunktion“ können dann die gewünschten Strukturen visualisiert werden (***Abbildung 8***).

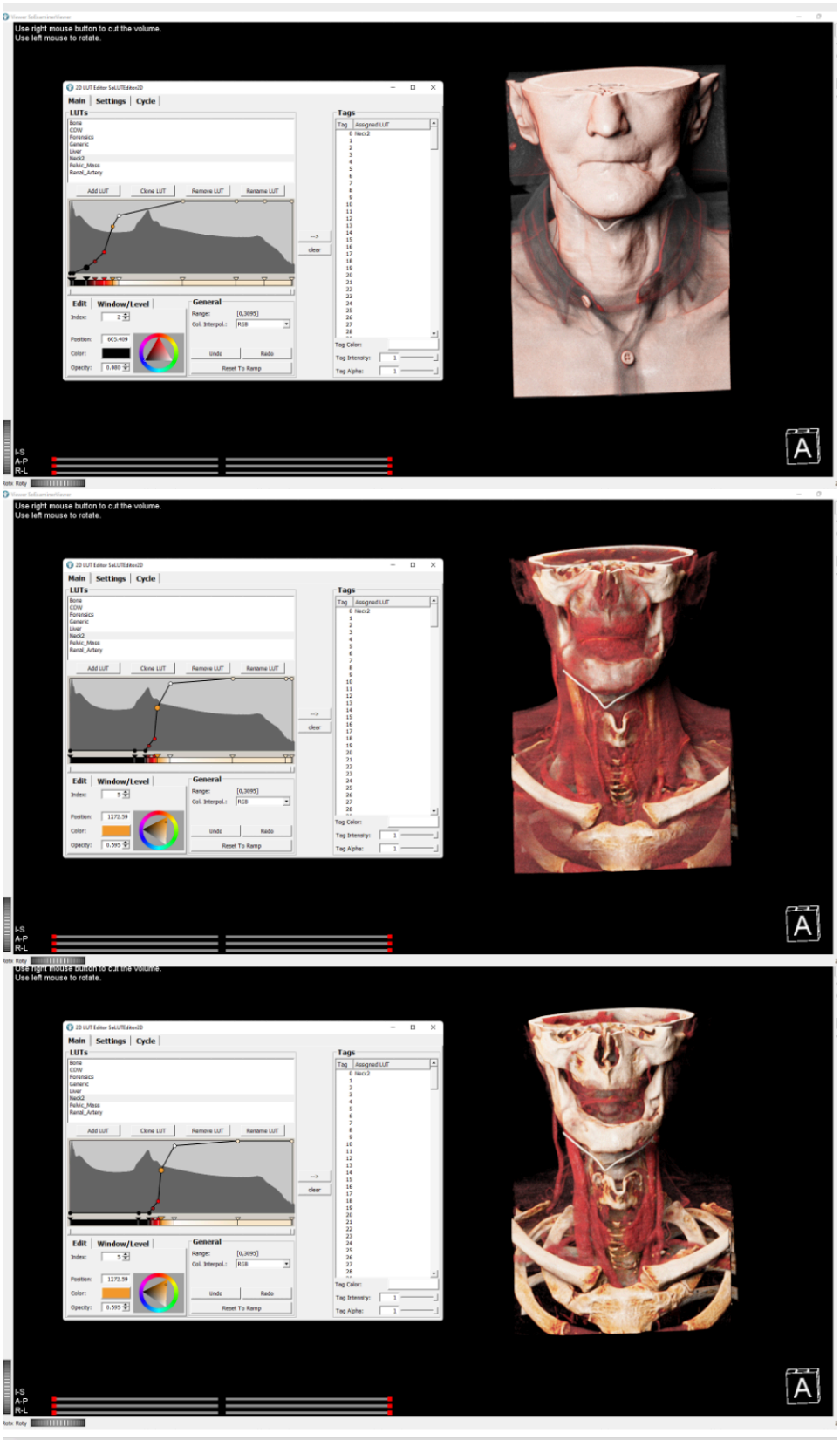

Abbildung 8. Das Histogramm des 2D LUT Editor SoLUTEditior2D (links) zeigt die Verteilung der Hounsfield-Einheiten. Die Änderung der Auswahl („Gradientenfunktion“) führt zu einer Veränderung der dargestellten Bildinformation (rechts). Bei diesem Fall aus unserer Klinik handelt es sich um die Planung einer Unterkieferrekonstruktion bei einer infizierten Osteoradionekrose des linken Unterkiefers nach Oropharynxkarzinom.
Anmerkung: A, Anterior.

3.7.2. Die Herausforderung unvollständiger Verknöcherung

Das Problem der unvollständigen Verknöcherung der Übergangsbereiche zwischen Mandibula und Fibulatransplantat und einzelner Fibulasegmenten selbst haben wir identifiziert. Als Konsequenz wurden sowohl die Plattenstärke als auch das Osteosyntheseprinzip geändert. Die physiologische Knochenstimulation wird durch lastteilende patienten-spezifische Platten der Stärke 1,5 mm erhöht. Weitere klinische Studien sind notwendig, um den erwarteten Benefit dieser Modifikation beurteilen zu können. Ein klinisches Beispiel zeigt **Abbildung 9**.

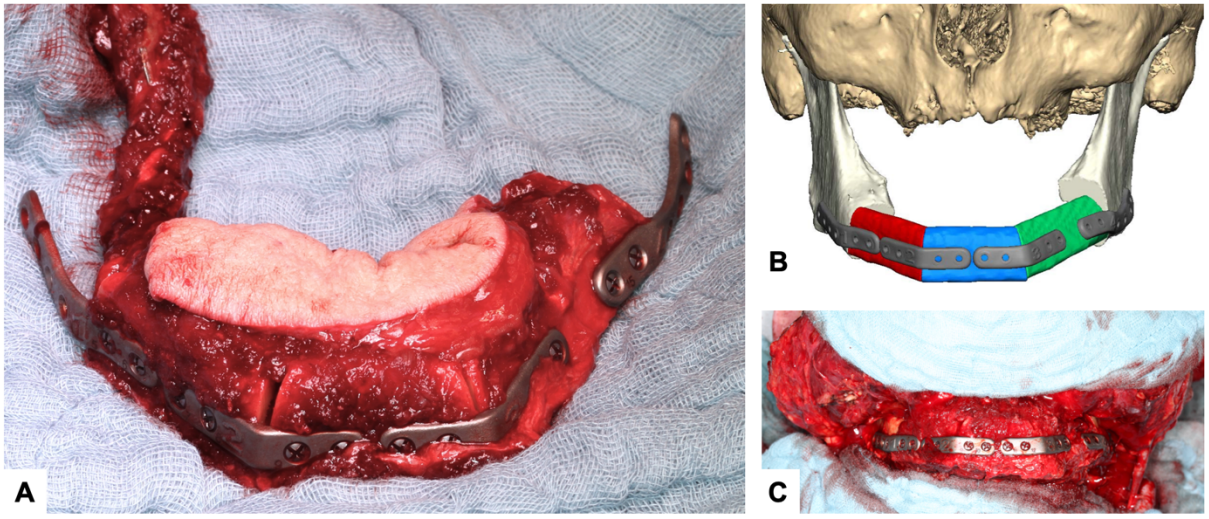

Abbildung 9. Trisegmentale einzeitige Mandibularekonstruktion bei einem 62-jährigen Patienten aufgrund eines cT3 cN0 cM0 Plattenepithelkarzinoms des anterioren Mundboden aus unserer Klinik. (**A**) Zusammengesetztes Fibulatransplantat mit aufliegender Hautinsel mit separaten, lastteilenden patienten-spezifischen Platten (Stärke: 1,5 mm). Das proximale Gefäßstielende liegt dorsal auf der Lingualseite des IV. Quadranten. (**B**) Ergebnis der virtuellen Planung (Verwendung mit freundlicher Genehmigung von KLS Martin) und (**C**) die finale Neo-Mandibula.

Ein weiterer relevanter Aspekt in diesem Zusammenhang ist, nach welcher Zeitspanne eine vollständige radiologische Ossifikation beobachtet werden kann bzw. eintritt. Diese Frage ist aktuell Gegenstand weiterer Forschungsarbeit. Im Detail wird dabei untersucht, wie sich der natürliche Verlauf einer unvollständigen Verknöcherung im Follow-up und im klinischen Verlauf bemerkbar macht. Es werden Anzahl und Art chirurgischer Revisionseingriffe sowie die Rate erfolgreicher dentaler (implantologischer) Rehabilitationen analysiert. Erste Datenauswertungen auf der

Basis von 133 mikrovaskulären Rekonstruktionen mit freiem Fibulatransplantat (PSI: *n* = 64; Konventionell: *n* = 69) zeigen, dass der in Originalarbeit 6 [154] beschriebene signifikant höhere Anteil unvollständiger Verknöcherungen zum Zeitpunkt 12±3 Monate postoperativ auch über die Intervalle 12-24, 24-36 und >36 Monate post OP erhalten bleibt (**Abbildung *10***). In die Auswertung gingen – im Gegensatz zur genannten Originalarbeit 6 – auch Oberkieferrekonstruktionen ein. Aktuell erfolgt die statistische Auswertung der Daten.

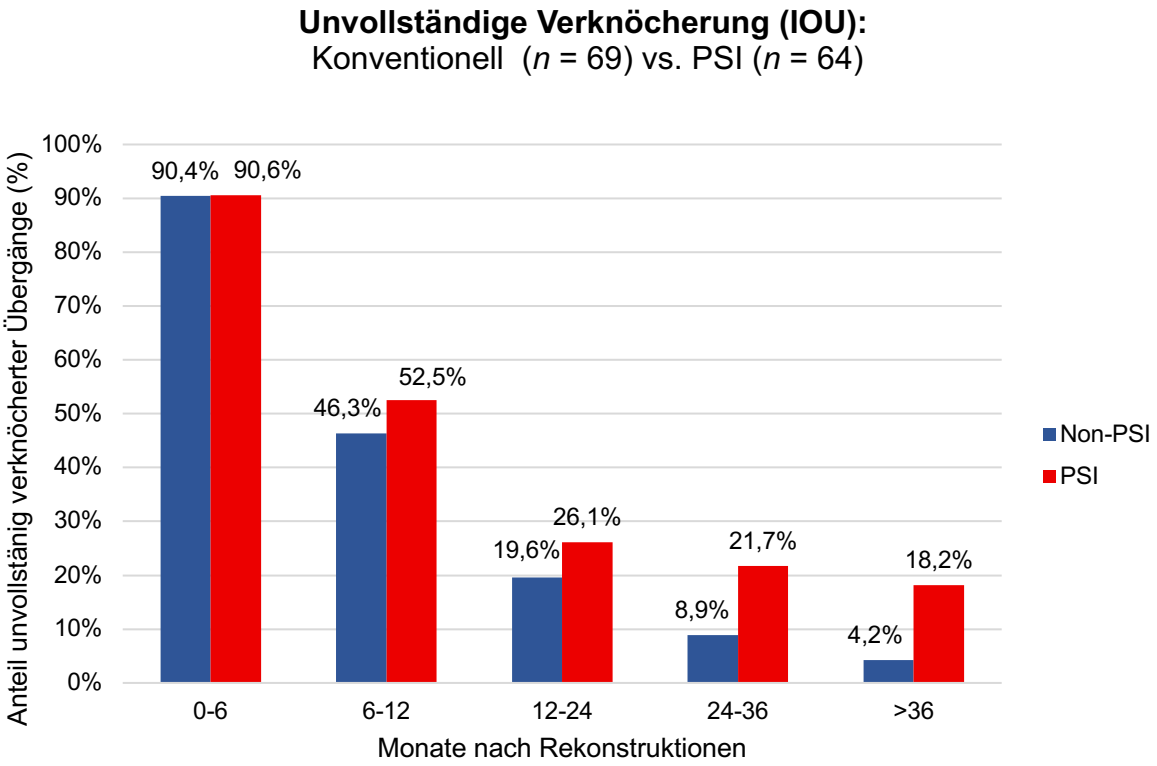

Abbildung 10. Vergleich der Osteosyntheseverfahren Konventionell vs. PSI. Das Diagramm zeigt die relativen Anteile mindestens eines unvollständig (IOU) verknöcherten Überganges je Patient gruppiert nach Zeitintervall post Kieferrekonstruktion mit einem Fibulatransplantat (Monate).

4. Diskussion

4.1. Wie hoch ist die Rate der Lappenverluste und in welcher Form treten sie auf?

Die Originalarbeit 1 (Partial and Total Flap Failure after Fibula Free Flap in Head and Neck Reconstructive Surgery: Retrospective Analysis of 180 Flaps over 19 Years) [155] setzte sich mit dieser Fragestellung auseinander und explorierte Risikofaktoren sub- und totalen Lappenverlusts.

In dem Zeitraum von Januar 2002 bis Juni 2020 wurden 180 Kieferrekonstruktionen mit einem freien Fibulatransplantat durchgeführt. Vollständige Lappenerfolge traten in 80,0 % (*n* = 144) und (sub-)totale Lappenverluste in 20,0 % (*n* = 36) der Fälle auf. Totale Lappenverluste (*TFF*) wurden definiert als solche, die auf einen Verschluss der Makroperfusion (Thrombose bzw. Embolie, Strangulation und Abknicken des Gefäßstiels) und im unmittelbaren postoperativen Verlauf auftraten. Als partielle Lappenverluste (*PFF*) hingegen wurden solche definiert, die Teil- oder Totalverluste der Hautinsel und/oder Verlust einzelner knöcherner Segmente bei polysegmentalen Rekonstruktionen im kurz- bis mittelfristigen postoperativen Verlauf nach sich zogen. Sie sind die Folge von Mikroperfusionsstörungen. *PFF* trat in 8,9 % (*n* = 16) und TFF in 11,1 % (*n* = 20) des Gesamtkollektivs auf. Dabei setzte sich die Gruppe PFF aus Teilverlusten der Hautinsel (*n* = 11), dem Verlust einzelner Transplantatsegmente (*n* = 4) sowie einer Kombination beider Komponenten (*n* = 1) zusammen. Für Details sei auf **Tabelle 3 und 4** im Anhang sowie auf Table 1 der Originalarbeit 1 (Page 8 of 21) verwiesen.

a. <u>Faktor Alter</u>

In der spezifischen Analyse wurden keine statistisch signifikanten Unterschiede in Bezug auf den Faktor *Alter* bei Fibula-Transplantation zwischen den Gruppen *PFF* und *TFF* festgestellt. Auch unter Einbeziehung der Gruppe *Erfolg* (**Tabelle 3**) ergab die asymptotische Signifikanz im Kruskal-Wallis-Test ebenfalls keinen signifikanten Unterschied (*p* = 0,165). Einen statistischen Trend zeigte der Mann-Whitney-U-Test (*p* = 0,101), wenn die Gruppen *Erfolg* und *PFF (*57,3 ± 13,5 Jahren) zusammengefasst und mit TFF (62,5 ± 9,5 Jahren) verglichen wurden (**Tabelle *4***).

In der Literatur sind allgemeine Verlustraten für mikrovaskuläre, freie Lappen zwischen 0,8 - 6,0 % beschrieben [156]. Fokussiert auf ältere Patientengruppen ergeben sich etwas höhere Raten von 1,8 % - 7,0 % [157-162]. Die Datenlage zu Erfolgsraten nach Rekonstruktionen mit dem freien Fibulatransplantat im Kopf-Hals-Bereich ist in diesem Punkt lückenhaft und neuere Studien berichten über Misserfolgsraten zwischen 7 – 12,4 % [132, 134, 163]. Altersgruppenspezifische Erfolgs- bzw. Misserfolgsraten für das Fibulatransplantat liegen in der Literatur nicht vor. Die eigene Auswertung hat ergeben, dass in der Altersgruppe zwischen 70 < 80 Jahren die Rate totaler Lappenverluste (TFF) 20,8 % und die partieller (PFF) 16,7 % betrug. Es zeigte sich ein Trend einer zunehmenden Rate von TFF zwischen den Altersgruppen der 4. und 8. Lebensdekade (**Abbildung *11***).

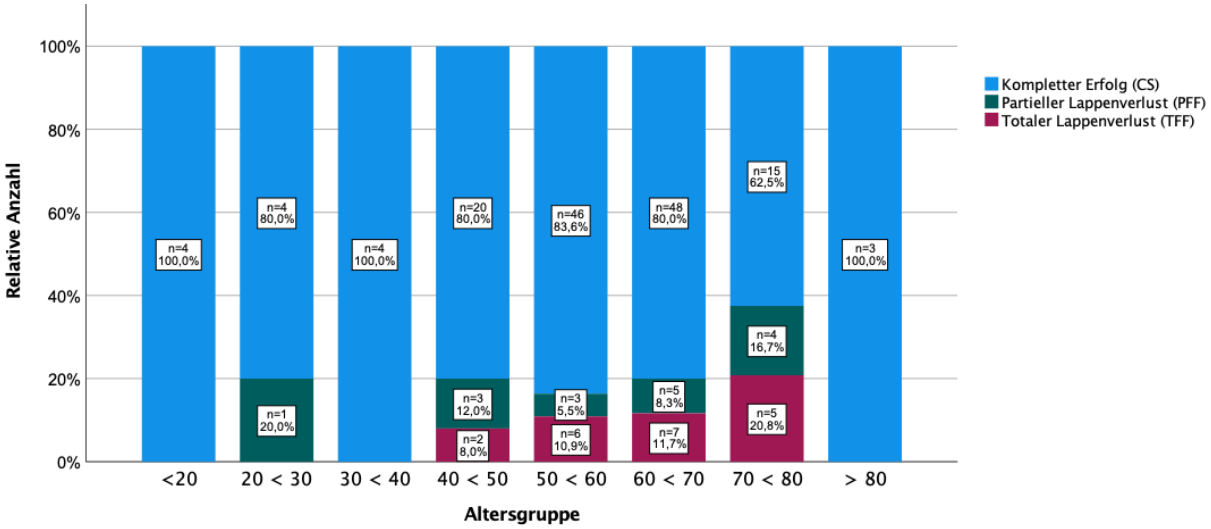

Abbildung 11. Ergebnisse des mikrovaskulären Fibula-Transfers aufgeteilt nach Altersgruppen.

Jubbal et al. analysierten die Ergebnisse freier Lappentransplantate. Sie nutzten die Datenbank des *American College of Surgeons National Surgical Quality Improvement Programs* (ACS NSQIP) und konnten 5951 Fälle in die Auswertung einschließen [164]. Im Ergebnis fanden sie, dass das Alter nicht signifikant mit der Rate chirurgischer oder medizinischer Komplikationen, Lappenversagen oder Reoperationen verbunden war. Mit zunehmendem Lebensalter beobachteten sie einen Anstieg der chirurgischen (p = 0,001) und medizinischen (p < 0,001) Komplikationsraten und folgerten, dass der Faktor *Alter* nicht als alleinige Grundlage für eine Kontraindikation herangezogen werden sollte. Der präoperativen Beurteilung von Komorbiditäten und des

physiologischen Alters solle mehr Augenmerk geschenkt werden, da sich die Optimierung der Komorbiditäten positiv auf die Ergebnisse mikrochirurgischer freier Lappenrekonstruktionen in der älteren Bevölkerung auswirkt. Eine britische Arbeitsgruppe um *Sierakowski et al.* untersuchte retrospektiv die Ergebnisse mikrovaskulärer Transplantate bei über 70-jährigen Patienten [165] und ermittelte eine Verlustrate von 4,5 % (n = 5 von 110). Sie fanden keine statistisch signifikanten Unterschiede der Komplikationsraten zwischen Patienten im Alter von 70-79 und ≥ 80 Jahren. Die Anästhesiezeit wurde als statistisch signifikanter Prädiktor für postoperative medizinische Komplikationen (Odds Ratio 1,345, 95% Konfidenzintervall 1,117-1,663, p = 0,001) beschrieben. Ein freier Gewebetransfer kann bei älteren Patienten mit einem hohen Maß an technischem Erfolg und geringer operativer Sterblichkeit durchgeführt werden, jedoch sollte die Operationsdauer (Narkosedauer) auf ein Minimum begrenzt werden. Einschränkend muss zu den beiden letztgenannten Untersuchungen ergänzt werden, dass dabei nicht ausschließlich mikrovaskuläre Rekonstruktionen der Kopf-Hals-Region ausgewertet wurden. Lediglich freie Lappen nach Tumorresektionen der Kopf-Hals-Region untersuchten *Ferrari et al.* [166] und gaben dabei eine Lappenverlustrate von 3,5 % (n = 13 von 373) an. Der mikrovaskuläre Gewebetransfer könne bei älteren Patienten mit hoher Sicherheit und Erfolg durchgeführt werden [166]. Das mittlere Alter wurde mit 59,7 Jahren (Spanne: 25 – 87 Jahre) angegeben. Sie bestätigen damit das Ergebnis anderer Studien, dass das chronologische Alter allein nicht als ausschließliches Entscheidungskriterium für oder gegen eine mikrovaskuläre Rekonstruktion angesehen werden soll und betonen den Stellenwert der Berücksichtigung von Komorbiditäten. Im Vergleich dazu wies die hier untersuchte Kohorte ein mittleres Alter von 57,9 ± 13,2 Jahren (Spanne: 14,75 – 82,75 Jahre) auf. Die französische Multicenter-Studie um *Poisson et al.* erhob an 215 Patienten nach Rekonstruktion im Kopf-Hals-Bereich nach ablativer Tumorchirurgie eine Lappenverlustrate von 5,6 % [167]. Das mittlere Alter ihres Kollektivs betrug 58,6 Jahre (Spanne: 25 – 85 Jahre). *Kesting et al*. fanden, dass das Alter ein Risikofaktor für einen längeren Intensivstationsaufenthalt und eine höhere Komplikationsrate war. Sie konnten aber keinen Einfluss auf die Dauer des Krankenhausaufenthalts und den Gesamterfolg mikrovaskulärer Rekonstruktionen durch das Alter feststellen [168].

Zusammenfassend kann festgestellt werden, dass der Faktor *Alter* in der untersuchten Gruppe keinen statistisch signifikanten Einfluss auf das Fibula-Transplantationsergebnis aufwies.

b. <u>Faktor BMI</u>

Für den gruppierten Faktor *Body Mass Index* (Körpergewicht [kg| / Körpergröße^2 [m]) konnte kein statistisch signifikanter Unterschied zwischen den Gruppen *PFF* und *TFF* festgestellt werden. Der direkte Rangvergleich aller drei Gruppen (**Tabelle *3***) ergab im Kruskal-Wallis-Test keinen signifikanten Unterschied (p = 0,814). Auch nach Gruppenzusammenschluss von *Erfolg* und *PFF* konnte im Vergleich mit *TFF* im Mann-Whitney-U-Test kein statistisch signifikanter Zusammenhang zwischen BMI und dem Transplantationsergebnis (p = 0,685) beobachtet werden (**Tabelle *4***).

Die Literatur berichtet uneinheitlich über die Auswirkungen eines erhöhten BMI auf die chirurgische Komplikationsrate. Patienten mit einem höheren BMI und Operationen an der *Gl. thyroidea* bzw. *Gl. parathyroidea* weisen eine höhere postoperative Morbidität und insbesondere mehr Wundkomplikationen auf. Klinisch scheint das unerheblich zu sein, daher empfehlen die Autoren betroffene Patienten ähnlich zu behandeln wie solche mit Normalgewicht [169]. Andere Studien bestätigen dieses Vorgehen [170]. Bei Eingriffen im Bereich des Mittel- und Innenohres fanden sich keine nachweisbaren Auswirkungen eines erhöhten BMI auf die chirurgische Komplikationsrate [171]. Eine retrospektive Untersuchung von Patienten mit Kopf-Hals-Tumoren ergab, dass solche mit einem höheren BMI gar sowohl eine niedrigere krankheitsbedingte Sterblichkeitsrate als auch eine Gesamtsterblichkeitsrate aufwiesen und so eine Verlängerung der Gesamtüberlebenszeit im Vergleich zu untergewichtigen oder normalgewichtigen Patienten beobachtet werden konnte [172]. Untersuchungen bei verschiedenen chirurgischen Eingriffen zeigten, dass ein erhöhter BMI mit einem erhöhten Risiko für chirurgische Infektionen in Verbindung gebracht werden konnte [173, 174]. Ein niedriger BMI bzw. Untergewicht bei der Diagnose war ein unabhängiger, prognostisch ungünstiger Faktor [175, 176]. Über die Auswirkungen eines isoliert erhöhten BMI auf die Ergebnisse des freien Gewebetransfers und lokale Wundinfektionen bei Patienten mit Kopf- und Halstumoren ist bislang wenig in der Literatur veröffentlicht [174, 177].

Adipositas (BMI > 30) war mit einem besseren Ergebnis assoziiert und war kein unabhängiger Risikofaktor für postoperative Komplikationen bei freiem Gewebetransfer im Kopf-Hals-Bereich [178, 179]. *Patel et al.* fanden, dass der BMI, Alter, ASA-Klasse, präoperative Hämoglobinkonzentration und Tracheotomie unabhängige Risikofaktoren für größere Komplikationen sind [180]. Ein höherer BMI/Adipositas ist ein Risikofaktor für peri- und postoperative medizinische Komplikationen [181]. Ein hoher BMI, Diabetes mellitus, arterielle Hypertension, Atherosklerose und arterielle oder venöse Transplantate wurden von *Kopp et al.* als Risikofaktoren für einen Lappenverlust identifiziert ($p < 0,05$) [182].

Die Auswertung der gewonnen Daten zeigt, dass der Faktor *BMI* in unserem Patientenkollektiv keinen statistisch signifikanten Einfluss auf den Lappenerfolg hatte.

c. <u>Faktor ASA-Klasse</u>

Nach Zusammenschluss der Gruppen *Erfolg* und *partieller Lappenverlust (PFF)* konnte im Vergleich mit der Gruppe *totaler Lappenverlust (TFF)* im Mann-Whitney-U-Test ein statistisch signifikanter Zusammenhang zwischen ASA-Klasse und dem Transplantationsergebnis ($p = 0,034$) beobachtet werden (**Tabelle *4***). Lappenerfolge (*Erfolg und PFF*) wurden in 42,5 % ($n = 62$) vs. *TFF* in 65 % ($n = 13$) der Fälle beobachtet, wenn sie als ≥ ASA-Klasse 3 bewertet worden waren.

Die Literatur weist darauf hin, dass die ASA-Klasse mit schwerwiegenden medizinischen und chirurgischen Komplikationen in Verbindung steht [183, 184]. *Ferrari et al.* [166] berichten, dass die ASA-Klasse mit einer statistisch signifikant höheren Inzidenz von Komplikationen bei Patienten < 75 Jahren verbunden war ($p < 0,0001$). Ein Alter von mehr als 70 Jahren war in einer prospektiven Studie an 215 Patienten mit einer signifikant höheren ASA-Klasse und einer kürzeren Operationsdauer vergesellschaftet [168]. ASA-Klasse und Operationsdauer erwiesen sich als unabhängige Risikofaktoren für operative Revisionen, und es konnte ein statistischer Trend hinsichtlich des Lappenversagens bei längeren Operationszeiten beobachtet werden [185]. In der Literatur korreliert die ASA-Klasse mit einer höheren Anzahl von postoperativen Komplikationen nach mikrovaskulären Rekonstruktionen [186, 187] und dem Gesamtüberleben [188]. *Poisson et al.* beschrieben als Ergebnis ihrer Multicenterstudien, dass die ASA-Klasse kein prädiktiver Faktor für ein Versagen des freien Lappens oder größere chirurgische Komplikationen war [167].

Die Ergebnisse unserer Untersuchung bestätigen, dass ein statistisch signifikanter Unterschied zwischen den Ergebnissen nach freiem Fibula-Transplantat und ASA-Klasse ≥ 3 vorliegt.

d. <u>Faktor Planungs- und Rekonstruktionsverfahren (analog vs. digital)</u>

Die Auswertung zeigte keine statistisch signifikanten Unterschiede hinsichtlich des Planungs- und Rekonstruktionsverfahrens zwischen den Gruppen *teilweisen (PFF)* und *totalen Lappenverlustes (TFF)*. Auch unter Einbeziehung der Gruppe *Erfolg* (**Tabelle *3***) ergab die asymptotische Signifikanz im Kruskal-Wallis-Test ebenfalls keinen signifikanten Unterschied (p = 0,678). Nach Zusammenschluss der Gruppen *Erfolg* und *partieller Lappenverlust (PFF)* konnte im Vergleich mit der Gruppe *totaler Lappenverlust (TFF)* im Mann-Whitney-U-Test ebenfalls kein statistisch signifikanter Zusammenhang zwischen Planungs- und Rekonstruktionsmethode und dem Transplantationsergebnis (p = 0,393) beobachtet werden (**Tabelle *4***).

Die durchgeführte Auswertung hat eine totale Lappenverlustrate (*TFF*) von 9,4 % für die konventionelle (Non-VSP) und 13,5 % für die virtuell geplante (VSP) Gruppe mikrovaskulärer Kieferrekonstruktionen mit freiem Fibulatransplantat des untersuchten Patientenpools ergeben. Damit sind die Erfolgsraten mit denen der Literatur vergleichbar. Aus einer Meta-Analyse mit insgesamt 713 eingeschlossenen Patienten von *Tang et al.* geht hervor, dass keine statistisch signifikanten Unterschiede hinsichtlich des Lappenversagens, Fisteln und lokalen Wundinfektionen zwischen den Gruppen VSP und Non-VSP gefunden wurden [100]. Sie schlussfolgern damit, dass die Methode VSP zu ähnlichen Komplikationsraten wie die Non-VSP führt. Angaben bezüglich partieller Transplantatverluste wurden nicht gemacht.

In der Analyse der Studiengruppe wurden *PFF* in der Non-VSP in 9,4 % (n = 10) und in 8,1 % (n = 6) in der VSP-Gruppe registriert. Die hier gefundenen isolierten, sub- bzw. totalen Verluste der Hautinsel traten in insgesamt n = 11 Fällen, davon n = 9 in der Non-VSP-Gruppe, auf. Als Gründe hierfür sind mechanische Traumata und Manipulationen während der Transplantatpräparation und -formgebung zu sehen, wie bei der Präparation der Knochensegmente und der Anpassung der Osteosynthese. Die Freihandanpassung ist als gewebetraumatischer zu bewerten. Die Anwendung von individuellen Sägeschablonen hat sich als vorteilhaft erwiesen, da insbesondere bei polysegmentalen Rekonstruktionen sie die Transplantatglieder sicher fixieren und

ein Abscheren bzw. Torquieren des Gefäßstiels verhindern und die Handhabung während der Präparation deutlich erleichtern [97]. Dabei ist beachtenswert, dass hierzu eine ausgedehntere Präparation der lateralen Fibulafläche für einen präzisen Schablonensitz unumgänglich ist. Damit ist eine deutlich umfangreichere Präparation der dort inserierenden Muskulatur notwendig, was sich auf peri- und endostale Durchblutung auswirken kann [189-192]. Selbst zur Schablonenfixation temporär eingedrehte, monokortikale Schrauben können zu Durchblutungsstörungen und Gewebequetschungen führen (**Abbildung *13*** und **Abbildung *14***) [48, 193, 194].
Alle partiellen Knochentransplantatverluste ($n = 4$) wurden in der VSP-Gruppe dokumentiert. Die Hälfte der Knochensegmentverluste trat nach einer adjuvanten Strahlentherapie im Sinne einer Osteoradionekrose auf. In den beiden anderen Fällen ließ sich keine Strahlentherapie als Ursache für die Mikrozirkulationsstörung, bei intraoperativ Handdoppler-sonographisch gesicherter Perfusion der Transplantatarterie, ausmachen. Die Originalarbeit 1 beschreibt den klinischen und radiologischen Verlauf eines Falls in den Figuren 3 – 5 [155]. Es wird die Hypothese aufgestellt, dass sowohl die Anlage von Sägeschablonen als auch die Fixierung des Knochensegments an der patienten-spezifischen Osteosyntheseplatte (PSI) mit Non-Locking-Schrauben ein perfusionsrelevantes Trauma für das periostale Gewebe des Transplantatsegments darstellt. Die Hypothese wird durch Ergebnisse von Tierversuchen gestützt, die ergeben haben, dass sich die periostale Blutgefäßdichte an und unter einer Osteosyntheseplatte signifikant in Abhängigkeit des knochenoberflächennahen Plattendesigns unterscheidet [195]. Somit ergibt sich, dass eine Beeinträchtigung der Durchblutung des knöchernen Fibulasegments resultieren kann. Zur Bewertung dieser These wurde die Dichte und Verteilung der periostalen und septo-kutanen Abgänge, die sog. „kleinen“ Gefäße, der *A. fibularis* anhand der präoperativen CTA-Untersuchungen für VSP erarbeitet (Originalarbeiten 4 und 5) und im Kapitel 4.3. diskutiert.

Zusammenfassend kann festgestellt werden, dass *Teilverluste (PFF)* der Hautinsel in der Non-VSP und partielle Knochensegmentverluste *(PFF)* in der VSP-Gruppe dominierten.

e. <u>Faktor Rekonstruktionszeitpunkt</u>

Der Parameter *Rekonstruktionszeitpunkt* (ein- vs. zweizeitig) übte keinen statistisch signifikanten Unterschied im Vergleich der Gruppen *partiellen (PFF)* und *totalen Transplantatverlustes (TFF)* aus (p = 0,610). Im weiteren Vergleich mit der Gruppe *Erfolg* (**Tabelle *3***) ergab die asymptotische Signifikanz im Kruskal-Wallis-Test keinen signifikanten Unterschied (p = 0,488). Nach Zusammenschluss der Gruppen *Erfolg* und *partieller Lappenverlust (PFF)* konnte im Vergleich mit *TFF* im Mann-Whitney-U-Test kein statistisch signifikanter Zusammenhang (p = 0,479) bestimmt werden (**Tabelle *4***).

Wurden in der Vergangenheit noch die Methode [196] und der Zeitpunkt für die Rekonstruktion der Kiefer diskutiert, so dominiert inzwischen das Verfahren der einzeitigen Rekonstruktion des Unterkiefers [197] mit mikrovaskulären Transplantaten wie dem hier untersuchten Fibulatransplantat. Für Oberkieferrekonstruktionen zeichnet sich in der Literatur ebenfalls ein Trend zu einzeitigen Rekonstruktionen ab [198]. Seine Beliebtheit fußt u.a. – wie bereits eingangs erwähnt – auf der Vielseitigkeit und den Vorteilen bei kaufunktioneller Rehabilitation mit dentalen Implantaten [53, 54, 199]. Zudem wird über die Möglichkeit der zeitgleich mit der Rekonstruktion stattfindenden Implantateinbringung in der Literatur berichtet [200-204] und dies auch im Zusammenhang mit einzeitigen onkologischen Rekonstruktionen [205].

Für einzeitige mikrovaskuläre Rekonstruktionen sprechen ideale anatomische Verhältnisse während der Präparation der Gefäße, fehlende Vernarbung, schnellere kaufunktionelle Rehabilitation und Verbesserung der Lebensqualität [206]. Die Befürworter der zweizeitigen Rekonstruktion betonen, dass zur Beurteilung der knöchernen Resektionsränder kein adäquates intraoperativ anwendbares Verfahren – analog der pathohistologischen Schnellschnittuntersuchung – zur Verfügung steht. *Schaaf et al.* berichten in diesem Zusammenhang über die Anwendung der *flat-panel Volume Computed Tomography* (fpVCT) [207], einer Methode, die zur hochauflösenden Darstellung knöcherner Strukturen geeignet ist [208-210]. In einer Untersuchung fanden sie in 95,7 % übereinstimmende Ergebnisse für eine Knocheninfiltration in der fpVCT und dem histologischen Befund. Bezogen auf die knöchernen Absetzungsränder ergab sich eine Übereinstimmung von 100 %. Die Autoren folgerten daher, dass die Methode die diagnostische intraoperative Lücke schließen kann [207]. Andererseits müsste sonst nach erfolgter Rekonstruktion im Falle positiver knöcherner Absetzungsränder das bereits eingebrachte

Knochentransplantat verworfen werden [211]. Wir bevorzugen im Oberkiefer die zweizeitige Rekonstruktion nach konventioneller pathohistologischer Beurteilung der Absetzungsränder und der Unversehrtheit des Halses für die Mikrochirurgie, die dann im Anschluss an die Lymphadenektomie (Neck dissection) durchgeführt werden kann. Einen einzeitigen Rekonstruktionsmodus präferieren wir bei histologisch gesicherten, benignen Raumforderungen. Die einzeitige Rekonstruktion des Unterkiefers mit einem Fibulatransplantat stellt hingegen unsere Standardtherapie dar. Bei kompromittiertem Gefäßstatus der Unterschenkel, begrenzter Belastbarkeit des Patienten und Patientenwunsch werden alternative Rekonstruktionstechniken, wie unter anderem mit einer patienten-spezifischen Rekonstruktionsplatte, zumeist in Kombination mit einer regionalen oder gestielten Fernlappenplastik, gewählt.

In Zusammenschau der Ergebnisse kann festgehalten werden, dass in der ausgewerteten Studienpopulation der Zeitpunkt der Rekonstruktion keinen Einfluss auf das Transplantationsergebnis hatte.

4.2. Wie unterscheiden sich die Komplikationsraten zwischen analog und digital geplanten Rekonstruktionen?

4.2.1. Einfluss des Planungs- und Rekonstruktionsmodus auf das Auftreten von heterotopen Ossifikation (HO)

Die heterotope Ossifikation (HO) ist ein beschriebenes Phänomen u.a. nach rekonstruktiven Eingriffen im Mund-, Kiefer- und Gesichtsbereich mit mikrovaskulärem Fibulatransplantat (FFF). Das Auftreten von extraossären HO in der CT-Schichtbildgebung wird in der Literatur mit einer beachtlichen Spanne von bis zu 65 % bei andererseits sehr variabler klinischer Beschwerdesymptomatik angegeben [212-214]. Die ektopen knöchernen Massen können zu Funktionsstörungen wie Dysphagie, Sprechbeschwerden, Mundöffnungseinschränkungen (Trismus) sowie zu tast- und sichtbaren, störenden Befunden im Bereich des Gefäßstiels führen. Die durchgeführte eigene Studie an 102 Patienten ergab eine radiologisch nachgewiesene HO-Frequenz von 28,4 % (n = 29) [215]. Klinische Symptome traten in 9,8 % (n = 10) des untersuchten Kollektivs in Form von Dysphagie (n = 5), Trismus (n = 3) und

knöchernen Massen (*n* = 2) auf. Darüber hinaus können sie zu einer erheblichen Verlegung des Mundraums führen, wie in der Originalarbeit 2 dargestellt ist [215]. Letztlich bestand nur in 4,9 % (*n* = 5) der gesamten Studiengruppe chirurgischer Interventionsbedarf, bei denen die verkalkten Strukturen im Bereich des Halses (*n* = 1, non-VSP) zur Verbesserung der Mundöffnung (*n* = 2, beide VSP) und Dysphagie (*n* = 2, beide VSP) entfernt wurden. Der Gruppenvergleich brachte hervor, dass ein signifikanter Altersunterschied vorlag und HO häufiger bei jüngeren Patienten beobachtet wurde (HO-: 58,69 ± 11,92 vs. HO+: 52,30 ± 14,39 Jahre; *p* = 0,002). In der untersuchten Kohorte konnte kein signifikanter Zusammenhang zwischen dem Auftreten von HO und dem Planungs- bzw. Rekonstruktionsverfahren (HO+: VSP: 33,3 % (*n* = 14) vs. Non-VSP: 25,0 % (*n* = 15); *p* = 0,381) sowie der Anzahl der verwendeten Segmente bestimmt werden.

Der Untersuchung der HO als Komplikation wurde im Rahmen dieser Arbeit berücksichtigt, weil dem Periost der Fibula, neben lokalen mechanischen Faktoren und Zytokin-Interaktionen [216], eine Schlüsselrolle bei der Entstehung der HO beigemessen wird [217-219]. Für die Hauptrolle des Periostes in der Genese der HO spricht insbesondere, dass bei Modifikationen der Operationstechnik, bei denen der Gefäßstiel vollständig vom Periost separiert wird, keinerlei Bildung von HO beobachtet werden konnte [220, 221]. Andererseits wird in der Literatur anhand von Einzelfallberichten eines faszio-kutanen Radialislappens [222] und eines seitlichen Oberarmlappens [223] aufgezeigt, das HO des Gefäßstiels auch ohne Periostbeteiligung auftreten kann. *Sierra et al*. beschreiben das osteogene Potential des Periosts eindrucksvoll in Form eines vaskularisierten Fibula-Periost-Lappens (VFPF) in Kombination mit einem Allotransplantat nach Resektion eines Ewing-Sarkoms am rechten Unterkieferkörper eines 11-jährigen Mädchens [224]. *Trignano et al.* berichten über eine interessante Modifikation für unisegmentale Fibulatransplantate, um die Rate der knöchernen Vereinigung zu erhöhen. Sie empfehlen insbesondere bei einer kleinen Knochenkontaktfläche zwischen Fibulatransplantat und Unterkiefer die Verwendung eines periostalen Überschusses, um eine ausreichende Blutversorgung des rekonstruierten Unterkiefers und der Hautinsel zu gewährleisten, was zu einer geringeren Komplikationsrate und einer verbesserten Verknöcherung führte [225].

Insbesondere im Zusammenhang mit der Methode VSP mit PSI, und dem damit verbundenen schablonengeführten Transfer, wird dem Periost der Fibula eine Schlüsselrolle zuteil.

1. Die Geometrie der (korrespondierenden) Osteotomieflächen wird mittels Übertragungsschablonen kodiert. Zum präzisen Sitz müssen diese flächenschlüssig auf die Fibula aufgesetzt und mittels Schrauben fixiert werden. Das Periost bedeckende Weichgewebe (**Abbildung *13***) und die darin verlaufenden „kleinen Gefäßen“ können hierdurch kritisch traumatisiert werden (**Abbildung *14*** und **Abbildung *17***) [190].

2. Eine Zunahme des Spaltes zwischen Schablone und Knochenoberfläche durch eine „schützende“ periostale Weichgewebsmanschette führt zu einer Abnahme der Transplantatsegmentlänge. Mittels Trigonometrie kann gezeigt werden, dass bei einem Schablonen-Knochenabstand pro 1 Millimeter sich das Segment an jeder Schnittfläche bei einem Winkel von 60° um 0,577 mm, bei 45° um 1 mm und bei 30° um 1,73 mm verkürzt.

$$\tan\alpha = \frac{Gegenkathete}{Ankathete} \tag{1}$$

$$\text{Ankathete} = \frac{Gegenkathete}{\tan\alpha} \tag{2}$$

Eine Fehlpositionierung der Schablone führt zu einem vergrößerten Schablonen-Knochenabstand. Er entspricht der Gegenkathete (roter Pfeil in D, **Abbildung *12***). In dem Beispiel der **Abbildung *12*** würde ein Abstand von 1 mm bei $\alpha_1 = 58°$, $\alpha_2 = 55°$, $\alpha_3 = 56°$ und $\alpha_4 = 87°$

$$\sum_{i=1}^{4} \frac{1}{\tan\alpha_i} = \frac{1}{1{,}6} + \frac{1}{1{,}43} + \frac{1}{1{,}48} + \frac{1}{19{,}08} = 2{,}07 \tag{3}$$

zu einer Verkürzung von insgesamt 2,07 mm führen.

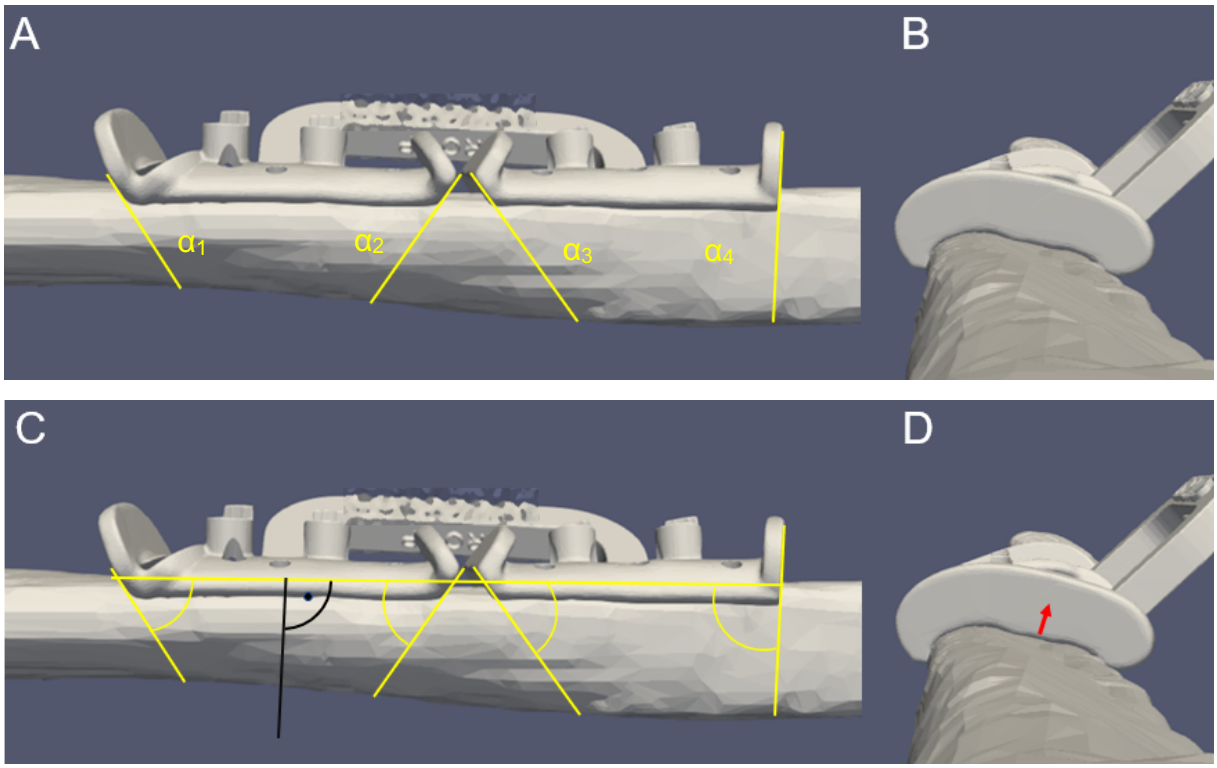

Abbildung 12. Einfluss der Schablonenposition auf die Segmentlänge. **(A)** Exakt dem Knochen aufsitzende Sägeschablone. In Gelb sind die Osteotomielinien bzw. -ebenen eingezeichnet. **(B)** Flächenbündiger Schablonensitz in der Ansicht von schräg axial. **(C)** Die Winkel α_1, α_2, α_3 und α_4 definieren die Osteotomieebene. **(D)** Jede Inkongruenz führt zu einem Offset - einem vergrößerten Schablonen-Knochenabstand (roter Pfeil).

3. Das Periost wird bei intersegmentaler Präparation (Anlage der Gehrungsschnitte) nicht exzidiert. Es wird an den Flanken der Sägeschablone inzidiert und aus der Osteotomiezone herausgehalten (**Abbildung *14*** und **Abbildung *15***).

4. Der später verworfene proximale Anteil der Fibula wird im Rahmen der Präparation des Gefäßpedikels von Periost befreit, sodass Anteile dessen an der Gefäßachse verbleiben (**Abbildung *14***). In diesem Punkt bestehen keine Unterschiede im präparatorischen Vorgehen zwischen der konventionellen Freihand- und der schablonengeführten Methode.

5. Das PSI wird oberflächenkongruent gefertigt. Daraus leitet sich ein gewölbter Querschnitt mit gratartigen Rändern über der Fibulasektion ab, die die periostale Perfusion in Kombination mit transplantatseitigen, nicht-verriegelnden (non-locking) Schrauben beeinträchtigen können (**Abbildung *18***

und C2-4 in Figure 5 in Originalarbeit 1). Bei Verwendung von non-locking Schrauben besteht somit die Gefahr, dass die Platte das bedeckende Weichgewebe und gleichzeitig die Blutversorgung des darunter liegenden Periosts schädigt [191]. Schließlich werden die Knochensegmente bei Verwendung von non-locking Schrauben durch das Prinzip „Zugschraube“ gegen die Unterseite der Platte herangezogen, was zu einer Knochenresorption unter der Platte und zu einer Lockerung der Schrauben führen kann bzw. führt [192]. PSI sind zwar ideal oberflächenkongruent modelliert, jedoch führt bereits eine geringe Fehlpositionierung der Schablone zu einer Positionsabweichung und damit zu Störstellen unter der Platte. Die lokale Minderdurchblutung wiederum führt zu Resorptionen, bis ausreichend Raum für das Wachstum des Periosts vorliegt [190].

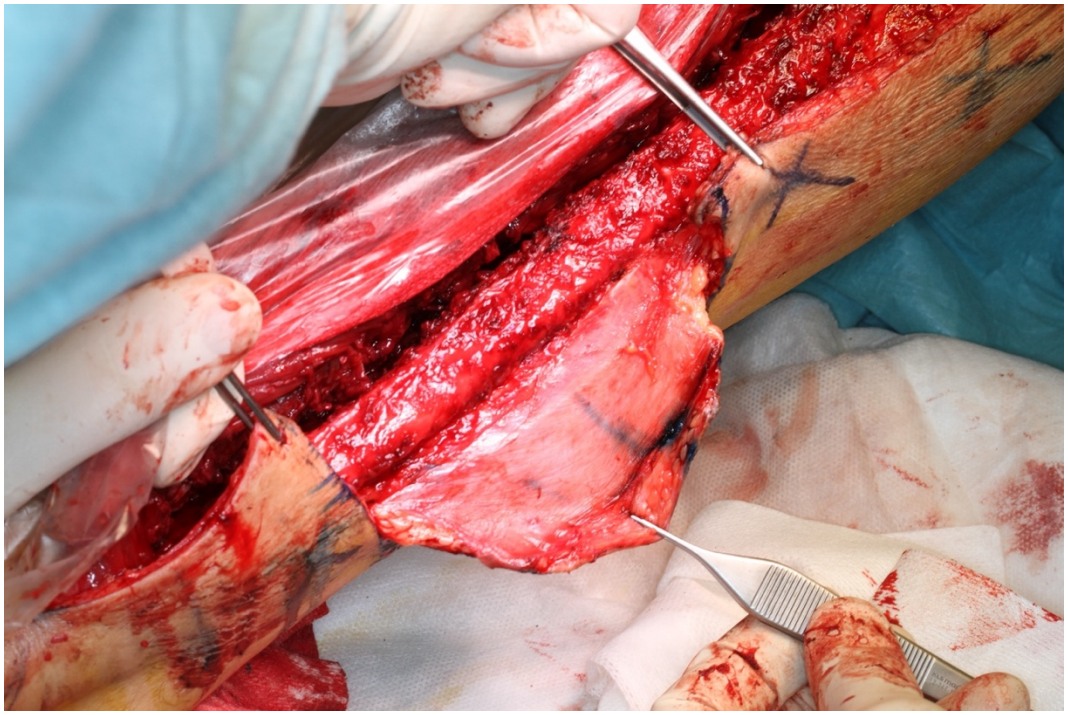

Abbildung 13. Definition der septo-kutanen Hautinsel nach Präparation der peronealen Muskulatur. Die blauen Kreuze auf der Haut markieren den Austritt von Perforatoren, die mit einem Handdoppler gefunden wurden. Beachte, dass die Fibula von einer verbleibenden Weichgewebemaschette bedeckt wird.

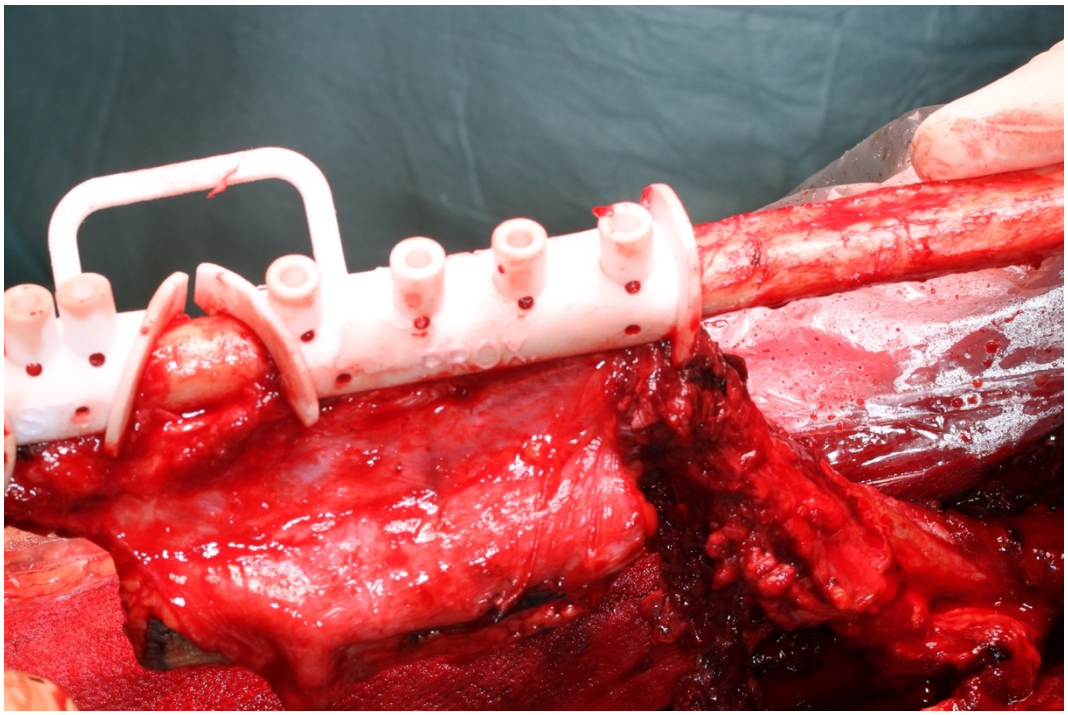

Abbildung 14. Die Schablone wurde aufgesetzt und fixiert. Der Gefäßstiel wird vom Fibulasegment mitsamt Periost gelöst. Das intersegmentale Periost wird eröffnet und für die Osteotomie zur Seite verdrängt (Verwendung mit freundlicher Genehmigung von KLS Martin).

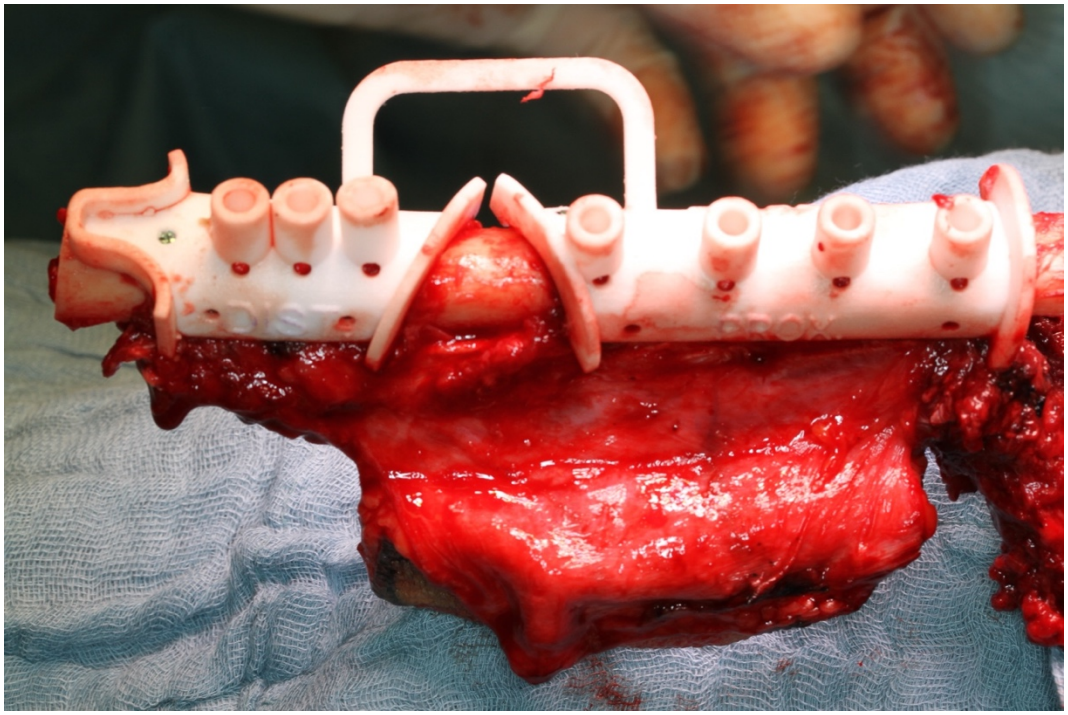

Abbildung 15. Vor intersegmentaler Osteotomie der Fibula. Das Periost wurde inzidiert und zur Seite verdrängt (Verwendung mit freundlicher Genehmigung von KLS Martin).

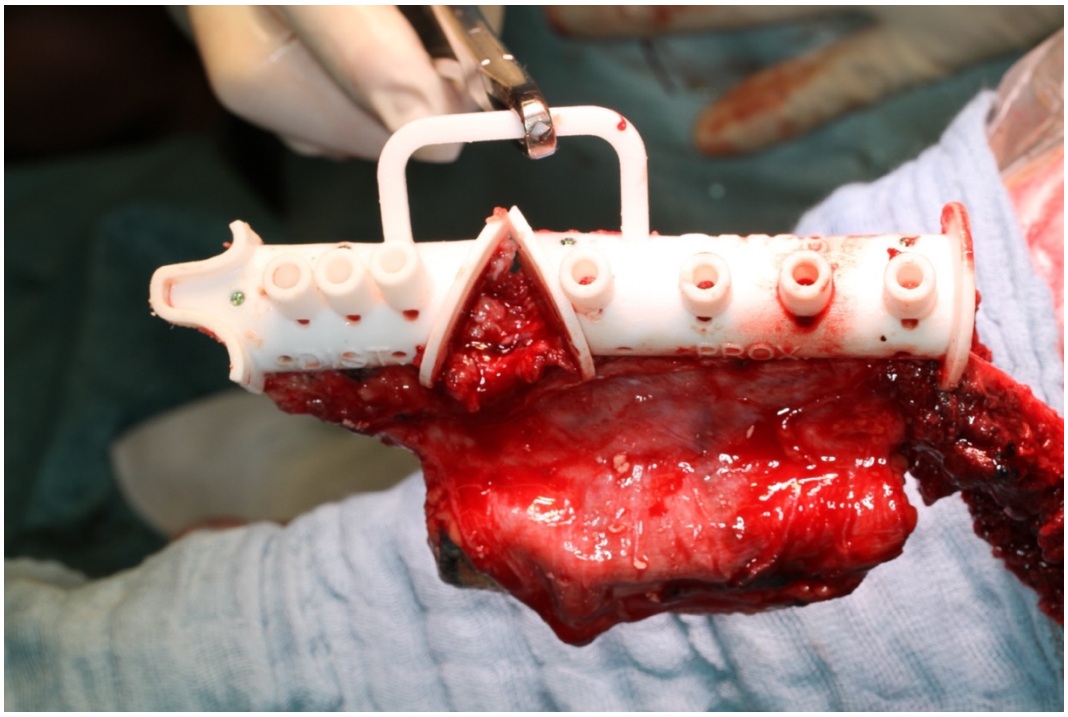

Abbildung 16. Nach intersegmentaler Osteotomie der Fibula. Das Periost des osteotomierten Knochenkeils wurde inzidiert und zur Seite verdrängt (Verwendung mit freundlicher Genehmigung von KLS Martin).

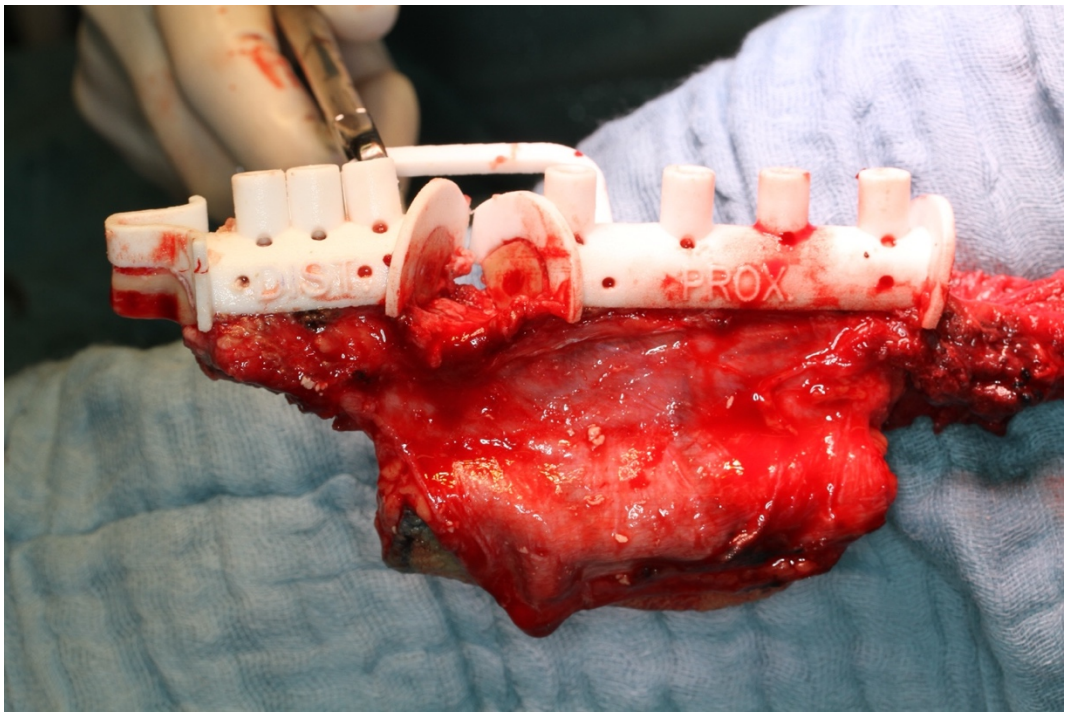

Abbildung 17. Nach der intersegmentalen Osteotomie stützt die Sägeschablone die Gefäßachse und verhindert ein unkontrolliertes Abknicken bzw. Traumatisieren des Gewebes. Zwischen der Schablonenunterseite und dem Knochen ist Weichgewebe eingequetscht (Verwendung mit freundlicher Genehmigung von KLS Martin).

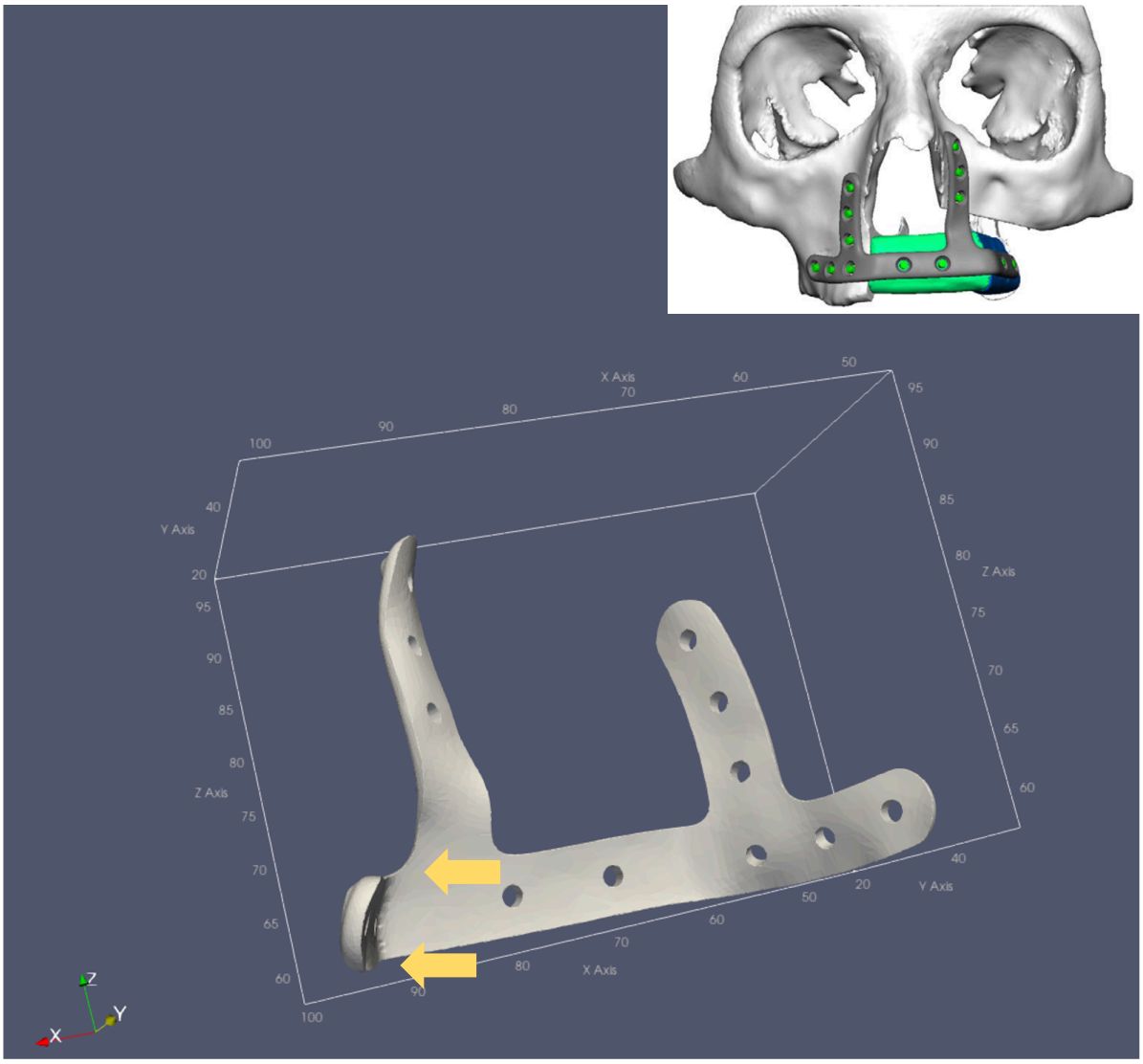

Abbildung 18. Blick auf die Rückseite eines patientenspezifischen Implantats (Osteosyntheseplatte). Der gewölbte Querschnitt zeigt gratartige Ausläufer an den Plattenrändern (gelbe Pfeile). Das Oberflächen-Modell (oben rechts) visualisiert den geplanten Sitz des PSI und die Position der Transplantatsegmente (Verwendung mit freundlicher Genehmigung von KLS Martin).

Zusammenfassend muss der Gefäßversorgung der Fibula und dem Periost während der Präparation große Beachtung eingeräumt werden. Es scheint angezeigt zu sein, ausschließlich verriegelnde (locking) Schrauben bei der PSI-Anwendung zu benutzen [191]. Da das Periost bei intersegmentalen Osteotomien (Gehrungsschnitte) nicht verworfen wird, wäre in Anlehnung an *Trigano et al*. ein gehäuftes Auftreten von ektopen Knochenmassen (HO Typ 3, siehe 4.2.2) zu erwarten [225].

4.2.2. Einführung einer Klassifikation für HO nach Kieferrekonstruktion

Die Datenanalyse ergab vier unterscheidbare Muster heterotoper Ossifikationen nach Kieferrekonstruktion. Damit konnte eine neue Klassifikation für HO nach mikrovaskulären Rekonstruktionen mit Fibulatransplantat vorgeschlagen werden (**Tabelle 2**).

Tabelle 2. Klassifizierungsvorschlag heterotoper Ossifikationen [215]

HO Typ-Definition	
Typ 1: HO der Übergangszone Fibula-transplantat zum Gefäßstiel	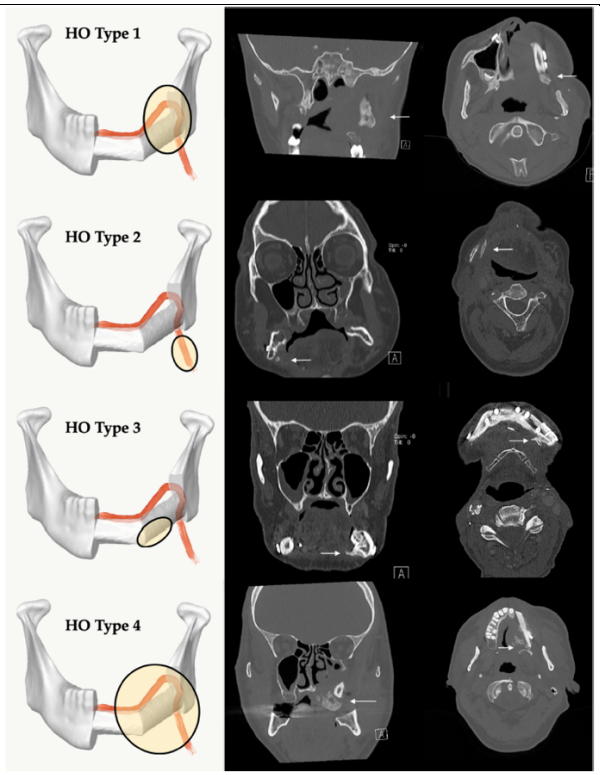
Typ 2: HO isoliert am Gefäßstiel ohne Kontakt zur Fibula	
Typ 3: HO erscheint isoliert am periossären Gewebe ohne Beteiligung des Gefäßstiels	
Typ 4: Kombination mit Verknöcherung des Pedikels und des periossären Gewebes.	

Die HO-Typ 1 ist im untersuchten Patientenkollektiv die am häufigsten beobachtete Variante heterotoper Knochenbildung, und zwar unabhängig vom Kiefer und der Rekonstruktionsmethode. Die sog. Knochenheilungs-/Frakturreparaturtheorie beschreibt die Ätiologie der HO an der Resektionsstelle. Die funktionelle Belastung des stabilisierten Knochentransplantats induziert Mikrobewegungen und fördert die Kallusbildung und die Knochenheilung [220]. Wir stellen die Hypothese auf, dass es sich bei dem kalzifizierten Gewebe um eine Form der exzessiven Knochenheilung handelt, die von der Resektionsstelle ausgeht und durch molekulare Stimulation der Rekrutierung von Osteoprogenitorzellen entlang des verbleibenden Periosts am Pedikel verläuft [216, 226, 227].

Das isolierte Auftreten von HO-Typ 2 (**Abbildung *19***) entlang des Gefäßstiels ist auf verbliebene, isolierte Periostzellen und Kontakt mit Osteozyten entlang des Gefäßpedikels des Fibulatransplantats zurückzuführen [228-231]. Ein langer Gefäßstiel mit verbleibenden Periostzellen bietet daher mehr Potenzial für die Entwicklung von HO [232]. Lokale Faktoren, molekulare Interaktionen und der Einfluss von BMPs auf die Induktion der Wundheilung fördern zudem die Entwicklung von HO [216]. Somit erwarteten wir, dass HO-Typ 2 insbesondere nach Oberkieferrekonstruktionen, bei denen ein langer Gefäßstiel zur Anastomose in der bevorzugten submandibulären Region bevorzugt wird, dominierend auftritt, was sich in der Auswertung aber nicht bestätigte.

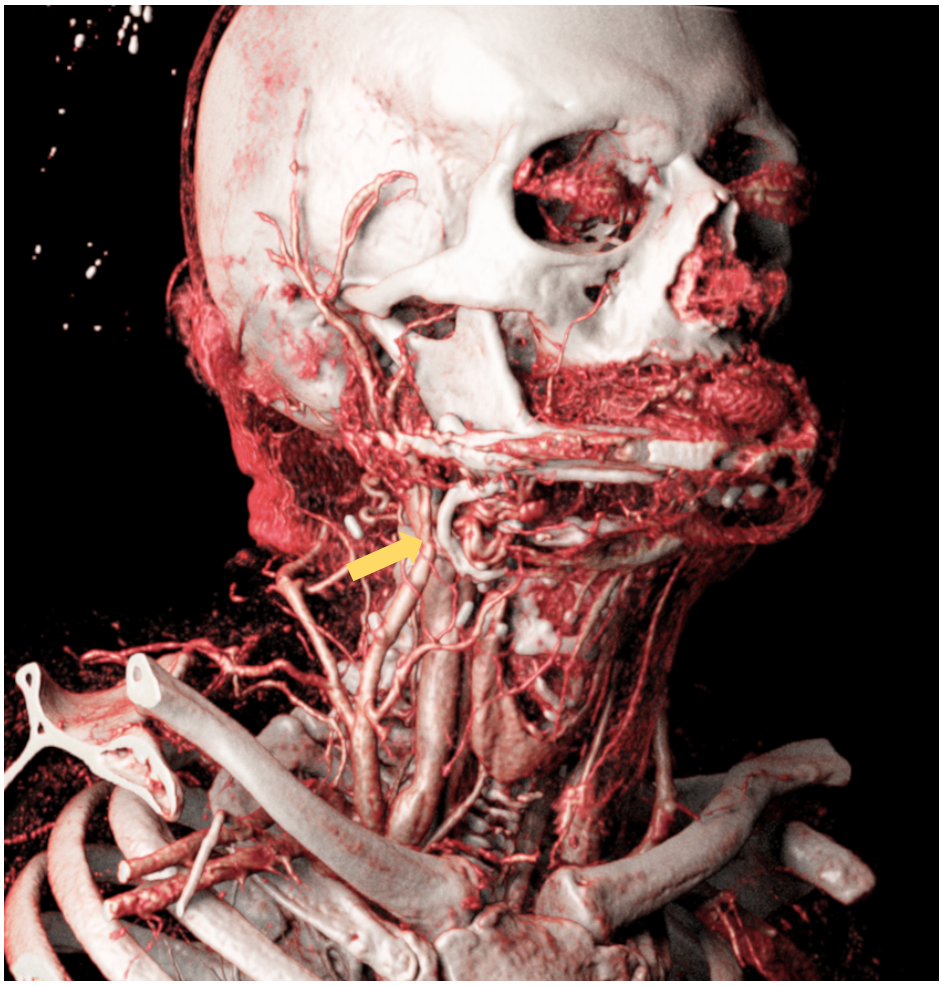

Abbildung 19. *Cinematic volume rendering* Rekonstruktion einer KM-CT nach Kieferrekonstruktion mit freiem Fibulatransplantat nach VSP mit PSI mit MeVisLab (MeVis Medical Solutions AG, Bremen, Deutschland). Das tri-segmentale Fibulatransplantat war bei einem ausgedehnten T4-Karzinom des anterioren Mundbodens angezeigt. Es bestand die Indikation zur adjuvanten Strahlentherapie des Tumorbettes und des Lymphabflussgebietes mit einer kumulativen Gesamtdosis

von 70,4 Gy. Trotzdem entwickelte sich eine spangenförmige HO-Typ 2 im Bereich des Gefäßstiels (gelber Pfeil).

HO-Typ 3 wurde in unserem Kollektiv in nur *n* = 2 Fällen nach Unterkieferrekonstruktion beobachtet. Sein klinisches Erscheinungsbild ähnelt dem Torus mandibularis. Das Auftreten ektoper oraler Knochenbildung ist auf kaufunktionelle Reize zurückzuführen [233, 234]. Dieser HO-Typ scheint durch Manipulation bei der Periostpräparation ausgelöst (siehe 4.2.1.) und durch funktionelle Faktoren, wie kaufunktionelle Stimuli, induziert und aufrechterhalten zu werden. Mechanische Reize fördern den BMP-Signalweg [216]. Vor diesem Hintergrund wäre jedoch zu erwarten, dass der HO-Typ 3 deutlich häufiger bei poly-segmentalen Rekonstruktionen im Bereich der Transitionszonen der einzelnen Fibulasegmente als an den Übergängen des originären Kiefers zum Fibulatransplantat auftritt. Letztlich handelt es sich daher bei dem HO-Typ 3 um ein zufälliges Auftreten des von *Trignano et al.* berichteten Effekts der Verknöcherung bei Verwendung eines periostalen Überschusses [225]. Lokale Faktoren (Gewebewiderstand) könnten dazu beitragen, dass Typ 3 nur nach Unterkieferrekonstruktionen beobachtet wurde.

Veränderungen des Blutflusses und des -drucks lösen wahrscheinlich HO-Typ 4 aus [220]. Einen eindrucksvollen Fall beschrieben wir in der Originalarbeit 2 [215]. Das Gewebe erscheint wie aufgebläht, was einer Dilatation der Mikrogefäße entspricht. Während der Kallusheilung kommt es sodann zu einer Neubildung von Knochen und Blutgefäßen, wie sie normalerweise bei stabilisierten Frakturen beobachtet wird [235]. Während dem Gewebe bei der freien Granulation im Oberkiefer keine komprimierenden Kräfte – bis auf die Zunge – entgegenwirken, übt das den Gefäßstiel umgebende Weichgewebe des Halses einen ausreichend hohen Gegendruck aus. Damit kann den veränderten Perfusionsdrücken nach Lappentransfer begegnet werden [220]. Dies ist eine Erklärung dafür, warum derartige HO-Typ 4 Auftreibungen im parapharyngealen Gefäßstieltunnel [236] und im Hals nicht beobachtet werden konnten.

Die HO-Typen 1 und 2 wurden vor allem nach einer Unterkieferrekonstruktion und Typ 4 in *n* = 3 von insgesamt 4 Fällen nach Oberkieferrekonstruktion beobachtet. In dem untersuchten Studienkollektiv von 102 ergab sich nur in 4,9 % chirurgischer Interventionsbedarf. Dabei wurden verkalkte Strukturen im Bereich des Halses (*n* = 1,

non-VSP) zur Verbesserung der Mundöffnung (*n* = 2, beide VSP) und Dysphagie (*n* = 2, beide VSP) entfernt. Es fällt ins Auge, dass nur die HO im Oberkiefer eine klinische Symptomatik verursachte, die eine chirurgische Therapie notwendig machte (Typ 1 und 2: je *n* = 1 und Typ 4: *n* = 3). Kein Fall eines radiologischen, klinisch stummen bzw. symptomatischen HO-Verlaufs führte zu einem Lappenverlust

4.2.3. Analyse der Komplikationsraten konventioneller vs. CAD/CAM (PSI) Osteosyntheseplatten zur Kieferrekonstruktion mit FFF

Im Allgemeinen stehen konventionelle Osteosyntheseplatten (Miniplatten), Rekonstruktionsplatten und patienten-spezifische Implantate (PSI) mit jeweils spezifischen Vor- und Nachteilen zur Kieferrekonstruktion zur Verfügung [237]. Die nachfolgenden Ausführungen beziehen sich hauptsächlich auf Originalarbeit 6, in der konventionelle, handgebogene Unilock-Platten (**Abbildung *20***) mit CAD/CAM gefertigten PSI verglichen wurden.

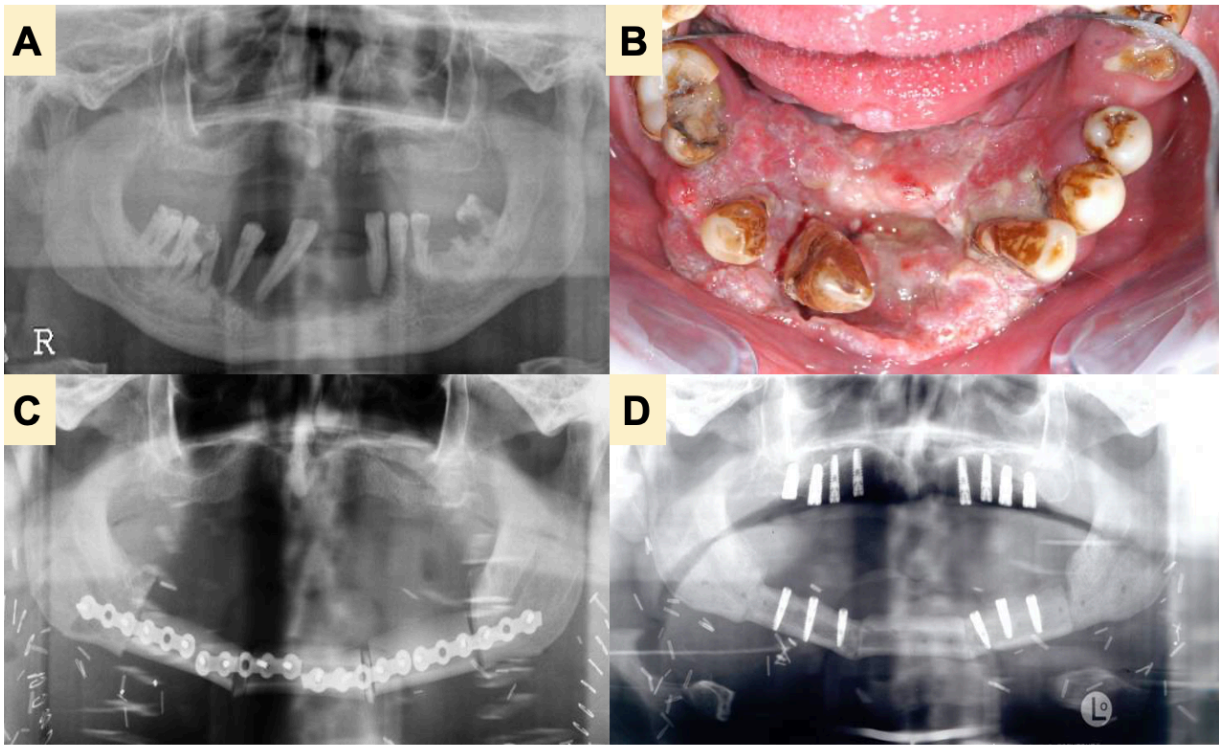

Abbildung 20: T4a Plattenepithelkarzinom des anterioren Unterkiefers eines 60-jährigen Patienten. Der präoperative radiologische Befund (**A**) zeigt eine deutliche Osteolyse des Unterkiefers. Der klinische Befund ist in (**B**) dargestellt. Die Rekonstruktion wurde auf konventionellem Wege mit einem tri-segmentalen Fibulatransplantat und mit Unilock-Platten

(2.0) segmental durchgeführt (**C**). Die abschließende prothetische Rehabilitation erfolgte mit enossalen Implantaten (**D**).

i. Komplikation: Unvollständige Verknöcherung der Übergangsbereiche Mandibula – Fibula und intersegmental

Die Knochen- und intersegmentale Spaltheilung kann radiologisch bereits zwei Monate postoperativ aufgrund strukturellen Knochenumbaus beobachtet werden [238]. Unvollständige Verknöcherungsraten (IOU) werden in der Literatur mit 5 - 45,9 % nach mikrovaskulären Kieferrekonstruktionen angegeben [137, 239-245]. Besonderes Augenmerk sei auf die Arbeit von *Rendenbach et al.* gelenkt, die bei der Verwendung von PSI eine Rate unvollständiger Verknöcherungen von 45,9 % in ihrem Kollektiv fanden [137]. Die eigene Auswertung ergab eine Rate unvollständiger Verknöcherungen von 24,7 % auf der Basis von 89 Patienten (PSI: 35,6 % vs. konventionell: 13,6 %; $p = 0{,}017$) bzw. eine Rate bezogen auf 249 Osteotomiespalten zwischen Mandibula und Fibula sowie intersegmental von 12,4 % (PSI: 19,4 % ($n = 25$) vs. konventionell: 5,0 % ($n = 6$); $p < 0{,}001$). Ausschließlich bezogen auf $n = 176$ Übergangsbereiche Mandibula-zu-Fibula entspricht das einer Rate unvollständiger Verknöcherungen von 13,1 % (PSI: 19,3 % ($n = 17$) vs. konventionell: 6,8 % ($n = 6$); $p = 0{,}014$). Intersegmentale unvollständige Verknöcherungen wurden nur bei poly-segmentalen Rekonstruktionen in der PSI-Gruppe in 16,0 % ($n = 8$; $p = 0{,}015$) festgestellt. Bei Verwendung von PSI ist die Rate unvollständiger Verknöcherungen somit stets höher als in der konventionellen Gruppe und zwar unabhängig davon, ob es sich um intersegmentale Übergänge oder die Bereiche Mandibula-zu-Fibula handelt.

Unvollständig verknöcherte Übergänge traten in unserer Auswertung bei mono- und poly-segmentalen sowie bei lateralen (nicht-Mittellinienüberschreitenden) und anterioren (Mittellinienüberschreitenden) Rekonstruktionen am proximalen und distalen Ende des Fibulatransplantats auf. In der PSI-Gruppe zeigten sich unvollständig verknöcherte Übergänge signifikant häufiger bei poly-segmentalen ($p = 0{,}041$) und bei lateralen Rekonstruktionen ($p = 0{,}016$).

Verschiedene Kräfte wirken bei Mundöffnung und Kaubewegungen auf den Unterkiefer. Zug- und Druck-, Scher-, Biege- und Torsionskraft führen zu einer Verformung des Unterkiefers, die sich als Kombination aus sagittaler Biegung, Torsion und lateraler Querbiegung beschreiben lässt [246]. Patienten mit reduziertem

Zahnstatus bzw. fehlender postoperativer Okklusion weisen eine geringe kaufunktionelle Belastung und eine höhere Rate unvollständig verknöcherter Übergänge auf [137, 141]. Das unterstreicht die Bedeutung mechanischer Stimuli auf die Knochenheilung [247]. Die höhere Rate unvollständiger Verknöcherungen in der PSI-Gruppe wird auf die höhere Plattensteifigkeit der CAD/CAM-Platten zurückgeführt [140]. Eine Abschirmung der mechanischen Kräfte durch rigide Plattensysteme reduziert die Mikrobewegungen unter ein kritisches Schwellenniveau, das für die Stimulation der Knochenheilung notwendig ist [141-144]. Über erfolgreiche segmentale Unterkieferrekonstruktionen mit dem Fibulatransplantat wurde auch berichtet, wenn Miniplatten verwendet wurden [140, 248]. Unvollständige Verknöcherungen für diese werden mit 14 % in der Literatur angegeben [143]. Ist im Anschluss an die Rekonstruktion jedoch eine adjuvante Strahlentherapie wahrscheinlich bzw. geplant, so wird von der Verwendung von Miniplatten abgeraten [249, 250].

Im Gegensatz zur untersuchten konventionellen Unilock 2.0 mm Platte verringert das PSI durch seine höhere Rigidität Mikrobewegungen zwischen allen Knochensegmenten der Rekonstruktion und dem originären Kiefer. Darüber hinaus ist die Kontaktfläche zwischen Knochen bzw. Periost und der PSI-Unterseite größer [140]. Gerade aufgrund dieser idealen knochenoberflächenkongruenten Form des PSI kann die periostale Blutversorgung durch Kompression geschädigt werden, wenn non-locking Schrauben zu Einsatz kommen [190, 191]. In der Folge können Knochenresorption mit Schraubenlockerung [192] und partielle Transplantatverluste auftreten [155]. Ein weiterer Unterschied ist die funktionelle Kraftleitung in den Knochen bei den verwendeten Systemen. Konventionelle Unilock-Platten wurden in der Hauptzahl segmental angebracht, sodass jeder Übergang (Mandibula – Fibula sowie Fibula – Fibula) mit einer separaten, winkelstabilen Osteosynthese adressiert wurde. Die einwirkende Kaukraft wird so durch jedes Glied der „Knochenkette“ geleitet und trägt zu einer funktionellen Stimulation bei. Das ist bei der Anwendung von PSI nicht der Fall. Die Knochensegmente werden an die Platte adaptiert und eingeleitete Kräfte werden von der überspannenden, last-tragenden (load-bearing) PSI-Rekonstruktionsplatte aufgenommen. Der funktionelle Reiz auf die einzelnen Knochensegmente muss daher zwangsläufig geringer sein. *Kreutzer et al.* haben daher vorgeschlagen, die PSI, die bislang als patienten-spezifische

Rekonstruktionsplatten zu bewerten sind, gegen patienten-spezifische Miniplatten zu ersetzen [251]. Eine durchgeführte Machbarkeitsstudie hierzu ist jüngst publiziert worden [252]. Zur Verbesserung der bei der Anwendung von patienten-spezifischen Implantaten signifikant häufiger beobachteten unvollständigen Verknöcherung der Übergänge Mandibula-zu-Fibula bzw. zwischen einzelnen Fibulasegmenten, scheint eine Trennung der durchgehenden Platte im Sinne einer segmentalen Osteosynthese sinnvoll, um eine physiologische Knochenremodellation zu stimulieren.

Zusammenfassend lässt sich feststellen, dass eine unvollständige Verknöcherung (IOU) der Übergangsbereiche (n = 249) Mandibula-zu-Fibula und intersegmental signifikant häufiger in der PSI-Gruppe beobachtet (PSI: 19,4 % (n = 25) vs. konventionell: 5,0 % (n = 6); p < 0,001) wurde. Bei mehrgliederigen Rekonstruktionen wurden unvollständige Verknöcherungen ausschließlich in der PSI-Gruppe gefunden (p = 0,015). Wahrscheinlich ist die mechanische Rigidität und der damit geringere funktionelle Stimulus zwischen den Knochensegmenten hierfür die Ursache.

ii. Komplikation: Plattenexposition und -lockerung

In der Literatur werden nach segmentalen Unterkieferrekonstruktionen Plattenexpositionsraten von 4 – 46 % angegeben [253]. In dem untersuchten Patientenkollektiv wurde eine Rate von 23,6 % ermittelt (PSI: 24,4 % vs. konventionell: 22,7 %; p = 1,000), was mit den in der Literatur berichteten Ergebnissen (PSI: 29,7 % vs. konventionell: 18,7 %) vergleichbar ist [137]. Eine Infektion an der Operationsstelle wird als unabhängiger Risikofaktor für eine Plattenexposition angegeben [253-257]. Das Risiko, eine Plattenexposition zu erleiden, ist mit postoperativer Infektion an der Operationsstelle, Art des Kieferdefekts sowie Plattenprofil und -dicke assoziiert [253]. Die Auswertung des Faktors *Plattenexpositionen* hat ergeben, dass bis auf den Fall eines PSI alle innerhalb der Mundhöhle und trotz Weichteilbedeckung durch die septo-kutane Hautinsel eines Fibulatransplantates auftraten. Der Benefit einer intraoralen Hautinsel zur Vermeidung intraoral freiliegenden Osteosynthesematerials wird von *Kreutzer et al*. kritisch gesehen, da dieser in ihrer Untersuchung nicht bestand. Die Vermeidung einer Hautinsel würde sich sogar positiv auf die Morbidität der Entnahmestelle und auf das künftige periimplantäre Gewebe auswirken [251]. Zur Vermeidung freiliegender Platten sollte aus unserer Erfahrung darauf geachtet

werden, Überkonturierungen der Kinnprojektion des Neounterkiefers zu vermeiden, intersegmentale Übergänge zu glätten und für eine stabile Weichteilabdeckung z.B. mit der septo-kutanen Hautinsel des Fibulatransplantats zu sorgen. Die narbige Retraktion des Weichgewebes kann mitunter nur begrenzt kontrolliert werden. Im Verlauf – u.a. im Rahmen der implantologischen Rehabilitation – können Korrektureingriffe wie z.B. Vestibulumplastiken notwendig werden [53, 54]. Technische Weiterentwicklungen erhöhen die Biokompatibilität der Rekonstruktionsplatten und tragen ebenso wie Modifikationen des Plattendesigns (z.B. flacheres Plattenprofil) zu einer Verringerung des Risikos einer Plattenexposition bei [258, 259].

Platten- bzw. Schraubenlockerungen wurden in der durchgeführten Untersuchung in 12,3 % gefunden (PSI: 15,6 % vs. konventionell: 9,1 %; p = 0,522). Damit ist die Rate etwas höher als in der Literatur (PSI: 8,1 % vs. konventionell: 6,6 %) [137]. Die postoperative Bestrahlungsrate ist in der PSI-Gruppe höher (PSI: 53,3 % vs. konventionell: 34,1 %).

Das Risiko für die Entstehung einer Osteoradionekrose in einem Fibulatransplantat steigt um das 21-fache bei einer Strahlendosis > 60 Gy [260]. Nach unserer klinischen Erfahrung erhöht die Strahlentherapie die postoperative Komplikationsrate erheblich. Dies lässt sich an bestrahlten Fibulatransplantaten bei unseren Studienteilnehmern mit einer Schraubenlockerungsrate von 42,8 % in der PSI-Gruppe (n = 3 von 7) und 25 % in der konventionellen Osteosynthesegruppe (n = 1 von 4) bestätigen und darstellen. In zwei PSI-Fällen trat eine Osteoradionekrose des Fibulatransplantats auf, was als Grund für die Schraubenlockerung gelten kann. Es konnte jedoch kein statistisch signifikanter Zusammenhang zwischen Schraubenlockerung und Strahlentherapie festgestellt werden, vermutlich aufgrund der begrenzten Anzahl der betroffenen Patienten. Dennoch sind plattenbedingte Probleme bei der Verwendung von patienten-spezifischen Rekonstruktionsplatten weit verbreitet und treten nicht nur bei Patienten mit signifikanten Risikofaktoren wie Bestrahlung oder polysegmentalen Rekonstruktionen auf [252].

Zur Frage der idealen Befestigungsform eines Fibulatransplantats besteht im Schrifttum Uneinigkeit. *Likhterov et al.* berichten über die routinemäßige Osteosynthese mit winkelstabilen 2,0 mm- oder 2,4 mm-Platten und mit bis zu 4 bikortikalen Locking-Schrauben zur Befestigung am nativen Unterkiefer sowie 1 - 2 monokortikalen Schrauben zur Befestigung der Knochensegmente an der Platte [249].

Für die PSI-Befestigung werden monokortikale Locking [251] oder Non-Locking-Schrauben [137] für die Fibula-Segmente und bikortikale Non-Locking-Schrauben am Unterkiefer beschrieben. Die Verwendung von Locking-Schrauben zur PSI-Fixierung am Kiefer und der Transplantatsegmente wurde in einer Finite-Elemente-Analyse einer tri-segmentalen anterioren Unterkieferrekonstruktion positiv bewertet [191]. Wir bevorzugen bikortikale Locking-Schrauben zur Befestigung des PSI am originären Kiefer und in der Regel Non-Locking-Schrauben für die Transplantat-Segmente. Aus unserer Erfahrung sind bei polysegmentalen Rekonstruktionen die Gehrungsschnitte eine häufige Quelle von Passungenauigkeiten und Störkontakten. Zur Korrektur sind mitunter wiederholte Anpassungen - mit dem Risiko von Verletzungen des Gefäßstiels - mittels Diamantschleifern oder der oszillierenden Säge - notwendig. Die Verwendung von Locking-Schrauben hat sich in unserem Arbeitsablauf daher als eher ungünstig erwiesen. Non-Locking-Schrauben bieten den Vorteil, dass die Knochensegmente an die Platte herangezogen bzw. die Gehrungsschnitte zusammengezogen werden. In Kombination mit einer empfohlenen, periostalen Weichteildeckung [189] besteht die Gefahr, dass die Oberflächenkongruenten PSI bei geringfügigen Passungsungenauigkeiten kritische Durchblutungsstörungen auslösen können [190, 191]. Ein Lösungsansatz besteht im sequenziellen Austausch der Non-Locking- gegen Locking-Schrauben, nachdem die Segmente an die Platte adaptiert worden sind.

Die Untersuchung hat ergeben, dass kein statistisch signifikanter Zusammenhang bezüglich des verwendeten Plattentyps und den Faktoren *Plattenexposition* (PSI: 24,4 % vs. Konventionell: 22,7 %; $p = 1.000$) sowie *Platten- bzw. Schrauben-lockerungen* (PSI: 15,6 % vs. konventionell: 9,1 %; $p = 0,522$) besteht. Jedoch hat die multivariate Analyse ergeben, dass die Parameter *Plattensystem* (OR = 3,682; 95%-CI: 1,236-10,966; $p = 0,019$) und *Plattenexposition* (OR = 3,389; 95%-CI: 1,118-10,275; $p = 0,031$) unabhängige Risikofaktoren für eine unvollständige Verknöcherung sind.

iii. Aspekt: Segmentorientierung (proximales und distales Ende)

Wie bereits erwähnt, wird in der Literatur über unvollständige Verknöcherungsraten (IOU) nach mikrovaskulärer Unterkieferrekonstruktionen zwischen 5 – 37,0 % berichtet [239-245]. Die Auswertung ergab kumulative Raten unvollständiger

Verknöcherungen am proximalen Transplantatende von 10,6 % (PSI: 19,5 % vs. konventionell: 2,2 %; $p = 0{,}009$) und am distalen von 16,3 % (22,2 % vs. 11,4 %; $p = 0{,}190$). Es konnten keine Regionen ermittelt werden, in der unvollständige Verknöcherungen signifikant häufiger auftrat. Kritisch muss angemerkt werden, dass die untersuchte PSI-Gruppe eine höhere Anzahl von polysegmentalen Rekonstruktionen und damit intersegmentale Lücken aufwies (PSI: $n = 50$ vs. konventionell: $n = 32$).

Tierexperimentelle Untersuchungen an der Schweinefibula ergaben einen Zusammenhang zwischen der Anzahl segmentaler Osteotomien, eingebrachter Osteosyntheseschrauben und einem verringerten Blutfluss zum distalen Fibulasegment hin [261, 262]. Es konnte ein Zusammenhang zwischen der Segmentlänge und der Anzahl der proximalen Osteotomien mit der Knochendurchblutung herausgearbeitet werden. Längere Segmente und weniger Osteotomien waren mit einer höheren Perfusion des distalen Segments verbunden [145]. Diese Ergebnisse stehen im Einklang mit der Beobachtung, dass bei polysegmentalen Unterkieferrekonstruktion die Komplikations- und Nichtverwachsungsrate am distalen Segment höher war [146]. Während in der PSI-Gruppe unvollständige Verknöcherungen gleichermaßen am proximalen (19,5 %) und distalen (22,2 %) Ende beobachtet wurden, stellt sich Frage, warum die Rate unvollständig verknöcherter Übergänge in der konventionellen Gruppe deutlich niedriger war. Die Art der Osteosynthese, das Spaltmaß sowie die Flächenkongruenz der Übergangszone und funktionelle Stimuli sind offensichtlich relevante Faktoren. In den Punkten Form- und Flächenkongruenz liegen gerade die Stärken der Methode VSP mit CAD/CAM-PSI, jedoch scheint die Minderung der funktionellen Stimulation durch das PSI diesen Vorteil schwinden zu lassen. Eine retrospektive Studie an 104 Unter- und Oberkieferrekonstruktionen mit (zum weit überwiegenden Teil) Fibulatransplantaten ergab eine Rate unvollständiger Verknöcherungen von 47 %. Die Autoren beobachteten signifikant ($p = 0{,}0006$) höhere Raten einer vollständigen knöchernen Vereinigung von 65 % zwischen einzelnen Fibulasegmenten als an den Übergängen Fibula-zu-Kieferstumpf (53 %) [243]. Angaben zum Planungsmodus und Osteosyntheseverfahren gehen aus der Publikation nicht hervor [243]. Die eigene Auswertung ergab eine Rate unvollständiger Verknöcherungen von 16,0 % ($n = 8$) für intersegmentale Übergänge in der PSI-Gruppe ($n = 8$ von 50). In der konventionellen

Gruppe (n = 32) wurden keine unvollständigen Verknöcherungen zwischen einzelnen Fibulasegmenten festgestellt (p = 0,015).
Die primäre Knochenheilung läuft bei einer Spaltbreite < 1 mm ab. Breitere Lücken verknöchern sekundär über den Mechanismus der Kallusbildung [263]. Eine Untersuchung zu mikrovaskulären Unterkieferrekonstruktionen erkannte radiologisch keine vollständige knöcherne Vereinigungen, wenn die intersegmentale Spaltbreite > 1 mm betrug. Die Autoren empfahlen daher eine präzise Präparation, um die intersegmentale Spaltbreite auf ein Minimum zu reduzieren [243]. Vor diesem Hintergrund ist es jedoch umso erstaunlicher, dass in der untersuchten konventionellen Osteosynthesegruppe kein Fall unvollständig verknöcherter intersegmentaler Übergängen ermittelt wurde. Gerade VSP ermöglicht in Verbindung mit CAD/CAM-Schablonen geführten Osteotomien präzise Rekonstruktionen. Der funktionelle Reiz, Stress und Scherung spielen eine entscheidende Rolle in der physiologischen Stimulation der Knochenheilung [264]. Rigide CAD/CAM-Platten schirmen funktionelle Kräfte stärker ab und verringern die physiologische Stimulation der Knochenbildung.

Nach Frakturen und/oder Osteotomien verändert die Größe des interfragmentären Spalts das mechanische Umfeld. Eine zunehmende Spaltbreite führt zu einer signifikant geringeren mechanischen Festigkeit und Steifigkeit, was in tierexperimentellen, mechanischen, histologischen und radiologischen Auswertungen gezeigt werden konnte [264-266]. In Abschnitt 4.2.1. wurde der Einfluss des Schablonenabstands zur Knochenoberfläche dargestellt, wonach es mit zunehmendem Abstand zu einer Verkürzung der Transplantatrekonstruktion kommt. In dem aufgeführten Beispiel einer bi-segmentalen Rekonstruktion in **Abbildung *12*** kommt es zu einer Gesamtverkürzung von > 2 mm, wenn der Knochen-Schablonenabstand 1 mm beträgt. Jede Aufpassungsinkongruenz auf der Donorseite führt zu einer Verkürzung der Segmente und kann damit zu einem kritischen intersegmentalen Spalt > 1 mm beitragen. Bei breiteren Spalten bleibt die primäre Knochenheilung aus [243]. Zu diesem Fehler addieren sich dann noch Ungenauigkeiten durch die Osteotomie mit der Pendelsäge, die durch die unilaterale Führung der Säge an der Schablone entstehen können. Die schablonengestützte Osteotomie muss damit auch als Ursache für unvollständige Verknöcherungen

aufgrund möglicher verbreiterter intersegmentaler Spaltmaße auf der Donorseite berücksichtigt werden.

Zusammenfassend kann gesagt werden, dass sich die Raten unvollständig verknöcherter Übergänge zwischen konventionellen und CAD/CAM-Platten signifikant unterscheiden. Bei Verwendung von PSI traten unvollständige Verknöcherungen in rund einem Fünftel der Fälle am proximalen wie auch distalen Ende auf, was auf eine systematische Ursache hinweist. In der konventionellen Vergleichsgruppe konnte nur in jedem zehnten Fall eine unvollständige Verknöcherung am distalen Ende und nur ein Fall proximal identifiziert werden. Überdies fanden sich unvollständige Verknöcherungen bei polysegmentalen Rekonstruktionen ausschließlich in der PSI-Gruppe. Das Zusammenspiel aus vermindertem funktionellen Reiz zur physiologischen Stimulierung der Osteogenese und einer Spaltbreite > 1 mm, was durch die Verwendung von Präparationsschablonen und Ungenauigkeiten bei der einseitig geführten Osteotomie bedingt sein kann, begünstigen das Auftreten von unvollständiger Verknöcherungen in der PSI-Gruppe.

iv. <u>Aspekt: Segmentanzahl und Defektlokalisation (anterior vs. lateral)</u>

Die multivariate logistische Regressionsanalyse identifizierte nur die Faktoren Plattentyp und -exposition als unabhängige Risikofaktoren für das Auftreten einer unvollständigen Verknöcherung. Die Anzahl der verwendeten Transplantat-Segmente erreichte in der Auswertung keine statistische Signifikanz (p = 0,800; OR = 0,919, 95%-CI: 0,479-1,765). Im Gruppenvergleich konventionell vs. CAD/CAM-PSI-Osteosynthese zeigte sich ein signifikanter Unterschied für polysegmentale Rekonstruktionen (p = 0,041), nicht jedoch für unisegmentale Rekonstruktionen (p = 0,215). Die weitere Auswertung hat (teils) signifikante Unterschiede zwischen Plattentyp, Defektlokalisation und dem Vorliegen unvollständiger Verknöcherungen ergeben. Rekonstruktionen der lateralen – nicht-Mittellinienüberschreitenden – Unterkieferregion zeigten signifikant häufiger unvollständige Verknöcherungen in der CAD/CAM-PSI-Gruppe (PSI: 44,0 % vs. konventionell: 14,3 %; p = 0,016). Unvollständig verknöcherte Übergänge wurden ebenfalls in der PSI-Gruppe häufiger nach anteriorer, mittelinienüberschreitender Rekonstruktionen beobachtet, wenn auch nicht auf signifikantem Niveau (PSI: 25,0 % vs. konventionell: 12,5 %; p = 0,346).

Anatomische Studien haben gezeigt, dass die Knochendurchblutung des Skeletts durch ein System von drei Gefäßarten aufrechterhalten wird [267, 268]: endostale Vasa nutritia, penetrierende periostale Gefäße und nicht-penetrierende periostale Gefäße [42, 269]. Während die Vasa nutricia zur periostalen und endostalen Blutversorgung beitragen [270], scheinen die nicht-penetrierenden Äste keinen Beitrag zur endostalen Perfusion zu leisten [268, 271]. Das Fibulatransplantat wird versorgt von nicht-penetrierenden Perforatorgefäßen vom Typ periostal und muskulo-periostal und den Vasa nutritia [42, 269]. Mehrere Studien unterstützten die These, dass nicht-penetrierende Äste nur die äußere Kompakta perfundieren [271, 272].

In Röhrenknochen ist die endostale Blutversorgung für mehr als zwei Drittel des Blutflusses in der Kortikalis verantwortlich [194]. Bei der Präparation und bei multiplen Osteotomien verringert sich durch mechanisches Trauma der endostale Blutfluss im distalen Segment [262]. Segmentale Osteotomien und Osteosyntheseschrauben verringerten in Tierstudien an der vaskularisierten Fibula des Schweins den Blutfluss zum distalen Fibulasegment [261, 262]. Im klinischen Verlauf kann es daher zu Schraubenlockerungen kommen [192]. Ein entsprechender Fall ist in Originalarbeit 1 beschrieben. Die Anzahl von Osteotomien und somit die Anzahl der Segmente sollte so gering wie möglich gehalten werden, um die segmentale Periostperfusion wenig zu beeinträchtigen und um die Operationszeit auf ein Minimum beschränken zu können [273, 274]. In einer experimentellen Untersuchung an humanen Fibulapräparaten wurde die Segmentlänge ermittelt, ab der eine kritische Blutversorgung auftritt. Für Fibulasegmente, denen *Foramina nutricia* und damit eintretende endostale *Vasa nutritia* fehlen, konnte eine Revaskularisierung im Empfängerbett festgestellt werden, wenn sie mindestens 2 cm lang waren. Bei kürzeren Segmenten war eine partielle Revaskularisierung wahrscheinlich. Trotz angemessener Präparation und suffizienter Mikroanastomose wurden Segmente mit einer Länge von 0,5 cm wahrscheinlich nicht revaskularisiert und werden im Wesentlichen zu nicht vaskularisierten Transplantaten [275]. Trotz Kollateralen zwischen den periostalen und endostalen Gefäßen scheint eine unzureichende Perfusion ursächlich [193]. Bei der VSP muss darauf geachtet werden, kurze Fibulasegmente zu vermeiden, um eine ausreichende Durchblutung des Knochensegments zu gewährleisten und (sub-)totale Segmentverluste zu vermeiden [276]. Nach unserer Erfahrung sollten Segmente, die kürzer als 3,0 cm

sind, möglichst vermieden werden. Weitere eigene Erkenntnisse über die vaskuläre Versorgung der Fibula und kleiner Gefäße werden im Abschnitt 4.3. diskutiert.

Es bestehen charakteristische Unterschiede zwischen den Defektformen anterior (mittellinienüberschreitend) und lateral (nicht-mittellinienüberschreitend). Beim lateralen Typ (Brown I-II(c)) ist der funktionelle Reiz durch die suprahyoidale Muskulatur auf der Innenseite der ventralen Unterkieferspange zumeist erhalten, aber die Integrität der masseterico-pterygoidalen Muskelschlinge kompromittiert. Bei dem anterioren Defekttyp (Brown III – IV(c)) verhält es sich gegensätzlich. Der funktionelle Reiz durch die suprahyoidale Muskulatur ist aufgrund der fehlenden Insertion erheblich vermindert, während der Reiz durch die masseterico-pterygoidale Muskelschlinge zumeist erhalten bleibt. Damit scheint die höhere Rate unvollständiger Verknöcherungen nach lateraler Rekonstruktion durch Funktionseinschränkung bzw. Verlust des funktionellen Reizes der masseterico-pterygoidalen Muskulatur mit erklärbar zu sein, über dessen Einfluss auf die Knochenheilung kein Zweifel besteht [141-144]. Zudem können durch VSP mit PSI auch ausgedehnte Kieferdefekte erfolgreich rekonstruiert werden. Das wiederum begünstigt das Auftreten ausgedehnter postoperativer Vernarbungen und Funktionseinschränkungen bzw. -störungen wie eine eingeschränkte Mundöffnung (Trismus). Dieser Effekt überlagert die „Funktionsabschirmung“ des CAD/CAM-PSI und aggraviert den verminderten funktionellen Stimulus. Es ist daher anzunehmen, dass load-bearing PSI bei lateralen Rekonstruktionen funktionelle Reize stärker abschirmen, als dies bei anterioren Rekonstruktionen der Fall ist. Weitere Einflussfaktoren sind die verbliebene Bezahnung, auch des Gegenkiefers, der Resektionsumfang und mögliche postoperativ durchgeführte adjuvante Maßnahmen, beispielsweise eine Strahlentherapie.

Unvollständige Verknöcherungen traten nach lateraler und polysegmentaler Rekonstruktion signifikant häufiger in der CAD/CAM-PSI Gruppe auf. Die Rigidität des PSI ist in Kombination mit der Defekttopographie, der Rekonstruktionsform und veränderten mechanischen Reizen die ursächliche Konstellation für die verminderte Verknöcherung. Weitere klinische Follow-up-Untersuchungen sind notwendig, um den natürlichen „zeitlichen“ Verlauf einer IOU am Patienten erfassen zu können und das Verknöcherungsmuster beurteilen zu können.

4.2.4. Einfluss der Prozesszeit des digitalen Planungs- und Rekonstruktionsverfahrens auf einzeitige, onkologische Unterkieferrekonstruktionen

Das Verfahren VSP mit PSI findet zunehmend Verbreitung zur einzeitigen Kieferrekonstruktion bei knöcherner Infiltration durch Tumore der Mundhöhle. Der pathohistologische Residualstatus (R-Kategorie) ist in der Literatur als prognostischer Faktor für ein Tumorrezidiv beschrieben worden [277-281]. Ziel der chirurgischen Therapie ist die Exzision der Neoplasie mit einem umgebenden Sicherheitsabstand von ≥ 5 mm (R0-Resektion) [282]. Die Resektion wird mit einem Abstand von 10 mm um den sicht- und tastbaren Tumor empfohlen [211]. Um den onkologischen Sicherheitsabstand zu erhöhen, muss somit - je nach Lage des Tumors - eine segmentale Resektion (Kasten- oder Spangenresektion) oder eine Kontinuitätsresektion des Unterkiefers durchgeführt werden [283-285].
Eine Resektion wird als ‚knapp R0' (close margin) bezeichnet, wenn der Abstand zum Tumorrand zwischen 1 – 5 mm beträgt [286, 287]. Eine R1-Resektion ist gegeben, wenn der Abstand Tumorrand zu Exzisionsrand < 1 mm misst. Involvierte (R1) oder knappe R0-Resektionsränder erhöhen das Risiko für ein lokales Tumorrezidiv und die Entwicklung von Fernmetastasen [288]. Eine Infiltration des Knochens korreliert mit einer schlechteren Prognose [289]. Die Anwendung des VSP-Verfahrens ermöglicht das Einhalten eines onkologischen (pathohistologischen) Sicherheitsabstandes [98, 112, 138, 290-292]. Literaturdaten zeigen, dass etwa 3 % der Resektionen von Mundhöhlenkarzinomen als R1 und 16,3 % als ‚knapp R0' kategorisiert wurden [293]. Andere Untersucher erreichten nur bei der Hälfte ihres Kollektivs (*n* = 896) eine R0-Resektion [294].

Neben den oben benannten Vorteilen der VSP ist ein gravierender Nachteil die Planungs- und Fertigungszeit des CAD/CAM-PSI [113]. Die Auswirkungen der systemimmanenten „Vorlaufzeit" auf den Resektionsstatus der Weich- und Hartgewebeschnittränder wurde in einer retrospektiven, monozentrischen Originalarbeit 3 erarbeitet [295]. Insgesamt wurden 104 Patienten (Non-VSP: *n* = 63 und VSP: *n* = 41) nach einer einzeitigen Kieferrekonstruktion mit Fibulatransplantat aufgrund eines Mundhöhlenkarzinoms in die Studie eingeschlossen. Die Ergebnisse

zeigen eine signifikante Verzögerung vom Erstkontakt in der Universitätsambulanz bis zum chirurgischen Therapiebeginn bei Anwendung der Methode VSP mit PSI von im Median 11 Tagen (VSP: 47,2 ± 24,5 Tage, Median: 42,0 Tage vs. Non-VSP: 35,7 ± 18,6 Tage, Median: 31,0 Tage; p = 0,008).

In der VSP-Gruppe wurde häufiger eine Knocheninfiltration (VSP: 56,1 % vs. Non-VSP: 50,8 %; p = 0,372) und in der Non-VSP-Gruppe häufiger eine Knochenarrosion festgestellt (VSP: 19,0 % vs. Non-VSP: 14,6 %; p = 0,559). Knöcherne R0-Resektion wurde in der Nicht-VSP-Gruppe unwesentlich häufiger befundet (96,8 % vs. 95,1 %). Die Beurteilung der Weichgewebeabsetzungsränder ergab sichere Resektionsränder (R0) nach virtueller in 63,4 % und nach konventioneller Planung in 73,0 %. Im Gruppenvergleich waren die Unterschiede bei den Resektionsrändern des Knochens (p = 0,516) und der Weichteile (p = 0,470) statistisch nicht signifikant. Es wurde eine signifikant verlängere Zeit bis zum Therapiebeginn (TTI) festgestellt, wenn VSP für die einzeitige Unterkieferrekonstruktion angewandt wurde. In Bezug auf die TTI betonen Autoren die Notwendigkeit einer Tumorresektion innerhalb weniger Tage bis zu drei Wochen nach der Diagnose und zweifeln an, ob das mit einem digitalen Arbeitsablauf erreicht werden kann [98]. Eine irische Arbeitsgruppe um *Barry et al.* fandt eine kürzere (nicht signifikante) TTI von 59 ± 16 Tagen, wenn VSP anstatt der etablierten, konventionellen Sofortrekonstruktion (65 ± 30 Tage) eingesetzt wurde [138]. Im Vergleich dazu ermittelten wir den chirurgischen Therapiebeginn für VSP mit PSI mit 47,2 ± 24,5 Tagen. Dabei ergab sich eine signifikante Zeitverzögerung von rund 11 Tagen im Vergleich zur konventionellen Methode (Non-VSP: 35,7 ± 18,6 Tage; p = 0,008). Veröffentlichte Daten aus der National Cancer Database der Vereinigten Staaten legen dar, dass eine TTI von mehr als 46 – 52 Tagen die Mortalität erhöht und noch stärker, wenn die TTI > 60 Tage betrug. Eine verlängerte TTI wirkte sich auf die krankheitsspezifische Überlebensrate aus [296]. Die TTI hat aber keinen Einfluss auf das Gesamtüberleben [297]. Bei fortgeschrittenen Tumoren der Kopf-Hals-Region ist häufig eine multidisziplinäre Behandlung erforderlich, und ein verzögerter Beginn der adjuvanten Strahlentherapie ist mit einer höheren Mortalität assoziiert. Unter Berücksichtigung des gesamten Behandlungszeitraums tritt die Verzögerung bei Therapiebeginn jedoch in den Hintergrund [298]. Die aktuelle Leitlinie Mundhöhlenkarzinom empfiehlt den Abschluss einer adjuvanten Radiatio nach Beginn der chirurgischen Therapie innerhalb eines Zeitrahmens von maximal 11 Wochen [211]. Dieses Zeitfenster korreliert signifikant mit der lokoregionären Tumorkontrolle

und dem Over-all-survival [299, 300]. Partielle und totale Lappenverluste treten gerade in dieser vulnerablen Periode auf und können so zu einer relevanten Verzögerung der onkologischen Therapiesequenz beitragen [155], wenn weitere Eingriffe mit Sekundärlappenplastiken wie *Pectoralis major* [301, 302] und *Delto-pectoral*-Lappen [303] zum Einsatz kommen.

Bei einzeitigen Kieferrekonstruktionen basiert die VSP auf der Momentaufnahme der CT-Diagnostik der onkologisch relevanten Tumor- und damit geplanten Empfängerregion. Diese Diagnostik steht am Beginn der Staging-Prozedur, was als Krux der Methode VSP hinsichtlich der Ausdehnung und des weiteren Tumorwachstums diskutiert werden kann. *Waech et al.* untersuchten den Aspekt Tumorinfiltrationstiefe in der CT- und MRT-Bildgebung im Vergleich mit der histopathologischen Aufarbeitung. Alle Diagnoseverfahren tendierten zu einer Überschätzung der histopathologischen Infiltrationstiefe (DOI) von etwa 5 - 15 %. Dieser Trend war bei dünnen, flächig wachsenden Tumoren am stärksten ausgeprägt, bei denen sowohl CT- als auch MRT-Beurteilung in mehr als 50 % der Fälle zu einem Up-staging führten [304]. Die Überschätzung der Invasionstiefe scheint bei flachen Tumoren mit einer Invasionstiefe < 5 mm tendenziell stärker ausgeprägt zu sein [304]. Eine Diskrepanz zwischen der histologischen und der radiologischen Invasionstiefe ist methodisch bedingt, da die histologische Invasionstiefe von der Basalmembran bis zum tiefsten Punkt der Tumorinfiltration gemessen wird [305]. Auch andere Studien berichten eine Überschätzung der Tumorinvasionstiefe um etwa 10 % in der Schichtbildgebung [305-309]. Dies steht im Einklang mit früheren Berichten, die eine schlechte Übereinstimmung bei flachen Tumoren ergaben [310]. In frühen Stadien führt das zu Unterschieden der initialen radiologischen **c**T-Kategorisierung und der finalen pathologischen **p**T-Einordnung. Die Diskrepanz ist größer bei exophytischen Tumoren, während endophytische Tumore durch die bildgebungsbasierte Invasionstiefe gefährlich unterschätzt werden. Der Unterschied zwischen der schichtbildbasierten und der histologischen Invasionstiefe ist bei endophytischen, ulzerierten Tumoren größer [311, 312]. Weitere Aspekte sind die Schrumpfung des Präparates während des Transports und der Formalinfixierung [313]. Bis zur pathologischen Beurteilung auf dem Objektträger können so Diskrepanzen von bis zu 30 % auftreten [313, 314]. Interessanterweise verringern sich die Abmessungen des

Tumors und die der Ränder zwischen chirurgischer Resektion und pathologischer Analyse [313].

Das Zeitintervall zwischen der CT-Untersuchung der Tumor- bzw. Empfängerregion und der Festlegung der virtuellen Resektionsebenen sollte bis zur Operation so kurz wie möglich sein [103]. Eine verlängerte Zeit bis zum Therapiebeginn (TTI) ist ein Nachteil der VSP und führt zu weiterem Tumorwachstum [291, 315-317]. Tumorwachstum über die geplanten Resektionsgrenzen hinweg kann intraoperative Änderungen des virtuellen Operationsplans auslösen. Veränderungen der geplanten und „programmierten" Resektionsränder haben bei einem Two-Team-Approach zur Folge, dass die Präparation und Formgebung des Fibulatransplantates zurückgestellt werden muss, bis der betroffene Knochenabschnitt beurteilt worden ist. Zur intraoperativen Beurteilung der knöchernen Resektionsränder kann die bereits erwähnte fpVCT eingesetzt werden [207]. Es besteht immer das Risiko ein vorbereitetes CAD/CAM-PSI modifizieren oder sogar verwerfen zu müssen, wenn sich die knöchernen Resektionsränder verändern oder eine unvorhergesehene Situation auf der Weichgewebsebene auftritt.
Unsere Daten bestätigen die Ergebnisse anderer Studien, wonach sich die Operationsdauer signifikant verkürzt [113, 317, 318], was auf die schablonengeführten, präzisen Segmentosteotomien und die erleichterte Formgebung der Neo-Mandibula durch das PSI bei Wegfall der freihändigen Konturierung und der schrittweisen Plattenanbiegung zurückzuführen ist [290, 319, 320].

CT-Aufnahmen der Empfängerstelle waren zum Zeitpunkt der Operation in der VSP-Gruppe (VSP: 34,8 ± 17,6 Tage) im Durchschnitt rund zehn Tage älter als in der Non-VSP-Gruppe (Non-VSP: 25,1 ± 17,2 Tage) aufgrund der verlängerten Vorlaufzeit für die Planung und Herstellung des CAD/CAM-PSI. Dieser signifikante Unterschied (p = 0,008) zeigte keinen Einfluss auf die Rate lokaler Tumorrezidive (LTR) aufgrund knapper (closed) R0- oder involvierter R1-Ränder innerhalb der Follow-up-Periode.
Die Rate lokaler Tumorrezidive nach R0-Resektion wird in der Literatur zwischen 16 % und 20 % angegeben [321]. Werden keine sicheren R0-Ränder erreicht, erhöht sich das Risiko für ein Lokalrezidiv deutlich [322]. Das Auftreten einer R1- oder R2-Situation ist beim oralen Plattenepithelkarzinom 1,7-mal häufiger als bei anderen Kopf-Hals-Tumoren [323-325]. Die erhobenen lokalen Tumorrezidivraten bei R0-Resektion

(Weichgewebe) betrugen in der Non-VSP-Gruppe 20,63 %, was gut mit der Literatur vergleichbar war, und in der VSP-Gruppe 4,87 %. Ein Grund für die niedrigere lokale Tumorrezidivrate in der VSP-Gruppe ist die Möglichkeit der umfangreichen Resektion und optimaler Rekonstruktion aufgrund der notwendigen präoperativen Operationsplanung und prospektiven, großzügigen Festlegung der Resektionslinien. In unseren Augen ist dies neben der erreichbaren Präzision der Rekonstruktion ein entscheidender Vorteil der virtuellen Methode. Nicht außer Acht gelassen werden darf in diesem Punkt die unterschiedlich lange Follow-up-Periode der beiden Gruppen, auch wenn kein signifikanter Unterschied ermittelt wurde (VSP: 20,6 ± 16,4 vs. Non-VSP: 64,9 ± 52,1 Monate; p = 0,502). Die Zeitverzögerung durch die Methode VSP mit PSI zur Sofortrekonstruktion des Unterkiefers hatte keinen signifikanten Einfluss auf die Qualität des Knochen- oder Weichgeweberesektionsstatus in einer Studie mit n = 53 [138]. Unsere Befunde bestätigen diese Ergebnisse hinsichtlich der Auswirkungen von VSP auf die Resektionsränder.

Ein weiterer Aspekt ist der Zeitpunkt der diagnosesichernden Probebiopsie, die entweder bereits extern erfolgte oder im Rahmen bzw. im Verlauf nach der Erstvorstellung in der Klinik durchgeführt wurde. In beiden Studiengruppen stellte sich ein Drittel der Patienten bereits mit einer auswärtig histologisch gesicherten Diagnose eines Malignoms vor. Die Zeitspanne nach externer Biopsie bis zur Operation war in beiden Rekonstruktionsgruppen nahezu identisch und betrug unabhängig von der Planungsmethode im Median 46 Tage (p = 0,995). Im Gegensatz dazu ergab sich bei einer in-domo-Biopsie eine kürzere TTI in der Non-VSP Gruppe von im Median 34,5 Tagen (34,5 ± 20,6 Tage) und in der VSP-Gruppe von 43 Tagen (47,7 ± 25,2 Tage). Der Unterschied zwischen den Planungsgruppen war signifikant (p = 0,022). Dieser Zeitvorteil spricht somit für die Empfehlung zur Biopsie im onkologischen und rekonstruktiven Zentrum.

Kritisch muss angemerkt werden, dass mehrere Einflussgrößen die TTI in der VSP-Gruppe verzerrt darstellen. So findet seit 2015 die eingerichtete interdisziplinäre onkologische Konferenz nur einmal wöchentlich statt. In der spezifischen Umgebung der Abteilung war die planbare Kapazität eines Intensivbetts im Allgemeinen auf einen Tag pro Woche beschränkt. Die gesamte Prozess- und Produktionszeit beträgt im Median 15 Tage nach VSP-Kickoff und initialem Web-Meeting. Die längere TTI kann

also durch den VSP-Workflow, die im Wochenrhythmus stattfindende onkologische Konferenz und die begrenzte Anzahl valenter Intensivbettplätze mit bedingt sein. Die Zeitverzögerung ist der kritische Aspekt der VSP-Methode, da die Tumorprogression zeitabhängig ist [326].

Wie bereits erläutert, wurde in der Datenanalyse für die VSP-Gruppe eine niedrigere Rate an Lokalrezidiven (LTR) (VSP: R0 = 4,87%, *n* = 2, close/R1 = 9,76%, *n* = 4 vs. Non-VSP: R0 = 20,63%, *n* = 13, close/R1 = 6,34%, *n* = 4) bei einer etwa 10 % geringeren Quote sicherer R0-Resektion auf Weichgewebsebene gefunden (VSP: 63,4 % vs. Non-VSP: 73,0 %; *p* = 0,206). Während des Follow-up-Zeitraums hat sich dieser Unterschied nicht auf die Frequenz von Lymphknoten- (LNM) und Fernmetastasen (DM) ausgewirkt. Dieses Ergebnis muss mit deutlicher Einschränkung vor dem Hintergrund der geringen Fallzahl, der Länge des Follow-up und Unterschieden in der Therapie beispielsweise einer adjuvanten Strahlentherapie beurteilt werden.

Die planungs- und fertigungsbedingte Zeitverzögerung der Methode VSP mit CAD/CAM-PSI hatte gegenüber der konventionellen Methode keinen statistisch signifikanten Einfluss auf den Resektionsstatus der Weich- und Hartgewebeabsetzungsränder. VSP ermöglicht eine präzise einzeitige Rekonstruktion nach ablativer onkologischer Chirurgie und verkürzt die Schnitt-Naht-Zeit signifikant im Vergleich zur konventionellen Methode. Die Auswertung hat ergeben, dass sich in der mit dem VSP-Verfahren geplanten Gruppe eine geringere Rate an lokalen Tumorrezidiven bei fast gleicher Rate an Lymphknotenmetastasen und Fernmetastasen ergeben hat. Statistisch waren die Unterschiede jedoch ohne Signifikanz im Vergleich zur Non-VSP-Gruppe. Die Methode VSP mit PSI-Rekonstruktion ist daher aus onkologischer Sicht in unserem Umfeld als sicher und keinesfalls nachteilig zu beurteilen.

4.3. Wie kann der klinisch tätige Chirurg den funktionellen Lappenerfolg in der Planungsphase positiv beeinflussen?

Voraussetzung für eine erfolgreiche mikrovaskuläre Transplantation sind arterielle und venöse Anschlussgefäße der Empfängerregion und eine geeignete Gefäßanatomie der Donorregion [327]. Konkret wird hierunter eine regelrechte Drei-Gefäßversorgung des Unterschenkels durch die *Aa. tibialis anterior*, *tibialis posterior* und *fibularis* verstanden (**Abbildung *21***).

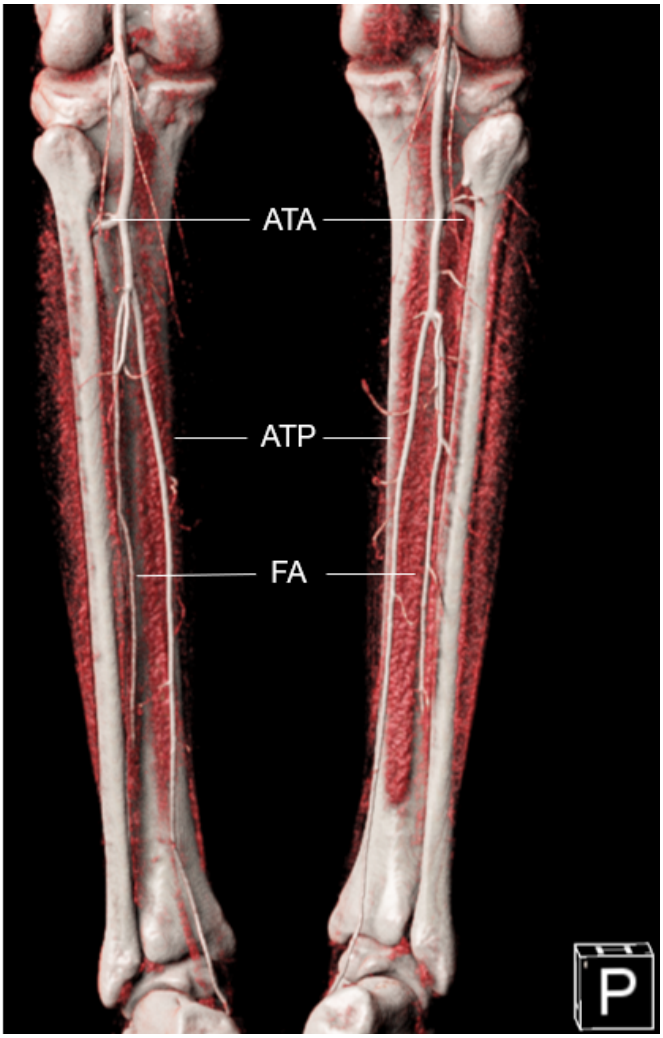

Abbildung 21. Dargestellt ist eine CVR eines 27-jährigen Patienten von posterior [P] aus unserer Klinik im Rahmen der präoperativen Planung bei einem Ameloblastom des Unterkiefers. Im Patientenfall liegt eine geeignete Gefäßversorgung der Unterschenkel beidseits vor. Regelhaft ausgebildet sind die ATA, ATP und FA. Damit liegt beidseitig ein infra-popliteales Versorgungsmuster nach der Klassifikation von Kim et al. [328] vom Typ I-a vor. Deutlich sind septo-kutanen Perforatoren der FA und ATP zu erkennen. Software: MeVisLab (MeVis Medical Solutions AG, Bremen, Deutschland). (ATA, *A. tibialis anterior;* ATP, *A. tibialis posterior*; FA, *A. fibularis*)

Zur präoperativen Beurteilung des „makrovaskulären“ Gefäßstatus der Donorseite können eine invasive Angiographie- (DSA) [329, 330] und nicht-invasive Verfahren wie MR- [329, 331-334] oder CT-Angiographie [331, 335-337] durchgeführt werden. CT-Untersuchungen der Donor- und Empfängerregion werden bei der Methode VSP zur virtuellen Resektion und der digitalen Rekonstruktionsplanung benötigt. Auf der Basis der CT-Daten können dann segmentierte Computermodelle erstellt werden und patientenspezifische Implantate bzw. Osteosyntheseplatten mit entsprechenden Präparierschablonen geplant werden [110, 111, 113]. Die CT-Angiographie (CTA) ermöglicht die gleichzeitige Untersuchung und Beurteilung der knöchernen und vaskulären Strukturen [338]. Sie bietet als nicht-invasives Bildgebungsverfahren im Vergleich zur DSA unter anderem den Vorteil der Vermeidung von Komplikationen der intraarteriellen Anwendung, wie z.B. die Bildung von Pseudoaneurysma und arteriovenösen Fisteln [339]. Als Standardbildgebung des infra-poplitealen Systems hat sich die CT-Angiographie in der pAVK-Diagnostik etabliert [340]. Zudem ist sie der MR-Angiographie in der Visualisierung des Perforatorensystems überlegen [341]. Die CT- ist breiter verfügbar, ausreichend präzise und überdies kostengünstiger im Vergleich zur MR-Angiographie [336, 342, 343].

Im Gegensatz zum klinischen Allen-Test, dessen Erstbeschreibung auf *Edgar Allen* im Jahr 1929 zurückgeht und eine suffiziente Beurteilung der Perfusion der Hand über die *A. radialis* und *ulnaris* darstellt [344, 345], steht kein klinisches Verfahren für die sichere Evaluation der infra-poplitealen Gefäßversorgung zur Verfügung. Zur Diagnostik der peripheren arteriellen Verschlusskrankheit (pAVK) wird der Ankle-Brachial-Index (ABI) als kostengünstiger und nicht-invasiver Test genannt [139]. Werte von 0,9 oder weniger werden als pathologisch eingestuft. Sie implizieren eine weitere Diagnostik der pAVK [346-348] durch eine MR- oder CT-Angiographie [349, 350]. In der Literatur wird berichtet, dass pathologische Ergebnisse der präoperativen ABI Untersuchung mit Problemen bei der arteriellen Anastomose korrelieren [351]. Die Kombination aus klinischer ABI- und Handgerät-Doppler-Sonographie-Untersuchung ist nicht ausreichend für eine präoperative Beurteilung des Gefäßsystems zur Planung eines freien Fibulatransplantats [352]. Die CT-Angiographie bietet damit in einem Untersuchungsgang eine suffiziente Beurteilung des vaskulären Status des infra-poplitealen Gefäßsystems zum Ausschluss relevanter Pathologien und anatomischer

Varianten, die eine kritische Durchblutungssituation mit Verlust der Extremität auslösen könnten [331, 353-356].

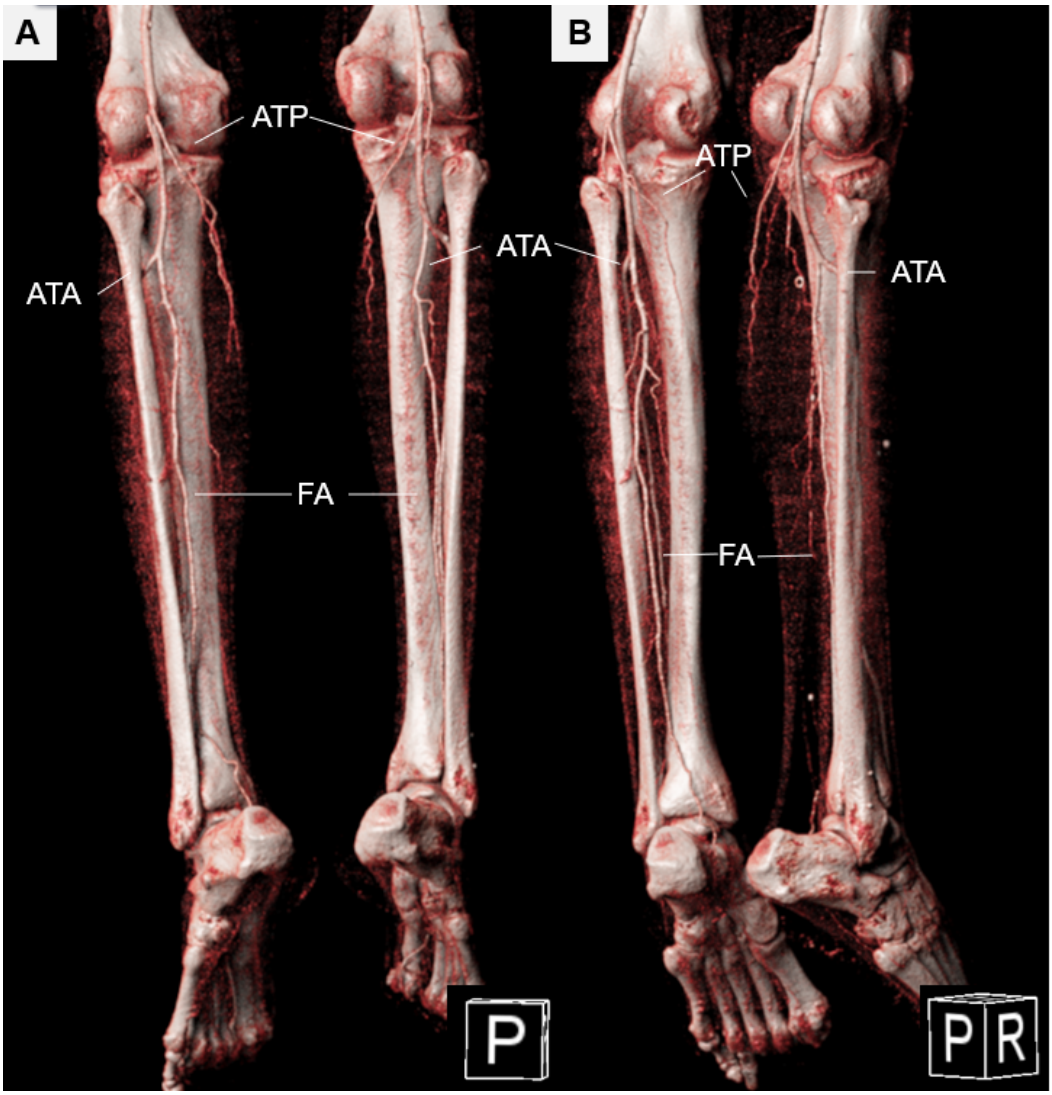

Abbildung 22. Dargestellt ist eine CVR einer 67-jährigen Patientin aus der Perspektive von posterior [P] in (A) und schräg posterior-rechts [P|R] in (B) aus unserer Klinik im Rahmen der präoperativen Planung bei einem Plattenepithelkarzinom des Alveolarfortsatzes in regio 46-47. Im präsentierten Fallbeispiel liegt eine nicht geeignete Gefäßversorgung der Unterschenkel beidseits vor. Regelhaft ausgebildet sind die ATA und FA, während die ATP auf Höhe des Kniegelenks entspringt und im proximalen Unterschenkeldrittel bereits verdämmert. Damit liegt beidseitig ein infra-popliteales Versorgungsmuster nach der Klassifikation von Kim et al. [328] vom Typ III-a vor. Software: MeVisLab (MeVis Medical Solutions AG, Bremen, Deutschland). (ATA, *A. tibialis anterior;* ATP, *A. tibialis posterior*; FA, *A. fibularis*)

Ergänzend zu der Beurteilung einer geeigneten Gefäßanatomie (**Abbildung *22***) ergibt sich die Frage, inwiefern die CT-Angiographie-Daten genutzt werden könnten, um zum

einen in der Diagnostik- und Planungsphase drohende Komplikationen zu erkennen und zum anderen diese Aspekte bei der VSP individuell hinsichtlich Segmentlänge und Hautinseldesign einfließen zu lassen.

4.3.1. Analyse des makro- und mikrovaskulären infra-poplitealen Systems mit besonderem Fokus auf Äste der *A. fibularis*

Der Originalarbeit 4 [357] liegen Untersuchungen zur darstellbaren Gefäßversorgung der Fibula in der „Routine"-CT-Angiographie-Bildgebung für VSP zugrunde. Besonderes Augenmerk lag dabei auf der „Architektur" des infra-poplitealen Gefäßsystems sowie der Dichte und Verteilung der kleinen Gefäße der *A. fibularis* - der periostalen Äste (PB) und der septo-kutanen Perforatoren (SCPs). Der im Folgenden verwendete Begriff „periostale Äste" (PB, *periosteal branch*) umfasst die penetrierenden *Vasa nutricia* und die nicht-penetrierenden Gefäße der *A. fibularis*.

Insgesamt wurden 144 Unterschenkel verblindet analysiert (Durchschnittsalter: 58,5 ± 15,3 Jahre; Frauen: n = 28, 38,9 %; Männer: n = 44, 61,1 %). Zur Qualitätssicherung war für den Untersucher nicht erkennbar, welcher Unterschenkel als spätere Fibula-Donorseite gewählt wurde.
Das Gefäßsystem wurde in 140 Fällen (97,2 %) gemäß der Klassifizierung von *Kim et al.* [328] als regelrecht (Typ I-A bis II-C) eingestuft. Vaskuläre Auffälligkeiten traten in Form hypoplastischer *A. tibialis anterior* (Typ III-A, n = 2) und jeweils ein Fall einer hypo- und aplastischen *A. tibialis posterior* (Typ III-B, n = 2) auf. In diesen Fällen lagen dominante FA-Varianten vor. Stenosen wurden in n = 14 Fällen gefunden, wovon n = 11 in der *A. fibularis*, n = 1 in der *A. tibialis anterior* und n = 2 in der *A. tibialis posterior* registriert wurden.

Ribuffo et al. fanden, dass die CT-Angiographie Größe, Verlauf und das Penetrationsmuster der Perforatoren der *A. fibularis* (PB und SCP) mit einem Durchmesser von mehr als 0,3 mm abbilden kann [336]. Deutlicher gelingt die Darstellung ab einem Durchmesser ≥ 1 mm [358, 359]. Unsere Ergebnisse bestätigen das Auflösungs- und Darstellungsvermögen der CT-Angiographie [336, 357]. Für septo-kutane Perforatoren beobachteten wir einen Durchmesser von 0,93 ± 0,30 mm

(Spanne: 0,52 - 2,43 mm) und für periostale Äste 0,87 ± 0,25 mm (Spanne: 0,35 - 2,26 mm). Insgesamt konnten 361 periostale Äste (PB) und 231 septo-kutane Perforatoren (SCP) der FA erfasst werden. Für die Verteilung der PB wurde ein Verteilungsmuster mit zwei und für die septo-kutane Perforatoren mit drei Häufigkeitsgipfeln gefunden. Für PB wurde ein schmaler Häufigkeitsgipfel bei 0,30 RD (relativer Abstand: 0 = Malleolus lateralis; 1 = Caput fibulae) und im mittleren Drittel ein breiter zwischen 0,55 RD und 0,70 RD gefunden. Bei den SCPs wurde ein dreigeteiltes Verteilungsmuster aufgezeichnet. Distal wurde ein schmaler Häufigkeitsgipfel bei 0,30 RD, im mittleren Drittel ein breiterer zwischen 0,45 und 0,60 RD und ein weiterer schmaler im proximalen Drittel bei 0,70 RD gefunden. Eine ähnliche Verteilung konnten *Gaillard et al.* für SCP ermitteln. Sie beobachteten in einer anatomischen Untersuchung an zehn Unterschenkeln 126 SCP und stellten fest, dass sich diese auf das mediane und proximale Fibuladrittel konzentrierten. Die suprafasziale Gefäßachse stellt somit die anatomische Grundlage für einen faszio-kutanen Lappen lateral der Fibula (sog. Perforator flap) dar [360]. Während die Lokalisationen der Perforatoren mit Ergebnissen anderer Studien vergleichbar waren [64, 334, 343], ergaben sich Unterschiede in der Dichteverteilung [361]. So demonstrierten *Fry et al.* anhand von CT-Untersuchungen, nach Applikation eines Barium-Latex-Gemisches an frischen humanen Fibulapräparaten, im Durchschnitt 12,8 periostale Äste (PB) der FA mit einem mittleren Abstand von 1,36 cm [361]. Sie beobachteten in 65,1 % auf einem 1,0 cm-Abschnitt, in 83,4 % auf einem 1,5 cm und in 94 % der 2,0 cm langen Fibulasegment einen PB [361]. Die hier ausgewerteten Routine-CT-Angiographien zeigen nur in 10,8 % einen periostalen Ast auf einem 1,0 cm langen Fibulaabschnitt. Die Wahrscheinlichkeit, mindestens einen periostalen Ast finden zu können, steigt auf einem 2,0 cm langen Abschnitt auf 21,1 % und in einem 3,0 cm-Segment auf 29,17 %. Ein Vergleich unserer Ergebnisse mit der Präparate-Studie ist jedoch nur eingeschränkt möglich aufgrund der methodischen Unterschiede, der applizierten Strahlendosis und der Art des verwendeten Kontrastmittels [361].

In der Zusammenschau mit den Forschungsergebnissen anderer Arbeitsgruppen muss konstatiert werden, dass die Zahl der periostalen Äste und septo-kutanen Perforatoren in der CT-Angiographien im Vergleich zu anatomischen Untersuchungen in der Routine- CT-Angiographien unterschätzt wird [275, 334, 336, 343, 360, 361].

Die Diskrepanz zwischen anatomischen und radiologischen Befunden ist hierbei zunächst auf die Qualität der CT-Angiographien zurückzuführen. Die Faktoren Zeitpunkt, Dosierung und Abstimmung des Kontrastmittel-Bolus auf die Bildabfolge beeinflussen die Genauigkeit der CT-Angiographien [362]. Dennoch ermutigen die Ergebnisse, da es aus anatomischer Sicht somit möglich scheint, kürzere Segmente in die Kieferrekonstruktion einzubeziehen, was eine größere Flexibilität in der Rekonstruktion der Empfängerregion bedeutet. Bei der VSP vermeiden wir möglichst Segmentlängen unter 30 mm, um eine suffiziente Knochensegmentperfusion zu gewährleisten und damit einen partiellen bzw. totalen Lappenverlust zu vermeiden.

Aus der Untersuchung können als Fazit drei Kernaspekte abgeleitet werden.

1. Die Routine-CTA für die VSP kann die infra-popliteale Gefäßarchitektur zuverlässig darstellen.
2. Die Fibula wird von periostalen Ästen gespeist. Die Wahrscheinlichkeit, mindestens einen PB auf einem 2,0 cm langen Fibulaabschnitt einzuschließen, beträgt 94 % in anatomisch-radiologischen Untersuchungen [361]. Die durchgeführte CT-Angiographie-Auswertung registrierte auf einem 2,0 cm-Abschnitt in 21,1 % einen periostalen Ast. Anzahl und Dichte der in der Routine-CTA erkennbaren periostalen Äste müssen als geringer als in Wirklichkeit vorliegend angenommen werden.
3. Je weiter proximal ein Fibulaabschnitt untersucht wurde, desto häufiger wurden periostale Äste im Vergleich zu weiter distal gelegenen Sektionen erfasst. Eine Verschiebung der Fibula-Donorregion nach distal zu Gunsten einer Maximierung der Gefäßstiellänge verlagert die Hautinselentnahmeregion in weniger dicht mit septo-kutanen Perforatoren versorgtes Gebiet.

4.3.2. Einfluss in der CTA sichtbarer „kleiner Gefäße“ auf den Lappenerfolg?

Die Kenntnis über die Lage und den Verlauf der kleinen Gefäße (PB und SCP) kann bei der VSP und dem Design einer Hautinsel helfen, um drohende Komplikationen im Sinne von (sub-)totalen Transplantatverlusten zu vermeiden. Beim mikrovaskulären

Fibulatransplanat wurde festgestellt, dass die Blutversorgung von Segmenten nicht gefährdet ist, solange die Verbindung zum Gefäßstiel erhalten, das segmentale Periost intakt und von einer dünnen Muskelgewebemanschette bedeckt ist [48]. Längere Fibulassegmente und eine geringe Anzahl von Osteotomien korrelieren mit einer höheren Perfusion des distalen Fibulasegmentes [145]. Vorangegangene Untersuchungen unserer Forschungsgruppe an der Studienstichprobe ergaben unterschiedliche Verteilungsmuster und Häufigkeiten für periostale Äste (PB) und septo-kutane Perforatoren (SCP) der FA auf der Basis der CT-Angiographie beider Beine [357]. Darüber hinaus wurden im Vergleich zu anatomischen Studien signifikante Unterschiede in Bezug auf die Anzahl und Dichte der periostalen Äste pro Knochensegment festgestellt [361]. Je proximaler das Fibulatransplantat-Segment, desto häufiger wurde ein potenzieller periostaler Ast in der CT-Angiographie gefunden. In einer auf die Originalarbeit 4 aufbauenden Untersuchung wurde ein Matching der radiologischen Verteilung der kleinen Gefäße der *A. fibularis* mit den finalen virtuellen Planungen und den operativen Ergebnissen unseres Patientenkollektivs durchgeführt (Originalarbeit 5, [276]).

1. Welchen Einfluss haben das infra-popliteale Verzweigungsmuster und Stenosen der *A. fibularis* auf das Ergebnis des freien Fibulatransfers?

Die Auswertung der Gefäßarchitektur des Donorunterschenkels ergab, dass nach der Klassifizierung von *Kim et al.* [328] in 93,1 % ein Typ I-A vorlag (Nicht-Spenderstelle: 84,7 %). Zwei Gefäßsysteme der Donorseite wurden als Typ I-B klassifiziert, und je ein Fall wurde den Kategorien I-C bis II-B zugeordnet. Vier Unterschenkel der Nicht-Spenderstelle wiesen dominante FA-Varianten auf (III-A: $n = 2$; III-B: $n = 2$). Die ***Abbildung 23*** zeigt exemplarisch *Cinematic Volume Rendering* (CVR)-Rekonstruktionen der Unterschenkel aus CT-Angiographien und verschiedene infra-popliteale Aufzweigungsmuster der *A. poplitea*. Die postprozedurale Erstellung dieser Bilder wurde mit einem eigens dafür erstellen Modul mit der Software (Freeware) MeVisLab (MeVis Medical Solutions AG, Bremen, Deutschland) durchgeführt. CVR erlaubt ein intuitives, plastisches Verständnis der radiologisch erhobenen Bilddaten. Weitere Ausführungen hierzu sind im Abschnitt 3.7.1. darlegt.

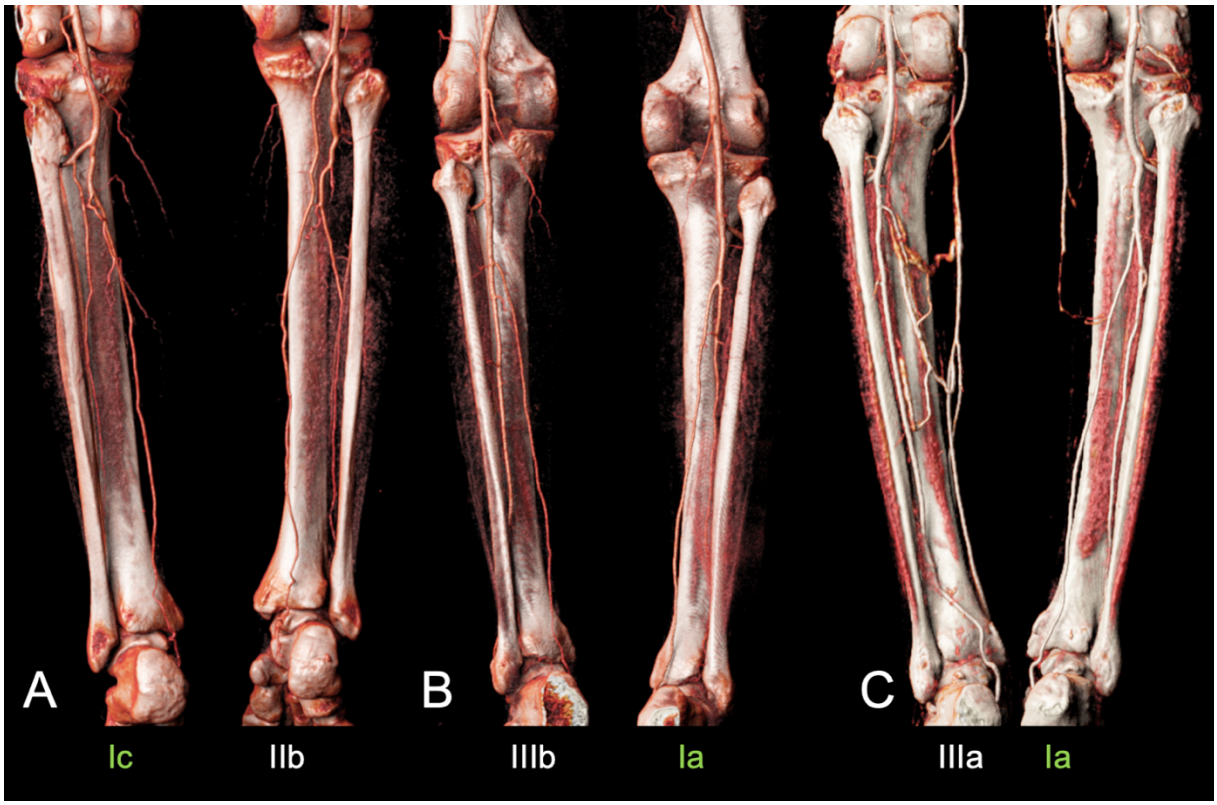

Abbildung 23: Fallbeispiele aus unserer Klinik. Cinematic Volume Rendering (CVR) der Unterschenkel aus CT-Angiographien mit MeVisLab (MeVis Medical Solutions AG, Bremen, Deutschland). Die infra-poplitealen Gefäßsysteme der Patienten A, B und C sind nach der Klassifikation vom *Kim et al. [328]* eingeteilt. Grün unterlegt ist die gewählte Donorseite des Fibulatransplantats. Die CVR-Rekonstruktionen wurden mittels eines eigen entwickelten Moduls generiert.

Die Blutversorgung des Fußes wird dann zwischen der *A. fibularis* und nicht-hypoplastischer ATA oder ATP bei Typ III-A und B geteilt, und die FA ist infolgedessen vergrößert [363-365]. In 5,2 % der Fälle scheint eine dominante FA-Variante (Typ III-A oder III-B) vorzuliegen [331]. In der untersuchten Studienstichprobe war weder auf der Donor- noch auf der Non-Donorseite eine *A. peronea magna* (Typ III-C) vorhanden, bei der die *A. fibularis* den Unterschenkel und den Fuß mit Blut versorgt. Die beobachtete Verteilung der infra-poplitealen Verzweigungsvarianten der *Arteria poplitea* ist damit vergleichbar mit den Beobachtungen anderer Studien [366]. Vor der Entnahme eines Fibulatransplantates ist es erforderlich, einen Versorgungstypus III-C auszuschließen, um eine kritische Ischämie der unteren Gliedmaßen und des Fußes zu verhindern [353, 355, 356]. So ergab unsere Untersuchung, dass bis auf einen Fall eines Typ I-B alle partiellen (*PFF*) und totalen Lappenverluste (*TFF*) dem Verzweigungsmuster Typ I-A zugeordnet werden konnten. In Übereinstimmung mit der Literatur ist der Typ I-A das häufigste Verzweigungsmuster. Lappentransfers konnten

bei Vorliegen eines Typs I-B, I-C, II-A und II-B (jeweils *n* = 1) ebenfalls erfolgreich durchgeführt werden.
In der Untersuchungsgruppe wurden in 9,7 % kalzifizierende Stenosen (*n* = 14) des infra-poplitealen Systems identifiziert, von denen *n* = 11 die FA betrafen. In fünf Fällen wurde trotz Vorliegen kalzifizierender Stenosen im distalen Verlauf der FA die Fibula der betroffenen Seite als Donorregion gewählt. In zwei Fällen kam es zum vollständigen Lappenverlust (*TFF*), während in drei Fällen die beobachteten kalzifizierenden Stenosen keinen Einfluss auf den Lappenerfolg hatten. Bemerkenswert ist, dass die Mehrzahl der festgestellten Stenosen in der *A. fibularis* lokalisiert war, da andere Studien ergaben, dass die beiden Tibia-Arterien-Gefäße häufiger von pAVK als die FA betroffen sind [353, 355, 356].

Lee et al. führten trotz kalzifizierender Stenosen der Lappenstielgefäße erfolgreiche mikrovaskuläre Fibulatransplantationen durch. Sie registrierten im postoperativen Verlauf 7 % partielle Lappenverluste, jedoch keinen Fall eines totalen Lappenverlustes [367]. Die präoperative Optimierung der Unterschenkelperfusion durch endovaskuläre Interventionen wird als therapeutische Option bei kritischer Extremitätenperfusion vor Entnahme eines Fibulatransplantates beschrieben [368].
Weitere Studienergebnisse zeigten signifikante Unterschiede in Bezug auf die Länge des *Truncus tibio-fibularis,* des gemeinsamen Stamms der *A. fibularis* und *A. tibialis posterior* nach Abzweigung der *A. tibialis anterior* aus der *A. poplitea.* Der *Truncus tibio-fibularis* war in der *TFF* Gruppe mit 40,1 ± 14,9 mm signifikant länger im Vergleich mit der Erfolgsgruppe ($p = 0{,}034$). Ein längerer *Truncus tibio-fibularis* impliziert eine Verkürzung der *A. fibularis* und damit des freien Gefäßstiels des Fibulatransplantates. Während ein kurzer Gefäßstiel die mikrochirurgische Anastomose technisch erschweren kann [369], ist ein langer Gefäßstiel gefährdet abzuknicken und sich zu verdrehen. Beides kann zu einer kritischen Durchblutung führen [370]. In der Literatur wird ein Zusammenhang zwischen der Länge und dem Verlauf der *Truncus tibio-fibularis* und einem hohen Körpergewicht aufgezeigt. Ein hyperalimentärer Zustand kann einen gestreckten und gedrehten *Truncus tibio-fibularis* begünstigen und die Entstehung lokaler Atherosklerose fördern, was in letzter Folge die Mikrochirurgie erschwert [371].

Zusammenfassend kann gesagt werden, dass ein infra-popliteales Verzweigungsmuster vom Typus I-A bis II-B in der vorliegenden Studie keinen Einfluss auf das Ergebnis des Lappentransfers hatte. Trotz präoperativ festgestellter kalzifizierender Stenosen der *A. fibularis* verlief in mehr als der Hälfte der von Stenosen betroffenen Fälle der freie Fibula-Lappentransfer erfolgreich.

2. Wie beeinflusst die Verteilung periostaler Äste und septo-kutaner Perforatoren das chirurgische Ergebnis von mono- und polysegmentalen Kieferrekonstruktionen und (sub-)totalen Lappenverlust?

Beim Abgleich der geplanten Fibulasegmente mit den ermittelten periostalen Ästen auf Grundlage der CTA waren 38,5 % aller virtuell geplanten Fibulasegmente (*n* = 143 bei 72 Patienten) mit der Lage mindestens eines periostalen Astes kongruent. Wurden die durch mindestens einen periostalen Ast deutlich versorgten Segmente den Lappenergebnisgruppen zugeordnet, zeigte sich, dass die Gruppe vollständiger Lappenerfolg (*CS*) mit 37,2 % die niedrigste und die Gruppe partieller Lappenverlust (*PFF*) mit 50,0 % die höchste Quote aufweist, die Gruppe vollständiger Lappenverlust (*TFF*) mit 42,9 % liegt zwischen beiden. Es gelang also nur in etwa der Hälfte der geplanten Fibulasegmente, einen periostalen Ast auf diesem Fibulaabschnitt in der CT-Angiographie zu registrieren. Mono- und polysegmentale Rekonstruktionen verliefen erfolgreich, auch wenn in der CT-Angiographie-Auswertung kein distinkter periostaler Ast retrospektiv in dem geplanten Segment registriert wurde. Umgekehrt traten Misserfolge auf, obwohl periostale Äste und septo-kutane Perforatoren in einem geplanten Segment nachweisbar waren.

Battaglia et al. berichteten über 20 Patienten, bei denen anhand von präoperativer CT-Angiographie die Lage der septo-kutanen Perforatoren verortet und mit dem intraoperativen Befund während der Fibula-Präparation korreliert wurde [335]. Dabei fanden sie in allen Fällen in der CT-Angiographie septo-kutane Perforatoren und intraoperativ eine durchschnittliche Abweichung der Perforatorposition von 1 mm (Spanne: 0 - 2 mm) gegenüber der Lage in der CT-Angiographie. Die präoperative CT-Angiographie-Analyse kann zum Mapping der Lage und des Verlaufs der septo-kutanen Perforatoren bei VSP eine hilfreiche Ergänzung zur Planung der Hautinsel sein [335]. Bestehende CT-Angiographie-Protokolle und Abläufe der VSP müssen

weiterentwickelt werden, um die Lage der septo-kutanen Perforatoren im Rahmen der VSP berücksichtigen zu können [337]. Sie weisen aber darauf hin, dass die Berücksichtigung der septo-kutanen Perforatoren im Rahmen der VSP bei der Planung der polysegmentalen Rekonstruktion und der Hautinsel möglich erscheint [337].

Die Untersuchung erbrachte damit keinen Informationszugewinn bezüglich des späteren Lappenoutcomes, wenn die Quote der in der CT-Angiographie erfassten periostalen Äste pro Segment rückblickend ermittelt wurde. Mono- und polysegmentale Rekonstruktionen waren erfolgreich, wenn bei der CT-Angiographie-Auswertung keine periostalen und septo-kutanen Abgänge gefunden wurden, und waren sogar erfolglos, wenn periostale und septo-kutane Abgänge erfasst wurden.

3. Beeinflusst die beobachtete Verteilung periostaler Äste und septo-kutaner Perforatoren die Wundheilung der Entnahmestelle?

Wundheilungsstörungen der Donorregion wurden ausnahmslos nach Entnahme einer septo-kutanen Hautinsel festgestellt. Alle Hautinselentnahmedefekte wurden in unserem Kollektiv mit einem autologen, 400 µm dicken Spalthauttransplantat verschlossen. Die Rate an Wundheilungsstörungen betrug in der Gruppe vollständiger Lappenverlust (*TFF*) 55,5 % (n = 5 von 9), während die Rate in der Gruppe Lappenerfolg (*CS*) mit 52,5 % (n = 31 von 59) bestimmt wurde. Der marginale Unterschied ist aufgrund der geringen Fallzahl kritisch zu sehen. Die Ergebnisse wurden differenziert nach Wundheilungsstörungen vom Minor- und Major-Typ. Der Minor-Typ wurde definiert durch eine kleine Wundfläche, die ausschließlich einer lokalen Therapie bedurfte. Eine Wundheilungsstörung vom Major-Typ ist charakterisiert durch eine Wunde mit freiliegender Sehne und der Notwendigkeit einer chirurgischen Therapie (z.B. Debridement) und wiederholter Spalthauttransplantation. Wundheilungsstörungen vom Major-Typ traten in der Gruppe vollständiger Lappenerfolge mit 33,9 % rund doppelt so häufig auf wie solche vom Minor-Typ mit 18,6 %. Kumulativ betrachtet wurden Wundheilungsstörungen in 52,8 % der untersuchten Studiengruppe festgestellt, während in der Literatur Komplikationsraten von 2 % bis 38 % für die Donorregion angegeben werden [372-375]. Die breite Spanne für lokale Komplikationen kann mehrere Ursachen haben. Es gibt unterschiedliche Techniken zur Entnahme des Fibulatransplantates wie verschiedene operative

Zugangswege oder die Möglichkeit zur Präparation in Blutleere. Hinsichtlich der Defektdeckung der Entnahmeregion reicht die Bandbreite von primärem Wundverschluss über freie Granulation, Spalt- oder Vollhauttransplantationen [376] unter anderem in Kombination mit der Anwendung von Niederdruckwundverbänden (VAC-Therapie) [377], ggf. temporärer Unterschenkel-Immobilisation (Gipsschiene) bis hin zu mikrovaskulären Lappentransplantaten [378]. Neben dieser technischen Heterogenität ist es auch eine Frage der Definition, wann eine Wundheilung als gestört bewertet wird. In der durchführten Untersuchung erfolgte die Datenerhebung retrospektiv, was zumeist zu einer Unterschätzung der Fallzahl aufgrund von Dokumentationslücken führt. Die hier gewählte Unterscheidung von Wundheilungsstörungen vom Major-Typ und Minor-Typ hat dabei praktische Gründe, da chirurgische Wundrevisionen, die eine erneute Spalthauttransplantation bedurften, als operative Prozedur im Patienteninformationssystem hinterlegt sind. Solche vom Minor-Typ hingegen lassen sich nur anhand von Aktenrecherche bzw. klinischen Fotos erheben. Aus diesem Blickwinkel betrachtet erscheint die genannte Major-Typ-Komplikationsrate in der Gruppe vollständiger Lappenerfolge mit 33,9 % mit der in der Literatur angegebenen Spanne vergleichbar zu sein.

Es wurde die Matching-Rate für septo-kutane Perforatoren pro Segment, für Fibulatransplantate mit eingeschlossener Hautinsel, erhoben. Eine Gesamtzahl von 126 Segmenten bei 64 Patienten hat gezeigt, dass insgesamt nur 28,6 % aller virtuell geplanten Segmente mit einer oder mehreren Lokalisationen septo-kutaner Perforatoren übereinstimmten, was daher keine statistischen Rückschlüsse hinsichtlich des Auftretens einer Wundheilungsstörung erlaubte. Das Problem der donorseitigen Morbidität ist in der Literatur bekannt und der ideale Verschluss der Entnahmestelle nach wie vor Gegenstand reger Diskussion [378]. Die Methoden reichen dabei von primärem Verschluss, offener Wundheilung, Spalthauttransplantation, Vollhauttransplantation bis zu freien, mikrovaskulären Lappen [372, 376, 378]. Multiple Inzisionen, welche zirkulär in die den Entnahmedefekt umgebende Haut erfolgen, dienen der Verkleinerung der Wundfläche und führen zu zufriedenstellenden ästhetischen Ergebnissen [379]. Die Anwendung von Niederdrucksaug-Systemen wird ebenfalls beschrieben. Sie ermöglichen eine frühere Mobilisierung der Patienten und führen zu einer akzelerierten Wundheilung [377]. Letztlich spielen die Größe der Hautinsel und des Entnahmedefekts sowie der

Allgemeinzustand und die Komorbiditäten des Patienten eine entscheidende Rolle bei der Wundheilung. Darüber hinaus haben viele andere Faktoren einen wichtigen Einfluss auf die Wundheilung der Donorregion nach Entnahme einer Hautinsel [376]. *Li et al*. verwendeten eine bivariate Korrelationsanalyse, um die Risikofaktoren für frühe und späte Komplikationen der Donorregion von Fibulatransplantaten zu bewerten [380]. Sie fanden heraus, dass die entnommene Segmentlänge, die Operationszeit und die Follow-up-Zeit wichtige Faktoren für die späte Morbidität an der Donorregion waren. Keiner dieser Faktoren für sich zeigte einen statistisch signifikanten Effekt auf die Wundheilung [380]. In der Auswertung von *Shindo et al.* wiesen starke Raucher eine signifikant erhöhte Inzidenz von Komplikationen an der Donorregion auf [221]. Die Arbeitsgruppe vermutete außerdem, dass der Zeitpunkt des Muskelödems und die Lage der Hautinsel zwei weitere wichtige Variablen sind, die Morbidität und Wundheilungsrate der Donorregion beeinflussen [221]. Die Lage der Hautinsel wird durch die intraoperativ sichtbaren septo-kutanen Perforatoren im Bereich des *Septum intermusculare posterius* bestimmt. Je mehr septo-kutane Äste für die Versorgung eben dieser in die Lappenpräparation eingeschlossen werden, desto sicherer ist zwar eine zuverlässige Versorgung der Hautinsel, kompromittiert aber dadurch die vaskuläre Versorgung des Entnahmebetts und trägt zu Wundheilungsstörungen bei.

Die Verteilung der in der präoperativen CT-Angiographie erfassten septo-kutanen Perforatoren pro Segment erlaubte keinen Rückschluss auf Wundheilungsstörungen der Donorregion nach Entnahme einer Hautinsel.

Fazit:

Patienten, bei denen ein Malignom mit Kieferbeteiligung diagnostiziert wurde, werden nach ablativer Tumorchirurgie - wenn möglich - einer einzeitigen Kieferrekonstruktion, und von uns bevorzugt mit einem Fibulatransplantat, zugeführt. Die digitale Technologie ermöglicht es rekonstruktiven Kieferchirurgen, die operative Rekonstruktion ideal zu simulieren und dann im Operationssaal mithilfe von Schablonen und PSI auf den Patienten zu übertragen. Anatomische Untersuchungen anderer Arbeitsgruppen haben gezeigt, dass Fibulasegmente mit einer Länge von 2 cm mit sehr hoher Wahrscheinlichkeit von mindestens einem periostalen Ast der *A. fibularis* versorgt sind [361]. Im Vergleich dazu haben unsere - auf konventionellen CT-

Angiographie-Untersuchungen basierenden Daten - eine geringere Anzahl von Perforatoren ergeben, was einer geringen Auflösung gegenüber der anatomischen Realität entspricht. Im Ergebnis ergab sich weder eine positive noch eine negative Korrelation bezüglich der Verteilung der kleinen Gefäße und dem Lappenergebnis [276].

Abschließend bleibt festzuhalten, dass sowohl der Einsatz von *Cinematic Volume Rendering* als Planungshilfe als auch die Verwendung von patienten-spezifischen Implantaten im Sinne von Mini-Platten wesentliche Impulse für künftige Kieferrekonstruktionen sind.

5. Zusammenfassung

Das freie mikrovaskuläre Fibulatransplantat (FFF) ist in der plastisch-rekonstruktiven Mund-, Kiefer- und Gesichtschirurgie (MKG) zur Wiederherstellung ausgedehnter Kieferdefekte etabliert. Es wurden retrospektiv Patientendaten aus der Klinik für MKG-Chirurgie der Justus-Liebig-Universität Gießen erhoben, bei denen zwischen 01/2002 und 12/2020 eine Kieferrekonstruktion mit einem Fibulatransplantat durchgeführt wurde. Die hier präsentierten klinischen Versorgungsstudien untersuchten zum einen die Einflussfaktoren für das Auftreten partieller und totaler Lappenverluste. Weiterhin konnte eine Klassifikation für die heterotope Ossifikationen nach Kieferrekonstruktion mit dem Fibulatransplantat erarbeitet und publiziert werden. Ein weiterer Fokus lag in der vergleichenden Analyse von konventionellen/analogen versus virtuellen/digitalen Planungen (VSP) mit patienten-spezifischen Implantaten (PSI). Zwar hat sich die VSP mit PSI als effektives und präzises Instrument zur Kieferrekonstruktion erwiesen, jedoch bestehen noch Defizite hinsichtlich der Komplikationsraten wie unvollständige Verknöcherungen der Übergangsbereiche Kieferknochen zu Transplantat und einer Exposition von Osteosynthesematerial. Für die rekonstruktive Tumorchirurgie wurde ein zusätzlicher Bedarf von rund 11 Tagen für die planungs- und fertigungsbedingte Vorlaufzeit von patienten-spezifischen Implantaten festgestellt. Der Einfluss dieser hinzukommenden verfahrensbedingten Zeitverzögerung von Erstvorstellung bis zur Operation wurde anhand des Residualstatus untersucht. Es konnte kein negativer Einfluss auf das Tumorgeschehen dokumentiert werden. Im Weiteren konnte auf Basis der präoperativen CT-Angiographien für die Methode VSP die vaskuläre Architektur der infra-poplitealen Gefäße und der kleinen Äste der *A. fibularis* mit den Ergebnissen des Lappentransfers korreliert werden. Die Berücksichtigung der kleinen Äste der *A. fibularis* im Rahmen der virtuellen Planung zur Gestaltung kleinerer Transplantatsegmente und einer „maßgeschneiderten“ Hautinsel scheint mit den bislang zur Verfügung stehenden Visualisierungsmethoden nicht vielversprechend.

<u>Ausblick:</u>

Totale Transplantatverluste nach mikrovaskulären Kieferrekonstruktionen mit einem Fibulatransplantat treten unabhängig von der verwendeten Planungs- und Rekonstruktionsmethode auf. Die Verwendung von Präparationsschablonen im

Rahmen der Transplantathebung und -formung scheint einen protektiven Effekt auf die Verlustrate der septo-kutanen Hautinsel zu haben. Dieser Effekt basiert dabei neben dem mechanischen Schutz durch die Osteotomieschablone auch auf der dadurch verkürzten Präparationsdauer der Rekonstruktion. Die zum korrekten Aufsitz der Schablone und des späteren PSI notwendige Präparation der Weichgewebsmanschette kann zu einer kritischen Durchblutung und damit zu einem partiellen Verlust knöcherner Transplantatanteile führen. Durch patientenspezifische Implantate können kürzere Schnitt-Naht-Zeiten bei gleichzeitig komplexeren Rekonstruktionen erreicht werden. Aus onkologischer Sicht ergab sich trotz der verfahrensbedingt verlängerten Vorlaufzeit eine geringere Rate an Lokalrezidiven. Zur Verbesserung der bei der Anwendung von patientenspezifischen Implantaten signifikant häufiger beobachteten unvollständigen Verknöcherung der Übergänge von Mandibula zu Fibula bzw. zwischen den einzelnen Fibulasegmenten scheint eine Trennung der durchgehenden Platte im Sinne einer segmentalen Osteosynthese sinnvoll, um eine physiologische Knochenremodellation zu stimulieren.

Da die Darstellung „kleiner Äste“ der *A. fibularis* mit den bislang zur Verfügung stehenden Visualisierungsmethoden nicht ausreichend gelingt, ist der Einsatz von *Cinematic Volume Rendering* (CVR) zur Visualisierung aus konventionellen CT-Schichtbildgebungen und deren Anwendung zur Planung von Hautinseln aktuell Gegenstand einer klinischen Machbarkeitsstudie.

6. Summary

The free microvascular fibular flap (FFF) is well established in oral and maxillofacial reconstructive plastic surgery for jaw reconstruction. Retrospective patient data were collected from the Department of Maxillofacial Surgery at Justus Liebig University in Giessen, Germany, who underwent jaw reconstruction with a fibular flap between 01/2002 and 12/2020. The presented studies investigated influencing factors on the occurrence of partial and total flap loss. Furthermore, a classification for heterotopic ossifications after jaw reconstruction with the fibula graft was developed and published. Another focus was the comparative analysis of conventional/analog versus virtual/digital planning (VSP) with patient-specific implants (PSI). Although VSP with PSI has been shown to be an effective and accurate tool for jaw reconstruction, there are still deficits in terms of complication rates when using PSI, such as incomplete ossification of the jawbone-to-graft transition areas and plate exposure. For reconstructive tumor surgery, an additional period of approximately 11 days was determined for the planning and fabrication-related lead time of patient-specific implants. For reconstructive surgery of the jaws, an additional requirement of approximately 11 days was identified for the planning and fabrication-related lead time of patient-specific implants. The influence of this added procedure-related time delay from initial presentation to surgery was investigated using the residual status. No negative influence on tumor progression could be documented. Furthermore, based on the preoperative CT angiographies for the method VSP, the vascular architecture of the infra-popliteal vessels and the small branches of the fibular artery could be correlated with the results of the flap transfer. Consideration of fibular arteries "small branches" in the context of virtual planning to design smaller graft segments and a "tailored" skin island does not seem promising with the visualization methods available to date.

Perspective:
Total graft loss after microvascular jaw reconstruction with a fibular graft occurs regardless of the planning and reconstruction method used. The use of preparation templates as part of graft elevation and shaping appears to have a protective effect on the rate of loss of the septo-cutaneous skin paddle. This effect is based not only on the mechanical protection provided by the osteotomy template but also on the resulting

shorter preparation time for the reconstruction. The preparation of the soft tissue cuff necessary for correct seating of the template and the subsequent PSI can lead to critical blood flow and thus to partial loss of bony graft components. Patient-specific implants can achieve shorter incision-suture times with more complex reconstructions. From an oncologic perspective, a lower rate of local recurrence was found despite the procedure-related prolonged lead time. To improve the incomplete ossification of the transitions from mandible to fibula or between the individual fibula segments, which is observed significantly more frequently when using patient-specific implants, a separation of the continuous plate in the sense of a segmental osteosynthesis seems to be useful to stimulate physiological bone remodeling.

The visualization of fibular arteries "small vessels" in the context of virtual planning to design smaller graft segments and a "customized" skin paddle does not seem promising with the visualization methods available so far. The use of *cinematic volume rendering* (CVR) for visualization from conventional CT-imaging and its application for planning skin paddle is currently the subject of a clinical feasibility study.

7. Erklärung

„Hiermit erkläre ich, dass ich die vorliegende Arbeit bzw. die mir zuzuordnenden Teile im Rahmen einer kumulativen Habilitationsschrift, selbstständig und ohne unzulässige Hilfe oder Benutzung anderer als der angegebenen Hilfsmittel angefertigt habe. Alle Textstellen, die wörtlich oder sinngemäß aus veröffentlichten oder nichtveröffentlichten Schriften entnommen sind, und alle Angaben, die auf mündlichen Auskünften beruhen, sind als solche kenntlich gemacht. Ich versichere, dass ich für die nach §2 (3) der Habilitationsordnung angeführten bereits veröffentlichten Originalarbeiten als Erst- oder Seniorautor fungiere, da ich den größten Teil der Daten selbst erhoben habe, für das Design der Arbeiten verantwortlich bin und die Manuskripte maßgeblich gestaltet habe. Für alle von mir erwähnten Untersuchungen habe ich die in der „Satzung der Justus-Liebig-Universität zur Sicherung guter wissenschaftlicher Praxis“ niedergelegten Grundsätze befolgt. Ich versichere, dass alle an der Finanzierung der Arbeiten beteiligten Geldgeber in den jeweiligen Publikationen genannt worden sind. Ich versichere außerdem, dass die vorgelegte Arbeit weder im Inland noch im Ausland in gleicher oder ähnlicher Weise einer anderen Prüfungsbehörde vorgelegt wurde oder Gegenstand eines anderen Prüfungsverfahrens war. Mit der Überprüfung meiner Arbeit durch eine Plagiatserkennungssoftware bzw. ein internetbasiertes Softwareprogramm erkläre ich mich einverstanden.“

Dr. med. Dr. med. dent. Heinz Michael Knitschke

8. Danksagung

Größter Dank gilt Herrn Univ.-Prof. Dr. med. Dr. med. dent. Hans-Peter Howaldt für seine Unterstützung bei diesem Projekt. Er ist mein chirurgischer Ausbilder und akademisch-wissenschaftlicher Förderer. Nur durch die Freiräume, die er mir während des klinischen Alltags gegeben hat, war dieser akademische Schritt möglich. Ohne seine kompetente Beratung und Expertise wäre diese Arbeit nicht möglich gewesen. Die wissenschaftliche Zusammenarbeit war zu jeder Zeit freundschaftlich und motivierend.

Unserer Arbeitsgruppe: Dr. Sameh Attia, MSc, Dr. Dr. Sebastian Böttger, apl. Prof. Dr. Dr. Philipp Streckbein, Dr. Daniel Schmermund, Christina Bäcker und Dr. Fritz Roller.

Mein großer Dank gilt dem gesamten Team der MKG-Chirurgie Gießen. Meinen ärztlichen Kollegen, die mir in der Phase des Schreibens Freiräume geschaffen und den Rücken freigehalten haben, den Kolleginnen aus der Anmeldung und Administration bei der Aktensuche, dem OP-Personal bei allen Fragen rund um das Material und den Doktorand*innen für Datenerhebung und Auswertung.

Danken möchte ich meinen Freunden Prof. Dr. Michael Stelzel für seinen unermüdlichen Zuspruch und seine Unterstützung, Dr. Dr. Stephan Hauk für seine Unterstützung während meines Zweitstudiums und Dr. Stephen Kalden für seinen großartigen und fortwährenden Optimismus. Björn, Jessica und Ben danke ich für die zahlreichen Wanderungen und die Erkenntnis, dass die Motivation immer eine Frage der Perspektive ist. Dem gesamten Team der ZNA größten Dank für die zahl- und lehrreichen Nachtdienste.

Ganz besonderer Dank geht an Frau Dr. Annika Trümner für das Korrekturlesen des Manuskripts.

Gewidmet ist diese Arbeit meiner Frau Rebekka und unseren wunderbaren Kindern Ole und Inga, die nicht nur mein großer Rückhalt sind, sondern mir täglich zeigen, was wirklich entscheidend im Leben ist. Ich danke Euch von ganzem Herzen.

9. Anhang

Tabelle 3. Klinische Daten der untersuchten Studiengruppe und Kategorisierung in die Gruppen: Erfolg, partiellen (PFF) und totalen Lappenverlust (TFF). Anmerkungen: BMI, Body mass index; E, Entlassung MRONJ, Medication-related osteonecrosis of the jaw; ND, Neck dissection; OPINT, operative Intensivstation; ORN, Osteoradionekrose; SD, Standardabweichung; VSP, virtual surgical planning. [a], asymptotische Signifikanz im Kruskal-Wallis-Test.

n = 180	Erfolg n = 144 (80,0 %)	PFF n = 16 (8,9 %)	TFF n = 20 (11,1 %)	p-Wert
Alter [y] ± SD	57,1 ± 13,4	59,9 ± 14,4	62,5 ± 9,5	0,165[a]
Follow-up [mo] ± SD	51,9 ± 51,6	48,0 ± 42,9	31,5 ± 31,6	0,341 [a]
PFF, Hautinsel	-	11	-	
PFF, Knochensegment	-	4	-	
PFF, Beides	-	1	-	
Weiblich	55 (38,2)	5 (31,3)	6 (30,0)	
Männlich	89 (61,8)	11 (68,8)	14 (70,0)	0,696 [a]
Diagnose				
Benigner Tumor	17 (11,8)	1 (6,3)	-	
Maligner Tumor	114 (79,2)	15 (93,8)	15 (75,0)	
MRONJ	2 (1,4)	-	2 (10,0)	
ORN	5 (3,5)	-	3 (15,0)	
Osteomyelitis	4 (2,8)	-	-	
Sonstige	2 (1,4)	-	-	0,039 [a]
Einzeitige Rekonstruktion	111 (77,1)	14 (87,5)	17 (85,0)	
Zweizeitige Rekonstruktion	33 (22,9)	2 (12,5)	3 (15,0)	0,488 [a]
Analog (Non-VSP)	86 (59,7)	10 (62,5)	10 (50,0)	
Digital (VSP)	58 (40,3)	6 (37,5)	10 (50,0)	0,678 [a]
Unilaterale ND	70 (48,6)	11 (68,8)	13 (65,0)	
Bilaterale ND	38 (26,4)	3 (18,8)	3 (15,0)	
Keine ND	36 (25,0)	2 (12,5)	4 (20,0)	0,181 [a]
Tracheostomie				
Keine	53 (36,8)	6 (37,5)	8 (40,0)	
Primär	89 (61,8)	9 (56,3)	11 (55,0)	
Sekundär	2 (1,4)	1 (6,3)	1 (5,0)	0,979 [a]
Strahlentherapie				
Präoperative	18 (12,5)	1 (6,3)	3 (15,0)	
Postoperativ	52 (36,1)	8 (50,0)	4 (20,0)	
Keine	74 (51,4)	7 (43,8)	13 (65,0)	0,643 [a]
Alkoholkonsum	48 (33,3)	5 (31,3)	9 (45,0)	0,568 [a]
Nikotinabusus	84 (58,3)	9 (56,3)	13 (65,0)	0,831 [a]
Schnitt-Naht-Zeit [min] ± SD	517,3 ± 108,5	546,2 ± 94,9	524,4 ± 97,2	0,493 [a]
Verweildauer OPINT [d] ± SD	2,1 ± 1,8	2,1 ± 1,3	2,1 ± 1,7	0,878 [a]
Verweildauer OP – E [d] ± SD	17,2 ± 9,0	22,6 ± 9,7	33,8 ± 18,8	**0,001** [a]
BMI				
≤18	9 (6,3)	-	1 (5,0)	
18 – ≤ 25	69 (47,9)	9 (56,3)	9 (45,0)	
25 – ≤ 30	50 (34,7)	3 (18,8)	7 (35,0)	
30 – ≤ 35	10 (6,9)	4 (25,0)	2 (10,0)	
> 35	6 (4,2)	-	1 (5,0)	0,814 [a]
ASA-Score				
ASA 1	13 (9,0)	-	-	
ASA 2	69 (47,9)	10 (62,5)	7 (35,0)	
ASA 3	59 (41,0)	6 (37,5)	12(60,0)	
ASA 4	3 (2,1)	-	1 (5,0)	0,105 [a]

Tabelle 4. Klinische Daten der untersuchten Studiengruppe und Kategorisierung in die Gruppen: Erfolg inklusive PFF und totalen Lappenverlust (TFF). Anmerkungen: BMI, Body mass index; E, Entlassung MRONJ, Medication-related osteonecrosis of the jaw; ND, Neck dissection; OPINT, operative Intensivstation; ORN, Osteoradionekrose; SD, Standardabweichung; VSP, virtual surgical planning. [a], asymptotische Signifikanz im Mann-Whitney-U-Test.

n = 180	Erfolg + PFF n = 160 (88,9 %)	TFF n = 20 (11,1 %)	p-Wert
Alter [y] ± SD	57,3 ± 13,5	62,5 ± 9,5	0,101[b]
Follow-up [mo] ± SD	51,5 ± 50,7	31,5 ± 31,6	0,157 [b]
Weiblich	55 (38,2)	6 (30,0)	
Männlich	89 (61,8)	14 (70,0)	0,513 [b]
Diagnose			
Benigner Tumor	18 (11,3)	-	
Maligner Tumor	129 (80,6)	15 (75,0)	
MRONJ	2 (1,3)	2 (10,0)	
ORN	5 (3,1)	3 (15,0)	
Osteomyelitis	4 (2,5)	-	
Sonstige	2 (1,3)	-	0,011 [b]
Einzeitige Rekonstruktion	125 (78,1)	17 (85,0)	
Zweizeitige Rekonstruktion	35 (21,9)	3 (15,0)	0,479 [b]
Analog (Non-VSP)	96 (60,0)	10 (50,0)	
Digital (VSP)	64 (40,0)	10 (50,0)	0,393 [b]
Unilaterale ND	81 (50,6)	13 (65,0)	
Bilaterale ND	41 (25,6)	3 (15,0)	
Keine ND	38 (23,8)	4 (20,0)	0,306 [b]
Tracheostomie			
Keine	59 (36,9)	8 (40,0)	
Primär	98 (61,3)	11 (55,0)	
Sekundär	3 (1,9)	1 (5,0)	0,926[b]
Strahlentherapie			
Präoperativ	19 (11,9)	3 (15,0)	
Postoperativ	60 (37,5)	4 (20,0)	
Keine	81 (50,6)	13 (65,0)	0,368[b]
Alkoholkonsum	53 (33,1)	9 (45,0)	0,293 [b]
Nikotinabusus	93 (58,1)	13 (65,0)	0,557[b]
Schnitt-Naht-Zeit [min] ± SD	520,2 ± 107,3	524,4 ± 97,2	0,717 [b]
Verweildauer OPINT [d] ± SD	2,1 ± 1,8	2,1 ± 1,7	0,731 [b]
Verweildauer OP – E [d] ± SD	17,7 ± 9,2	33,8 ± 18,8	**0,001** [b]
BMI			
≤18	9 (5,6)	1 (5,0)	
18 – ≤ 25	78 (48,8)	9 (45,0)	
25 – ≤ 30	53 (33,1)	7 (35,0)	
30 – ≤ 35	14 (8,8)	2 (10,0)	
> 35	6 (3,8)	1 (5,0)	0,685 [b]
ASA-Score			
ASA 1	13 (8,1)	-	
ASA 2	79 (49,4)	7 (35,0)	
ASA 3	65 (40,6)	12(60,0)	
ASA 4	3 (1,9)	1 (5,0)	0,034 [b]

10. Abbildungsverzeichnis

Zustimmung zur Verwendung von Abbildungen der KLS-Martin Group:

LV **van Meenen, Lutz** Gestern um 15:49
AW: Freigabe Photos, Abbildungen für Habilitationsschrift
An: Dr. Dr. Michael Knitschke, Kopie: UKGM Mkg Dr. Dr. Michael Knitschke Details

Sehr geehrter Herr Dr. Knitschke,

vielen Dank für diese Rückmeldung und Abklärung. Ich kann mich noch gut an das Telefonat mit Ihnen erinnern.
Ich habe die entsprechenden Seiten durchgeschaut und konnte unsererseits keine Einwände oder Beanstandungen feststellen.
Dies können Sie somit gerne als freundliche Genehmigung durch KLS Martin vermerken.

Mit freundlichen Grüßen und viel Erfolg

Lutz van Meenen
Director Individual Patient Solutions
Implants

KLS martin GROUP

Karl Leibinger Medizintechnik GmbH & Co. KG
Ein Unternehmen der KLS Martin Group

Kolbinger Str. 10
78570 Mühlheim/Donau, Deutschland

Telefon	+49 7463 838-3846
Fax	+49 7463 838-298
Mobil	+15172636008
Mail	Lutz.vanMeenen@klsmartin.com
Web	www.klsmartin.com

Registergericht: Stuttgart HRA 450721
Geschäftsführer: Karl Leibinger, Christian Leibinger
Persönlich haftende Gesellschafterin: Karl Leibinger Verwaltungs- und Beteiligungsgesellschaft mbH
Registergericht: Stuttgart HRB 450285
USt.-Id-Nr. DE 142933208

11. Tabellenverzeichnis

12. Literaturverzeichnis

1. Straßburg, M. and H. Böttger, *Die Geschichte der Westdeutschen Kieferklinik. Deutscher Zahnärztekalender 1994*. 1994: Hanser Verlag München Wien.
2. Meikle, M.C., *Reconstructing Faces, The art and wartime surgery of Gillies, Pickerill, McIndoe and Mowlem*. 2013: Otago University Press.
3. Meekeren, J.v., *Heelen genees konstige aanmerkkingen*. 1668, Amsterdam: Commelijin.
4. Hjorting-Hansen, E., *Bone grafting to the jaws with special reference to reconstructive preprosthetic surgery. A historical review.* Mund Kiefer Gesichtschir, 2002. **6**(1): p. 6-14.
5. Haeseker, B., *Van Meekeren and his account of the transplant of bone from a dog into the skull of a soldier.* Plast Reconstr Surg, 1991. **88**(1): p. 173-4.
6. Walther, P.v., *Wiedereinheilung der bei der Trepanation ausgebohrten Knochenscheibe.* Journal der Chirurgie und Augenheilkunde, 1821. **2**: p. 571–583.
7. Ollier, L., *Traité expérimental et clinique de la régénération des os et de la production artificielle du tissu osseux*. Vol. 2. 1867: V. Masson.
8. Axhausen, G., *Die pathologisch-anatomischen Grundlagen der Lehre von der freien Knochentransplantation beim Menschen und beim Tiere*. 1908: Urban & Schwarzenberg.
9. Lexer, E., *Die freien Transplantationen*. Vol. 1. 1919: Enke.
10. Leriche, R. and A. Policard, *Some fundamental principles in the pathology of bone.* Surg. Gynec. obstet, 1926. **43**: p. 308-309.
11. Axhausen, W., *Die Knochenregeneration, ein zweiphasiges Geschehen.* Zentralbl Chir, 1952. **77**(11): p. 435-442.
12. Axhausen, W., *Die Bedeutung der Individual und Artspezifität der Gewebe für die freie Knochenüberpflanzung.* 1962.
13. Bardenheuer, F., *Verhandlung der Deutsch Gesellschaft Zentrabilothek.* Chirurgie, 1892. **21**(68).
14. Walther, C., *Résection de l'extrémité inférieure du radius pour ostéosarcome*. 1911.
15. Saraf, S. and S. Goel, *Complications of resection and reconstruction in giant cell tumour of distal end of radius-An analysis.* Indian Journal of Orthopaedics, 2005. **39**(4): p. 206.
16. Steel, B.J. and M.R. Cope, *A brief history of vascularized free flaps in the oral and maxillofacial region.* J Oral Maxillofac Surg, 2015. **73**(4): p. 786 e1-11.
17. Baadsgaard, K. and S. Medgyesi, *Muscle-pedicle bone grafts: an experimental study.* Acta Orthopaedica Scandinavica, 1965. **35**(1-4): p. 279-293.
18. McDowell, F. and D. Ohlwiler, *Mandibular resection and replacement.* SURGERY GYNECOLOGY & OBSTETRICS, 1962. **115**(2): p. 103-&.
19. Parmar, S., *Defect-based reconstruction: mandible and oral cavity.* Shell and Maran's testbook of Head and Neck Surgery and Oncology, 2012: p. 959.
20. Prein, J., A. Eschmann, and B. Spiessl, *[Results of follow-up examinations in 81 patients with functionally stable mandibular osteosynthesis].* Fortschr Kiefer Gesichtschir, 1976. **21**: p. 304-7.
21. McKee, D.M., *Microvascular bone transplatation.* Clin Plast Surg, 1978. **5**(2): p. 283-92.

22. McCullough, D.W. and J.M. Fredrickson, *Composite neovascularized rib grafts for mandibular reconstruction.* Surg Forum, 1972. **23**(0): p. 492-4.
23. Buncke, H.J., D.W. Furnas, L. Gordon, and B.M. Achauer, *Free osteocutaneous flap from a rib to the tibia.* Plast Reconstr Surg, 1977. **59**(6): p. 799-804.
24. Eck, N., *On the question of ligature of the portal vein.* Voyennomed Zh 1877. **130**: p. 1.
25. Jassinowski, A., *Die Arteriennhat: Eine experimentelle Studie.* Inaug Diss Dorpat, 1889.
26. Carrel, A., *La technique operatoire des anastomoses vasculaires et la transplantation des visceres.* Lyon Med., 1902. **98**: p. 859-863.
27. Höpfner, E., *Über Gefässnhaht, Gefässtransplantationen und Replantation von amputierten Extremitäten.* Arch Klin Chir., 1903. **70**: p. 417-471.
28. Tamai, S., *History of microsurgery.* Plast Reconstr Surg, 2009. **124**(6 Suppl): p. e282-e294.
29. McLean, J., *The thromboplastic action of cephalin.* Am J Physiol, 1916. **41**: p. 250-257.
30. Howell, W.H. and E. Holt, *Two new factors in blood coagulation: Heparin and pro-antithrombin.* Am J Physiol, 1918. **47**: p. 328-341.
31. Charles, A.F. and D.A. Scott, *Studies on heparin.The preparation of heparin.* J Biol Chem, 1933. **102**: p. 425-429.
32. Nylen, C.O., *The microscope in aural surgery, its first use and later development.* Acta Otolaryngol Suppl, 1954. **116**: p. 226-40.
33. Holmgren, G., *Some experiences in surgery of otosclerosis.* Acta Otolaryngol, 1923. **5**: p. 460-466.
34. Suarez, E.L. and J.H. Jacobson, 2nd, *Results of small artery endarterectomy-microsurgical technique.* Surg Forum, 1961. **12**: p. 256-7.
35. Jacobson, J.H., 2nd and E.L. Suarez, *Microvascular surgery.* Dis Chest, 1962. **41**: p. 220-4.
36. Jacobson, J.H., 2nd and E.L. Suarez, *Microsurgery in anastomosis of small vessels.* Surg Forum, 1960. **11**: p. 243-245.
37. Krizek, T.J., T. Tani, J.D. Desprez, and C.L. Kiehn, *Experimental transplantation of composite grafts by microsurgical vascular anastomoses.* Plast Reconstr Surg, 1965. **36**(5): p. 538-46.
38. Strauch, B., A.E. Bloomberg, and M.L. Lewin, *An experimental approach to mandibular replacement: island vascular composite rib grafts.* Br J Plast Surg, 1971. **24**(4): p. 334-41.
39. Harii, K., K. Omori, and S. Omori, *Successful clinical transfer of ten free flaps by microvascular anastomoses.* Plast Reconstr Surg, 1974. **53**(3): p. 259-70.
40. Daniel, R.K. and G.I. Taylor, *Distant transfer of an island flap by microvascular anastomoses. A clinical technique.* Plast Reconstr Surg, 1973. **52**(2): p. 111-7.
41. Taylor, G.I. and J.H. Palmer, *The vascular territories (angiosomes) of the body: experimental study and clinical applications.* Br J Plast Surg, 1987. **40**(2): p. 113-41.
42. Taylor, G.I., G.D. Miller, and F.J. Ham, *The free vascularized bone graft. A clinical extension of microvascular techniques.* Plast Reconstr Surg, 1975. **55**(5): p. 533-44.
43. Baudet, J., J.C. Guimberteau, and E. Nascimento, *Successful clinical transfer of two free thoraco-dorsal axillary flaps.* Plast Reconstr Surg, 1976. **58**(6): p. 680-8.

44. Yang, G.F., P.J. Chen, Y.Z. Gao, X.Y. Liu, J. Li, S.X. Jiang, and S.P. He, *Forearm free skin flap transplantation: a report of 56 cases. 1981.* Br J Plast Surg, 1997. **50**(3): p. 162-5.
45. Song, R., Y. Gao, Y. Song, Y. Yu, and Y. Song, *The forearm flap.* Clin Plast Surg, 1982. **9**(1): p. 21-6.
46. Ueba, Y. and S. Fujikawa, *Nine years' follow-up of a free vascularized fibular graft in neurofibromatosis: a case report and literature review.* Jpn J Orthop Trauma Surg, 1983. **26**: p. 595-600.
47. Gilbert, A., *Vascularized transfer of the fibular shaft.* Int J Microsurg, 1979. **1**(2): p. 100-102.
48. Wei, F.C., H.C. Chen, C.C. Chuang, and M.S. Noordhoff, *Fibular osteoseptocutaneous flap: anatomic study and clinical application.* Plast Reconstr Surg, 1986. **78**(2): p. 191-200.
49. Kansy, K., A.A. Mueller, T. Mücke, J.B. Kopp, F. Koersgen, K.D. Wolff, . . . D.C.G.f.M. Reconstruction, *Microsurgical reconstruction of the head and neck--current concepts of maxillofacial surgery in Europe.* J Craniomaxillofac Surg, 2014. **42**(8): p. 1610-3.
50. Cordeiro, P.G., J.J. Disa, D.A. Hidalgo, and Q.Y. Hu, *Reconstruction of the mandible with osseous free flaps: a 10-year experience with 150 consecutive patients.* Plast Reconstr Surg, 1999. **104**(5): p. 1314-20.
51. Brown, J.S., C. Barry, M. Ho, and R. Shaw, *A new classification for mandibular defects after oncological resection.* Lancet Oncol, 2016. **17**(1): p. e23-30.
52. Hanasono, M.M. and D.W. Chang, *Discussion: Jaw in a day: total maxillofacial reconstruction using digital technology.* Plast Reconstr Surg, 2013. **131**(6): p. 1392-3.
53. Attia, S., J. Wiltfang, J. Pons-Kühnemann, J.F. Wilbrand, P. Streckbein, C. Kähling, . . . H. Schaaf, *Survival of dental implants placed in vascularised fibula free flaps after jaw reconstruction.* J Craniomaxillofac Surg, 2018. **46**(8): p. 1205-1210.
54. Attia, S., J. Wiltfang, P. Streckbein, J.F. Wilbrand, T. El Khassawna, K. Mausbach, . . . H. Schaaf, *Functional and aesthetic treatment outcomes after immediate jaw reconstruction using a fibula flap and dental implants.* J Craniomaxillofac Surg, 2019. **47**(5): p. 786-791.
55. Levine, J.P., J.S. Bae, M. Soares, L.E. Brecht, P.B. Saadeh, D.J. Ceradini, and D.L. Hirsch, *Jaw in a day: total maxillofacial reconstruction using digital technology.* Plast Reconstr Surg, 2013. **131**(6): p. 1386-91.
56. Hakim, S.G., H. Kimmerle, T. Trenkle, P. Sieg, and H.C. Jacobsen, *Masticatory rehabilitation following upper and lower jaw reconstruction using vascularised free fibula flap and enossal implants-19 years of experience with a comprehensive concept.* Clin Oral Investig, 2015. **19**(2): p. 525-34.
57. Patel, A., S. Motakef, and R.L. Agag, *Reply: Emerging Paradigms in Perioperative Management for Microsurgical Free Tissue Transfer: Review of the Literature and Evidence-Based Guidelines.* Plast Reconstr Surg, 2015. **136**(2): p. 279e-281e.
58. Qaisi, M., H. Kolodney, G. Swedenburg, R. Chandran, and R. Caloss, *Fibula Jaw in a Day: State of the Art in Maxillofacial Reconstruction.* J Oral Maxillofac Surg, 2016. **74**(6): p. 1284 e1-1284 e15.
59. Bluebond-Langner, R. and E.D. Rodriguez, *Application of skeletal buttress analogy in composite facial reconstruction.* Craniomaxillofac Trauma Reconstr, 2009. **2**(1): p. 19-25.

60. Attia, S., J. Diefenbach, D. Schmermund, S. Bottger, J. Pons-Kuhnemann, C. Scheibelhut, . . . H.P. Howaldt, *Donor-Site Morbidity after Fibula Transplantation in Head and Neck Tumor Patients: A Split-Leg Retrospective Study with Focus on Leg Stability and Quality of Life.* Cancers (Basel), 2020. **12**(8).
61. Löfstrand, J., M. Nyberg, T. Karlsson, A. Thórarinsson, G. Kjeller, M. Lidén, and V. Fröjd, *Quality of Life after Free Fibula Flap Reconstruction of Segmental Mandibular Defects.* J Reconstr Microsurg, 2018. **34**(2): p. 108-120.
62. Tarsitano, A., L. Ciocca, R. Cipriani, R. Scotti, and C. Marchetti, *Mandibular reconstruction using fibula free flap harvested using a customised cutting guide: how we do it.* Acta Otorhinolaryngol Ital, 2015. **35**(3): p. 198-201.
63. Schusterman, M.A., G.P. Reece, M.J. Miller, and S. Harris, *The osteocutaneous free fibula flap: is the skin paddle reliable?* Plast Reconstr Surg, 1992. **90**(5): p. 787-93; discussion 794-8.
64. Jones, N.F., S. Monstrey, and B.A. Gambier, *Reliability of the fibular osteocutaneous flap for mandibular reconstruction: anatomical and surgical confirmation.* Plast Reconstr Surg, 1996. **97**(4): p. 707-16; discussion 717-8.
65. Winters, H.A. and G.J. de Jongh, *Reliability of the proximal skin paddle of the osteocutaneous free fibula flap: a prospective clinical study.* Plast Reconstr Surg, 1999. **103**(3): p. 846-9.
66. Wong, C.H., B.K. Tan, F.C. Wei, and C. Song, *Use of the soleus musculocutaneous perforator for skin paddle salvage of the fibula osteoseptocutaneous flap: anatomical study and clinical confirmation.* Plast Reconstr Surg, 2007. **120**(6): p. 1576-84.
67. Yadav, P.S., Q.G. Ahmad, V.K. Shankhdhar, and G.I. Nambi, *Skin paddle vascularity of free fibula flap - A study of 386 cases and a classification based on contribution from axial vessels of the leg.* Indian J Plast Surg, 2012. **45**(1): p. 58-61.
68. Ahmad, Q.G., P. Yadav, V.K. Shankhdhar, and G.I. Nambi, *Use of fibula pedicle as a composite interposition vascular graft to salvage large skin paddle with anomalous vascular supply.* Eur J Plast Surg, 2011. **34**(5): p. 413-6.
69. Tan, B.K. and C.H. Wong, *An anomalous septocutaneous perforator to the skin paddle of the fibula osteocutaneous flap originating from the posterior tibial artery.* J Plast Reconstr Aesthet Surg, 2009. **62**(5): p. 690-2.
70. Yadav, P.S., Q.G. Ahmad, V.K. Shankhdhar, and G.I. Nambi, *Successful management of free osteocutaneous fibula flap with anomalous vascularity of the skin paddle.* Indian J Plast Surg, 2009. **42**(2): p. 255-7.
71. Chen, Z.W. and W. Yan, *The study and clinical application of the osteocutaneous flap of fibula.* Microsurgery, 1983. **4**(1): p. 11-6.
72. Jones, N.F., W.M. Swartz, D.C. Mears, J.B. Jupiter, and A. Grossman, *The "double barrel" free vascularized fibular bone graft.* Plast Reconstr Surg, 1988. **81**(3): p. 378-85.
73. Hidalgo, D.A., *Fibula free flap: a new method of mandible reconstruction.* Plast Reconstr Surg, 1989. **84**(1): p. 71-9.
74. Nakayama, B., H. Matsuura, Y. Hasegawa, O. Ishihara, H. Hasegawa, and S. Torii, *New reconstruction for total maxillectomy defect with a fibula osteocutaneous free flap.* Br J Plast Surg, 1994. **47**(4): p. 247-9.
75. Bähr, W., P. Stoll, and R. Wächter, *Use of the "double barrel" free vascularized fibula in mandibular reconstruction.* J Oral Maxillofac Surg, 1998. **56**(1): p. 38-44.

76. Chang, E.I., K.R. Zeidler, B. Schmidt, and P. Leon, *Experience with Free Fibula Peroneal Osteofascial Flap for Composite Head and Neck Reconstruction.* Plastic and Reconstructive Surgery, 2010. **126**: p. 116.
77. Fan, S., Y.Y. Wang, D.H. Wu, D.L. Lai, Y.H. Feng, X. Yu, . . . J.S. Li, *Intraoral lining with the fibular osteomyofascial flap without a skin paddle during maxillary and mandibular reconstruction.* Head Neck, 2016. **38 Suppl 1**: p. E832-6.
78. Eckardt, A. and G.R. Swennen, *Virtual planning of composite mandibular reconstruction with free fibula bone graft.* J Craniofac Surg, 2005. **16**(6): p. 1137-40.
79. Ciocca, L., S. Mazzoni, M. Fantini, F. Persiani, C. Marchetti, and R. Scotti, *CAD/CAM guided secondary mandibular reconstruction of a discontinuity defect after ablative cancer surgery.* J Craniomaxillofac Surg, 2012. **40**(8): p. e511-5.
80. Marchetti, C., A. Bianchi, S. Mazzoni, R. Cipriani, and A. Campobassi, *Oromandibular reconstruction using a fibula osteocutaneous free flap: four different "preplating" techniques.* Plast Reconstr Surg, 2006. **118**(3): p. 643-51.
81. Hirsch, D.L., E.S. Garfein, A.M. Christensen, K.A. Weimer, P.B. Saddeh, and J.P. Levine, *Use of computer-aided design and computer-aided manufacturing to produce orthognathically ideal surgical outcomes: a paradigm shift in head and neck reconstruction.* J Oral Maxillofac Surg, 2009. **67**(10): p. 2115-22.
82. Thankappan, K., N.P. Trivedi, P. Subash, S.K. Pullara, S. Peter, M.A. Kuriakose, and S. Iyer, *Three-dimensional computed tomography-based contouring of a free fibula bone graft for mandibular reconstruction.* J Oral Maxillofac Surg, 2008. **66**(10): p. 2185-92.
83. Lanning, C., S.Y. Chen, A. Hansgen, D. Chang, K.C. Chan, and R. Shandas, *Dynamic three-dimensional reconstruction and modeling of cardiovascular anatomy in children with congenital heart disease using biplane angiography.* Biomed Sci Instrum, 2004. **40**: p. 200-5.
84. Levy, R.A., T.M. Chu, J.W. Halloran, S.E. Feinberg, and S. Hollister, *CT-generated porous hydroxyapatite orbital floor prosthesis as a prototype bioimplant.* AJNR Am J Neuroradiol, 1997. **18**(8): p. 1522-5.
85. Migaud, H., B. Cortet, R. Assaker, C. Fontaine, J.F. Kulik, and A. Duquennoy, *[Value of a synthetic osseous model obtained by stereo-lithography for preoperative planning. Correction of a complex femoral deformity caused by fibrous dysplasia].* Rev Chir Orthop Reparatrice Appar Mot, 1997. **83**(2): p. 156-9.
86. Berger, F., L.C. Ebert, R.A. Kubik-Huch, K. Eid, M.J. Thali, and T. Niemann, *Application of Cinematic Rendering in Clinical Routine CT Examination of Ankle Sprains.* AJR Am J Roentgenol, 2018. **211**(4): p. 887-890.
87. Dappa, E., K. Higashigaito, J. Fornaro, S. Leschka, S. Wildermuth, and H. Alkadhi, *Cinematic rendering - an alternative to volume rendering for 3D computed tomography imaging.* Insights Imaging, 2016. **7**(6): p. 849-856.
88. Stadlinger, B., S. Valdec, L. Wacht, H. Essig, and S. Winklhofer, *3D-cinematic rendering for dental and maxillofacial imaging.* Dentomaxillofac Radiol, 2020. **49**(1): p. 20190249.
89. Chen, P. and L. Nikoyan, *Guided Implant Surgery: A Technique Whose Time Has Come.* Dent Clin North Am, 2021. **65**(1): p. 67-80.
90. Deeb, G.R., D.Q. Tran, and J.G. Deeb, *Computer-Aided Planning and Placement in Implant Surgery.* Atlas Oral Maxillofac Surg Clin North Am, 2020. **28**(2): p. 53-58.

91. Farrell, B.B., P.B. Franco, and M.R. Tucker, *Virtual surgical planning in orthognathic surgery.* Oral Maxillofac Surg Clin North Am, 2014. **26**(4): p. 459-73.
92. Perez, D.E. and R. Garza, Jr., *Computer-Assisted Design and Manufacturing in Combined Orthognathic and Temporomandibular Joint Surgery.* Atlas Oral Maxillofac Surg Clin North Am, 2020. **28**(2): p. 83-93.
93. Ramanathan, M., E. Panneerselvam, and V.B. Krishna Kumar Raja, *3D planning in mandibular fractures using CAD/CAM surgical splints - A prospective randomized controlled clinical trial.* J Craniomaxillofac Surg, 2020. **48**(4): p. 405-412.
94. Seier, T., L. Hingsammer, P. Schumann, T. Gander, M. Rücker, and M. Lanzer, *Virtual planning, simultaneous dental implantation and CAD/CAM plate fixation: a paradigm change in maxillofacial reconstruction.* Int J Oral Maxillofac Surg, 2020. **49**(7): p. 854-861.
95. Wilde, F., O. Krauß, A. Sakkas, F. Mascha, S. Pietzka, and A. Schramm, *Custom wave-shaped CAD/CAM orbital wall implants for the management of post-enucleation socket syndrome.* J Craniomaxillofac Surg, 2019. **47**(9): p. 1398-1405.
96. Rana, M., B. Singh, and N.C. Gellrich, *Einsatz von im Laserschmelzverfahren hergestellten patientenspezifischen Implantaten in der Mund-, Kiefer- und Gesichtschirurgie.* OP-JOURNAL, 2016. **32**: p. 241-246.
97. Seruya, M., M. Fisher, and E.D. Rodriguez, *Computer-assisted versus conventional free fibula flap technique for craniofacial reconstruction: an outcomes comparison.* Plast Reconstr Surg, 2013. **132**(5): p. 1219-28.
98. Han, H.H., H.Y. Kim, and J.Y. Lee, *The Pros and Cons of Computer-Aided Surgery for Segmental Mandibular Reconstruction after Oncological Surgery.* Arch Craniofac Surg, 2017. **18**(3): p. 149-154.
99. Saini, V., S. Gaba, S. Sharma, P. Kalra, and R.K. Sharma, *Assessing the Role of Virtual Surgical Planning in Mandibular Reconstruction With Free Fibula Osteocutaneous Graft.* J Craniofac Surg, 2019. **30**(6): p. e563-e566.
100. Tang, N.S.J., I. Ahmadi, and A. Ramakrishnan, *Virtual surgical planning in fibula free flap head and neck reconstruction: A systematic review and meta-analysis.* J Plast Reconstr Aesthet Surg, 2019. **72**(9): p. 1465-1477.
101. Barr, M.L., C.S. Haveles, K.S. Rezzadeh, I.T. Nolan, R. Castro, J.C. Lee, . . . M.J. Pfaff, *Virtual Surgical Planning for Mandibular Reconstruction With the Fibula Free Flap: A Systematic Review and Meta-analysis.* Ann Plast Surg, 2020. **84**(1): p. 117-122.
102. Zheng, G.S., Y.X. Su, G.Q. Liao, Z.F. Chen, L. Wang, P.F. Jiao, . . . Y.J. Liang, *Mandible reconstruction assisted by preoperative virtual surgical simulation.* Oral Surg Oral Med Oral Pathol Oral Radiol, 2012. **113**(5): p. 604-11.
103. Roser, S.M., S. Ramachandra, H. Blair, W. Grist, G.W. Carlson, A.M. Christensen, . . . M.B. Steed, *The accuracy of virtual surgical planning in free fibula mandibular reconstruction: comparison of planned and final results.* J Oral Maxillofac Surg, 2010. **68**(11): p. 2824-32.
104. Zheng, G.S., Y.X. Su, G.Q. Liao, P.F. Jiao, L.Z. Liang, S.E. Zhang, and H.C. Liu, *Mandible reconstruction assisted by preoperative simulation and transferring templates: cadaveric study of accuracy.* J Oral Maxillofac Surg, 2012. **70**(6): p. 1480-5.
105. Al-Nawas, B. and E. Goetze, *3-D-Druck in der MKG-Chirurgie.* MKG-Chirurg, 2017. **10**: p. 234-243.

106. Zimmerer, R.M., J. Dittman, and N.C. Gellrich, *Virtuelle Techniken in der Traumatologie.* MKG-Chirurg, 2017. **10**: p. 252-262.
107. Modabber, A., N. Ayoub, S.C. Mohlhenrich, E. Goloborodko, T.T. Sonmez, M. Ghassemi, . . . F. Holzle, *The accuracy of computer-assisted primary mandibular reconstruction with vascularized bone flaps: iliac crest bone flap versus osteomyocutaneous fibula flap.* Med Devices (Auckl), 2014. **7**: p. 211-7.
108. Wilde, F., C.P. Cornelius, and A. Schramm, *Computer-Assisted Mandibular Reconstruction using a Patient-Specific Reconstruction Plate Fabricated with Computer-Aided Design and Manufacturing Techniques.* Craniomaxillofac Trauma Reconstr, 2014. **7**(2): p. 158-66.
109. Cornelius, C.P., W. Smolka, G.A. Giessler, F. Wilde, and F.A. Probst, *Patient-specific reconstruction plates are the missing link in computer-assisted mandibular reconstruction: A showcase for technical description.* J Craniomaxillofac Surg, 2015. **43**(5): p. 624-9.
110. Wilde, F., K. Winter, K. Kletsch, K. Lorenz, and A. Schramm, *Mandible reconstruction using patient-specific pre-bent reconstruction plates: comparison of standard and transfer key methods.* Int J Comput Assist Radiol Surg, 2015. **10**(2): p. 129-40.
111. Wilde, F. and A. Schramm, *[Computer-aided reconstruction of the facial skeleton : Planning and implementation in clinical routine].* HNO, 2016. **64**(9): p. 641-9.
112. Liu, X.J., L. Gui, C. Mao, X. Peng, and G.Y. Yu, *Applying computer techniques in maxillofacial reconstruction using a fibula flap: a messenger and an evaluation method.* J Craniofac Surg, 2009. **20**(2): p. 372-7.
113. Wilde, F., H. Hanken, F. Probst, A. Schramm, M. Heiland, and C.P. Cornelius, *Multicenter study on the use of patient-specific CAD/CAM reconstruction plates for mandibular reconstruction.* Int J Comput Assist Radiol Surg, 2015. **10**(12): p. 2035-51.
114. Weitz, J., F.J. Bauer, A. Hapfelmeier, N.H. Rohleder, K.D. Wolff, and M.R. Kesting, *Accuracy of mandibular reconstruction by three-dimensional guided vascularised fibular free flap after segmental mandibulectomy.* Br J Oral Maxillofac Surg, 2016. **54**(5): p. 506-10.
115. Rustemeyer, J., A. Busch, and A. Sari-Rieger, *Application of computer-aided designed/computer-aided manufactured techniques in reconstructing maxillofacial bony structures.* Oral Maxillofac Surg, 2014. **18**(4): p. 471-6.
116. Deek, N.F. and F.C. Wei, *Computer-Assisted Surgery for Segmental Mandibular Reconstruction with the Osteoseptocutaneous Fibula Flap: Can We Instigate Ideological and Technological Reforms?* Plast Reconstr Surg, 2016. **137**(3): p. 963-70.
117. Ilankovan, V., L.C. Hsing, and A. Webb, *Microvascular anastomosis.* Br J Oral Maxillofac Surg, 2002. **40**(6): p. 510-1.
118. Markiewicz, M.R. and M. Miloro, *The Evolution of Microvascular and Microneurosurgical Maxillofacial Reconstruction.* J Oral Maxillofac Surg, 2018. **76**(4): p. 687-699.
119. Mason, K.A., E. Theodorakopoulou, G. Pafitanis, A.M. Ghanem, and S.R. Myers, *Twelve tips for postgraduate or undergraduate medics building a basic microsurgery simulation training course.* Med Teach, 2016. **38**(9): p. 872-8.
120. Mavrogenis, A.F., K. Markatos, T. Saranteas, I. Ignatiadis, S. Spyridonos, M. Bumbasirevic, . . . P.N. Soucacos, *The history of microsurgery.* Eur J Orthop Surg Traumatol, 2019. **29**(2): p. 247-254.

121. Senthil Murugan, M., P. Ravi, K. Mohammed Afradh, V. Tatineni, and V.B. Krishnakumar Raja, *Comparison of the efficacy of venous coupler and hand-sewn anastomosis in maxillofacial reconstruction using microvascular fibula free flaps: a prospective randomized controlled trial.* Int J Oral Maxillofac Surg, 2018. **47**(7): p. 854-857.
122. Wang, W.M., L. Huang, X. Gao, Y.X. Yuan, X.Q. Chen, and X.C. Jian, *Use of a microvascular coupler device for end-to-side venous anastomosis in oral and maxillofacial reconstruction.* Int J Oral Maxillofac Surg, 2018. **47**(10): p. 1263-1267.
123. Baumeister, R.G., W. Mayo, M. Notohamiprodjo, J. Wallmichrath, S. Springer, and A. Frick, *Microsurgical Lymphatic Vessel Transplantation.* J Reconstr Microsurg, 2016. **32**(1): p. 34-41.
124. Campisi, C.C., L.P. Jiga, M. Ryan, P.G. di Summa, C. Campisi, and M. Ionac, *Mastering Lymphatic Microsurgery: A New Training Model in Living Tissue.* Ann Plast Surg, 2017. **79**(3): p. 298-303.
125. Pons, G. and J.B. Tang, *Major Changes in Lymphatic Microsurgery and Microvascular Surgery in Past 20 Years.* Clin Plast Surg, 2020. **47**(4): p. 679-683.
126. Adam, D., D. Broderick, P. Kyzas, and L. Vassiliou, *Microvascular anastomotic coupler devices versus hand-sewn technique for arterial anastomosis: a systematic review.* Br J Oral Maxillofac Surg, 2021. **59**(5): p. 524-533.
127. Ardehali, B., A.N. Morritt, and A. Jain, *Systematic review: anastomotic microvascular device.* J Plast Reconstr Aesthet Surg, 2014. **67**(6): p. 752-5.
128. Bank, J., E. Teng, and D.H. Song, *Microvascular coupler-induced intimal crimping causing venous thrombosis.* J Reconstr Microsurg, 2015. **31**(2): p. 157-8.
129. Head, L.K. and D.R. McKay, *Economic Comparison of Hand-Sutured and Coupler-Assisted Microvascular Anastomoses.* J Reconstr Microsurg, 2018. **34**(1): p. 71-76.
130. Chae, M.P., W.M. Rozen, I.S. Whitaker, D. Chubb, D. Grinsell, M.W. Ashton, . . . W.C. Lineaweaver, *Current evidence for postoperative monitoring of microvascular free flaps: a systematic review.* Ann Plast Surg, 2015. **74**(5): p. 621-32.
131. Thiem, D.G.E., R.W. Frick, E. Goetze, M. Gielisch, B. Al-Nawas, and P.W. Kämmerer, *Hyperspectral analysis for perioperative perfusion monitoring-a clinical feasibility study on free and pedicled flaps.* Clin Oral Investig, 2021. **25**(3): p. 933-945.
132. Shroff, S.S., S.C. Nair, A. Shah, and B. Kumar, *Versatility of Fibula Free Flap in Reconstruction of Facial Defects: A Center Study.* J Maxillofac Oral Surg, 2017. **16**(1): p. 101-107.
133. Hölzle, F., M.R. Kesting, G. Hölzle, A. Watola, D.J. Loeffelbein, J. Ervens, and K.D. Wolff, *Clinical outcome and patient satisfaction after mandibular reconstruction with free fibula flaps.* Int J Oral Maxillofac Surg, 2007. **36**(9): p. 802-6.
134. Colletti, G., L. Autelitano, D. Rabbiosi, F. Biglioli, M. Chiapasco, M. Mandala, and F. Allevi, *Technical refinements in mandibular reconstruction with free fibula flaps: outcome-oriented retrospective review of 99 cases.* Acta Otorhinolaryngol Ital, 2014. **34**(5): p. 342-8.

135. Heller, M., H.K. Bauer, E. Goetze, M. Gielisch, K.E. Roth, P. Drees, . . . B. Al-Nawas, *Applications of patient-specific 3D printing in medicine.* Int J Comput Dent, 2016. **19**(4): p. 323-339.
136. Toto, J.M., E.I. Chang, R. Agag, K. Devarajan, S.A. Patel, and N.S. Topham, *Improved operative efficiency of free fibula flap mandible reconstruction with patient-specific, computer-guided preoperative planning.* Head Neck, 2015. **37**(11): p. 1660-4.
137. Rendenbach, C., C. Steffen, H. Hanken, K. Schluermann, A. Henningsen, B. Beck-Broichsitter, . . . C. Precht, *Complication rates and clinical outcomes of osseous free flaps: a retrospective comparison of CAD/CAM versus conventional fixation in 128 patients.* Int J Oral Maxillofac Surg, 2019. **48**(9): p. 1156-1162.
138. Barry, C.P., C. MacDhabheid, K. Tobin, L.F. Stassen, P. Lennon, M. Toner, . . . J.R. Clark, *'Out of house' virtual surgical planning for mandible reconstruction after cancer resection: is it oncologically safe?* Int J Oral Maxillofac Surg, 2021. **50**(8): p. 999-1002.
139. Doobay, A.V. and S.S. Anand, *Sensitivity and specificity of the ankle-brachial index to predict future cardiovascular outcomes: a systematic review.* Arterioscler Thromb Vasc Biol, 2005. **25**(7): p. 1463-9.
140. Rendenbach, C., K. Sellenschloh, L. Gerbig, M.M. Morlock, B. Beck-Broichsitter, R. Smeets, . . . H. Hanken, *CAD-CAM plates versus conventional fixation plates for primary mandibular reconstruction: A biomechanical in vitro analysis.* J Craniomaxillofac Surg, 2017. **45**(11): p. 1878-1883.
141. Claes, L.E., C.A. Heigele, C. Neidlinger-Wilke, D. Kaspar, W. Seidl, K.J. Margevicius, and P. Augat, *Effects of mechanical factors on the fracture healing process.* Clin Orthop Relat Res, 1998(355 Suppl): p. S132-47.
142. Kennady, M.C., M.R. Tucker, G.E. Lester, and M.J. Buckley, *Stress shielding effect of rigid internal fixation plates on mandibular bone grafts. A photon absorption densitometry and quantitative computerized tomographic evaluation.* Int J Oral Maxillofac Surg, 1989. **18**(5): p. 307-10.
143. Robey, A.B., M.L. Spann, T.M. McAuliff, J.L. Meza, R.R. Hollins, and P.J. Johnson, *Comparison of miniplates and reconstruction plates in fibular flap reconstruction of the mandible.* Plast Reconstr Surg, 2008. **122**(6): p. 1733-1738.
144. Zoumalan, R.A., D.L. Hirsch, J.P. Levine, and P.B. Saadeh, *Plating in microvascular reconstruction of the mandible: can fixation be too rigid?* J Craniofac Surg, 2009. **20**(5): p. 1451-4.
145. Fichter, A.M., L.M. Ritschl, R. Georg, A. Kolk, M.R. Kesting, K.D. Wolff, and T. Mücke, *Effect of Segment Length and Number of Osteotomy Sites on Cancellous Bone Perfusion in Free Fibula Flaps.* J Reconstr Microsurg, 2019. **35**(2): p. 108-116.
146. Mücke, T., L.M. Ritschl, M. Roth, F.D. Güll, A. Rau, S. Grill, . . . D.J. Loeffelbein, *Predictors of free flap loss in the head and neck region: A four-year retrospective study with 451 microvascular transplants at a single centre.* J Craniomaxillofac Surg, 2016. **44**(9): p. 1292-8.
147. Fishman, E.K., D.R. Ney, D.G. Heath, F.M. Corl, K.M. Horton, and P.T. Johnson, *Volume rendering versus maximum intensity projection in CT angiography: what works best, when, and why.* Radiographics, 2006. **26**(3): p. 905-22.

148. Li, Y., Y. Zheng, J. Chen, X. Chen, J. Lin, A. Cai, and X. Zhou, *Determining the organ of origin of large pelvic masses in females using multidetector CT angiography and three-dimensional volume rendering CT angiography.* Eur Radiol, 2015. **25**(4): p. 1032-9.
149. Mirka, H., J. Ferda, and J. Baxa, *Multidetector computed tomography of chest trauma: indications, technique and interpretation.* Insights Imaging, 2012. **3**(5): p. 433-49.
150. Wang, H., F. Wang, S. Newman, Y. Lin, X. Chen, L. Xu, and Q. Wang, *Application of an innovative computerized virtual planning system in acetabular fracture surgery: A feasibility study.* Injury, 2016. **47**(8): p. 1698-701.
151. Guo, Y., Y. Liu, Q.H. Lu, K.H. Zheng, L.J. Shi, and Q.J. Wang, *CT two-dimensional reformation versus three-dimensional volume rendering with regard to surgical findings in the preoperative assessment of the ossicular chain in chronic suppurative otitis media.* Eur J Radiol, 2013. **82**(9): p. 1519-24.
152. Sun, W., L. Jia, Y. Dong, H. Zhao, H. Liu, K. Yang, and Y. Li, *Morphological study of surgical approach by superior temporal sulcus-temporal horn of lateral ventricle approach using volume rendering.* J Craniofac Surg, 2014. **25**(2): p. 611-3.
153. Graidis, C., D. Dimitriadis, V. Karasavvidis, G. Dimitriadis, E. Argyropoulou, F. Economou, . . . G. Karakostas, *Prevalence and characteristics of coronary artery anomalies in an adult population undergoing multidetector-row computed tomography for the evaluation of coronary artery disease.* BMC Cardiovasc Disord, 2015. **15**: p. 112.
154. Knitschke, M., S. Sonnabend, F.C. Roller, J. Pons-Kühnemann, D. Schmermund, S. Attia, . . . S. Böttger, *Osseous Union after Mandible Reconstruction with Fibula Free Flap Using Manually Bent Plates vs. Patient-Specific Implants: A Retrospective Analysis of 89 Patients.* Current Oncology, 2022. **29**(5): p. 3375-3392.
155. Knitschke, M., S. Sonnabend, C. Bäcker, D. Schmermund, S. Böttger, H.P. Howaldt, and S. Attia, *Partial and Total Flap Failure after Fibula Free Flap in Head and Neck Reconstructive Surgery: Retrospective Analysis of 180 Flaps over 19 Years.* Cancers (Basel), 2021. **13**(4).
156. Bianchi, B., C. Copelli, S. Ferrari, A. Ferri, and E. Sesenna, *Free flaps: outcomes and complications in head and neck reconstructions.* J Craniomaxillofac Surg, 2009. **37**(8): p. 438-42.
157. Beausang, E.S., E.E. Ang, J.E. Lipa, J.C. Irish, D.H. Brown, P.J. Gullane, and P.C. Neligan, *Microvascular free tissue transfer in elderly patients: the Toronto experience.* Head Neck, 2003. **25**(7): p. 549-53.
158. Bridger, A.G., C.J. O'Brien, and K.K. Lee, *Advanced patient age should not preclude the use of free-flap reconstruction for head and neck cancer.* Am J Surg, 1994. **168**(5): p. 425-8.
159. Howard, M.A., P.G. Cordeiro, J. Disa, W. Samson, M. Gonen, R.N. Schoelle, and B. Mehrara, *Free tissue transfer in the elderly: incidence of perioperative complications following microsurgical reconstruction of 197 septuagenarians and octogenarians.* Plast Reconstr Surg, 2005. **116**(6): p. 1659-68; discussion 1669-71.
160. Nao, E.E., O. Dassonville, E. Chamorey, G. Poissonnet, C.S. Pierre, J.C. Riss, . . . A. Bozec, *Head and neck free-flap reconstruction in the elderly.* Eur Ann Otorhinolaryngol Head Neck Dis, 2011. **128**(2): p. 47-51.

161. Serletti, J.M., J.P. Higgins, S. Moran, and G.S. Orlando, *Factors affecting outcome in free-tissue transfer in the elderly.* Plast Reconstr Surg, 2000. **106**(1): p. 66-70.
162. Turrà, F., S. La Padula, S. Razzano, P. Bonavolontà, G. Nele, S. Marlino, . . . F. Schonauer, *Microvascular free-flap transfer for head and neck reconstruction in elderly patients.* BMC Surg, 2013. **13 Suppl 2**(Suppl 2): p. S27.
163. Verhelst, P.J., F. Dons, P.J. Van Bever, J. Schoenaers, L. Nanhekhan, and C. Politis, *Fibula Free Flap in Head and Neck Reconstruction: Identifying Risk Factors for Flap Failure and Analysis of Postoperative Complications in a Low Volume Setting.* Craniomaxillofac Trauma Reconstr, 2019. **12**(3): p. 183-192.
164. Jubbal, K.T., D. Zavlin, and A. Suliman, *The effect of age on microsurgical free flap outcomes: An analysis of 5,951 cases.* Microsurgery, 2017. **37**(8): p. 858-864.
165. Sierakowski, A., A. Nawar, M. Parker, and B. Mathur, *Free flap surgery in the elderly: Experience with 110 cases aged >/=70 years.* J Plast Reconstr Aesthet Surg, 2017. **70**(2): p. 189-195.
166. Ferrari, S., C. Copelli, B. Bianchi, A. Ferri, T. Poli, T. Ferri, and E. Sesenna, *Free flaps in elderly patients: outcomes and complications in head and neck reconstruction after oncological resection.* J Craniomaxillofac Surg, 2013. **41**(2): p. 167-71.
167. Poisson, M., J. Longis, M. Schlund, M. Pere, G. Michel, A. Delagranda, . . . H. Bertin, *Postoperative morbidity of free flaps in head and neck cancer reconstruction: a report regarding 215 cases.* Clin Oral Investig, 2019. **23**(5): p. 2165-2171.
168. Kesting, M.R., F. Holzle, K.D. Wolff, S. Wagenpfeil, R.J. Hasler, C.J. Wales, . . . N.H. Rohleder, *Use of microvascular flap technique in older adults with head and neck cancer: a persisting dilemma in reconstructive surgery?* J Am Geriatr Soc, 2011. **59**(3): p. 398-405.
169. Buerba, R., S.A. Roman, and J.A. Sosa, *Thyroidectomy and parathyroidectomy in patients with high body mass index are safe overall: analysis of 26,864 patients.* Surgery, 2011. **150**(5): p. 950-8.
170. Norman, J. and K. Aronson, *Outpatient parathyroid surgery and the differences seen in the morbidly obese.* Otolaryngol Head Neck Surg, 2007. **136**(2): p. 282-6.
171. Stevens, S.M., B.P. O'Connell, and T.A. Meyer, *Obesity related complications in surgery.* Curr Opin Otolaryngol Head Neck Surg, 2015. **23**(5): p. 341-7.
172. Hollander, D., E. Kampman, and C.M. van Herpen, *Pretreatment body mass index and head and neck cancer outcome: A review of the literature.* Crit Rev Oncol Hematol, 2015. **96**(2): p. 328-38.
173. Dotters-Katz, S.K., C. Feldman, A. Puechl, C.A. Grotegut, and R.P. Heine, *Risk factors for post-operative wound infection in the setting of chorioamnionitis and cesarean delivery.* J Matern Fetal Neonatal Med, 2016. **29**(10): p. 1541-5.
174. Sebastian, A., P. Huddleston, 3rd, S. Kakar, E. Habermann, A. Wagie, and A. Nassr, *Risk factors for surgical site infection after posterior cervical spine surgery: an analysis of 5,441 patients from the ACS NSQIP 2005-2012.* Spine J, 2016. **16**(4): p. 504-9.
175. Crippen, M.M., J.S. Brady, A.M. Mozeika, J.A. Eloy, S. Baredes, and R.C.W. Park, *Impact of Body Mass Index on Operative Outcomes in Head and Neck Free Flap Surgery.* Otolaryngol Head Neck Surg, 2018. **159**(5): p. 817-823.

176. Gama, R.R., Y. Song, Q. Zhang, M.C. Brown, J. Wang, S. Habbous, . . . G. Liu, *Body mass index and prognosis in patients with head and neck cancer.* Head Neck, 2017. **39**(6): p. 1226-1233.
177. Ubags, N.D., R.D. Stapleton, J.H. Vernooy, E. Burg, J. Bement, C.M. Hayes, . . . B.T. Suratt, *Hyperleptinemia is associated with impaired pulmonary host defense.* JCI Insight, 2016. **1**(8).
178. de la Garza, G., O. Militsakh, A. Panwar, T.L. Galloway, J.B. Jorgensen, L.G. Ledgerwood, . . . N.A. Pagedar, *Obesity and perioperative complications in head and neck free tissue reconstruction.* Head Neck, 2016. **38 Suppl 1**: p. E1188-91.
179. Khan, M.N., J. Russo, J. Spivack, C. Pool, I. Likhterov, M. Teng, . . . B.A. Miles, *Association of Body Mass Index With Infectious Complications in Free Tissue Transfer for Head and Neck Reconstructive Surgery.* JAMA Otolaryngol Head Neck Surg, 2017. **143**(6): p. 574-579.
180. Patel, R.S., S.A. McCluskey, D.P. Goldstein, L. Minkovich, J.C. Irish, D.H. Brown, . . . R.W. Gilbert, *Clinicopathologic and therapeutic risk factors for perioperative complications and prolonged hospital stay in free flap reconstruction of the head and neck.* Head Neck, 2010. **32**(10): p. 1345-53.
181. Thai, L., K. McCarn, W. Stott, T. Watts, M.K. Wax, P.E. Andersen, and N.D. Gross, *Venous thromboembolism in patients with head and neck cancer after surgery.* Head Neck, 2013. **35**(1): p. 4-9.
182. Kopp, Q., D. Montoya, M. Brix, G. Dautel, and E. Simon, *[Analysis of microsurgical reconstruction activity in a university hospital: A 14-year historical cohort].* Ann Chir Plast Esthet, 2019. **64**(4): p. 311-319.
183. Chen, Y.W., C.Y. Chen, S.C. Chiang, M.T. Lui, S.Y. Kao, and M.H. Yang, *Predictors and impact of microsurgical complications in patients with locally advanced oral squamous cell carcinoma.* Cancer Sci, 2012. **103**(9): p. 1672-8.
184. Suh, J.D., J.A. Sercarz, E. Abemayor, T.C. Calcaterra, J.D. Rawnsley, D. Alam, and K.E. Blackwell, *Analysis of outcome and complications in 400 cases of microvascular head and neck reconstruction.* Arch Otolaryngol Head Neck Surg, 2004. **130**(8): p. 962-6.
185. Wolfer, S., R. Wohlrath, A. Kunzler, T. Foos, C. Ernst, and S. Schultze-Mosgau, *Scapular free flap as a good choice for mandibular reconstruction: 119 out of 280 cases after resection of oral squamous cell carcinoma in a single institution.* Br J Oral Maxillofac Surg, 2020. **58**(4): p. 451-457.
186. Grill, F.D., M. Wasmaier, T. Mucke, L.M. Ritschl, K.D. Wolff, G. Schneider, . . . V. Kadera, *Identifying perioperative volume-related risk factors in head and neck surgeries with free flap reconstructions - An investigation with focus on the influence of red blood cell concentrates and noradrenaline use.* J Craniomaxillofac Surg, 2020. **48**(1): p. 67-74.
187. Clark, J.R., S.A. McCluskey, F. Hall, J. Lipa, P. Neligan, D. Brown, . . . R. Gilbert, *Predictors of morbidity following free flap reconstruction for cancer of the head and neck.* Head Neck, 2007. **29**(12): p. 1090-101.
188. Loeffelbein, D., L.M. Ritschl, F.D. Gull, M. Roth, K.D. Wolff, and T. Mucke, *Influence of possible predictor variables on the outcome of primary oral squamous cell carcinoma: a retrospective study of 392 consecutive cases at a single centre.* Int J Oral Maxillofac Surg, 2017. **46**(4): p. 413-421.
189. Pitak-Arnnop, P., A. Hemprich, K. Dhanuthai, and N.C. Pausch, *Fibular flap for mandibular reconstruction: are there old tricks for an old dog?* Rev Stomatol Chir Maxillofac Chir Orale, 2013. **114**(1): p. 15-8.

190. Kristina, H., *Finite Element Analysis of Orthopaedic Plates and Screws to Reduce the Effects of Stress Shielding*. 2009, Ottawa-Carleton Institute for Mechanical and Aerospace Engineering, : University of Ottawa, Ottawa.
191. Zhong, S., Q. Shi, Y. Sun, S. Yang, J. Van Dessel, Y. Gu, . . . C. Politis, *Biomechanical comparison of locking and non-locking patient-specific mandibular reconstruction plate using finite element analysis.* J Mech Behav Biomed Mater, 2021. **124**: p. 104849.
192. Coletti, D.P., R. Ord, and X. Liu, *Mandibular reconstruction and second generation locking reconstruction plates: outcome of 110 patients.* Int J Oral Maxillofac Surg, 2009. **38**(9): p. 960-3.
193. Menck, J. and A. Sander, *[Periosteal and endosteal blood supply of the human fibula and its clinical importance].* Acta Anat (Basel), 1992. **145**(4): p. 400-5.
194. Strachan, R.K., I. Mccarthy, R. Fleming, and S.P.F. Hughes, *The Role of the Tibial Nutrient Artery - Microsphere Estimation of Blood-Flow in the Osteotomised Canine Tibia.* Journal of Bone and Joint Surgery-British Volume, 1990. **72**(3): p. 391-394.
195. Antabak, A., D. Papes, D. Haluzan, S. Seiwerth, N. Fuchs, I. Romic, . . . T. Luetic, *Reducing damage to the periosteal capillary network caused by internal fixation plating: An experimental study.* Injury, 2015. **46 Suppl 6**: p. S18-20.
196. Bede, S.Y.H., W.K. Ismael, and E.A. Hashim, *Reconstruction plate-related complications in mandibular continuity defects.* Oral Maxillofac Surg, 2019. **23**(2): p. 193-199.
197. Pang, J.H., S. Brooke, M.W. Kubik, R.L. Ferris, M. Dhima, M.M. Hanasono, . . . M.G. Solari, *Staged Reconstruction (Delayed-Immediate) of the Maxillectomy Defect Using CAD/CAM Technology.* J Reconstr Microsurg, 2018. **34**(3): p. 193-199.
198. Santamaria, E. and E. de la Concha, *Lessons Learned from Delayed Versus Immediate Microsurgical Reconstruction of Complex Maxillectomy and Midfacial Defects: Experience in a Tertiary Center in Mexico.* Clin Plast Surg, 2016. **43**(4): p. 719-27.
199. Zlotolow, I.M., J.M. Huryn, J.D. Piro, E. Lenchewski, and D.A. Hidalgo, *Osseointegrated implants and functional prosthetic rehabilitation in microvascular fibula free flap reconstructed mandibles.* Am J Surg, 1992. **164**(6): p. 677-81.
200. Chang, Y.M. and F.C. Wei, *Fibula Jaw-in-a-Day with Minimal Computer-Aided Design and Manufacturing: Maximizing Efficiency, Cost-Effectiveness, Intraoperative Flexibility, and Quality.* Plast Reconstr Surg, 2021. **147**(2): p. 476-479.
201. Garrido-Martinez, P., J.F. Pena-Cardelles, J.J. Pozo-Kreilinger, G. Esparza-Gomez, N. Montesdeoca-Garcia, and J.L. Cebrian-Carretero, *Jaw in a day: Osseointegration of the implants in the patient's leg before reconstructive surgery of a maxilla with ameloblastoma. A 4-year follow-up case report.* J Clin Exp Dent, 2021. **13**(1): p. e81-e87.
202. Khatib, B., A. Cheng, F. Sim, B. Bray, and A. Patel, *Challenges With the Jaw in a Day Technique.* J Oral Maxillofac Surg, 2020. **78**(10): p. 1869 e1-1869 e10.
203. Patel, A., P. Harrison, A. Cheng, B. Bray, and R.B. Bell, *Fibular Reconstruction of the Maxilla and Mandible with Immediate Implant-Supported Prosthetic Rehabilitation: Jaw in a Day.* Oral Maxillofac Surg Clin North Am, 2019. **31**(3): p. 369-386.

204. Sukato, D.C., D. Hammer, W. Wang, T. Shokri, F. Williams, and Y. Ducic, *Experience With "Jaw in a Day" Technique.* J Craniofac Surg, 2020. **31**(5): p. 1212-1217.
205. Allen, R.J., Jr., J.A. Nelson, T.O. Polanco, M.G. Shamsunder, I. Ganly, J. Boyle, . . . E. Matros, *Short-Term Outcomes following Virtual Surgery-Assisted Immediate Dental Implant Placement in Free Fibula Flaps for Oncologic Mandibular Reconstruction.* Plast Reconstr Surg, 2020. **146**(6): p. 768e-776e.
206. Rogers, S.N., J. Devine, D. Lowe, P. Shokar, J.S. Brown, and E.D. Vaugman, *Longitudinal health-related quality of life after mandibular resection for oral cancer: a comparison between rim and segment.* Head Neck, 2004. **26**(1): p. 54-62.
207. Schaaf, H., T. Wahab-Göthe, H. Kerkmann, P. Streckbein, M. Obert, J. Pons-Kuehnemann, . . . S. Attia, *Comparison between flat-panel volume computed tomography and histologic assessments of bone invasion of maxillofacial tumors: utility of an instantaneous radiologic diagnostic tool.* Oral Surg Oral Med Oral Pathol Oral Radiol, 2017. **124**(2): p. 191-198.
208. Cheung, A.C., M.A. Bredella, M. Al Khalaf, M. Grasruck, C. Leidecker, and R. Gupta, *Reproducibility of trabecular structure analysis using flat-panel volume computed tomography.* Skeletal Radiol, 2009. **38**(10): p. 1003-8.
209. Obert, M., B. Ahlemeyer, E. Baumgart-Vogt, and H. Traupe, *Flat-panel volumetric computed tomography: a new method for visualizing fine bone detail in living mice.* J Comput Assist Tomogr, 2005. **29**(4): p. 560-5.
210. Schaaf, H., P. Streckbein, M. Obert, B. Goertz, P. Christophis, H.P. Howaldt, and H. Traupe, *High resolution imaging of craniofacial bone specimens by flat-panel volumetric computed tomography.* J Craniomaxillofac Surg, 2008. **36**(4): p. 234-8.
211. Wolff, K.D., *Leitlinienprogramm Onkologie (Deutsche Krebsgesellschaft, Deutsche Krebshilfe, AWMF): S3-Leitlinie Diagnostik und Therapie des Mundhöhlenkarzinoms, Langversion 3.01 (Konsultationsfassung), 2019, AWMF Registernummer: 007/100OL https://www.leitlinienprogramm-onkologie.de/leitlinien/mundhoehlenkarzinom/ (abgerufen am: 7.2.2021).* 2019.
212. Glastonbury, C.M., A. van Zante, and P.D. Knott, *Ossification of the vascular pedicle in microsurgical fibular free flap reconstruction of the head and neck.* AJNR Am J Neuroradiol, 2014. **35**(10): p. 1965-9.
213. Karagozoglu, K.H., H.A. Winters, T. Forouzanfar, and E.A. Schulten, *Periosteal ossification of the vascular pedicle after reconstruction of continuity defects of the mandible and the maxilla with fibular free flaps: a retrospective study.* Br J Oral Maxillofac Surg, 2013. **51**(8): p. 965-7.
214. DeConde, A.S., D. Vira, K.E. Blackwell, J.M. Moriarty, J.A. Sercarz, and V. Nabili, *Neck mass due to pedicle ossification after oromandibular reconstruction.* Laryngoscope, 2011. **121**(10): p. 2095-9.
215. Knitschke, M., K. Siu, C. Bäcker, S. Attia, H.P. Howaldt, and S. Böttger, *Heterotopic Ossification of the Vascular Pedicle after Maxillofacial Reconstructive Surgery Using Fibular Free Flap: Introducing New Classification and Retrospective Analysis.* J Clin Med, 2020. **10**(1).
216. Yu, Y.Y., S. Lieu, C. Lu, and C. Colnot, *Bone morphogenetic protein 2 stimulates endochondral ossification by regulating periosteal cell fate during bone repair.* Bone, 2010. **47**(1): p. 65-73.
217. Tarsitano, A., R. Sgarzani, E. Betti, C.M. Oranges, F. Contedini, R. Cipriani, and C. Marchetti, *Vascular pedicle ossification of free fibular flap: is it a rare*

phenomenon? Is it possible to avoid this risk? Acta Otorhinolaryngol Ital, 2013. **33**(5): p. 307-10.
218. Wang, T., X. Zhang, and D.D. Bikle, *Osteogenic Differentiation of Periosteal Cells During Fracture Healing.* J Cell Physiol, 2017. **232**(5): p. 913-921.
219. Kim, B.B., A. Kaleem, S. Alzahrani, M. Yeoh, and W. Zaid, *Modified fibula free flap harvesting technique for prevention of heterotopic pedicle ossification.* Head Neck, 2019. **41**(7): p. E104-E112.
220. Myon, L., J. Ferri, M. Genty, and G. Raoul, *Consequences of bony free flap's pedicle calcification after jaw reconstruction.* J Craniofac Surg, 2012. **23**(3): p. 872-7.
221. Shindo, M., B.P. Fong, G.F. Funk, and L.H. Karnell, *The fibula osteocutaneous flap in head and neck reconstruction: a critical evaluation of donor site morbidity.* Arch Otolaryngol Head Neck Surg, 2000. **126**(12): p. 1467-72.
222. Gangidi, S.R. and D. Courtney, *"You reap what you sow"--a case of heterotopic ossification within a fasciocutaneous radial forearm free flap reconstruction.* Int J Oral Maxillofac Surg, 2013. **42**(4): p. 458-9.
223. Jehn, P., R. Zimmerer, J. Dittmann, M. Fedchenko, N.C. Gellrich, and S. Spalthoff, *Ossification of the Vascular Pedicle After Microsurgical Soft Tissue Transfer of the Lateral Upper Arm Free Flap.* Ann Plast Surg, 2019. **83**(6): p. e39-e42.
224. Sierra, N.E., P. Diaz-Gallardo, J. Knorr, V. Mascarenhas, E. Garcia-Diez, M. Munill-Ferrer, . . . F. Soldado, *Bone Allograft Segment Covered with a Vascularized Fibular Periosteal Flap: A New Technique for Pediatric Mandibular Reconstruction.* Craniomaxillofac Trauma Reconstr, 2018. **11**(1): p. 65-70.
225. Trignano, E., N. Fallico, M. Faenza, C. Rubino, and H.C. Chen, *Free fibular flap with periosteal excess for mandibular reconstruction.* Microsurgery, 2013. **33**(7): p. 527-33.
226. Kwong, F.N. and M.B. Harris, *Recent developments in the biology of fracture repair.* J Am Acad Orthop Surg, 2008. **16**(11): p. 619-25.
227. Shirley, D., D. Marsh, G. Jordan, S. McQuaid, and G. Li, *Systemic recruitment of osteoblastic cells in fracture healing.* J Orthop Res, 2005. **23**(5): p. 1013-21.
228. Autelitano, L., G. Colletti, R. Bazzacchi, and F. Biglioli, *Ossification of vascular pedicle in fibular free flaps: a report of four cases.* Int J Oral Maxillofac Surg, 2008. **37**(7): p. 669-71.
229. Burstein, F.D. and R.F. Canalis, *Studies on the osteogenic potential of vascularized periosteum: behavior of periosteal flaps transferred onto soft tissues.* Otolaryngol Head Neck Surg, 1985. **93**(6): p. 731-5.
230. Ortak, T., R. Ozdemir, A. Uysal, M.G. Ulusoy, N. Sungur, B. Sahin, . . . O. Sensoz, *Osteogenic capacities of periost grafts, periost flaps and prefabricated periosteal flaps: experimental study.* J Craniofac Surg, 2005. **16**(4): p. 594-600.
231. Takato, T., K. Harii, T. Nakatsuka, K. Ueda, and T. Ootake, *Vascularized periosteal grafts: an experimental study using two different forms of tibial periosteum in rabbits.* Plast Reconstr Surg, 1986. **78**(4): p. 489-97.
232. Gonzalez-Garcia, R., D. Manzano, L. Ruiz-Laza, C. Moreno-Garcia, and F. Monje, *The rare phenomenon of vascular pedicle ossification of free fibular flap in mandibular reconstruction.* J Craniomaxillofac Surg, 2011. **39**(2): p. 114-8.
233. Cortes, A.R., Z. Jin, M.D. Morrison, E.S. Arita, J. Song, and F. Tamimi, *Mandibular tori are associated with mechanical stress and mandibular shape.* J Oral Maxillofac Surg, 2014. **72**(11): p. 2115-25.

234. Morrison, M.D. and F. Tamimi, *Oral tori are associated with local mechanical and systemic factors: a case-control study.* J Oral Maxillofac Surg, 2013. **71**(1): p. 14-22.
235. Claes, L., K. Eckert-Hubner, and P. Augat, *The effect of mechanical stability on local vascularization and tissue differentiation in callus healing.* J Orthop Res, 2002. **20**(5): p. 1099-105.
236. McCarthy, C.M. and P.G. Cordeiro, *Microvascular reconstruction of oncologic defects of the midface.* Plast Reconstr Surg, 2010. **126**(6): p. 1947-59.
237. Möllmann, H.L., L. Apeltrath, N. Karnatz, M. Wilkat, E. Riedel, D.D. Singh, and M. Rana, *Comparison of the Accuracy and Clinical Parameters of Patient-Specific and Conventionally Bended Plates for Mandibular Reconstruction.* Front Oncol, 2021. **11**: p. 719028.
238. Sharan, R., S. Iyer, S.S. Chatni, J. Samuel, K.R. Sundaram, R.F. Cohen, . . . M.A. Kuriakose, *Increased plate and osteosynthesis related complications associated with postoperative concurrent chemoradiotherapy in oral cancer.* Head Neck, 2008. **30**(11): p. 1422-30.
239. Chang, E.I., M.P. Jenkins, S.A. Patel, and N.S. Topham, *Long-Term Operative Outcomes of Preoperative Computed Tomography-Guided Virtual Surgical Planning for Osteocutaneous Free Flap Mandible Reconstruction.* Plast Reconstr Surg, 2016. **137**(2): p. 619-623.
240. Foster, R.D., J.P. Anthony, A. Sharma, and M.A. Pogrel, *Vascularized bone flaps versus nonvascularized bone grafts for mandibular reconstruction: an outcome analysis of primary bony union and endosseous implant success.* Head Neck, 1999. **21**(1): p. 66-71.
241. Jung, J.P., K. Haunstein, H.H. Müller, I. Fischer, and A. Neff, *Intensive Care as an Independent Risk Factor for Infection after Reconstruction and Augmentation with Autologous Bone Grafts in Craniomaxillofacial Surgery: A Retrospective Cohort Study.* J Clin Med, 2021. **10**(12).
242. Mehra, P. and H. Murad, *Internal fixation of mandibular angle fractures: a comparison of 2 techniques.* J Oral Maxillofac Surg, 2008. **66**(11): p. 2254-60.
243. Swendseid, B., A. Kumar, L. Sweeny, T. Zhan, R.A. Goldman, H. Krein, . . . J.M. Curry, *Natural History and Consequences of Nonunion in Mandibular and Maxillary Free Flaps.* Otolaryngol Head Neck Surg, 2020. **163**(5): p. 956-962.
244. Yeh, D.H., D.J. Lee, A. Sahovaler, K. Fung, D. MacNeil, A.C. Nichols, and J. Yoo, *Shouldering the load of mandible reconstruction: 81 cases of oromandibular reconstruction with the scapular tip free flap.* Head Neck, 2019. **41**(1): p. 30-36.
245. Yla-Kotola, T.M., E. Bartlett, D.P. Goldstein, K. Armstrong, R.W. Gilbert, and S.O. Hofer, *Union and bone resorption of free fibular flaps in mandibular reconstruction.* J Reconstr Microsurg, 2013. **29**(7): p. 427-32.
246. Wong, R.C., H. Tideman, L. Kin, and M.A. Merkx, *Biomechanics of mandibular reconstruction: a review.* Int J Oral Maxillofac Surg, 2010. **39**(4): p. 313-9.
247. Ghiasi, M.S., J. Chen, A. Vaziri, E.K. Rodriguez, and A. Nazarian, *Bone fracture healing in mechanobiological modeling: A review of principles and methods.* Bone Rep, 2017. **6**: p. 87-100.
248. Hidalgo, D.A., *Titanium miniplate fixation in free flap mandible reconstruction.* Ann Plast Surg, 1989. **23**(6): p. 498-507.
249. Likhterov, I., A.M. Roche, and M.L. Urken, *Contemporary Osseous Reconstruction of the Mandible and the Maxilla.* Oral Maxillofac Surg Clin North Am, 2019. **31**(1): p. 101-116.

250. Zavattero, E., M. Fasolis, P. Garzino-Demo, S. Berrone, and G.A. Ramieri, *Evaluation of plate-related complications and efficacy in fibula free flap mandibular reconstruction.* J Craniofac Surg, 2014. **25**(2): p. 397-9.
251. Kreutzer, K., C. Steffen, S. Nahles, S. Koerdt, M. Heiland, C. Rendenbach, and B. Beck-Broichsitter, *Removal of patient-specific reconstruction plates after mandible reconstruction with a fibula free flap: is the plate the problem?* Int J Oral Maxillofac Surg, 2021.
252. Kreutzer, K., C. Steffen, S. Koerdt, C. Doll, T. Ebker, S. Nahles, . . . C. Rendenbach, *Patient-Specific 3D-Printed Miniplates for Free Flap Fixation at the Mandible: A Feasibility Study.* Frontiers in Surgery, 2022. **9**.
253. Yao, C.M., H. Ziai, G. Tsang, A. Copeland, D. Brown, J.C. Irish, . . . J.R. de Almeida, *Surgical site infections following oral cavity cancer resection and reconstruction is a risk factor for plate exposure.* J Otolaryngol Head Neck Surg, 2017. **46**(1): p. 30.
254. Day, K.E., R. Desmond, J.S. Magnuson, W.R. Carroll, and E.L. Rosenthal, *Hardware removal after osseous free flap reconstruction.* Otolaryngol Head Neck Surg, 2014. **150**(1): p. 40-6.
255. Knott, P.D., J.D. Suh, V. Nabili, J.A. Sercarz, C. Head, E. Abemayor, and K.E. Blackwell, *Evaluation of hardware-related complications in vascularized bone grafts with locking mandibular reconstruction plate fixation.* Arch Otolaryngol Head Neck Surg, 2007. **133**(12): p. 1302-6.
256. Tsang, G.F.Z., H. Zhang, C. Yao, M. Kolarski, P.J. Gullane, J.C. Irish, . . . J.R. de Almeida, *Hardware complications in oromandibular defects: Comparing scapular and fibular based free flap reconstructions.* Oral Oncol, 2017. **71**: p. 163-168.
257. Wood, C.B., J.R. Shinn, S.N. Amin, S.L. Rohde, and R.J. Sinard, *Risk of plate removal in free flap reconstruction of the mandible.* Oral Oncol, 2018. **83**: p. 91-95.
258. Zhang, Z.L., S. Wang, C.F. Sun, and Z.F. Xu, *Miniplates Versus Reconstruction Plates in Vascularized Osteocutaneous Flap Reconstruction of the Mandible.* J Craniofac Surg, 2019. **30**(2): p. e119-e125.
259. Militsakh, O.N., D.I. Wallace, J.D. Kriet, D.A. Girod, M.S. Olvera, and T.T. Tsue, *Use of the 2.0-mm locking reconstruction plate in primary oromandibular reconstruction after composite resection.* Otolaryngol Head Neck Surg, 2004. **131**(5): p. 660-5.
260. Dziegielewski, P.T., S. Bernard, W.M. Mendenhall, K.E. Hitchock, C. Parker Gibbs, J. Wang, . . . R. Sawhney, *Osteoradionecrosis in osseous free flap reconstruction: Risk factors and treatment.* Head Neck, 2020. **42**(8): p. 1928-1938.
261. Gur, E., A. Chiodo, C.Y. Pang, M. Mendes, K.P. Pritzker, P.C. Neligan, . . . C.R. Forrest, *The vascularized pig fibula bone flap model: effects of multiple segmental osteotomies on growth and viability.* Plast Reconstr Surg, 1999. **103**(5): p. 1436-42.
262. Chiodo, A.A., E. Gur, C.Y. Pang, P.C. Neligan, J.B. Boyd, P.M. Binhammer, and C.R. Forrest, *The vascularized pig fibula bone flap model: effect of segmental osteotomies and internal fixation on blood flow.* Plast Reconstr Surg, 2000. **105**(3): p. 1004-12.
263. Yoda, N., K. Zheng, J. Chen, Z. Liao, S. Koyama, C. Peck, . . . Q. Li, *Biomechanical analysis of bone remodeling following mandibular reconstruction using fibula free flap.* Med Eng Phys, 2018. **56**: p. 1-8.

264. Bartnikowski, N., L.E. Claes, L. Koval, V. Glatt, R. Bindl, R. Steck, . . . D.R. Epari, *Modulation of fixation stiffness from flexible to stiff in a rat model of bone healing.* Acta Orthop, 2017. **88**(2): p. 217-222.
265. Augat, P., K. Margevicius, J. Simon, S. Wolf, G. Suger, and L. Claes, *Local tissue properties in bone healing: influence of size and stability of the osteotomy gap.* J Orthop Res, 1998. **16**(4): p. 475-81.
266. Claes, L., P. Augat, G. Suger, and H.J. Wilke, *Influence of size and stability of the osteotomy gap on the success of fracture healing.* J Orthop Res, 1997. **15**(4): p. 577-84.
267. Panje, W. and C. Cutting, *Trapezius osteomyocutaneous island flap for reconstruction of the anterior floor of the mouth and the mandible.* Head Neck Surg, 1980. **3**(1): p. 66-71.
268. Sparks, D.S., D.B. Saleh, W.M. Rozen, D.W. Hutmacher, M.A. Schuetz, and M. Wagels, *Vascularised bone transfer: History, blood supply and contemporary problems.* J Plast Reconstr Aesthet Surg, 2017. **70**(1): p. 1-11.
269. Schmidt, A.B. and G.A. Giessler, *The muscular and the new osteomuscular composite peroneus brevis flap: experiences from 109 cases.* Plast Reconstr Surg, 2010. **126**(3): p. 924-932.
270. Simpson, A.H., *The blood supply of the periosteum.* J Anat, 1985. **140 (Pt 4)**: p. 697-704.
271. Rhinelander, F.W., *Tibial blood supply in relation to fracture healing.* Clin Orthop Relat Res, 1974(105): p. 34-81.
272. Kofoed, H., E. Sjontoft, S.O. Siemssen, and H.P. Olesen, *Bone marrow circulation after osteotomy. Blood flow, pO2, pCO2, and pressure studied in dogs.* Acta Orthop Scand, 1985. **56**(5): p. 400-3.
273. Strackee, S.D., F.H. Kroon, J.E. Jaspers, and K.E. Bos, *Modeling a fibula transplant in mandibular reconstructions: evaluation of the effects of a minimal number of osteotomies on the contour of the jaw.* Plast Reconstr Surg, 2001. **108**(7): p. 1915-21; discussion 1922-3.
274. Wei, F.C., E. Santamaria, Y.M. Chang, and H.C. Chen, *Mandibular reconstruction with fibular osteoseptocutaneous free flap and simultaneous placement of osseointegrated dental implants.* J Craniofac Surg, 1997. **8**(6): p. 512-21.
275. Bähr, W., *Blood supply of small fibula segments: an experimental study on human cadavers.* J Craniomaxillofac Surg, 1998. **26**(3): p. 148-52.
276. Knitschke, M., A.K. Baumgart, C. Bäcker, C. Adelung, F. Roller, D. Schmermund, . . . S. Attia, *Impact of Periosteal Branches and Septo-Cutaneous Perforators on Free Fibula Flap Outcome: A Retrospective Analysis of Computed Tomography Angiography Scans in Virtual Surgical Planning.* Front Oncol, 2021. **11**: p. 821851.
277. Chang, A.M., S.W. Kim, U. Duvvuri, J.T. Johnson, E.N. Myers, R.L. Ferris, . . . S.I. Chiosea, *Early squamous cell carcinoma of the oral tongue: comparing margins obtained from the glossectomy specimen to margins from the tumor bed.* Oral Oncol, 2013. **49**(11): p. 1077-82.
278. Hinni, M.L., A. Ferlito, M.S. Brandwein-Gensler, R.P. Takes, C.E. Silver, W.H. Westra, . . . L. Barnes, *Surgical margins in head and neck cancer: a contemporary review.* Head Neck, 2013. **35**(9): p. 1362-70.
279. Maxwell, J.H., L.D. Thompson, M.S. Brandwein-Gensler, B.G. Weiss, M. Canis, B. Purgina, . . . S.I. Chiosea, *Early Oral Tongue Squamous Cell Carcinoma:*

Sampling of Margins From Tumor Bed and Worse Local Control. JAMA Otolaryngol Head Neck Surg, 2015. **141**(12): p. 1104-10.
280. Meier, J.D., D.A. Oliver, and M.A. Varvares, *Surgical margin determination in head and neck oncology: current clinical practice. The results of an International American Head and Neck Society Member Survey.* Head Neck, 2005. **27**(11): p. 952-8.
281. Thomas Robbins, K., A. Triantafyllou, C. Suarez, F. Lopez, J.L. Hunt, P. Strojan, . . . A. Ferlito, *Surgical margins in head and neck cancer: Intra- and postoperative considerations.* Auris Nasus Larynx, 2019. **46**(1): p. 10-17.
282. Muller, S., S.C. Boy, T.A. Day, K.R. Magliocca, M.S. Richardson, P. Sloan, . . . L.D.R. Thompson, *Data Set for the Reporting of Oral Cavity Carcinomas: Explanations and Recommendations of the Guidelines From the International Collaboration of Cancer Reporting.* Arch Pathol Lab Med, 2019. **143**(4): p. 439-446.
283. Friedland, P.L., B. Bozic, J. Dewar, R. Kuan, C. Meyer, and M. Phillips, *Impact of multidisciplinary team management in head and neck cancer patients.* Br J Cancer, 2011. **104**(8): p. 1246-8.
284. Gou, L., W. Yang, X. Qiao, L. Ye, K. Yan, L. Li, and C. Li, *Marginal or segmental mandibulectomy: treatment modality selection for oral cancer: a systematic review and meta-analysis.* Int J Oral Maxillofac Surg, 2018. **47**(1): p. 1-10.
285. Abler, A., M. Roser, and D. Weingart, *[On the indications for and morbidity of segmental resection of the mandible for squamous cell carcinoma in the lower oral cavity].* Mund Kiefer Gesichtschir, 2005. **9**(3): p. 137-42.
286. Looser, K.G., J.P. Shah, and E.W. Strong, *The significance of "positive" margins in surgically resected epidermoid carcinomas.* Head Neck Surg, 1978. **1**(2): p. 107-11.
287. Ribeiro, N.F., D.R. Godden, G.E. Wilson, D.M. Butterworth, and R.T. Woodwards, *Do frozen sections help achieve adequate surgical margins in the resection of oral carcinoma?* Int J Oral Maxillofac Surg, 2003. **32**(2): p. 152-8.
288. Slootweg, P.J., G.J. Hordijk, Y. Schade, R.J. van Es, and R. Koole, *Treatment failure and margin status in head and neck cancer. A critical view on the potential value of molecular pathology.* Oral Oncol, 2002. **38**(5): p. 500-3.
289. Ebrahimi, A., R. Murali, K. Gao, M.S. Elliott, and J.R. Clark, *The prognostic and staging implications of bone invasion in oral squamous cell carcinoma.* Cancer, 2011. **117**(19): p. 4460-7.
290. Antony, A.K., W.F. Chen, A. Kolokythas, K.A. Weimer, and M.N. Cohen, *Use of virtual surgery and stereolithography-guided osteotomy for mandibular reconstruction with the free fibula.* Plast Reconstr Surg, 2011. **128**(5): p. 1080-1084.
291. Ciocca, L., S. Mazzoni, M. Fantini, F. Persiani, P. Baldissara, C. Marchetti, and R. Scotti, *A CAD/CAM-prototyped anatomical condylar prosthesis connected to a custom-made bone plate to support a fibula free flap.* Med Biol Eng Comput, 2012. **50**(7): p. 743-9.
292. Rodby, K.A., S. Turin, R.J. Jacobs, J.F. Cruz, V.J. Hassid, A. Kolokythas, and A.K. Antony, *Advances in oncologic head and neck reconstruction: systematic review and future considerations of virtual surgical planning and computer aided design/computer aided modeling.* J Plast Reconstr Aesthet Surg, 2014. **67**(9): p. 1171-85.
293. Fridman, E., S. Na'ara, J. Agarwal, M. Amit, G. Bachar, A.B. Villaret, . . . C. Neck, *The role of adjuvant treatment in early-stage oral cavity squamous cell*

carcinoma: An international collaborative study. Cancer, 2018. **124**(14): p. 2948-2955.
294. Jayasooriya, P.R., T.N. Pitakotuwage, B.R. Mendis, and T. Lombardi, *Descriptive study of 896 Oral squamous cell carcinomas from the only University based Oral Pathology Diagnostic Service in Sri Lanka.* BMC Oral Health, 2016. **16**: p. 1.
295. Knitschke, M., C. Bäcker, D. Schmermund, S. Böttger, P. Streckbein, H.P. Howaldt, and S. Attia, *Impact of Planning Method (Conventional versus Virtual) on Time to Therapy Initiation and Resection Margins: A Retrospective Analysis of 104 Immediate Jaw Reconstructions.* Cancers (Basel), 2021. **13**(12).
296. Murphy, C.T., T.J. Galloway, E.A. Handorf, B.L. Egleston, L.S. Wang, R. Mehra, . . . J.A. Ridge, *Survival Impact of Increasing Time to Treatment Initiation for Patients With Head and Neck Cancer in the United States.* J Clin Oncol, 2016. **34**(2): p. 169-78.
297. DeGraaff, L.H., A.J. Platek, A.J. Iovoli, K.E. Wooten, H. Arshad, V. Gupta, . . . A.K. Singh, *The effect of time between diagnosis and initiation of treatment on outcomes in patients with head and neck squamous cell carcinoma.* Oral Oncol, 2019. **96**: p. 148-152.
298. Ho, A.S., S. Kim, M. Tighiouart, A. Mita, K.S. Scher, J.B. Epstein, . . . Z.S. Zumsteg, *Quantitative survival impact of composite treatment delays in head and neck cancer.* Cancer, 2018. **124**(15): p. 3154-3162.
299. Bagnardi, V., M. Blangiardo, C. La Vecchia, and G. Corrao, *Alcohol consumption and the risk of cancer: a meta-analysis.* Alcohol Res Health, 2001. **25**(4): p. 263-70.
300. Awwad, H.K., M. Lotayef, T. Shouman, A.C. Begg, G. Wilson, S.M. Bentzen, . . . S. Eissa, *Accelerated hyperfractionation (AHF) compared to conventional fractionation (CF) in the postoperative radiotherapy of locally advanced head and neck cancer: influence of proliferation.* Br J Cancer, 2002. **86**(4): p. 517-23.
301. Ariyan, S., *The pectoralis major myocutaneous flap. A versatile flap for reconstruction in the head and neck.* Plast Reconstr Surg, 1979. **63**(1): p. 73-81.
302. Ariyan, S., *Pectoralis major, sternomastoid, and other musculocutaneous flaps for head and neck reconstruction.* Clin Plast Surg, 1980. **7**(1): p. 89-109.
303. Bakamjian, V.Y. and M. Poole, *Maxillo-facial and palatal reconstructions with the deltopectoral flap.* Br J Plast Surg, 1977. **30**(1): p. 17-37.
304. Waech, T., S. Pazahr, V. Guarda, N.J. Rupp, M.A. Broglie, and G.B. Morand, *Measurement variations of MRI and CT in the assessment of tumor depth of invasion in oral cancer: A retrospective study.* Eur J Radiol, 2021. **135**: p. 109480.
305. Morand, G.B., K. Ikenberg, D.G. Vital, I. Cardona, H. Moch, S.J. Stoeckli, and G.F. Huber, *Preoperative assessment of CD44-mediated depth of invasion as predictor of occult metastases in early oral squamous cell carcinoma.* Head Neck, 2019. **41**(4): p. 950-958.
306. Lwin, C.T., R. Hanlon, D. Lowe, J.S. Brown, J.A. Woolgar, A. Triantafyllou, . . . R.J. Shaw, *Accuracy of MRI in prediction of tumour thickness and nodal stage in oral squamous cell carcinoma.* Oral Oncol, 2012. **48**(2): p. 149-54.
307. Madana, J., F. Laliberte, G.B. Morand, D. Yolmo, M.J. Black, A.M. Mlynarek, and M.P. Hier, *Computerized tomography based tumor-thickness measurement is useful to predict postoperative pathological tumor thickness in oral tongue squamous cell carcinoma.* J Otolaryngol Head Neck Surg, 2015. **44**(1): p. 49.

308. Noorlag, R., T.J.W. Klein Nulent, V.E.J. Delwel, F.A. Pameijer, S.M. Willems, R. de Bree, and R.J.J. van Es, *Assessment of tumour depth in early tongue cancer: Accuracy of MRI and intraoral ultrasound.* Oral Oncol, 2020. **110**: p. 104895.
309. Shah, J.P. and Z. Gil, *Current concepts in management of oral cancer--surgery.* Oral Oncol, 2009. **45**(4-5): p. 394-401.
310. Alsaffar, H.A., D.P. Goldstein, E.V. King, J.R. de Almeida, D.H. Brown, R.W. Gilbert, . . . J.C. Irish, *Correlation between clinical and MRI assessment of depth of invasion in oral tongue squamous cell carcinoma.* Journal of Otolaryngology - Head & Neck Surgery, 2016. **45**(1): p. 61.
311. de Lima, J.M., G.B. Morand, C.C.S. Macedo, L. Diesel, M.P. Hier, A. Mlynarek, . . . S.D. da Silva, *NDRG1 deficiency is associated with regional metastasis in oral cancer by inducing epithelial-mesenchymal transition.* Carcinogenesis, 2020. **41**(6): p. 769-777.
312. Mao, M.-H., S. Wang, Z.-e. Feng, J.-Z. Li, H. Li, L.-z. Qin, and Z.-x. Han, *Accuracy of magnetic resonance imaging in evaluating the depth of invasion of tongue cancer. A prospective cohort study.* Oral Oncology, 2019. **91**: p. 79-84.
313. Umstattd, L.A., J.C. Mills, W.A. Critchlow, G.J. Renner, and R.P. Zitsch, 3rd, *Shrinkage in oral squamous cell carcinoma: An analysis of tumor and margin measurements in vivo, post-resection, and post-formalin fixation.* Am J Otolaryngol, 2017. **38**(6): p. 660-662.
314. Johnson, R.E., J.D. Sigman, G.F. Funk, R.A. Robinson, and H.T. Hoffman, *Quantification of surgical margin shrinkage in the oral cavity.* Head Neck, 1997. **19**(4): p. 281-6.
315. Bosc, R., B. Hersant, R. Carloni, J. Niddam, J. Bouhassira, H. De Kermadec, . . . J.P. Meningaud, *Mandibular reconstruction after cancer: an in-house approach to manufacturing cutting guides.* Int J Oral Maxillofac Surg, 2017. **46**(1): p. 24-31.
316. Smithers, F.A.E., K. Cheng, R. Jayaram, P. Mukherjee, and J.R. Clark, *Maxillofacial reconstruction using in-house virtual surgical planning.* ANZ J Surg, 2018. **88**(9): p. 907-912.
317. Wang, Y.Y., H.Q. Zhang, S. Fan, D.M. Zhang, Z.Q. Huang, W.L. Chen, . . . J.S. Li, *Mandibular reconstruction with the vascularized fibula flap: comparison of virtual planning surgery and conventional surgery.* Int J Oral Maxillofac Surg, 2016. **45**(11): p. 1400-1405.
318. Mazzola, F., F. Smithers, K. Cheng, P. Mukherjee, T.H. Hubert Low, S. Ch'ng, . . . J.R. Clark, *Time and cost-analysis of virtual surgical planning for head and neck reconstruction: A matched pair analysis.* Oral Oncol, 2020. **100**: p. 104491.
319. Bell, R.B., *Computer planning and intraoperative navigation in cranio-maxillofacial surgery.* Oral Maxillofac Surg Clin North Am, 2010. **22**(1): p. 135-56.
320. Modabber, A., C. Legros, M. Rana, M. Gerressen, D. Riediger, and A. Ghassemi, *Evaluation of computer-assisted jaw reconstruction with free vascularized fibular flap compared to conventional surgery: a clinical pilot study.* Int J Med Robot, 2012. **8**(2): p. 215-20.
321. Yanamoto, S., S. Yamada, H. Takahashi, I. Yoshitomi, G. Kawasaki, H. Ikeda, . . . M. Umeda, *Clinicopathological risk factors for local recurrence in oral squamous cell carcinoma.* Int J Oral Maxillofac Surg, 2012. **41**(10): p. 1195-200.
322. Zanoni, D.K., J.C. Migliacci, B. Xu, N. Katabi, P.H. Montero, I. Ganly, . . . S.G. Patel, *A Proposal to Redefine Close Surgical Margins in Squamous Cell*

Carcinoma of the Oral Tongue. JAMA Otolaryngol Head Neck Surg, 2017. **143**(6): p. 555-560.
323. Chen, W.C., C.H. Lai, C.C. Fang, Y.H. Yang, P.C. Chen, C.P. Lee, and M.F. Chen, *Identification of High-Risk Subgroups of Patients With Oral Cavity Cancer in Need of Postoperative Adjuvant Radiotherapy or Chemo-Radiotherapy.* Medicine (Baltimore), 2016. **95**(22): p. e3770.
324. Magliocca, K.R., *Surgical Margins: The Perspective of Pathology.* Oral Maxillofac Surg Clin North Am, 2017. **29**(3): p. 367-375.
325. Smits, R.W., S. Koljenovic, J.A. Hardillo, I. Ten Hove, C.A. Meeuwis, A. Sewnaik, . . . R.J. Baatenburg de Jong, *Resection margins in oral cancer surgery: Room for improvement.* Head Neck, 2016. **38 Suppl 1**: p. E2197-203.
326. Xiao, R., M.C. Ward, K. Yang, D.J. Adelstein, S.A. Koyfman, B.L. Prendes, and B.B. Burkey, *Increased pathologic upstaging with rising time to treatment initiation for head and neck cancer: A mechanism for increased mortality.* Cancer, 2018. **124**(7): p. 1400-1414.
327. Onoda, S. and K. Masahito, *Microsurgery for Head and Neck Reconstruction.* J Craniofac Surg, 2020. **31**(5): p. 1441-1444.
328. Kim, D., D.E. Orron, and J.J. Skillman, *Surgical significance of popliteal arterial variants. A unified angiographic classification.* Ann Surg, 1989. **210**(6): p. 776-81.
329. Hölzle, F., E.P. Franz, V.H. von Diepenbroick, and K.D. Wolff, *[Evaluation of the lower leg vessels before microsurgical fibula transfer. Magnetic resonance angiography versus digital subtraction angiography].* Mund Kiefer Gesichtschir, 2003. **7**(4): p. 246-53.
330. Wales, C.J., J. Morrison, R. Drummond, J.C. Devine, and J. McMahon, *Pre-operative evaluation of vascularised fibula donor sites: a UK maxillofacial e-survey.* Br J Oral Maxillofac Surg, 2010. **48**(3): p. 192-4.
331. Abou-Foul, A.K. and F. Borumandi, *Anatomical variants of lower limb vasculature and implications for free fibula flap: Systematic review and critical analysis.* Microsurgery, 2016. **36**(2): p. 165-72.
332. Akashi, M., T. Nomura, S. Sakakibara, A. Sakakibara, and K. Hashikawa, *Preoperative MR angiography for free fibula osteocutaneous flap transfer.* Microsurgery, 2013. **33**(6): p. 454-9.
333. Kelly, A.M., P. Cronin, H.K. Hussain, F.J. Londy, D.B. Chepeha, and R.C. Carlos, *Preoperative MR angiography in free fibula flap transfer for head and neck cancer: clinical application and influence on surgical decision making.* AJR Am J Roentgenol, 2007. **188**(1): p. 268-74.
334. Schuderer, J.G., J.K. Meier, C. Klingelhöffer, M. Gottsauner, T.E. Reichert, C.M. Wendl, and T. Ettl, *Magnetic resonance angiography for free fibula harvest: anatomy and perforator mapping.* Int J Oral Maxillofac Surg, 2020. **49**(2): p. 176-182.
335. Battaglia, S., V. Maiolo, G. Savastio, M. Zompatori, F. Contedini, E. Antoniazzi, . . . A. Tarsitano, *Osteomyocutaneous fibular flap harvesting: Computer-assisted planning of perforator vessels using Computed Tomographic Angiography scan and cutting guide.* J Craniomaxillofac Surg, 2017. **45**(10): p. 1681-1686.
336. Ribuffo, D., M. Atzeni, L. Saba, M. Guerra, G. Mallarini, E.B. Proto, . . . W.M. Rozen, *Clinical study of peroneal artery perforators with computed tomographic angiography: implications for fibular flap harvest.* Surg Radiol Anat, 2010. **32**(4): p. 329-34.

337. Ettinger, K.S., A.E. Alexander, and K. Arce, *Computed Tomographic Angiography Perforator Localization for Virtual Surgical Planning of Osteocutaneous Fibular Free Flaps in Head and Neck Reconstruction.* J Oral Maxillofac Surg, 2018. **76**(10): p. 2220-2230.
338. Ma, C., L. Wang, Z. Tian, X. Qin, D. Zhu, J. Qin, and Y. Shen, *Standardize routine angiography assessment of leg vasculatures before fibular flap harvest: lessons of congenital and acquired vascular anomalies undetected by color Doppler and physical examinations.* Acta Radiol, 2021: p. 284185120980001.
339. Napoli, A., M. Anzidei, F. Zaccagna, B. Cavallo Marincola, C. Zini, G. Brachetti, . . . R. Passariello, *Peripheral arterial occlusive disease: diagnostic performance and effect on therapeutic management of 64-section CT angiography.* Radiology, 2011. **261**(3): p. 976-86.
340. Shwaiki, O., B. Rashwan, M.A. Fink, L. Kirksey, S. Gadani, K. Karuppasamy, . . . S. Partovi, *Lower extremity CT angiography in peripheral arterial disease: from the established approach to evolving technical developments.* Int J Cardiovasc Imaging, 2021.
341. Rozen, W.M., T.J. Phillips, M.W. Ashton, D.L. Stella, R.N. Gibson, and G.I. Taylor, *Preoperative imaging for DIEA perforator flaps: a comparative study of computed tomographic angiography and doppler ultrasound.* Plast Reconstr Surg, 2008. **121**(1 Suppl): p. 1-8.
342. Abdel Razek, A.A., A.T. Denewer, M.A. Hegazy, and M.T. Hafez, *Role of computed tomography angiography in the diagnosis of vascular stenosis in head and neck microvascular free flap reconstruction.* Int J Oral Maxillofac Surg, 2014. **43**(7): p. 811-5.
343. Garvey, P.B., E.I. Chang, J.C. Selber, R.J. Skoracki, J.E. Madewell, J. Liu, . . . M.M. Hanasono, *A prospective study of preoperative computed tomographic angiographic mapping of free fibula osteocutaneous flaps for head and neck reconstruction.* Plast Reconstr Surg, 2012. **130**(4): p. 541e-549e.
344. Fuhrman, T.M., W.D. Pippin, L.A. Talmage, and T.E. Reilley, *Evaluation of collateral circulation of the hand.* J Clin Monit, 1992. **8**(1): p. 28-32.
345. Wood, J.W., K.C. Broussard, and B. Burkey, *Preoperative testing for radial forearm free flaps to reduce donor site morbidity.* JAMA Otolaryngol Head Neck Surg, 2013. **139**(2): p. 183-6.
346. Yao, S.T., J.T. Hobbs, and W.T. Irvine, *Ankle pressure measurement in arterial disease of the lower extremities.* Br J Surg, 1968. **55**(11): p. 859-60.
347. Fowkes, F.G., *The measurement of atherosclerotic peripheral arterial disease in epidemiological surveys.* Int J Epidemiol, 1988. **17**(2): p. 248-54.
348. Fowkes, F.G., E. Housley, C.C. Macintyre, R.J. Prescott, and C.V. Ruckley, *Variability of ankle and brachial systolic pressures in the measurement of atherosclerotic peripheral arterial disease.* J Epidemiol Community Health, 1988. **42**(2): p. 128-33.
349. Anzidei, M., P. Lucatelli, A. Napoli, S. Jens, L. Saba, G. Cartocci, . . . C. Catalano, *CT angiography and magnetic resonance angiography findings after surgical and interventional radiology treatment of peripheral arterial obstructive disease.* J Cardiovasc Comput Tomogr, 2015. **9**(3): p. 165-82.
350. Mishra, A., N. Jain, and A. Bhagwat, *CT Angiography of Peripheral Arterial Disease by 256-Slice Scanner: Accuracy, Advantages and Disadvantages Compared to Digital Subtraction Angiography.* Vasc Endovascular Surg, 2017. **51**(5): p. 247-254.

351. Bartella, A.K., C. Luderich, M. Kamal, T. Braunschweig, J. Steegmann, A. Modabber, . . . B. Lethaus, *Ankle Brachial Index Predicts for Difficulties in Performing Microvascular Anastomosis.* J Oral Maxillofac Surg, 2020. **78**(6): p. 1020-1026.
352. Klein, S., J.J. Hage, C.M. van der Horst, and M. Lagerweij, *Ankle-arm index versus angiography for the preassessment of the fibula free flap.* Plast Reconstr Surg, 2003. **111**(2): p. 735-43.
353. Rosson, G.D. and N.K. Singh, *Devascularizing complications of free fibula harvest: peronea arteria magna.* J Reconstr Microsurg, 2005. **21**(8): p. 533-8.
354. Sarkar, D.F., N. Mishra, D. Samal, D. Pati, I.B. Kar, D. Mohapatra, and A. Mishra, *Locking versus non-locking plating system in the treatment of mandibular fractures: A randomized comparative study.* J Craniomaxillofac Surg, 2021. **49**(3): p. 184-190.
355. Futran, N.D., B.C. Stack, Jr., and A.P. Zachariah, *Ankle-arm index as a screening examination for fibula free tissue transfer.* Ann Otol Rhinol Laryngol, 1999. **108**(8): p. 777-80.
356. Astarci, P., S. Siciliano, R. Verhelst, V. Lacroix, P. Noirhomme, J. Rubay, . . . G. El Kourhy, *Intra-operative acute leg ischaemia after free fibula flap harvest for mandible reconstruction.* Acta Chir Belg, 2006. **106**(4): p. 423-6.
357. Knitschke, M., A.K. Baumgart, C. Bäcker, C. Adelung, F. Roller, D. Schmermund, . . . S. Attia, *Computed Tomography Angiography (CTA) before Reconstructive Jaw Surgery Using Fibula Free Flap: Retrospective Analysis of Vascular Architecture.* Diagnostics (Basel), 2021. **11**(10).
358. Chiu, W.K., W.C. Lin, S.Y. Chen, W.D. Tzeng, S.C. Liu, T.P. Lee, and S.G. Chen, *Computed tomography angiography imaging for the chimeric anterolateral thigh flap in reconstruction of full thickness buccal defect.* ANZ J Surg, 2011. **81**(3): p. 142-7.
359. Prokop, M., *Multislice CT angiography.* Eur J Radiol, 2000. **36**(2): p. 86-96.
360. Gaillard, J., L.M. Bourcheix, and A.C. Masquelet, *Perforators of the fibular artery and suprafascial network.* Surg Radiol Anat, 2018. **40**(8): p. 927-933.
361. Fry, A.M., D. Laugharne, and K. Jones, *Osteotomising the fibular free flap: an anatomical perspective.* Br J Oral Maxillofac Surg, 2016. **54**(6): p. 692-3.
362. Chang, E.I., C.K. Chu, and E.I. Chang, *Advancements in imaging technology for microvascular free tissue transfer.* J Surg Oncol, 2018. **118**(5): p. 729-735.
363. Abou-Foul, A.K., A. Fasanmade, S. Prabhu, and F. Borumandi, *Anatomy of the vasculature of the lower leg and harvest of a fibular flap: a systematic review.* Br J Oral Maxillofac Surg, 2017. **55**(9): p. 904-910.
364. Carroll, W.R. and R. Esclamado, *Preoperative vascular imaging for the fibular osteocutaneous flap.* Arch Otolaryngol Head Neck Surg, 1996. **122**(7): p. 708-12.
365. Seres, L., J. Csaszar, L. Borbely, and E. Voros, *[Donor site digital subtraction angiography before mandible reconstruction with free fibula transplantation].* Fogorv Sz, 2001. **94**(1): p. 15-20.
366. Yanik, B., E. Bulbul, and G. Demirpolat, *Variations of the popliteal artery branching with multidetector CT angiography.* Surg Radiol Anat, 2015. **37**(3): p. 223-30.
367. Lee, M.K., K.E. Blackwell, B. Kim, and V. Nabili, *Feasibility of microvascular head and neck reconstruction in the setting of calcified arteriosclerosis of the vascular pedicle.* JAMA Facial Plast Surg, 2013. **15**(2): p. 135-40.

368. Kim, R.Y., J.N. Burkes, H.S. Broker, and F.C. Williams, *Preoperative Vascular Interventions to Improve Donor Leg Perfusion: A Report of Two Fibula Free Flaps Used in Head and Neck Reconstruction.* J Oral Maxillofac Surg, 2019. **77**(3): p. 658-663.
369. Lorenz, R.R. and R. Esclamado, *Preoperative magnetic resonance angiography in fibular-free flap reconstruction of head and neck defects.* Head Neck, 2001. **23**(10): p. 844-50.
370. Bui, D.T., P.G. Cordeiro, Q.Y. Hu, J.J. Disa, A. Pusic, and B.J. Mehrara, *Free flap reexploration: indications, treatment, and outcomes in 1193 free flaps.* Plast Reconstr Surg, 2007. **119**(7): p. 2092-100.
371. Wood, N.B., S.Z. Zhao, A. Zambanini, M. Jackson, W. Gedroyc, S.A. Thom, . . . X.Y. Xu, *Curvature and tortuosity of the superficial femoral artery: a possible risk factor for peripheral arterial disease.* J Appl Physiol (1985), 2006. **101**(5): p. 1412-8.
372. Momoh, A.O., P. Yu, R.J. Skoracki, S. Liu, L. Feng, and M.M. Hanasono, *A prospective cohort study of fibula free flap donor-site morbidity in 157 consecutive patients.* Plast Reconstr Surg, 2011. **128**(3): p. 714-20.
373. Zimmermann, C.E., B.I. Borner, A. Hasse, and P. Sieg, *Donor site morbidity after microvascular fibula transfer.* Clin Oral Investig, 2001. **5**(4): p. 214-9.
374. Babovic, S., C.H. Johnson, and S.J. Finical, *Free fibula donor-site morbidity: the Mayo experience with 100 consecutive harvests.* J Reconstr Microsurg, 2000. **16**(2): p. 107-10.
375. Ling, X.F. and X. Peng, *What is the price to pay for a free fibula flap? A systematic review of donor-site morbidity following free fibula flap surgery.* Plast Reconstr Surg, 2012. **129**(3): p. 657-74.
376. Fang, H., F. Liu, C. Sun, and P. Pang, *Impact of wound closure on fibular donor-site morbidity: a meta-analysis.* BMC Surg, 2019. **19**(1): p. 81.
377. Bach, C.A., L. Guillere, S. Yildiz, I. Wagner, S. Darmon, and F. Chabolle, *Comparison of negative pressure wound therapy and conventional dressing methods for fibula free flap donor site management in patients with head and neck cancer.* Head Neck, 2016. **38**(5): p. 696-9.
378. Shimbo, K., Y. Okuhara, and K. Yokota, *Closure of a free osteofasciocutaneous fibula flap donor site using local skin grafts or flaps: A systematic review and meta-analysis.* Microsurgery, 2022. **42**(2): p. 192-198.
379. Fry, A.M., A. Patterson, R.L. Orr, and G.B. Colver, *Open wound healing of the osseocutaneous fibula flap donor site.* Br J Oral Maxillofac Surg, 2014. **52**(9): p. 861-3.
380. Li, P., Q. Fang, J. Qi, R. Luo, and C. Sun, *Risk Factors for Early and Late Donor-Site Morbidity After Free Fibula Flap Harvest.* J Oral Maxillofac Surg, 2015. **73**(8): p. 1637-40.